USC
UNIVERSIDADE DE SANTIAGO DE COMPOSTELA

INTERNATIONAL DOCTORAL SCHOOL OF THE USC

Miguel
Cobo Golpe

PhD Thesis

Mass spectrometry coupled to chromatographic techniques and direct sample injection. Toxicological and environmental applications

Santiago de Compostela, 2024

Doctoral Programme in Chemical Science and Technology

USC
UNIVERSIDADE
DE SANTIAGO
DE COMPOSTELA

INTERNATIONAL DOCTORAL
SCHOOL OF THE USC

DOCTORAL THESIS

MASS SPECTROMETRY COUPLED TO CHROMATOGRAPHIC TECHNIQUES AND DIRECT SAMPLE INJECTION. TOXICOLOGICAL AND ENVIRONMENTAL APPLICATIONS

Miguel Cobo Golpe

Supervisor/s: Isaac Rodríguez Pereiro

María Ramil Criado

Tutor: Isaac Rodríguez Pereiro

PHD PROGRAMME IN CHEMICAL SCIENCE AND TECHNOLOGY.

SANTIAGO DE COMPOSTELA

2024

USC
UNIVERSIDADE
DE SANTIAGO
DE COMPOSTELA

ACKNOWLEDEGEMENTS

I would like to acknowledge the financial support by the Spanish government through the FPI contract (ref: PGC2018-094613-B-10) to develop this doctoral Thesis

Furthermore, research developed along this Thesis has received economic support from projects TED2021-129962B-C42, funded by the Spanish Ministry of Science and Innovation, through the UE Next Generation program; and ED431C2021/06, from Xunta de Galicia, co-financed the EU FEDER program.







ATRIBUTION TO FIGURES

All the original figures and charts present in this Thesis were prepared by the PhD student using Chemdraw (22.0 version), Microsoft® Powerpoint® (version 2021).

Data (figures and tables) from the publications included in this Thesis were shown or adapted using the above-mentioned software. Journal permissions are given at the end of the document.

USC
UNIVERSIDADE
DE SANTIAGO
DE COMPOSTELA

USC
UNIVERSIDADE
DE SANTIAGO
DE COMPOSTELA

AGRADECIMIENTOS

Parece mentira que ya hayan pasado cinco años desde que empecé la etapa de la tesis. En estos cinco años ha pasado de todo, desde el comienzo de nuevas amistades hasta el transcurso de una pandemia, quién lo hubiese dicho. A lo largo de todos estos años he tenido a mucha gente que me ha apoyado incondicionalmente, incluyendo a aquellos que nos han dejado; por ello me gustaría agradecer a todos ellos el apoyo que me han prestado.

En primer lugar, me gustaría agradecer a mis directores de tesis: **Isaac** y **María** por ofrecerme la oportunidad de hacer la tesis bajo su tutela y toda la ayuda y el apoyo que me han prestado a lo largo de los años, ya que, sin ellos, nada de esto sería posible. Muchas gracias por apretarme las tuercas cuando era necesario y estar siempre ahí para resolver las dudas que me surgieron durante los experimentos más complejos.

Muchas gracias, **Andrea** por todos los años que hemos compartido juntos desde que empezamos la carrera, siempre has estado ahí para mi durante los 4 años de carrera, el año del máster y durante estos largos años de la tesis, ayudándome a ver la luz al final del túnel; muchas gracias también por recomendarme que viniese a este laboratorio a hacer el trabajo de fin de máster, lo que acabó provocando que llegase este momento, quiero que sepas que pase lo que pase, me tendrás a sólo una llamada de distancia para lo que necesites.

Muchas gracias, **Leti** y **Gabi** por toda la ayuda que me disteis cuando empecé siendo sólo un estudiante de máster, y también todas las veces que me seguisteis ayudando durante el doctorado, muchas gracias, **Javi** por las risas y las divertidas conversaciones que tuvimos a lo largo de estos años, eres un trabajador nato y creo que va siendo hora de que deje de llamarte "casual" que te lo has ganado, gracias, **Vicky** por la ayuda en el trabajo de laboratorio y mucho ánimo, que ya no te queda nada. Gracias **Carlos** y **Sandra** por estar ahí siempre dispuestos a ayudar y por amenizar los descansos del café y mucho ánimo, que la tesis se pasa volando. Tampoco puedo olvidarme de agradecerle a **Sara** y a **Rafa** por su inestimable ayuda en algunas de mis publicaciones y por mantener siempre una sonrisa en la cara o de **Beni**, por siempre ayudar cuando había problemas en los equipos o las amenas conversaciones sobre juegos de Nintendo durante los cafés, tampoco olvidarme de **Tito** y **Charo**, con Charo ayudando con el tema de la normativa del doctorado y Tito ayudando cuando había problemas y por el buen trato de ambos en el laboratorio. Quería hacer también una mención a las personas que hicieron el TFG o TFM conmigo, muchas gracias a **Jose**, **Sandra**, **Jenny**, **Gloria**, **Alba** y **Tania**; sin vuestra ayuda, no hubiese llegado tan lejos, todos sois unos grandes trabajadores y solo os deseo lo mejor de ahora en adelante, en especial en el caso de Tania, quién se quedaba a ayudar fuera del trabajo de su TFG. Muchas gracias a todos, ya que el trabajo en el laboratorio no hubiese sido el mismo sin todos vosotros.

I want to give my thanks and best regards to **Thomas**, **Felix**, **Philipp**, **Karel** and everyone else at Agroscope for looking out for me and helping me with a smile whenever I needed help during the three months I spent there, you turned the whole stay into a really special and fond memory for me, I hope we can work together again in the future.

USC DE COMPOSTELA

I can't forget about **Rim**, who may have stayed on our lab for only a month, but that month is filled with great memories and are some of my most special memories during the realization of my PhD, not only was a pleasure working with her, it is also thanks to her that we were able to open some investigation lines we didn't think about before. I hope we can meet again soon and work together again.

También quiero agradecer a los amigos que he hecho a lo largo de mi vida, empezando por **Iago**, mi mejor amigo y el mejor amigo que nadie pueda tener, gracias por estar siempre ahí cuando te he necesitado y por todos los buenos momentos que hemos vivido desde que éramos pequeños. **Manuel** y **Rubén**, gracias por hacer mi vida universitaria toda una aventura y por toda la ayuda que me habéis brindado durante todos estos años; os deseo mucha suerte en vuestras Tesis. Muchas gracias, **Andrea Chaves** y **Sandra** por haberme querido en los grupos de trabajo de la carrera junto con Andrea, hemos pasado muchas cosas juntos los cuatro, hemos reído mucho juntos y siempre era un placer trabajar con vosotras, mucho ánimo con todo, siempre tendréis mi apoyo. Muchas gracias Xulián por los buenos momentos durante la carrera y la paciencia que tienes, sobre todo con el proyecto de PPQ, espero que sigas así y tengas un gran futuro.

Por último, pero no menos importante, sino todo lo contrario, muchas gracias a toda mi familia por vuestro apoyo incondicional desde el principio. **Papá** y **mamá**, muchas gracias por haber estado siempre ahí en todo momento, ayudándome siempre en todo y haciendo siempre lo mejor por mí. Muchas gracias, **Luis** y **María** por ser los mejores hermanos que uno puede pedir, gracias por todos los buenos momentos que pasamos juntos desde pequeños. Muchas gracias abuela **Ana**, por siempre creer en mí y animarme, muchas gracias abuelo **Antonio**, aunque ya no estés con nosotros, sé que te alegraría saber que tu químico lo ha conseguido. Muchas gracias a ambos por ayudar a mamá a cuidarnos y por aseguraros siempre de nuestro bienestar.

Muchas gracias a toda la gente que he conocido y me ha ayudado a llegar hasta aquí, me ha brindado su amistad y me ha apoyado en los tiempos difíciles. Nunca lo hubiese logrado de no ser por todos ellos.

USC
UNIVERSIDADE DE SANTIAGO DE COMPOSTELA

“Life is like a video game. You come into the game, push the power on, you face trials and tribulations, ups and downs and each time the failures make you stronger, the wins make you stronger and you grow.
Then you realize at the end of the game you’ve been the hero the whole way, so be your hero”

Charles Martinet

USC
UNIVERSIDADE DE SANTIAGO DE COMPOSTELA

USC
UNIVERSIDADE
DE SANTIAGO
DE COMPOSTELA

INDEX

INDEX....11
Abbreviations and acronyms....14
List of Figures....23
List of Tables....25
Abstract....27
Resumo....29
1 Introduction....37
1.1 Mass spectrometry....37
1.1.1 Mass analysers....37
1.1.2 Tandem mass spectrometry....38
1.1.2.1 Non-target screening....41
1.1.2.2 Target and suspect screening....42
1.2 Chromatographic and direct sample introduction methodologies....44
1.2.1 Liquid chromatography (LC)....44
1.2.1.1 Liquid chromatography coupled to mass spectrometry (LC-MS)....46
1.2.1.2 Screening strategies employed in LC-ESI-QTOF-MS....47
1.2.1.3 Data processing from MS and MS/MS spectra for structure elucidation and identification....49
1.2.1.4 Applications of LC-MS to the determination of emerging pollutants in environmental samples....50
1.2.2 Supercritical fluid chromatography....51
1.2.2.1 Supercritical fluid chromatography coupled to mass spectrometry....52
1.2.2.2 Applications of SFC-MS to the separation of chiral pollutants in environmental samples....53
1.2.3 Gas chromatography....55
1.2.3.1 Gas chromatography coupled to mass spectrometry.....57
1.2.3.2 Data acquisition and processing in GC-QTOF-EI-MS....57
1.2.3.3 Applications of GC-MS to the determination of emerging pollutants in air samples.....58
1.2.4 Direct sample injection. Direct analysis in real time....59

USC UNIVERSIDADE DE SANTIAGO DE COMPOSTELA

1.2.4.1 Direct analysis in real time (DART) source coupled to mass spectrometry 60
1.2.4.2 Applications of DART-MS for the analysis of emerging pollutants. 61
1.3 Sample preparation 62
1.3.1 Solid-phase extraction 62
1.3.2 Matrix solid-phase dispersion 66
1.3.3 Pressurized liquid extraction 68
1.3.4 Ultrasound assisted extraction 69
1.4 Studied compounds 70
1.4.1 Volatile and semi-volatile organic compounds in indoor air 70
1.4.2 Electronic cigarette refill characterization 71
1.4.3 Emerging pollutants 72
1.4.3.1 Pharmaceuticals 73
1.4.3.1.1 Tertiary treatments applied in wastewater treatment plants 73
1.4.3.2 Pesticides and plastic litter 76
References 78
2 Justification and objectives 87
3 Material and methods 89
4 Results 93
Chapter 1. Development of non-target screening methodologies using high resolution mass spectrometry for a comprehensive characterization of environmental and commercially available samples. 93
Publication I: Portable dehumidifiers condensed water: A novel matrix for the screening of semi-volatile compounds in indoor air 97
Publication II: Predicting concentrations of volatile and semi-volatile compounds in indoor areas through analysis of condensed water samples. A proof of concept 121
Publication III: Comprehensive characterization of volatile and semi-volatile compounds in e-liquids for electronic cigarette using gas chromatography accurate mass spectrometry 143
Publication IV: Comparison of UV, chlorination, UV-hydrogen peroxide and UV-chlorine processes for tramadol removal: Kinetics study and transformation products identification 175
Chapter 2. Target analysis of selected pollutants in complex environmental matrices 201

USC UNIVERSIDADE DE SANTIAGO DE COMPOSTELA

Publication V: Chlorhexidine residues in sludge from municipal wastewater treatment plants: analytical determination and toxicity evaluation 203

Publication VI: Assessment of direct analysis in real time accurate mass spectrometry for the determination of triclosan in complex matrices..... 221

Publication VII: Supercritical fluid chromatography time-of-flight mass spectrometry enantiomeric determination of basic drugs in sewage samples..... 239

Publication VIII: Assessment of the occurrence and interaction between pesticides and plastic litter from vineyard plots..... 257

5 Integrative discussion 287

Chapter 1: Development of non-target screening methodologies using high resolution mass spectrometry for a comprehensive characterization of environmental and commercially available samples..... 290

Chapter 2: Target analysis of selected pollutants in complex environmental matrices. 294

6 CONCLUSIONS.....299

Annex 1: List of publications and contribution statements 303

Annex 2: Reproduction Permissions 307

USC
UNIVERSIDADE DE SANTIAGO DE COMPOSTELA

ABBREVIATIONS AND ACRONYMS

1

1,2-DBP	1,2-dibromopropane

A

AC	Alternating current
ACN	Acetonitrile
AcOEt	Ethyl acetate
AME	Ametoctradin
AOP	Advanced Oxidation Process
APCI	Atmospheric Pressure Chemical Ionization
API	Atmospheric Pressure Ionization
APPI	Atmospheric Pressure Photoionization
ASE	Accelerated Solvent Extraction
ATR	Total Attenuated Reflectance
AZO	Azoxystrobin

B

BEN	Benalaxyl
BPR	Back-Pressure Regulator

C

CAR	Carbendazim
CBA	p-Chlorobenzoic acid
CBC	Cannabichromene
CBE	Cannabielsoin
CBZ	Climbazole
CDB	Cannabidiol
CE	Collision energy

USC UNIVERSIDADE DE SANTIAGO DE COMPOSTELA

CFU	Colony forming units
CHLOF	Chlofentezine
CHLOR	Chlorpyrifos
CHLORM	Chlorpyrifos methyl
CN	Cyannopropylsilane
CYF	Cyflufenamid
CYP	Cyprodinil

D

DART	Direct Analysis in Real Time
DBP	Dibutyl Phthalate
DC	Direct Current
DCM	Dichloromethane
DDA	Data Dependent Acquisition
DEA	Diethyl Amine
DIA	Data Independent Acquisition
DIF	Difenoconazole
DIM	Dimethomorph
DOM	Dissolved Organic Matter
DWTP	Drinking Water Treatment Plant

E

E-cig	Electronic Cigarette
EE	Extraction Efficiencies
EF	Enantiomeric Fraction
EP	Emerging Pollutants
ESI	Electrospray Ionization
EtOH	Ethanol

F

FA	Formic Acid

USC UNIVERSIDADE DE SANTIAGO DE COMPOSTELA

FDA	Federal Drug Administration
FLUO	Fluopicolide
FTZ	Fenticonazole

G

GC	Gas Chromatography
GFF	Glass Fibre Filter

H

HClO	Hypochlorous Acid
Hex	Hexane
HILIC	Hydrophilic Interaction Liquid Chromatography
HLB	Hydrophilic-Lipophilic Balanced
HPLC	High Performance Liquid Chromatography
HRMS	High Resolution Mass Spectrometry

I

ICP	Inductive Coupled Plasma
IEC	Ion exchange chromatography
IMI	Imidacloprid
IPROV	Iprovalicarb
IUPAC	International Union of Pure and Applied Chemistry

L

LC	Liquid Chromatography
LD50	Median Lethal Dose
LLE	Liquid-Liquid Extraction
LOD	Limit of Detection
LOQ	Limit of Quantification

M

m/z	Mass Charge Ratio

USC UNIVERSIDADE DE SANTIAGO DE COMPOSTELA

MAN	Mandipropamid
MAX	Mixed-mode Anionic eXchanger
MCX	Mixed-mode Cationic eXchanger
MCZ	Miconazole
ME	Matrix Effect
MeOH	Methanol
MET	Metalaxyl
METR	Metrafenone
MHB	Mueller-Hinton Broth
MIP	Molecularly Imprinted Polymer
MRM	Multiple Reaction Monitoring
MS	Mass Spectrometry
MSPD	Matrix-Solid Phase Dispersion
MTBSTFA	N-methyl-N-(tert-butyldimethylsilyl)-trifluoroacetamide
MYC	Myclobutanil

N

NB	Nitrobenzene
NH4AC	Ammonium acetate
NIC	Nicotine
NMR	Nuclear Magnetic Resonance
NORMAN	European Commission Network of Reference Laboratories and Related Organisations for Monitoring and Bio-monitoring of Emerging Environmental Pollutants
NTS	Non-Target Screening

O

OECD	Organisation for Economic Co-operation and Development

P

PAH	Polycyclic Aromatic Hydrocarbon
PCDL	Personal Compound Database Library

USC UNIVERSIDADE DE SANTIAGO DE COMPOSTELA

PCP	Personal Care Products
PE	Polyethylene
PEC_{soil}	Predicted Environmental Concentrations in Amended Soils
PEN	Penconazole
PFAS	Perfluoroalkyl Substances
PFTBA	Perfluorotributyl Amine
PG	Propylene Glycol
PLE	Pressurized Liquid Extraction
PNEC	Predicted Non-Effect Concentration
PP	Polypropylene
PPT	Plant Protection Tube
PRO	Propranolol
PROP	Propiconazole
PS	Pore-Shell
PSA	Primary and Secondary Amine
PTFE	Polytetrafluoroethylene
PTV	Programmed Temperature Volatilization
PUF	Polyurethane Foam
PYR	Pyrimethanil
PYRA	Pyraclostrobin

Q

Q	Quadrupole
QqQ	Triple Quadrupole
Q-RAI	Quadrupole-Resolved All-Ions
QuEChERS	Quick, Easy, Cheap, Effective, Rugged and Safe
QUIN	Quinoxyfen

R

RAM	Restricted Access Material

USC UNIVERSIDADE DE SANTIAGO DE COMPOSTELA

RCS	Reactive Chlorine Species
RI	Retention Index
RPLC	Reversed-Phase Liquid Chromatography
Rs	Resolution Factor
RSD	Relative Standard Deviation
RT	Retention Time
RW	Raw Wastewater

S

S/N	Signal to Noise ratio
SAX	Strong Anionic eXchanger
SEM	Scanning Electron Microscopy
SFC	Supercritical Fluid Chromatography
SIM	Selected Ion Monitoring
SPE	Solid-Phase Extraction
SS	Surrogate Standard
STP	Sewage Treatment Plant
STZ	Sertaconazole
SVOC	Semi-Volatile Organic Compound
SWATH	Sequential Window Acquisition of All Theoretical Fragment Ion Spectra

T

TCPP	Tris(1-Chloro-2-propyl) Phosphate
TCS	Triclosan
TCZ	Tioconazole
TD	Thermal Desorption
TEBU	Tebuconazole
TETRA	Tetraconazole
THC	Tetrahydrocannabinol
TIC	Total Ion Current Chromatogram

USC UNIVERSIDADE DE SANTIAGO DE COMPOSTELA

TOC	Total Organic Compounds
TOF	Time Of Flight
TP	Transformation Product
TRA	Tramadol
TRIAF	Triadimefon
TRIAL	Triadimenol
TRIF	Trifloxystrobin
TT	Tying Tape
TW	Treated Wastewater

U

UAE	Ultrasound Assisted Extraction
UA	Unknowns Analysis
UHPLC	Ultra-High Performance Liquid Chromatography
UV	Ultraviolet

V

VFX	Venlafaxine
VG	Vegetal Glycerine
VOC	Volatile Organic Compounds
VVOC	Very Volatile Organic Compounds

W

WAX	Weak Anionic eXchanger
WCX	Weak Cationic eXchanger
WHO	World Health Organization
WMS	Waterloo Membrane Sampler
WWTP	Wastewater Treatment Plant

Y

YPD	Yeast-Extract-Peptone-Dextrose
YPDA	Yeast-Extract-Peptone-Dextrose Agar

USC UNIVERSIDADE DE SANTIAGO DE COMPOSTELA

YPDB	Yeast-Extract-Peptone-Dextrose Broth

Z

ZOX	Zoxamide

USC UNIVERSIDADE DE SANTIAGO DE COMPOSTELA

USC
UNIVERSIDADE
DE SANTIAGO
DE COMPOSTELA

LIST OF FIGURES

Figure 1: Scheme of a quadrupole mass analyser 37
Figure 2: Scheme of a Time-of-flight mass analyser 38
Figure 3: Scheme of a triple quadrupole mass analyser 39
Figure 4: Summary of the 4 possible MS/MS operational modes of a QqQ MS analyser. 40
Figure 5: Scheme of a quadrupole time of flight MS analyser 41
Figure 6: Screening methodologies workflow 43
Figure 7: Basic scheme of a LC-MS system. 45
Figure 8: Scheme of the Electrospray ionization. 47
Figure 9: Operating scheme of DDA and DIA modes 49
Figure 10: Components of a supercritical fluid chromatograph coupled to a mass spectrometer (SFC-MS) system by Agilent technologies® 52
Figure 11: General scheme of the components of a gas chromatography (GC) system combined with a MS spectrometer. 56
Figure 12: Structure of a DART source (IonSense) 60
Figure 13: Scheme of a solid phase extraction procedure. 63
Figure 14: Scheme of a matrix solid phase dispersion extraction 67
Figure 15: Scheme of a pressurized liquid extraction device. 69
Figure 16: Disassembled e-cigarette head 71
Figure 17: Aged plastic items and plastic debris found in vineyards. 77
Figure 18: Setup used for direct sampling of indoor air 89
Figure 19: Scheme of the MSPD elution protocol followed during this PhD Thesis 90
Figure 20: Structure of a polar C18 column. Phenomenex® 91
Figure 21: Scheme of the coupling between SFC and MS used during this Thesis 91
Figure 22: Sample holders for DART sources, 12 *Dip-it* (A) and *quick-strip* (B) 92
Figure 23**:** Workflow for compound identification followed in **Publication I** 94
Figure 24: Set up of degradation experiments using *UV* radiation 95
Figure 25: Scheme of the studies carried out during the current Thesis. 289

USC UNIVERSIDADE DE SANTIAGO DE COMPOSTELA

USC
UNIVERSIDADE
DE SANTIAGO
DE COMPOSTELA

LIST OF TABLES

Table 1.1 Applications of LC-MS to analysis of emerging pollutants 51
Table 1.2 Applications of SFC-MS for the separation of pesticides in environmental matrices 54
Table 1.3 Applications of SFC-MS for the separation of chiral pharmaceuticals in environmental matrices 55
Table 1.4 Applications of GC-MS in air characterization 59
Table 1.5 Applications of DART-MS in different fields 62

USC
UNIVERSIDADE DE SANTIAGO DE COMPOSTELA

USC
UNIVERSIDADE
DE SANTIAGO
DE COMPOSTELA

ABSTRACT

In recent years the use of chemicals has become commonplace in daily life, from food additives and personal care products to pharmaceuticals, flame retardants and pesticides. The development of new additives and active ingredients by the chemical and pharmacological industries resulted in a higher quality of life for the population; however, the abuse and/or poor management of these substances proved to have an adverse effects in human health, and the environment. Substances present in furniture to prevent their ignition or to avoid decolouration catalysed by sunlight can migrate to the air and be inhaled by humans or animals present on the same room. On the same vein, a pesticide designed for the protection of crops can persist in the environment and harm non-target organisms or be transported to different environmental compartments.

As a result of the growing use of new synthetic compounds, it has become a necessity to study their presence and toxicity in environmental matrices, investigating their degradation routes in wastewater treatment plants to avoid their release to the environment and/or their recirculation to drinking water sources; as well as to identify the potential impact of their transformation products in living organisms. Studies regarding Persistence, distribution, migration, exposition, etc. need analytical tools capable of both screening and quantitative analysis.

In this context, in my PhD thesis I carried out an evaluation of the performance of different mass spectrometry platforms, combined with various ionisation sources and chromatographic separation techniques, for the determination of potentially hazardous compounds in multiple complex matrices, including indoor air samples, wastewater, sludge, and end-of-life plastics from agriculture; as well as for the characterisation of the components of complex commercial mixtures of e-cigarette refill liquids, and the identification of transformation products after degradation of the drug tramadol in river water and wastewater samples. Depending on the objective of each of these studies, priority was given to the identification of new compounds, or their quantification, in the case of already known species, for which potential negative impacts are assumed, either on the environment, or on individuals exposed to them.

The main objective of this Thesis was the assessment of different mass spectrometry platforms (based on nominal resolution and accurate mass analysers), coupled to several ionization sources, and chromatographic separation techniques for the determination of pollutants and chemicals of interest in many different and complex matrices, including plastic litter and soil from agricultural fields, wastewater samples and sludge from sewage treatment plants, as well as complex fluids obtained from indoor air to commercial solutions, as e-cigarette refill liquids. Depending on the considered issue, quantitative target methods, comprehensive screening approaches or enantiomeric, sensitive determinations were developed and applied to analysis of a range of samples with different features. Thus, possibilities, and limitations, of mass spectrometry, to face real-life problems demanding high quality analytical information were thoroughly explored.

USC
UNIVERSIDADE
DE SANTIAGO
DE COMPOSTELA

This main objective was developed in two chapters according to the main purpose of the mass spectrometry application: quantification or screening. Each chapter encompasses 4 publications

Chapter 1: Development of non-target screening methodologies using high resolution mass spectrometry for a comprehensive characterization of environmental and commercially available samples.

- Publication I: Portable dehumidifiers condensed water: A novel matrix for the screening of semi-volatile compounds in indoor air
- Publication II: Predicting concentrations of volatile and semi-volatile compounds in indoor areas through analysis of condensed water samples. A proof of concept
- Publication III: Comprehensive characterization of volatile and semi-volatile compounds in e-liquids for electronic cigarette using gas chromatography accurate mass spectrometry
- Publication IV: Comparison of UV, chlorination, UV-hydrogen peroxide and UV-chlorine processes for tramadol removal: Kinetics study and transformation products identification

Chapter 2: Target analysis of selected pollutants in complex environmental matrices.

- Publication V: Chlorhexidine residues in sludge from municipal wastewater treatment plants: analytical determination and toxicity evaluation
- Publication VI: Assessment of direct analysis in real time accurate mass spectrometry for the determination of triclosan in complex matrices
- Publication VII: Supercritical fluid chromatography time-of-flight mass spectrometry enantiomeric determination of basic drugs in sewage samples
- Publication VIII: Assessment of the occurrence and interaction between pesticides and plastic litter from vineyard plots

This Thesis was able to assess the capabilities of mass spectrometry for both quantitative analysis compounds known to be present in samples, as well as providing ample information about the composition of complex matrices and mixtures.

USC UNIVERSIDADE DE SANTIAGO DE COMPOSTELA

RESUMO

Na actualidade, o uso de substancias químicas pasou a formar parte de todos os aspectos da vida diaria, dende aditivos alimentarios e produtos de hixiene e coidado persoal, ata fármacos, retardantes de chama e pesticidas. O desenrolo de novos aditivos, e principios activos por parte da industria química e farmacéutica deu como resultado unha maior calidade de vida para a poboación; sen embargo, o abuso e/ou a xestión deficiente destas substancias demostrou ter un efecto adverso sobre a saúde humana, e sobre o medio ambiente. Por exemplo, compostos presentes en mobiliario para incrementar a resistencia o lume, previr procesos de decoloración debido a reaccións catalizadas pola luz, e outras, poden pasar ao aire e ser inhalados pola poboación ou animais que se atope na mesma estancia. Na mesma liña, un pesticida deseñado para a protección dos cultivos, pode persistir no medio ambiente, e causar danos a organismos non obxectivo; ou ser transportado a compartimentos ambientais diferentes a aquel no que foi aplicado.

Como resultado do crecente uso de novos produtos químicos de síntese, fíxose necesario estudar a súa presencia, persistencia e toxicidade en matrices ambientais, investigar a súas vías de degradación en estacións depuradoras de augas residuais; para evitar a súa liberación ao medio ambiente e/ou a súa recirculación ata fontes de auga potable, ademais do impacto potencial dos seus produtos de transformación en distintos organismos. Os estudos de distribución, persistencia, migración, exposición, etc., precisan de ferramentas analíticas, con diferentes capacidades dende o punto de vista cuantitativo como de *screening*.

Neste contexto, na miña Tese de Doutoramento levei a cabo unha avaliación das prestacións de diferentes plataformas de espectrometría de masas, combinadas a diversas fontes de ionización e técnicas cromatográficas de separación, para a determinación de compostos potencialmente perigosos en múltiples matrices complexas, incluíndo mostras de aire de interiores, augas residuais, lodos, e residuos de plásticos usados na agricultura; así como para a caracterización dos compoñentes das mesturas comerciais complexas de líquidos de recarga para cigarros electrónicos, e a caracterización dos produtos de transformación tras a degradación do fármaco tramadol en, mostras de auga de río e auga residual. Dependendo do obxectivo de cada un destes estudos, priorizouse a identificación de novos compostos, ou ben a súa cuantificación no caso de especies xa coñecidas para as que se asumen potenciais impactos negativos, ben sobre o medio ambiente, ben sobre os individuos expostos os mesmos.

Esta memoria de Tese atópase dividida en seis seccións principais para poder abranguer todos os traballos realizados durante a etapa doutoral e cumprir as directivas da escola de doutoramento da USC relativa a organización da tese na modalidade de presentación por artigos.

USC
UNIVERSIDADE DE SANTIAGO DE COMPOSTELA

Na **Sección I** realizase unha extensa introdución sobre os distintos tipos de instrumentación de espectrometría de masas que foron avaliadas, e empregadas na presente Tese, así coma o seu funcionamento e as combinacións máis comúns entre eles. Posto que esta Tese centrouse no estudo de matrices complexas, é necesario levar a cabo etapas previas de preparación de mostra, ademais do emprego de diferentes técnicas de separación que permitan simplificar a complexidade das mesturas que entran nas fontes de ionización, ademais de discriminar entre compostos con patróns de fragmentación comúns, tal como ocorre no caso dos enantiómeros de compostos quirais. De forma resumida, as técnicas de separación empregadas na tese, foron a cromatografía de líquidos (LC) para a análise de compostos pouco volátiles, a cromatografía de gases (GC) con fins maiormente de identificación de compostos volátiles e/ou semi-volátiles, e a cromatografía de fluídos supercríticos (SFC) aplicada a separación enantiomérica de compostos quirais. Por último, a fonte de ionización de análise directa en tempo real denominada DART, en base ao seu acrónimo en inglés (DART), foi avaliada dende o punto de vista da súa utilidade na identificación e determinación de compostos minoritarios en matrices complexas. A última parte desta sección da Tese céntrase nunha breve revisión dos diferentes grupos de compostos e matrices, para os que foron desenvoltos cada unha das aplicacións experimentais.

Na **Sección II** atópanse recollidos as xustificacións dos diversos traballos levados a cabo durante a realización da Tese, contextualizando cada un dos problemas analíticos abordados. Ademais, nesta sección recóllense os obxectivos principais a desenvolver:

Obxectivo 1: Análise *non-target* de compostos volátiles, e semi-volátiles, en mostras gaseosas e líquidas, por exemplo aire de interiores e líquidos de cigarros electrónicos a partir de datos obtidos con GC-QTOF-MS, coa axuda de LC-QqQ-MS, esta última empregada como técnica complementaria que permita despexar dúbidas relacionadas con potenciais artefactos analíticos, intrínsecos as condicións de traballo empregadas en cromatografía de gases.

Obxectivo 2: Estudos *non-target* baseados na información complementaria obtida mediante LC-QTOF-MS e GC-QTOF-MS aplicada á caracterización das rutas de degradación do fármaco tramadol baixo distintos tratamentos oxidativos, aplicados a escala de laboratorio, para a súa eliminación do ambiente acuático.

Obxectivo 3: Avaliación do rendemento da SFC, combinada con espectrometría de masas, usando una fonte de ionización de electrospray (ESI), para o análise enantiomérico, multianalito e sensible dunha selección de contaminantes emerxentes quirais en mostras relacionadas con augas residuais.

Obxectivo 4: Desenvolvemento de métodos cuantitativos centrados na cuantificación de compostos preseleccionados, en base a toxicidade e/ou potenciais riscos, en matrices de complexidades variables usando LC-QqQ-MS, ionización directa seguida por detección mediante QTOF-MS e GC-QTOF-MS.

Na **Sección III** levase a cabo unha breve descrición dos procedementos experimentais empregados nos diferentes traballos realizados no transcurso da Tese.

As mostras líquidas foron procesadas mediante SPE en modo descontinuo *(SPE-offline)* usando diferentes adsorbentes para a extracción e concentración dos analitos seleccionados. Os materiais mais empregados foron os polímeros de modo mixto (tipo MCX) para a concentración, e/ou purificación, de compostos de natureza básica presentes en mostras de augas e/ou extractos de lodos, e polímeros de tipo hidrofílico-lipofílico para a concentración non-selectiva de compostos orgánicos en estudos de screening, e de tipo cuantitativo, en distintos tipos de fluídos. No caso de mostras sólidas, traballouse con diferentes técnicas de

extracción que van desde a extracción sólido-líquido, a asistida por ultrasóns, para liberar compostos asociados a matrices de plásticos agrícolas; a extracción con fluídos presurizados (PLE), previamente optimizada no grupo de investigación, para a extracción de solos agrícolas, e a dispersión de matriz en fase sólida (MSPD), combinada cunha etapa de purificación en liña, no caso da extracción de fármacos dende mostras de lodos de depuradora.

Para as determinacións analíticas dos pesticidas e o bactericida chlorhexidine, utilizouse un equipo de LC, capaz de operar con columnas tipo UPLC, combinado con un analizador de triplo cuadrupolo; sendo a separación cromatográfica en fase reversa. Para a determinación enantiomérica dos compostos quirais, a metodoloxía utilizada foi a cromatografía de fluídos supercríticos (SFC) combinada con un detector de cuadrupolo tempo de voo (QTOF), empregando columnas quirais derivadas de polisacáridos. A identificación dos produtos de transformación do fármaco tramadol foi levada a cabo empregando cromatografía de líquidos en fase reversa (RPLC), combinada cun analizador de masas de tipo QTOF. Este sistema permitiu seguir tanto as cinéticas de disipación do analxésico, baixo diferentes condicións de traballo, como investigar a formación de produtos de transformación empregando os seus espectros de tipo barrido de ión produto, rexistrados a distintas enerxías de colisión. Asemade, a formación de produtos de transformación haloxenados e volátiles investigouse mediante GC-TOF-MS, empregando ionización de tipo electrónica. Os extractos correspondentes a mostraxe activo, de aire, auga condensada de deshumidificador e líquidos de cigarros electrónicos foron caracterizados tamén usando un equipo de cromatografía de gases (GC), acoplado a un detector TOF. Para obter unha mellor caracterización dos extractos, empregáronse dúas columnas de diferente polaridade: unha columna polar (tipo Carbowax), en unha columna semi-polar (tipo BP-5).

Por último, o bactericida e funxicida triclosan foi analizado mediante análise directo en tempo real (DART) conectado a un espectrómetro de masas QTOF.

Na **Sección IV** recóllense as publicacións acadadas durante o período da realización da Tese. Ditas publicacións atópanse agrupadas en dous capítulos dependendo do modo de operación da espectrometría de masas.

Capítulo 1: Desenvolvemento de metodoloxías non dirixidas empregando espectrometría de masas exactas, para unha caracterización exhaustiva de mostras comerciais e ambientais.

Neste capítulo inclúense 4 publicacións nas que se desenvolveron diferentes metodoloxías para levar a cabo unha caracterización exhaustiva de mostras complexas. Dependendo do tipo de mostra e do obxectivo, a técnica de separación utilizada é diferente.

A primeira publicación centrase no estudo das augas de condensación, obtidas empregándose un deshumidificador portátil, como posible matriz para a caracterización indirecta da composición de compostos volátiles e semi-volátiles en aire de atmosferas interiores. Para iso, tomáronse mostras de forma simultánea de aire e de auga condensada. No primeiro caso empregouse un sistema de mostraxe activa. No segundo concentrouse a auga condensada a partir do aire. Ambos tipos de mostras foron caracterizadas mediante GC-TOF-MS, empregando ionización electrónica e procesando os extractos con dúas columnas capilares con fases estacionarias diferentes. Mediante a combinación de índices de retención e espectros de masas identificáronse mais de 140 compostos orgánicos presentes en atmosferas interiores. O traballo fai una avaliación, a nivel cualitativo, da detectabilidade destes compostos en función do sistema de mostraxe empregado, avalía diferencias na composición en función do lugar de mostraxe e das actividades, e os dispositivos existentes nos lugares de mostraxe.

USC
DE SANTIAGO
DE COMPOSTELA

Na segunda publicación recollida neste capítulo, continuación do traballo anterior, realizouse unha proba de concepto sobre a posibilidade de utilizar auga obtida dun deshumidificador para a estimación de concentracións de compostos semi-volátiles presentes en aire. No traballo investigouse de maneira sistemática os efectos de diferentes variables na distribución dunha selección de compostos entre aire e auga condensada, obtivéronse coeficientes de distribución auga-aire para 14 compostos, de diferentes familias químicas, e validouse a exactitude dos mesmos para a predición das concentracións en fase gas en novos lugares de mostraxe.

A terceira publicación consistiu na caracterización exhaustiva de líquidos de cigarros electrónicos mediante o uso de GC-QTOF-MS. Posto que estes líquidos son mesturas moi complexas, con potenciais efectos adversos na saúde dos consumidores, o obxectivo do estudo foi obter una visión o mais ampla posible da súa composición. Asemade da información resumida na publicación científica, elaboráronse dúas bases de datos, en formato aberto, cos espectros de EI-MS dos compostos identificados. No caso de especies químicas sospeitosas de efectos non desexados sobre o sistema respiratorio dos consumidores (tales como acetais, alcaloides relacionadas coa nicotina, ou en xeral sobre a súa saúde, cannabinoides), leváronse a cabo determinacións de tipo semi-cuantitativo, ben baseadas unicamente en datos de GC-TOF-MS, ben empregando LC-MS como técnica complementaria.

Na cuarta e última publicación deste capítulo levouse a cabo unha serie de experimentos para a eliminación do fármaco tramadol en mostras de auga ultrapura, auga de río e auga residual; así como a caracterización dos seus posibles produtos de transformación en cada un dos experimentos de eliminación e tamén se realizou unha proposta de posibles rutas de degradación do composto.

Capítulo 2: Análise dirixido de contaminantes seleccionados en matrices ambientais complexas.

Este capítulo tamén consta de 4 publicacións, neste caso baseadas en métodos de MS diana para a determinación de contaminantes emerxentes de interese, pertencentes a diferentes familias químicas e a súa optimización e aplicación para avaliar os seus niveis en distintos nichos medioambientais.

A primeira das publicacións consistiu na determinación do bactericida chlorhexidine en mostras de lodo obtidas de estacións de tratamento de augas residuais mediante RPLC-QqQ-MS; neste caso a columna empregada foi unha C_{18} polar funcionalizada con cargas positivas para evitar a unión irreversible do analito, fortemente básico, coa fase estacionaria. Unha vez validado o método, aplicouse a un número representativo de mostras para coñecer a súa distribución nesta matriz. Estes datos serviron de base a para a realización de experimentos adicionais de toxicidade fronte a diferentes organismos, empregado ensaios in-vitro, ben feitos dentro do grupo de investigación (ensaios de fitotoxicidade), ben en colaboración con investigadores do departamento de microbioloxía, no caso de estudos toxicidade fronte a bacterias e fungos.

Na segunda publicación desenvolveuse unha metodoloxía de análise directa en tempo real (DART) para a determinación do bactericida, e funxicida, triclosan en matrices complexas, como mostras de lodo, augas residuais e produtos de coidado persoal (pasta de dentes e colutorios). Optimizáronse múltiples parámetros, empezando pola posibilidade de derivatizar, ou non, o composto de cara a mellorar a súa ionización; o tipo de portador da mostra, a distancia entre a fonte de ionización e a mostra e a temperatura dos gases da fonte. As mostras foron tratadas segundo a súa natureza. A auga residual foi extraída mediante SPE usando un cartucho HLB, as mostras de lodo e pasta de dentes foron extraídas mediante MSPD e por último, o

colutorio foi diluído ata que a concentración de triclosan entrase no rango de resposta lineal do equipo. As determinacións de tipo cuantitativo, levadas a cabo mediante a técnica DART-TOF-MS, foron verificadas mediante o uso de LC-TOF-MS cunha concordancia aceptable entre os valores acadados con ambas ferramentas. As dúas principais conclusións do estudo foron (1) a elevada sensibilidade do sistema DART-TOF-MS, e (2) a saturación espectral que limita a súa aplicabilidade a matrices complexas, agás no caso de compostos de tipo haloxenado, cun defecto de masas negativo, tal que da lugar a ións en rexións espectrais relativamente limpas.

A terceira publicación centrouse na optimización dunha metodoloxía de separación de enantiómeros de fármacos básicos, con grupos funcionais de tipo azólico e amino, baseada na cromatografía de fluídos supercríticos (SFC), empregando columnas quirais. Durante este estudo analizáronse mostras de augas residuais e lodos procedentes de estacións depuradoras de augas residuais (EDARs). As mostras de augas residuais foron extraídas mediante SPE utilizando un intercambiador catiónico de modo mixto, eliminando as interferencias con metanol contendo 0,1% de ácido fórmico, deseguido os compostos de interese foron eluidos con metanol con 2% de amoníaco. As mostras de lodo foron extraídas mediante MSPD usando C_{18} como dispersante e amina primaria e secundaria (PSA) como coadsorbente; ademais o cartucho de MSPD foi eluído en serie cun cartucho intercambiador catiónico forte (SCX) primeiro con metanol, e despois o cartucho SCX foi eluido coa mestura de metanol e amoníaco mencionada anteriormente. Os dous obxectivos básicos do estudo foron (1) desenvolver un método multiresiduo, relativamente rápido, con suficiente sensibilidade para a súa aplicación a mostras ambientais; e (2) investigar a posible presenza de cambios nas fraccións enantioméricas de fármacos recoñecidos como compostos resistentes a procesos de biodegradación, e ubicuos en augas residuais e lodos de estacións depuradoras.

Na cuarta publicación deste capítulo estudiouse a presencia, e persistencia, de pesticidas en plásticos empregados en agricultura, así como a capacidade dos mesmos para actuar como portadores de pesticidas. O traballo deriva dun estudo previo, en colaboración con investigadores do CNRS (Francia) no que se detectou a presenza de pesticidas en microplásticos recollidos do medio mariño. A hipótese de partida do estudo incluído na miña Tese de doutoramento foi que, nalgúns casos, estes pesticidas poderían estar presentes xa en plásticos de uso agrícola, antes da súa fragmentación física e transporte o medio acuático. Dada a importancia da viticultura dentro do sector primario en Galicia, e as evidencias físicas de uso diferentes materiais plásticos en viñedos, en combinación con tratamentos de funxicidas e insecticidas, centrouse o traballo en mostras de residuos plásticos recollidos de viñedos. As mostras utilizadas neste estudio consistiron en cintas de atado de polietileno, e fragmentos de tubos de protección de polipropileno empregados na protección de plantas xoves. Os polímeros plásticos foron caracterizados mediante FTIR-ATR e extraídos mediante extracción asistida por ultrasóns (UAE), empregando como disolvente extractante unha mestura de diclorometano e hexano en proporción 1:1. Para a estimación do seu potencial como portadores de pesticidas leváronse a cabo diversas probas de absorción/adsorción e de desorción poñendo os plásticos en contacto con auga, en axitación magnética, tomando alícuotas de auga cada certo tempo e realizando unha extracción dos plásticos tras 72 horas. A determinación de pesticidas nos plásticos, solos agrícolas e nos estudos de absorción/desorción levouse a cabo mediante UPLC-MS/MS empregando un equipo de tipo QqQ-MS.

Na **Sección V** faise unha discusión integradora dos traballos incluídos na Tese, explicando en profundidade o desenvolvemento das metodoloxías levadas a cabo en cada unha das publicacións. Ademais nesta sección explícase a relación entre as publicacións; por exemplo, a metodoloxía para a caracterización de aire a partir de auga condensada de deshumidificador

desenvolvida na primeira publicación é validada como proba de concepto para a cuantificación de compostos semi-volátiles en ambientes interiores; outro exemplo é o emprego da metodoloxía de minado de datos, desenvolvida na primeira publicación, posteriormente empregada para a caracterización exhaustiva dos líquidos de cigarros electrónicos e os produtos de transformación volátiles formados durante a eliminación do tramadol.

Por último, a **Sección VI** describe as conclusións obtidas ao longo dos traballos presentados na presente Tese doutoral, ditas conclusións atópanse recollidas a continuación:

Capítulo 1: Desenvolvemento de metodoloxías non dirixidas empregando espectrometría de masas de alta resolución para obter unha caracterización exhaustiva de mostras comerciais e ambientais.

- Un total de 141 compostos foron identificados en aire de atmósferas interiores mediante análise por GC-EI-QTOF-MS. A existencia de correlacións entre os compostos presentes en aire de interiores e os acumulados en mostras de auga condensada foron confirmadas con: (1) rexistros GC-TOF-MS repetibles obtidos durante mostraxes consecutivos levados a cabo na mesma habitación; e (2) grazas aos diferentes perfiles de GC-MS de mostras de auga de deshumidificador de diferentes zonas interiores.
- A utilidade de deshumidificadores portátiles para a caracterización de aire de interiores foi avaliada en profundidade respecto a posibilidade da obtención de análises semi-cuantitativos para un grupo de 14 compostos volátiles e semi-volátiles, xeralmente presentes en aire de oficinas e diferentes estancias en fogares particulares. A súas constantes de distribución aire-auga foron calculadas mediante mostraxes sistemáticos, utilizando diferentes volumes de aire e temperaturas ambientes para asegurar valores máis fiables. As constantes calculadas foron empregadas para a estimación de concentracións en aire para ditos compostos, presentes nun total de 13 pares de mostras recollidas en sete puntos de mostraxe distintos. Todos os compostos mostraron unha correlación moi alta, o que demostra o potencial dos deshumidificadores portátiles para a análise semi-cuantitativa de mostras de aire. Outra conclusión do traballo e que, unha vez obtida a proba de concepto con resultados satisfactorios, o seguinte paso consiste no deseño dun sistema (deshumidificador) profesional, cun control mais exhaustivo da temperatura do condensador, no que se minimice o emprego de materiais plásticos, fonte posible de contaminación para algúns dos compostos identificados na fase vapor de ambientes interiores, caso de ftalatos volátiles, compostos organofosforados e/ou derivados de benzofenona.
- Identificáronse máis de 250 compostos presentes na formulación de mostras de e-liquids mediante GC-EI-QTOF-MS empregando dúas columnas diferentes. Entre eles, compostos pro-inflamatorios, como acetais de propilenglicol e glicerina con aldehidos; alcaloides relacionados e non relacionados coa nicotina, e cannabinoides psicoactivos, presentes nas mostras de e-liquids, incluso previamente o proceso de vapeo (xeración de aerosol), durante o cal os seus niveis poderían verse incrementados.
- Entre as metodoloxías ensaiadas para a eliminación de tramadol en mostras de auga, a mais eficaz foi a combinación de luz ultravioleta e cloro libre, acadando porcentaxes de eliminación pretos ao 100% en 30 minutos. Entre os produtos de transformación identificados, o mais perigoso pola súa toxicidade foi o tramadol-

USC UNIVERSIDADE DE SANTIAGO DE COMPOSTELA

N-oxide. Os datos obtidos no estudo indicaron que o porcentaxe de conversión de tramadol a tramadol-N-oxide mantívose por debaixo do 3%. Outros produtos de transformación clorados mantivéronse por debaixo do 2% da concentración de tramadol. En base os resultados obtidos, propuxéronse as rutas de transformación do tramadol para os dous tratamentos oxidativos mais efectivos identificados: a combinación de radiación UV con peróxido de hidróxeno e con cloro libre. A ruta de transformación do tramadol durante os tratamentos con UV/peróxido diferenciábanse na ausencia de produtos de transformación clorados e na formación de produtos de transformación di- e tri-hidroxilados, non presentes na reacción con UV/cloro libre.

Capítulo 2: Análise dirixida de contaminantes seleccionados en matrices ambientais complexas.

- A chlorhexidine confirmouse como ubicua en mostras de lodo do Noroeste de España, chegándose a rexistrar concentracións de ata 16 µg g^{-1}. A alta basicidade e características lipofílicas deste bactericida son os maiores desafíos para a súa determinación mediante LC-MS.
- Tras varios ensaios para determinar a súa eco-toxicidade, demostrouse que as concentracións de chlorhexidine presentes en lodo non causaban ningún efecto na xerminación de diferentes plantas. Sen embargo, a chlorhexidine demostrou ser moi tóxica para os tres microorganismos modelo fronte os que se avalió, xa que produciu unha gran mortalidade a concentracións menores nas presentes en lodos. Con estes datos, pódese asumir que a chlorhexidine pode causar un importante impacto na poboación microbiana presente en lodo de estacións de tratamento de augas residuais, e polo tanto, afectar a bio-degradabilidade doutras especies químicas
- O uso de DART-MS permitiu a determinación selectiva e sensible de triclosan en mostras ambientais complexas. Isto foi debido, principalmente, ao defecto de masa do átomo de cloro, presente na estrutura química deste composto. Empregando un análogo marcado isotópicamente, como subrogado interno, obtívose unha boa concordancia entre os datos cuantitativos proporcionados por DART-TOF-MS e LC-TOF-MS. A vantaxe obvia da primeira aproximación é a súa rapidez.
- Acadouse a separación enantiomérica de oito fármacos diferentes grazas ao uso de SFC-ESI-QTOF-MS; a súa cuantificación foi feita en mostras de augas residuais e de lodos. O procedemento da separación cromatográfica podería considerarse como parte da "química verde" posto que nas condicións de separación optimizadas, o compoñente maioritario na fase móbil empregada foi o CO_2. Sen embargo, os fluxos de fase móbil utilizados son máis altos que en análises de cromatografía de líquidos de fase reversa; ademais, foi preciso empregar unha disolución adicional, chamada de "*make-up*" para mellorar a eficacia de ionización dos analitos. En conclusión, ambas aproximacións (SFC-MS quiral e LC-MS quiral, operada en condicións de fase reversa) consomen volumes similares de disolventes orgánicos. En xeral, o método desenvolvido en SFC-ESI-QTOF-MS foi realmente efectivo en termos de tempo total de análise, resolución enantiomérica e límites de cuantificación.
- Puideron observarse diferencias nas fracción enantioméricas entre os fármacos comerciais e os presentes en augas residuais, tratadas e sen tratar, para tres dos oito fármacos estudados. Estas diferencias foron atribuídas a procesos de

USC UNIVERSIDADE DE SANTIAGO DE COMPOSTELA

metabolización de tipo enantioselectivo, mais que a unha biodegradación enantioselectiva durante os tratamentos de augas residuais.

- Os fragmentos de plásticos recollidos de viñedos, identificados como polietileno e polipropileno, contiñan niveis elevados de diversos pesticidas, moi por encima dos atopados en mostras de solo das mesmas parcelas, o que demostra o papel dos plásticos coma almacéns e portadores de pesticidas. Entre eles atópanse incluso compostos considerados como lábiles en condicións ambientais, tal e como ocorre co Folpet.
- As capacidades dos plásticos para acumular e liberar pesticidas, dende e ata, a fase acuosa foron avaliadas vía experimentos de adsorción e desorción. Os resultados obtidos mostraron que, canto máis degradado estivese o plástico, maior eran as súas capacidades de adsorción; tamén observáronse que diferentes polímeros presentaban diferentes afinidades polos pesticidas. Como regra xeral, os residuos de polietileno son capaces de reter máis os pesticidas que os residuos de polipropileno. Polo tanto, a combinación dos procesos térmicos e mecánicos que ten lugar durante o reciclado de cintas de polietileno de uso agricultural, previamente lavadas, pode resultar de pouca utilidade para a eliminación de residuos de pesticidas asociados a plásticos de agricultura no final do seu ciclo de vida útil.

USC UNIVERSIDADE DE SANTIAGO DE COMPOSTELA

1 INTRODUCTION

1.1 MASS SPECTROMETRY

Mass spectrometry (MS) is an analytical methodology that allows the identification and quantification of molecules, previously turned into ions [1]. Mass spectrometers are generally combined with a previous separation step (usually LC and GC, but more recently SFC has seen an increase in use as separation technique); moreover, they can also be used with a direct ionization methodology, as in the case of Direct Analysis in Real Time (DART). These techniques and their coupling to MS will be explained in more detail in chapter 1.2. Mass spectrometers generally consist of three elements: a ionization source, a mass analyser and a detector.

1.1.1 Mass analysers

In this section, the configuration and the operational modes of the different kinds of mass analysers, employed in my PhD Thesis, are discussed. Among them, the *quadrupole* (Q) is still the most popular one. It consists of four elongated, hyperbolic, cylinders that serve as electrodes. Ions generated at the source are introduced in the quadrupole by using a small potential (from 5 to 15 eV). The opposing cylinders are electrically connected, one pair to the positive side of a source of direct current (DC), while the other pair is connected to the negative one. In addition to this voltage, an alternating current (AC), that is generally known as radiofrequency voltage, is also applied to all the bars [2]. A scheme of this analyser is shown in figure 1.

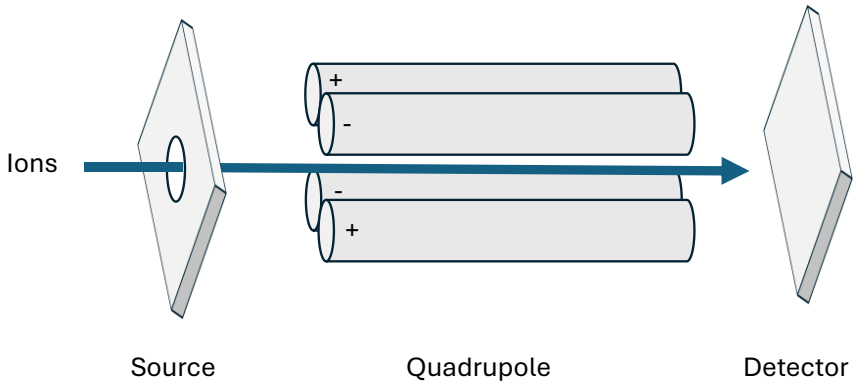


Figure 1: Scheme of a quadrupole mass analyser

USC
UNIVERSIDADE DE SANTIAGO DE COMPOSTELA

Quadrupole mass analysers can work in two different modes. In *Selected Ion Monitoring* (SIM) a constant potential is applied to the quadrupole bars, this potential allows only for ions with specific *m/z* ratios to pass through and reach the detector, the other ions either collide with the quadrupole bars, or are shot outside the mass analyser entirely. In the *Scan* mode, a potential gradient, from 0 V to its maximum value is applied to the quadrupole bars throughout the analysis, filtering all ions with an increasing *m/z* ratio. This allows conventional quadrupole mass analysers to easily resolve ions with *m/z* differences of 1 Da, reaching up to ions with a *m/z* ratio of 4000 Da.

In *Time of flight* (TOF) mass analysers, ions coming from the source are also accelerated, with a voltage much higher than those normally used in Q analysers, into a drift region, which is a long tube, generally 1 m tall, devoid of any electric or magnetic fields. As we assume that the initial kinetic energy of all ions is the same, their speed is going to be dependent on their respective mass, as such, lighter ions travel faster than heavier ones. Based in this principle, it can allow for a virtually limitless mass range, which can be useful to determine substance composition or structure. To further improve resolving power, ions are turned around by a reflectron, placed at the end of the TOF tube. The reflectron consists of a series of hollow rings, with a potential more positive than the ion pulser, at the source; thus, ions are reflected towards the detector doubling the flighting path [2]. The scheme of this mass analyser is presented below in figure 2.

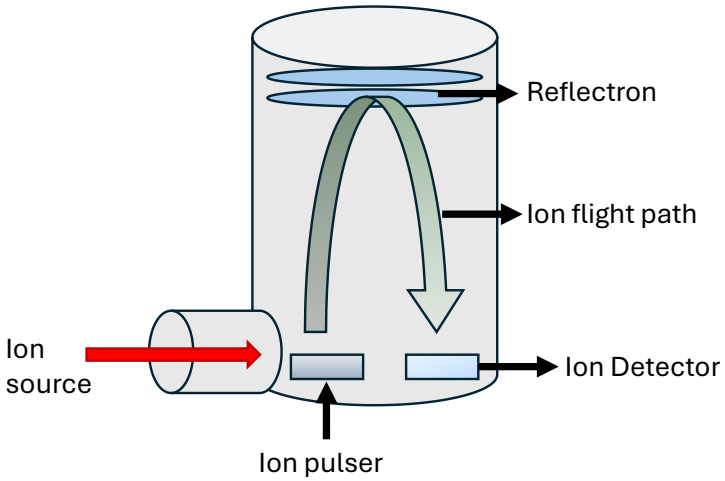


Figure 2: Scheme of a Time-of-flight mass analyser

The above-mentioned mass analysers can also be employed in combination with themselves or with each other, to create hybrid instruments, employed in tandem mass spectrometry determinations.

1.1.2 Tandem mass spectrometry

By combining mass analysers together, a better sensitivity and higher selectivity can be achieved. In this section, the two most popular couplings of mass analysers will be discussed.

The *triple quadrupole* (QqQ) is the most widely spread of the MS/MS analysers, regardless of the previous separation technique. In QqQ systems, two linear quadrupoles are connected by

USC
SANTIAGO
DE COMPOSTELA

a third quadrupole. When working on MS/MS mode, both the first (Q1) and third (Q3) quadrupoles work as ion filters while the second (Q2) works as a collision chamber, producing the collision-induced dissociation (CID) of the precursor ions, proceeding from Q1, and generating product ions sent to Q3 for further filtering. A scheme of this analyser is shown in figure 3 [3].

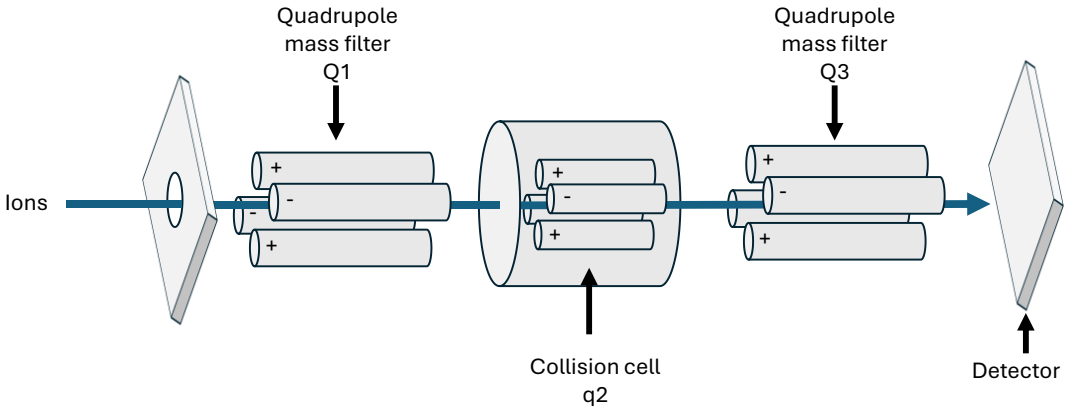


Figure 3: Scheme of a triple quadrupole mass analyser

The different MS/MS operational modes for QqQ are described below.

- *Product ion scan*: Q1 works in SIM mode selecting an ion with a known *m/z*, which is fragmented in Q2, and is finally filtered in Q3 working in scan mode to acquire its full-product ion spectrum.
- *Precursor scan*: Q1 works in scan mode, letting all ions through to Q2, where they are fragmented and Q3 works in SIM mode. This mode is useful to find different precursors for known product ions.
- *Neutral loss scan*: Q1 and Q3 operate in full scan. This mode is helpful in the selective recognition of the ions that break down in Q2 producing the same neutral fragment (as NH_3, CO_2, or H_2O)
- *Multiple reaction monitoring*: Q1 and Q3 operate in SIM mode, selecting a precursor ion to be fragmented in Q2, and in Q3, a selection of product ions is filtered (normally 2 or 3 product ions per precursor). This mode reduces the interferences and the chemical noise; therefore, it increases the selectivity and sensibility of the analysis. This approach was employed in the present Thesis as our methodology for quantification of pre-selected compounds in different matrices

Figure 4 shows a graphical representation of the differences of these operational modes.

USC
UNIVERSIDADE
DE SANTIAGO
DE COMPOSTELA

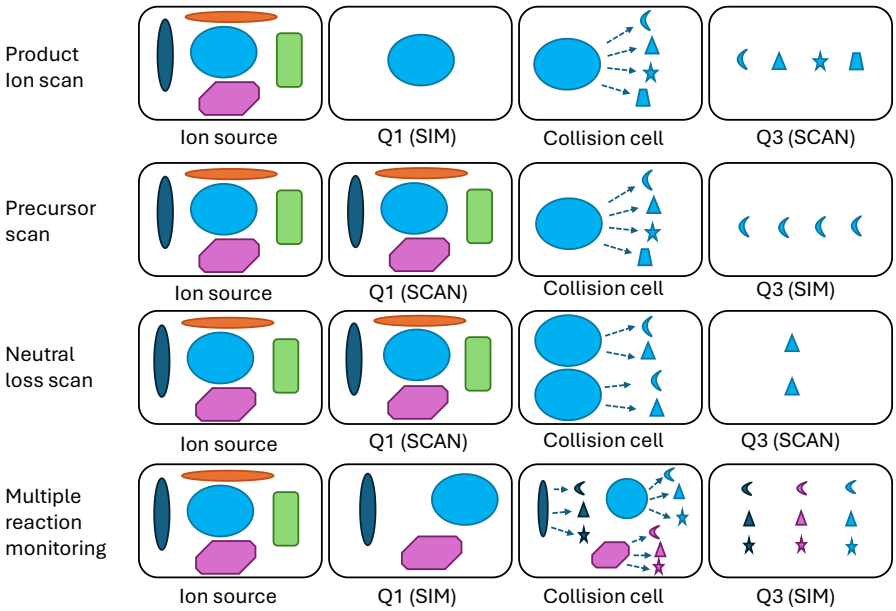


Figure 4: Summary of the 4 possible MS/MS operational modes of a QqQ MS analyser.

Quadrupole time of flight (QTOF) MS instruments are able to provide high resolution mass spectrometry (HRMS) records thanks to the *high m/z* selectivity of the Q and the high resolution provided by the TOF. Despite this generic statement, a more suitable term to refer to it should be accurate MS. Although the resolution can vary between systems, it rarely goes over 50000 [3]. On the other hand, m/z ratios, in single MS or product ion scan modes, can be determined with an error of a few ppm. A scheme of these detectors can be seen in figure 5.

These hybrid detectors are widely used in screening methodologies because of their fast obtention of complete and accurate spectral data. When combined with a soft ionization source, like electrospray ionization (ESI) or atmospheric pressure chemical ionization (APCI), they can provide two different types of data in a single experiment: the empirical formula of the studied compounds, thanks to the single MS mode; as well as their possible structure, thanks to the accurate *m/z* ratios in their product ion spectra obtained from the MS/MS mode. Thanks to these properties, QTOF instruments are extremely useful on the analysis of unknown species, and to remove isobaric interferences from compounds with the same nominal m/z ratios, but different molecular formulae. In addition to MS and target MS/MS data, a number of additional signal acquisition functions are available for these hybrid MS systems, such as the so-called *All ions* (also known as MS^E), and the auto MS/MS modes. In the *All-ions* mode, the quadrupole works as an ion guide, letting all ions reach the collision cell, where they are broken using pre-selected collision energies; thereafter, these ions are separated in the TOF mass analyser. The auto MS/MS mode follows a preestablished set of rules to record precursor and product ion data. These modes will be explained in more detail in further sections. In brief, the collision cell is activated when the signal of a given ion, recorded in the MS channel, stays above a given threshold.

USC UNIVERSIDADE DE SANTIAGO DE COMPOSTELA

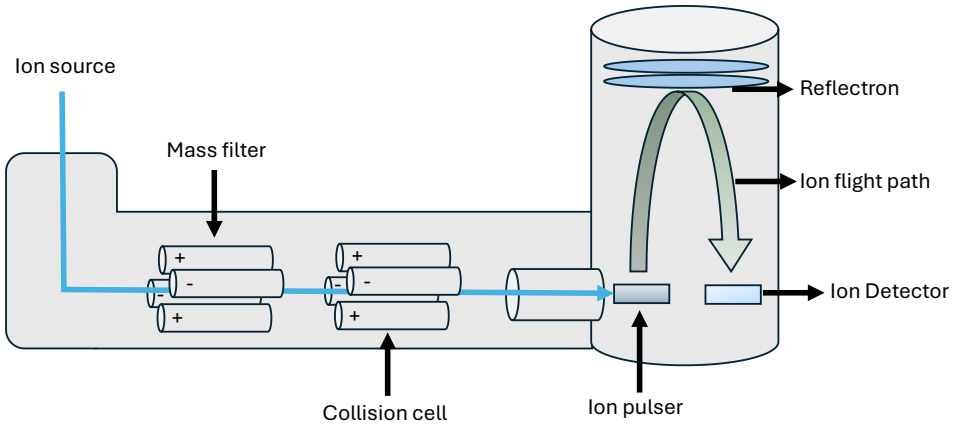


Figure 5: Scheme of a quadrupole time of flight MS analyser

1.1.2.1 Non-target screening

The main advantage of non-target screening (NTS), when compared to other kinds of data acquisition modes (target and suspect screening, which will be explained in more detail later), is the possibility to identify unknown species in complex environmental matrices. Since there is no prior information on the composition of the samples, the identification can only be done by matching the information of the detected species (retention behaviour; mass spectrum; exact mass and isotopic pattern) with data present in spectral databases. HRMS, with its high mass accuracy, resolution and wide mass range, provides exact masses and can resolve ions with very small mass differences, which makes them suitable for the identification of a great variety of substances. Due to the lack of standards for confirmation, the reliability of identifications is normally sorted according to their confidence level using the scale proposed by Schymansky et. al. [4]. This scale is divided into 5 levels of confidence, with level 5 being a compound identified only by its empirical formula, which means it is the lowest level of confidence; meanwhile level 1 corresponds to full confirmation against a standard of the candidate compound, this being the highest level of confidence.

- Level 1: Confirmed structure against a standard by matching of retention time, MS and MS/MS spectra.
- Level 2: Probable structure. There is an exact structure proposed based on two different possibilities:
  - Level 2a: Library; the proposed structure matches with a library or literature spectrum, and the spectrum-structure match is unambiguous.
  - Level 2b: Diagnostic; when no other structure matches the experimental data, but there are no literature or standards available.
- Level 3: Tentative candidate. There is a structure proposed, but there is not sufficient data for it, to be just a single structure.
- Level 4: Unequivocal empirical formula. An empirical formula is presented but there is not enough information to propose a possible structure.
- Level 5: The exact mass is presented because of the research interest, but there is no information to propose a molecular formula.

When developing a non-target screening methodology, there are some considerations that must be taken into account. First, blanks must be analysed regularly between samples to exclude, or to dismiss, the possible carryover between samples or the possibility of a false

USC DE COMPOSTELA

positive on the samples. Another important consideration is that when doing NTS, compounds that show low intensity are excluded from analysis, which can make the data easier to interpret, but this can also cause false negatives to appear; as such, the sensitivity of the instrument can be a limiting factor in NTS.

The strategies used for NTS are very different depending on the ionization source (soft or hard), which means that data acquisition modes, and data mining workflows are very different in case of GC-QTOF-MS and LC-QTOF-MS instruments.

In the current Thesis, NTS studies were carried out in combination with an LC-QTOF-MS instrument for the identification of tramadol transformation products (TPs) following its degradation at laboratory scale, under different experimental conditions; in this case, a data independent acquisition (DIA) methodology was used, followed by confirmation using standards and target MS/MS experiments for the estimation of several TPs that had not been previously reported.

Other applications of NTS were carried out using a GC-QTOF-MS instrument for the characterization of electronic cigarette refill liquids, compiling the confirmed volatile compounds into two different accurate MS libraries containing their retention index (RI), for two columns with different polarities. A second NTS method dealt with the characterization of indoor air compounds and the validation of an alternative, indirect method to assess the presence of semi-volatile compounds in this matrix. In the case of GC-TOF-MS screening methodologies, accurate EI spectra were first compared to the NIST17 EI spectra database for tentative identification; some compound identities were later confirmed using standards.

1.1.2.2 Target and suspect screening

Target and suspect screening consist of the analysis of a sample, with prior knowledge, or a suspicion, of the families of compounds present in the sample. The whole process for the analysis has been previously optimized taking into account the properties of the different compounds (including sample preparation and column separation). The name target screening is normally used for analysis where standards for the selected analytes are available. When the analysis is done for a list of suspect compounds, but there are no standards available, the employed term is suspect screening.

Figure 6 shows a general workflow of screening analysis.

USC
UNIVERSIDADE DE SANTIAGO DE COMPOSTELA

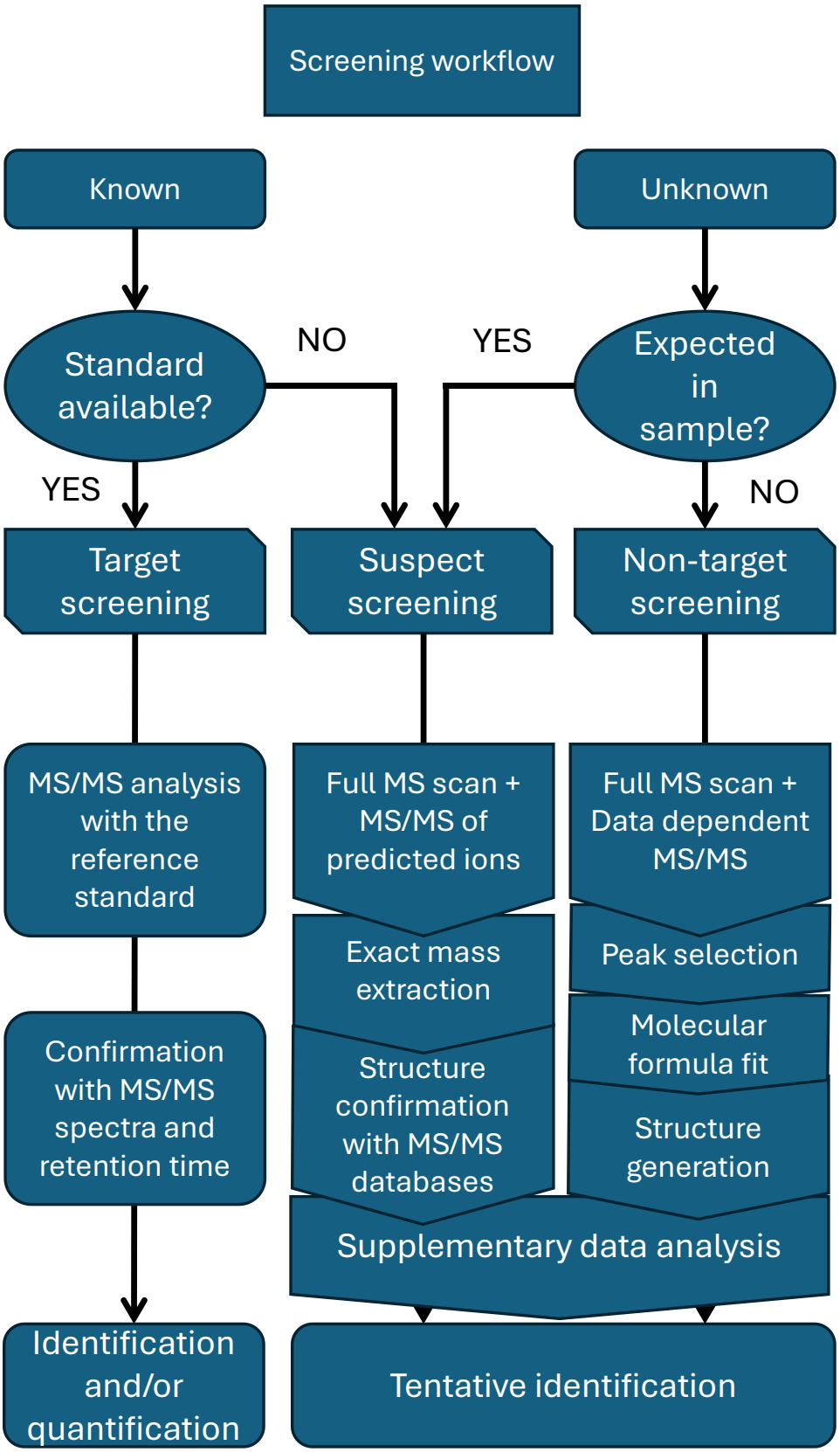


Figure 6: Screening methodologies workflow

USC UNIVERSIDADE DE SANTIAGO DE COMPOSTELA

1.2 CHROMATOGRAPHIC AND DIRECT SAMPLE INTRODUCTION METHODOLOGIES

One of the biggest challenges faced by analytical chemists is the determination of trace organic pollutants in complex environmental matrices, such as sludge, dust, and wastewater samples. To solve such problems, a selective sample preparation step followed by a powerful determination technique are normally combined. Chromatographic techniques coupled to mass spectrometry are the most resorted determination techniques to face complex problems. Liquid chromatography (LC) is the most used due to its versatility, gas chromatography (GC) also provides a lot of advantages, although its application field is more limited. In addition, supercritical fluid chromatography (SFC) has recently gained popularity in environmental analyses.

During this Thesis, the three aforementioned chromatographic techniques were employed to some extent, coupled to MS and tandem MS, depending on the aim of each application. An attempt to simplify analysis by applying direct analysis in real time coupled to a mass spectrometer (DART-MS) to complex environmental samples was also evaluated. The most important characteristics of these techniques will be explained in the following sections, as well as their combination with MS and some outstanding applications.

1.2.1 Liquid chromatography (LC)

Liquid chromatography pursues the separation of the different components of a sample based on their interactions between a solid stationary phase and a liquid mobile phase. The use of smaller particle sizes in LC gave way to high performance liquid chromatography (HPLC), with particle sizes between 2 and 5 μm; and the ultra-high performance liquid chromatography (UHPLC) (size < 2 μm) which allows the use of higher pressures to obtain faster separations, better resolution and narrow, symmetric peak shapes. Figure 7 shows a scheme of the components of a liquid chromatography system, combined with MS detection.

USC UNIVERSIDADE DE SANTIAGO DE COMPOSTELA

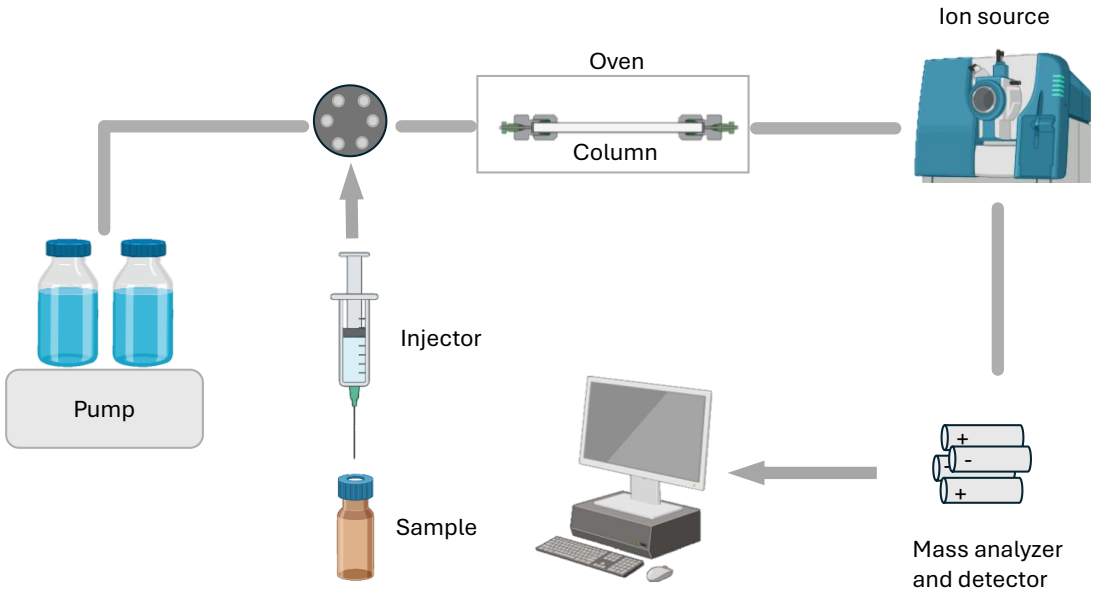


Figure 7: Basic scheme of a LC-MS system.

Different types of LC modes exist according to their separation mechanism, such as partition chromatography, size exclusion, ion exchange, affinity or chiral chromatography. Partition chromatography is the most often employed, and depending on the polarity of its stationary phase, it can be classified in two types: normal phase (polar stationary phase: i.e. diol, amino, nitrile) and reversed phase (apolar stationary phase: C_8, C_{18}, cyclohexyl, phenyl). Most of the LC applications to environmental samples employ C_{18} reversed-phase columns for their strong retention and separation efficiency of non-polar compounds. Common polar solvents used as mobile phase in reversed-phase LC (RPLC) include weak ones like water, or stronger mobile phases like acetonitrile (ACN) or methanol (MeOH) for a faster separation. When using a gradient while working in RPLC, it must always start on the most polar one and slowly change to the least polar one; this will result in the most polar components eluting first.

The separation of highly polar compounds by normal-phase LC combined with MS is challenging due to the poor compatibility of pure organic phase with ESI ionization sources. To help with this problem, hydrophilic interaction liquid chromatography (HILIC) was proposed. HILIC is a slightly modified version of normal-phase chromatography, employing polar stationary phases, while using the same mobile phase as RPLC. The most used stationary phase consists of silica or silica gel functionalized with polar groups. HILIC is a good choice for the separation of uncharged hydrophilic compounds that are too polar for RPLC. In HILIC separations, gradients usually start with a relatively high percentage of organic solvent, increasing then the percentage of the aqueous phase. As a general statement, HILIC columns cannot be run in 100% of organic phase.

Ion exchange chromatography (IEC) is used to separate compounds by their interaction with a stationary phase that contains fixed charges. There are two types of IEC: cationic exchangers and anionic exchangers. Cationic exchanger columns use a negatively charged stationary phase to separate positive ions, while anionic exchangers use positively charged particles to separate negative ions instead. Elution of the charged analytes is normally achieved

by using a high concentration of competing ions on the mobile phase. Obviously, when IEC is combined with MS detection, these ions need to be relatively volatile species.

In recent years there have been developments in chiral separation using LC and SFC techniques, both combined with MS detection. Chiral stationary phases (CSPs) have been lately classified as coated or immobilized, depending on the type of bond between the support particle (usually silica) and the chiral selector, crosslinking or covalent bond, respectively. Generally, coated phases are easier to prepare and have a better selectivity than their immobilized analogue; however, they show limited solvent compatibility. As a general statement, reversed-phase chiral LC analysis and SFC separations using polar solvents (i.e. methanol, acetonitrile, ethanol or isopropanol) as modifiers of supercritical CO_2, can be developed with coated columns.

1.2.1.1 Liquid chromatography coupled to mass spectrometry (LC-MS)

Liquid chromatography coupled to mass spectrometry (LC-MS) is considered the most important analytical technique of the last decades. It combines the great separation efficiency and versatility of LC analysis, with the sensitivity of MS, providing qualitative and quantitative information of time-resolved analytes in complex matrices after their ionization.

The hardest challenge in the hyphenation of LC and MS was turning molecules in solution into ions, in gas phase, while avoiding their thermal degradation, and removing the solvent before entering the high vacuum region in the mass analyser. The solution found were the atmospheric pressure ionization (API) processes, which include atmospheric pressure photoionization (APPI), atmospheric pressure chemical ionization (APCI) and electrospray ionization (ESI), which was the ionization technique employed throughout this Thesis.

The ESI source was first reported by Fenn and co-workers [5]. Its main feature is the simultaneous volatilisation and ionization of analytes as they exit the LC column. The ESI process for ion generation is comprised of three steps: in the first one, a fine spray of electrically charged droplets (with the same polarity as the voltage applied) is formed, simultaneously; a nebulising gas (normally nitrogen) helps creating a higher sample flow rate. The charged droplets are guided by pressure and voltage gradients to the analyser region of the mass spectrometer; a stream of heated nitrogen, flowing in the opposite direction assists the evaporation of the solvent, reducing the size of the droplets, and thus, increasing the surface charge density. Finally, the superficial electrical charge reaches a point in which the surface charges can escape from the solvent into the gas phase and are guided into the mass analyser for separation of ions as function of their m/z ratios. A generic scheme of the ESI process is shown in figure 8.

USC UNIVERSIDADE DE SANTIAGO DE COMPOSTELA

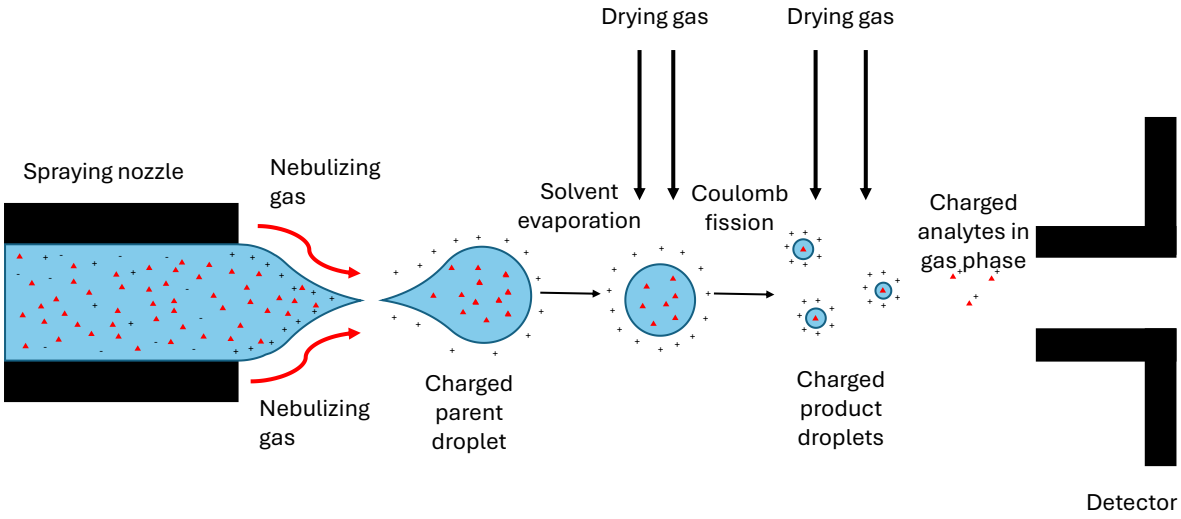


Figure 8: Scheme of the Electrospray ionization.

During this Thesis several LC-MS instruments have been employed. An LC instrument coupled to a triple quadrupole (QqQ) was used to acquire quantification data for a selection of different pollutants present in environmental samples. Another LC instrument coupled to a quadrupole time-of-flight (QTOF) analyser was used to obtain comprehensive information about the different transformation products of a certain pharmaceutical after its controlled degradation at laboratory scale.

1.2.1.2 Screening strategies employed in LC-ESI-QTOF-MS

The recent advances in mass spectrometry technologies have seen a notable improvement in selectivity, sensitivity and specificity; at the same time, software improvements allow for the acquisition of both, MS and product ion scan data in the same injection, with or without the selection of a previous list of precursor ions. This last option is the best one for screening analysis. According to literature, the functions used to record ion scan spectra using QTOF-MS systems can be divided in two categories: data dependent analysis (DDA), which is the most employed methodology, and data independent analysis (DIA) [6][7].

(i) Data dependent acquisition mode: Target-MS/MS and auto-MS/MS

DDA analysis is recommended for target analysis. In this mode, the instrument first performs an MS scan of the precursor ions, registering their m/z ratio and intensity and generates a list. Different ions are then selected following a set of preestablished rules and are guided to the collision chamber, for the formation of product ions. In this mode, the instrument generates both MS scan and MS/MS spectra in the same chromatographic run. The change between both modes is automatically controlled by the intensity of the precursor ion. Alternatively, it can be defined by a list of included/excluded ions, or by other different criteria like charge state, and/or the presence/absence of isotopic patterns.

USC UNIVERSIDADE DE SANTIAGO DE COMPOSTELA

According to the needs of the carried-out screening, there are two different strategies available:

- Target MS/MS experiments: a list of target precursor ions, including m/z ratios and retention times (RTs) is created for each compound; after that, the instrument registers the full MS spectra during the whole chromatographic run, while the target MS/MS analysis is performed during the set retention time windows; allowing for the acquisition of the information related to the molecular ion cluster (MS mode) and the accurate product ion scan spectra using one or more collision energies in the same chromatographic run.
- Auto-MS/MS experiments: A list of excluded or preferred ions can be added to the method in the same way as with target-MS/MS (excluding their retention time windows). Alternatively, precursor ions can be selected automatically according to their intensity, charge state or isotopic profile. To avoid the loss of information, a list of preferred/excluded ions is usually accompanied by the list of precursor ions selected by the instrument.

The main limitations of DDA are: (1) the loss of MS/MS information for the ions with lower abundance, since MS/MS data acquisition is normally triggered by the detection of precursor ions above a certain intensity threshold in the MS spectra; and (2) the loss of sensitivity produced by the simultaneous use of multiple acquisition functions in the same time window. When following narrow peaks, like those obtained by UHPLC, the simultaneous fragmentation of multiple precursor ions, requires the reduction of the number of transients accumulated in each MS and product ion scan spectrum. This has an important, negative effect in the LOQs of QTOF-MS instruments. The lower the number of transients accumulated in each spectra, the higher the LOQs.

(ii) Data independent acquisition mode: all-ions.

In all-ions mode, the QTOF instrument is always recording accurate spectral data without any pre-selection on the Q analyser, losing the specificity of DDA mode. Data acquisition can be obtained using different energies at the collision cell, low, high or even a collision energy (CE) ramp can be performed during a single chromatographic run.

All-ions mode is usually called pseudo-MS/MS since it does not provide authentic product spectra, but the combined product ion spectra of all the ions that reach the collision chamber at the same time. All-ions spectra of a mixture of standards properly separated in the LC column is equivalent to MS/MS spectra obtained after precursor ion selection in the Q analyser. Depending on the CE applied, different types of information can be obtained; using low CE values it is possible to acquire more data about the precursor ion, when using high CE values, more data about the product ions is obtained. The main strength of the all-ions mode is the fast acquisition of pseudo-MS/MS spectra; however, its main weakness is the high amount of interferences caused by the fragmentation of all co-eluting species. To avoid this limitation, the so-called quadrupole-resolved all-ions (Q-Rai), which is a DIA method that allows the obtention of cleaner MS/MS spectra without the loss of accuracy or quality of the data, is often used. The main difference between Q-Rai and all-ions is the pre-selection of ions creating different m/z windows in the Q analyser, before introduction into the collision cell with the

USC DE SANTIAGO DE COMPOSTELA

objective of reducing the amount of possible interferences in the chromatograms. Larger m/z window sizes means that the amount of precursor ions that will be fragmented will increase, thus, the complexity of the MS/MS spectra will also increase; in consequence, the narrower the m/z window, the cleaner the MS/MS spectra will be, and the number of m/z windows needed to cover a set m/z range will increase. [8] Depending on the vendor, Q-Rai mode is called SWATH (sequential window acquisition of all theoretical fragment ion spectra).

DIA mode presents some advantages over DDA mode since it allows the comprehensive fragmentation of all ions generated in the ion source and the obtention of the corresponding MS/MS spectra without the need to define any m/z or intensity threshold before the analysis. In combination with an accurate spectra database, the all-ions mode provides information for confirming the presence of database compounds in complex samples. Figure 9 shows the scheme of the DDA and DIA operation modes in a QTOF instrument.

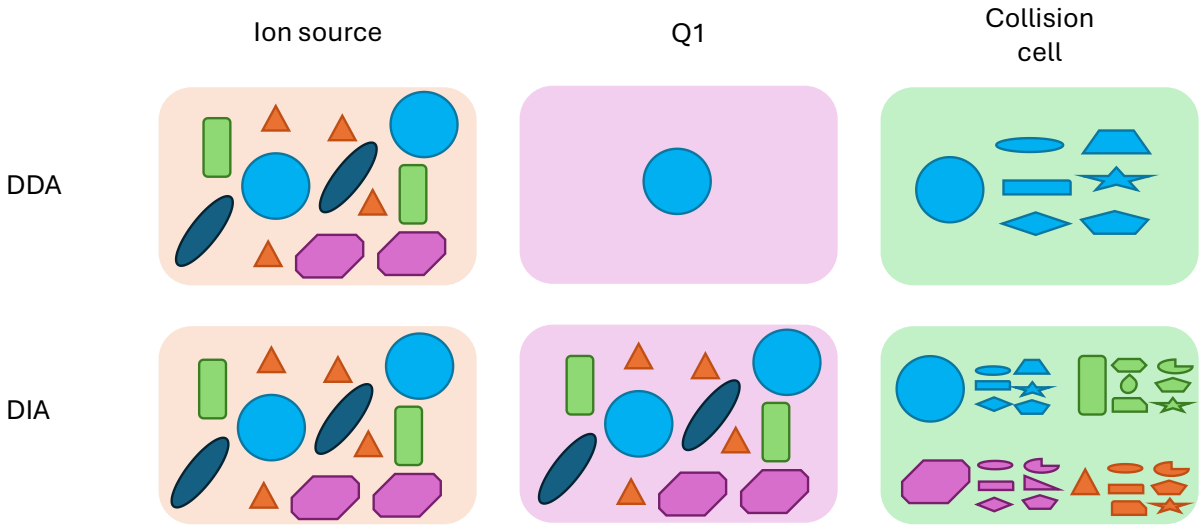


Figure 9: Operating scheme of DDA and DIA modes

1.2.1.3 Data processing from MS and MS/MS spectra for structure elucidation and identification

When data is acquired in auto MS/MS mode, the information contained in MS and MS/MS can be readily extracted. Once a relevant peak is detected, a molecular formula can be generated according to the accurate masses and the isotopic profile observed in the MS spectra. Both the molecular formulae and the MS/MS spectra can be compared to those existing in databases for confirmation.

In the same way, there are algorithms that can associate the data corresponding to precursor and product ions recorded in all-ions mode and compare them with an accurate database. Usually, these algorithms search for pseudo-molecular ions present in the database (i.e. $[M+H]^+$, $[M+NH_4]^+$,$[M+Na]^+$), obtained through LC-ESI-MS recorded with the collision cell inactive for a tentative identification. These tentative identifications are later confirmed checking if the product ions obtained from a spectral database are present at the same retention time as the parent ion in the high energy collision function.

There are several accurate MS spectral libraries available that contain data obtained using QTOF and Orbitrap instruments in combination with soft ionization sources, mainly ESI. Databases can be open-source, like MassBank [9], m/z cloud [10], or METLIN [11]; as well as commercial ones, like Personal Compound Database and Library (PCDL) from Agilent Technologies. Comparison between experimental spectra with those existing in databases is a useful strategy to help with the identification of unknown compounds present in complex matrices during screening in real samples or in laboratory degradation experiments. However, the number of inputs in these databases is still limited.

Nowadays most instruments include these databases in their software to help streamline screening methodologies. Experimental MS/MS spectra are automatically compared with the data present in the database and ranked on a confidence score based on the concordance of their m/z ratios, retention times (when available), and the relative intensity of their precursor and product ions between the experimental data and the ones recorded in the database.

1.2.1.4 Applications of LC-MS to the determination of emerging pollutants in environmental samples

Thanks to the above-described advantages, LC-MS(MS) has been widely used in combination with low resolution MS (LRMS) and HRMS for the quantification of emerging organic pollutants in many different matrices, as well as for the non-targeted screening of unknown pollutants in a variety of environmental matrices.

Most LC-MS applications involve multianalyte separations, they can range from only a few pollutants corresponding to the same family [12], [13], to procedures regarding more than 400 substances with completely different uses, chemical properties and structures [14].

The main matrices in environmental analysis of emerging pollutants include surface waters [15][16], wastewater and sludges [17][18], drinking water [19][20] and soils [21][22], since the presence of said pollutants can impact both human and animal health, as well as cause unpredicted damage to the environment. Aqueous type samples are normally extracted by Solid-phase extraction (SPE) before injection into the LC-MS, while soil or sludge samples are extracted using different techniques, such as matrix solid phase dispersion (MSPD), pressurized liquid extraction (PLE) or, more recently, the quick, easy, cheap, effective, rugged and safe (QuEChERS) methodology.

Table 1.1 summarizes some applications of LC-MS to different environmental samples.

USC
UNIVERSIDADE DE SANTIAGO DE COMPOSTELA

Table 1.1 Applications of LC-MS to analysis of emerging pollutants

Analytes	Matrix	sample pre-treatment	Column	Recoveries (%)	LOD	LOQ	Mass analyser	Ref
74 Pharmaceuticals	Ground water, Surface water, Wastewater	SPE (OASIS HLB)	BEH C18	50-150	0.01-8.98 ng L^{-1}	n.a.	QqQ	[16]
11 Organophosphate esters	Environmental waters	SPE (OASIS HLB)	Waters BEH C8	70-110	n.a.	2-6 ng L^{-1}	QqQ	[23]
50 Antibiotics	Environmental waters, Sludge, sediments, Manure	SPE (OASIS HLB) for liquid samples, Solid-liquid extraction + SPE (SAX) for solid samples	Agilent zorbax XDB	50-150	n.a.	0.52-65.8 ng L^{-1}; 0.64-28.6 ng g^{-1}	QqQ	[18]
26 Pesticides	Sediments	PLE+ SPE (OASIS HLB)	Aquitiy purospher STAR RP-18e	33-107	0.02-16.98 ng g^{-1}	n.a.	QqQ	[24]
430 Contaminants	Surface water and Wastewater	SPE (OASIS HLB)	Zorbax Eclipse plus C18	50-130	n.a.	<10 ng L^{-1}	QqTOF	[14]
7 Antimycotic drugs	River water, Treated water, raw Wastewater	Mixed mode SPE (OASIS MCX)	Zorbax Eclipse XDB C18	63-111	n.a.	2-15 ng L^{-1}	QqTOF	[13]
100 Pharmaceuticals and their degradation products	Drinking water, Groundwater, Surface water and Wastewater	SPE (OASIS HLB)	Zorbax Eclipse XDB C8	-	<10 ng L^{-1}µg L^{-1}	n.a.	QqTOF	[20]
42 Pharmaceuticals, Azole biocides, and Fungicides	Soil and plants	PLE + SPE (STRATA X)	Acquity U-HPLC column C18	>70	≤10 µg kg^{-1}	n.a.	Orbitrap	[22]

1.2.2 Supercritical fluid chromatography

Supercritical fluid chromatography (SFC) is a separation technique very similar to UHPLC that replaces most mobile phases components with a gas compressed to supercritical conditions. Thanks to its low toxicity and its relatively easy to achieve supercritical conditions, CO_2 is the major component of the mobile phase, in combination with other co-solvents that help with the separation of the analytes by modifying the polarity of the CO_2. A backpressure regulator (BPR) is necessary to ensure that the CO_2 stays in supercritical conditions throughout the whole chromatographic system (column and connection with the atmospheric pressure ionization source of the MS system). The main advantages of SFC over HPLC are its higher flowrates, which provide faster separations due to the higher diffusivity and low viscosity of supercritical CO_2, and a lower organic solvent usage, which is why it is considered a green analytical technique. SFC also shows higher efficiency and shorter equilibration times than those required in separations done in HPLC. A scheme of the different parts of an Agilent® SFC-MS are shown below in figure 10. The configuration commercialized by this vendor uses a pre-BPR splitter, after addition of the make-up solution.

USC UNIVERSIDADE DE SANTIAGO DE COMPOSTELA

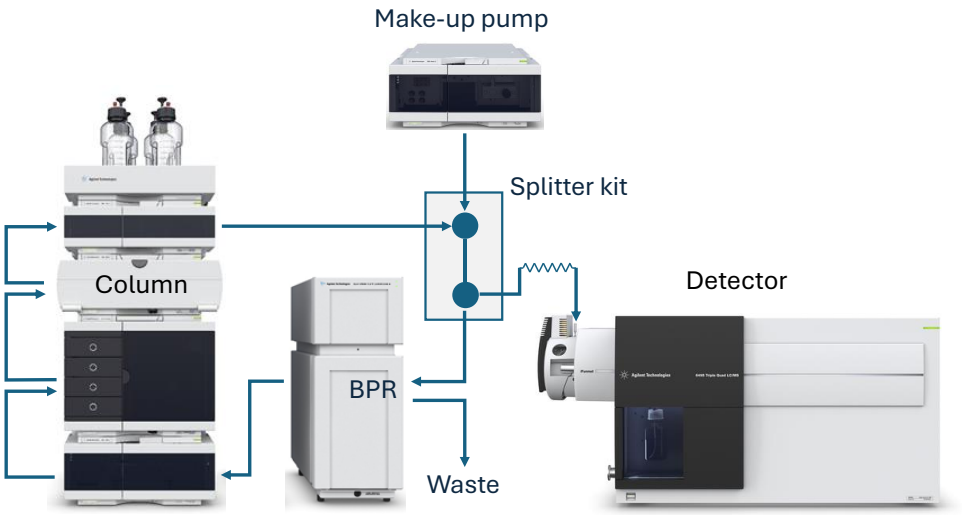


Figure 10: Components of a supercritical fluid chromatograph coupled to a mass spectrometer (SFC-MS) system by Agilent technologies®

The first reported use of SFC for chiral separations was done in 1985 by Mourier et.al. [25] and it has been widely used for chiral separations since then. In fact, one of the main uses of SFC is in the pharmaceutical industry, for the separation of enantiomers of chiral pharmaceuticals. For instance, Michael Hayes et. al. [26] developed an ultra-fast purification methodology that allowed the separate recovery of the two different enantiomers of given pharmaceuticals and allowed for subsequent biological testing with the intention of identifying its most active enantiomer. The main types of CSPs used in SFC are derivatives of cellulose and amylose (coated or silica-based), brush type (Pirkle-type) CSPs, native and derivatized cyclodextrins and cyclofructans, quinine-based and macrocyclic antibiotic-based CSPs. Among them, the derivates of cellulose and amylose cover the enantiomeric analysis of a large number of compounds and are commercially available from different vendors.

1.2.2.1 Supercritical fluid chromatography coupled to mass spectrometry

The coupling of SFC to MS (SFC-MS) has seen a recent increase in attention because of its status as a green methodology, as well as its higher efficiency and selectivity in the separation of chiral compounds when compared to reversed-phase HPLC applications. In addition, it presents a better compatibility with ESI ionization than organic solvents employed in normal-phase LC chiral analysis. However, its hyphenation to MS has its own challenges, due to the different features of SFC. When using an ESI source, an additional make-up auxiliary solution must be added at the end of the separation, and before the ionization source (Fig. 10), to improve the ionization of the analytes, as well as to prevent their precipitation after CO_2 passes to gas phase, beyond the split point (Fig. 10); its composition and flow rate can have a very important effect in the ionization efficiency.

During this Thesis, SFC-MS has been employed for the enantiomeric separation and subsequent study of the potentially enantioselective degradation of a selection of pharmaceuticals in sludge and wastewater samples.

1.2.2.2 Applications of SFC-MS to the separation of chiral pollutants in environmental samples

The applications of SFC-MS cover a wide range of substances with different chemical structures and origins, for different purposes. The main applications for chiral SFC covered in this Thesis correspond to the two major types of chiral pollutants in the context of environmental samples: pesticides and pharmaceuticals.

Table1.2 summarizes the conditions for chiral analysis of pesticide residues in environmental samples by SFC-MS. In most of these articles, the authors focused on the separation of the enantiomers of a single pesticide [27][28][29]. In these cases, chromatographic conditions were optimized for the fast separation of a few peaks, usually under isocratic conditions, with analysis times below 5 min. For these simple separations, the selection of the SFC column and the modifier were the most important variables controlling the selectivity of the separation process. In addition, the use of a mobile phase additive plays a relevant role for chiral analysis of acid or basic compounds. As further commented in the results and discussion section, the peak shape of basic species improves when adding a small percentage of ammonia to the organic modifier mixed with supercritical CO_2. In case of neutrals or slightly acidic species, formic acid (FA) and ammonium acetate (NH_4Ac) have been proposed to improve the separation of several azolic compounds [30], acylalanine species [31] and the insecticide dinotefuran [32]. The most employed CSPs are amylose-1 [tris(3,5-dimethylphenylcarbamate)], cellulose-1 [tris(3,5-dimethylphenylcarbamate)] and cellulose-2 [tris(3-chloro-4-methylphenylcarbamate)].

USC UNIVERSIDADE DE SANTIAGO DE COMPOSTELA

Table 1.2 Applications of SFC-MS for the separation of pesticides in environmental matrices

Compound	Matrix	Column	Sample pre-treatment	CO_2 modifier and additive	Run time (min)	Make-up solution	ref
Myclobutanyl, penconazole	Wine and Soil	Cellulose-5	SPE; PLE	ACN, NH_4Ac (5 mM)	10	MeOH:FA (0.5%), 0.1 mL min^{-1}	[31]
Metalaxyl, Benalaxyl, Tebuconazole	Wine and Soil	Amylose 1	SPE; PLE	MeOH, NH_4Ac (5 mM)	10	MeOH:FA (0.5%), 0.3 mL min^{-1}	[31]
Cyproconazole	Earthworms and Soil	Cellulose-2	QuEChERS	MeOH	5	MeOH: FA (0.1%): NH_4F (5 mM), 0.1 mL min^{-1}	[33]
Flutriafol	Vegetables and Soil	Amylose 1	QuEChERS	MeOH	5	MeOH: FA (1%), 0.1 mL min^{-1}	[34]
Fenbuconazole and metabolite	Vegetables and Soil	Amylose 1	QuEChERS	EtOH	4	MeOH: FA (0.1%), 0.4 mL min^{-1}	[35]
Uniconazole	Earthworms and Soil	Cellulose-2	QuEChERS	MeOH	1	MeOH: FA (0.1%): NH_4F (5 mM), 0.1 mL min^{-1}	[27]
Propiconazole	Wheat grapes and soil	Amylose 1	QuEChERS, SPE as clean-up	MeOH	5	MeOH: FA (0.1%), 0.1 mL min^{-1}	[28]
Pyrisoxazole	Spiked Soiland water	Amylose 1	QuEChERS	MeOH	4	MeOH: FA (0.1%)	[29]
Tebuconazole	Water and Biota	Amylose 1	SPE; QuEChERS	MeOH	5	MeOH: FA (0.1%), 0.15 mL min^{-1}	[36]

The reactivity of chiral drugs can differ significantly between enantiomers. Frequently, one of the enantiomers is biologically active while the other is either inactive or can lead to unexpected reactions or produce toxic effects [37]. Chiral analysis of drugs in environmental samples is of great importance, since it can help discriminating the source of some compounds, such as certain drugs of abuse or prescription pharmaceuticals that show different Enantiomeric fractions (EFs) in urine, faeces or wastewater samples, than those present in their commercial preparations [38]. Table 1.3 shows separation conditions for SFC separations of drug residues in different environmental samples.

USC UNIVERSIDADE DE SANTIAGO DE COMPOSTELA

Table 1.3 Applications of SFC-MS for the separation of chiral pharmaceuticals in environmental matrices

Compound	Matrix	Column	Sample pre-treatment	CO_2 modifier & additive	Run time (min)	Make-up solution	ref
Atenolol, Metoprolol, Propranolol, Metoprolol acid	Wetland microcosms	Cellulose-1	SPE	MeOH, TFAA (0.5%), NH3 (0.25%)	9	MeOH: FA (99.9:0.1), 0.3 mL min^{-1}	[39]
Aminorex, Carprofen, Chloramphenicol 3-N-Dechloroethylfosfamide, Flurbiprofen, 2-Hydroxy ibuprofen, Ifosfamide, Imazalil, Naproxen, Ofloxacin, Omeprazole, Praziquante, Tetramisole	Wastewater	Amylose-1, Cellulose-2	SPE	MeOH:ACN:IPA (1:1:1), NH4Ac (10 mM), NH3 (0.1%)	10	MeOH: FA (99.9:0.1), MeOH: NH4OH (99.8:0.2), 0.3 mL min-1	[38]
Alprenolol, Atenolol, Bisoprolol, Metoprolol, Mirtazapine, Ozaxepan, Propanol, Tramadol, 10,11-dihydro-10-hydroxy carbamazepine	River ater, Wastewater	Cellulose-1	SPE	MeOH: ACN :IPA (1:1:1)	9	MeOH (0.1%) FA, 0.3 mL min-1	[38]

1.2.3 Gas chromatography

Gas chromatography (GC) is an analytical technique that allows the separation of different compounds based on their volatility, and their interactions with the stationary phase.

The main difference between GC and LC is that the gaseous analytes in GC are carried through the column using a carrier gas (normally helium) as the mobile phase. The stationary phase in GC columns is normally a non-volatile liquid, that covers the interior of the column, or the surface of a solid support. This technique is generally used for the separation of volatile and semi-volatile analytes that are also thermally stable. Liquid samples (normally prepared on a volatile organic solvent) are volatilized by maintaining the GC injector at high temperatures. The carrier gas then takes the volatilized compounds to the head of the column. To increase the scope of applications of GC separations, a derivatization step can be employed to increase the stability or volatility of compounds not amenable to direct analysis by GC. This approach was very common on the early days of LC-MS, when not all laboratories had the necessary equipment to

USC UNIVERSIDADE DE SANTIAGO DE COMPOSTELA

address the determination of these compounds. The main components of GC-MS system are shown in figure 11.

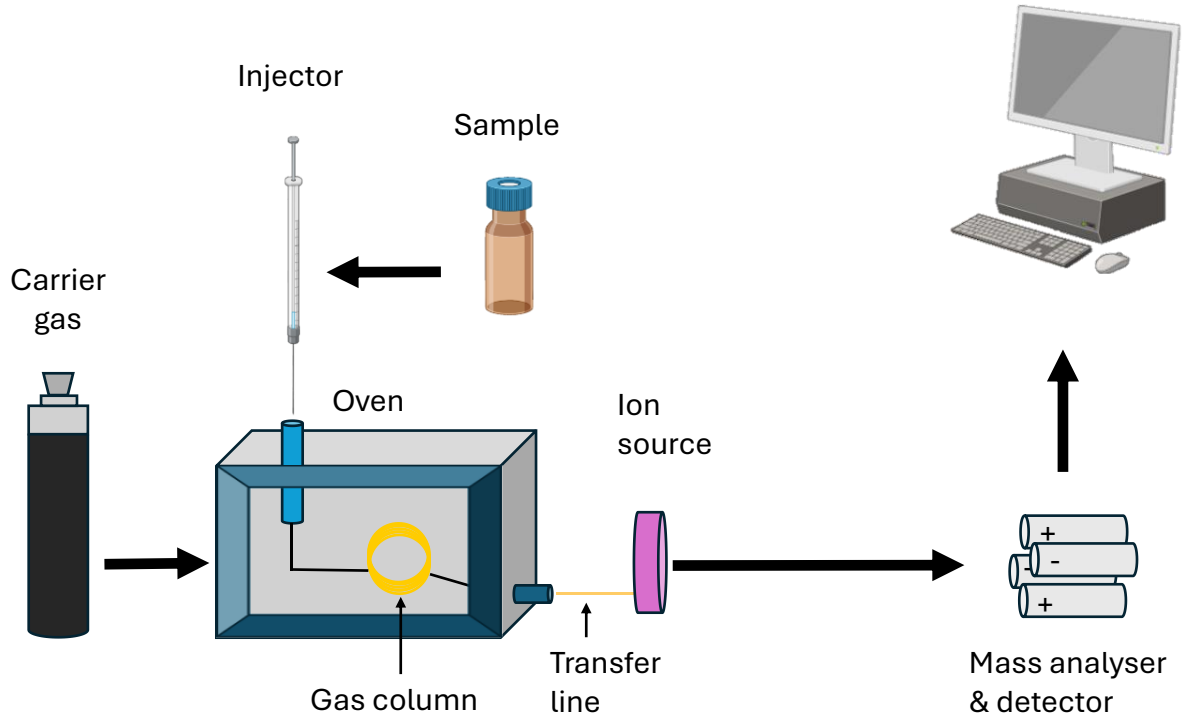


Figure 11: General scheme of the components of a gas chromatography (GC) system combined with a MS spectrometer.

Liquid samples are generally introduced in the GC column by a syringe. There are four different modes of injection of liquid samples in GC: volatilization at constant temperature with or without flow division, named split and splitless respectively, on-column injection and volatilization using a temperature program (PTV).

- Split and splitless injection: these modes are normally used for trace analysis, when the analytes present comprise less than 0.1 and 0.01% of the sample, respectively. Normally, only 1-2 µL of sample are injected, and the temperature of the injector is usually held around 50 ºC above the boiling point of the less volatile of the analytes. The main difference between split and splitless modes is that during split injection, only the 0.2-2 % of the volatilized analytes enter the column while in splitless mode, most of the volatilized sample enters the GC column.
- On-column injection: This injection mode is used when the sample components suffer decomposition at temperatures above the boiling point of the solvent. It is the best mode to transfer all components of the sample to the head of the chromatographic column; however, it is not recommended for complex matrices, as low volatility compounds may end up trapped in the initial part of the column.

USC UNIVERSIDADE DE SANTIAGO DE COMPOSTELA

- Temperature program volatilization: It is very similar to split and splitless injection but it has the possibility to create a temperature program for the volatilization and venting of most of the solvent whilst less volatile components of the sample remain in the liner, within the injection port. Its main advantage is that it can be used with high sample volumes to achieve higher sensitivity without peak deformation.

1.2.3.1 Gas chromatography coupled to mass spectrometry.

The same as what happened with the coupling between LC and MS, the coupling of gas chromatography and mass spectrometry (GC-MS) joins the advantages of both techniques, combining the selectivity and resolution of the separation technique with the sensitivity and structural information associated to the MS spectrum. Although GC separations can be applied to a narrower range of compounds than LC (this is the reason behind the growing popularity of LC), GC-MS still has some advantages over LC-MS, such as the higher spectral information that electron ionization (EI) provides versus ESI ionization, and the availability of EI-MS databases.

The GC-MS coupling consists of a gas chromatograph equipped with a capillary column, directly connected to the mass spectrometer. The most used ionization source is the electron ionization one (EI). In an EI source, the neutral molecules that exit the chromatographic column are impacted by electrons, generally with an associated energy around 70 eV, and form the ion $[M]^+$ called the molecular ion; usually these ions fragment further, creating fragment ions and sometimes, they can be completely missing from the GC-MS spectra.

In the present Thesis, GC was coupled to a QTOF mass analyser and further employed for the non-target screening of both environmental samples, and liquids used as refills for electronic cigarettes.

1.2.3.2 Data acquisition and processing in GC-QTOF-EI-MS

Since some emerging pollutants are not amenable to LC-ESI-MS determination, GC-EI-MS is a complementary methodology for the analysis of these non-polar compounds. Quite often, the information contained in EI-MS spectra is enough for the unequivocal identification of a given compound, or at the very least, to assign it to a chemical structure. As far as we know, the software controlling the GC-EI-QTOF-MS does not offer the possibility to work in the previously described auto MS/MS and all-ions modes, so in most cases, data is acquired only in scan MS mode and records of product ion scan spectra are limited to a pre-selection of target compounds.

The data mining strategy for GC-EI-TOF-MS is completely different to the one described for LC-ESI-TOF-MS. The main advantage of EI-TOF-MS spectra is that MS data normally provides enough information for the identification of a given peak. Its main problems, however, are that (1) the molecular ion is very often absent from the spectra and, (2) the presence of fragment ions from coeluting species creates interferences. For these reasons, the first step in screening studies based on this technique is the de-convolution of the whole chromatogram to obtain a list of components, with their accurate EI-MS spectra not interfered by fragments of coeluting compounds. The next step is a spectral search in EI-MS databases. Since EI

fragmentation is very reproducible in different instruments, reliable, nominal resolution mass spectral libraries for over 15000 compounds have been developed (NIST 17). Unfortunately, as of now, there are no high-resolution EI-MS spectral databases available apart from small libraries focused on certain families of compounds (e.g. pesticides). For these reasons, most identifications are done using the low resolution NIST EI-MS library. Further comparison of experimental m/z ratios with calculated values from fragments with known structure present in the NIST database can be useful for the discrimination of compounds with different empirical formula, but same nominal masses.

Although these data mining methodologies can be very useful for the identification of unknown substances, user verification for most candidate structures is needed; when a screening produces a high amount of identifications, these verification processes can be time-consuming. To help with this problem, some software packages incorporate automated workflows for searching different molecular formulas in different databases during the same workflow, resulting in more accurate identifications and saving a lot of time; however, user verification is still required to avoid errors made by the program.

1.2.3.3 Applications of GC-MS to the determination of emerging pollutants in air samples.

Given the volatile and semi-volatile nature of the substances present in air, GC-MS has been the most widely used technique for their determination and quantification. There has been an increase on the interest of air composition due to the possible adverse health effects that different volatile and semi-volatile pollutants present can cause [40][41]. There are two different approaches for air sampling: active sampling, which uses a vacuum pump and an activated sorbent capable of retaining the different pollutants; and passive sampling, in which a sorbent is left in the selected area for a specific amount of time, or until an equilibrium between the air and the sampler is reached.

Most air quality measurements are done using the passive sampling approach due to the lower cost of the sorbents, compared to that of vacuum pumps; their versatility, as they can be used for monitoring both indoor and outdoor areas and they are also less intrusive for the sampling of indoor areas (workplaces or households). Passive samplers have been successfully used in a variety of different environments like hair salons [41], and vehicles [42]. Common passive samplers include polyurethane foam (PUF); which can be used for both active and passive sampling, tube-type passive samplers, which can be filled with a variety of sorbents depending on their application, XAD-resin based samplers and the waterloo membrane sampler (WMS) [43].

The most widely used introduction method of passive samplers to the GC instrument is the thermal desorption (TD). TD-GC-MS permits the overriding of the solvent delay, required during analysis of liquid samples (extracts), which allows the instrument to start registering the EI-MS spectra right after injection to record very volatile organic compounds (VVOCs) that are otherwise lost within the solvent delay window [44].

Table 1.4 shows some examples of GC applications for the characterization of organic volatile compounds in indoor air.

USC DE COMPOSTELA

Table 1.4 Applications of GC-MS in air characterization

Compound	Sampling method	matrix	Sample pre-treatment	LOD	LOQ	Ref
Pesticides	Active sampling	Outdoor air	Thermal desorption	n.a.	0.02-0.21 ng m-3	[45]
PAHs	Active sampling	Outdoor air	MIP-SPE	0.03-0.09 ng m-3	0.12-0.33 ng m-3	[46]
Persistent organic pollutants	Active sampling	Outdoor air particulate matter	UAE-MSC	0.5-2.7 pg m-3	1.7-9.0 pg m-3	[47]
Volatile organic compounds	Passive sampling	Indoor air	Thermal desorption	0.015-0.446 µg m -3	0.045-1.35 µg m -3	[41]
Volatile organic compounds	Passive sampling	Outdoor air	Thermal desorption	0.00082-0.023 µg m -3	0.0042-0.047 µg m -3	[48]

1.2.4 Direct sample injection. Direct analysis in real time

Direct analysis in real time (DART) is an ambient ion source, first presented by Cody et. al. in 2005 [49]. This technique was developed for the fast and non-contact analysis of materials at ambient pressure and has succeeded in the determination of hundreds of substances present on the surface of samples of very different natures.

Ion formation in DART ionization is based on the ambient air-chemical reactivity activated by a gas stream of species in an excited metastable state. The ionization mechanism is variable and depends on (1) the carrier gas used, (2) the proton affinity and ionization potential of the analyte, and (3) the presence of additives or dopants. Normally the ionization takes place after the analyte volatilization and its mechanism is a charge transfer reaction with reactive ions or through Penning ionization. Penning ionization involves energy transfer between the excited metastable gas M* to an analyte, S, whose ionization potential is lower than the energy of M*. (Eq.1)

$$\boldsymbol{M^* + S \rightarrow S^{+\cdot} + M + e^- \; Eq.1}$$

The DART source structure is shown in figure 12. In this source, the ionization starts when a carrier gas stream, normally Helium (other gases such as Argon and Nitrogen have been studied as ionization sources) is introduced in a discharge zone, where it is subjected to an electrical discharge creating ions, electrons and excited metastable molecules. Afterwards, the gas is transferred to a ceramic heater that heats it to the desired temperature and passes through an electrically charged grid filters, where only the neutral and metastable excited molecules remain, discarding the rest of the charged species. Lastly, the heated gas reacts with the surrounding atmosphere containing nitrogen (N_2), oxygen (O_2) and water (H_2O), generating water clusters that further ionize analytes through a series of sequential reactions[50].

When helium is used, the dominant positive ion formation mechanism involves the formation of water clusters followed by proton transfer reactions [50]. (Eqs. 2-5)

$$He(2^3S) + H_2O \rightarrow H_2O^{+\cdot} + He(1^1S) + e^- \; Eq.2$$
$$H_2O^{+\cdot} + H_2O \rightarrow H_3O^+ + OH^- \; Eq.3$$
$$H_3O^+ + n\,H_2O \rightarrow [(H_2O)nH]^+ \; Eq.4$$
$$[(H_2O)nH]^+ + M \rightarrow MH^+ + nH_2O \; Eq.5$$

Negative ion formation follows a different mechanism. Electrons are produced by Penning ionization, these electrons are then thermalized by atmospheric gas and are later captured by atmospheric oxygen to form $O_2^{\cdot}$, which reacts with the analytes to form anions. [eq 6-8]

$$M^* + surface \rightarrow M + surface + e^- \; Eq.6$$
$$e^-_{fast} + gas \rightarrow e^-_{slow} \; Eq.7$$
$$e^-_{slow} + O_2 \rightarrow O_2^{\cdot} \; Eq.8$$

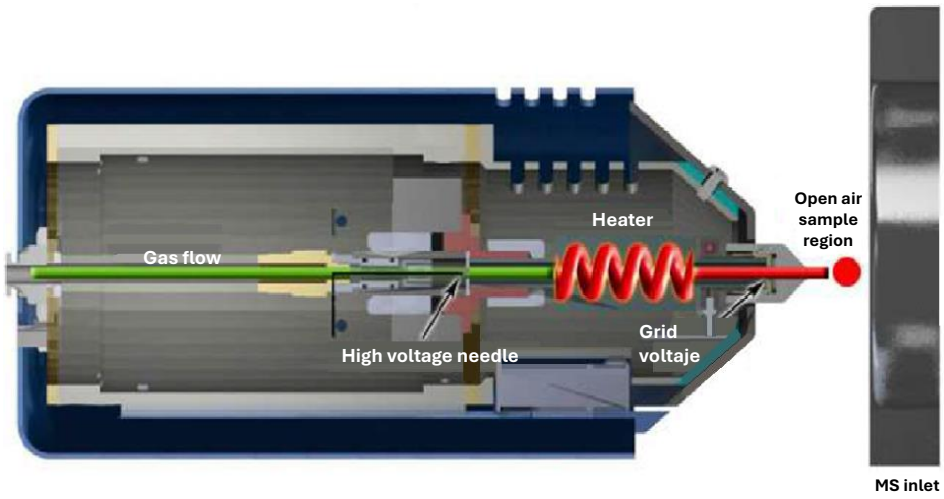


Figure 12: Structure of a DART source (IonSense)

1.2.4.1 Direct analysis in real time (DART) source coupled to mass spectrometry.

The DART source has been successfully employed in combination with several types of mass spectrometers (DART-MS), from QqQ to QTOF and Orbitrap instruments, for the analysis of many different materials in several phases (solid, liquid and gas), demonstrating its value as a powerful technique for the selective and fast qualitative characterization of different analytes in complex samples.

The main advantage and selling point of DART-MS is that it allows for the characterization of complex matrices without, or with minimal, sample treatment and skipping the chromatographic separation step, allowing for faster and simpler analysis of a greater number of samples.

As with any other analysis technique, DART-MS has some parameters that need to be optimized to ensure a better selectivity, sensitivity, and reproducibility. Some parameters have a significant effect in the signal intensity and signal-to-noise ratio. The quality of the signal and intensity depend on the production of metastable atoms, the volatilization of the target analytes and the formation of the water clusters. During the development of this Thesis, the parameters that had the biggest impact on signal intensity were:

- Ionization mode. Both positive and negative ions are formed in the DART source, and they can be filtered by changing the polarity of the grid, improving the formation of positive or negative ions of the analytes.
- Carrier gas and gas flow rate. Different carrier gases can yield different ionization efficiencies, according to the energy of their metastable state.
- Gas heater temperature. Some analytes might thermally degrade at higher temperatures, while others may not be able to be desorbed at lower temperatures.
- Grid voltage.
- Sample movement speed. The speed at which the sample holder moves influences the amount of time that the sample is in contact with the stream of excited atoms coming from the source, increasing or decreasing sample signal in the detector, and increasing or decreasing the width of the chronographic peak.
- Distance between the DART exit and the MS. This parameter affects the transfer efficiency of the ions into the MS detector, the efficiency increases as the distance decreases.

During this Thesis, DART-MS was evaluated for the quantification of a commonly used bactericide in complex environmental samples such as wastewater and sludge from wastewater treatment plants (WWTPs), validating its accuracy using samples of known concentration and considering LC-MS as alternative, reference technique.

1.2.4.2 Applications of DART-MS for the analysis of emerging pollutants.

DART-MS is well suited for the analysis of compounds present, deposited or absorbed into the surface of the sample or that are being released into the atmosphere. DART-MS has been used in many different fields like forensics [51][52], food quality and safety [53], environmental analysis, [54][55] or quality control [56][57] mostly for qualitative purposes.

Some quantitative methods have been developed for DART-MS as is the case of Castro et. al. [58] where the authors developed and validated a method for the determination of bisphenol A in thermal printing paper, with a previous ultrasound assisted extraction of the samples, reporting recoveries in the range from 90 to 110% and an LOQ of 0.04 mg g^{-1}. In all these applications the selectivity of the determination relies mostly on the performance of the MS technique. Thus, the higher the complexity of the sample and the lower the concentration of the target species, the more likely the existence of isobaric interferences.

Table 1.5 summarizes some applications of DART-MS in different fields for the analysis of a wide variety of compounds.

USC UNIVERSIDADE DE SANTIAGO DE COMPOSTELA

Table 1.5 Applications of DART-MS in different fields

Field of application	Compound	Matrix	Sample pre-treatment	Quantitative /Qualitative	Ref
Forensics	Synthetic cannabinoids	Blood	ACN/MeOH extraction	Qualitative	[59]
	Synthetic cannabinoids	Herbal samples	Direct analysis	Qualitative	[52][60]
	Ink composition	Ink lines drawn in paper	Direct analysis	Qualitative	[51]
Environmental analysis	UV filters	Water and cosmetics	Direct analysis	Quantitative	[54]
	UV filters	Water	Stir bar sorptive extraction	Quantitative	[55]
	Aspirin, Acetaminophen	Soil	Direct analysis	Semi-quantitative	[61]
	7 herbicides	Water	SPME	Quantitative	[62]
	Melamine, cyanuric acid, D-Glucose, Dimethyl sulfoxide and 5 phthalates	Water	Stir bar sorptive extraction	Quantitative	[63]
Food quality and safety	Mycotoxins	Beer	ACN extraction, Direct analysis and sediment redissolution	Qualitative	[56]
	Fingerprint analysis	Peppers	Direct analysis	Qualitative	[64]
Quality control	Bisphenol A	Thermal printing paper	UAE	Quantitative	[58]
	21 stabilisers	Polypropylene	Reflux extraction and Direct analysis	Qualitative	[57]

1.3 SAMPLE PREPARATION

1.3.1 Solid-phase extraction

Solid-phase extraction (SPE) is a simple methodology and the most used one for the extraction of analytes from a liquid sample in contact with a solid sorbent. Its action mechanism is very similar to that of chromatography, with the different components of the sample interacting in different ways with the selected sorbent. The main objective of SPE is to retain the selected analytes while the rest of the sample components pass through the SPE syringe, without interacting with the sorbent, allowing the obtention of a cleaner extract.

The different steps of a standard SPE protocol, based on a reversed-phase mechanism, are listed below and a scheme of this process can be seen in figure 13:

- Conditioning: The first step of most SPE protocols is to use a water miscible organic solvent (normally the one that is going to be used for the subsequent elution of the samples, i.e. MeOH, ACN) to clean the cartridge, eliminating possible residues of its manufacturing and activating the sorbent surface to improve analyte interaction. Afterwards, the excess of organic solvent must be eliminated using a solvent with a lower elution power, normally water.

USC UNIVERSIDADE DE SANTIAGO DE COMPOSTELA

- Sample loading: The sample is passed through the sorbent and the analytes get retained. The sample flowrate should be very slow to ensure more time for the analyte-sorbent interactions to happen. This step is generally performed by gravity, however, when high volumes of sample need to be extracted, the sample loading can be helped using a vacuum pump connected to an SPE station, while ensuring that the flowrate of the sample is still low enough, to guarantee that compounds are properly retained.
- Cleaning: After loading the sample, a solvent with low eluting power is used to rinse the sample container and ensure all the analytes have reached the cartridge. Depending on the features of the sorbent material, and the type of cleaning solvent, sometimes, certain sample components can be rinsed from the SPE cartridge, or syringe.
- Drying: The loaded cartridge is completely dried under a low flow of nitrogen to eliminate all the excess water (or cleaning solvent) so that it does not affect the efficiency of the analyte elution.
- Analyte elution: A suitable solvent with higher affinity to the analytes than the sorbent is used to break the sorbent-analyte interaction, while leaving the remaining impurities retained. The chosen solvent should also be compatible with the selected determination technique whenever possible. Analyte elution can be performed directly or in various steps like using a different solvent to eliminate interferences before eluting the analytes, or using different solvents to selectively elute analytes with different properties.

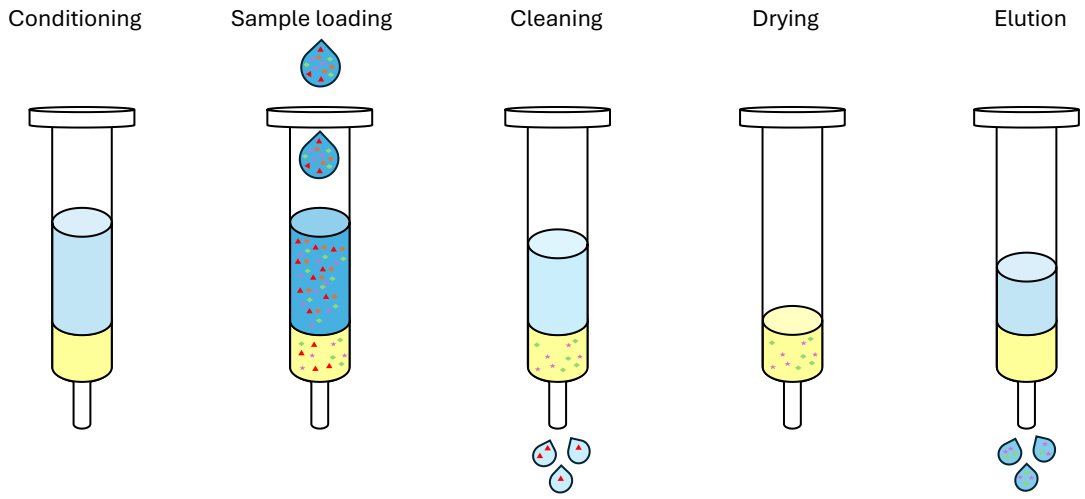


Figure 13: Scheme of a solid phase extraction procedure.

The critical steps that define the performance of the SPE are the sample loading and analyte elution steps, in which the interactions between the analytes, the solid phase and the elution solvent are the most important factor. The factors that can impact the efficiency and the selectivity of the SPE process are the nature of the sample, the nature of the analytes, the sample pH, and ionic strength.

USC
UNIVERSIDADE DE SANTIAGO DE COMPOSTELA

SPE sorbents have been organized into three main groups according to Poole [65].

- **Inorganic oxides.**

Silica gel, alumina, Florisil (synthetic magnesium silicate) and diatomaceous earth are the most important of this kind of sorbents. Their selectivity is controlled by the functional group linked to their surface, in general the most polar compounds (i.e. sulfonic acids, carboxylic acids, phenols, hydroxylated compounds) are the ones that show the highest retention, aromatic or less polar compounds show the lowest retention, and those with a dipole character (nitro, ester, ketone) show intermediate results [66]. Inorganic oxide cartridges have been successfully used for the separation of polar compounds from oils and fats; however, their applicability to water samples is limited. Another problem they pose is that they can catalyse the degradation of, or form irreversible bonds with, certain analytes limiting their applications further.

- **Low specificity sorbents.**

This group includes silica-based sorbents, porous polymers and carbon-based sorbents. All of them are commonly used for the isolation of contaminants from aqueous solutions. Their separation efficiency depends on dispersive and polar intermolecular interactions.

  - Silica-based sorbents: They are generally synthetized by reaction of mono or trifunctional organosilanes with silica gel, followed, in some cases by endcapping of the free small silanol groups, to avoid possible undesired interactions. Depending on the functionalization performed, three different separation mechanisms according to their major interactions with target compounds can be achieved:

    - *Normal phase:* This kind of sorbents focuses on the extraction of polar components from non-polar samples via hydrogen bonds, dipole-dipole or induced dipole-dipole interactions. A polar solvent is used for the analyte elution. This kind of interaction is displayed by materials like N-propylethylene diaminosilane (PSA), (PSA can also be used as a weak anionic exchanger), or cyanopropylsilane (CN).

    - *Reversed phase:* They allow the extraction of non-polar components present in polar samples. The interactions that reign in these extractions are mainly Van der Waals forces. Analytes are normally eluted using a low volume of organic, polar solvents. Reversed-phase materials commonly used are silica functionalized with octyl (C_8) or octadecyl (C_{18}) groups.

    - *Ion exchange:* They specialize in the extraction of ionic species from the sample. They can contain cationic or anionic exchange groups, as such, sorption-desorption processes are based on electrostatic interactions between the analytes and the sorbents. Common anionic exchangers

USC UNIVERSIDADE DE SANTIAGO DE COMPOSTELA

include quaternary amines, as the ones present in (trimethylamine) propylsilane (SAX) or secondary amines as (diethylamino) propylsilane phases. Cationic exchangers present acidic groups such as sulphonates (benzenesulphonyl) propylsilane (SCX) or carboxylates as (carboxy) methylsilane.

For the elution of the analytes, there are two different strategies, the first one is neutralizing the charged groups, either those in the analytes, or in the surface of the sorbent, using an appropriate solvent, and the other one is displacement, using a solvent containing a high amount of ions that bind more strongly than the analytes to the sorbent.

- Carbon-based sorbents: The main types of carbon-based materials employed in SPE processes are graphitized carbon black, carbon nanotubes, activated carbon and porose graphitic carbon. They show a high retention for planar molecules with systems rich in polarizable electrons, and highly polar functional groups. As drawback, quite often these interactions are not reversible, making difficult to recover the sorbed compounds during the elution step.
- Porous polymeric sorbents: They are generally copolymers of styrene and divinylbenzene processed to enhance their properties for SPE. They show a high retention due to their high surface area and high degree of crosslinking. The most common porous polymer sorbents are those formed by poly (styrene-divinylbenzene) copolymers (PS-DVB); however, due to their low capacity to retain more polar analytes, a combination of the PS-DVB skeleton with hydrophilic monomers, adding a polar group, helps overcome this limitation. One of the most popular of these new porous sorbents is the microporous poly (divinylbenzene-co-N-vinylpyrrolidone), often referred as the hydrophilic-lipophilic balanced (HLB) sorbent.

- **Compound-specific and class-specific sorbents.**

They are sorbents developed with a higher selectivity in mind for the analysis of specific analytes in very complex samples. They include mixed-mode sorbents, immunosorbents, restricted access materials and molecularly imprinted polymers.

- Mixed mode sorbents: They were created as an alternative to reversed-phase sorbents to improve their selectivity. They consist of a polymeric skeleton with ionic groups, which allows them to have two kinds of interactions: reversed-phase and ionic exchange. They are normally used in very complex samples to extract a variety of analytes (charged or not). The elution of the desired analytes is done by adjusting several parameters like the pH, or the polarity of the eluent to obtain the cleanest extract.

  Some of these sorbents are based on the above-mentioned HLB sorbent by functionalization with strong cation exchangers like sulfonic groups OASIS®

USC UNIVERSIDADE DE SANTIAGO DE COMPOSTELA

MCX materials (Mixed-mode Cationic eXchangers), weak cation exchange groups like carboxylic groups OASIS® WCX (Weak Cationic eXchangers), or with strong and weak anionic exchangers like quaternary amines and piperazines OASIS® MAX (Mixed-mode Anionic eXchangers) and OASIS® WAX (Weak Anionic eXchangers) respectively. During elution, this kind of sorbents allows the fractionation of compounds retained by the reversed-phase mechanism, from those showing electrostatic interactions with charged groups present in the sorbent.

- Immunosorbents: They are the most employed in medicine, biology and food sciences and they are considered the first specific sorbents. They are formed by a silica base with an immobilized antibody which presents exclusive selectivity for the analyte that works as an antigen.
- Molecularly imprinted polymers (MIPS): They are synthetic analogues for immunosorbents; they are prepared using a specific molecule as a template, obtaining a polymer with specific recognition sites for that analyte, or for a family of compounds, allowing their selective extraction from very complex matrices.
- Restricted access materials (RAM): They were developed for the retention of low molecular weight molecules. The selection mechanism for these sorbents depends on both size and affinity. The only analytes that will be retained are the ones small enough to fit into the functionalized pores, which means that the bigger analytes will pass through the sorbent without interacting with it, leading to cleaner extracts.

In this Thesis, different types of sorbents were used depending on the complexity of the analysed matrix. For example, HLB cartridges were employed when working with the relatively simple condensed water matrix, its hydrophilic-lipophilic nature allowed the retention of a wide variety of volatile organic compounds.

Mixed mode MCX cartridges were employed when working on the extraction of basic compounds from wastewater samples, allowing quantitative recoveries and obtaining a relatively clean extract; when working with more complex organic extracts from sludge samples, an SCX cartridge was used as a clean-up step after the sample extraction using matrix solid-phase dispersion (explained in detail below).

1.3.2 Matrix solid-phase dispersion

Matrix solid-phase dispersion (MSPD) is an extraction method proposed by Barker et al in 2007 [67]. This technique consists of the dispersion and homogenization of a sample in a solid sorbent to ensure better analyte-sorbent-solvent interactions. MSPD involves three steps that are shown in Figure 14.

- Dispersion of the sample in the matrix: Both the sample and the sorbent are placed in a mortar and the sample is dispersed with the help of a pestle, until a

USC UNIVERSIDADE DE SANTIAGO DE COMPOSTELA

homogeneous mixture is obtained. Both, mortar and pestle should be made from glass, or agate, since porous materials might lead to material and analyte losses, or future contaminations.

- Packaging: Once the sample has been homogenised, it is transferred to the MSPD cartridge (normally a polypropylene syringe) containing a polypropylene frit at the bottom to avoid sample loss. Another frit is usually added on top of the sample to help compacting it. Another sorbent can be added at the bottom of the cartridge, acting as a co-sorbent (not used in the dispersion) to help with the fractionation of the sample, or it can be used to help cleaning up the extract.
- Elution: The elution solvent is passed through the dispersed sample and clean-up sorbent, either by gravity or with a slight vacuum, and it interacts with the analytes, eluting them. Any parameter that affects the solubility of the analytes, like pH or temperature can have significant effects on the MSPD extraction yield. Two strategies can be considered for the elution of a MSPD packed cartridge: (1) direct elution of the analytes, using a solvent that does not release the interferences, or (2) considering a first clean-up step, selecting a solvent that does not elute the analytes, but eliminates the interferences (this extract is discarded), before recovering the analytes.

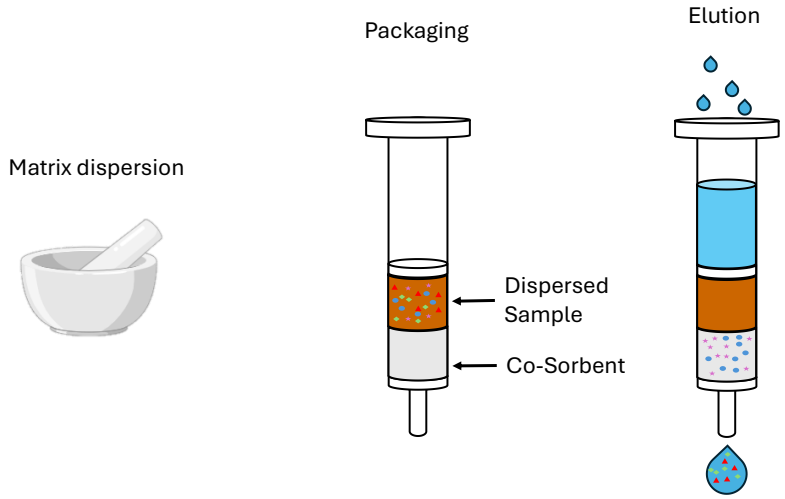


Figure 14: Scheme of a matrix solid phase dispersion extraction

During this Thesis, MSPD was applied to the selective extraction of basic analytes from complex sludge samples. To this end, the MSPD cartridge was on-line combined with a clean-up SCX cartridge. During elution of organic compounds contained in the sludge matrix, neutrals and acidic species flow through the cationic exchange sorbent to waste, whilst the basic, target drugs were retained in the second sorbent. After removing the upper cartridge, compounds were released from the SCX sorbent using a mixture of MeOH and ammonia [68][69][70].

USC
UNIVERSIDADE DE SANTIAGO DE COMPOSTELA

1.3.3 Pressurized liquid extraction

The pressurized liquid extraction (PLE), also known as accelerated solvent extraction (ASE), was first reported by Richter et al. in 1996 [71]. This technique uses solvents and mixtures of solvents at high temperatures, and high pressure, for the extraction of solid samples. The physical properties and polarity of the solvent, or mixtures of solvents, affect the efficiency of the extraction. The high temperatures during the extraction promote analyte desorption, by increasing their solubility and breaking the matrix-analyte interactions; on the other hand, the high pressures prevent the solvent from boiling. Both factors decrease the viscosity and surface tension of the solvent, promoting the extraction of the analytes from the matrix pores, while reducing the amount of solvent needed.

The parameters that affect PLE extraction are the type of matrix, the type of compound and the extraction mode used. There are two types of extraction modes in PLE: dynamic and static, both with their advantages and inconveniences [72]. In the dynamic mode, the extraction solvent is continuously pumped through the extraction cell, accelerating the diffusion rate, it is theoretically the most favourable for the complete extraction of the sample; however, a higher volume of solvent is used, resulting in the dilution of the final extract. Static mode is the one employed by most commercial instruments. In this case, the extraction cell is loaded with solvent and maintained at a selected temperature and pressure for a specific amount of time before being replaced by a fresh volume of solvent (flush volume) to repeat the process. Static mode allows the concentration of the sample while using a lower volume of solvent; however, the conditions in this mode need to be optimized to avoid the degradation of the analytes and undesirable chemical reactions. A scheme of the PLE system is shown in figure 15. The steps for the operation of the PLE instrument in static mode are as follows:

- Cell preparation: the sample is weighed and loaded into a stainless-steel cell, filling the extra space with an inert material and compressing them, closing both sides with frits to avoid sample loss.
- Sample loading: The instrument moves the cell into the oven and seals it under pressure (1500-3000 psi).
- Cell filling and sample heating: The instrument fills the cell and heats it to the specified temperature, maintaining it for some time to ensure the sample reaches the set temperature.
- Flushing with fresh solvent: The static valve opens and the extraction solvent flows into the collection vial as new solvent enters the cell. Multiple cycles can be performed if needed.
- Purge: The remaining solvent gets displaced into the collection vial using nitrogen as purge gas.
- End relief and unloading the cell: The pressure is released and the cell is taken out of the oven and back into the tray.

Even though most stages in this procedure are done automatically by the instrument, all the parameters, like temperature, pressure, solvent flow or equilibration time need to be optimized to ensure a quantitative extraction.

USC UNIVERSIDADE DE SANTIAGO DE COMPOSTELA

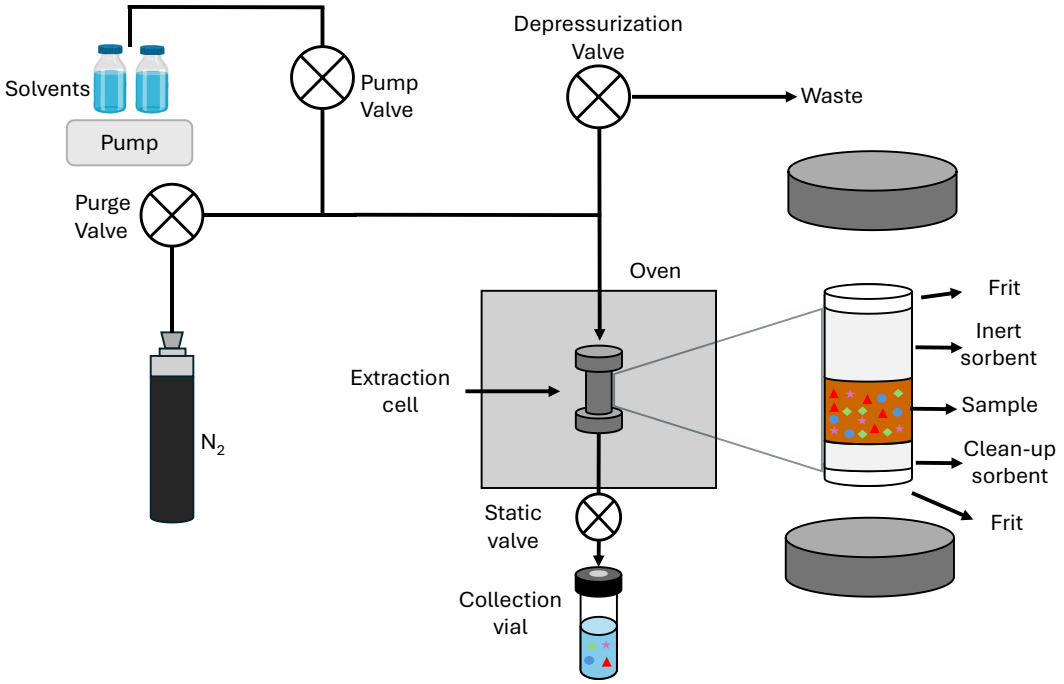


Figure 15: Scheme of a pressurized liquid extraction device.

1.3.4 Ultrasound assisted extraction

The ultrasound assisted extraction (UAE) is a sample preparation technique based on the use of ultrasonic waves combined with organic solvents to help analyte extraction in different matrices. Ultrasounds are mechanical waves with a frequency higher than the audible frequency range of human hearing (20 Hz to 20 kHz). These waves consist of a series of compression and rarefaction cycles and can be propagated through solid, liquid and gas mediums, and induce displacements and dislodgements of the molecules from their original positions. At high intensity sound waves, the negative pressure during rarefaction exceeds the attractive force that joins molecules together, pulling them apart and creating cavitation bubbles [73]. These bubbles have a larger area during the rarefaction cycle, which increases gas diffusion, causing the bubbles to enlarge. During compression, a critical point is reached where the energy provided is not enough to retain the vapor phase in the bubble, causing a rapid condensation and the release of high amounts of energy. The condensed bubbles then collide and create shockwaves that create high temperature and pressure regions (up to 5000 K and 50 MPa). Cavitation can produce micro-streams in the solvent which can enhance heat and mass transfer, creating spots that can accelerate the chemical reactivity in the medium. When these bubbles collide with a solid surface, the high pressure and temperature is released against said surface, which depending on the material, can cause a located erosion, pore formation or the penetration of the solvent into the sample material, promoting a better extraction of analytes that are found in the deeper layers of the sample [73] [74].

Ultrasonication can be done using ultrasound baths, ultrasound probes or cup-horn sono-reactors. Taking into account the complexity of the matrix, the number and size of the samples and the operating costs, ultrasound baths are the most widely employed ones due to their low

USC DE COMPOSTELA

cost, and the possibility of extracting multiple samples at the same time. Despite its advantages and wide usage, ultrasonic baths do not have a uniform energy distribution, which is solved by mapping the high cavitation regions, resulting in satisfactory relative standard deviation (RSD) values. In addition to the high analytical efficiency, UAE allows for the use of low amounts of both solvent and sample, and the possibility to replace or eliminate toxic or dangerous solvents, reducing the risk of the analysis and complying with several principles of the green analytical chemistry [17]

The parameters to optimize during UAE extractions include the sonication time, the solvent or mixture of solvents, the extraction temperature, the ultrasounds frequency and ultrasound power; since most UAE extraction methods have been developed using ultrasound baths, instead of more powerful equipment, these last two parameters could not be adjusted.

1.4 STUDIED COMPOUNDS

1.4.1 Volatile and semi-volatile organic compounds in indoor air

Air composition has been proven to have effects in human health. The gas phase in indoor air contains a wide range of both, volatile and semi-volatile compounds, that come from different sources, such as human activities, fragrance diffusers, household products and even building materials and furniture [75] [76]. Since indoor areas present low ventilation and volatile substances are more protected from photodegradation than their outdoors counterparts, this creates a very different composition between indoor and outdoor environments. Since many people spend most of their lives in indoor areas, being at home, at school or at work, it is impossible to avoid the inhalation of this mixture of compounds. When entering the respiratory system, the harm they can cause to human health ranges from allergic reactions, to asthma, including the sick-building syndrome [77]. Eventually, these compounds can be transferred between air and arterial blood at the lungs, causing even more damage.

Traditionally, the analysis of these volatile and semi-volatile compounds was done using gas chromatography as the gold standard for their determination. In addition, for their sensitive analysis, a previous sampling step is needed. The most common sampling methodologies for indoor air include active sampling, using a vacuum pump to capture the highest variety and amount of the analytes present in air in a solid sorbent; equilibrium techniques, based on diffusion of compounds from air to a solid sorbent; and lastly indirect approaches, analysing a substrate in contact with air [48] [47].

During this Thesis, water condensates obtained from a dehumidifier system were evaluated for their possibility to be used as a matrix for the indirect analysis of volatile and semi-volatile compounds present in indoor air. During the initial studies, the aim was to carry out a comprehensive non-target screening of the compounds present in water condensates, by comparing the GC-EI-TOF-MS accurate spectra with the low-resolution library NIST17, and a subsequent confirmation of suspect compounds using an in-house accurate spectra personal compound database library (PCDL), and the use of standards. Afterwards, a new PCDL containing all the confirmed substances and their linear retention indexes (LRI) was created.

During a second study, the possibility of air characterization using water condensates was studied. To that end, active air sampling was conducted at the same time as the indirect approach

USC DE COMPOSTELA

via water condensation. A first set of samples were used to calculate the air/water partition coefficients (K_{aw}) of selected compounds, which later allowed for the semiquantitative evaluation of their concentration in air samples from different locations.

1.4.2 Electronic cigarette refill characterization

Electronic cigarettes (e-cigs) were introduced in the United States, in 2007, as a healthier alternative to conventional tobacco cigarettes, limiting human exposure to harmful compounds generated during the combustion of tobacco, such as tar or polycyclic aromatic hydrocarbons (PAHs), while also being advertised as helpful for stopping tobacco addiction; nevertheless, considering their increase of usage and prevalence in recent years, this was not the case, as some studies point out, they instead serve as a gateway for non-smokers to start smoking [78]:

E-cigs are small devices, reminiscent of regular cigarettes that consist of an e-liquid storage, a power supply and a heater (which can be in direct contact with the e-liquid). During each puff, the power supply heats the e-liquid turning it into an aerosol containing the different flavours and other components of the e-liquid. If the heater is in direct or indirect contact with the e-liquid, some metal nanoparticles may get sorbed into the liquid, be transferred to the gas phase and enter the respiratory tract during vaping [79] [80]. Figure 16 shows a picture of the disassembled head (e-liquid reservoir containing the heating element) of a vaping device, in this case, the heater was in direct contact with the e-liquid.

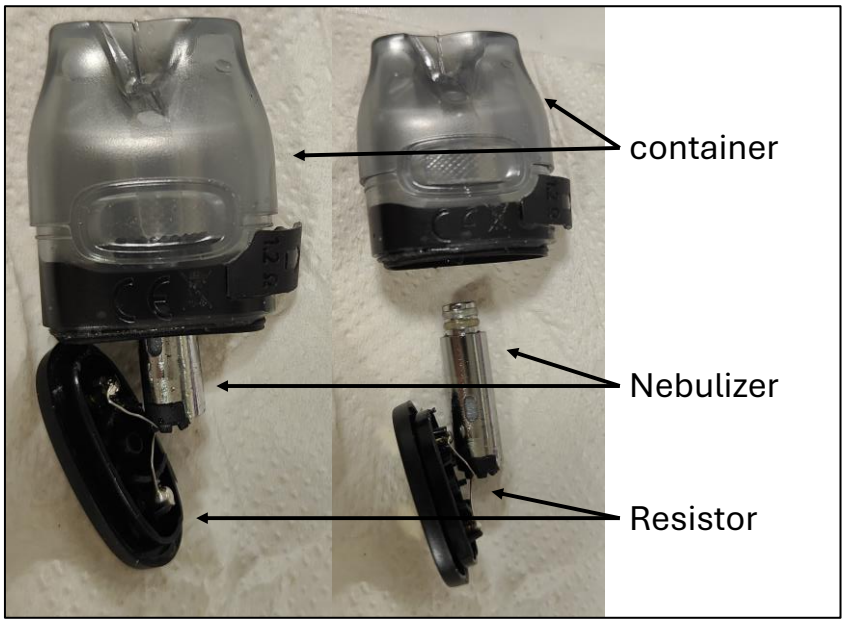


Figure 16: Disassembled e-cigarette head

Little is known about e-cig refill liquid (e-liquid) comprehensive composition, as the ingredients stated by the suppliers normally only include the solvents (ethylene glycol and vegetal glycerine), and a few high concentration allergens (i.e. limonene in lemon flavoured e-liquid), and some other major components of interest, such as nicotine or cannabidiol (CBD), which have their concentrations explicitly stated. In addition to these major components, the e-liquids are very complex mixtures of unknown substances from many different families, such

as fragrances, flavours, stabilizers, or additives that are considered safe for human ingestion by organisms like the Federal Drug Administration (FDA), but can be harmful, or at least irritants, to the respiratory tract. Understanding the composition of e-liquids can help us to better understand the possible impact they may have on human health, as well as their possible reactivity, and formation of harmful transformation products during the act of e-smoking. The source of the components included in the formulation of e-liquids can also affect the final composition and the complexity of these formulations. This statement applies to e-liquids containing nicotine or CBD, if these compounds are added from natural sources, some congeners (different alkaloids and terpenoids) also present in their natural source will also appear in the e-liquid, making their composition even more complex and potentially more harmful [81].

Previous studies of e-liquid composition normally consist of analysis of a selection of target compounds and their quantification in both the e-liquid, headspace vapor, as well as in the aerosol obtained by simulated smoking; these quantifications are normally done using a GC-MS equipment, usually a single Q mass analyser [82][83]. These methodologies do not allow for the obtention of HRMS spectra and thus, they are not suitable for the comprehensive, non-target screening and the full characterization of e-liquid composition.

During this Thesis, a non-target screening regarding several e-liquid composition was performed using a dilute-and-shoot approach, employing a GC-TOF-MS instrument. The non-target screening was performed using both a semi-polar and a polar column, with complementary selectivities, as a means to acquire the most comprehensive characterization possible. During this screening, two separate in-house libraries were created, each one including the accurate mass spectra, LRI, molecular formula and structure of the identified compounds for each of the columns. Since the GC-MS was operating at very high temperatures, confirmatory, additional experiments were conducted using LC-MS to verify the presence in the e-liquids of certain compounds, which might be artifacts formed in the hot injector of GC-MS instruments.

1.4.3 Emerging pollutants

Emerging pollutants (EPs) can be defined as “chemical substances that have been detected in the environment, but which are currently not included in the routine monitoring programs at the European level, however they should be considered as candidates for future regulations due to their (eco)toxicity, potential health effects and public perception” [84] according to the European Commission Network of Reference Laboratories and Related Organisations for Monitoring and Bio-monitoring of Emerging Environmental Pollutants (NORMAN).

These kinds of compounds have been reported worldwide in a large variety of matrices, such as soils, wastewaters, air or sediments. The number of publications reporting their concentrations was so vast that in 2015 the NORMAN network released a list of the most important based on the number of scientific publications for each. This list includes some pharmaceuticals, drugs of abuse, plasticisers, surfactants, enzymes and hormones, personal care products (PCPs), perfluoroalkyl substances (PFAS), flame retardants, some pesticides and some transformation products (TPs).

USC UNIVERSIDADE DE SANTIAGO DE COMPOSTELA

Due to their potential harmful effects and persistence after their release to the environment, this Thesis has also addressed the development and application of MS based methodologies aiming to understand the occurrence, the interaction of some selected pollutants with different matrices, and their dissipation and transformation routes under oxidative conditions. Moreover, development of direct analysis methods and quantitative LC-MS/MS approaches for some less studied EPs were also considered.

1.4.3.1 Pharmaceuticals

Pharmaceuticals are chemicals synthetised with the objective of treating different illnesses or reducing their symptoms, as such, they are designed to have high stability for their intended effects on humans; this may cause their incomplete degradation in WWTPs. They have been extremely beneficial helping extend human life expectancy and eradicating dangerous illnesses[85]; however, they also present some very important problems. Since they are intended for use against certain organisms or to treat certain injuries/symptoms, they have been thoroughly tested to be safe on humans, however their effects on non-target living beings are unknown [86], so they can cause serious problems to them due to unforeseen effects. Moreover, their transformation products can also be the ones released to the environment showing a higher ecotoxicity than the pharmaceutical itself [87].

The overuse, or environmental discharge, of certain pharmaceuticals, like bactericides can also result in the proliferation of bacteria resistance. Some bactericides, such as triclosan and chlorhexidine are used as additives in PCPs like mouth-wash or toothpastes, and are poorly degraded in WWTPs, so they remain in water and sludge after their treatments, potentially modifying the microbiome of soils, if treated wastewater and/or sludge are regarded for agricultural and/or gardening uses.

Since most pharmaceuticals are chiral compounds both their therapeutical and/or toxicological effects for target and non-target organisms vastly differ between enantiomers. As most pharmaceuticals are marketed as racemates, their metabolization rates and environmental degradability could be enantioselective processes. As a result, their enantiomeric fraction (EF) in environmental (i.e. wastewater and/or sludge) samples might be different than the one existing in their commercial formulations [88].

During this Thesis an enantioselective separation for a group of selected pharmaceuticals, that showed high occurrence in wastewater and sludge samples, was explored to ascertain the possible changes in the EF before and after wastewater treatment, and in treated sludge samples, compared to their commercial formulations. The analysed pharmaceuticals included a group of five antimycotics and three basic drugs, including a beta-blocker, an opioid and an antidepressant. To this end, SFC-MS was chosen as determination technique.

1.4.3.1.1 Tertiary treatments applied in wastewater treatment plants

The occurrence of organic pollutants, including conventional and EPs, and their TPs in water resources has been an important problem in recent years. These pollutants, either from natural or anthropogenic origin, belong to many different classes, such as pesticides, pharmaceuticals, PCPs or drugs of abuse to name a few. These substances pose a serious environmental problem, as their persistent nature (or pseudo-persistent due to their constant

USC UNIVERSIDADE

introduction into the environment) makes their presence ubiquitous in water and terrestrial matrices.

The treatment of wastewaters in WWTPs should help in getting rid of these pollutants; however, their main biological degradation process often fails to eliminate most EPs which are then discharged into surface water, one of the main sources of drinking water. As a result, high concentrations of EPs have been found even in tap water samples (i.e. imidacloprid and tebuconazole in the range between 0.7-20.68 ng/L and 0.66-21.61 ng/L respectively) [89] due to their incomplete elimination during treatment of wastewater and further in drinking water treatment plants (DWTPs) disinfection procedures.

In order to solve this problem, WWTPs have started to implement new technologies with the objective of obtaining higher quality effluents. To this end, oxidation processes, generally referred to as tertiary treatments, are implemented after the biological step, which transform organic pollutants into less complex compounds. The main types of tertiary treatments applied at WWTPs are free chlorine and UV-photolysis.

Advanced oxidation processes (AOPs) consist of the formation of highly reactive radicals that attack the organic pollutants. The high efficiency of AOPs is due to the formation of hydroxy radicals ($OH^{\bullet}$) which are non-selective, high energy oxidizing species capable of mineralizing organic pollutants forming CO_2, H_2O and inorganic ions as final products. Some of the most used AOPs include Fenton processes, direct photolysis, photolysis with the addition of hydrogen peroxide or free chlorine, ozonisation, etc. These processes can be categorised in photochemical and non-photochemical processes.

According to the International Union of Pure and Applied Chemistry (IUPAC), the photodegradation process is defined as the transformation of a molecule into smaller fragments, usually through an oxidation process. They can be classified into two groups depending on the different pathways they can take:

- Direct photolysis: Direct photolysis consists of the absorption of light by the pollutant, causing its degradation without the help of other compounds.
- Indirect photolysis: Light is absorbed by other substances, creating reactive radicals that produce the target degradation. In water environments, light irradiation can produce hydroxyl radicals capable of transforming the pollutant.

In this Thesis, a study to improve the selective degradation of the pharmaceutical tramadol was performed using a series of photodegradation based AOPs which will be described below. Tramadol was selected as model species for this study as it is ubiquitous in wastewater samples at concentrations around 900 ng/L, with an estimated removal of 4% in regular wastewater treatments [90] and is not degraded during conventional wastewater treatments [91][92].

- **Photolysis**

In every photolysis degradation, the most important factor is the compound ability to absorb radiation. For that reason, the most important photochemical processes use light, either UV or visible light, which is a selective reagent capable of producing chemical reactions, breaking the analyte bonds and forming simpler molecules. In this regard, the use of UV light for the disinfection of water has been successfully used for the last few decades [93].

USC UNIVERSIDADE DE SANTIAGO DE COMPOSTELA

Direct photolysis requires the use of light emitters, of which, the most used one is the low-pressure mercury lamp operating at 254 nm. In many cases, direct photolysis does not lead to the complete elimination of organic pollutants but to the formation of new substances called transformation products (TPs). In real samples with complex matrices, complementary reactions may happen during photolysis that can improve the removal of the organic pollutants. In these processes, light is absorbed by other substances that form TPs, or unstable intermediates, capable of reacting with the pollutants, leading to their degradation. In natural water samples, this is caused by the presence of dissolved organic matter (DOM)

- **UV/H_2O_2**

The combination of UV irradiation with an H_2O_2 leads to a more efficient and faster degradation of emerging pollutants in contaminated samples than just the use of UV light. This methodology is based on the formation of $HO^{\bullet}$ radicals during the H_2O_2 photolysis and the subsequent reactions (Eq 9-10):

$$H_2O_2 + h\upsilon \rightarrow 2HO^{\bullet}, Eq\ 9$$

$$HO^{\bullet} + organic\ compound \rightarrow Products, Eq\ 10$$

One of the main advantages of UV/ H_2O_2 is that H_2O_2 is commercially available and thermally stable.

- **Reactions with free chlorine**

Water chlorination is a method normally used for the disinfection and elimination of bacteria and harmful pathogens, as well as for the degradation of contaminants. This is usually the last step in the disinfection treatment, to eliminate contaminants and microorganisms that may have survived the other steps of the process.

The application of free chlorine to polluted samples renders two reactions: hydrolysis and dissociation.

$$Cl_2 + H_2O \rightarrow HClO + H^+ + Cl^-, Eq\ 11$$

$$HClO \leftrightarrow H^+ + ClO^-, Eq\ 12$$

Chlorine hydrolyses to hypochlorous acid (HClO) in the presence of water. The dissociation constant of HClO is K_{HClO}= 2.9*10^{-8} (pK_a=7.54 at 25 ºC). Thus, at the normal pH of natural waters (between 6 and 9), the main species present are hypochlorous acid and hypochlorite.

Disinfection of waters using free chlorine has been a matter of great concern in the last decades, because although it has many advantages, like its low cost and reactivity with organic pollutants and pharmaceuticals, leading to their degradation and mineralization, these treatments can also create by-products that can be more toxic than their precursor due to the possibility of the formation of halogenated compounds, which are known to show carcinogenic activities, such as trihalomethanes [94].

The chlorination process can also be combined with UV radiation to achieve better removal rates at a lower cost. In addition to hydroxyl radicals ($HO^{\cdot}$), the photodecomposition of free chlorine (eq. 13) generates a series of reactive chlorine species (RCS) with the chlorine radical ($Cl^{\cdot}$) being the most abundant one. Both radical species show high redox potential and present

complementary reactivity towards organic compounds, thus, it is expected that UV/chlorine treatment is more effective than UV/H_2O_2, which only produces $OH^{\cdot}$.

$$ClOH/ClO^- + UV\ (254\,nm) \rightarrow HO^{\cdot}/O^{\cdot -} + Cl^{\cdot}, Eq\ 13$$

During this Thesis, the efficiency for the removal of the pharmaceutical tramadol using direct photolysis, UV/H_2O_2 and UV/chlorine was compared at a laboratory scale. During the different degradation experiments, aliquots were taken at different times (stopping the reaction) to assess the kinetics of tramadol degradation. Moreover, a comprehensive assessment of the degradation products formed under different oxidative conditions was carried out. To this end, LC-QTOF-MS and GC-TOF-MS were employed as complementary techniques to screen the potential formation of non-volatile and volatile disinfection by-products, respectively.

1.4.3.2 Pesticides and plastic litter

Pesticides can be defined as any chemical used to repel, control or attack any organism that may hinder the correct development of plants, or animals. Pesticides can be classified in many different ways, according to their target organisms, mode of action, toxicity or chemical structure. Their categorization regarding their target organism is the most common one, it includes fungicides, herbicides, insecticides, rodenticides, biocides, acaricides and nematicides. According to their mode of action against target compounds, they can be classified as contact or systemic pesticides, depending on whether they only persist on the treated surface, or they reach the internal tissues of vegetables and crops.

Their classification according to their chemical structure is the most important from the analytical perspective, as compounds with similar structures tend to show similar behaviour regarding their extraction and determination conditions; some known chemical families include organophosphates, neonicotinoids, organochlorines, carbamates and azoles.

However, the World Health Organization (WHO) recommends the use of a pesticide acute toxicity as their classification criteria. According to this criterion, pesticides are classified in five different levels according to their estimated lethal dose LD50 (dose required to kill half of the tested animals when entering their body):

Ia – Extremely hazardous
Ib – Highly hazardous
II – Moderately hazardous
III – Slightly hazardous
U – Unlikely to present acute hazard

Pesticides have become a key component of modern-day, intensive agriculture. In recent times, pesticide use has seen an increment due to the increased food needs caused by population growth. Since the pesticide industry started around a century ago, most natural pesticides have been replaced by synthetic ones; in recent times, development strategy for new pesticides is focused on reducing the dosage, increasing their degradability and increasing their selectivity; all to reduce their potential impact in the environment and against non-target organisms.

Viticulture is a very important economic activity, with 80% of worldwide wine production centred around well-defined areas of nine countries [95]; this concentration of vineyards makes them especially susceptible to pests, particularly to fungi and insect transmitted diseases. In

USC DE COMPOSTELA

order to combat these threats, winegrowers make intensive use of pesticides, and particularly of fungicides and insecticides.

The use of plastics in agriculture has also become a common practice due to their positive effect in crop production and in the reduction of costs [96]; however, these plastics will degrade under environmental conditions, spreading smaller fragments to the agriculture field, which will end in the formation of micro and nano plastics. By themselves, plastic debris are already a hazard, since they can enter the food chain by accidental ingestion by soil invertebrates, wild and livestock animals, or they can migrate to surface or groundwater. In addition to these concerns, plastic debris are recognized as vectors of concerning pollutants, either used in their formulation or sorbed to them while in contact with crops.

While it is a well-known issue that microplastics can act as carriers for many different pollutants, most of these studies were centred around microplastics present in the aquatic medium [97][98] or focused on mulching plastics used in agriculture [99].

The studies in this Thesis were focused on the analysis of pesticides in two types of plastic items frequently used in viticulture: plant protection tubes (PPTs) and tying tapes (TTs), and comparing those results with the ones obtained from soils sampled from the same vineyards during the same period. Figure 17 shows a picture of plastic items and plastic litter noticed in many vineyards in the Northwest Spain. In this study, we employed a target LC-MS/MS method addressing the determination of a suite of fungicides and insecticides often found in wines and vineyard soils.



Figure 17: Aged plastic items and plastic debris found in vineyards.

USC UNIVERSIDADE DE SANTIAGO DE COMPOSTELA

REFERENCES

[1] D.A. Skoog, Fundamentals of analytical chemistry, 9th ed., Cengage learning, 2013.

[2] D.C. Harris, Quantitative Chemical Analysis, 7th ed., 2007. https://doi.org/10.1016/B978-0-444-40826-6.50009-1.

[3] E. de Hoffmann, V. Stroobant, Mass Spectrometry Principles and applications, 3rd editio, John Wiley & Sons Ltd, 2007.

[4] E.L. Schymanski, J. Jeon, R. Gulde, K. Fenner, M. Ruff, H.P. Singer, J. Hollender, Identifying small molecules via high resolution mass spectrometry: Communicating confidence, Environ. Sci. Technol. 48 (2014) 2097–2098. https://doi.org/10.1021/es5002105.

[5] M. Yamashita, J.B. Fenn, Electrospray ion source. Another variation on the free-jet theme, J. Phys. Chem. 88 (1984) 4451–4459. https://doi.org/10.1021/j150664a002.

[6] C. Moschet, B.M. Lew, S. Hasenbein, T. Anumol, T.M. Young, LC- and GC-QTOF-MS as Complementary Tools for a Comprehensive Micropollutant Analysis in Aquatic Systems, Environ. Sci. Technol. 51 (2017) 1553–1561. https://doi.org/10.1021/acs.est.6b05352.

[7] M.J. Martínez-Bueno, M.J. Gómez Ramos, A. Bauer, A.R. Fernández-Alba, An overview of non-targeted screening strategies based on high resolution accurate mass spectrometry for the identification of migrants coming from plastic food packaging materials, TrAC - Trends Anal. Chem. 110 (2019) 191–203. https://doi.org/10.1016/j.trac.2018.10.035.

[8] J.K. Chang, G. Teo, Y. Pewzner-Jung, D.J. Cuthbertson, A.H. Futerman, M.R. Wenk, H. Choi, F. Torta, Q-RAI data-independent acquisition for lipidomic quantitative profiling, Sci. Rep. 13 (2023) 1–15. https://doi.org/10.1038/s41598-023-46312-8.

[9] Massbank, (2006). https://massbank.eu/MassBank/Search (accessed June 11, 2024).

[10] mz cloud, (2013). https://www.mzcloud.org/ (accessed June 11, 2024).

[11] Metlin, (n.d.). https://metlin.scripps.edu/landing_page.php?pgcontent=mainPage (accessed June 11, 2024).

[12] J. Martín, W. Buchberger, J.L. Santos, E. Alonso, I. Aparicio, High-performance liquid chromatography quadrupole time-of-flight mass spectrometry method for the analysis of antidiabetic drugs in aqueous environmental samples, J. Chromatogr. B Anal. Technol. Biomed. Life Sci. 895–896 (2012) 94–101. https://doi.org/10.1016/j.jchromb.2012.03.023.

[13] J. Casado, I. Rodríguez, M. Ramil, R. Cela, Selective determination of antimycotic drugs in environmental water samples by mixed-mode solid-phase extraction and liquid chromatography quadrupole time-of-flight mass spectrometry, J. Chromatogr. A. 1339 (2014) 42–49. https://doi.org/10.1016/j.chroma.2014.02.087.

[14] J. Robles-Molina, F.J. Lara-Ortega, B. Gilbert-López, J.F. García-Reyes, A. Molina-Díaz, Multi-residue method for the determination of over 400 priority and emerging pollutants in water and wastewater by solid-phase extraction and liquid chromatography-time-of-flight mass spectrometry, J. Chromatogr. A. 1350 (2014) 30–43. https://doi.org/10.1016/j.chroma.2014.05.003.

[15] L. Colzani, C. Forni, L. Clerici, S. Barreca, P. Dellavedova, Determination of pollutants, antibiotics, and drugs in surface water in Italy as required by the third EU Water Framework Directive Watch List: method development, validation, and assessment, Environ. Sci. Pollut. Res. 31 (2024) 14791–14803. https://doi.org/10.1007/s11356-024-

USC DE COMPOSTELA

32025-6.
[16] R. López-Serna, M. Petrović, D. Barceló, Development of a fast instrumental method for the analysis of pharmaceuticals in environmental and wastewaters based on ultra high performance liquid chromatography (UHPLC)-tandem mass spectrometry (MS/MS), Chemosphere. 85 (2011) 1390–1399. https://doi.org/10.1016/j.chemosphere.2011.07.071.
[17] S. Santana-Viera, P.A. Lara-Martín, E. González-Mazo, High resolution mass spectrometry (HRMS) determination of drugs in wastewater and wastewater based epidemiology in Cadiz Bay (Spain), J. Environ. Manage. 341 (2023). https://doi.org/10.1016/j.jenvman.2023.118000.
[18] L.J. Zhou, G.G. Ying, S. Liu, J.L. Zhao, F. Chen, R.Q. Zhang, F.Q. Peng, Q.Q. Zhang, Simultaneous determination of human and veterinary antibiotics in various environmental matrices by rapid resolution liquid chromatography-electrospray ionization tandem mass spectrometry, J. Chromatogr. A. 1244 (2012) 123–138. https://doi.org/10.1016/j.chroma.2012.04.076.
[19] M. Di Carro, A. Lluveras-Tenorio, B. Benedetti, E. Magi, An innovative sampling approach combined with liquid chromatography–tandem mass spectrometry for the analysis of emerging pollutants in drinking water, J. Mass Spectrom. 55 (2020). https://doi.org/10.1002/jms.4608.
[20] I. Ferrer, E.M. Thurman, Analysis of 100 pharmaceuticals and their degradates in water samples by liquid chromatography/quadrupole time-of-flight mass spectrometry, J. Chromatogr. A. 1259 (2012) 148–157. https://doi.org/10.1016/j.chroma.2012.03.059.
[21] R. Rao Pasupuleti, Y.J. Ku, T.Y. Tsai, H.T. Hua, Y.C. Lin, J. Shiea, P.C. Huang, G. Andaluri, V.K. Ponnusamy, Novel fast pesticides extraction (FaPEx) strategy coupled with UHPLC-MS/MS for rapid monitoring of emerging pollutant fipronil and its metabolite in food and environmental samples, Environ. Res. 217 (2023) 114823. https://doi.org/10.1016/j.envres.2022.114823.
[22] C.L. Chitescu, E. Oosterink, J. De Jong, A.A.M. Stolker, Ultrasonic or accelerated solvent extraction followed by U-HPLC-high mass accuracy MS for screening of pharmaceuticals and fungicides in soil and plant samples, Talanta. 88 (2012) 653–662. https://doi.org/10.1016/j.talanta.2011.11.054.
[23] X. wei Wang, J. fu Liu, Y. guang Yin, Development of an ultra-high-performance liquid chromatography-tandem mass spectrometry method for high throughput determination of organophosphorus flame retardants in environmental water, J. Chromatogr. A. 1218 (2011) 6705–6711. https://doi.org/10.1016/j.chroma.2011.07.067.
[24] M. Köck-Schulmeyer, M. Olmos, M. López de Alda, D. Barceló, Development of a multiresidue method for analysis of pesticides in sediments based on isotope dilution and liquid chromatography-electrospray-tandem mass spectrometry, J. Chromatogr. A. 1305 (2013) 176–187. https://doi.org/10.1016/j.chroma.2013.07.036.
[25] P.A. Mourier, E. Eliot, M.H. Caude, R.H. Rosset, A.G. Tambute, Supercritical and Subcritical Fluid Chromatography on a Chiral Stationary Phase for the Resolution of Phosphine Oxide Enantiomers, Anal. Chem. 57 (1985) 2819–2823. https://doi.org/10.1021/ac00291a017.
[26] M. Hayes, K. Hettiarachchi, S. Lang, J. Wang, T.J. Greshock, Ultra-fast microscale purification of chiral racemates and achiral pharmaceuticals with analytical supercritical fluid chromatography, J. Chromatogr. A. 1665 (2022) 462829. https://doi.org/10.1016/j.chroma.2022.462829.
[27] C. Teng, Y. Li, T. Cang, H. Xu, Z. Liu, P. Qi, Z. Wang, H. Zhao, S. Di, X. Wang, Study

USC

on the enantioselective bioaccumulation and dissipation of uniconazole enantiomers in earthworm-soil microcosm through supercritical fluid chromatography-tandem mass spectrometry (SFC-MS/MS), Environ. Sci. Pollut. Res. 30 (2023) 29432–29441. https://doi.org/10.1007/s11356-022-24023-3.

[28] Y. Cheng, Y. Zheng, F. Dong, J. Li, Y. Zhang, S. Sun, N. Li, X. Cui, Y. Wang, X. Pan, W. Zhang, Stereoselective analysis & dissipation of propiconazole in wheat, grapes, & soil by supercritical fluid chromatography-tandem mass spectrometry, J. Agric. Food Chem. 65 (2017) 234–243. https://doi.org/10.1021/acs.jafc.6b04623.

[29] X. Pan, F. Dong, N. Liu, J. Xu, X. Liu, X. Wu, Y. Zheng, Development of RS-pyrisoxazole for reduction of pesticide inputs: A new insight from systemic evaluation of pyrisoxazole at the stereoisomeric level, J. Hazard. Mater. 407 (2021) 124359. https://doi.org/10.1016/j.jhazmat.2020.124359.

[30] D. Jiang, F. Dong, J. Xu, X. Liu, X. Wu, X. Pan, Y. Tao, R. Li, Y. Zheng, Enantioselective Separation and Dissipation of Prothioconazole and Its Major Metabolite Prothioconazole-desthio Enantiomers in Tomato, Cucumber, and Pepper, J. Agric. Food Chem. 67 (2019) 10174–10184. https://doi.org/10.1021/acs.jafc.9b03607.

[31] L. Pérez-Mayán, M. Ramil, R. Cela, I. Rodríguez, Supercritical fluid chromatography-mass spectrometric determination of chiral fungicides in viticulture-related samples, J. Chromatogr. A. 1644 (2021). https://doi.org/10.1016/j.chroma.2021.462124.

[32] Z. Chen, F. Dong, S. Li, Z. Zheng, Y. Xu, J. Xu, X. Liu, Y. Zheng, Response surface methodology for the enantioseparation of dinotefuran and its chiral metabolite in bee products and environmental samples by supercritical fluid chromatography/tandem mass spectrometry, J. Chromatogr. A. 1410 (2015) 181–189. https://doi.org/10.1016/j.chroma.2015.07.067.

[33] S. Di, T. Cang, Y. Li, L. Xu, P. Qi, Z. Wang, H. Zhao, Z. Liu, X. Wang, Stereoselective bioaccumulation and dissipation of four stereoisomers of cyproconazole in earthworm-soil microcosm, Sci. Total Environ. 907 (2024). https://doi.org/10.1016/j.scitotenv.2023.168111.

[34] Y. Tao, F. Dong, J. Xu, X. Liu, Y. Cheng, N. Liu, Z. Chen, Y. Zheng, Green and sensitive supercritical fluid chromatographic-tandem mass spectrometric method for the separation and determination of flutriafol enantiomers in vegetables, fruits, and soil, J. Agric. Food Chem. 62 (2014) 11457–11464. https://doi.org/10.1021/jf504324t.

[35] Y. Tao, Z. Zheng, Y. Yu, J. Xu, X. Liu, X. Wu, F. Dong, Y. Zheng, Supercritical fluid chromatography–tandem mass spectrometry-assisted methodology for rapid enantiomeric analysis of fenbuconazole and its chiral metabolites in fruits, vegetables, cereals, and soil, Food Chem. 241 (2018) 32–39. https://doi.org/10.1016/j.foodchem.2017.08.038.

[36] N. Liu, F. Dong, J. Xu, X. Liu, Z. Chen, Y. Tao, X. Pan, X. Chen, Y. Zheng, Stereoselective Determination of Tebuconazole in Water and Zebrafish by Supercritical Fluid Chromatography Tandem Mass Spectrometry, J. Agric. Food Chem. 63 (2015) 6297–6303. https://doi.org/10.1021/acs.jafc.5b02450.

[37] M. Garzotti, M. Hamdan, Supercritical fluid chromatography coupled to electrospray mass spectrometry: A powerful tool for the analysis of chiral mixtures, J. Chromatogr. B Anal. Technol. Biomed. Life Sci. 770 (2002) 53–61. https://doi.org/10.1016/S1570-0232(01)00582-7.

[38] J.C. Barreiro, M.E. Tiritan, Q.B. Cass, Challenges and innovations in chiral drugs in an environmental and bioanalysis perspective, TrAC - Trends Anal. Chem. 142 (2021) 116326. https://doi.org/10.1016/j.trac.2021.116326.

[39] I. Ilisz, A. Bajtai, I. Szatmári, F. Fülöp, W. Lindner, A. Péter, Enantioseparation of ß-carboline, tetrahydroisoquinoline and benzazepine analogues of pharmaceutical importance: Utilization of chiral stationary phases based on polysaccharides and sulfonic acid modified Cinchonaalkaloids in high-performance liquid and s, J. Chromatogr. A. 1615 (2020) 1–10. https://doi.org/10.1016/j.chroma.2019.460771.

[40] N. Ninyà, L. Vallecillos, R.M. Marcé, F. Borrull, Evaluation of air quality in indoor and outdoor environments: Impact of anti-COVID-19 measures, Sci. Total Environ. 836 (2022). https://doi.org/10.1016/j.scitotenv.2022.155611.

[41] C. Kaikiti, M. Stylianou, A. Agapiou, TD-GC/MS analysis of indoor air pollutants (VOCs, PM) in hair salons, Chemosphere. 294 (2022) 133691. https://doi.org/10.1016/j.chemosphere.2022.133691.

[42] A. Besis, T. Katsaros, C. Samara, Concentrations of volatile organic compounds in vehicular cabin air – Implications to commuter exposure, Environ. Pollut. 330 (2023) 121763. https://doi.org/10.1016/j.envpol.2023.121763.

[43] F. Salim, T. Górecki, Theory and modelling approaches to passive sampling, Environ. Sci. Process. Impacts. 21 (2019) 1618–1641. https://doi.org/10.1039/c9em00215d.

[44] T. Salthammer, Very volatile organic compounds: An understudied class of indoor air pollutants, Indoor Air. 26 (2016) 25–38. https://doi.org/10.1111/ina.12173.

[45] C. Décuq, M. Bourdat-Deschamps, P. Benoit, C. Bertrand, R. Benabdallah, B. Esnault, B. Durand, B. Loubet, C. Fritsch, C. Pelosi, S. Gaba, V. Bretagnolle, C. Bedos, A multiresidue analytical method on air and rainwater for assessing pesticide atmospheric contamination in untreated areas, Sci. Total Environ. 823 (2022). https://doi.org/10.1016/j.scitotenv.2022.153582.

[46] M.C. Pietrogrande, G. Demaria, M. Russo, Determination of particulate polycyclic aromatic hydrocarbons in ambient air by gas chromatography-mass spectrometry after molecularly imprinted polymer extraction, J. Environ. Sci. (China). 124 (2023) 644–654. https://doi.org/10.1016/j.jes.2021.11.021.

[47] E. Beristain-Montiel, R. Villalobos-Pietrini, G.E. Arias-Loaiza, S.L. Gómez-Arroyo, O. Amador-Muñoz, An innovative ultrasound assisted extraction micro-scale cell combined with gas chromatography/mass spectrometry in negative chemical ionization to determine persistent organic pollutants in air particulate matter, J. Chromatogr. A. 1477 (2016) 100–107. https://doi.org/10.1016/j.chroma.2016.11.043.

[48] L. Vallecillos, J. Riu, R.M. Marcé, F. Borrull, Air monitoring with passive samplers for volatile organic compounds in atmospheres close to petrochemical industrial areas. The case study of Tarragona (2019–2021), Atmos. Pollut. Res. 15 (2024). https://doi.org/10.1016/j.apr.2023.101986.

[49] R.B. Cody, J.A. Laramée, H.D. Durst, Versatile new ion source for the analysis of materials in open air under ambient conditions, Anal. Chem. 77 (2005) 2297–2302. https://doi.org/10.1021/ac050162j.

[50] S. Otles, V. Hazal Ozyurt, Direct Analysis in Real Time Mass Spectrometry, Ambient Mass Spectrosc. Tech. Food Environ. (2019) 95–104. https://doi.org/10.1201/9781315146836-5.

[51] R.W. Jones, R.B. Cody, J.F. McClelland, Differentiating writing inks using direct analysis in real time mass spectrometry, J. Forensic Sci. 51 (2006) 915–918. https://doi.org/10.1111/j.1556-4029.2006.00162.x.

[52] R.A. Musah, M.A. Domin, R.B. Cody, A.D. Lesiak, A. John Dane, J.R.E. Shepard, Direct analysis in real time mass spectrometry with collision-induced dissociation for structural analysis of synthetic cannabinoids, Rapid Commun. Mass Spectrom. 26 (2012)

USC UNIVERSIDADE DE SANTIAGO DE COMPOSTELA

2335–2342. https://doi.org/10.1002/rcm.6354.
[53] J.H. Gross, Direct analysis in real time-a critical review on DART-MS, Anal. Bioanal. Chem. 406 (2014) 63–80. https://doi.org/10.1007/s00216-013-7316-0.
[54] M. Haunschmidt, W. Buchberger, C.W. Klampfl, R. Hertsens, Identification and semi-quantitative analysis of parabens and UV filters in cosmetic products by direct-analysis-in-real-time mass spectrometry and gas chromatography with mass spectrometric detection, Anal. Methods. 3 (2011) 99–104. https://doi.org/10.1039/c0ay00588f.
[55] M. Haunschmidt, C.W. Klampfl, W. Buchberger, R. Hertsens, Determination of organic UV filters in water by stir bar sorptive extraction and direct analysis in real-time mass spectrometry, Anal. Bioanal. Chem. 397 (2010) 269–275. https://doi.org/10.1007/s00216-009-3438-9.
[56] M. Marinas, E. Sa, M.M. Rojas, M. Moalem, F.J. Urbano, C. Guillou, L. Rallo, A nuclear magnetic resonance (1 H and 13 C) and isotope ratio mass spectrometry (d 13 C , d 2 H and d 18 O) study of Andalusian olive oils, Rapid Commun. Mass Spectrom. 24 (2010) 1457–1466. https://doi.org/10.1002/rcm.
[57] M. Haunschmidt, C.W. Klampfl, W. Buchberger, R. Hertsens, Rapid identification of stabilisers in polypropylene using time-of-flight mass spectrometry and DART as ion source, Analyst. 135 (2010) 80–85. https://doi.org/10.1039/b911040b.
[58] G. Castro, I. Rodríguez, M. Ramil, R. Cela, Direct analysis in real time accurate mass spectrometry determination of bisphenol A in thermal printing paper, Talanta. 205 (2019) 120086. https://doi.org/10.1016/j.talanta.2019.06.086.
[59] J. Ji, J. Wang, Y. Zhang, Rapid screening of 23 synthetic cannabinoids in blood by direct analysis in real time - Tandem mass spectrometry, Int. J. Mass Spectrom. 469 (2021) 116667. https://doi.org/10.1016/j.ijms.2021.116667.
[60] R.A. Musah, M.A. Domin, M.A. Walling, J.R.E. Shepard, Rapid identification of synthetic cannabinoids in herbal samples via direct analysis in real time mass spectrometry, Rapid Commun. Mass Spectrom. 26 (2012) 1109–1114. https://doi.org/10.1002/rcm.6205.
[61] A.H. Grange, Semi-quantitative analysis of contaminants in soils by direct analysis in real time (DART) mass spectrometry, Rapid Commun. Mass Spectrom. 27 (2013) 305–318. https://doi.org/10.1002/rcm.6450.
[62] J. Wang, Q. Du, X. You, Y. Lv, W. Bi, H. Li, D.D.Y. Chen, Solvent-free high-throughput analysis of herbicides in environmental water, Anal. Chim. Acta. 1071 (2019) 8–16. https://doi.org/10.1016/j.aca.2019.04.024.
[63] W. Jing, Y. Zhou, J. Wang, Y. Zhu, Y. Lv, W. Bi, D.D.Y. Chen, Sorbent and solvent co-enhanced direct analysis in real time-mass spectrometry for high-throughput determination of trace pollutants in water, Talanta. 208 (2020) 1–9. https://doi.org/10.1016/j.talanta.2019.120378.
[64] T.J. Mason, H.M. Bettenhausen, J.M. Chaparro, M.E. Uchanski, J.E. Prenni, Evaluation of ambient mass spectrometry tools for assessing inherent postharvest pepper quality, Hortic. Res. 8 (2021). https://doi.org/10.1038/s41438-021-00596-x.
[65] C.F. Poole, New trends in solid-phase extraction, TrAC - Trends Anal. Chem. 22 (2003) 362–373. https://doi.org/10.1016/S0165-9936(03)00605-8.
[66] C.F. Poole, Core concepts and milestones in the development of solid-phase extraction, Elsevier Inc., 2020. https://doi.org/10.1016/B978-0-12-816906-3.00001-7.
[67] S.A. Barker, Matrix solid phase dispersion (MSPD), J. Biochem. Biophys. Methods. 70 (2007) 151–162. https://doi.org/10.1016/j.jbbm.2006.06.005.
[68] G. Castro, I. Carpinteiro, I. Rodríguez, R. Cela, Determination of cardiovascular drugs

in sewage sludge by matrix solid-phase dispersion and ultra-performance liquid chromatography tandem mass spectrometry, Anal. Bioanal. Chem. 410 (2018) 6807–6817. https://doi.org/10.1007/s00216-018-1268-3.

[69] J. Casado, G. Castro, I. Rodríguez, M. Ramil, R. Montes, R. Cela, Liquid chromatography quadrupole time-of-flight mass spectrometry identification and determination of tri- and hexaaryl chloro imidazoles in sewage sludge, J. Mass Spectrom. 52 (2017) 69–77. https://doi.org/10.1002/jms.3903.

[70] G. Castro, M. Roca, I. Rodríguez, M. Ramil, R. Cela, Identification and determination of chlorinated azoles in sludge using liquid chromatography quadrupole time-of-flight and triple quadrupole mass spectrometry platforms, J. Chromatogr. A. 1476 (2016) 69–76. https://doi.org/10.1016/j.chroma.2016.11.020.

[71] B.E. Richter, B.A. Jones, J.L. Ezzell, N.L. Porter, N. Avdalovic, C. Pohl, Accelerated solvent extraction: A technique for sample preparation, Anal. Chem. 68 (1996) 1033–1039. https://doi.org/10.1021/ac9508199.

[72] G. Alvarez-Rivera, M. Bueno, D. Ballesteros-Vivas, J.A. Mendiola, E. Ibañez, Pressurized liquid extraction, Liq. Extr. (2019) 375–398. https://doi.org/10.1016/B978-0-12-816911-7.00013-X.

[73] K. Kumar, S. Srivastav, V.S. Sharanagat, Ultrasound assisted extraction (UAE) of bioactive compounds from fruit and vegetable processing by-products: A review, Ultrason. Sonochem. 70 (2021) 105325. https://doi.org/10.1016/j.ultsonch.2020.105325.

[74] Y. Picó, Ultrasound-assisted extraction for food and environmental samples, TrAC - Trends Anal. Chem. 43 (2013) 84–99. https://doi.org/10.1016/j.trac.2012.12.005.

[75] A.L. Hodshire, E. Carter, J.M. Mattila, V. Ilacqua, J. Zambrana, J.P.D. Abbatt, A. Abeleira, C. Arata, P.F. Decarlo, A.H. Goldstein, L.H. Ruiz, M.E. Vance, C. Wang, D.K. Farmer, Detailed Investigation of the Contribution of Gas-Phase Air Contaminants to Exposure Risk during Indoor Activities, Environ. Sci. Technol. 56 (2022) 12148–12157. https://doi.org/10.1021/acs.est.2c01381.

[76] T. Salthammer, J. Gu, S. Wientzek, R. Harrington, S. Thomann, Measurement and evaluation of gaseous and particulate emissions from burning scented and unscented candles, Environ. Int. 155 (2021) 106590. https://doi.org/10.1016/j.envint.2021.106590.

[77] C. Veenaas, M. Ripszam, B. Glas, I. Liljelind, A.S. Claeson, P. Haglund, Differences in chemical composition of indoor air in rooms associated/not associated with building related symptoms, Sci. Total Environ. 720 (2020) 137444. https://doi.org/10.1016/j.scitotenv.2020.137444.

[78] X. Liu, A. Lugo, E. Davoli, G. Gorini, R. Pacifici, E. Fernández, S. Gallus, Electronic cigarettes in Italy: A tool for harm reduction or a gateway to smoking tobacco?, Tob. Control. 29 (2020) 148–152. https://doi.org/10.1136/tobaccocontrol-2018-054726.

[79] M. Williams, A. Villarreal, K. Bozhilov, S. Lin, P. Talbot, Metal and Silicate Particles Including Nanoparticles Are Present in Electronic Cigarette Cartomizer Fluid and Aerosol, PLoS One. 8 (2013) 1–11. https://doi.org/10.1371/journal.pone.0057987.

[80] M. Halstead, N. Gray, N. Gonzalez-Jimenez, M. Fresquez, L. Valentin-Blasini, C. Watson, R. Steven Pappas, Analysis of Toxic Metals in Electronic Cigarette Aerosols Using a Novel Trap Design, J. Anal. Toxicol. 44 (2019) 149–155. https://doi.org/10.1093/jat/bkz078.

[81] K.E. Farsalinos, I. Gene Gillman, M.S. Melvin, A.R. Paolantonio, W.J. Gardow, K.E. Humphries, S.E. Brown, K. Poulas, V. Voudris, Nicotine levels and presence of selected tobacco-derived toxins in tobacco flavoured electronic cigarette refill liquids, Int. J.

USC UNIVERSIDADE DE SANTIAGO DE COMPOSTELA

Environ. Res. Public Health. 12 (2015) 3439–3452. https://doi.org/10.3390/ijerph120403439.
[82] S. Barhdadi, B. Mertens, M. Van Bossuyt, J. Van De Maele, R. Anthonissen, M. Canfyn, P. Courselle, V. Rogiers, E. Deconinck, T. Vanhaecke, Identification of flavouring substances of genotoxic concern present in e-cigarette refills, Food Chem. Toxicol. 147 (2021) 111864. https://doi.org/10.1016/j.fct.2020.111864.
[83] C. Hutzler, M. Paschke, S. Kruschinski, F. Henkler, J. Hahn, A. Luch, Chemical hazards present in liquids and vapors of electronic cigarettes, Arch. Toxicol. 88 (2014) 1295–1308. https://doi.org/10.1007/s00204-014-1294-7.
[84] Norman, Emerging substances, (n.d.). https://www.norman-network.net/?q=node/19 (accessed May 22, 2024).
[85] E.Y. Guzel, F. Cevik, N. Daglioglu, Determination of pharmaceutical active compounds in Ceyhan River, Turkey: Seasonal, spatial variations and environmental risk assessment, Hum. Ecol. Risk Assess. 25 (2019) 1980–1995. https://doi.org/10.1080/10807039.2018.1479631.
[86] E.A. Asare, Status of pharmaceuticals in the Korle Lagoon and their toxicity to non-target organisms, Ecotoxicology. 31 (2022) 299–311. https://doi.org/10.1007/s10646-021-02507-1.
[87] M. Antonopoulou, I. Konstantinou, Photocatalytic degradation and mineralization of tramadol pharmaceutical in aqueous TiO2 suspensions: Evaluation of kinetics, mechanisms and ecotoxicity, Appl. Catal. A Gen. 515 (2016) 136–143. https://doi.org/10.1016/j.apcata.2016.02.005.
[88] Z. Wang, Q. Huang, Y. Yu, C. Wang, W. Ou, X. Peng, Stereoisomeric profiling of pharmaceuticals ibuprofen and iopromide in wastewater and river water, China, Environ. Geochem. Health. 35 (2013) 683–691. https://doi.org/10.1007/s10653-013-9551-x.
[89] Y. Cai, T. Tian, Y. Huang, H. Yao, X. Qi, J. Fan, Y. Kuang, J. Chen, X. Li, K. Kadokami, Occurrence and Health Risks of Organic Micropollutants in Tap Water in Dalian, Chem. Res. Toxicol. 36 (2023) 1938–1946. https://doi.org/10.1021/acs.chemrestox.3c00221.
[90] B. Petrie, J. Youdan, R. Barden, B. Kasprzyk-Hordern, Multi-residue analysis of 90 emerging contaminants in liquid and solid environmental matrices by ultra-high-performance liquid chromatography tandem mass spectrometry, J. Chromatogr. A. 1431 (2016) 64–78. https://doi.org/10.1016/j.chroma.2015.12.036.
[91] M. Etesam, H. Jalili, M. Barshan, M. Bahman, A. Amrane, E. Borhani Fard, Removal of pharmaceutical compounds (ranitidine, tramadol, and gabapentin) from wastewater by Trichormus variabilis microalgae, Biofuels, Bioprod. Biorefining. 18 (2024) 543–554. https://doi.org/10.1002/bbb.2581.
[92] R. Tanoue, L. Margiotta-Casaluci, B. Huerta, T.J. Runnalls, A. Eguchi, K. Nomiyama, T. Kunisue, S. Tanabe, J.P. Sumpter, Protecting the environment from psychoactive drugs: Problems for regulators illustrated by the possible effects of tramadol on fish behaviour, Sci. Total Environ. 664 (2019) 915–926. https://doi.org/10.1016/j.scitotenv.2019.02.090.
[93] M. Gmurek, M. Olak-Kucharczyk, S. Ledakowicz, Photochemical decomposition of endocrine disrupting compounds – A review, Chem. Eng. J. 310 (2017) 437–456. https://doi.org/10.1016/j.cej.2016.05.014.
[94] J.L. Acero, F.J. Benitez, F.J. Real, G. Roldan, E. Rodriguez, Chlorination and bromination kinetics of emerging contaminants in aqueous systems, Chem. Eng. J. 219 (2013) 43–50. https://doi.org/10.1016/j.cej.2012.12.067.
[95] Top Fifteen Wine-Producing Countries, (2024). https://italianwinecentral.com/top-

fifteen-wine-producing-countries/ (accessed May 22, 2024).

[96] F. Wang, J. Gao, W. Zhai, D. Liu, Z. Zhou, P. Wang, The influence of polyethylene microplastics on pesticide residue and degradation in the aquatic environment, J. Hazard. Mater. 394 (2020) 122517. https://doi.org/10.1016/j.jhazmat.2020.122517.

[97] E. Concha-Graña, C.M. Moscoso-Pérez, P. López-Mahía, S. Muniategui-Lorenzo, Adsorption of pesticides and personal care products on pristine and weathered microplastics in the marine environment. Comparison between bio-based and conventional plastics, Sci. Total Environ. 848 (2022). https://doi.org/10.1016/j.scitotenv.2022.157703.

[98] R. Elseblani, M. Cobo-Golpe, S. Godin, J. Jimenez-Lamana, M. Fakhri, I. Rodríguez, J. Szpunar, Study of metal and organic contaminants transported by microplastics in the Lebanese coastal environment using ICP MS, GC-MS, and LC-MS, Sci. Total Environ. 887 (2023). https://doi.org/10.1016/j.scitotenv.2023.164111.

[99] X. Bao, Y. Gu, L. Chen, Z. Wang, H. Pan, S. Huang, Z. Meng, X. Chen, Microplastics derived from plastic mulch films and their carrier function effect on the environmental risk of pesticides, Sci. Total Environ. 924 (2024) 171472. https://doi.org/10.1016/j.scitotenv.2024.171472.

[100] L. Pérez-Mayán, M. Ramil, R. Cela, I. Rodríguez, Multiresidue procedure to assess the occurrence and dissipation of fungicides and insecticides in vineyard soils from Northwest Spain, Chemosphere. 261 (2020). https://doi.org/10.1016/j.chemosphere.2020.127696.

[101] M. Cobo-Golpe, M. Ramil, R. Cela, I. Rodríguez, Portable dehumidifiers condensed water: A novel matrix for the screening of semi-volatile compounds in indoor air, Chemosphere. 251 (2020). https://doi.org/10.1016/j.chemosphere.2020.126346.

USC UNIVERSIDADE DE SANTIAGO DE COMPOSTELA

USC
UNIVERSIDADE
DE SANTIAGO
DE COMPOSTELA

2 JUSTIFICATION AND OBJECTIVES

In current times, the use of chemicals has become common place in almost every aspect of everyday life, from cooking seasonings and personal care products, to pharmaceuticals, fire-retardants and pesticides. This increased use of chemicals, although it has allowed a better and comfier lifestyle and greater health quality for humans, has been proven to also have its share of problems, in both human health and on the environment. For instance, some components present in furniture to protect them can become airborne and be inhaled by people and animals present in the building, or a given pesticide, designed for the protection of crops, can persist on the environment, cause harm for non-target organisms, or be transported to unexpected compartments.

As a result of this widespread use of potentially concerning chemicals, it becomes a necessity to understand their presence, prevalence and toxicity in environmental matrices, their potential pathways to enter the human body and their degradation pathways in wastewater treatment plants to avoid their discharge to the environment and/or their recirculation into drinking water sources, as well as the potential impact of their transformation products in living organisms. Analytical Chemistry plays a central role in assessing the distribution, interaction and transformation routes of these chemicals in different environments, from fluids (such as air, water masses, complex commercial mixtures) to solid environmental matrices, such as sludge, and man-made polymers. In summary, Analytical Chemistry provides the tools for the comprehensive study of the cycle of man-made chemicals in the media. Among these tools, mass spectrometry, combined with different separation techniques and sample preparation approaches, offers the possibility to investigate and to understand the above commented scenarios.

The main objective of this Thesis was the assessment of different mass spectrometry platforms (based on nominal resolution and accurate mass analysers), coupled to several ionization sources, and chromatographic separation techniques for the determination of pollutants and chemicals of interest in many different and complex matrices, including plastic litter and soil from agricultural fields, wastewater samples and sludge from sewage treatment plants, as well as complex fluids obtained from indoor air to commercial solutions, as e-cigarette refill liquids. Depending on the considered issue, quantitative target methods,

USC UNIVERSIDADE DE SANTIAGO DE COMPOSTELA

comprehensive screening approaches or enantiomeric determinations were developed and applied to analysis of a range of samples with different features. Thus, possibilities, and limitations, of mass spectrometry, to face real-life problems demanding high quality analytical information were thoroughly explored. Through the different phases of this PhD Thesis the following tasks were developed:

- Non-target screening analysis of volatile and semi-volatile compounds in gas and liquid samples, like indoor air and e-liquids, mainly derived from GC-QTOF-MS records, with the aid of LC-QqQ-MS as complementary technique for quantification of selected targets.
- Non-target screening studies based on complementary information offered by LC-QTOF-MS and GC-QTOF-MS applied to the comprehensive characterization of degradation routes of the emerging pollutant tramadol under different oxidative treatments intended to remove the compound from the aquatic environment.
- Assessment of the performance of supercritical fluid chromatography (SFC) followed by mass spectrometry for sensitive, multianalyte, enantiomeric analysis of a pre-selection of chiral emerging pollutants in wastewater related samples.
- Development of a range of target, quantitative methods focussed on the quantification of pre-selected compounds in different complexity matrices by using LC-QqQ-MS, direct ionization followed by QTOF-MS detection, and GC-QTOF-MS.

Apart from providing efficient analytical solutions to different relevant problems, a major aim of this PhD Thesis was to acquire a deep, practical knowledge and understanding of mass spectrometry to develop further activities within the private and/or the public sector.

USC
UNIVERSIDADE DE SANTIAGO DE COMPOSTELA

3 MATERIAL AND METHODS

In this doctoral Thesis, a variety of analytical methods and sample preparation processes were developed, validated and applied to samples of different natures. Each one of these methods was optimized, or adapted from previous studies, considering the particular features of the different combinations of analytes and matrices. The next paragraphs present a summary of the employed sample preparation methodologies and determination techniques.

Offline-SPE, using different sorbents, was employed when working with liquid samples, to extract and to concentrate selected analytes. Particularly, Mixed mode Cation eXchanger cartridges (MCX) were employed for selective extraction of basic compounds (pesticides and pharmaceuticals) from wastewater samples. Removal of neutrals and acidic species was achieved by rinsing the sorbent with methanol, before breaking electrostatic interactions between sorbent and analytes with methanol:ammonia. [13]. Thus, lower complexity extracts were obtained in comparison with non-selective sorbent elution and/or direct concentration of basic compounds using reversed-phase sorbents. Concentration of volatile and semi-volatile compounds present in water condensates originating for dehumidifiers, was carried out using a hydrophilic-hydrophobic balance reversed-phase (HLB). The same sorbent was also used to trap volatile compounds present in indoor air, the setup for the direct sampling of indoor air is shown in figure 18. The aim of this study was a comprehensive characterization of the organic composition of both matrices; thus, a non-selective sample concentration step was used. In both cases, compounds were recovered from the sorbent using ethyl acetate before analysis by GC-MS.

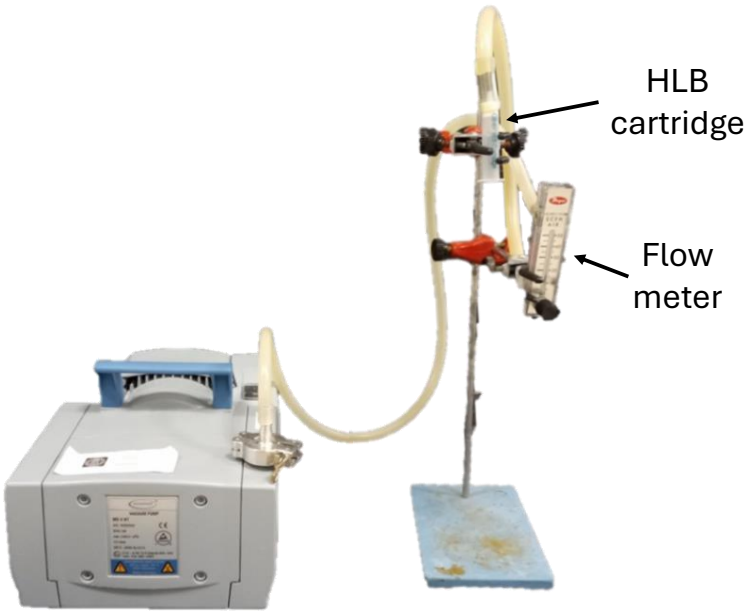


Figure 18: Setup used for direct sampling of indoor air

USC
UNIVERSIDADE
DE SANTIAGO
DE COMPOSTELA

For the determination of basic compounds in sludge samples, MSPD was the selected sample preparation process, using C_{18} as matrix dispersant. The extract was cleaned using a Strong Cation eXchanger, connected on-line to the MSPD syringe, using a procedure previously optimized in the research group. In brief, target analytes were separated from the rest of extracted compounds using the electrostatic interaction between basic groups in their structure and the anionic functionalities of the SCX sorbent, as shown in figure 19. For the extraction of pesticides from agricultural plastics, a non-selective ultrasound assisted extraction was developed, considering different combinations of organic solvents depending on the nature of the polymer, followed by concentration via nitrogen flow to improve the detection of said pesticides; for the extraction of soils related to these plastics, PLE conditions were also adopted from a previous study [100].

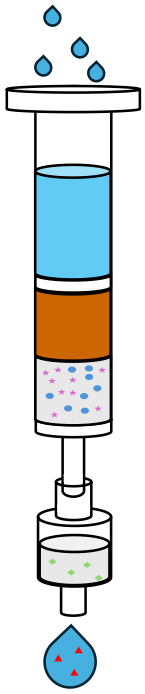


Figure 19: Scheme of the MSPD elution protocol followed during this PhD Thesis

A simple dilute-and-shoot approach was employed for the analysis of e-cigarette liquids. Finally, photodegradation experiments for the pharmaceutical Tramadol were performed in quartz tubes, using sodium hypochlorite and hydrogen peroxide as degradation starters (source of reactive radical species), with, or without, exposure to UV light from a mercury vapor lamp.

For the analytical determination of pesticides and the bactericide chlorhexidine, an LC system, able to operate with UPLC type columns, coupled to a QqQ mass spectrometer (Waters, XEVO, TQD) was used. The chromatographic separation was performed in reversed-phase UHPLC columns, either C_{18}-type columns, or C_{18}-polar ones, modified with positively charged groups, to prevent non-reversible sorption of strong basic compounds on free silanol groups existing in conventional C_{18} columns, the structure of this kind of column is shown in figure 20. Chiral determination of basic drugs was developed using an SFC system coupled to a QTOF mass spectrometer (Agilent, 6550 model), through a pre-back pressure regulator, split interface connected to the electrospray ionization source of the QTOF instrument. Fig 21 shows the configuration used in the present Thesis. Chiral analysis under SFC conditions was carried out

using polysaccharide type columns, containing different chiral selectors. The identification of tramadol transformation products was carried away using an LC system coupled to a QTOF mass spectrometer. A reversed-phase UHPLC column was used to separate the precursor tramadol from its TPs based on their different physicochemical properties. A targeted MSMS approach allowed the structural identification of these TPs.

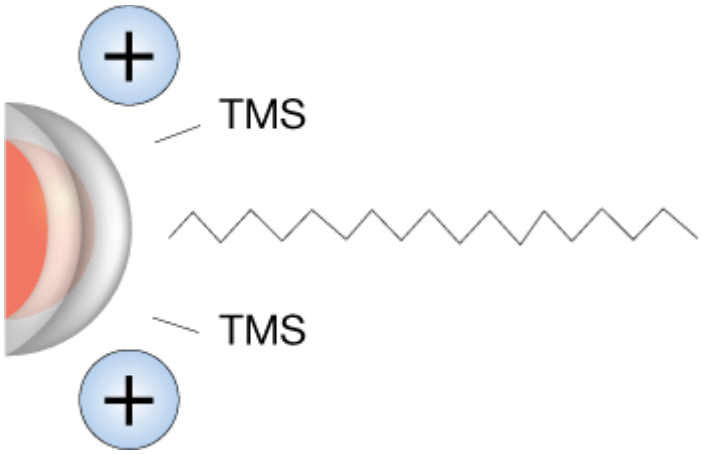


Figure 20: Structure of a polar C18 column. Phenomenex®

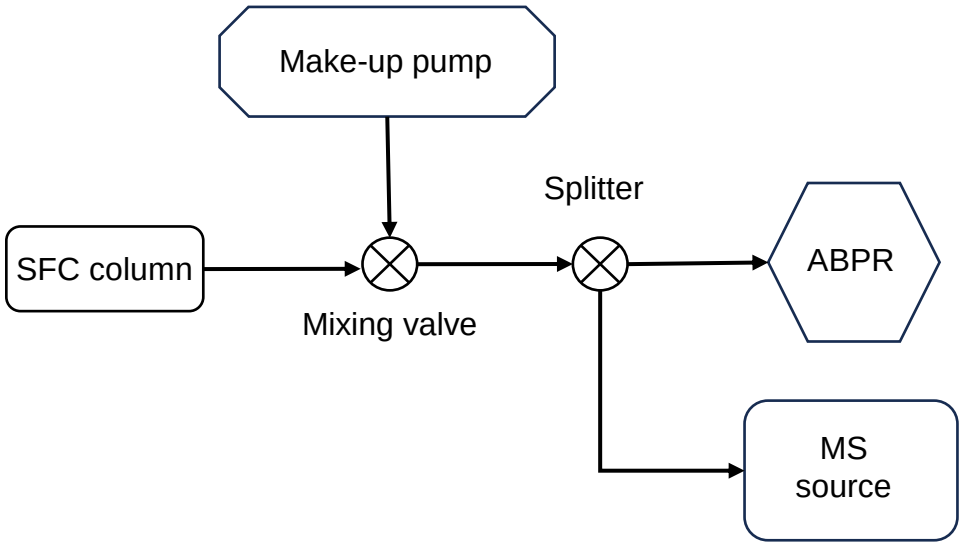


Figure 21: Scheme of the coupling between SFC and MS used during this Thesis

Extracts corresponding to active sampling of indoor air, water condensates obtained from dehumidifiers, and diluted e-liquid extracts were analyzed using a CG system coupled to a QTOF mass spectrometer (Agilent 7200). For the chromatographic analysis of these samples, both a polar (Carbowax type) and a semi-polar (BP-5 type) column were employed to ensure a more in-depth characterization. The anti-bacterial and fungicide triclosan was analyzed in multiple matrices using a DART source coupled to a QTOF mass spectrometer (Agilent, 6520 model). The DART source employed was equipped with a linear rail that was used to carry the two different kinds of sample holders tested in this Thesis: a *Quick Strip* transmission sample cards, with a 12-position frame of stainless steel and a *Dip It* with 12 positions for glass capillaries, both holders can be seen in figure 22. The interface between the two systems was a commercial Vapur interface, connected to a membrane vacuum pump, which permits to reduce

USC UNIVERSIDADE DE SANTIAGO DE COMPOSTELA

the entrance of helium and nitrogen into the high-vacuum region of the MS instrument, enhancing the sensitivity of the technique.

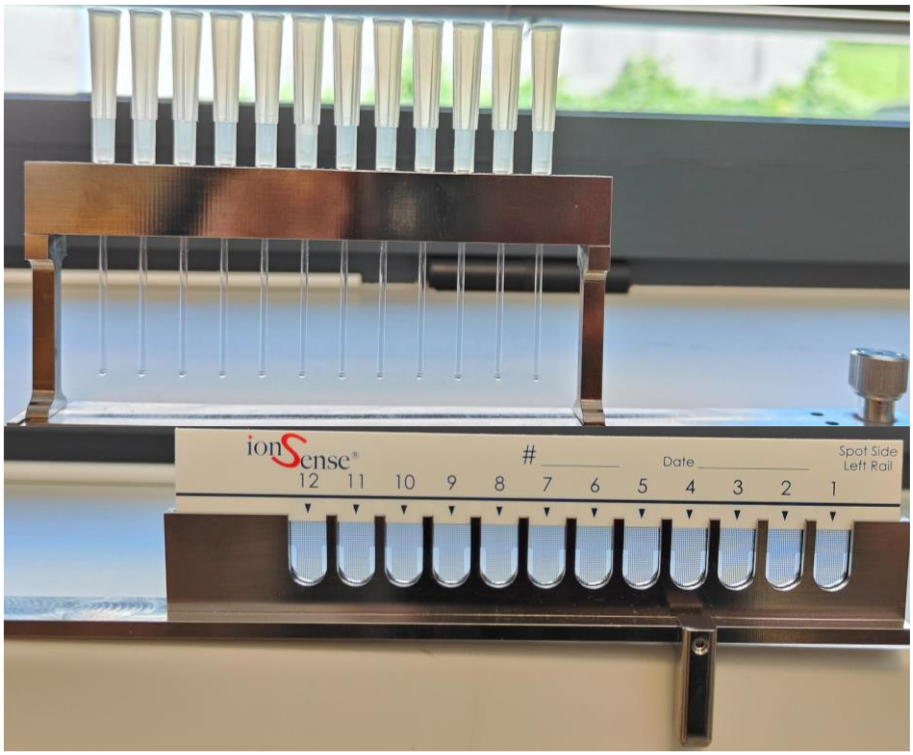


Figure 22: Sample holders for DART sources, 12 *Dip-it* (A) and *quick-strip* (B)

USC
UNIVERSIDADE DE SANTIAGO DE COMPOSTELA

4 RESULTS

CHAPTER 1. DEVELOPMENT OF NON-TARGET SCREENING METHODOLOGIES USING HIGH RESOLUTION MASS SPECTROMETRY FOR A COMPREHENSIVE CHARACTERIZATION OF ENVIRONMENTAL AND COMMERCIALLY AVAILABLE SAMPLES.

Throughout their entire life, humans are exposed to all kinds of substances existing in air (indoor or outdoor) via inhalation, as well as to man-made compounds present in drinking water due to their incomplete degradation in wastewater and drinking water treatment plants. Moreover, this exposure to unknown, and possibly harmful substances, can be voluntary, like in the case of e-cigarette vaping, whose composition remains mostly unknown, and as such, its potential medium-, and long-term effects in the health of consumers is difficult to predict.

In this chapter, different methodologies for the non-target screening characterization of several matrices, employing complementary chromatographic separation techniques, coupled to accurate mass spectrometry through electrospray (ESI), and electronic ionization (EI) sources were assessed. First, the characterization of air composition was carried out by simultaneous direct and indirect sampling of indoor spaces, using a vacuum pump connected to an activated sorbent, and a dehumidifier placed next to said pump, respectively. The sorbent was directly eluted with ethyl acetate and injected into the GC instrument while the condensed water was concentrated by solid-phase extraction using ethyl acetate as the elution solvent. Once GC-MS records were obtained, a spectral search was performed against the low resolution NIST17 database, after deconvolution of accurate EI-MS spectra. The workflow of the non-target screening performed in this study is shown in figure 22. Tentative identifications were later confirmed against standards and the spectra of confirmed substances were compiled in a personal library database, along with their linear retention indexes. Thereafter, in a second publication, the air/water constants of some of the most widely present compounds were calculated. Afterwards, these values were used to assess the suitability of condensed water analysis to predict concentrations of semi-volatile compounds in the vapor phase of indoor atmospheres. Said work describes the advantages and limitations of both approaches (direct and indirect sampling) to determine trace amounts of organic compounds in air from confined indoor environments.

USC UNIVERSIDADE DE SANTIAGO DE COMPOSTELA

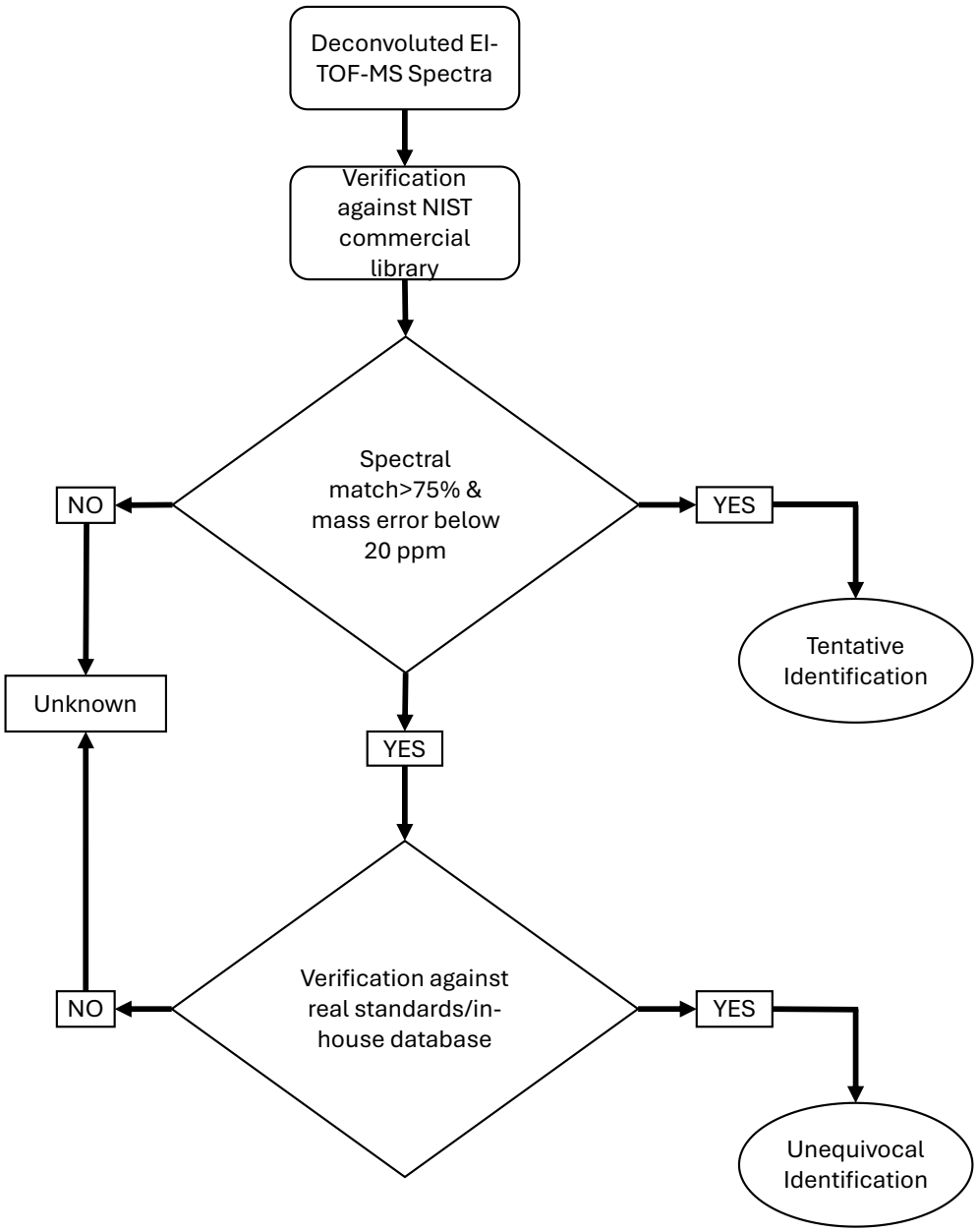


Figure 23: Workflow for compound identification followed in **Publication I**

For the characterization of e-liquids, samples were analysed using a dilute and shoot approach, this ensured that all the components of the liquids would be reflected in the corresponding GC-MS records. Given the differences among concentrations of volatile components of e-liquids, some of them might be hampered by large responses obtained for the base solvents employed in these formulations: propylene glycol and vegetal glycerine. To prevent this problem, a liquid-liquid extraction was evaluated as sample clean-up; however, even though the interferences due to base alcohols were avoided, a lot of information regarding volatile polar compounds was lost as a result; so, eventually, the dilute-and-shoot approach was preferred. To gain a bigger knowledge of e-liquid composition, a total of 39 samples were analysed using two columns with different polarity. The accurate EI-MS spectra of tentatively

identified, and confirmed, species were compiled in a database made accessible to the scientific community through Zenodo on-line repository (https://zenodo.org; doi: 10.5281/zenodo. 7738079). In addition, this research employed the complementary features of GC-EI-MS and LC-ESI-MS/MS to confirm some findings derived from GC-TOF-MS records, such as the existence of acetals in e-liquids. Also, the presence of delta-9-tetrahidrocannabinol in cannabidiol containing e-liquids, excluding the risk of data misinterpretation associated to potential reactions in the hot injector of the GC-TOF-MS instrument, was confirmed from complementary information provided by both techniques.

Finally, a non-target study of the degradation by-products of the pharmaceutical tramadol was developed. Several advanced oxidative processes were applied to spiked samples of ultrapure water, river water and wastewaters; these include UV photolysis, UV/H_2O_2 and UV/Free chlorine (figure 24). During these experiments, aliquots were taken at specific times, quenching the reactions with methanol. The different reaction time aliquots were directly injected in a liquid chromatograph coupled to a QTOF mass spectrometer to assess the efficiency of tramadol removal for each treatment, as well as to understand the transformation routes of the parent pharmaceutical under the different oxidative treatments. Transformation routes were inferred from identified TPs and their time-course evolution.

Identification of the TPs of tramadol was carried out following a two-step data acquisition strategy. First, reaction time aliquots were injected in the single LC-MS mode. Differences between records for control (zero time) and different reaction times experiments were used to identify potential TPs and to propose their empirical formula. Then, in a 2nd injection, product ion accurate spectra of pre-selected compounds were acquired and employed to propose their chemical structures. Information provided by LC-QTOF-MS spectra was completed with that obtained by GC-TOF-MS, using a non-target mode, for identification of volatile TPs related to degradation of tramadol. In this case, reaction time aliquots were extracted with pentane before GC-TOF-MS analysis.

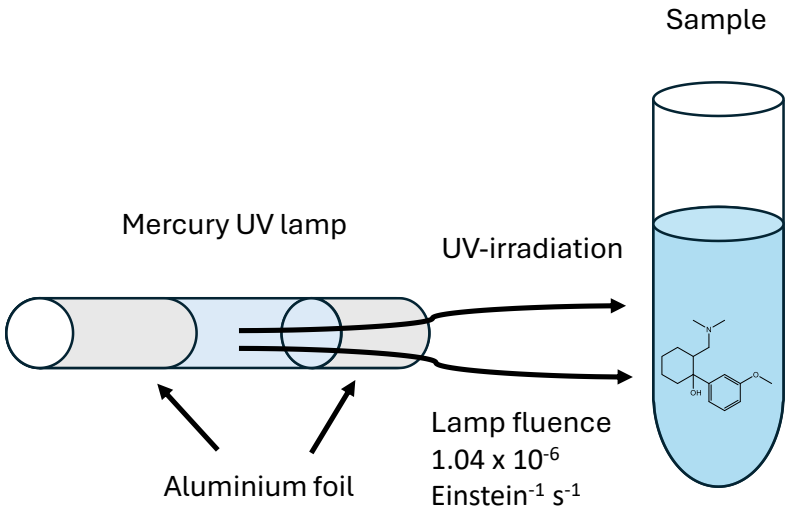


Figure 24: Set up of degradation experiments using *UV* radiation

The publications regarding these four works are shown in the following pages.

USC UNIVERSIDADE DE SANTIAGO DE COMPOSTELA

USC
UNIVERSIDADE
DE SANTIAGO
DE COMPOSTELA

PUBLICATION I: PORTABLE DEHUMIDIFIERS CONDENSED WATER: A NOVEL MATRIX FOR THE SCREENING OF SEMI-VOLATILE COMPOUNDS IN INDOOR AIR

M. Cobo-Golpe , M. Ramil , R. Cela , I. Rodríguez

Chemosphere 251 (2020) 126346
DOI: 10.1016/j.chemosphere.2020.126346



Impact factor: 7.086
Category: environmental sciences
Position: 30/274
Quartile: Q1

USC
UNIVERSIDADE DE SANTIAGO DE COMPOSTELA

Chemosphere 251 (2020) 126346

Contents lists available at ScienceDirect

Chemosphere

journal homepage: www.elsevier.com/locate/chemosphere

Portable dehumidifiers condensed water: A novel matrix for the screening of semi-volatile compounds in indoor air

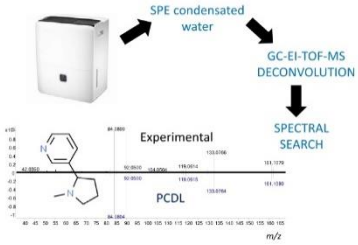
M. Cobo-Golpe , M. Ramil , R. Cela , I. Rodríguez *

Department of Analytical Chemistry, Nutrition and Food Sciences, Institute of Research on Chemical and Biological Analysis (IAQBUS), Universidade de Santiago de Compostela, 15782, Santiago de Compostela, Spain

HIGHLIGHTS

- Dehumidifier condensates contain qualitative information of indoor pollutants.
- Above 140 compounds identified following a non-target data mining approach.
- Variable condensate composition depending on the investigated environment.
- Acceptable repeatability between samples obtained with different dehumidifiers.
- Extraction efficiency correlated to Henry's law constant.

GRAPHICAL ABSTRACT



ARTICLE INFO

Article history:
Received 16 January 2020
Received in revised form
20 February 2020
Accepted 25 February 2020
Available online 25 February 2020

Handling Editor: Keith Maruya

Keywords:
Indoor air
Semi-volatile compounds
Dehumidifiers
Non-target screening
Gas chromatography accurate mass spectrometry

ABSTRACT

The comprehensive identification of organic species existing in indoor environments is a key issue to understand their impact in human health. This study proposes the analysis of condensed water samples, collected with portable dehumidifiers, to characterize semi-volatile compounds in the gas phase of confined areas. Water samples are concentrated by solid-phase extraction (SPE). The obtained extracts are analysed by gas chromatography (GC) time-of-flight mass spectrometry (TOF-MS), following a non-target screening data mining approach. In first term, spectra of deconvoluted compounds are compared with those in NIST low resolution library; thereafter, tentative identifications are verified using an in-house database of accurate electron ionization (EI) MS spectra. Chromatographic (retention index) and spectral data are combined for unambiguous species identification. The potential of condensed water samples to reflect changes in the composition of indoor atmospheres, the match between data obtained using different dehumidifiers, and the relative concentration efficiency of condensed water compared to that attained by active sampling of moderate air volumes are discussed. A total of 141 semi-volatile compounds were identified (98 confirmed against authentic standards) in a set of 21 samples obtained from different homes and working places. This list contains more than 40 fragrances (including several potential allergens), solvents and intermediates in the production of polymeric materials, plasticizers and flame retardants.

© 2020 Elsevier Ltd. All rights reserved.

1. Introduction

Indoor environments contain rich, complex mixtures of organic

* Corresponding author.
E-mail address: isaac.rodriguez@usc.es (I. Rodríguez).

https://doi.org/10.1016/j.chemosphere.2020.126346
0045-6535/© 2020 Elsevier Ltd. All rights reserved.

USC UNIVERSIDADE DE SANTIAGO DE COMPOSTELA

chemicals which have been correlated with allergies, respiratory and dermal diseases (Araki et al., 2018; Steinemann and Goodman, 2019). Some of these compounds have a natural (human) origin (Liu et al., 2017); however, most of them are related to building materials, upholstery, personal care and household products (Lamas et al., 2010; Lucattini et al., 2018), and even with life habits (i.e. smoking and consumption of illict drugs) (Cecinato et al., 2017; Pandey and Kim, 2010). In addition to parent compounds released from above sources, their degradation products might also impair the quality of air in indoor environments (Wakayama et al., 2019).

Compounds released in indoor areas are distributed between dust particles and the gas phase. Analysis of dust is useful to evaluate human exposure through accidental ingestion, whilst the identification of compounds existing in air is required to understand inhalation exposure (Geens et al., 2009). Dust samples are available from domestic vacuum cleaners; however, air sampling requires the use of dedicated gadgets. Active sampling devices employ a vacuum pump forcing a stream of air through a trapping unit, usually consisting of a filter followed by a sorbent (Laboire et al., 2016). Their concentration efficiency depends on the sampling time, the flow of air through the trapping unit (measured using a flowmeter or volumetric counter), and the retention efficiency of the sorbent. Low density sorbents, offering a low pressure drop, such as polyurethane foam (PUF), permit high flow rates of air for effective concentration of semi-volatile compounds (Melymuk et al., 2016). Carbonaceous materials, Amberlite polymers and Tenax display a high affinity for volatile compounds (Hoang et al., 2017). In this case, the flow rate of air through the sorbent and the sampled volume are reduced in comparison with protocols dealing with semi-volatile compounds. To compensate for a lower enrichment factor, trapped compounds are totally transferred to a gas chromatography (GC) instrument through thermal desorption of the sorbent (Ramírez et al., 2010). Passive sampling devices, such as semipermeable membranes filled with liquid or solid sorbents (Gale et al., 2009), microextraction techniques (Esteve-Turrillas et al., 2009) and PUF disks (Soheib and Harner, 2002) represent another option to investigate the presence of volatile compounds in confined atmospheres. In this approach, the uptake mass of a given compound depends on thermodynamic factors (affinity for the sorbent) and kinetic variables (diffusion rate from air to the active sorbent).

Portable dehumidifiers are appliances designed to reduce the concentration of water in air from interior environments. They incorporate a fan to create a stream of air, which passes first through a filter (to remove coarse particles), and then gets in contact with a cold region (usually the evaporator of a previously compressed cryogenic fluid), where water vapor condenses to be recovered in a draining tank. The high flow rate of air circulating through the dehumidifier, controlled by the turning speed of the fan, is expected to lead to a significant concentration of semi-volatile compounds in the condensed water. A previous study has described the presence of more than 40 compounds in condensed water obtained from the heater exchanger units of central air conditioning systems (Roll et al., 2015). Authors demonstrated the repeatability of chromatographic profiles for samples obtained from the same building in different dates; moreover, they showed how changes in daily activities affected the composition of water condensates (Roll et al., 2015). Unfortunately, central air conditioning facilities are not available everywhere, they do not provide information regarding the spatial distribution of organic compounds in different rooms from the same house, and the potential effect of each air conditioning facility in the composition of water condensates is not easy to evaluate.

The aim of this manuscript is to investigate comprehensively the range of organic compounds existing in condensed water samples obtained from portable dehumidifiers. To this end, samples were concentrated by solid-phase extraction (SPE). Thereafter, the SPE extracts were characterized by GC combined with accurate mass spectrometry (MS), based on a time-of-flight (TOF) instrument. Compounds identification was carried out by comparison of accurate electron ionization (EI) MS spectra of deconvoluted compounds with those included in the low resolution NIST database; followed by additional confirmation with an in-house database (personal compound database library, PCDL) of suspected targets (Castro et al., 2019; Gómez-Ramos et al., 2019). Concordance of results obtained using different dehumidifiers, placed in the same room, and major changes in the composition of drained water depending on the sampling place are reported. In addition, the concentration efficiencies attained using portable dehumidifiers and active sampling, of moderate air volumes, are compared and correlated with the properties of identified compounds.

2. Material and methods

2.1. Solvents, standards and sorbents

Ethyl acetate (AcOEt) (trace analysis grade) and methanol (MeOH) (LC gradient quality) were obtained from Merck (Darmstadt, Germany). Standards of compounds employed in the current study were provided by Sigma Aldrich (St. Louis, MO, USA), Riedel de Häen (Seelze, Germany) and Restek (Bellefonte, PA, USA). Compounds were acquired either as individual species, or as technical mixtures (case of some fragrances and other ingredients of personal care products). Stock solutions of each substance were prepared in MeOH. Further dilutions and mixtures were made in AcOEt. The concentrations of standards employed to build the PCDL of accurate EI-MS spectra were in the range from 0.5 to 2 $\mu g\ mL^{-1}$. A standard mixture of n-alkanes (C_8–C_{40}) in dichloromethane was provided by Supelco (Bellefonte, PA, USA). This solution was used to calculate the linear retention index (LRI) of compounds in chromatograms of sample extracts and those for standards included in the PCDL. LRI and accurate EI-MS spectra were employed for confirmation of tentative identifications derived from search of deconvoluted experimental spectra in the NIST database. PCB-30 (2,4,6-trichloro biphenyl) was used as injection standard, added to SPE extracts before GC-MS analysis.

OASIS HLB (200 mg) cartridges were purchased from Waters. This polymer was employed for the concentration of condensed water, and also as trapping sorbent for active air sampling. Dehumidifiers employed to obtain water samples from different indoor areas were purchased in local markets. They were furnished with a cryogenic fluid evaporator where water vapor condensates. A grid in the back side of these appliances served as a filter to limit the entrance of coarse particles into the evaporator unit. In some experiments, the grid was covered with glass fibre filters (GFF), pore size of 0.7 μm, provided by Sigma-Aldrich.

The membrane pump employed for active sampling of indoor air was purchased from Vaccubrand (model MD 4NT). It was connected to an HLB cartridge, followed by a rotameter. Air was sampled at a flow rate of 16.5 $L\ min^{-1}$, similar to values considered in previous studies dealing with determination of fragrances (10 $L\ min^{-1}$) (Lamas et al., 2010) and other semi-volatile compounds from indoor air (12 $L\ min^{-1}$) (Laboire et al., 2016). Unless otherwise stated, the pump was operated 5 h to concentrate 5 m^3 of air.

2.2. Samples and sample preparation

Dehumidifiers were placed in several indoor environments, including private houses and working places. After a given

USC UNIVERSIDADE DE SANTIAGO DE COMPOSTELA

MIGUEL COBO GOLPE

sampling time (5–12 h) condensed water samples were transferred to glass vessels, transported to the laboratory and stored at 4 °C, for a maximum of 24 h, before SPE extraction. Table 1 summarizes some data regarding the sampling places, and the codes assigned to the obtained samples. In brief, samples were taken in 10 different homes, two administrative buildings, a hair dressing in a shopping centre, and the research laboratory where SPE extractions were carried out. Additional information, including temperature and relative air humidity at the beginning of the sampling step, and the collected water volume are provided as supplementary material, Table S1.

Field blanks were prepared filling the drain vessel of dehumidifiers with ultrapure water. After a contact time of 12 h, water was concentrated by SPE. Another set of blanks corresponded to SPE of ultrapure water without contact with dehumidifiers.

Water samples (300 mL) were concentrated using HLB cartridges previously conditioned with AcOEt, MeOH and ultrapure water (2 mL each). Following the concentration step, the sorbent was rinsed with 5 mL of ultrapure water, dried using a gentle stream of nitrogen and eluted with 2 mL of AcOEt. This extract was fortified with PCB-30 as injection standard, at 1000 ng mL^{-1}, to check the stability in the responses of the GC-MS system. Potential breakthrough problems were investigated by passing the water sample (300 mL) through two cartridges connected in series. After the concentration step, they were disconnected and eluted separately.

HLB cartridges employed in active sampling experiments were conditioned with AcOEt (2 mL). Thereafter, they were dried and wrapped in aluminium foil. During active air sampling experiments, the open edge of the cartridge was faced to floor (floor distance was 0.5 m, similar to that existing in the air entrance of dehumidifiers) to prevent direct deposition of particulate matter on the frit above the sorbent. Breakthrough studies were carried out by spiking a standard mixture of fragrances, with different volatilities, in a plug of glass wool placed inside the barrel of the SPE cartridge, above the sorbent. In these experiments, a 2nd cartridge was connected in series. After sampling a given volume of air, cartridges were eluted separately with 2 mL of ethyl acetate. The plug of glass wool was sonicated with the same volume of solvent for 5 min. In order to compare the range of compounds concentrated using active sampling and dehumidifiers, both systems were simultaneously operated in the same room.

2.3. GC-MS system and data analysis

Identification of compounds in indoor air related extracts was performed with a GC-QTOF-MS instrument, obtained from Agilent (Wilmington, DE, USA). The system was comprised of a 7890A gas chromatograph connected to a 7200 QTOF MS spectrometer, which was furnished with an EI source. The TOF was operated in the 2 GHz mode, offering typical mass resolution values (FWHM) of 6500 at *m/z* 131. The GC-QTOF-MS system was employed in the single MS mode, that is, as a GC-TOF-MS instrument. MS spectra were obtained at 2.5 Hz (5430 scans accumulated per spectrum) in the range of *m/z* values from 40 to 600. The *m/z* axis in the mass analyser was automatically recalibrated, every 3 injections, by infusion of perfluorotributyl amine (PFTBA) in the EI source.

Two different columns were tested for the separation of compounds exiting in SPE extracts. They were a BP-5 MS (30 m × 0.25 mm i.d., 0.25 μm film thickness) and a DB-WAXETR one (30 m × 0.25 mm i.d., 0.5 μm film thickness). Both were acquired from Agilent. The carrier gas (Helium) flow rate was 1.2 mL min^{-1}. Standards and sample extracts (2 μL) were injected in the splitless mode, with the injector maintained at 260 °C. The splitless time and the split flow were 1 min and 50 mL min^{-1}, respectively. The quadrupole and the EI source temperatures were 150 °C and 230 °C, respectively. Two different oven temperature programs were employed. For the BP-5 column the gradient was 50 °C (1 min), rated at 10 °C min^{-1} to 290 °C (15 min). When using the DB-WAXETR one, temperature varied as follows: 60 °C (1 min), 1st rate at 5 °C min^{-1} to 220 °C, 2nd rate at 20 °C min^{-1} to 240 °C (15 min). The temperature of the transfer line between the GC and the MS spectrometer was the same as the upper value employed with each column.

The *MassHunter* software was used to control the acquisition parameters in the GC-QTOF-MS system and to process the obtained data. *MassHunter Qualitative* software (version B.08.00) was employed during inspection of raw GC-TOF-MS chromatograms, to

Table 1
Codes of dehumidifier water samples, indicating the sampling place and the identities of the three most intense peaks in the GC-EI-TOF-MS chromatograms for their SPE extracts.

Sample code	Sampling Place	Room	1st most intense peak	2nd most intense peak	3rd most intense peak
S1	Home 1	Laundry	Diethylene glycol butyl ether	Texanol	TXIB
S2	Home 1	Bedroom	Diethylene glycol butyl ether	Texanol	TXIB
S3	Home 1	Living room	Diethylene glycol butyl ether	Texanol	TXIB
S4	Home 1	Kitchen	Alfa-Terpineol	Diethylene glycol butyl ether	Texanol
S5	Home 2	Entrance	Nonanoic acid	Diisobutyl phthalate	2-Phenoxyethanol
S6	Home 3	Living room	Diisobutyl phthalate	Diethyl phthalate	Nonanoic acid
S7	Home 4	Living room	TCPP	Nonanoic acid	Diethylene glycol butyl ether
S8	Home 4	Office	Diethylene glycol butyl ether	TCPP	Hexanoic acid
S9	Home 5	Living room	2-Phenoxyethanol	Diethyl phthalate	Diethylene glycol butyl ether
S10	Home 6	Living room	Nicotine	Methyl Dihydrojasmonate	Dodecanoic acid
S11	Home 7	Laundry	Linalool	4,7-Methano-1H-indenol, hexahydro-	2-Phenoxyethanol
S12	Shopping centre	Hair dressing	2-Phenoxyethanol	Methyl Dihydrojasmonate	Dodecanoic acid
S13	Home 8	Living room	[a]Glycol	[a]Glycol	Nonanoic acid
S14	Administrative building 1	Reception area	Texanol	TXIB	Diethyl phthalate
S15	Administrative building 2	Office	Diethyl phthalate	Nonanoic acid	Diisobutyl phthtalate
S16	Administrative building 1	Office	Benzyl alcohol	2-Phenoxyethanol	Texanol
S17	Home 1	Garage	Benzothiazole	TXIB	Texanol
S18	Home 9	Garage	Benzothiazole	2-phenoxyl ethanol	[a]Glycol
S19	Home 10	Living room	2-Phenoxyethanol	Methyl Dihydrojasmonate	Diethyl phthalate
S20	Research building	Sample peparation laboratory	Nonanoic acid	Diisobutyl phthalate	Diethyl phthalate
S21	Home 11	Living room	Texanol	Diethyl phthalate	Nonanoic acid

[a] The exact congener of the glycol series was not identified.

USC UNIVERSIDADE DE SANTIAGO DE COMPOSTELA

extract the accurate EI-MS spectra of standards and to transfer these spectra to a customized PCDL. In addition to accurate spectra, the PCDL database included LRI values.

Deconvolution of chromatograms obtained for indoor air related samples was carried out using the *Unknowns Analysis* (UA) function (based on the *SureMass* algorithm), integrated in the *MassHunter Quantitative* software (version B.08.00). Responses of deconvoluted species (peak areas corrected with that obtained for PCB30) were employed to evaluate the severity of contamination problems in procedural blanks, to compare the relative efficiencies of active air sampling versus concentrated dehumidifier water samples, to investigate the responses obtained for a given compound depending on the sampling place, and to evaluate the agreement between data obtained with different dehumidifiers.

The *MS Search (v. 2.3)* software was used to manage the spectra compiled in the NIST17 low resolution EI-MS library, and to calculate the theoretical *m/z* ratios of fragment ions with known structures, using the NIST-MS interpreter tool, in this database.

The workflow for the non-target identification of pollutants in sample extracts has been described in detail in a previous publication (Castro et al., 2019). In brief, it involves deconvolution of raw GC-TOF-MS chromatograms, followed by spectral comparison with the low resolution NIST17 and the accurate PCDL libraries. The 2nd database was updated continuously, taking into account tentative identifications derived from comparison with the NIST database. A scheme of the employed workflow is provided as supplementary information, Fig. S1. Currently, the created PCDL contains 265 inputs of volatile and semi-volatile species.

3. Results and discussion

3.1. Preliminary experiments

A typical chromatogram obtained with the DB-WAXETR column for dehumidifier condensed water is provided as supplementary information, Fig. S2A. One of the latter, intense eluting peaks corresponded to dibutyl phthalate (DBP). Less volatile species, such as di-(ethylhexyl) phthalate, tri-(butoxyethyl) phosphate, octocrylene and certain dyes (such as indigo), which are recognized as ubiquitous in dust from indoor areas (Castro et al., 2019; Fromme et al., 2004) were absent in this chromatogram. In order to verify that these less volatile compounds did not remain inside the employed column, the same extract was injected in the BP5-MS column, using a faster gradient and also a higher final temperature (290 °C versus 240 °C in the DB-WAXETR). DBP was again the latter intense peak in the BP-5 chromatogram, Fig. S2B. Thus, either less volatile species are mostly associated to indoor particles instead of to the gas phase (Weschler and Nazaroff, 2014), or they are not concentrated in condensed water samples. So, the more retentive and higher selectivity Carbowax-type column was selected for the rest of the study.

As regards SPE of dehumidifier water, considering a sample volume of 300 mL, rich chromatographic records (Fig. S2) were obtained without noticing breakthrough problems during the concentration step, just traces of some carboxylic acids were found in the security SPE cartridge (their peak areas represented between 1 and 2% of those observed in the extract from the first cartridge, figure not shown). Condensed water samples were concentrated without previous filtration to minimize the risk of losing any compound recovered from the indoor atmospheres. AcOEt was used for the elution of SPE cartridges considering its medium polarity and compatibility with GC-MS analysis. A volume of 2 mL was enough to recover species retained in the SPE sorbent.

The coarse grid of dehumidifiers might lead to the presence of dust particles in the drained water. Consequently, compounds in SPE extracts might correspond to species existing in the vapor phase, but also to those solubilised from dust particles. To investigate this possibility some experiments were carried out fitting a GFF filter behind the coarse grid of the dehumidifier. After operating the system for 48 h, filters were sonicated with ethyl acetate and the extract concentrated to 2 mL. The corresponding chromatograms were similar to those obtained for blank filters. Moreover, no significant peaks were noticed in the filter extract compared to those in the chromatogram of condensed water (Fig. S3). So, the stream of air created by the fan of the dehumidifier does not introduce particulate matter with a size larger than the cut-off of the filter (0.7 μm) in the cooling unit of the system.

Efficiency of the HLB polymer to trap volatile compounds during active sampling (16.5 L min^{-1}) of indoor air was investigated with a mixture of 16 terpenes with different volatilities (their chromatographic retention times varied from 7.81 min for limonene to 30.54 min for carvacrol, see Table S2). Experiments were performed as described in section 2.2. After sampling 5 m^3 of air, the extracted ion chromatograms (EIC), mass window 2 mDa, for their more representative ions (Table S2) corresponding to the glass wool plug, the retention and the security HLB cartridges were compared. Compounds were noticed only in the extract from the retention cartridge.

3.2. Database of accurate EI-MS spectra

Mass accuracy of the GC-EI-TOF-MS system employed in this study (first generation of Agilent TOF combined with GC) was in the range of 0.002 Da, equivalent to relative mass errors from 20 to 6.7 ppm for ions with *m/z* ratios in the range from 100 to 300. Although these errors have been lowered by 2nd generation TOF instruments (Stupak et al., 2018), and particularly by Orbitrap mass analyser (Gómez-Ramos et al., 2019), they sufficed to discriminate between ions with different empirical formula (considering C,H,O and N as their elements) and same nominal *m/z* values.

During non-target analysis of complex samples, ions from two or more compounds are often merged under the same chromatographic peak; thus, spectral deconvolution is mandatory previously to compounds identification. Even after deconvolution, more often than desired, spectral data alone are not enough for the unambiguous identification of a given compound. Fig. 1A depicts a region of a deconvoluted compounds chromatogram. Spectra assigned to peaks in blue are shown in Fig. 1B and C, whilst the accurate spectrum for the best candidate (benzaldehyde) appears in Fig. 1D. The normalized scores (0–100) corresponding to the match of deconvoluted spectra with that recorded for benzaldehyde remained above 90 in both cases (Fig. 1B and C); moreover, the differences with *m/z* values of ions in the PCDL spectra of benzaldehyde were lower than 1.3 mDa (absolute value, Fig. 1D). Thus, without using chromatographic data (retention times or LRI) it would be practically impossible to discriminate which of the two peaks corresponds to benzaldehyde. In this case, the component at 15.97 min matched the LRI of benzaldehyde. Another example of compounds with practically identical EI-MS spectra are the fragrances linalool ($C_{10}H_{18}O$, CAS number 78-70-6) and linalyl acetate ($C_{12}H_{20}O_2$, CAS number 115-95-7), Figs. S4A and S4B. In the latter case, the molecular ion ($M^{\cdot+}$) is absent and most fragment ions (Fig. S4A) match those in the spectrum of linalool. Additional problematic cases are positional isomers. Very often, they show practically identical EI-MS spectra, as they are the cases of ethylbenzene and xylenes, di-butyl and di-isopropyl phthalates, thymol and carvacrol (Figs. S4C and D).

In order to overcome limitations reported in the previous paragraph, the PCDL was implemented with LRI values. Thus, positive identifications were based on spectral and LRI matches

USC UNIVERSIDADE DE SANTIAGO DE COMPOSTELA

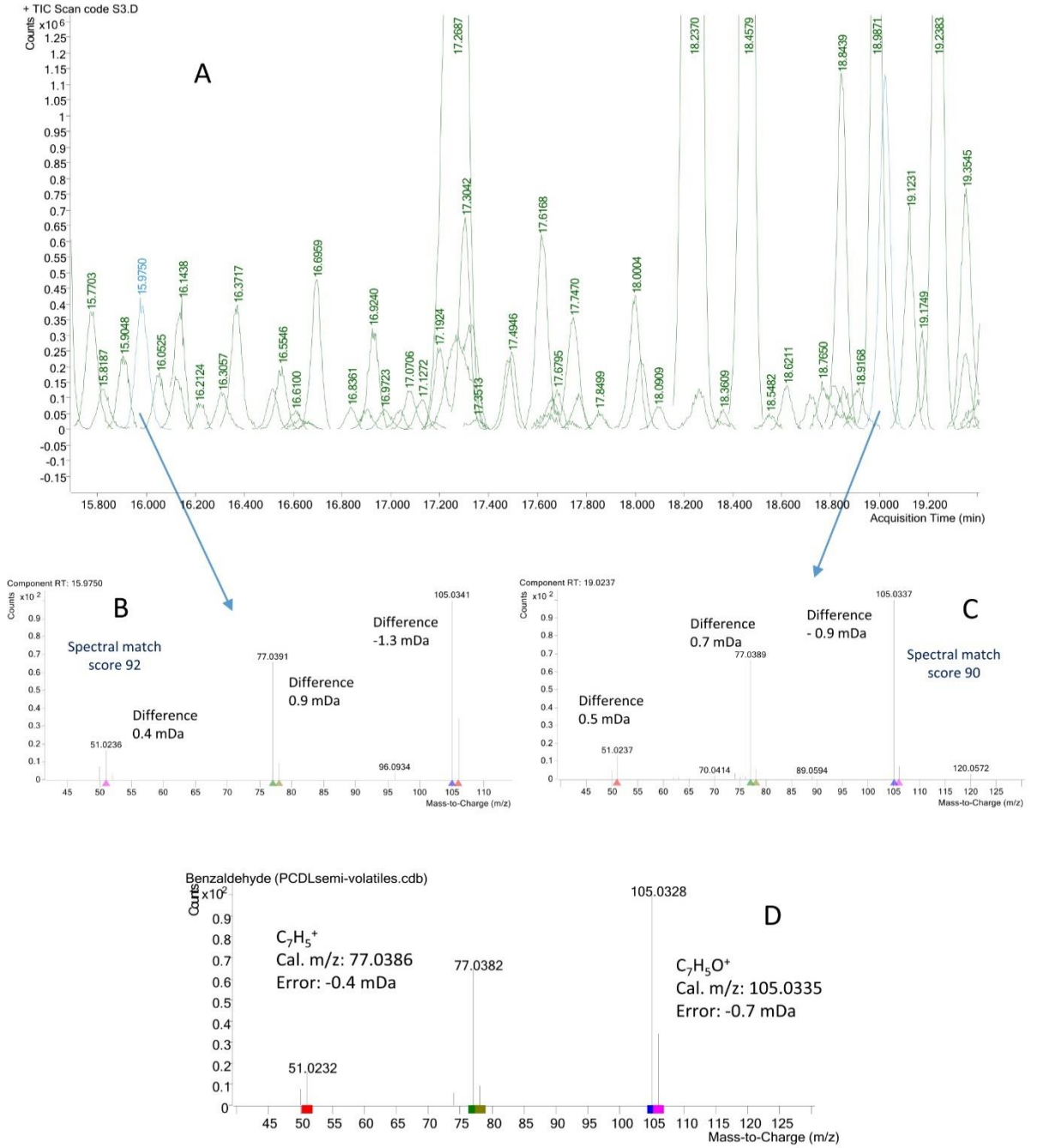


Fig. 1. Deconvoluted compound chromatogram (A), accurate EI-MS spectra of selected peaks (B and C) and PCDL spectrum for a standard of benzaldehyde (D).

between deconvoluted compounds in extracts from indoor air-related samples and the PCDL database. The minimum normalized score (0–100) for the spectral match was set at 70, and the maximum difference with database retention time 10 s (equivalent to a variation in LRI values of 8–10 units). A 3rd requirement for a positive identification was a maximum relative error of 20 ppm for any intense ion in the deconvoluted spectra compared to that in the PCDL spectrum of the candidate. These three conditions were verified by the *Unknowns Analysis* software during library search of deconvoluted components. Despite the restriction in the retention time window, in case of some isomeric species with very close retention times, such as the diastereomers of galaxolide, or *m*-

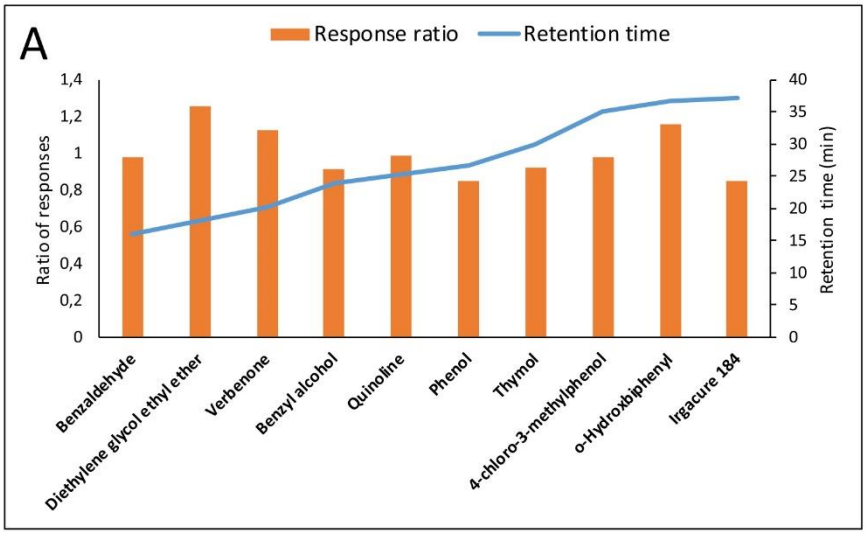
UNIVERSIDADE DE SANTIAGO DE COMPOSTELA

xylene and *p*-xylene, revision of identities assigned by *Unknowns Analysis* was required.

3.3. Dehumidifiers as samplers of semi-volatile compounds from indoor areas

The chromatograms of dehumidifier water samples contained a high number of peaks related to species existing in indoor air (Fig. S2 and Fig. 1); however, in order to demonstrate the usefulness of this matrix to characterize the composition of indoor air, several features need to be considered. Firstly, it is necessary to check that compounds in condensed water are not contaminants introduced by dehumidifiers. Changes in the composition of the indoor environment must be reflected in the presence of new chromatographic peaks, and/or in variations in their response intensities in dehumidifier water extracts. In addition, similar chromatographic profiles should be obtained for the same environment when using different dehumidifiers.

In general, the chromatograms of procedural blanks were very similar to those obtained for SPE of ultrapure water, not in contact with dehumidifier draining tanks. However, for two of the tested dehumidifiers we found traces of tris (1,3-dichloro-2-propyl) phosphate (TCPP) and tributyl acetylcitrate in procedural blanks, so these devices were not used in further experiments. In addition to substances released from the draining vessel, the stream of air and the condensed water drops might release organic compounds from



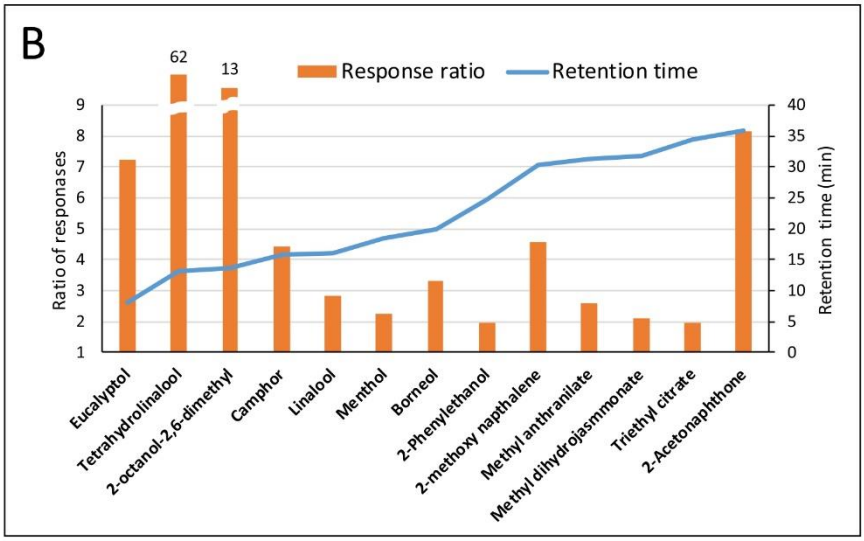


Fig. 2. Response ratios for compounds in condensed water samples obtained from the same room after and before installing an air freshener. A and B correspond to a selection of compounds not detected and detected in the freshener liquid, respectively.

USC UNIVERSIDADE DE SANTIAGO DE COMPOSTELA

other elements of dehumidifiers before reaching the draining vessel. Although this problem is difficult to detect, we have compared the normalized responses (peak area divided by the peak area of PCB30) for a series of potentially problematic species (plasticizers, flame retardants, curing agents, fragrances …) in the extracts of water samples taken, with the same dehumidifier, in the living room from 6 different homes. Responses of selected compounds showed significant variations (in some cases up to 10-fold) depending on the sampling site, Fig. S5. Thus, if occurs, the release of above compounds from the dehumidifier unit would not mask variations among samples obtained from different environments.

Fig. 2 shows the ratio of responses obtained for selected compounds in the extracts from two water samples obtained from the same room (46 m^3 volume). Samples were taken with the same dehumidifier, before and after installing an air freshener in the room (5 m distance from the dehumidifier). In addition to water extracts, the content of the freshener was diluted (10^5-fold dilution with AcOEt) and injected in the GC-TOF-MS system. In case of species not detected in the diluted freshener solution, response ratios from 0.8 to 1.2 were obtained, Fig. 2A. On the contrary, for compounds found in the freshener liquid, their responses increased between 2 and 62 times in the sample obtained after activation of the air aromatization device, Fig. 2B.

The effect of the dehumidifier device in the composition of condensed water samples was investigated operating simultaneously two different appliances in the same room. Chromatograms obtained at sampling point S21 (Table 1) are shown in Fig. 3A. The volumes of water recovered by each instrument differed around 20%; however, similar chromatographic profiles were observed for both extracts. Fig. 3B shows the correlation plot between responses (logarithms of peak areas) for 50 identified compounds (after deconvolution and comparison with the PCDL) in the chromatograms for both samples. An acceptable correlation (determination coefficient, R^2, 0.959) was observed; moreover, the slope of the plot (0.996) was close to the unit. Fig. 3C shows the equivalent plot for a second pair of dehumidifiers operating at sampling point S3. In this case, the graph compares the responses obtained for 70 positive identifications.

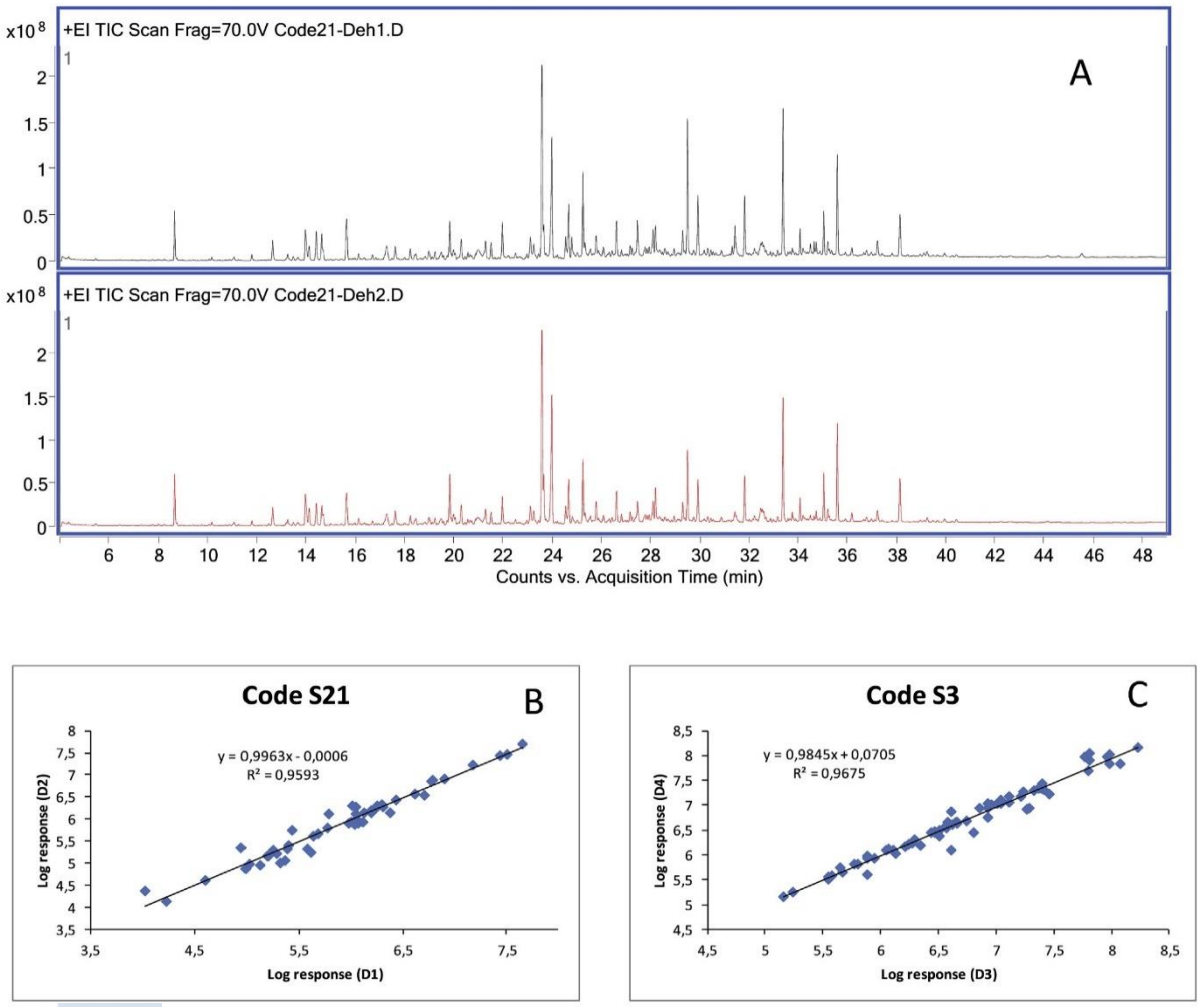


Fig. 3. A, Chromatograms for condensed water samples obtained in the same room with two different dehumidifiers operating simultaneously. B and C, correlation plots of logarithmic responses for identified compounds in sampling places S21 and S3 using different appliances.

USC UNIVERSIDADE DE SANTIAGO DE COMPOSTELA

3.4. Comprehensive identification of semi-volatile compounds in dehumidifier water samples

The list of substances identified in dehumidifier water from the 21 sampling points considered in the current study (Table 1) is compiled in Tables 2A and 2B. Compounds are classified attending to their applications (in most cases same species present different uses), and sorted accordingly to their increasing LRI values. Compounds detected in procedural blanks were included in the above tables only when their responses stayed above 10-times that observed in the procedural blank of the corresponding dehumidifier. Species such as toluene, styrene and dimethyl sulfoxide were ubiquitous in condensed water samples, however, they did not satisfy the above requirement; thus, they are not included in the list of positive identifications. Table 2A gathers compounds with applications as fragrances and flavors. They are usually incorporated in personal care, cleaning and other household products. Some of them are natural products whose empirical formulae derive from that of terpene ($C_{10}H_{16}$), with one or two atoms of oxygen and variations in the number of unsaturated bonds. In other cases, they show a phenolic structure, as it is the case of salicylates, vanillin, eugenol and thymol. The list includes also synthetic musks, such as galaxolide and tonalide. Many compounds in Table 2A have been included in the list of potential contact allergens (Shibuta et al., 2016).

Regarding substances compiled in Table 2B, most of them belong to the category of solvents and intermediates in the production of high volume chemicals, followed by those used as preservatives and plasticizers. Within the first group, 2-ethyl-1-hexanol was ubiquitous in the processed samples. This compound can be released from polymeric materials; moreover, it can arise from hydrolysis of di-ethylhexyl phthalate (Wakayama et al., 2019), which has been quantified in indoor dust at high concentrations (Castro et al., 2019). Another intermediate often noticed in samples was cyclohexanone, which is involved in the polyurethane foams (Glowacz-Czerwonka, 2017). Likely, phenol and aniline are released from adhesives, paints and cleaning fluids (Palmiotto et al., 2001). The most probable sources of compounds integrated in the category of preservatives are again personal and household products. The list of plasticizers whose presence was confirmed in dehumidifier water samples includes four phthalates, two citrates, a diisobutyrate (2,2,4-trimethyl-1,3-pentanediol diisobutyrate; TXIB) and diacetin. All of them are high production volume chemicals widely employed in building materials, and they have been previously detected in indoor air (Lucattini et al., 2018; Ueta et al., 2019).

Table 3 summarizes a list of 43 compounds tentatively identified (not confirmed by injection of authentic standards) in the processed samples. Compounds in this table showed spectral match scores higher than 90% when their experimental accurate MS spectra are compared with those in the NIST database. Moreover, the difference between *m/z* ratios in the de-convoluted spectra and the calculated values for ions with known structures in the NIST database remained below 2 mDa, at least for two intense fragment ions. When available, experimental LRI values of tentative identifications were compared with those obtained from Chemspider database (http://www.chemspider.com/), or directly for Carbowax-type columns in previous studies (Moniruzzaman et al., 2014). Most of them show similar applications to positive identifications compiled in Tables 2A and 2B. The largest families of compounds in Table 3 are benzene derivatives, carboxylic acids of natural origin, and several of their esters with industrial applications as plasticizers (particularly those of phthalic, hexanoic and isobutyric acid), glycols and terpene derivatives. Some compounds listed in Table 3 are closely related to those positively identified in Table 2. An example is 2-(methylthio) benzothiazole, which has been reported together with benzothiazole in vehicle tires (Zhang et al., 2018). Another case corresponds to the isomers of 1,3-pentanediol, 2,2,4-trimethyl-isobutyrate (Texanol) with similar applications to TXIB (Ueta et al., 2019).

Table 1 shows the identities assigned to the three most intense peaks in the chromatograms for condensed water samples from the 21 sampling sites involved in the current study. At least one plasticizer was within the above ranking for 14 out of 21 samples. Within the group of personal care and cleaning products, 2-phenoxyethanol was among the three most intense peaks in 5 sites. Nonanoic acid and diethylene glycol butyl ether were also often identified in the ranking of most intense peaks. Comparison of data for samples obtained at home 1 (sample codes S1, S2, S3, S4

Table 2 A
Fragrances and flavoring compounds identified in dehumidifier water samples.

Compound	Positive samples	CAS number	LRI	Compound	Positive samples	CAS number	LRI
Limonene	4	5989-27-5	1219	Beta-Ionone	5	14901-07-6	1972
Eucalyptol	13	470-82-6	1228	1-Dodecanol	5	112-53-8	1981
Octanal	8	124-13-0	1308	Methyleugenol	7	93-15-2	2044
3-Octanol	5	589-98-0	1406	Ethyl maltol	2	4940-11-8	2047
Tetrahydrolinalool	16	78-69-3	1442	Benzaldehyde, 4-methoxy	18	123-11-5	2065
2-Octanol, 2,6-dimethyl-	4	18479-57-7	1456	4-Ethylguaiacol	5	2785-89-9	2073
1-Heptanol	19	111-70-6	1471	Lilial	10	80-54-6	2080
Dihydromyrcenol	19	18479-58-8	1479	Cinnamal	2	104-55-2	2083
Camphor	16	76-22-2	1549	Eugenol	13	97-53-0	2207
Linalool	17	78-70-6	1564	Thymol	13	89-83-8	2213
Linalyl acetate	2	115-95-7	1573	Naphthalene, 2-methoxy	13	93-04-9	2232
1-Octanol	17	111-87-5	1574	Carvacrol	3	499-75-2	2245
Bornyl acetate	6	76-49-3	1604	Hexyl salicylate	7	6259-76-3	2247
Menthol	19	15356-70-4	1658	Naphthalene, 2-ethoxy	3	93-18-5	2265
Alfa-terpineol	20	98-55-5	1719	Piperonal	15	120-57-0	2279
Borneol	19	507-70-0	1726	Methyl anthranilate	17	134-20-3	2283
Verbenone	21	1196-01-6	1739	Methyl Dihydrojasmonate	18	24851-98-7	2316
Citronellol	11	106-22-9	1782	Galaxolide (two diastereomers)	9	1222-05-5	2358, 2365
Methylsalicylate	8	119-36-8	1815	Alfa-Hexylcinnamaldehyde	3	101-86-0	2395
Geraniol	9	106-24-1	1869	Tonalid	5	21145-77-7	2443
Alpha-isomethylionone	4	127-51-5	1877	Coumarin	21	91-64-5	2519
Benzyl alcohol	20	100-51-6	1912	Ethyl Vanillin	18	121-32-4	2570
2-Phenylethanol	21	60-12-8	1941	2-Acetonaphthone	20	93-08-3	2601
3,7-Dimethyl-7-hydroxyoctanal	12	107-75-5	1969				2601

USC UNIVERSIDADE DE SANTIAGO DE COMPOSTELA

and S5) revealed changes in the identities of the most intense chromatographic peaks between kitchen and garage (S4 and S17, respectively) with the other investigated rooms (S1, S2 and S3). Sample code S10 was obtained from the home of a smoker. In this case, the most intense chromatographic peak was identified as nicotine. In summary, even the major compounds in dehumidifier water extracts varied depending on the sampling area.

3.5. Dehumidifier condensed water versus active air sampling

Data in previous sections show that condensed water samples contain a cocktail of organic compounds potentially related with on-going activities, building materials and life style in indoor areas. The question is whether the qualitative information provided by dehumidifiers and active sampling are somehow correlated, or not. The raw chromatograms corresponding to active sampling (16.5 L min^{-1}) for 5 h through a HLB cartridge, and after concentration of condensed water sample obtained from a portable dehumidifier, both operating simultaneously in the same room, are shown in Fig. S6. The first part of the chromatogram for active sampling contains more intense peaks than those observed for condensed water (Fig. S6A). On the other hand, the latter chromatogram is richer in number and intensity of peaks with retention times above 17 min (Fig. S6B). Even when the sampling time was increased to 15 h, the 2nd half of the resulting chromatograms was relatively poor in peaks when compared to those obtained for dehumidifier condensed water (Fig. S6C).

Fig. 4 shows the logarithmic values of average response ratios for common compounds (sorted following their increasing retention times in the DB-WAXETR column), identified using both sampling approaches, at four different sampling points (S2, S3, S7 and S20, Table 1). In general, the response ratios plot follows a

Table 2 B
Summary of semi-volatile compounds identified in dehumidifier water samples, including their most relevant application.

Compound	Positive samples	CAS number	LRI	Application
Nicotine	8	54-11-5	1896	Alkaloids
Quinoline	19	91-22-5	1976	
Nonanoic acid[a]	18	112-05-0	2188	Carboxylic acid
Benzothiazole	20	95-16-9	1996	Curing agent
Tributyl phosphate	12	126-73-8	2141	Flame retardants
TCPP	17	13674-84-5	2735	
Tris(2-chloroethyl) phosphate	6	115-96-8	3026	
Irgacure 184	16	947-19-3	2684	Paint additives
Irgacure 651	18	24650-42-8	2794	
Diazinone	2	333-41-5	2463	Pesticides
Terbutryn	3	886-50-0	2992	
Ethyl benzene	10	100-41-4	1147	Petrol components
p-Xylene	16	106-42-3	1155	
m-Xylene	8	108-38-3	1163	
o-Xylene	10	95-47-6	1210	
Ibuprofen	4	15687-27-1	2863	Pharmaceutical
2,2,4-Trimethyl-1,3-pentanediol diisobutyrate (TXIB)	11	6846-50-0	1892	Plasticizers
1,2-Diacetin[a]	21	102-62-5	2096	
Dimethyl phthalate	19	131-11-3	2341	
Diethyl phthalate[a]	20	84-66-2	2409	
Triethyl citrate	20	77-93-0	2496	
Diisobutyl phthalate[a]	21	84-69-5	2577	
Dibutyl phthalate[a]	19	84-74-2	2735	
Tributyl acetylcitrate	13	77-90-7	2933	
Benzaldehyde[a]	21	100-52-7	1555	Preservatives
5-Chloro-2-methyl-3(2H)-isothiazolone	1	26172-55-4	2004	
2-Phenoxyethanol	19	122-99-6	2178	
Benzoic acid	6	65-85-0	2475	
o-Hydroxybiphenyl	17	90-43-7	2658	
Benzyl Benzoate	9	120-51-4	2693	
3(2H)-Isothiazolone, 2-octyl-	8	26530-20-1	2784	
Methylparaben	10	99-76-3	3000	
Cyclohexanone	17	108-94-1	1321	Solvents/intermediates
Ethylene glycol butyl ether	20	111-76-2	1419	
Furfural	6	98-01-1	1499	
2-Ethyl-1-hexanol[a]	21	104-76-7	1502	
Isophorone	18	78-59-1	1623	
Diethylene Glycol ethyl ether	7	111-90-0	1638	
1-Decanol	3	112-30-1	1775	
Aniline	9	62-53-3	1787	
Diethylene glycol monobutyl ether	14	112-34-5	1814	
2-Nitrophenol	3	88-75-5	1850	
Phenol[a]	10	108-95-2	2039	
2,3-Dimethylphenol	3	526-75-0	2112	
p-Cresol	15	106-44-5	2119	
4-Ethylphenol	18	123-07-9	2208	
Epsilon-Caprolactam	1	105-60-2	2225	
4-chloro-3-methylphenol	19	59-50-7	2548	
Benzoic acid, p-tert-butyl-	20	98-73-7	2794	
Phthalimide	13	85-41-6	2985	
Dibromochloromethane	4	124-48-1	1322	Trihalomethane

[a] Compounds also noticed in procedural blanks.

USC UNIVERSIDADE DE SANTIAGO DE COMPOSTELA

Table 3
Compounds tentatively identified in dehumidifier water samples, including the accurate *m/z* values of two intense ions with mass errors.

Compound	Formula	CAS number	Experimental LRI	Literature LRI	Chemical class	Positive samples	1st ion	2nd ion	Mass error (mDa) 1st ion	Mass error (mDa) 2nd ion
Pyridine, 3-ethenyl	C_7H_7N	1121-55-7	1501		Alkaloids	5	105.0575	78.0459	0.3	−0.4
Nicotyrine	$C_{10}H_{10}N_2$	487-19-4	2368			5	158.0844	130.0657	0.4	0.2
2-Butene, 2-methyl-	C_5H_{10}	513-35-9	1259		Alkanes	6	70.078	55.0542	0.3	−0.1
Cyclobutane, ethyl-	C_6H_{12}	4806-61-5	1363			10	69.0701	56.0625	0.3	0.4
Isopropylcyclobutane	C_7H_{14}	872-56-0	1467			17	83.0853	70.0775	−0.3	−0.3
Cyclopentane, 1,1-dimethyl-	C_7H_{14}	1638-26-2	1570			8	83.0852	69.0699	−0.4	0.1
Benzene, (1-methoxypropyl)-	$C_{10}H_{14}O$	59588-12-4	1783		Benzene derivatives	4	121.0646	91.0543	−0.2	0.1
1-phenyl ethanol	$C_8H_{10}O$	98-85-1	1838	1820[a]		5	122.0724	107.0488	−0.3	−0.4
1-(4-tert-Butylphenyl)propan-2-one	$C_{13}H_{18}O$	81561-77-5	2047			5	190.1373	175.1137	1.5	1.4
1-Phenoxypropan-2-ol	$C_9H_{12}O_2$	770-35-4	2073			8	152.0836	94.0409	0.4	−0.4
N-methyl phthalimide	$C_9H_7NO_2$	550-44-7	2328			4	161.0495	132.0474	1.8	2.5
Benzene, (3-methylcyclopentyl)-	$C_{12}H_{16}$	5078-75-1	2345			6	160.1257	131.0861	1.0	0.6
Dibenzyl ether	$C_{14}H_{14}O$	103-50-4	2423			13	92.0617	91.0546	−0.3	0.3
1,2-Ethanediol, monobenzoate	$C_9H_{10}O_3$	94-33-7	2554			6	123.0449	105.0344	0.8	0.9
Diphenyl methanol	$C_{13}H_{12}O$	91-01-0	2803			4	184.0904	105.0355	1.6	1.5
2-(Methylmercapto)benzothiazole	$C_8H_7NS_2$	615-22-5	2484	2422[a]	Benzothiazole derivative	4	181.0012	148.0217	−0.3	0.2
Hexanoic acid	$C_6H_{12}O_2$	142-62-1	1865	1851[a]	Carboxylic acids	7	87.0437	73.0277	−0.4	−0.6
Heptanoic acid	$C_7H_{14}O_2$	111-14-8	1972	1971[a]		8	101.0596	87.0438	−0.2	−0.3
Octanoic acid	$C_8H_{16}O_2$	124-07-2	2079	2086[a]		17	101.0592	87.0438	−0.6	−0.3
n-Decanoic acid	$C_{10}H_{20}O_2$	334-48-5	2292	2275[a]		4	129.0911	115.0753	0.1	−0.1
Tetradecanoic acid	$C_{14}H_{28}O_2$	544-63-8	2716	2716[a]		6	185.154	129.0914	0.4	0.4
Butanoic acid, ethyl ester	$C_6H_{12}O_2$	105-54-4	1071	1041[a]	Esters	3	101.0615	88.0536	1.2	1.2
Butanedioic acid, dimethyl ester	$C_6H_{10}O_4$	106-65-0	1616	1595[a]		10	115.0384	87.0441	−0.6	0.1
Hexanedioic acid, dimethyl ester	$C_8H_{14}O_4$	627-93-0	1842	1819[a]		10	143.0708	114.0675	0.5	−0.1
Hexanoic acid, 2-ethyl-	$C_8H_{16}O_2$	149-57-5	1968	1963[a]		8	101.0594	88.0515	−0.4	−0.4
3-hydroxy-2,2,4-trimethylpentyl isobutyrate (Texanol)	$C_{12}H_{24}O_3$	77-68-9	1889, 1909			9	173.1168	89.0593	−0.5	−0.5
Isobutyl methyl phthalate	$C_{13}H_{16}O_4$	1000373-89-3	2476			3	163.0391	149.0235	0.2	0.2
2(3H)-Furanone, 5-ethenyldihydro-5-methyl-	$C_7H_{10}O_2$	1073-11-6	1703	1689[a]	Furane	4	111.0431	98.0363	−0.9	0.1
2-Propanol, 1-butoxy-	$C_7H_{16}O_2$	5131-66-8	1354	1364[a]	Glycols	14	87.0805	57.0696	0.1	−0.3
1-Propanol, 2-(2-methoxypropoxy)-	$C_7H_{16}O_3$	13588-28-8	1584			3	117.0916	73.0644	0.6	−0.4
1,3-Pentanediol, 2,2,4-trimethyl-isobutyrate	$C_8H_{18}O_2$	144-19-4	1947			6	85.0646	73.0644	−0.2	−0.4
Ethanol, 2-[2-(2-butoxyethoxy) ethoxy]-	$C_{10}H_{22}O_4$	143-22-6	2217			4	85.0649	57.0697	0.2	−0.2
1H-Inden-1-one, 2,3-dihydro-	C_9H_8O	83-33-0	2055		Indene	17	132.0583	104.0626	1.3	0.5
Indole	C_8H_7N	120-72-9	2496	2445[a]	Indole	2	117.0585	90.0471	1.2	0.7
Tri-ethyl phosphate	$C_6H_{15}O_4P$	78-40-0	1675	1672[a]	Organophosphate	21	155.0469	127.0158	0.1	0.4
1H-Pyrrole-2-carboxaldehyde	C_5H_5NO	1003-29-8	2062	2044[a]	Pyrrole derivative	3	95.0374	94.029	0.8	0.3
cis-Furanoid linalool oxide	$C_{10}H_{18}O_2$	5989-33-3	1460	1462[b]	Terpenoids	7	111.0799	94.0774	−0.5	−0.4
trans-Furanoid linalool oxide	$C_{10}H_{18}O_2$	34995-77-2	1489	1483[a]		5	111.0803	94.0778	−0.2	0.1
3-Cyclohexen-1-ol, 1-methyl-4-(1-methylethyl)-	$C_{10}H_{18}O$	586-82-3	1593	1589[a]		9	136.1244	121.1012	−0.3	0.1
L-.alpha.-Terpineol	$C_{10}H_{18}O$	10482-56-1	1718	1722[b]		14	136.1247	121.1014	0.1	0.3
Cyclohexanol, 4-(1,1-dimethylethyl)-, trans-	$C_{10}H_{20}O$	21862-63-5	1766			6	123.1187	81.071	1.3	0.6
4,7-Methano-1H-indenol, hexahydro-	$C_{10}H_{14}O$	37275-49-3	2009			11	132.0939	117.0704	0.5	0.5
2,6-Di-tert-butyl-4-hydroxy-4-methylcyclohexa-2,5-dien-1-one	$C_{15}H_{24}O_2$	10396-80-2	2118	2049[a]		8	221.1538	180.114	0.2	−0.5

[a] LRI values obtained from ChemSpider database (http://www.chemspider.com/) for Carbowax-type GC columns.
[b] LRI obtained from Moniruzzaman et al. (2014).

USC UNIVERSIDADE DE SANTIAGO DE COMPOSTELA

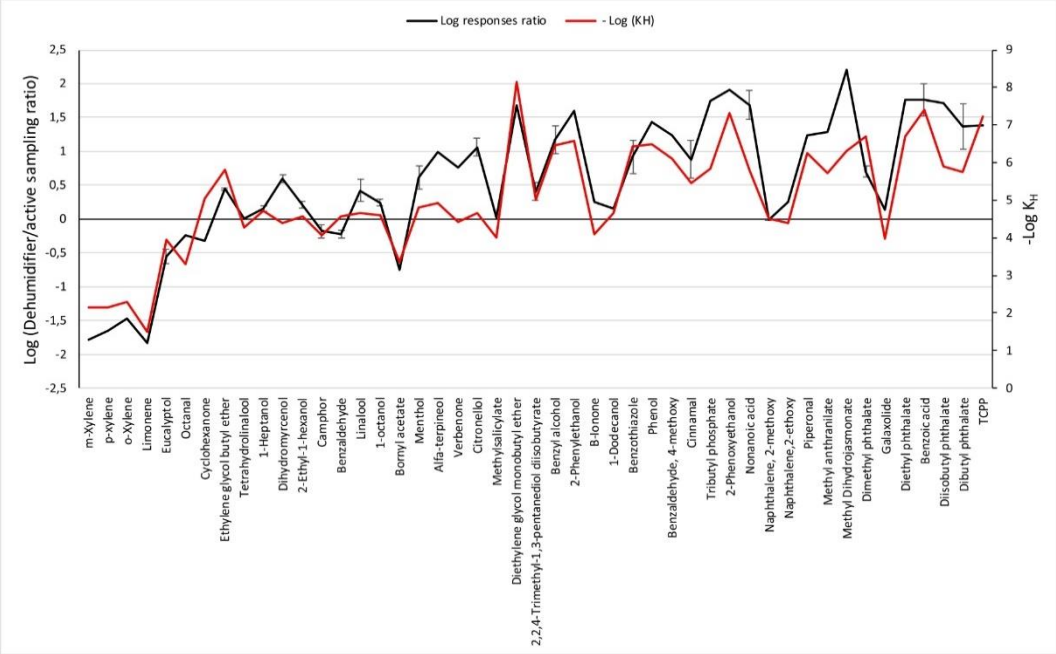


Fig. 4. Black, logarithmic values of response ratios for compounds identified in condensed water samples and in active sampling extracts (concentrated air volume 5 m^3) simultaneously obtained in the same room. Average data obtained in four different places. Red, negative logarithmic values of Henry's law constant (K_H, atm m^3 mol^{-1}) estimated using the bond method (values at 25 °C). (For interpretation of the references to colour in this figure legend, the reader is referred to the Web version of this article.)

similar trend that the negative logarithms of the Henry's law constants (K_H, atm m^3 mol^{-1}). That is, the relative extraction yield provided by dehumidifier condensed water samples increases with the decrease of the K_H values. Not surprisingly, K_H is defined as the ratio between the pressure of a given compound in the gas phase and its concentration in the equilibrium water phase. In general, for species with K_H values lower than 10^{-4} atm m^3 mol^{-1} higher responses are observed after SPE of 300 mL of condensed water than for direct sampling of 5 m^3 of air. In addition to compounds in Fig. 4, other species were only noticed using one of the two sampling techniques. For example, camphene and pinene (alpha and beta isomers), and the terpene-related species *p*-cymene were found in chromatograms corresponding to active air sampling, but not in the extracts from dehumidifier water. Their K_H values (data at 25 °C) stayed above 10^{-2} atm m^3 mol^{-1}. A list of compounds present in dehumidifier water, but not detected using active sampling, is provided as supplementary information, Table S3. Their K_H values varied between 10^{-6} and 10^{-11} atm m^3 mol^{-1}.

4. Conclusions

The GC-EI-TOF-MS chromatograms obtained for the extracts of dehumidifier water samples contain a large number of semi-volatile compounds. Variations among sampling places, and the reasonable agreement of data obtained in the same room, with different dehumidifiers, confirm that condensed water samples are useful for qualitative analysis of the chemical composition of indoor areas. Dehumidifier appliances are portable, relatively non-expensive and non-disrupting equipment compared to pumps involved in active sampling of indoor air. The concentration efficiency of indoor air compounds in dehumidifier water is correlated with the values of their Henry constants, being effective for species with values below 10^{-4} atm m^3 mol^{-1} at 25 °C. Compounds identified in this study (including tentative identifications) represent around 25% of deconvoluted peaks in the chromatograms of dehumidifier water samples; therefore, construction of larger EI-MS spectral databases is required to understand the complexity of the mixture of semi-volatile species existing in indoor areas.

Declaration of competing interest

The authors declare that they have no known competing financial interests or personal relationships that could have appeared to influence the work reported in this paper.

CRediT authorship contribution statement

M. Cobo-Golpe: Investigation, Validation. **M. Ramil:** Methodology, Validation, Writing - review & editing. **R. Cela:** Writing - review & editing, Supervision. **I. Rodríguez:** Conceptualization, Writing - original draft, Supervision, Project administration.

Acknowledgements

This study was supported by Xunta de Galicia and Spanish Government through grants GRC-ED431C 2017/36 and PGC2018-094613-B-I00, both co-funded by the EU.

Appendix A. Supplementary data

Supplementary data to this article can be found online at https://doi.org/10.1016/j.chemosphere.2020.126346.

USC UNIVERSIDADE DE SANTIAGO DE COMPOSTELA

References

Araki, A., Bastiaensen, M., Bamai, Y.A., Van den Eede, N., Kawai, T., Tsuboi, R., Ketema, R.M., Covaci, A., Kishi, R., 2018. Associations between allergic symptoms and phosphate flame retardants in dust and their urinary metabolites among school children. Environ. Int. 119, 438–446. https://doi.org/10.1016/j.envint.2018.07.018.

Castro, G., Rodríguez, I., Ramil, M., Cela, R., 2019. Assessment of gas chromatography time-of-flight mass spectrometry for the screening of semi-volatile compounds in indoor dust. Sci. Total Environ. 688, 162–173. https://doi.org/10.1016/j.jhazmat.2015.01.043.

Cecinato, A., Romagnoli, P., Perilli, M., Balducci, C., 2017. Psychotropric substances in house dusts: a preliminary assessment. Environ. Sci. Pollut. Res. 24, 21256–21261. https://doi.org/10.1007/s11356-017-9549-5.

Esteve-Turrillas, F.A., Ly-Verdú, S., Pastor, A., de la Guardia, M., 2009. Development of a versatile, easy and rapid atmospheric monitor for benzene, toluene, ethylbenzene and xylenes determination in air. J. Chromatogr. A 1216, 8549–8559. https://doi.org/10.1016/j.chroma.2009.10.001.

Fromme, H., Lahrz, T., Piloty, M., Gebhart, H., Oddoy, A., Rueden, H., 2004. Occurrence of phthalates and musk fragrances in indoor air and dust from apartments and kindergartens in Berlin (Germany). Indoor Air 14, 188–195. https://doi.org/10.1111/j.1600-0668.2004.00223.x.

Gale, R.W., Cranor, W.L., Alvarez, D.A., Huckins, J.N., Petty, J.D., Robertson, G.L., 2009. Semi-volatile organic compounds in residential air along the Arizona-Mexico Border. Environ. Sci. Technol. 43, 3054–3060. https://doi.org/10.1021/es803482u.

Geens, T., Roosens, L., Neels, H., Covaci, A., 2009. Assessment of human exposure to Bisphenol-A, Triclosan and Tetrabromobisphenol-A through indoor dust intake in Belgium. Chemosphere 76, 755–760. https://doi.org/10.1016/j.chemosphere.2009.05.024.

Glowacz-Czerwonka, D., 2017. The polyurethane foams based on melamine-formaldehyde-cyclohexanone. Cell. Polym. 36, 35–50. https://doi.org/10.1177/026248931703600103.

Gómez-Ramos, M.M., Ucles, S., Ferrer, C., Fernández-Alba, A.R., Hernando, M.D., 2019. Exploration of environmental contaminants in honeybees using GC-TOF-MS and GC-Orbitrap-MS. Sci. Total Environ. 647, 232–244. https://doi.org/10.1016/j.scitotenv.2018.08.009.

Hoang, T., Castorina, R., Gaspar, F., Maddalena, R., Jenkins, P.L., Zhang, Q., McKone, T.E., Benfenati, E., Shi, A.Y., Bradman, A., 2017. VOC exposures in California early childhood education environments. Indoor Air 27, 609–621. https://doi.org/10.1111/ina.12340.

Laboire, S., Moreau-Guigon, E., Alliot, F., Desportes, A., Oziol, L., Chevreuil, M., 2016. A new analytical protocol for the determination of 62 endocrine-disrupting compounds in indoor air. Talanta 147, 132–141. https://doi.org/10.1016/j.talanta.2015.09.028.

Lamas, J.P., Sánchez-Prado, L., García-Jares, C., Llompart, M., 2010. Determination of fragrance allergens in indoor air by active sampling followed by ultrasound-assisted solvent extraction and gas chromatography-mass spectrometry. J. Chromatogr. A 1217, 1882–1890. https://doi.org/10.1016/j.chroma.2010.01.055.

Liu, S., Thompson, S.L., Stark, H., Ziemann, P.J., Jimenez, J.L., 2017. Gas-phase carboxylic acids in a university classroom: abundance, variability and sources. Environ. Sci. Technol. 51, 5454–5463. https://doi.org/10.1021/acs.est.7b01358.

Lucattini, L., Poma, G., Covaci, A., de Boer, J., Lamoree, J.H., Leonards, P.E.G., 2018. A review of semi-volatile organic compounds (SVOCs) in the indoor environment: occurrence in consumer products. Chemosphere 201, 466–482. https://doi.org/10.1016/j.chemosphere.2018.02.161.

Melymuk, L., Bohlin-Nizzetto, P., Vojta, Š., Krátká, M., Kukučka, P., Audy, O., Přibylová, P., Klánová, J., 2016. Distribution of legacy and emerging semi-volatile organic compounds in five indoor matrices in a residential environment. Chemosphere 153, 179–186. https://doi.org/10.1016/j.chemosphere.2016.03.012.

Moniruzzaman, M., Rodríguez, I., Ramil, M., Cela, R., Sulaiman, S.A., Gan, S.H., 2014. Assessment of gas Chromatography time-of-flight accurate mass spectrometry for identification of volatile and semi-volatile compounds in honey. Talanta 129, 505–515. https://doi.org/10.1016/j.talanta.2014.06.019.

Palmiotto, G., Pieraccini, G., Moneti, G., Dolara, P., 2001. Determination of the levels of aromatic amines in indoor and outdoor air in Italy. Chemosphere 43, 355–361. https://doi.org/10.1016/S0045-6535(00)00109-0.

Pandey, S.K., Kim, K.H., 2010. A review of environmental tobacco smoke and its determination in air. Trends Anal. Chem. 29, 804–819. https://doi.org/10.1016/j.trac.2010.04.014.

Ramírez, N., Marcé, R.M., Borrull, F., 2010. Development of a thermal desorption-gas Chromatography-mass spectrometry method for determining personal care products in air. J. Chromatogr. A 1217, 4430–4438. https://doi.org/10.1016/j.chroma.2010.04.049.

Roll, I.B., Pycke, B.F.G., Halden, R.U., 2015. Indoor air condensate as a novel matrix for monitoring inhalable organic contaminants. J. Hazard Mater. 288, 89–96. https://doi.org/10.1016/j.jhazmat.2015.01.043.

Shibuta, S., Imasaka, T., Imasaka, T., 2016. Determination of fragrance allergens by ultraviolet femtosecond laser ionization mass spectrometry. Anal. Chem. 88, 10693–10700. https://doi.org/10.1021/acs.analchem.6b03229.

Soheib, M., Harner, T., 2002. Characterization and comparison of three passive air samplers for persistent organic compounds. Environ. Sci. Technol. 36, 4142–4151. https://doi.org/10.1021/es020635t.

Steinemann, A., Goodman, N., 2019. Fragranced consumer products and effects on asthmatics: an international population-based study. Air Qual. Atmos. Health 12, 643–649. https://doi.org/10.1007/s11869-019-00693-w.

Stupak, M., Goodall, I., Tomaniova, M., Pulkrabova, J., Hajslova, J., 2018. A novel approach to assess the quality and authenticity of Scotch whisky based on gas chromatography coupled to high resolution mass spectrometry. Anal. Chim. Acta 1042, 60–70. https://doi.org/10.1016/j.aca.2018.09.017.

Ueta, I., Takenaka, R., Fujimura, K., Narukami, S., Sasaki, T., Maeda, T., 2019. Quantitative determination of 2-ethyl-1-hexanol, Texanol and TXIB in in-door air using a solid-phase extraction-type collection device followed by gas chromatography-mass spectrometry. Anal. Sci. 35, 855–859. https://doi.org/10.2116/analsci.19P033.

Wakayama, T., Ito, Y., Sakai, K., Miyake, M., Shibata, E., Ohno, H., Kamijima, M., 2019. Comprehensive review of 2-ethyl-1-hexanol as an indoor air pollutant. J. Occup. Health 61, 19–35. https://doi.org/10.1002/1348-9585.12017.

Weschler, C.J., Nazaroff, W.W., 2014. Dermal uptake of organic vapors commonly found in indoor air. Environ. Sci. Technol. 48, 1230–1237. https://doi.org/10.1021/es405490a.

Zhang, J., Zhang, X., Wu, L., Wang, T., Zhao, J., Zhang, Y., Men, Z., Mao, H., 2018. Occurrence of benzothiazole and its derivates in tire wear, road dust, and roadside soil. Chemosphere 201, 310–317. https://doi.org/10.1016/j.chemosphere.2018.03.007.

USC UNIVERSIDADE DE SANTIAGO DE COMPOSTELA

Supplementary information to manuscript:

Portable dehumidifiers condensed water: a novel matrix for the screening of semi-volatile compounds in indoor air

M. Cobo, M. Ramil, R. Cela, I. Rodríguez*
Department of Analytical Chemistry, Nutrition and Food Sciences. Institute of Research on Chemical and Biological Analysis (IAQBUS). Universidade de Santiago de Compostela, 15782-Santiago de Compostela, Spain.

*corresponding author
e-mail: isaac.rodriguez@usc.es

USC
UNIVERSIDADE DE SANTIAGO DE COMPOSTELA

Table S1. Data corresponding to sampling places, temperature and relative humidity before dehumidifier operation.

Sample code	Dehumidifier system	Room volume (m^3)	Temperature (ºC)	Relative air humidity (%)	Volume of the condensed water sample (mL)
S1	1	46	21	72	650
S2	1	55	19	68	680
S3	1	90	19	68	700
S4	1	30	21	68	520
S5	1	50	18	65	800
S6	1	33	18	72	700
S7	1	53	21	62	1000
S8	1	25	22	65	850
S9	1	55	19	81	1000
S10	1	65	20	84	1000
S11	2	25	20	80	900
S12	1	105	22	56	400
S13	1	75	22	70	600
S14	1	35	20	75	500
S15	1	60	23	75	1900
S16	1	70	19	65	600
S17	1	150	16	75	1200
S18	3	150	17	75	1500
S19	4	35	19	80	600
S20	1	400	21	62	2000
S21	5	35	22	85	800

USC UNIVERSIDADE DE SANTIAGO DE COMPOSTELA

Table S2. Summary of compounds, including their retention times and a representative ion, used to investigate potential breakthrough problems during active sampling of indoor air in the HLB cartridge.

Compound	[a]Retention time (min)	Representative ion (*m/z*)
Limonene	7.81	93.0701
Eucalyptol	8.01	154.1354
Gamma-Terpinene	8.85	136.1252
Cymene	9.51	119.0847
Camphor	15.77	152.1195
Linalool	16.14	121.1017
Borneol acetate	17.17	136.1247
Neral	19.57	137.096
Alfa-Terpineol	19.84	121.1007
Verbenone	20.3	135.0801
Citral	20.71	137.096
Citronellol	21.26	95.0854
Geraniol	23.07	123.1176
Eugenol	29.78	164.0835
Thymol	29.77	135.0799
Carvacrol	30.54	135.0797

[a]Values corresponding to the DB-WAXETR column.

USC UNIVERSIDADE DE SANTIAGO DE COMPOSTELA

Table S3. Summary of compounds identified in condensed water extracts, and not detected after active sampling of 5 m^3 of indoor air. Henry´s law constant values (K_H) predicted using the bond method (http://www.chemspider.com/).

Compound	K_H (atm m^3 mol^{-1}, 25 ºC)
1,2-Diacetin	2.60e-11
2-Acetonaphthone	9.58e-7
4-chloro-3-methylphenol	4.58e-7
4-ethylphenol	8.21e-7
Coumarin	6.95e-6
Ethyl Vanillin	1.1e-10
Irgacure 184	2.78e-6
Isophorone	[a]6.64e-6
Phthalimide	1.02e-8
Quinoline	[a]1.67e-6
Tributyl acetylcitrate	3.78e-10
Triethyl citrate	[a]3.84e-9
Vanillin	[a]2.15e-9

[a]Experimental values.

USC UNIVERSIDADE DE SANTIAGO DE COMPOSTELA

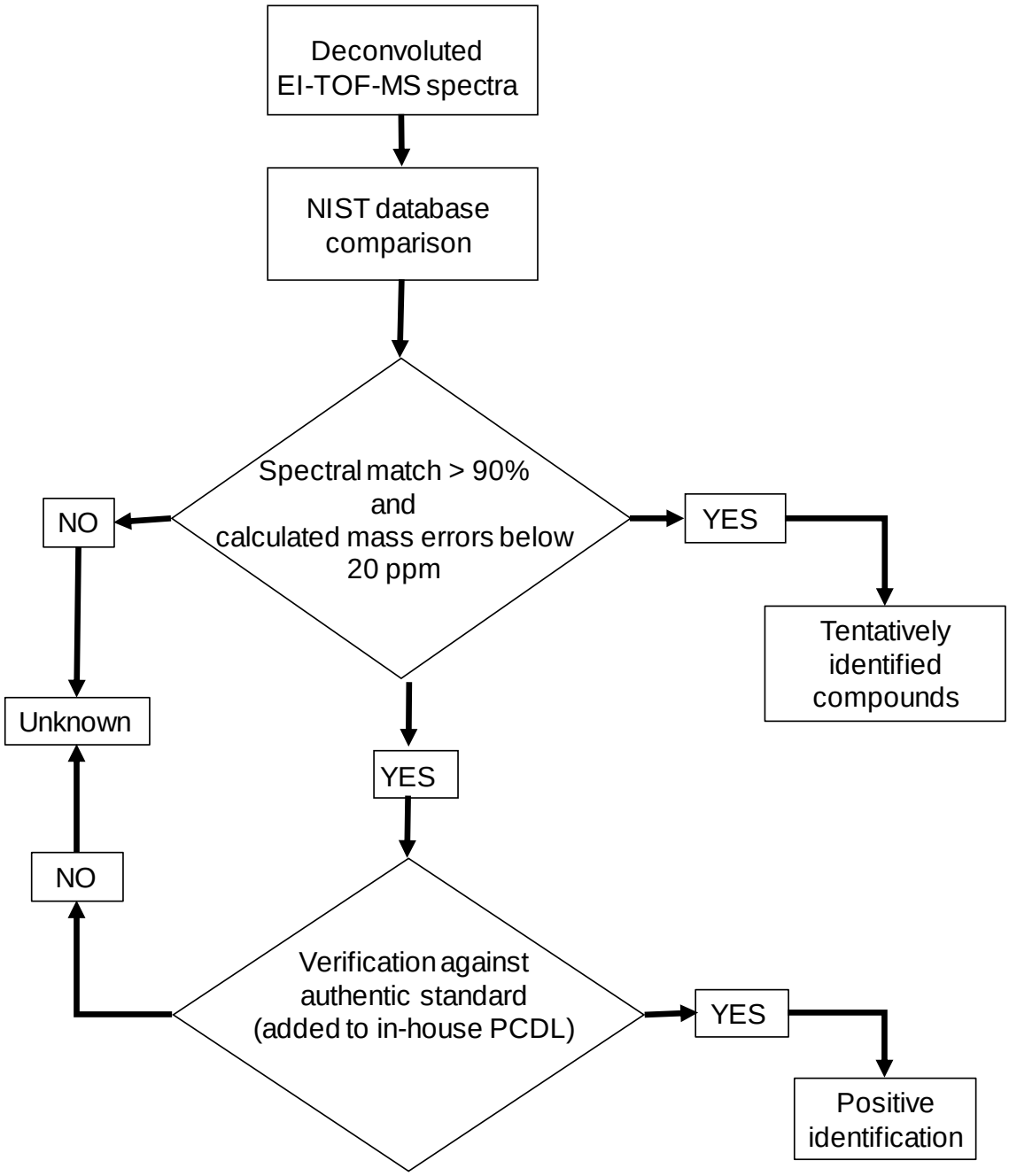


Fig. S1. Scheme of the workflow employed for non-target data mining of compounds existing in indoor air related samples.

USC UNIVERSIDADE DE SANTIAGO DE COMPOSTELA

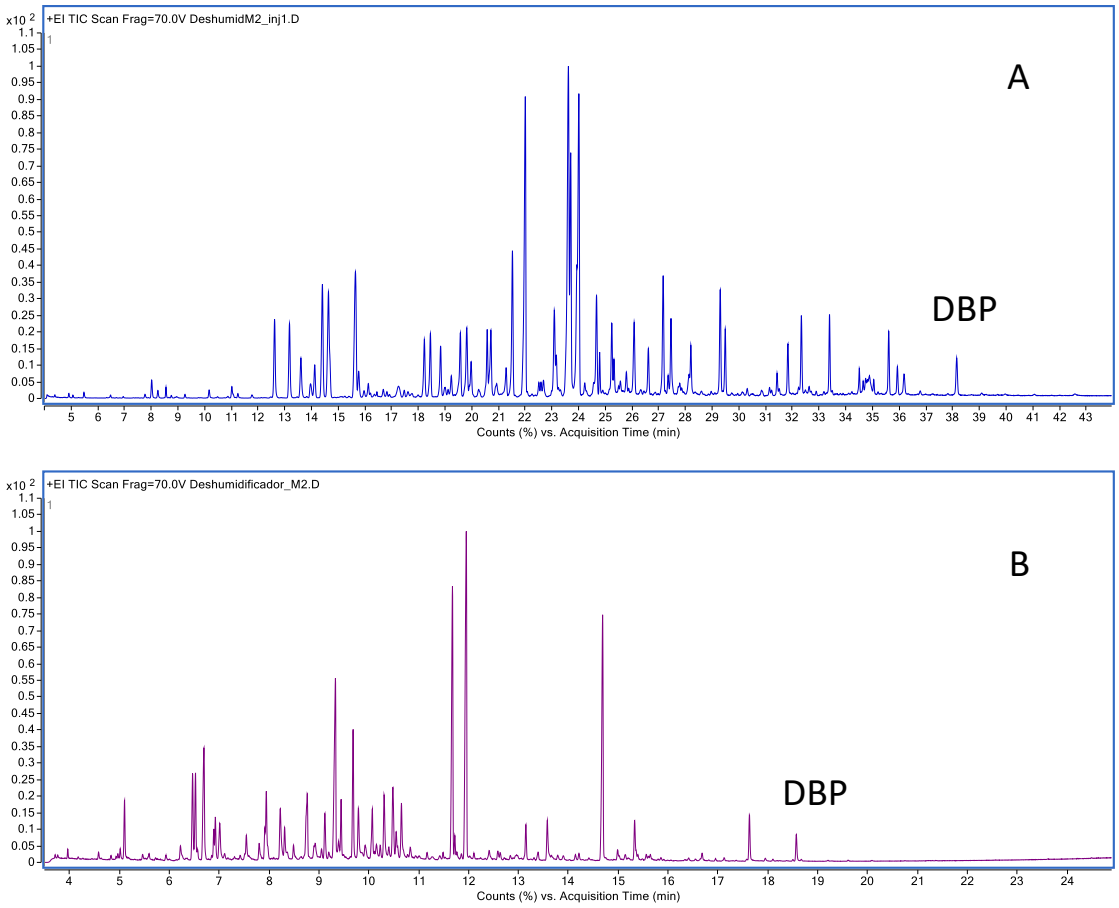


Fig. S2. GC-EI-TOF-MS chromatograms for the same SPE extract from dehumidifier water injected in the DB-WAXETR (A) and the BP-5 (B) column. DBP, dibutyl phthalate.

USC
UNIVERSIDADE DE SANTIAGO DE COMPOSTELA

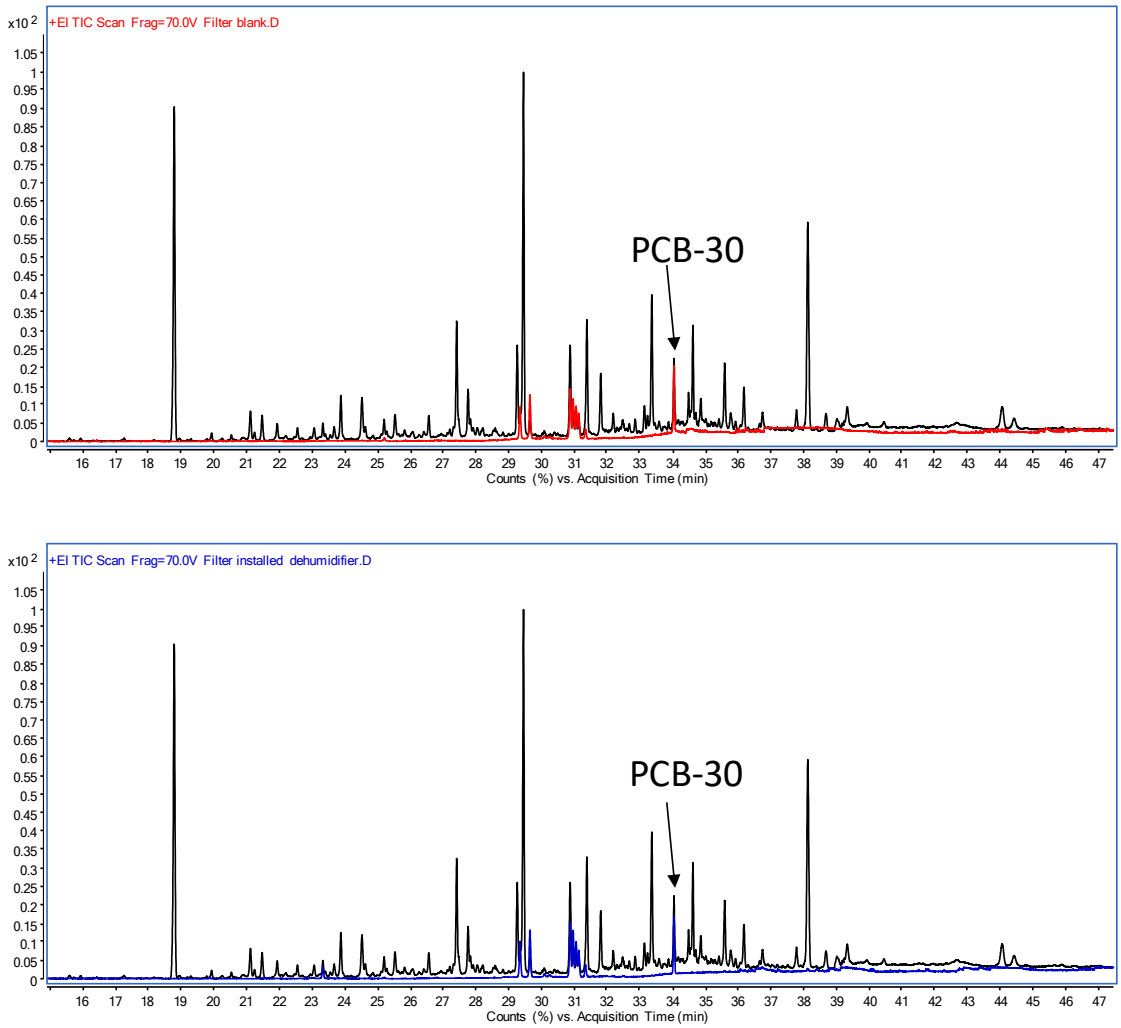


Fig. S3. Chromatograms obtained for condensed dehumidifier water (black), a blank of glass fiber filter (red), and a glass fiber filter placed before the coarse grid of the dehumidifier (blue) while collected the condensed water sample. Peaks in glass fiber filter extracts were tentatively identified as diisopropyl naphthalene isomers.

USC
UNIVERSIDADE DE SANTIAGO DE COMPOSTELA

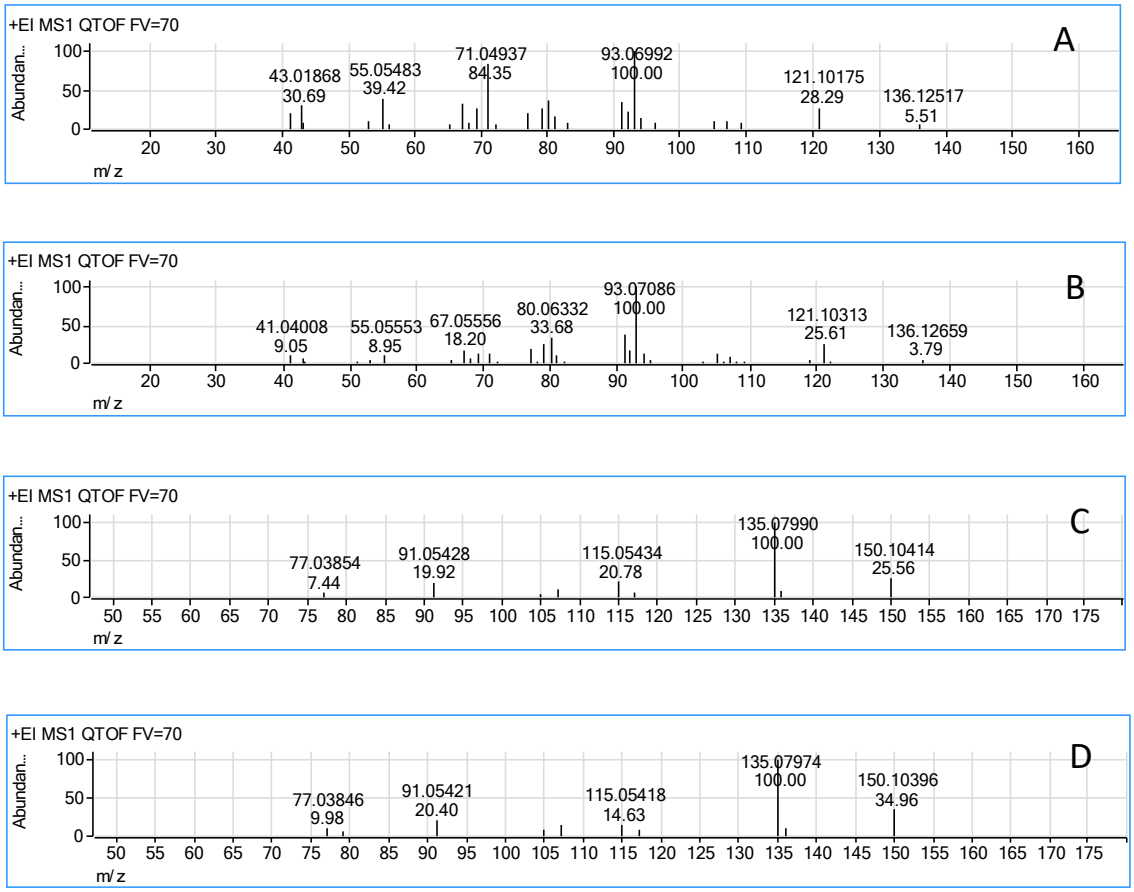


Fig. S4. Accurate EI-MS spectra for pairs of related species. A and B, Linalool ($C_{10}H_{18}O$) and Linalyl acetate ($C_{12}H_{20}O_2$). C and D, Thymol ($C_{10}H_{14}O$) and Carvacrol ($C_{10}H_{14}O$). Figures under *m/z* values correspond to the relative intensity of each ion.

USC UNIVERSIDADE DE SANTIAGO DE COMPOSTELA

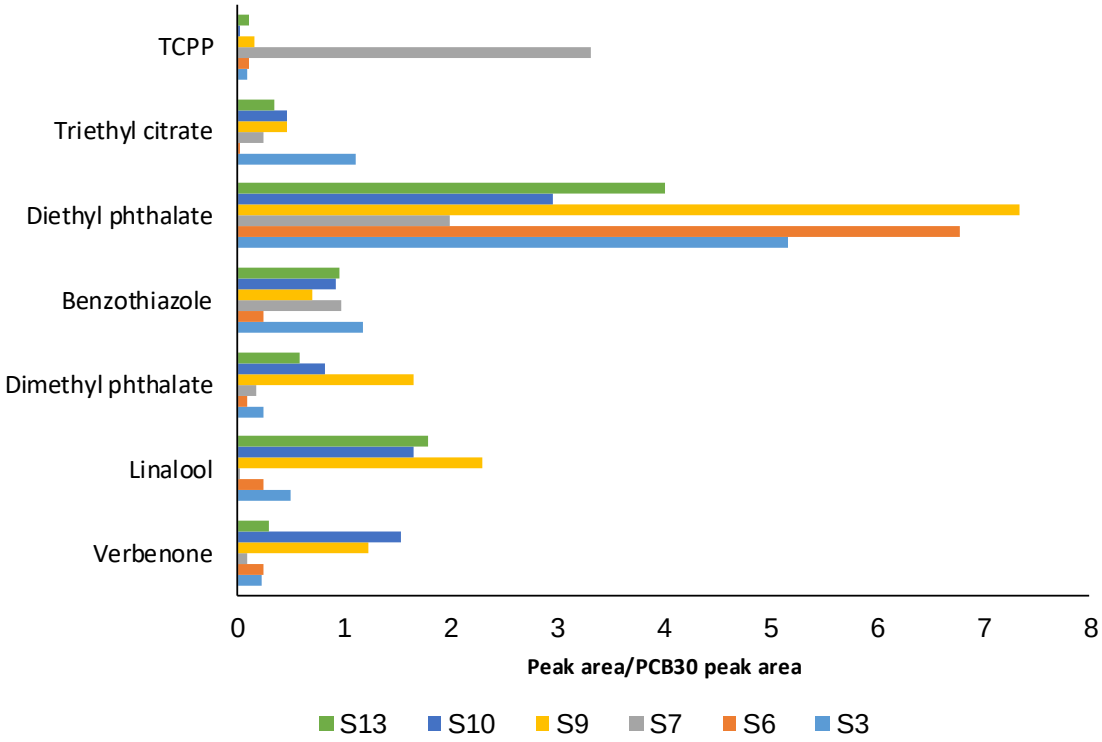


Fig. S5. Corrected responses (deconvoluted compound peak area/PCB 30 peak area) for selected compounds in the living room of different homes. Data corresponding to water samples obtained with the same dehumidifier.

USC
UNIVERSIDADE DE SANTIAGO DE COMPOSTELA

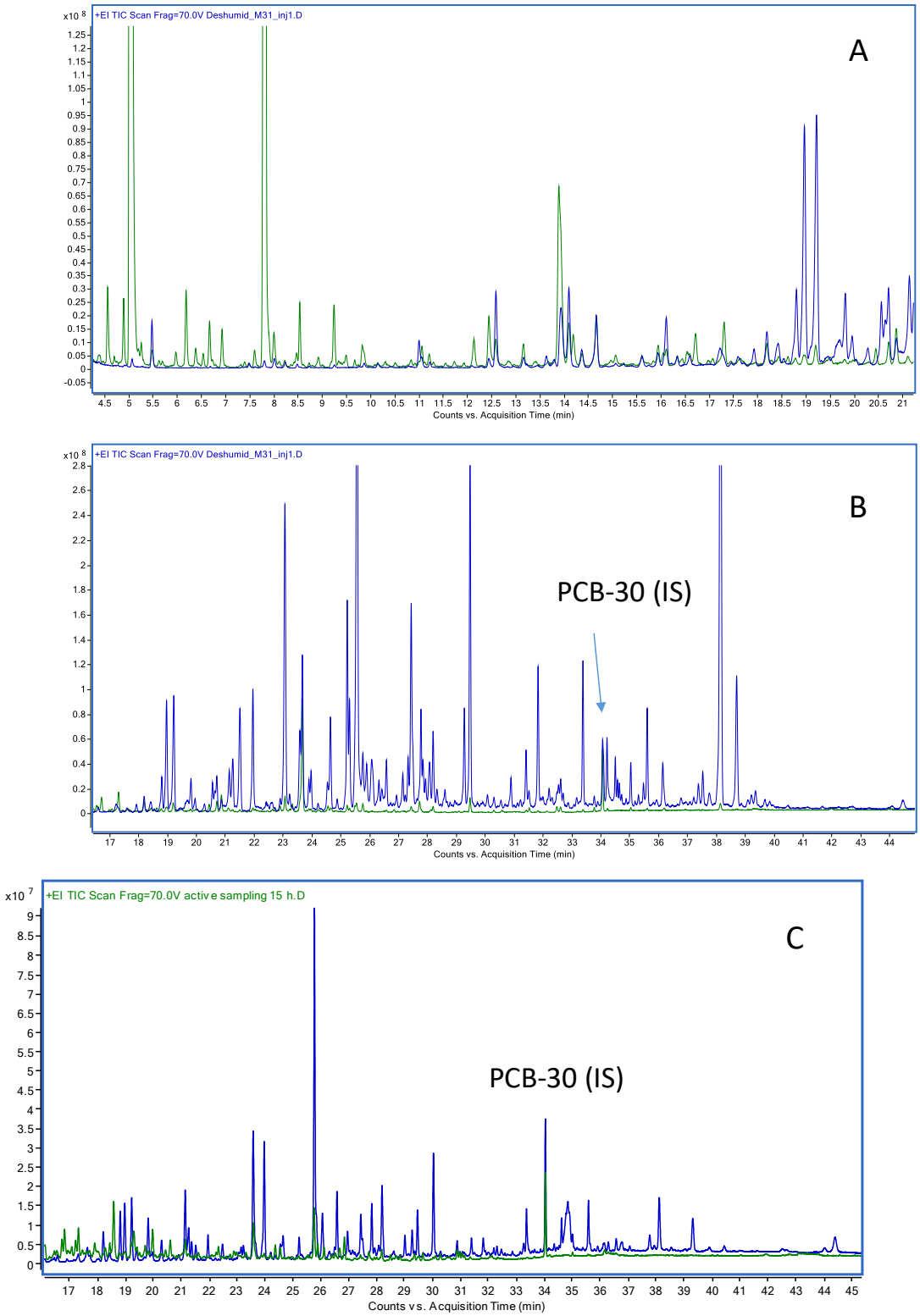


Fig. S6. GC-EI-TOF-MS chromatograms corresponding to active sampling (green) for 5 h at 16.5 L min^{-1} and the SPE extract from the dehumidifier water sample (blue) simultaneously obtained from the same room. A, retention time interval: 4-21 min. B, retention time range: 16-45 min. C, chromatograms after 15 h of active sampling (green) versus analysis of dehumidifier water (blue) obtained in a different room. Pairs of chromatograms are shown in the same scale

USC
UNIVERSIDADE DE SANTIAGO DE COMPOSTELA

USC
UNIVERSIDADE
DE SANTIAGO
DE COMPOSTELA

PUBLICATION II: PREDICTING CONCENTRATIONS OF VOLATILE AND SEMI-VOLATILE COMPOUNDS IN INDOOR AREAS THROUGH ANALYSIS OF CONDENSED WATER SAMPLES. A PROOF OF CONCEPT

M. Cobo-Golpe, M. Ramil, L. Pérez-Mayán, I. Rodríguez

Chemosphere 360 (2024) 142403
DOI: 10.1016/j.chemosphere.2024.142403

Impact factor: 8.1 (2023)
Category: Environmental sciences
Position: 32/358
Quartile: Q1

Chemosphere 360 (2024) 142403

Contents lists available at ScienceDirect

Chemosphere

journal homepage: www.elsevier.com/locate/chemosphere

Predicting concentrations of volatile and semi-volatile compounds in indoor areas through analysis of condensed water samples. A proof of concept

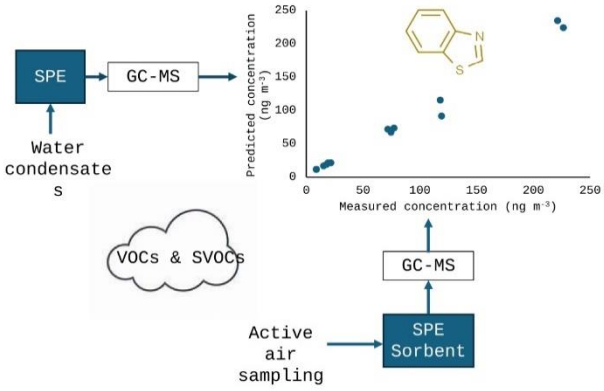
M. Cobo-Golpe [a], M. Ramil [a], L. Pérez-Mayán [b], I. Rodríguez [a,*]

[a] Department of Analytical Chemistry, Nutrition and Food Sciences, IAQBUS - Institute of Research on Chemical and Biological Analysis, Universidade de Santiago de Compostela, R/Constantino Candeira SN, 15782, Santiago de Compostela, Spain
[b] Mestrelab Research Center (CIM), Av. Barcelona 7, 15706, Santiago de Compostela, Spain

HIGHLIGHTS

- GC-MS quantification of volatile and semi-volatile species in water condensates.
- Assessment of parameters controlling concentrations in condensed water.
- Evaluation of air water partition coefficients for fourteen organic compounds.
- Prediction of concentrations in air from water condensates analysis.

GRAPHICAL ABSTRACT



ARTICLE INFO

Handling editor: Keith Maruya

Keywords:
Indoor pollutants
Air water partition coefficients
Gas chromatography
Mass spectrometry

ABSTRACT

Atmospheres from indoor areas contain a range of volatile and semi-volatile compounds to which inhabitants are exposed through breathing. Despite different qualitative approaches have been proposed for the identification of compounds associated to the vapor phase of confined areas, active sampling remains as the preferred technique when quantitative data is required. Herein, we investigate the correlations existing between concentrations in air and water condensates obtained from indoor areas. To this end, samples of both matrices were simultaneously collected and analyzed by gas chromatography mass spectrometry. After validation of sample concentration approaches for a selection of compounds, the effect of different operational conditions, and environmental variables, in their concentrations in condensed water was assessed. Levels in this matrix were hardly affected by sampling time, air flow through the dehumidifier device, and the environmental temperature and humidity. Thus, air water distribution coefficients (K_{aw}) could be estimated for fourteen out of sixteen pre-selected

* Corresponding author.
E-mail address: isaac.rodriguez@usc.es (I. Rodríguez).

https://doi.org/10.1016/j.chemosphere.2024.142403
Received 4 March 2024; Received in revised form 2 May 2024; Accepted 20 May 2024
Available online 23 May 2024
0045-6535/© 2024 The Author(s). Published by Elsevier Ltd. This is an open access article under the CC BY-NC-ND license (http://creativecommons.org/licenses/by-nc-nd/4.0/).

compounds. These values permitted a semiquantitative evaluation of their concentrations existing in air from different areas. In case of semi-volatile compounds (i.e. phenol, benzothiazole, phthalates), with log K_{aw} below −4.8, analysis of 50 mL water samples permitted to achieve lower limits of quantification than active air sampling for 3 h at a flowrate of 1 m^3 h^{-1}.

1. Introduction

The composition of air is known to play a major role in the health of the population. The vapor phase of indoor areas contains a range of volatile and semi-volatile substances related to ongoing activities, and different source emissions, from fragrance diffusers and household products (Hodshire et al., 2022; Karr et al., 2021; Temkin et al., 2023) to building materials, furniture and upholstery (Dodson et al., 2017; Salthammer et al., 2021). Limited ventilation and low contribution of photochemical processes to the degradation of organic species in confined areas contribute to create a different environment in indoor atmospheres compared to outdoors (González-Martín et al., 2021; Hernandez et al., 2020). Thus, characterization of air composition in confined areas is of interest to identify potential effects in the health of inhabitants spending significant periods of time in closed areas. In particular, inhalation of volatile and semi-volatile compounds existing in gas phase is unavoidable. As these compounds freely enter the respiratory system, they might be correlated with different diseases from allergies to asthma, including the sick-building syndrome (Idarraga et al., 2020; Veenaas et al., 2020). Eventually, compounds entering the respiratory tract might be exchanged between air and arterial blood at lungs (Jia et al., 2012).

Gas chromatography coupled to mass spectrometry (GC-MS) is the gold standard for the determination of organic compounds in air; however, this technique needs to be combined with a previous sampling step. Sample preparation methodologies applied to the analysis of chemicals in indoor air comprise active sampling, usually with retention of compounds in a solid sorbent (Balducci et al., 2022; Song et al., 2015; Wan et al., 2016); equilibrium techniques, based on diffusion of compounds from air to solid sorbent (Marć and Zabiegała, 2022; Wilford et al., 2004); and indirect approaches, involving the analysis of a substrate in contact with air (Kim et al., 2021). Among these substrates, condensed water, either obtained from central air conditioning facilities, or from portable dehumidifiers, is known to contain relevant concentrations of organic and inorganic chemicals existing in indoor areas (González-Martín et al., 2021; Roll et al., 2015). The distribution of compounds between the gas phase and condensed water is expected to be governed by their vapor pressure and water solubility. As temperature in the condenser unit of dehumidifiers, and air conditioning units, remains below that of the surrounding atmosphere, part of water vapor existing in indoor air turns into liquid phase concentrating the organic species existing in air. Qualitative studies dealing with identification of compounds dissolved in water condensates obtained from different indoor environments have already been published (Cobo-Golpe et al., 2020; Roll et al., 2015; Silva et al., 2021). On the other hand, the usefulness of this information to estimate concentrations in the vapor phase of confined areas remains unexplored.

In this context, the aim of the current study was to evaluate whether there is a correlation between the concentrations of volatile and semi-volatile compounds present in air from indoor, confined areas and those existing in condensed water samples obtained from the same environment. To this end, extracts corresponding to active sampling of air and condensed water samples, obtained using a portable, commercial dehumidifier were analyzed to determine the levels of a selection of compounds by GC combined with a time-of-flight (TOF) mass spectrometer. Efficiencies of active sampling and solid-phase extraction of condensed water were validated previously to estimate the air-water distribution coefficients (K_{aw}) under operational conditions employed in the research. The study investigates different parameters potentially affecting the K_{aw} values, and it assesses the usefulness of calculated K_{aw} for the semiquantitative determination of the levels of target compounds in a new set of samples. Advantages and limitations of water condensates analysis versus active air sampling are highlighted.

2. Material and methods

2.1. Solvents, standards, and samples

Trace analysis grade methanol and ethyl acetate were provided by Merck (Darmstadt, Germany). Ultrapure deionized water (18.2 MΩ cm^{-1}) was obtained using a Geni-U system (Rephile, Shanghai, China). Standards for a suite of semi-volatile compounds were purchased from Sigma-Aldrich (Milwaukee, WI, USA). The list of selected chemicals comprises natural origin compounds, fragrances included in the formulation of household cleaning products, and high-volume production chemicals used as plasticizers, flame retardants, and solvents, Table 1. Detection frequencies in condensed waters, obtained in a previous study (Cobo-Golpe et al., 2020), were considered to make the selection of species compiled in Table 1. Individual solutions of each compound were prepared in methanol. Further mixtures were made in ethyl acetate and stored at 4 °C.

Deuterated analogues for some of these compounds were obtained either from Sigma-Aldrich, or from Toronto Research Chemicals (North York, ON, Canada), Table S1. Individual and mixture solutions of labelled compounds were also made in methanol and ethyl acetate, respectively. Labelled compounds were added to condensed water samples before SPE extraction, and to sorbents employed for active air sampling. They were used as surrogate standards (SSs) to compensate non-quantitative recoveries and/or losses of compounds during air sampling, concentration of condensed water samples, and elution of SPE sorbents. Calibration standard solutions were prepared in ethyl acetate, at seven different concentration levels from 1 to 1000 ng mL^{-1}, with SSs maintained at 250 ng mL^{-1}.

OASIS HLB solid-phase extraction (SPE) syringes, containing 200 mg of sorbent, were obtained from Waters (Milford, MA, USA). Before use, the SPE sorbent was rinsed with MeOH followed by ultrapure water (5 mL, each). Those syringes employed for concentration of air samples were further dried using a gentle stream of dry nitrogen. Quartz glass filters (47 mm diameter, 0.7 μm cut-off limit) were purchased from Merck.

Air and condensed water samples were simultaneously obtained from indoor environments, corresponding to different rooms in private houses and offices, with the aid of a membrane pump (Vacuubrand GMBH, Wertheim, Germany) and using a portable dehumidifier, respectively. Access to sampling rooms was limited during the performed experiments (under final working conditions, the effective sampling time was limited to a maximum of 3 h) to minimize potential variations in the composition of these indoor atmospheres. Temperature and humidity levels in sampling areas were measured using an air quality monitoring multimeter purchased from Drogallega (Coruña, Spain). The temperature in the condenser of the dehumidifier was tested with a thermocouple type thermometer (Amzlab gmbh, Essen, Germany).

During active air sampling a flowmeter was installed between the SPE syringe and the entrance of the vacuum pump. The flowrate of air through the sorbent was limited to 1 m^3 h^{-1}. The open end of the SPE syringe was oriented to the floor (to prevent direct deposition of particulate matter), at a height of 0.5 m. The minimum distance between

USC UNIVERSIDADE DE SANTIAGO DE COMPOSTELA

the entrance of air in the dehumidifier and floor was also 0.5 m. Direct inputs of coarse particulate matter in the condenser of the dehumidifier was prevented with a metallic mesh (pore diameter 0.5 mm), placed in front of the fan responsible for circulating air through the system. To limit cross contamination problems between sampling sites (indoor rooms), the dehumidifier was operated in each place for 1 h and the condensed water was discarded. Thus, water collected in the pre-sampling step served to rinse the aluminium condenser and the receiver tank of the dehumidifier, preventing cross-contamination problems. This tank was rinsed twice with ultrapure water when the dehumidifier was changed to a different sampling site, and the metallic mesh was cleaned from particles using a Hoover. Sampling devices (membrane pump and dehumidifier) were operated for 90 min steps, switched off for 30 min (to extend the life of the membrane pump), and restarted until completing the desired sampling interval. Air volumes employed in the study varied from 1.5 m^3 to 5 m^3.

2.2. Efficiency of solid-phase concentration processes

The performance of the OASIS HLB sorbent for concentration of target compounds from water samples was evaluated with ultrapure water, acidified at a similar pH to that observed in condensed water (4.5 units), and spiked with target compounds at 5 ng mL^{-1}. Procedural blanks corresponded to ultrapure water spiked only with SSs (the addition level was equivalent to 250 ng mL^{-1} in the final extract). Efficiency of the retention-elution process was investigated considering water volumes from 50 mL to 300 mL. Under final working conditions, 50 mL and 2 mL were selected as the working volumes of water samples and sorbent elution solvent (ethyl acetate), respectively.

The efficiency of active air sampling on the HLB sorbent was assessed with two SPE syringes, connected in tandem. In a first series of experiments, samples (5 m^3) were passed through both sorbents. After the sampling step, they were disassembled and eluted separately. Responses for target compounds in the backward sorbent were normalized to those measured in the front one. This way, potential breakthrough problems for compounds existing in air could be identified. In a second series of experiments, efficiency of retention and elution steps were investigated by spiking the compounds in a plug of glass wool placed inside the barrel of the backward syringe. Thus, the stream of air sucked by the membrane pump volatilize and transport these compounds to the second syringe. After a given sampled air volume, the front cartridge loaded with species existing in indoor air was removed and the second one, containing glass wool, was eluted with 2 mL of ethyl acetate.

2.3. Determination conditions

Determination of compounds in the extracts from air and water samples was carried out by GC-MS, using a time-of-flight (TOF) instrument, Agilent model 7200. The system was furnished with a splitless injector and connected to the MS spectrometer equipped with an electronic ionization (EI) source. Compounds were separated in a Carbowax-type column (30 m length, i.d 0.250 mm, film thickness 0.50 μm). The transfer line and the EI source were maintained at 260 °C and 230 °C, respectively. Helium was used as carrier gas at a flowrate of 1 mL min^{-1}. Additional chromatographic and MS conditions are available elsewhere (Cobo-Golpe et al., 2020). Quantification and qualification ions for target compounds and their SSs were extracted using a mass window of 0.005 Da. Identification of compounds in the extracts from condensed water and air samples was based on retention times match with calibration standards (maximum difference 0.1 min), and response ratios

Table 1
Summary of compounds with vapor pressure values, GC-TOF-MS determination parameters, associated surrogate standards (SS), linearity and instrumental limits of quantification (LOQs).

Compound	CAS number	Vapor pressure (Pa) (25 °C)[a]	Retention time (min)	Quantification ion (Q1, *m/z*)	Qualification ion (Q2, *m/z*)	Q2/Q1 Ratio (%)	SS	R^2 (1–1000 ng mL^{-1})	LOQs (ng mL^{-1})
Cyclohexanone	108-94-1	533	9.9	98.0721	55.0179	110	Benzaldehyde-d5	0.999	5
Dihydromyrcenol	18479-58-8	16	14.0	123.116	59.0481	566	Benzophenone-d10	0.999	2.5
Camphor	76-22-2	87	15.5	152.1193	95.084	545	Benzophenone-d10	0.999	2.5
Benzaldehyde	100-52-7	160	15.7	105.0328	77.0376	97	Benzaldehyde-d5	0.999	1
Menthol	15356-70-4	8,5	18.2	123.116	95.0855	263	Menthol-d4	0.996	5
Triethyl phosphate	78-40-0	54.2/23.6	18.7	155.0453	127.0153	153	TCPP-d18	0.996	2.5
2,2,4-Trimethyl-1,3-pentanediol diisobutyrate	6846-50-0	<1.5	23.5	173.1153	71.076	400	Benzophenone-d10	0.997	1
2-Phenyl ethanol	60-12-8	9.88[b]	24.4	91.0532	122.0723	6	2-phenoxyethanol-d2	0.999	1
Benzothiazole	95-16-9	14	25.5	135.0116	108.0014	31	Benzothiazole-d4	0.998	1
Phenol	108-95-2	57	26.2	94.0423	66.0468	50	Phenol-d5	0.997	1
Methyl dihydrojasmonate	24851-98-7	0.094[b]	31.7	83.048	153.1275	24	Benzophenone-d10	0.998	1
Diethyl phthalate	84-66-2	0.28	33.2	149.0223	177.0541	12	Dibutyl phthalate-d4	0.999	1
Benzophenone	119-61-9	0.09	34.7	182.073	105.033	183	Benzophenone-d10	0.999	1
Diisobutyl phthalate	84-69-5	0.321	35.5	149.024	104.026	4	Dibutyl phthalate-d4	0.995	1
Tris (1-chloro-2-propyl) phosphate (TCPP)	13674-84-5	2.69E-03	37.9	124.9989	277.016	6	TCPP-d18	0.999	5
Dibutyl phthalate	84-74-2	3.60E-03	38.0	149.0217	121.0283	3	Dibutyl phthalate-d4	0.998	2.5

[a] Data obtained from Scifinder database.
[b] Predicted values.

UNIVERSIDADE DE SANTIAGO DE COMPOSTELA

between Q2 and Q1 ions ranging between ± 30% of average values obtained for calibration standards. Chromatographic and MS identification parameters for each compound are compiled in Table 1.

2.4. Air-water partition coefficients (K_{aw})

Air-water partition coefficients (K_{aw}), as dimensionless variables, were calculated as the ratio of concentrations measured in air (ng m^3) and those determined in condensed water (ng m^3). K_{aw} values were obtained for more than 20 pairs of samples corresponding to different indoor areas, with relative humidities above 40% and environmental temperature in the range from 16 °C to 24 °C.

3. Results and discussion

3.1. Characterization of the analytical procedure

Table 1 summarizes the determination coefficients (R^2) together with the instrumental limits of quantification (LOQs) of the GC-TOF-MS system for the selection of compounds considered in the study. The LOQs varied between 1 ng mL^{-1} and 5 ng mL^{-1}, with linear responses up to concentrations of 1000 ng mL^{-1} for each compound. For species prone to contamination problems (case of plasticizers), the instrumental LOQs were controlled by the stability of their responses in ethyl acetate employed to prepare calibration standards, and to desorb SPE sorbents used for concentration of air and water samples.

The efficiency of SPE for spiked water samples was compound dependent. Out of the initial selection of compounds, cyclohexanone could not be effectively retained by the HLB sorbent for any of the tested volumes (recoveries below 20%), due to its low affinity by the employed sorbent (breakthrough problems were noticed for every tested water volume). Other compounds that showed improved recoveries when reducing the volume of water passed through the HLB sorbent are triethyl phosphate, benzaldehyde, 2-phenyl ethanol and phenol, Table S2. In view of data compiled in Table S2, in further experiments, the volume of condensed water concentrated in the HLB sorbent was limited to 50 mL. Given aside cyclohexanone, the recoveries of the SPE process varied between 84% and 112%, with standard deviations from 2% to 9%, Table S2. Considering the linear response range of the GC-TOF-MS system, and the concentration factor (25-fold) provided by SPE step, the accurate determination of the concentrations of certain compounds in condensed water from some of the investigated areas required dilution of this extract. As regards minimum detectable values, they ranged from 0.04 ng mL^{-1} to 0.2 ng mL^{-1}, referred to the water matrix.

Respecting sorption efficiencies during air sampling, some volatile alcohols (identified in the GC-TOF-MS chromatograms corresponding to concentration of 5 m^3 of indoor air) were poorly retained by the HLB sorbent. Some examples are tetrahydrolinalool, 2-ethyl-1-hexanol and 1-octanol. Breakthrough values for these compounds accounted up to 30%. Thus, despite the GC-TOF-MS records for condensed water samples showed the presence of these species, the employed methodology did not allow to calculate the values of their K_{aw}. Less volatile compounds, as the plasticizer 2,2,4-trimethyl-1,3-pentanediol diisobutyrate were also found in the backward cartridge; however, the percentage of breakthrough was lower than 10% during concentration of 5 m^3 of air. Table 2 summarizes recoveries obtained for the initial selection of compounds spiked in a plug of glass wool located between the 1st and the 2nd SPE syringe after active sampling of 5 m^3 of air. This setup prevents inputs of compounds existing in the atmosphere of the sampling room; moreover, it guarantees continuous release of volatilized compounds in the sorbent contained in second SPE syringe. Experiments were carried out in triplicate, at two different addition levels, equivalent to concentrations in air of 200 ng m^{-3} and 40 ng m^{-3}, respectively. The concentrations of selected compounds in the room where these experiments were carried out varied from non-detected to more than 200 ng m^{-3} (values obtained for desorption of the front SPE syringe used in this series of experiments), Table S3. Despite the above reported breakthrough problems for 2,2,4-trimethyl-1,3-pentanediol diisobutyrate, acceptable recoveries were obtained for this compound. In case of cyclohexanone low recoveries (higher addition level) or high standard deviations (lower addition level) were observed, Table 2. Thus, this compound was excluded definitively from the selection of target compounds. Moreover, in further series of extractions, the volume of air passed through the HLB sorbent was limited to 3 m^3.

Table 2
Efficiency of compounds retention on the HLB sorbent during sampling of 5 m^3 of indoor air (flow rate 1 m^3 h^{-1}), n = 3 replicates.

Recoveries (%)	Addition level 200 ng m^{-3}		Addition level 40 ng m^{-3}	
	Retention efficiency (%)	SD	Retention efficiency (%)	SD
Cyclohexanone	53.6	4.2	94.2	20.4
Dihydromyrcenol	86.6	3.1	100.9	3.4
Camphor	80.5	2.2	98.1	4.0
Benzaldehyde	92.0	11.6	99.9	12.0
Menthol	89.6	2.2	98.7	0.6
Triethyl phosphate	82.4	1.3	96.0	4.0
2,2,4-Trimethyl-1,3-pentanediol diisobutyrate	96.8	5.4	122.4	14.6
2-Phenyl ethanol	96.4	8.3	120.0	13.1
Benzothiazole	96.9	11.3	95.4	6.0
Phenol	100.0	8.1	119.2	13.6
Methyl dihydrojasmonate	93.7	7.8	114.0	15.3
Diethyl phthalate	96.7	9.6	104.8	7.8
Benzophenone	94.7	6.8	114.0	9.6
Diisobutyl phthalate	94.2	6.3	136.0	8.0
TCPP	88.3	9.1	104.0	5.0
Dibutyl phthalate	84.1	1.9	116.0	3.0

Considering the instrumental LOQs compiled in Table 1, and the ratio between the volume of air (3 m^3) and that corresponding to the extract from the SPE cartridge (2 mL), the active sampling method showed a linear response range comprised between 0.7 ng m^{-3} and 667 ng m^{-3}.

3.2. Parameters affecting concentrations in water condensates

Levels of volatile and semi-volatile compounds transferred from indoor air to condensed water might be potentially affected by a significant number of variables, which could impair the estimation of K_{aw} values. The portable dehumidifier used in this study is furnished with a 0.5 mm mesh placed in front of the condenser element. Thus, particles below this size might end in the condensed water phase, increasing the concentration of certain compounds, such as high-volume production, semi-volatile species reported at high concentrations in indoor dust as it is the case of the organophosphate tris (1-chloro-2propyl)phosphate (TCPP) (Dou and Wang, 2023), vulcanization agents (i.e. benzothiazole) (Wan et al., 2016), and phthalates (Zhu et al., 2023). Analysis of 50 mL aliquots of filtered (using a 0.7 μm glass wool filter) and non-filtered fractions of the same condensed water sample lead to equivalent concentrations for all the investigated compounds, Table S4. Moreover, normalized responses obtained for desorption of filters (data obtained for filtration of 500 mL of condensates) ranged between 0.1% and 2.4% of those corresponding to SPE of filtered water, Table S5. This finding is in good agreement with the earlier data published by Roll and co-workers ((Roll et al., 2015)) supporting the fact that condensate water samples do not contain significant levels of particles above 0.7 μm. Additional studies have also confirmed the absence of particulate matter below 2.5 μm in condensed water from portable dehumidifiers (González-Martín et al., 2021). Thus, water samples were submitted to SPE concentration without filtration.

The volume of water obtained with a portable dehumidifier from a confined area depends on the operating time, as well as on the air

USC UNIVERSIDADE DE SANTIAGO DE COMPOSTELA

temperature and the relative humidity. Assuming that, temperature remains constant during sampling, the relative humidity of air decreases with the increase in the condensed volume of water. Thus, too long operational times might lead to more diluted water samples, if the concentrations of compounds in indoor areas are not under equilibrium conditions. To investigate the potential effect of this parameter, three consecutive condensed water samples were obtained from the same room (office during non-working days) for two periods of 4 h followed by a later one of 12 h (overnight). The experiment was repeated three times, in alternate days of the same week. On average, the volume of water corresponding to 1st and 2nd samplings was 500 mL, whilst up to 1500 mL were recovered operating the dehumidifier overnight. Table 3 summarizes the average normalized responses for each compound in the 2nd and 3rd sampling steps versus those measured in the 1st one. In general, normalized responses remained around 100%, except for triethyl phosphate. In this case, the normalized response increased in the consecutive samplings from the same room. It is worth noting that, during the study, neither the temperature nor the humidity of the room were controlled. On the other hand, the office was closed during the experiment, except a short period of time for collection of air sorbents and water condensates.

The volume of condensed water collected from an indoor environment might also depend on the flow of air through the condenser of the dehumidifier. Despite the system employed in this research not allowing to control this flowrate, the fan of the equipment can be operated at two different rotation speeds. Concentrations measured in water from the same room operating the fan at low and high speed are given as supplementary information, Table S6. The absolute value of relative differences for concentrations in water samples obtained under the two conditions remained below 20%, except in case of triethyl phosphate. For this compound, the concentration in the sample obtained operating the fan at the maximum speed was 33% higher than that obtained at low speed. Considering these data and those in Tables 3 and it cannot be excluded that the employed water dehumidifier device contributes to the presence of triethyl phosphate in condensed water. That is, there is a suspected significant contamination of condensed water with triethyl phosphate coming from any element of the portable dehumidifier. Whatever the exact source of the problem, this compound was no longer considered due to uncertainties associated to its concentrations in the condensed water matrix.

Environmental temperature was deemed to be a relevant parameter potentially affecting the levels of compounds in air from indoor environments (vapor phase concentrations of compounds emitted from furniture and building materials are expected to increase with temperature), but also the temperature of the condenser in the dehumidifier system. Within the range of temperatures from 16 °C to 29 °C, that measured in the same point of the condenser unit of the dehumidifier changed from 5 °C to 8 °C. That is, condenser temperature raised 1 °C when the environmental temperature increased 5 °C. Obviously, this change might affect distribution equilibrium between air and water. Fig. 1 summarizes experimental concentrations measured in air (ng m^{-3}) and condensed water (ng mL^{-1}) from the same room maintained at two different temperatures: 24 °C and 18 °C. Three consecutive sampling experiments were carried out at each temperature. For the most volatile compounds (see vapor pressure values compiled in Table 1) concentrations in air remained unaffected for variations in the indoor temperature, whilst higher levels of semi-volatile compounds (particularly phthalates and TCPP) were found when the environmental temperature increased from 18 °C to 24 °C, Fig. 1A. Relative concentrations in condensed water followed a similar trend, Fig. 1B and C. Thus, environmental temperature variations of 6 °C played a minor effect in the distribution of compounds between air and condensed water.

Table 3
Relative responses for consecutive samples of condensed water obtained from same room (18 m^2 office) for 4 h (1st and 2nd sampling) and 12 h (3rd sampling). Data corresponding to three series of experiments in the same week. Normalized values to those obtained in the 1st sample of each series.

Compound	Second sampling		Third sampling	
	Mean	SD	Mean	SD
Dihydromyrcenol	75.3	9.2	115.0	2.8
Camphor	96.0	14.0	92.7	15.3
Benzaldehyde	90.3	12.9	94.7	1.2
Menthol	87.7	14.8	91.3	9.1
Triethyl phosphate	131.7	7.2	149.0	15.5
2,2,4-Trimethyl-1,3-pentanediol diisobutyrate	96.0	23.5	94.3	17.5
2-Phenyl ethanol	93.7	8.0	90.3	9.5
Benzothiazole	93.7	15.0	91.0	4.6
Phenol	102.0	8.2	97.7	6.8
Methyl dihydrojasmonate	92.0	11.5	97.0	20.4
Diethyl phthalate	104.7	1.5	103.3	5.9
Benzophenone	105.0	4.6	104.7	7.5
Diisobutyl phthalate	105.3	2.5	104.3	0.6
TCPP	86.3	10.2	83.7	19.6
Dibutyl phthalate	105.3	0.6	103.7	2.1

3.3. Estimation of air water distribution coefficients

The unitless values for the air water distribution coefficients (K_{aw}) were calculated considering two different sampling periods of 3 h and 1.5 h, equivalent to concentrated volumes of air of 3 m^3 and 1.5 m^3, respectively. Pairs of samples (air and condensed water) were collected from different areas (office, bedroom, living room) at the beginning of autumn (end September-beginning October). The surface of sampled areas varied from 12 m^2 to 36 m^2 (equivalent to total air volumes from 31 m^3 to 94 m^3). Temperature was not controlled during the sampling process providing that it remained between 18 °C and 24 °C. Same comment is valid for the relative humidity in air, keeping in mind that the employed dehumidifier is designed to stop working when the relative humidity falls below 30%. Access to sampling rooms was restricted during the experiments. Table 4 summarizes the average values of K_{aw} in the two series of experiments, indicating the pairs of samples (n) considered for calculations. In some places, some of the selected compounds remained either below procedural LOQs, or very close to responses obtained for blanks (desorption of cleaned SPE cartridges and SPE of 50 mL of ultrapure water). This fact explains the different number of pairs of values as function of the considered compound. The Box Whisker plots for decimal logarithmic values of K_{aw} (Log K_{aw}) in both series of experiments are given as supplementary information, Fig. S1. As a general statement, similar mean and median values were attained for both series of experiments. Thus, a global mean value of Log K_{aw} was calculated with the associated standard deviation for the whole set of pairs of samples, Table 4. The pairs of samples employed to calculate the overall Kaw compiled in Table 4 ranged between 20 and 24.

The Log K_{aw} values varied between −4.04 for benzaldehyde to −6.31 for the chlorinated flame retardant TCPP. That is, the concentrations of compounds in condensed water stayed between 10^4 and 10^6 times higher than those in vapor phase. As a general statement, the calculated values of Log K_{aw} decreased with vapor pressures of tested compounds (Table 1). The lower the vapor pressure of a given compound the higher the affinity for the sample of condensed water. Comparison of Log K_{aw} values obtained in this study with EPA predicted dimensionless values of the Henry constant at 6 °C showed a reasonable agreement for phenol and diethyl phthalate, with average obtained values of Log Kaw of −5.83 ± 0.05 and −6.05 ± 0.12 (Table 4), versus −5.44 and −5.70 corresponding to the logarithmic values of the dimensionless Henry constant ("EPA, On-line Tools for site assessment calculation. Estimated Henry's Law Constants," n.d.). On the other hand, the calculated Log K_{aw} values of dibutyl phthalate (−6.11 ± 0.15) remained two orders of magnitude above the logarithm of the Henry constant compiled in the EPA database (−8.51) ("EPA On-line Tools for site assessment calculation. Estimated Henry's Law Constants," n.d.).

USC UNIVERSIDADE DE SANTIAGO DE COMPOSTELA

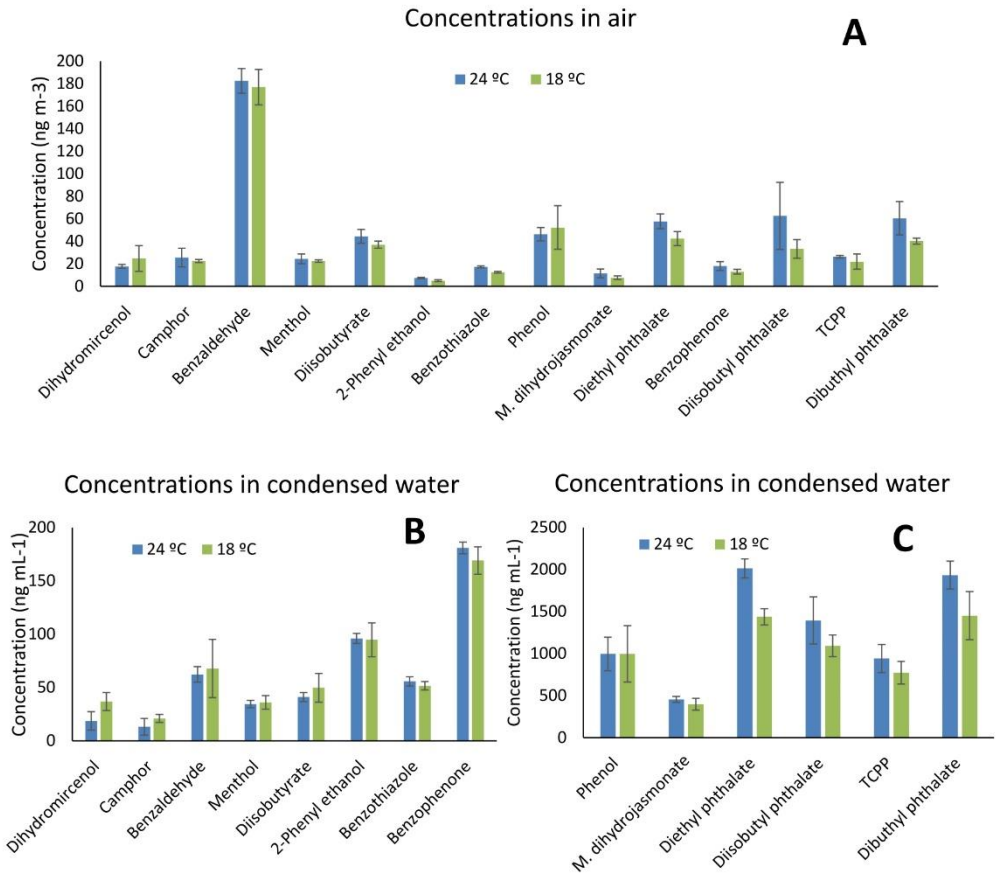


Fig. 1. Effect of environmental temperature on concentrations determined in air using active sampling (ng m^{-3}) (A), and those in condensed water (ng mL^{-1}) (B and C) obtained from same indoor area, n = 3 replicate sampling campaigns.

Table 4
Mean values of air water distribution coefficients (K_{aw}) with their relative standard deviations (RSDs) for two different air volumes, and overall decimal logarithmic coefficients (Log K_{aw}). N, represents the pairs of data used to calculate K_{aw} for each volume of air.

Compound	3 m^3			1.5 m^3			Overall values	
	Mean	RSD	n	Mean	RSD	n	Log K_{aw}	SD
Dihydromyrcenol	3.08E-05	18%	13	3.44E-05	13%	8	−4.50	0.08
Camphor	5.94E-05	13%	12	6.81E-05	11%	8	−4.20	0.06
Benzaldehyde	9.13E-05	20%	12	9.67E-05	17%	8	−4.04	0.08
Menthol	1.84E-05	17%	13	1.84E-05	22%	10	−4.74	0.08
2,2,4-Trimethyl-1,3-pentanediol diisobutyrate	4.16E-05	24%	13	4.67E-05	15%	8	−4.37	0.10
2-Phenyl ethanol	9.14E-07	27%	14	1.02E-06	24%	10	−6.03	0.11
Benzothiazole	7.48E-06	12%	14	7.86E-06	12%	10	−5.12	0.05
Phenol	1.48E-06	14%	12	1.48E-06	9%	10	−5.83	0.05
Methyl dihydrojasmonate	8.32E-07	29%	14	8.90E-07	17%	10	−6.08	0.10
Diethyl phthalate	8.97E-07	33%	13	9.46E-07	28%	10	−6.05	0.12
Benzophenone	3.47E-06	12%	13	3.62E-06	15%	9	−5.45	0.07
Diisobutyl phthalate	1.35E-06	38%	14	1.43E-06	38%	10	−5.88	0.14
TCPP	5.87E-07	40%	14	5.50E-07	57%	9	−6.31	0.28
Dibutyl phthalate	8.11E-07	37%	13	8.67E-07	40%	7	−6.11	0.15

3.4. Validation of predictions

The reliability of predicted air concentrations derived from Log K_{aw} compiled in Table 4 was assessed considering a new sampling campaign, in seven different indoor areas. In this case, samples were taken during wintertime, from rooms with surfaces comprised between 7 m^2 and 70 m^2. With the only exception of site S6, two consecutive samplings were carried out in the same room. Main characteristics of the sampling spaces, including a description of furniture, are given as supplementary information, Table S7. Predicted and measured air concentrations (ng m^{-3}), together with slopes and determination coefficients (R^2) of predicted versus measured values are given in Table S8. Slope values ranged

USC UNIVERSIDADE DE SANTIAGO DE COMPOSTELA

from a minimum of 0.85 for benzaldehyde (R^2 0.74) to 1.19 for dihydromyrcenol (R^2 0.995). Thus, the average error for predicted versus measured concentrations varied from −15% to +19%. The quality of the fitting between predicted versus measured concentrations, estimated with the R^2, depended not only on the match of values for each pair or samples, but also on the range of concentrations determined among the

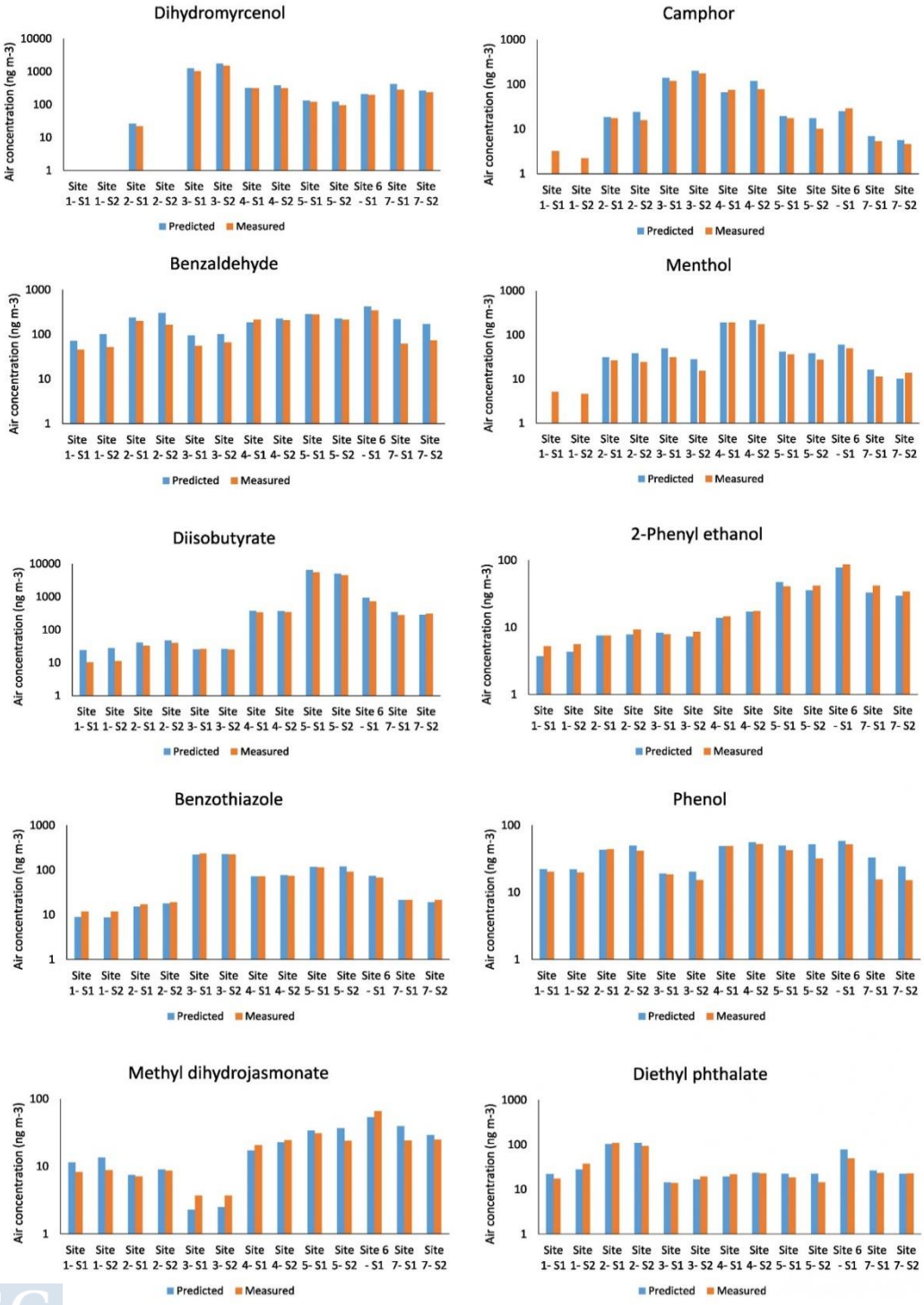


Fig. 2. Logarithmic plots of predicted versus measured concentrations of volatile and semi-volatile compounds in indoor air from seven different sites.

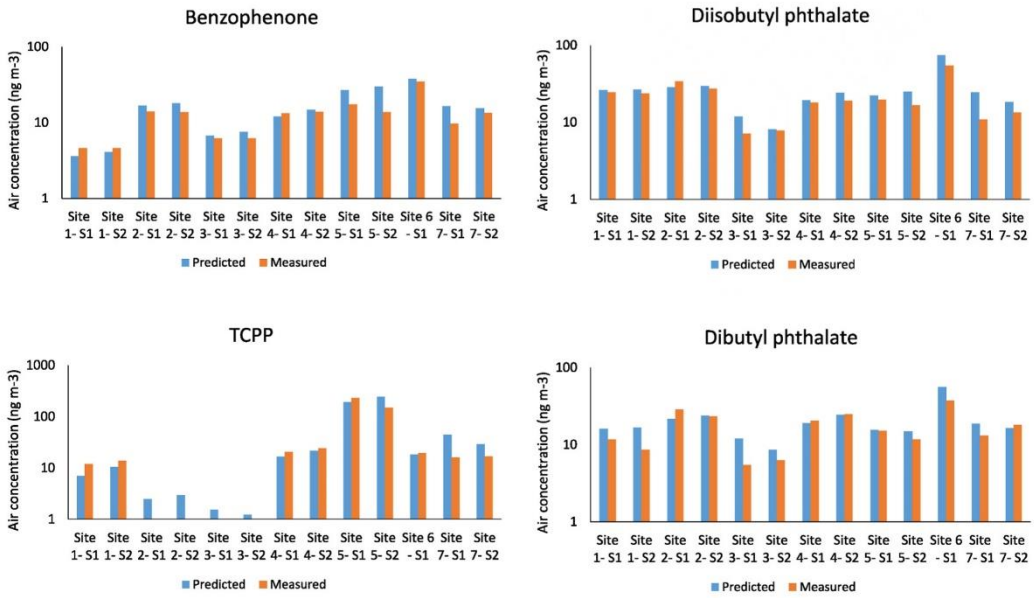


Fig. 2. (*continued*).

different sites. Fig. S2 illustrates this effect with data corresponding to dihydromyrcenol, with measured concentrations in the range from non-detected up to 1500 ng m^3 (Fig. S2A), and those of phenol with a narrow distribution of values between 15 ng m^3 and 53 ng m^3 (Fig. S2B).

Chart bars of predicted and measured concentrations (ng m^3) for the set of samples involved in the validation study are given in Fig. 2. At sampling site S1, camphor and menthol could be measured in the concentrated sample of air at values between 2 ng m^3 and 5 ng m^3, but not in the condensed water samples obtained from same sites, since estimated values are below to their LOQs (i.e. 0.031 ng mL^{-1} estimated for camphor in condensed water from 2 ng m^{-3} measured in air, versus a LOQ of 0.1 ng mL^{-1} for this compound in water using a 25-fold concentration factor). On the other hand, analysis of condensed water predicted concentrations of TCPP in air from sites S2 and S3 in the range of 1.3–2.5 ng m^3, whilst the procedural LOQ of the compound for active sampling of 3 m^3 of air corresponds to 3.3 ng m^3. For the rest of compounds, a reasonable agreement was found between predicted concentrations and those determined using active sampling.

Ranges of concentrations shown in Fig. 2 are in agreement with those obtained in previously published studies dealing with analysis of indoor air. As an example, Wan and co-workers (Wan et al., 2016) reported levels of benzothiazole in the range from 6 ng m^3 to 139 ng m^3 versus 8 ng m^3 to 220 ng m^3 given in Fig. 2. As regards the three phthalates considered in this research, a maximum concentration of 110 ng m^3 was observed for diethyl phthalate versus levels up to 1010 ng m^3 found in offices from China (Song et al., 2015). In case of fragrances median levels of benzaldehyde and camphor reported in previous studies were 170 ng m^3 (Warburton et al., 2023) and 157 ng m^3 (Balducci et al., 2022), respectively. Both values are within the range of concentrations reported in Fig. 2.

3.5. Limitations and advantages of condensed water analysis

Using condensed water samples to estimate concentrations of volatile compounds in indoor air avoids the need of relatively expensive, usually noisy, aspiration pumps required in active sampling methodologies. On the other hand, considering GC-MS as the standard technique for analysis of volatile and semi-volatile compounds, it is obvious that compounds need to be extracted from the water phase before injection in the chromatography system. Moreover, domestic dehumidifiers are programmed to operate at relative humidity values above 30%, as lower values are considered unhealthy. Given aside these issues, under conditions reported in this research (active sampling of 3 m^3 of air versus concentration of 50 mL of condensed water), direct air sampling will provide higher responses for compounds with values of Log K_{aw} higher than −4.78 (lower absolute values) than analysis of water condensates. This situation corresponded to the most volatile of the investigated compounds, Table 1. On the other hand, for semi-volatile species, with Log K_{aw} values lower than −4.78 (higher absolute values), analysis of water condensates permits achieving lower procedural LOQs than active sampling. If the concentrated volume of air is reduced from 3 m^3 to 1.5 m^3, the above threshold is reduced to −4.47. Fig. 3 shows the chromatograms for quantification (Q1) and qualification (Q2) ions of benzophenone (Log K_{aw} – 5.45), Fig. 3A, and phenol (Log K_{aw} – 5.83), Fig. 3B, corresponding to analysis of water condensates (50 mL of sample concentrated to 2 mL) and active sampling of 3 m^3. The improved response, and signal to noise ratio for peaks corresponding to water condensates versus active sampling is evident.

4. Conclusions

The existence of relatively stable correlations between concentrations existing in vapor phase and levels accumulated in condensed water samples has been demonstrated for a suite of organic compounds with vapor pressures ranging from 160 Pa (case of benzaldehyde) to 2.69 10^{-3} Pa (TCPP). Under operational conditions employed in this research, values of air-water partition coefficients were calculated. They were independent on sampling time and air flow through the condenser unit of the dehumidifier. Moreover, they succeeded to predict concentrations existing in air samples from indoor spaces with surfaces in the range from 7 m^2 to 70 m^2, without a rigorous control of environmental temperature (values from 16 °C to 24 °C). A refined evaluation of K_{aw} values would require an accurate control of the temperature in the condenser unit of dehumidifiers, independent of spatial and temporal variations (from 15 °C to 30 °C) of that existing in the sampled areas, and the use of a mass flow controlled to have an accurate value of the volume

USC UNIVERSIDADE DE SANTIAGO DE COMPOSTELA

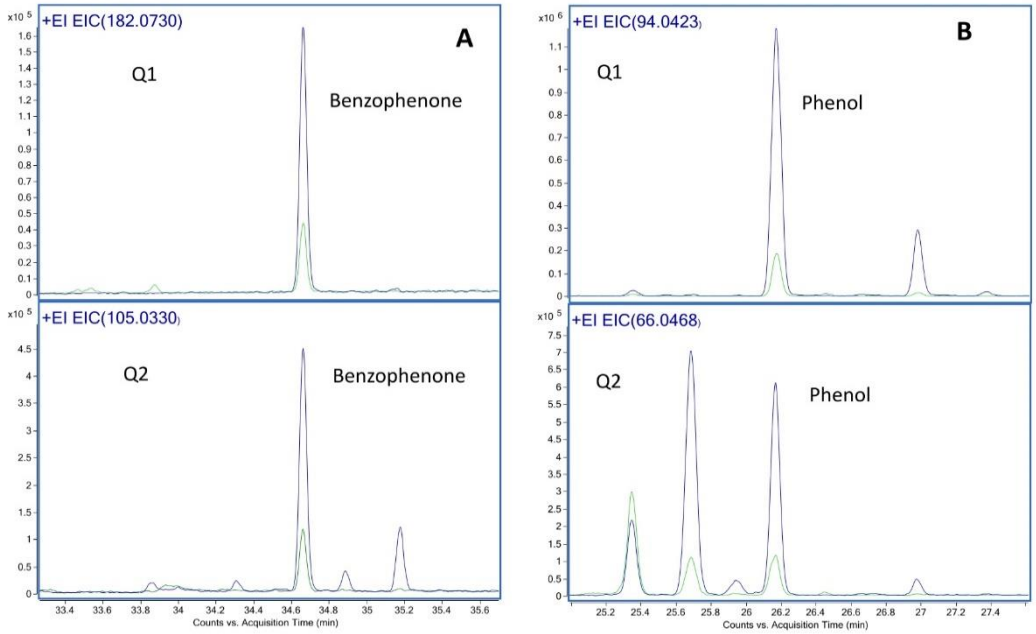


Fig. 3. GC-TOF-MS chromatograms for the quantification (Q1) and qualification (Q2) ions of benzophenone (A) and phenol (B) in water condensates (50 mL concentrated to 2 mL, blue trace) and air samples (3 m^3 passed through a SPE cartridge, green trace). Mass extraction window 0.005 Da. Measured air concentrations 5.7 ng m^{-3} and 13.0 ng m^{-3} for benzophenone and phenol, respectively.

of air passed through the SPE sorbent. Furthermore, replacing the polymeric housing of conventional dehumidifiers by metallic surfaces is highly advisable to prevent contamination of water samples with additives released from the device. To sum up, despite some technical limitations of the employed dehumidifier, results achieved in the manuscript might be considered as the conceptual basis to predict concentrations of organic semi-volatile species in confined areas through analysis of condensed water samples.

CRediT authorship contribution statement

M. Cobo-Golpe: Writing – review & editing, Writing – original draft, Methodology, Investigation. **M. Ramil:** Writing – review & editing, Supervision, Methodology, Funding acquisition. **L. Pérez-Mayán:** Writing – review & editing, Funding acquisition, Data curation. **I. Rodríguez:** Writing – review & editing, Writing – original draft, Supervision, Project administration, Funding acquisition, Conceptualization.

Declaration of competing interest

The authors declare that they have no known competing financial interests or personal relationships that could have appeared to influence the work reported in this paper.

Data availability

Data will be made available on request.

Acknowledgements

Economic support from project ED431C2021/06, from Xunta de Galicia, co-financed the EU FEDER program, is acknowledged. M.C. thanks a FPU contract to the Spanish Ministry of Science and Innovation. L.P.M. acknowledges funds received from Galician Innovation Agency, Xunta de Galicia, through project 001_IN853D-2022.

Appendix A. Supplementary data

Supplementary data to this article can be found online at https://doi.org/10.1016/j.chemosphere.2024.142403.

References

Balducci, C., Cerasa, M., Avino, P., Ceci, P., Bacaloni, A., Garofalo, M., 2022. Analytical determination of allergenic fragrances in indoor air. Separations 9, 99. https://doi.org/10.3390/separations9040099.

Cobo-Golpe, M., Ramil, M., Cela, R., Rodríguez, I., 2020. Portable dehumidifiers condensed water: a novel matrix for the screening of semi-volatile compounds in indoor air. Chemosphere 251, 126346. https://doi.org/10.1016/j.chemosphere.2020.126346.

Dodson, R.E., Udesky, J.O., Colton, M.D., McCauley, M., Camann, D.E., Yau, A.Y., Adamkiewicz, G., Rudel, R.A., 2017. Chemical exposures in recently renovated low-income housing: influence of building materials and occupant activities. Environ. Int. 109, 114–127. https://doi.org/10.1016/j.envint.2017.07.007.

Dou, M., Wang, L., 2023. A review on organophosphate esters: physiochemical properties, applications, and toxicities as well as occurrence and human exposure in dust environment. J. Environ. Manag. 325, 116601 https://doi.org/10.1016/j.jenvman.2022.116601.

EPA On-line Tools for site assessment calculation. Estimated Henry's Law Constants [WWW Document], n.d. URL https://www3.epa.gov/ceampubl/learn2model/part-two/onsite/esthenry.html (accessed 2.27.24).

González-Martín, J., Kraakman, N.J.R., Pérez, C., Lebrero, R., Muñoz, R., 2021. A state–of–the-art review on indoor air pollution and strategies for indoor air pollution control. Chemosphere 262, 128376. https://doi.org/10.1016/j.chemosphere.2020.128376.

Hernandez, G., Wallis, S.L., Graves, I., Narain, S., Birchmore, R., Berry, T.A., 2020. The effect of ventilation on volatile organic compounds produced by new furnishings in residential buildings. Atmos. Environ. X 6, 100069. https://doi.org/10.1016/j.aeaoa.2020.100069.

Hodshire, A.L., Carter, E., Mattila, J.M., Ilacqua, V., Zambrana, J., Abbatt, J.P.D., Abeleira, A., Arata, C., Decarlo, P.F., Goldstein, A.H., Ruiz, L.H., Vance, M.E., Wang, C., Farmer, D.K., 2022. Detailed investigation of the contribution of gas-phase air contaminants to exposure risk during indoor activities. Environ. Sci. Technol. 56, 12148–12157. https://doi.org/10.1021/acs.est.2c01381.

Idarraga, M.A., Guerrero, J.S., Mosle, S.G., Miralles, F., Galor, A., Kumar, N., 2020. Relationships between short-term exposure to an indoor environment and dry eye (De) symptoms. J. Clin. Med. 9, 1316. https://doi.org/10.3390/jcm9051316.

UNIVERSIDADE DE SANTIAGO DE COMPOSTELA

Jia, C., Yu, X., Masiak, W., 2012. Blood-air distribution volatile organic compounds. Sci. Total Environ. 419, 225–232. https://doi.org/10.1016/j.scitotenv.2011.12.055.

Karr, G., Nicolas, M., Maupetit, F., Ramel, M., 2021. Cleaning product emissions and indoor built environments: exposure and health risk assessments from experiments under realistic indoor conditions. Build. Environ. 206, 108384 https://doi.org/10.1016/j.buildenv.2021.108384.

Kim, K., Shin, H.M., Wong, L., Young, T.M., Bennett, D.H., 2021. Evaluating couch polyurethane foam for a potential passive sampler of semivolatile organic compounds. Chemosphere 271, 129349. https://doi.org/10.1016/j.chemosphere.2020.129349.

Marć, M., Zabiegała, B., 2022. Unconventional and user-friendly sampling techniques of semi-volatile organic compounds present in an indoor environment: an approach to human exposure assessment. TrAC – Trends Anal. Chem. 154, 116669 https://doi.org/10.1016/j.trac.2022.116669.

Roll, I.B., Halden, R.U., Pycke, B.F.G., 2015. Indoor air condensate as a novel matrix for monitoring inhalable organic contaminants. J. Hazard Mater. 288, 89–96. https://doi.org/10.1016/j.jhazmat.2015.01.043.

Salthammer, T., Gu, J., Wientzek, S., Harrington, R., Thomann, S., 2021. Measurement and evaluation of gaseous and particulate emissions from burning scented and unscented candles. Environ. Int. 155, 106590 https://doi.org/10.1016/j.envint.2021.106590.

Silva, L.F.O., Pinto, D., Enders, M.S.P., Hower, J.C., Flores, E.M.M., Müller, E.I., Dotto, G. L., 2021. Portable dehumidifiers as an original matrix for the study of inhalable nanoparticles in school. Chemosphere 262, 127295. https://doi.org/10.1016/j.chemosphere.2020.127295.

Song, M., Chi, C., Guo, M., Wang, X., Cheng, L., Shen, X., 2015. Pollution levels and characteristics of phthalate esters in indoor air of offices. J. Environ. Sci. (China) 28, 157–162. https://doi.org/10.1016/j.jes.2014.05.051.

Temkin, A.M., Geller, S.L., Swanson, S.A., Leiba, N.S., Naidenko, O.V., Andrews, D.Q., 2023. Volatile organic compounds emitted by conventional and "green" cleaning products in the U.S. market. Chemosphere 341, 139570. https://doi.org/10.1016/j.chemosphere.2023.139570.

Veenaas, C., Ripszam, M., Glas, B., Liljelind, I., Claeson, A.S., Haglund, P., 2020. Differences in chemical composition of indoor air in rooms associated/not associated with building related symptoms. Sci. Total Environ. 720, 137444 https://doi.org/10.1016/j.scitotenv.2020.137444.

Wan, Y., Xue, J., Kannan, K., 2016. Benzothiazoles in indoor air from Albany, New York, USA, and its implications for inhalation exposure. J. Hazard Mater. 311, 37–42. https://doi.org/10.1016/j.jhazmat.2016.02.057.

Warburton, T., Grange, S.K., Hopkins, J.R., Andrews, S.J., Lewis, A.C., Owen, N., Jordan, C., Adamson, G., Xia, B., 2023. The impact of plug-in fragrance diffusers on residential indoor VOC concentrations. Environ Sci Process Impacts 25, 805–817. https://doi.org/10.1039/d2em00444e.

Wilford, B.H., Harner, T., Zhu, J., Shoeib, M., Jones, K.C., 2004. Passive sampling survey of polybrominated diphenyl ether flame retardants in indoor and outdoor air in Ottawa, Canada: implications for sources and exposure. Environ. Sci. Technol. 38, 5312–5318. https://doi.org/10.1021/es049260x.

Zhu, L., Fauser, P., Mikkelsen, L., Sanderson, H., Vorkamp, K., 2023. Suspect and non-target screening of semi-volatile emerging contaminants in indoor dust from Danish kindergartens. Chemosphere 345, 140451. https://doi.org/10.1016/j.chemosphere.2023.140451.

USC UNIVERSIDADE DE SANTIAGO DE COMPOSTELA

Supplementary information to manuscript:

Predicting concentrations of volatile and semi-volatile compounds in indoor areas through analysis of condensed water samples. A proof of concept

M. Cobo-Golpe[a], M. Ramil[a], L. Pérez-Mayán[b], I. Rodríguez[a]*
[a]Department of Analytical Chemistry, Nutrition and Food Sciences, IAQBUS - Institute of Research on Chemical and Biological Analysis, Universidade de Santiago de Compostela, R/Constantino Candeira SN, 15782 Santiago de Compostela, Spain.
[b]Mestrelab Research Center (CIM), Av. Barcelona 7, 15706 Santiago de Compostela, Spain.

*Corresponding author
e-mail: isaac.rodriguez@usc.es

USC UNIVERSIDADE DE SANTIAGO DE COMPOSTELA

Fig S1. Log $k_{air/water}$ for the different analytes present in the study with values in the range between -3.96 and -5.10 (A) and between -5.46 and -6.35 (B). Data represented in blue were obtained for a volume of 3 m^3, data in red corresponds to a sample volume of 1.5 m^3.

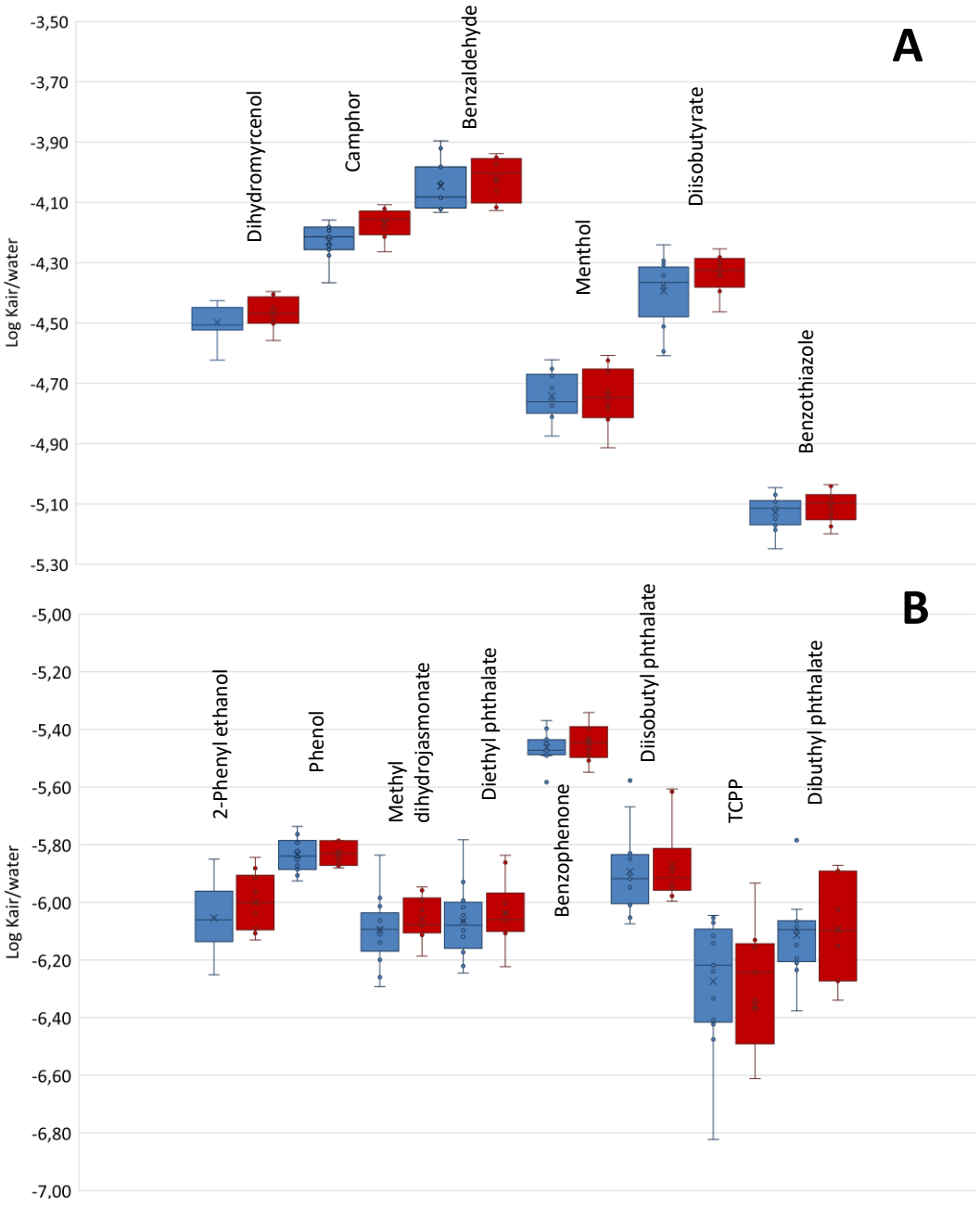
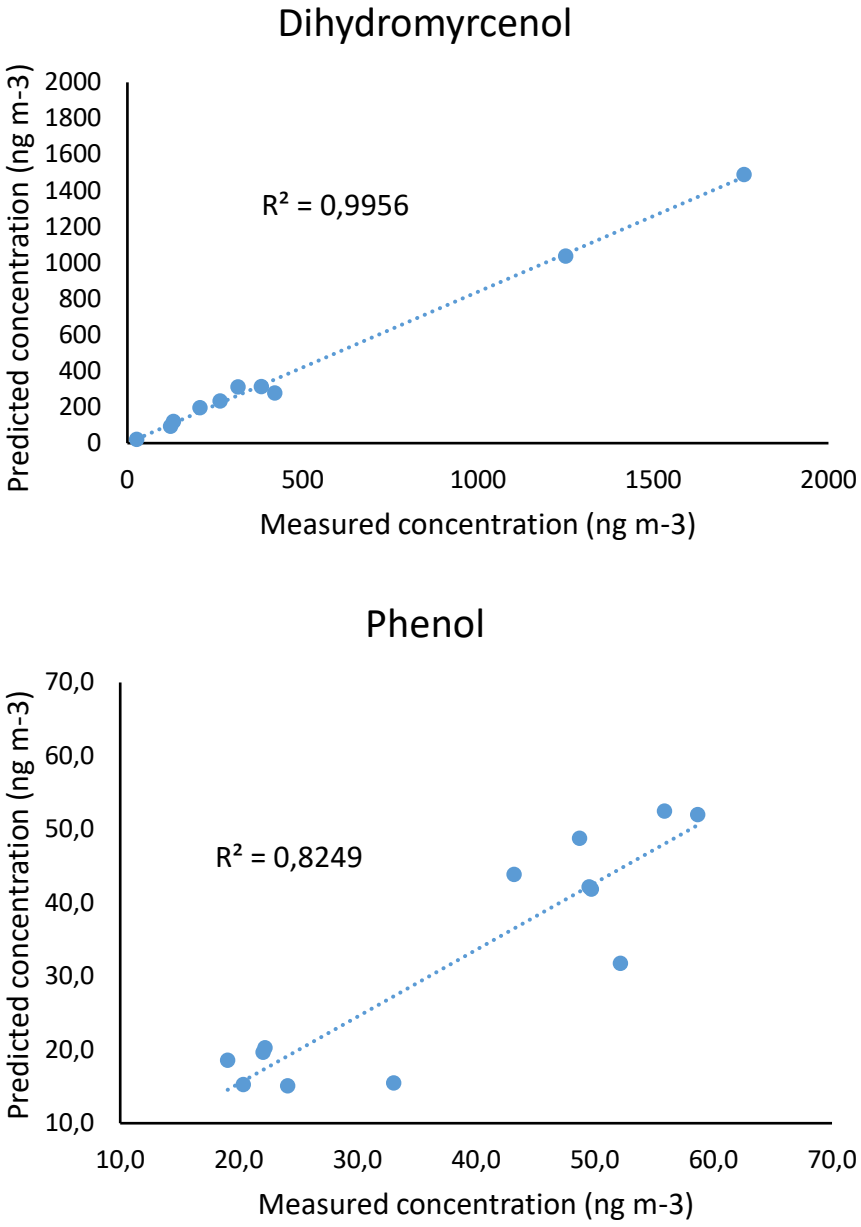


Fig S2. Correlation between analyte concentrations predicted in air from analysis of water condensates vs Air concentrations measured using active air sampling for dihydromyrcenol and phenol.



USC
UNIVERSIDADE DE SANTIAGO DE COMPOSTELA

Table S1. CAS number, retention times, quantification (Q1) and qualification (Q2) ions for the selection of surrogate standards.

Compound	CAS number	Retention time (min)	Q1 (m/z)	Q2 (m/z)	Q2/Q1 ratio (%)
Benzaldehyde-d5	14132-51-5	15.5	110.0646	82.0695	55
Menthol-d4	89-78-1	18.2	127.1413	127.1413	216
Benzothiazole-d4	194423-51-3	25.5	139.0388	112.0279	25
Phenol-d5	4165-62-2	26.3	99.0727	71.0776	31
2-phenoxyethanol-d2	21273-38-1	269.0	140.0799	94.0414	475
Benzophenone-d10	22583-75-1	34.8	192.1349	110.065	200
TCPP-d18	1447569-78-9	37.6	293.1162	212.0764	231
Dibutyl phthalate-d4	93952-11-5	38.0	153.0484	124.9992	2

USC UNIVERSIDADE DE SANTIAGO DE COMPOSTELA

Table S2. Recoveries of the SPE process (%), with standard deviations (SD), for spiked aliquots of ultrapure water adjusted at pH 4.5. Addition level 5 ng mL^{-1}, n=3 replicates.

Compound	300 mL		150 mL		50 mL	
	Recovery (%)	SD	Recovery (%)	SD	Recovery (%)	SD
Cyclohexanone	10.3	0.6	16.1	0.6	23.0	6.5
Dihydromyrcenol	95.0	3.0	93.3	1.6	90.8	5.1
Camphor	98.6	1.7	95.3	2.4	94.1	3.4
Benzaldehyde	56.4	3.8	89.3	3.1	91.7	4.9
Menthol	98.0	1.4	95.4	2.1	104.4	4.9
Triethyl phosphate	21.9	2.4	45.8	0.7	98.1	3.3
2,2,4-Trimethyl-1,3-pentanediol diisobutyrate	67.7	6.9	82.9	3.0	84.0	2.1
2-Phenyl ethanol	33.8	2.5	69.5	1.5	98.7	5.8
Benzothiazole	95.8	1.9	94.0	1.7	99.9	2.9
Phenol	58.6	4.5	84.4	2.2	98.5	2.2
Methyl dihydrojasmonate	96.1	3.8	96.8	3.5	95.3	3.6
Diethyl phthalate	96.6	2.9	97.9	2.2	112.2	9.1
Benzophenone	97.4	3.3	95.0	3.3	95.5	3.8
Diisobutyl phthalate	87.5	4.7	89.0	10.4	85.9	9.1
TCPP	101.4	2.5	101.5	2.1	94.0	4.6
Dibutyl phthalate	98.4	2.8	107.1	4.4	101.1	3.2

USC UNIVERSIDADE DE SANTIAGO DE COMPOSTELA

Table S3. Concentrations (ng m^{-3}) of selected compounds found in indoor air during assessment of the efficiency of active air sampling experiments.

Compound	Average	SD
Cyclohexanone	211.3	25.9
Dihydromyrcenol	nd	
Camphor	9.4	1.5
Benzaldehyde	86.1	14
Menthol	11.4	1.4
Triethyl phosphate	nd	
2,2,4-Trimethyl-1,3-pentanediol diisobutyrate	39.9	7.4
2-Phenyl ethanol	3.6	0.6
Benzothiazole	15.1	2.4
Phenol	31.3	5
Methyl dihydrojasmonate	10.8	0.5
Diethyl phthalate	18.9	2.2
Benzophenone	13.8	1.5
Diisobutyl phthalate	49.5	5.1
TCPP	nd	
Dibutyl phthalate	72.7	6.5

USC UNIVERSIDADE DE SANTIAGO DE COMPOSTELA

Table S4. Effect of filtration in the concentrations of compounds in the SPE extracts corresponding to 50 mL aliquots of condensed water from two different indoor areas. Data in ng mL^{-1} referred to SPE extracts, n=3 replicates.

Compound	Room 1				Room 2			
	Unfiltered		Filtered		Unfiltered		Filtered	
	Mean	SD	Mean	SD	Mean	SD	Mean	SD
Dihydromyrcenol	436.4	17.9	418.8	16.5	10.5	0.8	9.8	1.2
Camphor	27.7	7.3	23.4	4.3	6.7	0.5	6.9	0.5
Benzaldehyde	52.3	8.9	49.0	5.2	56.4	5.2	53.5	8.4
Menthol	34.4	1.7	33.9	1.2	29.6	2.4	30.3	1.5
Triethyl phosphate	117.1	6.1	111.7	2.3	129.5	9.7	116.9	1.4
2,2,4-Trimethyl-1,3-pentanediol diisobutyrate	20.2	1.7	21.9	1.5	42.0	4.6	39.3	2.9
2-Phenyl ethanol	417.5	30.4	403.9	24.2	93.3	6.6	91.4	7.8
Benzothiazole	1029.9	7.0	1056.3	2.3	51.6	0.6	50.7	2.1
Phenol	352.8	5.2	350.9	14.2	931.3	97.0	890.4	64.3
Methyl dihydrojasmonate	55.0	5.1	58.1	2.0	268.2	15.8	254.9	26.9
Diethyl phthalate	149.2	5.2	146.7	1.6	1937.3	32.9	1905.9	53.5
Benzophenone	64.1	3.2	60.5	1.7	166.6	9.4	162.3	10.8
Diisobutyl phthalate	396.6	22.8	334.7	14.8	1353.8	259.7	1235.8	350.8
TCPP	109.0	6.4	103.2	2.1	993.6	84.2	942.0	121.6
Dibutyl phthalate	939.1	57.7	793.3	42.2	2004.9	110.9	1859.2	177.4

USC UNIVERSIDADE DE SANTIAGO DE COMPOSTELA

Table S5. Normalized average responses in the extract from quartz glass filters (0.7 µm cut-off) versus SPE extracts from filtered water condensates, n=3 replicates.

Compound	Filter/Water ratio
Dihydromyrcenol	0.1%
Camphor	0.2%
Benzaldehyde	1.0%
Menthol	0.1%
Triethyl phosphate	0.3%
2,2,4-Trimethyl-1,3-pentanediol diisobutyrate	0.1%
2-Phenylethanol	0.1%
Benzothiazole	0.3%
Phenol	0.2%
Methyl dihydrojasmonate	0.3%
Diethyl phthalate	0.3%
Benzophenone	0.1%
Diisobutyl phthalate	0.6%
TCPP	0.1%
Dibutyl phthalate	2.4%

USC UNIVERSIDADE DE SANTIAGO DE COMPOSTELA

Table S6. Concentrations in condensed water samples, obtained from the same room operating the fan of the dehumidifier at low and high speed. Values in ng mL^{-1} of water extract. Average values for duplicate extraction of each water condensate.

Compound	Low	High	Variation
Dihydromyrcenol	322.5	284.8	-13%
Camphor	40.3	36.9	-9%
Benzaldehyde	62	69.1	10%
Menthol	212.5	232.8	9%
Triethyl phosphate	240.3	361	33%
2.2.4-Trimethyl-1.3-pentanediol diisobutyrate	312.7	349.6	11%
2-Phenyl ethanol	596.8	560.8	-6%
Benzothiazole	257.1	268.9	4%
Phenol	1846.1	1829.8	-1%
Methyl dihydrojasmonate	1510	1669.8	10%
Diethyl phthalate	1181.3	1249.3	5%
Benzophenone	188.1	232.4	19%
Diisobutyl phthalate	1718.9	1797.6	4%
TCPP	419.5	432.8	3%
Dibutyl phthalate	638	771	17%

USC UNIVERSIDADE DE SANTIAGO DE COMPOSTELA

Table S7. Surface and features of sampling rooms considered during validation of Kaw estimated values.

Site	Surface (m^2)	Uses	Floor type	Furniture
Site 1	71	Meeting room	Wood	Chairs, tables, and computers
Site 2	16	Office	Wood	Chairs, tables, computers, shelves and books
Site 3	8	Laundry room	Ceramic	Washing & drying machines and detergents
Site 4	36	Dining room	Wood	Sofa, chairs, tables, electric appliances
Site 5	20	Dining room	Wood	Sofa, chairs, tables, electronic devices
Site 6	40	Office	Wood	Chairs, tables, computers, shelves and books
Site 7	12	Kitchen	Ceramic	Kitchen furniture, and gas stove

USC UNIVERSIDADE DE SANTIAGO DE COMPOSTELA

Table S8 Predicted versus measured concentrations (ng m-3) of selected compounds in indoor air obtained from different sites. Average values in ng m-3 for duplicate injections of each sample

Site-sample		Site 1- S1	Site 1- S2	Site 2- S1	Site 2- S2	Site 3- S1	Site 3- S2	Site 4- S1	Site 4- S2	Site 5- S1	Site 5- S2	Site 6 - S1	Site 7- S1	Site 7- S2	Slope	R^2
Dihydromyrcenol	Predicted			26,4		1250,7	1759,5	315,4	382,7	131,4	122,9	207,6	421,0	264,4	1,188	0,996
	Measured			22,0		1038,3	1490,0	313,0	314,0	121,0	95,0	197,0	280,0	234,8		
Camphor	Predicted			18,5	23,9	138,3	198,8	66,0	118,9	19,4	17,3	25,2	6,9	5,6	1,149	0,966
	Measured	3,2	2,2	17,3	15,6	118,9	174,6	74,5	76,9	17,5	10,1	28,9	5,3	4,6		
Benzaldehyde	Predicted	71,6	102,0	237,8	299,4	95,4	101,5	185,7	223,7	287,6	227,5	418,9	220,3	170,3	0,852	0,739
	Measured	45,2	52,0	200,6	162,4	55,7	66,3	212,2	206,9	277,5	214,0	345,7	62,2	73,1		
Menthol	Predicted			30,8	38,0	49,0	27,9	190,5	214,6	41,1	38,1	59,3	16,1	10,2	1,080	0,975
	Measured	5,1	5,0	26,2	24,0	30,9	15,3	189,2	172,3	36,0	27,4	49,4	11,2	13,8		
Diisobutyrate	Predicted	24,4	27,6	40,4	47,0	25,6	26,1	376,3	364,1	6464,0	5073,7	925,5	347,0	286,4	1,152	0,999
	Measured	10,1	11,2	32,5	39,9	26,2	25,1	339,3	346,1	5511,0	4532,0	729,0	277,7	307,5		
2-Phenyl ethanol	Predicted	5,3	5,6	7,6	9,3	7,9	8,5	14,6	17,4	40,5	41,8	86,0	41,7	34,4	1,070	0,973
	Measured	3,7	4,4	7,6	7,8	8,3	7,3	13,8	17,0	47,3	35,5	77,8	32,8	29,5		
Benzothiazole	Predicted	8,9	8,7	15,2	17,9	221,4	226,5	71,8	77,3	118,0	119,2	74,6	21,6	19,1	0,990	0,986
	Measured	11,8	11,7	17,0	19,2	234,9	224,4	72,0	73,7	115,7	91,8	67,4	21,6	21,5		
Phenol	Predicted	22,2	22,0	43,2	49,7	19,1	20,4	48,7	55,9	49,5	52,2	58,7	33,1	24,1	0,908	0,825
	Measured	20,3	19,7	43,9	41,9	18,6	15,3	48,8	52,5	42,2	31,8	52,0	15,5	15,1		
Methyl dihydrojasmonate	Predicted	11,5	13,5	7,5	9,0	2,3	2,5	17,1	22,8	33,9	37,0	53,6	39,3	29,1	0,871	0,823
	Measured	8,3	8,8	7,1	8,6	3,7	3,7	20,6	24,5	31,0	24,1	65,6	24,3	24,8		
Diethyl phthalate	Predicted	21,9	28,2	103,0	110,4	14,1	16,7	19,2	23,3	22,3	22,3	78,8	26,5	22,3	1,059	0,917
	Measured	17,3	37,8	108,4	93,9	14,0	19,4	21,5	22,8	18,5	14,4	50,0	23,2	22,5		
Benzophenone	Predicted	3,6	4,1	16,9	18,1	6,8	7,6	12,0	14,8	26,8	29,8	37,7	16,4	15,4	1,153	0,787
	Measured	4,6	4,6	14,0	13,7	6,2	6,2	13,3	13,9	17,4	13,8	34,8	9,7	13,4		
Diisobutyl phthalate	Predicted	26,3	26,7	28,7	29,7	11,8	8,2	19,3	24,0	22,4	25,0	74,6	24,7	18,4	1,159	0,853
	Measured	24,7	23,7	34,3	27,5	7,2	7,8	18,0	18,9	19,7	16,6	54,5	10,9	13,5		
TCPP	Predicted	7,0	10,4	2,5	2,9	1,6	1,2	16,5	21,6	193,6	243,2	18,3	44,2	29,1	0,995	0,818
	Measured	11,9	13,9					20,6	24,1	231,1	149,8	19,4	16,1	16,9		
Dibutyl phthalate	Predicted	16,1	16,8	21,5	23,8	12,1	8,6	19,1	24,4	15,6	14,9	56,2	18,8	16,3	1,063	0,734
	Measured	11,7	8,6	28,5	23,5	5,5	6,3	20,5	24,8	15,2	11,7	37,6	13,1	18,1		

Empty cells correspond to compounds below method LOQs

USC UNIVERSIDADE DE SANTIAGO DE COMPOSTELA

PUBLICATION III: COMPREHENSIVE CHARACTERIZATION OF VOLATILE AND SEMI-VOLATILE COMPOUNDS IN E-LIQUIDS FOR ELECTRONIC CIGARETTE USING GAS CHROMATOGRAPHY ACCURATE MASS SPECTROMETRY

M. Cobo-Golpe, M. Ramil, I. Rodríguez

Journal of Chromatography A 1703 (2023) 464114
DOI: 10.1016/j.chroma.2023.464114



Impact factor: 3.8
Category: Analytical chemistry
Position: 26/196
Quartile: Q1

USC
UNIVERSIDADE DE SANTIAGO DE COMPOSTELA

Journal of Chromatography A 1703 (2023) 464114

Contents lists available at ScienceDirect

Journal of Chromatography A

journal homepage: www.elsevier.com/locate/chroma

Comprehensive characterization of volatile and semi-volatile compounds in e-liquids for electronic cigarette using gas chromatography accurate mass spectrometry

M. Cobo Golpe, M. Ramil, I. Rodríguez*

Department of Analytical Chemistry, Nutrition and Food Sciences. Research Institute on Chemical and Biological Analysis (IAQBUS). Universidade de Santiago de Compostela, 15782-Santiago de Compostela, Spain

ARTICLE INFO

Article history:
Received 31 March 2023
Revised 16 May 2023
Accepted 28 May 2023
Available online 29 May 2023

Keywords:
E-liquids
Non-target screening
Gas chromatography
Time-of-flight mass spectrometry

ABSTRACT

The consumption of electronic cigarettes is a habit with an increasing prevalence, particularly among youths. Knowing the composition of e-liquids used in these devices represents the first step to understand the potential impact of e-smoking in the health of consumers. Herein, a non-target screening methodology was applied to the identification of volatile and semi-volatile compounds in a set of e-liquids from different suppliers, with different flavors, and containing different kinds of additives, such as nicotine or cannabidiol. To this end, samples were characterized by gas chromatography accurate mass spectrometry, using a time-of-flight mass analyzer. Combination of deconvoluted electronic ionization mass spectra with linear retention index values, obtained for two columns with different selectivity, permitted the identification of more than 250 chemicals with different confidence levels. Among them, respiratory pro-inflammatory compounds, acetals of propylene glycol and glycerin with aldehydes, nicotine-related and non-related alkaloids, and psychoactive cannabinoids were confirmed as concerning compounds in e-liquid samples. Concentration ratios between propylene glycol acetals and parent aldehydes varied in the range from 2% (ethyl vanillin) to more than 80% (case of benzaldehyde). The ratios between the concentrations of delta-9-tetrahydrocannabinol and cannabidiol in e-liquids stayed in the range from 0.02% to 0.3%.

© 2023 The Author(s). Published by Elsevier B.V.
This is an open access article under the CC BY-NC-ND license
(http://creativecommons.org/licenses/by-nc-nd/4.0/)

1. Introduction

Electronic cigarettes (e-cig) were marketed as a safe alternative to conventional cigarettes, avoiding, or at least limiting, human exposure to harmful compounds generated during combustion of tobacco, such as tar and polycyclic aromatic hydrocarbons [1]. The power supply unit in e-cig devices is activated by each puff, heating the stream of air which gets in contact with the e-liquid to produce an aerosol containing different flavours and aromatic compounds [2]. Given that temperatures in e-cig devices remain far below those reached during conventional smoking, the formation of toxic combustion by-products is avoided. Composition of liquid solutions vaporized during e-smoking is also different to that of tobacco. Major components are propylene glycol (PG) and vegetal glycerine (VG). In addition, e-liquids contain a large variety of flavouring agents [3,4], and some formulations incorporate other compounds, such as nicotine (NIC) [5] and/or cannabidiol (CBD) [6]. Even in these cases, exposure to NIC during e-smoking is reduced compared to smoking, CBD lacks psychotropic effects, and the employed flavours have been approved as food additives.

Despite above assumptions, e-smoking rises some concerns, particularly after associations between this habit and outbreaks of lung injury [7]. Risks derived from e-cig consumption are related to several factors. On one hand, some common flavors in e-liquids, such as maltol, cinnamaldehyde and coumarin are known to produce oxidative stress in cultures of pleural cells [8], through modulation of the formation of reactive oxygen species during their vaporization [3,9]. Thus, they might damage different tissues of the respiratory tract, including oral [10] and lung cells [11]. Furthermore, it was suggested that flavoring agents are transported from lungs to bloodstream, exerting cytotoxic effects in the cardiovascular and immune systems [12]. Another risk factor is the novo formation of concerning chemicals due to reactions among sub-

* Corresponding author.
E-mail address: isaac.rodriguez@usc.es (I. Rodríguez).

https://doi.org/10.1016/j.chroma.2023.464114
0021-9673/© 2023 The Author(s). Published by Elsevier B.V. This is an open access article under the CC BY-NC-ND license
(http://creativecommons.org/licenses/by-nc-nd/4.0/)

stances mixed in e-liquids. In this vein, carbonyl species can react with alcohols (mainly with PG) to produce acetals, which are recognized as respiratory irritants. For very popular aldehyde flavors, such as benzaldehyde and vanillin, the rates of conversion to acetals have been estimated between 15% and 30% [13]. A third issue of concern is the generation of toxic species during the vaping process [14]. This latter group includes formaldehyde, acetaldehyde and glyoxal, which are produced from oxidation of base alcohols in e-liquids, as function of the voltage applied by the e-cig battery [15]. Finally, inclusion of addictive species in e-liquids, such as nicotine and cannabinoids, is regarded as an additional risk factor. In line with above concerns, the characterization of flavors existing in e-liquids, and those by-products formed during generation of the aerosol have become recurrent research topics [14]. Particularly, knowing the composition of e-liquids is the first step to identify concerning compounds attending to their toxicity, their addictive potential, and/or their role as precursors of toxic by-products, either generated directly in the e-liquid solutions, or produced during e-smoking.

Nuclear magnetic resonance (NMR) spectroscopy and liquid chromatography mass spectrometry (LC-MS) have been proposed for the quantification of major flavors [16], and the determination of specific families of compounds, such as volatile carbonyl species (after a derivatization reaction), and/or nicotine-related alkaloids in e-liquids [17,18]. However, gas chromatography (GC) MS is regarded as the gold standard for the analysis of e-liquids [2,19], either during quantitation of pre-selected compounds [20], or for the qualitative characterization of these mixtures [2,19,21].

So far, more than 140 volatile compounds have been reported in e-liquids [2]; however, considering the number of suppliers and the different available flavors, this number is likely below the figures of volatile and semi-volatile organic species included in these formulations. This statement is supported by several facts. First, most GC–MS studies rely on low-polarity, limited selectivity, siloxane-type columns, which fail to separate major components of e-liquids from minor flavors. Second, quadrupole-type MS instruments, employed in most of previous studies [2,11,21,22], offer a limited sensitivity when operated in the scan mode, so minor compounds might remain undetected, particularly if they co-elute with major e-liquid solvents. Finally, nominal resolution EI-MS spectra might lead to misidentification problems.

Despite the improved performance provided by accurate MS platforms, such as GC-TOF-MS and GC-Orbitrap-MS in non-target screening studies, as far as we could trace, they have not been used for the comprehensive characterization of e-liquids. Thus, the aim of the current study is to build a database of accurate EI-MS spectra for volatile and semi-volatile compounds often present in this matrix. To this end, a non-target data mining strategy was combined with the use of GC-TOF-MS, as main determination technique, under different chromatographic conditions. Particular attention was paid to (1) the identification of species related to well-known additives in e-liquids, such as minor alkaloids structurally related to NIC, and CBD-like compounds; and (2) the assessment of the presence of acetals in e-liquids and/or their potential formation as artefacts during GC–MS analysis. In addition to GC-TOF-MS, LC-MS was employed as complementary analytical technique to confirm those compounds prone to formation in the injector of the GC-TOF-MS instrument.

2. Material and methods

2.1. Samples and sample preparation

E-liquids (39 samples) were produced by nine different companies and purchased either from local retail markets, authorized for distribution of conventional cigarettes in Spain, or from on-line suppliers. Fourteen e-liquids contained nicotine (concentrations in the range from 3 to 12 mg mL^{-1}), and 6 samples declared the presence of cannabidiol (CBD). The range of flavors stated in e-liquids was relatively large, including tobacco, beverages, fruity and mint as main aroma descriptors. Table S1 summarizes the main features of the considered samples, including the ratio between PG and VG solvents. After acquisition, e-liquid samples were maintained at room temperature for a maximum of 1 month before opening. Thereafter, they were diluted with a suitable organic solvent (ethyl acetate and methanol for GC-TOF-MS and LC-MS analysis, respectively), and stored at −20 ºC until analysis. Unless otherwise stated, the dilution factor employed for GC-TOF-MS analysis was 1:100, whilst a 1:10 sample to solvent ratio was considered in LC-MS studies.

2.2. Solvents and standards

Ethyl acetate (trace analysis grade quality) was acquired from Merck (Darmstadt, Germany). Methanol (MeOH) and/or acetonitrile (ACN) for LC-MS, were provided by the same supplier. Ultrapure deionized water (18.2 MΩ cm^{-1}) was obtained from a Geni U system (Rephile, Shanghai, China). Standards of some tentatively identified flavors, and other volatile compounds detected in e-liquids were provided by Supelco (Bellefonte, PA, USA) and Sigma-Aldrich (St. Louis, Missouri USA). Mixtures of allergen fragrances were supplied by Restek (Bellefonte, PA, USA). Concentrated stock solutions of several cannabinoids, in MeOH, were also provided by Supelco. Individual stock standard solutions were prepared in MeOH, further dilutions and mixtures were made either in ethyl acetate, for GC-TOF-MS analysis, or in MeOH, when using LC-MS as determination technique. A mixture of n-alkanes (C_7 to C_{40}, 1000 µg mL^{-1} in dichloromethane) was provided by Supelco. Benzaldehyde-d_5 (deuterated in the aromatic ring) was purchased from Sigma-Aldrich.

2.3. GC-TOF-MS equipment

Identification of volatile compounds in e-liquids diluted solutions was carried out by GC–MS. The employed system was comprised of a 7200 quadrupole time-of-flight (QTOF) instrument (Agilent, Wilmington, DE), equipped with an EI source, and connected to a 7890 GC system from the same supplier. The ionization source and the quadrupole were maintained at 230 °C and 150 °C, respectively. The system was operated in the single MS mode (only the TOF analyzer was operative for separation of ions formed at the EI source), at 2.5 GHz, offering a typical mass resolution of 6000 (calculated as FWHM) at *m/z* 131. EI-TOF-MS spectra were recorded in the profile mode, within the range of masses comprised between 40 and 600 Da.

The e-liquids were analyzed using two capillary columns with different polarities. They were a semi-polar siloxane-type HP5-MS column (30 m x 0.25 mm, 0.25 µm), and a Carbowax, polyethylene glycol-type (DB-WAXetr), polar column with the same dimensions as the HP5-MS one, but a film thickness of 0.50 µm. Both were purchased from Agilent. They were operated using He as carrier gas, at a constant flow of 1 mL min^{-1}. The temperature of the injector was set at 280 ºC, and the transfer line with the MS instrument maintained at 270 ºC. For the HP5-MS column, a linear gradient at 5 ºC min^{-1}, from 65 ºC (1 min) to 260 ºC (8 min) was used. With the Carbowax one a first rate of 5 ºC min^{-1}, from 60 ºC (1 min) to 220 ºC, followed by a second one at 20 ºC min^{-1} to 240 ºC, were employed. In both cases, the final column temperature was held for different times to adjust the duration of chromatographic runs to 48 min.

USC UNIVERSIDADE DE SANTIAGO DE COMPOSTELA

2.4. Screening of volatile compounds in e-liquids from GC-TOF-MS data

GC-TOF-MS raw data were deconvoluted using the *Unknowns Analysis* (UA) tool, integrated in the Mass-Hunter software (version 10.0), which controlled all acquisition and data processing parameters of the GC-TOF-MS instrument. The workflow employed during data mining and compounds identification was similar to that described in previous articles [23,24]. In brief, chromatographic peaks with responses (peak heights) above a threshold of 10,000 counts were deconvoluted, and their accurate EI-MS spectra were compared to those compiled in NIST17 EI-MS library. Identifications were based on the following requirements: (1) spectral match above 75% between experimental and database spectra (spectral comparison was carried out using a mix of forward and reverse modes, with normalized contributions of 0.3 and 0.7, respectively); (2) differences between experimental and database linear retention index (LRI) values below 50 units for each chromatographic column; and (3) mass bias between deconvoluted spectra and calculated *m/z*, for known fragments in the NIST17 database, lower than 50 ppm, for a minimum of two intense ions. It is worth noting that, LRI values for Carbowax-type columns are relatively scarce compared to those existing for HP5 ones. In the first case, most LRI values were directly obtained from publications dealing with analysis of aroma and volatile compounds in vegetable origin foods [25] and beverages [26], or using the information accessible through the *Chemspider* database. In some cases, proposed identities were confirmed against standards.

Based on above statements, species in e-liquids were identified with different confidence levels. The highest one (level 1) was assigned to compounds fulfilling the three requirements (spectral, LRI and accurate mass match) and further confirmed against authentic standards with, at least, one of the columns. Level 2 corresponded to compounds not verified against standards, but matching spectral and retention time requirements in both columns. Finally, level 3 was assigned to compounds tentatively identified using just one of the columns. The latter situation mostly corresponds to, highly volatile species, poorly retained by the HP5-MS column; as well as to compounds detected in both columns, but without available reference LRI in one of them (usually the Carbowax one). The above confidence level identification scale was inspired in that proposed by Schymanski et al. [27], keeping in mind that, the latter has been proposed for MS and product ion scan accurate spectra obtained using soft ionization sources, such as ESI.

2.5. LC-MS confirmatory experiments

For certain compounds (identified by GC-TOF-MS at level 1), it was considered relevant to discriminate between their presence in the e-liquids, and their potential formation in the hot injector of the GC-TOF-MS system, through re-arrangements in the chemical structures of precursor species. In these cases, LC-MS was used as additional technique. Separations were carried out using a CORTECS Phenyl column (150 mm x 2.1 mm, 2.7 µm), acquired from Waters (Milford, MA, USA), and operated under reversed-phase conditions, with ultrapure water (A) and ACN (B), both 0.1% in FA, as mobile phases. The column was maintained at 40 ºC and the mobile phase flowrate was 0.3 mL min^{-1}. Different chromatographic gradients, and MS instruments, were considered depending on the investigated species: acetals of aldehydes, or cannabinoids. Further details on specific conditions for identification and/or determination of these compounds are given as supplementary information, Text S1 and S2. The complete data mining workflow, integrating data provided by GC-TOF-MS and LC-MS approaches, is provided as supplementary information, Fig. S1.

3. Results and discussion

3.1. Comprehensive overview of volatile organic compounds in e-liquids

Fig. 1A shows the total ion current (TIC) chromatogram for a diluted (1:100) e-liquid (sample code S3, Table S1) using the HP5-MS column. Several chromatographic items, of different intensities, are apparent. Moreover, the region below 11 min presents a broad chromatographic band (corresponding to VG) overlapping

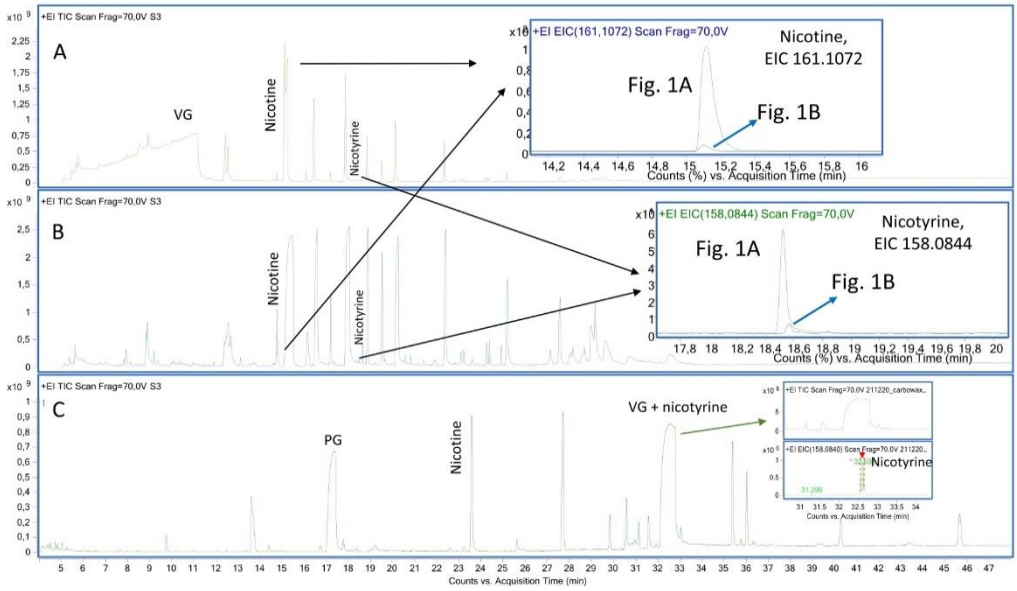


Fig. 1. GC-TOF-MS chromatograms for an e-liquid (sample code S3) under different conditions. A, Direct injection of a 100-times diluted sample using the HP5-MS column. B, Liquid-liquid extraction with ethyl acetate after water dilution (solvent to sample ratio 10:1) of same sample using the HP5-MS column. C, Direct injection of the diluted e-liquid (100-folds in ethyl acetate) using the Carbowax-type column.

UNIVERSIDADE DE SANTIAGO DE COMPOSTELA

the peaks of several compounds. Despite the data mining capabilities of the *Unknowns Analysis* deconvolution algorithm, this band might disturb the identification of minor species; moreover, it prevents the direct injection of e-liquids using lower dilution factors. Thus, different approaches were explored to allow a more comprehensive characterization of e-liquids. In first term, liquid-liquid extraction (LLE) of commercial samples with ethyl acetate (0.1 mL of e-liquids, diluted with 5 mL of ultrapure water and extracted with 1 mL of organic solvent) was assessed [2]. Fig. 1B shows the chromatogram obtained for same e-liquid as that in Fig. 1A after this process. LLE extraction removed the chromatographic band of VG and increased the number of noticeable peaks due to the use of a lower dilution factor; however, polar species present in some e-liquids, such as nicotine related alkaloids, remained mostly in the water phase, Fig. 1A and 1B. Table S2 summarizes the efficiency of the LLE process for a selection of compounds with different polarities. In addition to nicotine and nicotyrine, which were hardly recovered, extraction yields below 60% were observed for the acetals of vanillin with PG, several alcohols, such as maltol and benzyl alcohol, and the alkaloid acetyl pyrazine.

The second approach involved the testing of an alternative column for compound separation. Fig. 1C shows the chromatogram for same e-liquid (sample code S3, diluted 1:100 in ethyl acetate) with the Carbowax-type column. PG and VG increased their retention times and the latter rendered a narrower band than using the HP5-MS column. Moreover, chromatographic peaks for e-liquid components were distributed in a wider interval of retention times. Obviously, certain compounds could still be hindered by those of solvents, as illustrated for nicotyrine, Fig. 1C. In order to obtain a comprehensive characterization of e-liquids, retaining as much as possible of their original composition, LLE was not considered. Samples were just diluted 1:100 with ethyl acetate, injected by duplicate in both columns and the obtained chromatograms processed using the data mining workflow described in Material and Methods section.

Table 1 summarizes a list of 82 compounds observed in the chromatograms for the set of 39 e-liquid samples, using both columns, including their detection frequency ranges. These species were identified with a minimum confidence level of 2. Compounds are sorted attending to their increasing LRI in the HP5-MS column. In addition to CAS numbers and empirical formulae, the *m/z* ratios for the most intense peaks in their EI-MS spectra are provided. The largest number of species in Table 1 fit within the class of terpenes (including terpenes, sesquiterpenes and their hydroxylated terpenoids and sesquiterpenoids), followed by aromatic species and esters of carboxylic acids, Fig. 2A. Regarding their detection frequencies, vanillin and ethyl maltol were the compounds showing the highest prevalence in the set of processed e-liquids, Table 1.

Table S3 and S4 compile a selection of compounds mostly identified with a confidence level 3, and some that were confirmed with standards (confidence level 1). A total of 133 compounds fulfilled the criteria of mass accuracy, spectral match and agreement between experimental and database LRI values using the HP5-MS column, Table S3. In a few cases (i.e. quinolinamine), it was hard to discriminate between positional isomers, since the database LRI values for aminoquinoline analogues, substituted in different positions, differed in just 5–10 units. Most of these compounds were also apparent in the chromatograms corresponding to the Carbowax column; however, reference LRI values were not available for this stationary phase. On the other hand, limited volatility compounds, as it is the case of the cannabinoids and diterpenes, were not observed in chromatograms recorded with the Carbowax column. Likely, they were too strongly retained by this column, with thicker stationary phase and a lower maximum operational temperature than the HP5-MS one. As regards compounds identified only with the polar column, most of them are high volatility alcohols, aromatic compounds (including some solvents such as toluene and styrene), short chain carboxylic acids and some terpenes, Table S4. The latter ones likely co-eluted with more intense species, with several common ions in their spectra, when using the HP5-MS column, hampering their identification. It is worth noting that accuracy of EI-MS spectra was lost in case of saturated peaks; thus, the data mining strategy failed to identify some evident compounds, such as NIC and CBD, unless e-liquids were either injected in the split mode, or diluted up to 10,000 times.

The Venn diagram provided as supplementary information illustrates the advantage of combining the information provided by both columns for the comprehensive characterization of volatile compounds in e-liquids, Fig. S2. Globally, 253 compounds were identified in the processed e-liquids with confidence levels between 1 and 3. A recent review described the identification of 60 different compounds, including organic and inorganic species, in e-liquids [19]. Using a target GC–MS/MS method, 54 compounds, from a selection of 90 candidates, were confirmed in a set of 25 e-liquids from 5 different brands [20]. The pioneer study by Hutzler et al. [2] reported the identification of 140 organic substances in e-liquids. In summary, the number of compounds found using the non-target data-mining methodology reported in this research is larger than those so far compiled in the existing literature [2,19,20]. The accurate EI-MS spectra for compounds identified with confidence levels 1 and 2 have been made available through Zenodo repository (https://zendo.org; doi:10.5281/zenodo.7738079).

It is worth noting that, the processed e-liquids showed a high grade of heterogeneity, as regards their GC–MS profiles, see Fig. S3. This variability suggests that the number of species included in the formulation of e-liquids is likely even larger than those identified in this research. Within the set of tested samples, the detection frequency of a selection of aroma compounds suggested as respiratory pro-inflammatories, proved to display cytotoxic effects during in-vitro studies [12], and identified with a minimum confidence level of 2, are shown in Fig. 2B. Observed values varied from 13% for coumarin up to 68% for ethyl maltol.

3.2. Heterocyclic nitrogenated compounds

The main families of heterocyclic nitrogenated compounds identified in e-liquids were 3-pyrrol-pyridine compounds, 3-pyridine substituted species, and pyrazines. Occasionally, aminoquinolines, imidazoles, thiazoles and pyrimidine derivatives were also found. Fig. 3 shows their relative detection frequencies for the groups of nicotine (14 samples) and nicotine-free (25 samples) e-liquids. In addition to pyrrol-3-pyridine type compounds (cotinine, nicotine, myosmine, nicotyrine and nicotine-N-oxide) other heterocyclic species were mostly, or exclusively, found in nicotine-containing e-liquids, as it is the case of 3-pyridine carboxyaldehyde and 3-vinyl-pyridine, quinolinamine (the exact position of the amino group could not be identified), trimethylated-1,8-napthyridine (two isomers were detected) and pyrazino-pyrazine. Other alkaloids with a similar structure, such as anabasine and anatabine, previously reported in nicotine-containing e-liquids [17], were not found in this research. Minor nicotine related alkaloids might have either a natural origin, as it is the case of myosmine and cotinine [28], which are probably co-extracted together with nicotine from vegetable sources; or, they could be the result of the oxidation reactions occurring in e-liquid solutions, as reported for nicotyrine [22].

The rest of nitrogenated compounds included in Fig. 3 were less often detected, without a clear prevalence between nicotine-free and containing e-liquids. In the case of pyrazines, their presence was mostly associated to tobacco-flavored e-liquids, rather than to

USC UNIVERSIDADE DE SANTIAGO DE COMPOSTELA

USC UNIVERSIDADE DE SANTIAGO DE COMPOSTELA

Table 1
Summary of compounds identified using both columns. Compounds in bold were confirmed against authentic standards.

Compound	Chemical class	CAS number	Formula	[a]LRI, HP5-MS column		[a]LRI, Carbowax column		m/z ratios of relevant ions			[b]Detection Frequency
				Exp.	NIST17 database	Exp.	Database	Ion 1	Ion 2	Ion 3	
Camphene	Terpene	79-92-5	$C_{10}H_{16}$	960	952	1092	1092	93.0691	91.0532	121.0997	+
Benzaldehyde	Aldehyde	100-52-7	C_7H_6O	971	962	1551	1555	105.0329	77.0381	51.0224	+
Pyrazine, 2-methoxy-3-methyl-	Alkaloid	2847-30-5	$C_6H_8N_2O$	978	970	1394	1339	124.0618	106.048	95.0292	+
Bicyclo[3.1.0]hexane, 4-methylene-1-(1-methylethyl)- (	Terpene	3387-41-5	$C_{10}H_{16}$	984	974	1125	1120	93.0692	91.0533	77.0364	++
Hexanoic acid, ethyl ester	Ester	123-66-0	$C_8H_{16}O_2$	1001	1000	1247	1253	88.0497	73.027	99.0784	+
Thiazole, 4-methyl-2-(1-methylethyl)-	Alkaloid	15679-13-7	$C_7H_{11}NS$	1021	1022	1369	1339	126.0362	141.0599	70.9939	+
2-Acetylpyrazine	Alkaloid	22047-25-2	$C_6H_6N_2O$	1025	1023	1657	1646	94.0519	122.0476	80.0364	+
p-Cymene	Aromatic	99-87-6	$C_{10}H_{14}$	1027	1025	1291	1292	119.0845	134.1071	91.0538	+
D-Limonene	Terpene	5989-27-5	$C_{10}H_{16}$	1031	1018	1217	1219	67.0544	93.0693	121.1003	++
Eucalyptol	Terpenoid	470-82-6	$C_{10}H_{18}O$	1035	1032	1227	1228	93.0692	139.1113	154.1342	+
2-acetylpyridine	Alkaloid	1122-62-9	C_7H_7NO	1036	1035	1632	1603	79.0412	121.0516	93.0572	+
2-Cyclopenten-1-one, 2-hydroxy-3-methyl-	Ketone	80-71-7	$C_6H_8O_2$	1037	1034	1852	1839	112.052	84.0564	69.0335	++
Benzyl alcohol	Aromatic	100-51-6	C_7H_8O	1038	1036	1899	1917	79.0533	108.056	107.056	++
Butanoic acid, 3-methyl-, butyl ester	Ester	109-19-3	$C_9H_{18}O_2$	1047	1047	1261	1271	103.0748	57.0695	85.0642	+
Butanoic acid, 3-methylbutyl ester	Ester	106-27-4	$C_9H_{18}O_2$	1056	1056	1279	1256	70.0771	89.0587	115.074	+
Furaneol	Ketone	3658-77-3	$C_6H_8O_3$	1059	1070	2052	2050	128.0466	57.0331	85.0279	+
Gamma-Terpinene	Terpene	99-85-4	$C_{10}H_{16}$	1060	1060	1302	1263	93.0688	121.0998	136.1232	+
Pentanoic acid, 4-oxo-, ethyl ester	Ester	539-88-8	$C_7H_{12}O_3$	1063	1045	1636	1610	99.0434	129.0545	71.0481	+
Diethyl malonate	Ester	105-53-3	$C_7H_{12}O_4$	1072	1069	1597	1603	115.0381	133.0491	87.0069	+
Hexanoic acid, 2-propenyl ester	Ester	123-68-2	$C_9H_{16}O_2$	1082	1080	1387	1370	71.0849	99.0801	113.0597	+
Pyrazine, 2,3,5,6-tetramethyl-	Alkaloid	1124-11-4	$C_8H_{12}N_2$	1089	1089	1494	1466	136.0999	54.0466	94.0653	+
Terpinolene	Terpene	586-62-9	$C_{10}H_{16}$	1091	1088	1302	1293	93.0662	121.0986	136.1223	+
Butanoic acid, 2-methyl-, 3-methylbutyl ester	Ester	27625-35-0	$C_{10}H_{20}O_2$	1102	1101	1291	1276	103.0729	70.077	57.0695	+
Linalool	Terpenoid	78-70-6	$C_{10}H_{18}O$	1103	1099	1561	1565	93.0698	121.1002	71.0482	++
Butanoic acid, 3-methyl-, 3-methylbutyl ester	Ester	659-70-1	$C_{10}H_{20}O_2$	1107	1104	1308	1312	103.0736	85.0648	70.0772	+
(2R,4R)-4-Methyl-2-(2-methylprop-1-en-1-yl)tetrahydro-2H-pyran	Terpenoid	5258-11-7	$C_{10}H_{18}O$	1113	1127	1350	1371	139.1116	69.0326	83.0481	+
Maltol	ketone	118-71-8	$C_6H_6O_3$	1114	1110	1991	1991	126.0304	71.0117	97.0275	++
Phenyl ethyl alcohol	Aromatic	60-12-8	$C_8H_{10}O$	1120	1116	1935	1941	91.0541	92.0613	122.0731	+
Isophorone	Aldehyde	78-59-1	$C_9H_{14}O$	1125	1124	1623	1623	82.0413	54.0468	138.1045	+
Benzoic acid	Aromatic	65-85-0	$C_7H_6O_2$	1160	1170	2460	2475	105.0338	122.0371	77.0377	+
Benzene, 1,3-dimethoxy-	Aromatic	151-10-0	$C_8H_{10}O_2$	1170	1166	1775	1730	138.0677	109.0642	78.0453	+
endo-Borneol	Terpenoid	507-70-0	$C_{10}H_{18}O$	1171	1167	1723	1726	95.0851	67.054	110.1081	+
Benzenemethanol, .alpha.,.alpha.,4-trimethyl-	Aromatic	1197-01-9	$C_{10}H_{14}O$	1189	1183	1869	1851	135.0802	91.0534	115.0537	+
Butanoic acid, hexyl ester	Ester	2639-63-6	$C_{10}H_{20}O_2$	1193	1192	1430	1410	93.0691	121.1009	136.1245	+
Menthol	Terpenoid	89-78-1	$C_{10}H_{20}O$	1194	1174	1635	1626	81.0701	95.0859	123.1174	+
alpha.-Terpineol	Terpenoid	98-55-5	$C_{10}H_{18}O$	1195	1190	1718	1719	93.0672	121.1005	136.1247	++
Ethyl maltol	Ketone	4940-11-8	$C_7H_8O_3$	1200	1199	2041	2047	140.0463	139.0387	97.0282	+++
Gamma-Terpineol	Terpenoid	586-81-2	$C_{10}H_{18}O$	1202	1197	1690	1690	121.1006	93.0694	136.1244	+
2-Cyclohexen-1-ol, 2-methyl-5-(1-methylethenyl)-, cis-	Terpenoid	1197-06-4	$C_{10}H_{16}O$	1223	1229	1853	1845	109.0634	91.0525	84.0553	+
Citronellol	Terpenoid	106-22-9	$C_{10}H_{20}O$	1230	1228	1780	1776	67.0542	81.0699	123.116	+
Nerol	Terpenoid	106-25-2	$C_{10}H_{18}O$	1232	1228	1862	1818	69.0708	93.0705	121.1025	+
Pulegone	Terpenoid	89-82-7	$C_{10}H_{16}O$	1244	1237	1676	1665	81.0696	152.1199	137.0961	+
Benzeneacetic acid, ethyl ester	Aromatic	101-97-3	$C_{10}H_{12}O_2$	1248	1246	1783	1784	91.0536	164.0836	136.0538	+
Linalyl acetate	Ester	115-95-7	$C_{12}H_{20}O_2$	1257	1257	1561	1573	93.0703	121.102	80.0624	+
2-Cyclohexen-1-one, 3-methyl-6-(1-methylethyl)-	Terpenoid	89-81-6	$C_{10}H_{16}O$	1259	1253	1757	1841	110.0733	95.0495	137.097	+
Gamma-Octalactone	Lactone	104-50-7	$C_8H_{14}O_2$	1262	1261	1948	1946	85.0289	100.0526	57.0337	+
1,3-Dioxolane, 4-methyl-2-phenyl-	Acetal	2568-25-4	$C_{10}H_{12}O_2$	1271	1272	1840	1871	163.0752	105.0333	119.0464	++
Cinnamaldehyde, (E)-	Aldehyde	104-55-2	C_9H_8O	1274	1274	2043	2037	131.0507	103.0518	77.0381	+
5-Thiazoleethanol, 4-methyl	Alkaloid	137-00-8	C_6H_9NOS	1281	1288	2332	2311	112.0226	143.0417	85.0111	+
Anethole	Aromatic	4180-23-8	$C_{10}H_{12}O$	1289	1284	1854	1817	148.0897	147.0822	117.0708	+
Nonanoic acid, ethyl ester	Ester	123-29-5	$C_{11}H_{22}O_2$	1297	1296	1520	1526	88.0508	73.0272	61.0281	+
Thymol	Terpenoid	89-83-8	$C_{10}H_{14}O$	1303	1291	2234	2236	135.0798	150.1025	107.0836	+

(*continued on next page*)

Table 1 (*continued*)

Compound	Chemical class	CAS number	Formula	[a]LRI, HP5-MS column		[a]LRI, Carbowax column		m/z ratios of relevant ions			[b]Detection Frequency
				Exp.	NIST17 database	Exp.	Database	Ion 1	Ion 2	Ion 3	
Piperonal	Aldehyde	120-57-0	$C_8H_6O_3$	1337	1330	2268	2279	149.0224	150.0298	121.0274	+
Methyl anthranilate	Aromatic	134-20-3	$C_8H_9NO_2$	1345	1343	2271	2283	119.0371	151.0636	92.0268	+
Benzyl butyrate	Ester	103-37-7	$C_{11}H_{14}O_2$	1349	1345	1894	1866	108.0568	91.0538	178.087	+
4-Acetylanisole	Ketone	100-06-1	$C_9H_{10}O_2$	1356	1348	2173	2173	135.0441	150.0673	107.0489	+
Eugenol	Aromatic	97-53-0	$C_{10}H_{12}O_2$	1361	1357	2193	2207	164.0829	149.0582	131.0486	+
Nerol acetate	Ester	141-12-8	$C_{12}H_{20}O_2$	1385	1364	1774	1776	69.0698	93.0697	121.1008	+
Hydrocoumarin	Aromatic	119-84-6	$C_9H_8O_2$	1388	1387	2269	2269	148.0524	120.056	91.0537	+
2-Buten-1-one, 1-(2,6,6-trimethyl-1,3-cyclohexadien-1-yl)-, (E)-	Ketone	23726-93-4	$C_{13}H_{18}O$	1389	1386	1823	1847	121.1007	175.1108	105.069	+
beta.-Bourbonene	Sesquiterpene	5208-59-3	$C_{15}H_{24}$	1394	1384	1540	1539	81.0687	123.1158	161.1311	+
Vanillin	Aldehyde	121-33-5	$C_8H_8O_3$	1401	1404	2602	2623	151.0393	152.0467	123.044	+++
Diphenyl ether	Ether	101-84-8	$C_{12}H_{10}O$	1405	1404	2040	2017	170.0723	141.07	115.0541	+
2-Buten-1-one, 1-(2,6,6-trimethyl-1-cyclohexen-1-yl)-	Ketone	35044-68-9	$C_{13}H_{20}O$	1419	1417	1841	1836	177.1274	192.151	123.1158	+
Alpha-cedrene	Sesquiterpene	469-61-4	$C_{15}H_{24}$	1419	1411	1592	1599	119.0847	161.1306	204.1864	+
Myosmine	Alkaloid	532-12-7	$C_9H_{10}N_2$	1426	1427	2231	2236	145.0762	118.0536	146.0836	++
Cyclohexanepropanoic acid, 2-propenyl ester	Ester	2705-87-5	$C_{12}H_{20}O_2$	1426	1435	1820	1800	121.101	95.0851	113.0594	+
cis-Thujopsene	Sesquiterpene	470-40-6	$C_{15}H_{24}$	1438	1429	1627	1592	119.084	105.0685	91.0524	+
Coumarin	Aromatic	91-64-5	$C_9H_6O_2$	1441	1441	2501	2519	146.0354	118.0407	90.0456	+
Ethyl Vanillin	Aldehyde	121-32-4	$C_9H_{10}O_3$	1459	1453	2556	2570	137.0235	166.0626	109.028	+
Humulene	Sesquiterpene	6753-98-6	$C_{15}H_{24}$	1460	1454	1693	1682	93.0691	147.1155	121.0998	+
Gamma-decalactone	Lactone	706-14-9	$C_{10}H_{18}O_2$	1471	1470	2176	2179	85.029	57.0333	128.0824	++
(1*S*, 2*S*)-Nicotine-N-oxide	Alkaloid	29419-55-4	$C_{10}H_{14}N_2O$	1479	**n.a.**	2203	n.a.	118.0652	119.0722	60.0439	++
trans-.beta.-Ionone	Ketone	79-77-6	$C_{13}H_{20}O$	1491	1486	1841	1863	177.1264	91.053	135.0787	+
Delta-decalactone	Lactone	705-86-2	$C_{10}H_{18}O_2$	1499	1496	2228	2201	71.0484	99.0441	43.0542	+
Isoeugenol methyl ether	Aromatic	93-16-3	$C_{11}H_{14}O_2$	1500	1492	2118	2176	178.0985	107.0536	163.0752	+
2H-1-Benzopyran-2-one, 6-methyl-	Aromatic	92-48-8	$C_{10}H_8O_2$	1563	1574	2551	2629	160.0524	132.0561	131.0489	+
Gamma-undecalactone	Lactone	104-67-6	$C_{11}H_{20}O_2$	1576	1576	2289	2259	85.028	95.0482	57.033	+
Hedione	Ester	24851-98-7	$C_{13}H_{22}O_3$	1658	1649	2307	2229	83.0488	153.1275	156.0782	+
Delta.-Dodecalactone	Lactone	713-95-1	$C_{12}H_{22}O_2$	1712	1719	2465	2467	71.0481	99.0433	55.0533	+
Benzyl Benzoate	Ester	120-51-4	$C_{14}H_{12}O_2$	1770	1762	2672	2693	105.0329	194.0721	167.0833	+
Phytol	Diterpenoid	150-86-7	$C_{20}H_{40}O$	2090	2114	2621	2633	123.115	95.0845	81.0689	+

[a] LRI, linear retention index.

[b] Frequency of detection: + (< 30% of samples), ++ (30%– 60% samples), +++ (> 60% samples).

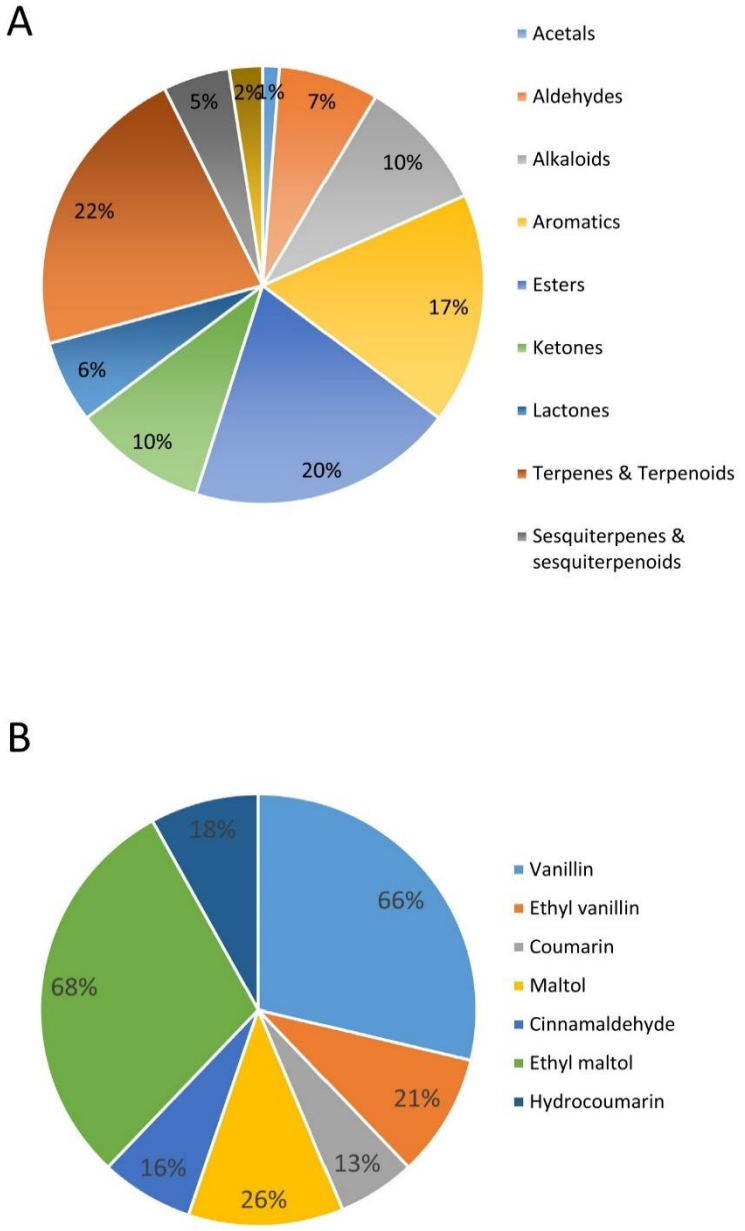


Fig. 2. A, Distribution of compounds identified with both column in chemical classes. B, Detection frequencies of respiratory pro-inflammatory compounds.

nicotine containing samples. Despite its similar chemical structure, methyl nicotinate appears to have a different origin than the rest of nicotine-like compounds, since it was identified in a limited number of both kinds of e-liquids. This compound has been correlated with dermatitis problems when included in topic use pharmaceutical preparations [29]; thus, it might behave also as an irritant of the respiratory system.

3.3. Acetals

Acetals are respiratory irritant compounds. Their presence in e-liquids is the result of reactions between aldehydes and alcohols. The data mining strategy described in the Material and Methods section, combined with manual inspection of GC-TOF-MS records, showed the frequent presence of two clusters of signals corresponding to the diastereomers of acetals formed between main aldehydes in e-liquids (i.e., vanillin and ethylvanillin) with PG (2 peaks) and VG (4 peaks). In the latter case, two different acetals corresponding to 5 and 6 member rings are possible. Fig. 4 plots the extracted ion chromatograms (obtained with the HP-5 MS column) and the accurate scan spectra for two representative species. Whatever their retention times, the congeners in both groups of vanillin acetals (with PG, or VG) showed identical spectra. They share the same fragment at *m/z* 151 (nominal mass) correspond-

USC UNIVERSIDADE DE SANTIAGO DE COMPOSTELA

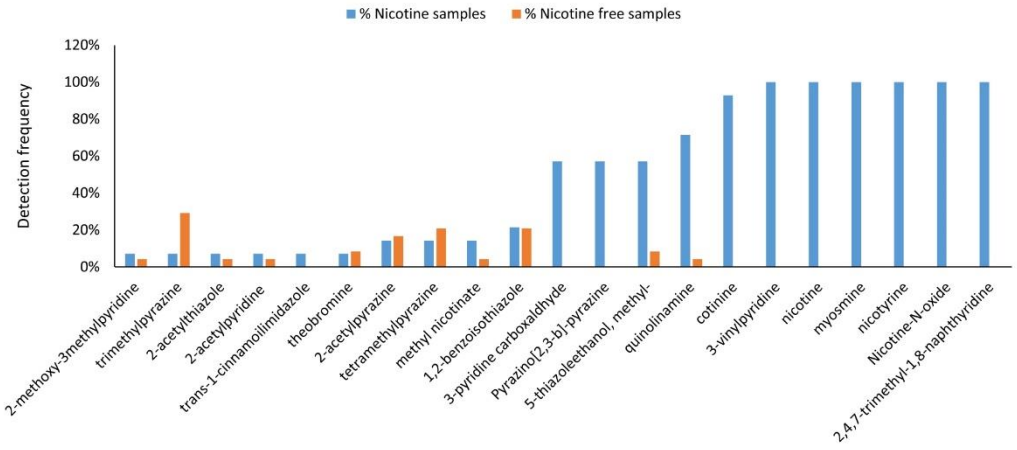


Fig. 3. Detection frequencies of heterocyclic nitrogenated compounds in nicotine and nicotine-free e-liquids.

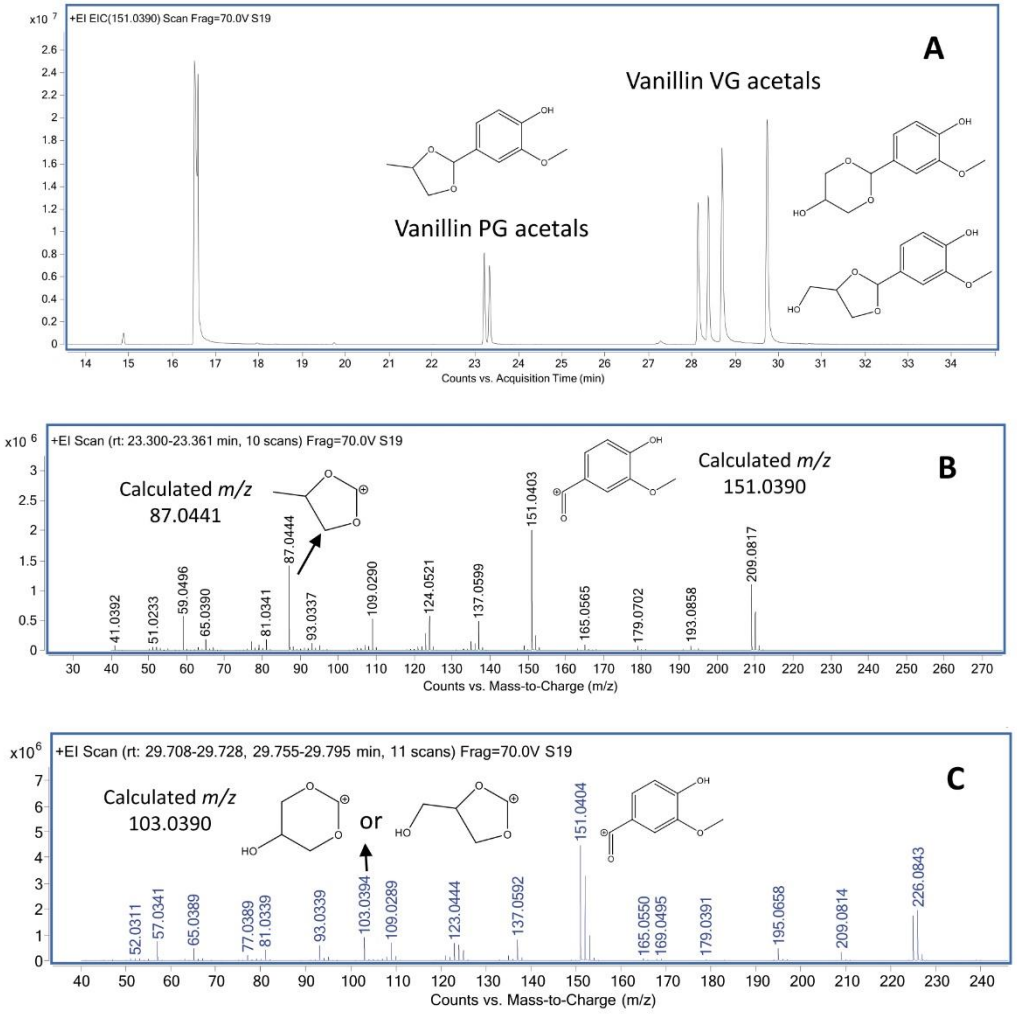


Fig. 4. A, EIC chromatogram at *m/z* 151.0390 (mass window 50 ppm) for sample S19. Accurate EI- MS spectra for the acetals of vanillin with PG (B) and VG (C).

USC UNIVERSIDADE DE SANTIAGO DE COMPOSTELA

Table 2
Concentrations of vanillin, ethyl vanillin, benzaldehyde and their acetals with PG in a selection of e-liquid samples. Average values for duplicate injections. Data in μg mL^{-1}.

Sample code	Brand	Vanillin	Ethyl Vanillin	Benzaldehyde	Vanillin Acetal	Ethyl Vanillin Acetal	Benzaldehyde acetal
1	A	754.3			33.4		
2	A	937.6			37.8		
3	A	1922.9	2447.0		77	121.1	
4	A	5365.0	1050.6		112.7	26.4	
5	B	467.8			15.6		
10	A	672.6		46.8	30.4		24.2
12	D	3752.9	625.5		217.1	29.6	
19	F	3923.0	485.4		225.1	23.4	
20	G	701.4			21.6		
21	G	4736.7	1051.1		283.8	58.2	
25	G	595.3			22.9		
30	G	487.8	289.5		13.5	9.6	
31	G	277.1		98.5	14.25		81.0
34	H	489.9			15.7		

ing to the deprotonated parent aldehyde ($[M\text{-}H]^+$ ion of vanillin); moreover, other ions, with calculated exact *m/z* values of 87.0441 and 103.0393, are compatible with the non-aromatic rings ($C_4H_7O_2$ and $C_4H_7O_3$ moieties) in the structures of vanillin-PG and vanillin-VG acetals. Same chromatographic and spectral behavior was observed for ethyl vanillin acetals. In case of benzaldehyde, a single peak corresponding to its acetal with PG was detected in the chromatograms for e-liquids, figure not shown.

The identities of the acetals of vanillin, ethyl vanillin and benzaldehyde with PG were confirmed with commercial standards. Verification of their presence in e-liquids, instead of formation at the injection of the GC–MS system, was achieved by LC-TOF-MS. Considering vanillin as potential precursor aldehyde, the acetals of this compound with PG and VG showed single peaks, at retention times slightly higher and lower than that of vanillin, respectively. The ESI (+) product ion (MS/MS) spectra of both acetals showed a product ion at *m/z* 153.0547, matching the $[M + H]^+$ ion of vanillin, Fig. S4. Further research to detect partial transformation of aldehydes to acetals, in the injector of the GC–MS instrument was carried out by adding benzaldehyde-d_5 (addition level 100 μg mL^{-1}) to ethyl acetate diluted e-liquids, just before GC–MS analysis. The obtained GC-TOF-MS chromatograms did not contain any extra peaks, neither at nominal *m/z* 168 not at *m/z* 184, corresponding to the acetals of benzaldehyde-d_5 with PG and VG, respectively. So, we concluded that acetals of the above aldehydes existed in e-liquids and that, they were not artifacts associated to thermally induced reactions in the injector of the GC-TOF-MS system.

Table 2 summarizes the concentrations of vanillin, ethyl vanillin and benzaldehyde together to those for their acetals with PG in the set of processed e-liquids. Concentrations were determined against solvent-based standards, considering split and splitless injection of diluted samples (1:100), for aldehydes and acetals respectively, and using benzaldehyde-d_5 as internal standard. Levels of vanillin and ethyl vanillin in positive samples varied between 0.3 mg mL^{-1} and 5.4 mg mL^{-1}, within the range of values reported in previous studies developed in Europe [20], and below maximum levels (33 mg mL^{-1} for vanillin) reported for samples purchased in USA [11]. The concentrations of their acetals with PG (as sum of diastereomers) represented between 2% and 6% of the content of parent aldehydes. These percentages are significantly lower than those reported in laboratory experiments, combining aldehydes with e-liquids containing different percentages of PG [13]. Benzaldehyde was found just in two out of 39 samples; however, the ratio between the concentration of its acetal with PG and the free aldehyde (values from 0.52 to 0.83) were higher than those observed for vanillin and ethyl vanillin.

3.4. Cannabinoids

Among commercially available e-liquids, those containing cannabidiol (CBD) are gaining popularity. This fact raises concerns in relation to consumers exposure to other cannabinoids, with potential psychotropic effects, either existing in cannabis extracts, or formed from transformation of CBD during consumption of e-cigarettes [30]. Fig. 5 shows the EI-MS spectra and the chemical structures assigned to cannabinoids identified in the GC-TOF-MS chromatograms for this type of e-liquids. Cannabinoids were detected only using the HP-5MS column due to their limited volatility. Fig. S5 shows the chromatographic profiles for the major congeners within this group of compounds. Two bicyclic species, with the same chemical structure of CBD, but shorter alkyl chains were identified as cannabidivarin (CBDV), and the homologue species with a butyl group bonded to carbon number 5 in the aromatic ring, Fig. 5A and 5B. Their structures were not confirmed with authentic standards; however little doubt exists on their identities considering differences between ions existing in their EI-MS spectra and that of CBD. To sum up, the radical cation $[(M^{\cdot+})]$ and the base peak in the spectra of these compounds are shifted in multiples of 14.0156 Da, versus those in the spectrum of CBD, Fig. 5A to 5C. The presence of cannabinol (CBN, $C_{21}H_{26}O_2$) was first identified, and then confirmed in e-liquids. Its spectrum is shown in Fig. 5D. A second group of cannabinoids, with the same empirical formula of CBD ($C_{21}H_{30}O_2$), were cannabichromene (CBC) Fig. 5E, with a similar spectrum but a most intense fragment at *m/z* 174, and a slightly higher retention time than CBD (Fig. S4), and delta-9-tetrahydrocannabinol (Δ9-THC) Fig. 5H. In addition, two relatively intense peaks, at longer retention times than that of CBD (Fig. S5), corresponding to three oxygenated species ($C_{21}H_{30}O_3$) with identical EI-MS spectra, were also detected, Fig. 5F and 5G. Identifications derived from NIST database search pointed out to cannabielsoin (CBE) as the most probable candidate for both peaks, whilst the retention time for a commercial CBE standard matched that obtained for the first species. CBE was already described by Tsujikawa et al. [31] in CBD-type e-liquids.

Taking into account reports describing the partial, and variable, decomposition of CBD in the injector of GC instruments (the percentage of CBD conversion to Δ9-THC varies depending on temperature and injection mode) [31], and the very low intensity of the peak assigned to Δ9-THC compared to that of CBD (Fig. S5), it was hard to determine whether the former compound (the only psychoactive cannabinol identified in this research) is present in e-liquids, or if it was an artifact generated in the injector of the GC-TOF-MS system. Thus, LC-MS/MS was used as complementary technique. Under conditions given in the supplementary informa-

USC UNIVERSIDADE DE SANTIAGO DE COMPOSTELA

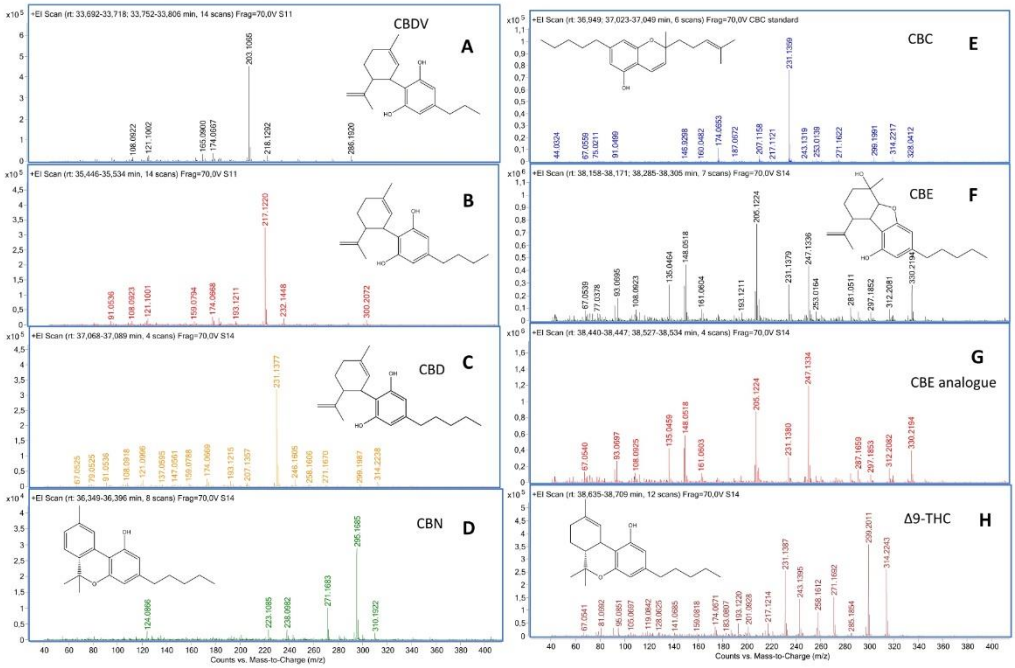


Fig. 5. Accurate EI-MS spectra and structures of cannabinoids identified in cannabidiol e-liquids. A, CBDV. B, homologue with a butyl bonded group bonded to carbon number 5 in the aromatic ring. C, CBD. D, CBN. E, CBC. F, CBE. G, CBE analogue. H, Δ9-THC.

Table 3
Concentrations (μg mL^{-1}) of delta-9-tetrahydrocannabinol (Δ9-THC) and cannabidiol (CBD) in e-liquids determined by LC-MS/MS, $n = 3$ replicates.

Sample code	Brand code	Δ9-THC	CBD	ratio
11	C	1.2	3202	0.04%
13	E	9.6	6814	0.14%
14	E	17.6	6163	0.29%
37	J	3.8	5984	0.06%
38	J	15.1	3718	0.41%
39	J	1.3	6183	0.02%

tion (Text S2), the retention times of CBD, Δ9-THC and CBC were 4.33, 6.34 and 7.34 min, respectively. The chromatograms for diluted e-liquids (1:10 dilution in methanol) confirmed the presence of CBC and Δ9-THC in e-liquids. Moreover, an extra species with same MRM transitions as Δ9-THC, and slightly higher retention time, was also evident, Fig. S6. The concentrations of CBD in e-liquids (obtained by LC-MS/MS) varied between 3.2 mg mL^{-1} and 6.2 mg mL^{-1}. The levels of Δ9-THC ranged from 1.2 μg mL^{-1} to 17.6 μg mL^{-1}, representing between 0.02% and 0.4% of those measured for CBD in the same e-liquids, Table 3. The therapeutic dose of Δ9-THC employed in commercial drugs, i.e. *marinol*, approved to treat side-effects of chemotherapy and in HIV infected patients, are in the range from 2.5 mg to 5 mg dose [32]. Considering a daily inhalation of 5 mL of e-liquids [11], direct exposure to Δ9-THC remains at least 20-times below the therapeutic value for oral administration. However, the potential conversion of CBD to Δ9-THC during e-smoking might increase the respiratory exposure to the latter species. Moreover, the bio-accessibility of the psychoactive compound probably differs depending on administration routes. So, possible therapeutic and/or addictive effects of Δ9-THC in consumers of CBD-containing e-liquids deserves further research.

4. Conclusions

E-liquids contain a large variety of volatile and semi-volatile compounds, at very different concentration levels, sometimes with same empirical formulae and/or with similar EI-MS spectra. Thus, the use of chromatographic retention index is mandatory to improve the confidence of tentative identifications derived from MS spectra. The enhanced sensitivity of the TOF mass analyzer, combined with accurate MS data, allowed the detection of a high number of volatile and semi-volatile features in e-liquids. Moreover, the employment of columns with different polarity improves the reliability of identifications derived from a non-target data mining strategy. Comprehensive characterization of e-liquids represents just the first step to understand possible risks associated to the e-smoking habit. Further studies should characterize the composition of their vaporized fraction, in order to determine the percentage of these compounds inhaled by consumers, and to identify potential transformation, and/or degradation processes, occurring during e-smoking. Spectral database created in this study are expected to be of usefulness in the further characterization of compounds present in vapors produced during e-smoking.

Declaration of Competing Interest

The authors declare that they have no known competing financial interests or personal relationships that could have appeared to influence the work reported in this paper.

CRediT authorship contribution statement

M. Cobo Golpe: Investigation, Methodology, Writing – review & editing. **M. Ramil:** Supervision, Writing – review & editing. **I. Rodríguez:** Conceptualization, Supervision, Funding acquisition, Writing – original draft.

USC UNIVERSIDADE DE SANTIAGO DE COMPOSTELA

Data availability

Data will be made available on request.

Acknowledgements

M.C.G. thanks a FPI pre-doctoral grant to the Spanish Ministry of Science & Innovation. This study was supported by Spanish Government and Xunta de Galicia through grants PGC2018–094613-B-I00 and ED431C 2021/06, respectively. Both projects are co-funded by the EU FEDER program.

Supplementary materials

Supplementary material associated with this article can be found, in the online version, at doi:10.1016/j.chroma.2023.464114.

References

[1] N. Beauval, S. Antherieu, M. Soyez, N. Gengler, N. Grova, M. Howsam, E.M. Hardy, M. Fischer, B.M.R. Appenzeller, J.F. Goossens, D. Allorge, G. Garçon, J.M. Lo-Guidice, A. Garat, Chemical evaluation of electronic cigarettes: multicomponent analysis of liquid refills and their corresponding aerosols, J. Anal. Toxicol. 41 (2017) 670–678, doi:10.1093/jat/bkx054.
[2] C. Hutzler, M. Paschke, S. Kruschinski, F. Henkler, J. Hahn, A. Luch, Chemical hazards present in liquids and vapors of electronic cigarettes, Arch. Toxicol. 88 (2014) 1295–1308, doi:10.1007/s00204-014-1294-7.
[3] Z.T. Bitzer, R. Goel, S.M. Reilly, R.J. Elias, A. Silakov, J. Foulds, J. Muscat, J.P. Richie, Effect of flavoring chemicals on free radical formation in electronic cigarette aerosols, Free Radic, Biol. Med. 120 (2018) 72–79, doi:10.1016/j.freeradbiomed.2018.03.020.
[4] X. Liu, A. Lugo, E. Davoli, G. Gorini, R. Pacifici, E. Fernández, S. Gallus, Electronic cigarettes in Italy: a tool for harm reduction or a gateway to smoking tobacco? Tob. Control. 29 (2020) 148–152, doi:10.1136/tobaccocontrol-2018-054726.
[5] K.E. Farsalinos, I.Gene Gillman, M.S. Melvin, A.R. Paolantonio, W.J. Gardow, K.E. Humphries, S.E. Brown, K. Poulas, V. Voudris, Nicotine levels and presence of selected tobacco-derived toxins in tobacco flavoured electronic cigarette refill liquids, Int. J. Environ. Res. Public Health. 12 (2015) 3439–3452, doi:10.3390/ijerph120403439.
[6] K. Dunn, A. Taylor, S. Turfus, A review of cannabidiol-containing electronic liquids—Current regulations and labelling accuracy, Drug Test. Anal. 13 (2021) 1490–1498, doi:10.1002/dta.3102.
[7] T.M. Falconer, F. Morales-Garcia, Rapid screening of vaping liquids by DART-MS, J. AOAC Int. (2022) 1–9, doi:10.1093/jaoacint/qsac103.
[8] T. Muthumalage, M. Prinz, K.O. Ansah, J. Gerloff, I.K. Sundar, I. Rahman, Inflammatory and oxidative responses induced by exposure to commonly used e-cigarette flavoring chemicals and flavored e-liquids without nicotine, Front. Physiol. 8 (2018) 1–13, doi:10.3389/fphys.2017.01130.
[9] C.A. Lerner, I.K. Sundar, R.M. Watson, A. Elder, R. Jones, D. Done, R. Kurtzman, D.J. Ossip, R. Robinson, S. McIntosh, I. Rahman, Environmental health hazards of e-cigarettes and their components: oxidants and copper in e-cigarette aerosols, Environ. Pollut. 198 (2015) 100–107, doi:10.1016/j.envpol.2014.12.033.
[10] M. Rouabhia, H.J. Park, A. Semlali, A. Zakrzewski, W. Chmielewski, J. Chakir, E-cigarette vapor induces an apoptotic response in human gingival epithelial cells through the caspase-3 pathway, J. Cell. Physiol. 232 (2017) 1539–1547, doi:10.1002/jcp.25677.
[11] P.A. Tierney, C.D. Karpinski, J.E. Brown, W. Luo, J.F. Pankow, Flavour chemicals in electronic cigarette fluids, Tob. Control. 25 (2016) e10–e15, doi:10.1136/tobaccocontrol-2014-052175.
[12] A.B. Stefaniak, R.F. LeBouf, A.C. Ranpara, S.S. Leonard, Toxicology of flavoring- and cannabis-containing e-liquids used in electronic delivery systems, Pharmacol. Ther. 224 (2021) 107838, doi:10.1016/j.pharmthera.2021.107838.
[13] H.C. Erythropel, S.V. Jabba, T.M. Dewinter, M. Mendizabal, P.T. Anastas, S.E. Jordt, J.B. Zimmerman, Formation of flavorant-propylene glycol adducts with novel toxicological properties in chemically unstable e-Cigarette liquids, Nicotine Tob. Res. 21 (2019) 1248–1258, doi:10.1093/ntr/nty192.
[14] K. Bekki, S. Uchiyama, K. Ohta, Y. Inaba, H. Nakagome, N. Kunugita, Carbonyl compounds generated from electronic cigarettes, Int. J. Environ. Res. Public Health 11 (2014) 11192–11200, doi:10.3390/ijerph111111192.
[15] S. Klager, J. Vallarino, P. MacNaughton, D.C. Christiani, Q. Lu, J.G. Allen, Flavoring chemicals and aldehydes in e-cigarette emissions, Environ. Sci. Technol. 51 (2017) 10806–10813, doi:10.1021/acs.est.7b02205.
[16] J. Hahn, Y.B. Monakhova, J. Hengen, M. Kohl-Himmelseher, J. Schössler, H. Hahn, T. Kuballa, D.W. Lachenmeier, Electronic cigarettes: overview of chemical composition and exposure estimation, Tob. Induc. Dis. 12 (2014) 1–12, doi:10.1186/s12971-014-0023-6.
[17] M. Famele, J. Palmisani, C. Ferranti, C. Abenavoli, L. Palleschi, R. Mancinelli, R.M. Fidente, G. de Gennaro, R. Draisci, Liquid chromatography with tandem mass spectrometry method for the determination of nicotine and minor tobacco alkaloids in electronic cigarette refill liquids and second-hand generated aerosol, J. Sep. Sci. 40 (2017) 1049–1056, doi:10.1002/jssc.201601076.
[18] S. Han, H. Chen, X. Zhang, T. Liu, Y. Fu, Levels of selected groups of compounds in refill solutions for electronic cigarettes, Nicotine Tob. Res. 18 (2016) 708–714, doi:10.1093/ntr/ntv189.
[19] E.A. Eshraghian, W.K. Al-Delaimy, A review of constituents identified in e-cigarette liquids and aerosols, Tob. Prev. Cessat 7 (2021) 1–15, doi:10.18332/tpc/131111.
[20] J. Aszyk, P. Kubica, M.K. Woźniak, J. Namieśnik, A. Wasik, A. Kot-Wasik, Evaluation of flavour profiles in e-cigarette refill solutions using gas chromatography–tandem mass spectrometry, J. Chromatogr. A. 1547 (2018) 86–98, doi:10.1016/j.chroma.2018.03.009.
[21] R.F. LeBouf, D.A. Burns, A. Ranpara, K. Attfield, L. Zwack, A.B. Stefaniak, Headspace analysis for screening of volatile organic compound profiles of electronic juice bulk material, Anal. Bioanal. Chem. 410 (2018) 5951–5960, doi:10.1007/s00216-018-1215-3.
[22] A. Larcombe, S. Allard, P. Pringle, R. Mead-Hunter, N. Anderson, B. Mullins, Chemical analysis of fresh and aged Australian e-cigarette liquids, Med. J. Aust. 216 (2022) 27–32, doi:10.5694/mja2.51280.
[23] G. Castro, I. Rodríguez, M. Ramil, R. Cela, Assessment of gas chromatography time-of-flight mass spectrometry for the screening of semi-volatile compounds in indoor dust, Sci. Total Environ. 688 (2019) 162–173, doi:10.1016/j.scitotenv.2019.06.192.
[24] M. Cobo-Golpe, M. Ramil, R. Cela, I. Rodríguez, Portable dehumidifiers condensed water: a novel matrix for the screening of semi-volatile compounds in indoor air, Chemosphere 251 (2020) 126346, doi:10.1016/j.chemosphere.2020.126346.
[25] M. Moniruzzaman, I. Rodríguez, M. Ramil, R. Cela, S.A. Sulaiman, S.H. Gan, Assessment of gas chromatography time-of-flight accurate mass spectrometry for identification of volatile and semi-volatile compounds in honey, Talanta 129 (2014) 505–515, doi:10.1016/j.talanta.2014.06.019.
[26] A. Fontana, I. Rodríguez, R. Cela, Dispersive liquid–liquid microextraction and gas chromatography accurate mass spectrometry for extraction and non-targeted profiling of volatile and semi-volatile compounds in grape marc distillates, J. Chromatogr. A. 1546 (2018) 36–45, doi:10.1016/j.chroma.2018.03.003.
[27] E.L. Schymanski, J. Jeon, R. Gulde, K. Fenner, M. Ruff, H.P. Singer, J. Hollender, Identifying small molecules via high resolution mass spectrometry: communicating confidence, Environ. Sci. Technol. 48 (2014) 2097–2098, doi:10.1021/es5002105.
[28] J.G. Lisko, H. Tran, S.B. Stanfill, B.C. Blount, C.H. Watson, Chemical composition and evaluation of nicotine, tobacco alkaloids, pH, and selected flavors in E-Cigarette cartridges and refill solutions, Nicotine Tob. Res. 17 (2015) 1270–1278, doi:10.1093/ntr/ntu279.
[29] S.F. de Andrade, C. Rocha, E.J. Pinheiro, C. Pereira-Leite, M. do C. Costa, L. Monteiro Rodrigues, Revealing the protective effect of topically applied cymbopogon citratus essential oil in human skin through a contact model, Cosmetics 10 (2023), doi:10.3390/cosmetics10010029.
[30] Z. Czégény, G. Nagy, B. Babinszki, Á. Bajtel, Z. Sebestyén, T. Kiss, B. Csupor-Löffler, B. Tóth, D. Csupor, CBD, a precursor of THC in e-cigarettes, Sci. Rep. 11 (2021) 8951, doi:10.1038/s41598-021-88389-z.
[31] Y.T.I. Kenji Tsujikawa, Yuki Okada, Hiroki Segawa, Tadashi Yamamuro, Kenji Kuwayama, Tatsuyuki Kanamori, Thermal decomposition of CBD to Delta-9-THC during GC-MS analysis: a potential cause of Delta-9-THC misidentification, Forensic Sci. Int. 37 (2022) 111366, doi:10.1016/j.forsciint.2022.111366.
[32] R. Likar, G. Nahler, The use of cannabis in supportive care and treatment of brain tumor, Neuro-Oncol. Pract. 4 (2017) 151–160, doi:10.1093/nop/npw027.

USC UNIVERSIDADE DE SANTIAGO DE COMPOSTELA

Supplementary information to manuscript:

Comprehensive characterization of volatile and semi-volatile compounds in e-liquids for electronic cigarette using gas chromatography accurate mass spectrometry

M. Cobo Golpe, M. Ramil, I. Rodríguez*

Department of Analytical Chemistry, Nutrition and Food Sciences. Research Institute on Chemical and Biological Analysis (IAQBUS). Universidade de Santiago de Compostela, 15782-Santiago de Compostela, Spain.

*e-mail: isaac.rodriguez@usc.es

USC UNIVERSIDADE DE SANTIAGO DE COMPOSTELA

List of abbreviations:

CBC, cannabichromene

CBD, cannabidiol

Δ9-THC, Delta-9-tetrahydrocannabinol

ESI, electrospray ionization

GC, gas chromatography

LC, liquid Chromatography

LLE, liquid-liquid extraction

LRI, linear retention index

MS, mass spectrometry

PG, propylene glycol

TIC, total ion current chromatogram

TOF, time of flight

VG, vegetal glycerine

USC UNIVERSIDADE DE SANTIAGO DE COMPOSTELA

Table S1. Summary of e-liquid samples with available information from suppliers

Sample code	Brand code	Flavor descriptor	PG:VG ratio	Nicotine content (mg mL^{-1})	Cannabidiol (CBD)
S1	A	Tobacco & ron	60:40	6	N
S2	A	Raspberry	70:30	6	N
S3	A	Yogurt mouse	50:50	3	N
S4	A	Anis	30:70		N
S5	B	Blond tobacco	70:30	6	N
S6	B	Mint	70:30	6	N
S7	A	Apple	70:30	12	N
S8	A	Gintonic	60:40	6	N
S9	A	Strawberry	30:70	12	N
S10	A	Hazelnut punch	70:30	3	N
S11	C	Blueberry	40:60		Y
S12	D	Black soul	30:70		N
S13	E	Not declared	100:0		Y
S14	E	Not declared	80:20		Y
S15	F	Classic tobacco	50:50		N
S16	F	Blond tobacco	50:50		N
S17	F	Menthol	50:50		N
S18	F	Tobacco	50:50		N
S19	F	Vainillin	50:50		N
S20	G	Banana	30:70		N
S21	G	Vainillin	30:70		N
S22	G	Blueberry	30:70		N
S23	G	Passion fruit	30:70		N
S24	G	Strawberry	30:70		N
S25	G	Watermelon	30:70		N
S26	G	Apple	30:70		N
S27	G	Mango	30:70		N
S28	G	Melon	30:70		N
S29	G	Mint	30:70		N
S30	G	Pineapple	30:70		N
S31	G	Cherry	30:70		N
S32	B	Peach	70:30	6	N
S33	B	Green lemon	70:30	3	N
S34	H	Chewing gum	50:50	3	N
S35	I	Lime & lemon	50:50	6	N
S36	I	Kiwi & strawberry	50:50	3	N
S37	J	Raspberry	70:30		Y
S38	J	Fresh grape soda	70:30		Y
S39	J	Grape fruit & lime	70:30		Y

Y, CBD declared e-liquids. N, not declared.

USC UNIVERSIDADE DE SANTIAGO DE COMPOSTELA

Table S2. Efficiency of LLE of e-liquids with ethyl acetate (0.1 mL of sample diluted with 5 mL of water and extracted with 1 mL of organic solvent) for selected compounds, n=6 replicates.

Compound	LLE efficiency	SD
Piperonal	105%	11%
Cinnamaldehyde (E)	120%	5%
Vanillin propylene glycol acetal isomer 1	18%	6%
Vanillin propylene glycol acetal isomer 2	27%	7%
Anethole	104%	6%
Maltol	18%	12%
Nicotine	< 5%	
Cinnamyl cinnamate	66%	7%
alpha-Terpineol	81%	4%
Benzyl alcohol	58%	2%
Benzyl benzoate	109%	4%
Vanillin	137%	8%
Nicotyrine	< 5%	
Hydrocoumarin	98%	2%
Ethyl vanillin	110%	2%
Trans beta-ionone	107%	2%
Isoeugenol methyl ether	110%	10%
Acetyl pyrazine	54%	2%

USC UNIVERSIDADE DE SANTIAGO DE COMPOSTELA

Table S3. Summary of compounds tentatively identified using the HP5-MS column. Species in bold were confirmed against authentic standards.

Compound	Chemical family	CAS number	Formula	LRI, exp.	LRI, NIST	Ion 1	Ion 2	Ion 3
1,3-Dioxolane, 4-methyl-2-pentyl-	Acetal	1599-49-1	C9H18O2	1083	1097	87.0437	59.0486	157.1205
1,3-Dioxolane, 4-methyl-2-(1-pentenyl)-, (E)-	Acetal	94089-21-1	C9H16O2	1120	1105	113.0595	127.0751	69.0332
1,3-Dioxolane, 2-heptyl-4-methyl-	Acetal	74094-61-4	C11H22O2	1285	1296	87.0433	59.0481	185.1525
1,3-Benzodioxole, 5-(4-methyl-1,3-dioxolan-2-yl)-	Acetal	61683-99-6	C11H12O4	1630	1617	149.0225	122.0342	207.0615
Vanillin propylene glycol acetal	Acetal	68527-74-2	C10H12N2O	1684	1686	98.0588	147.0683	176.0928
Benzaldehyde, 4-methoxy-	Aldehyde	123-11-5	C8H8O2	1257	1251	135.0455	107.0502	77.0386
Benzaldehyde, 3,4-dimethoxy-	Aldehyde	120-14-9	C9H10O3	1483	1495	166.0614	165.0545	137.0527
3-vinyl Pyridine	Alkaloid	1121-55-7	C7H7N	977	975	105.0573	104.0486	78.0440
2-amino-1,3-propanediol	Alkaloid	534-03-2	C3H9NO2	984	984	60.0206	42.0095	
3-Pyridinecarboxaldehyde	Alkaloid	500-22-1	C6H5NO	1004	976	106.0278	107.0358	78.0354
Trimethyl pyrazine	Alkaloid	14667-55-1	C7H10N2	1006	1004	122.0828	81.0568	
2-Acetylthiazole	Alkaloid	24295-03-2	C5H5NOS	1022	1022	99.0143	111.9842	127.0078
1H-Imidazole, 2-ethyl-4-methyl-	Alkaloid	931-36-2	C6H10N2	1111	1085	109.0987	95.0840	81.0686
Tetrahydro-1,3-oxazine-2-thione	Alkaloid	17374-18-4	C4H7NOS	1140	1163	117.0358	89.0399	59.0299
Methyl nicotinate	Alkaloid	93-60-7	C7H7NO2	1141	1139	136.0397	106.0290	78.0382
Oxazolidin-2-one	Alkaloid	497-25-6	C3H5NO2	1184	1164	87.0430	59.0480	41.0378
Pyrazino[2,3-b]pyrazine	Alkaloid	255-53-8	C6H4N4	1199	1207	133.0525	106.0310	78.0421
Benzothiazole	Alkaloid	272-16-2	C7H5NS	1228	1229	135.0135	108.0025	81.9867
2,4,5-Trihydroxypyrimidine	Alkaloid	496-76-4	C4H4N2O3	1241	1217	128.0513	85.0285	57.0339
Hidrazine 1-ethyl 2-phenyl	Alkaloid	622-82-2	C8H12N2	1279	1290	93.0689	107.0845	136.1242
Nicotyrine	Alkaloid	487-19-4	C10H10N2	1486	1488	158.0862	130.0646	116.0489
N-desmethyl nicotine	Alkaloid	5746-86-1	C9H12N2	1456	1435	119.0600	147.0915	70.0641
Quinolinamine (several positional isomers possible)	Alkaloid	580-17-6	C9H8N2	1562	1537	144.0700	117.0613	90.0446
1-8-Naphthyridine 2,4,7-trimethyl-	Alkaloid	14757-44-9	C11H12N2	1585	1559	171.0911	172.0986	130.0648
Cotinine	Alkaloid	15569-85-4	C10H12N2O	1717	1713	98.0592	147.0677	176.0938
trans-1-Cinnamoylimidazole	Alkaloid	1138-15-4	C12H10N2O	1761	1731	131.0489	103.0533	147.0462
Theobromine	Alkaloid	83-67-0	C7H8N4O2	1868	1874	180.0641	137.0565	109.0612
Cyclopropane, 1,2-dimethyl-3-pentyl-, (1.alpha.,2.alpha.,3.alpha.)-	Alkane	62238-10-2	C10H20	1014	1005	56.0613	69.0693	84.0919

USC DE COMPOSTELA

Compound	Chemical family	CAS number	Formula	LRI, exp.	LRI, NIST	Ion 1	Ion 2	Ion 3
Benzene, 4-ethenyl-1,2-dimethyl-	Aromatic	27831-13-6	C10H12	1092	1110	132.0919	117.0656	115.0531
Guaiacol	Aromatic	90-05-1	C7H8O2	1093	1090	124.0518	109.0288	81.0347
Benzene, 1-methyl-2-(1-methyl-2-propenyl)-	Aromatic	97664-19-2	C11H14	1149	1131	131.0846	146.1077	91.0526
Ethanone, 1-(4-methylphenyl)-	Aromatic	122-00-9	C9H10O	1188	1183	119.0477	91.0526	134.0711
Methyl salicylate	Aromatic	119-36-8	C8H8O3	1199	1192	120.0207	92.0259	152.0495
Catechol	Aromatic	120-80-9	C6H6O2	1201	1208	110.0359	81.0344	64.0355
Benzeneacetic acid	Aromatic	103-82-2	C8H8O2	1259	1262	91.0529	136.0517	65.0374
3-Ethoxy-4-methoxyphenol	Aromatic	65383-57-5	C9H12O3	1385	1379	125.0230	140.0467	168.0412
Benzeneacetic acid, 2-methylpropyl ester	Aromatic	102-13-6	C12H16O2	1394	1393	91.0530	136.0520	65.0375
Benzene, 1,2-dimethoxy-4-propenyl-, (Z)-	Aromatic	6380-24-1	C11H14O2	1459	1456	178.0983	163.0743	107.0486
Acetic acid, phenyl-, isopentyl ester	Aromatic	102-19-2	C13H18O2	1493	1490	91.0529	70.0758	136.0514
2,4-Di-tert-butylphenol	Aromatic	96-76-4	C14H22O	1514	1519	191.1457	206.1697	163.1134
Phenol, 2-ethoxy-5-(1-propenyl)-	Aromatic	94-86-0	C11H14O2	1528	1510	178.0979	149.0588	103.0529
2-Propanone, 1-(4-hydroxy-3-methoxyphenyl)-	Aromatic	2503-46-0	C10H12O3	1534	1536	137.0592	180.0772	122.0354
Phenol, 4-ethenyl-2,6-dimethoxy-	Aromatic	28343-22-8	C10H12O3	1568	1563	180.0791	165.0556	137.0595
Ethyl 3-(2-hydroxyphenyl)propanoate	Aromatic	20921-04-4	C11H14O3	1572	1576	120.0558	148.0518	194.0925
1-(4-Methoxyphenyl)propane-1,2-diol	Aromatic	51410-48-1	C10H14O3	1582	1582	137.0581	109.0630	94.0406
Butan-2-one, 4-(3-hydroxy-2-methoxyphenyl)-	Aromatic	303187-89-5	C11H14O3	1651	1638	137.0586	194.0931	119.0481
2-Propenoic acid, 3-phenyl-, phenylmethyl ester, (E)-	Aromatic	78277-23-3	C16H14O2	2097	2102	131.0483	192.0922	91.0530
2-Propenoic acid, 3-phenyl-, 3-phenylpropyl ester	Aromatic	122-68-9	C18H18O2	2312	2324	117.0671	118.0753	131.0479
Cannabidivarin	Cannabinoid	24274-48-4	C16H26O2	2190	n.a	203.1065	286.1920	218.1292
Cannabidiol	Cannabinoid	521-37-9	C21H30O2	2437	2405	231.1377	314.2238	246.1605
Cannabichromene	Cannabinoid	20675-51-8	C21H30O2	2450	2486	231.1367	314.2236	174.0653
Cannabielsoin	Cannabinoid	54002-78-7	C21H30O3	2493	2587	205.1224	247.1336	330.2194
Delta-9-tetrahydrocannabinol	Cannabinoid	1972-08-3	C21H30O2	2522	2468	299.2011	314.2243	271.1692
Benzylacetic acid	Carboxylic Acid	501-52-0	C9H10O2	1340	1359	91.0531	104.0604	150.0666
Carbamic acid	Carboxylic Acid	30379-59-0	C9H11NO2	1349	1358	108.0562	91.0529	79.0527

USC UNIVERSIDADE DE SANTIAGO DE COMPOSTELA

Compound	Chemical family	CAS number	Formula	LRI, exp.	LRI, NIST	Ion 1	Ion 2	Ion 3
cis-5-Dodecenoic acid	Carboxylic Acid	2430-94-6	C12H22O2	1577	1561	95.0496	110.0730	128.0841
Butanoic acid, 2-methylpropyl ester	Ester	539-90-2	C8H16O2	963	955	71.0473	43.0526	56.0610
4-Hexen-1-ol, acetate	Ester	72237-36-6	C8H14O2	1009	1020	67.0538	82.0766	
Acetic acid, hexyl ester	Ester	142-92-7	C8H16O2	1014	1011	56.0617	69.0696	61.0282
Acetic acid, phenylmethyl ester	Ester	140-11-4	C9H10O2	1167	1164	108.0572	91.0538	79.0540
Butanedioic acid, diethyl ester	Ester	123-25-1	C8H14O4	1183	1182	101.0238	129.0565	73.0278
cis-3-Hexenyl-.alpha.-methylbutyrate	Ester	53398-85-9	C11H20O2	1234	1234	67.0540	57.0695	82.0766
n-Caproic acid vinyl ester	Ester	3050-69-9	C8H14O2	1264	1244	99.0798	71.0845	43.0515
Hexanoic acid, hexyl ester	Ester	6378-65-0	C12H24O2	1387	1384	117.0871	99.0772	89.0581
2,6-Octadien-1-ol, 3,7-dimethyl-, propanoate, (Z)-	Ester	105-91-9	C13H22O2	1476	1455	69.0695	93.0687	121.1004
Crotonic acid, menthyl ester	Ester	114761-14-7	C14H24O2	1495	1511	83.0849	55.0541	95.0848
Citronellyl butyrate	Ester	141-16-2	C14H26O2	1530	1530	81.0686	95.0844	123.1156
Glycerin, 1,2-dicaprylate	Ester	502-54-5	C11H22O4	1680	1687	57.0688	127.1100	145.1201
Cinnamyl alcohol cinnamate	Ester	122-69-0	C18H16O2	2415	2447	131.0477	115.0523	219.1144
2-Propanol, 1,1'-oxybis-	Ether	110-98-5	C6H14O3	1030	1038	59.0488	89.0591	71.0479
1-Propanol, 2-(2-hydroxypropoxy)-	Ether	106-62-7	C6H14O3	1052	1046	59.0485	103.0743	45.0326
2-((3,3-Dimethyloxiran-2-yl)methyl)-3-methylfuran	furane	92356-06-4	C10H14O2	1178	1176	95.0487	151.0752	67.0542
.alpha.-Damascone	Ketone	31089-90-4	C13H20O	1397	1411	69.0332	192.1509	123.1161
2,4,4-Trimethyl-3-(3-methylbutyl)cyclohex-2-enone	Ketone	88725-82-0	C14H24O2	1545	1520	135.0595	95.0487	71.0483
.gamma.-Dodecalactone	Lactone	2305-05-7	C12H22O2	1682	1678	85.0278	57.0330	95.0482
Diethyl Phthalate	Phthalate	84-66-2	C12H14O4	1598	1594	149.0222	177.0531	121.0273
Dibutyl phthalate	Phthalate	84-74-2	C16H22O4	1966	1965	149.0241	121.0289	76.0303
Phthalic acid, di(2-ethylhexyl) ester	Phthalate	1000377-93-5	C24H38O4	2552	2539	149.0231	167.0325	71.0843
2H-Pyran, 2-ethenyltetrahydro-2,6,6-trimethyl-	Terpene	7392-19-0	C10H18O	979	972	139.1103	121.0992	71.0474
Tricyclo[5.3.0.0(4,8)]decane	Terpene	19485-20-2	C10H16	984	1003	79.0543	91.0539	121.1012
.beta.-Myrcene	Terpene	123-35-3	C10H16	994	991	93.0691	69.0691	79.0529
.alpha.-Phellandrene	Terpene	99-83-2	C10H16	1008	1005	93.0697	91.0538	136.1240
3-Carene	Terpene	13466-78-9	C10H16	1013	1011	93.0690	91.0531	79.0531
alpha-Terpinene	Terpene	99-86-5	C10H16	1020	1017	121.0999	136.1238	93.0683
.beta.-Ocimene	Terpene	13877-91-3	C10H16	1049	1037	93.0687	79.0532	121.1001

USC UNIVERSIDADE DE SANTIAGO DE COMPOSTELA

Compound	Chemical family	CAS number	Formula	LRI, exp.	LRI, NIST	Ion 1	Ion 2	Ion 3
1,3,8-p-Menthatriene	Terpene	18368-95-1	C10H14	1115	1119	134.1081	119.0838	91.0528
Fenchol	Terpene	1632-73-1	C10H18O	1119	1113	81.0696	93.0695	111.0799
2-Cyclohexen-1-ol, 1-methyl-4-(1-methylethenyl)-, trans-	Terpene	7212-40-0	C10H16O	1125	1123	91.0526	121.0999	137.0953
3-Cyclohexen-1-ol, 1-methyl-4-(1-methylethyl)-	Terpene	586-82-3	C10H18O	1138	1137	81.0693	107.0846	136.1241
Cis-Sabinol	Terpene	3310-02-9	C10H16O	1144	1143	91.0529	92.0529	119.0841
3-Thujanol	Terpene	7712-79-0	C10H18O	1149	1136	79.0538	93.0690	110.0720
(+)-2-Bornanone	Terpene	464-49-3	C10H16O	1150	1144	95.0844	108.0913	152.1185
Citronellal	Terpene	106-23-0	C10H18O	1155	1153	95.0860	121.1013	67.0543
l-Menthone	Terpene	14073-97-3	C10H18O	1158	1148	112.0886	139.1125	154.1353
Isoborneol	Terpene	124-76-5	C10H18O	1162	1157	95.0843	121.1000	67.0540
Isopulegol	Terpene	89-79-2	C10H18O	1168	1146	97.0647	139.1131	81.0701
Terpinen-4-ol	Terpene	562-74-3	C10H18O	1182	1177	111.0796	93.0691	71.0474
(-)-cis-Isopiperitenol	Terpene	96555-02-1	C10H16O	1206	1228	84.0557	56.0612	81.0692
Carveol	Terpene	99-48-9	C10H16O	1235	1219	84.0555	109.0634	119.0837
Oxiranecarboxaldehyde, 3-methyl-3-(4-methyl-3-pentenyl)-	Terpene	16996-12-6	C10H16O2	1236	1234	67.0541	109.0993	81.0686
Neral	Terpene	106-26-3	C10H16O	1245	1240	69.0705	83.0501	94.0790
Carvone	Terpene	99-49-0	C10H14O	1248	1242	82.0404	93.0690	108.0917
Geraniol	Terpene	106-24-1	C10H18O	1257	1255	69.0692	123.1159	93.0596
2-Cyclohexen-1-one, 2-hydroxy-6-methyl-3-(1-methylethyl)-	Terpene	54783-36-7	C10H16O2	1272	1274	125.0952	139.1114	168.1147
Citral	Terpene	5392-40-5	C10H16O	1273	1276	69.0694	84.0565	137.0961
Mentyl acetate	Terpene	89-48-5	C12H22O2	1297	1294	81.0695	95.0854	123.1167
(3R,6R)-3-Hydroperoxy-3-methyl-6-(prop-1-en-2-yl)cyclohex-1-ene	Terpene	77026-88-1	C10H16O2	1306	1324	91.0526	107.0834	135.0788
Menthyl formate	Terpene	2230-90-2	C11H20O2	1312	1302	81.0689	95.0846	123.1153
(-)-8-p-Menthen-2-yl, acetate, trans	Terpene	57287-13-5	C12H20O2	1317	1330	136.1248	121.1013	107.0860
Cyclohexene, 4-ethenyl-4-methyl-3-(1-methylethenyl)-1-(1-methylethyl)-, (3R-trans)-	Terpene	20307-84-0	C15H24	1342	1338	121.1007	93.0689	107.0846
6-Octen-1-ol, 3,7-dimethyl-, acetate	Terpene	150-84-5	C12H22O2	1355	1354	95.0862	109.1014	123.1167
Copaene	Terpene	3856-25-5	C15H24	1381	1376	105.0687	119.0836	161.1308
Bicyclo[7.2.0]undec-4-ene, 4,11,11-trimethyl-8-methylene-,[1R-(1R*,4Z,9S*)]-	Terpene	118-65-0	C15H24	1413	1406	91.0528	105.0687	133.0997

USC DE COMPOSTELA

Compound	Chemical family	CAS number	Formula	LRI, exp.	LRI, NIST	Ion 1	Ion 2	Ion 3
Bicyclo[5.2.0]nonane, 2-methylene-4,8,8-trimethyl-4-vinyl- (caryophyllene)	Terpene	87-44-5	C15H24	1426	1419	91.0530	133.1000	105.0686
10,10-Dimethyl-2,6-dimethylenebicyclo[7.2.0]undecane	Terpene	357414-37-0	C15H24	1434	1440	91.0528	120.0914	161.1307
cis-.alpha.-Bergamotene	Terpene	18252-46-5	C15H24	1440	1415	119.0838	93.0688	105.0686
1H-Benzocycloheptene, 2,4a,5,6,7,8,9,9a-octahydro-3,5,5-trimethyl-9-methylene-, (4aS-cis)-	Terpene	3853-83-6	C15H24	1456	1449	189.1623	119.0824	93.0686
.gamma.-Muurolene	Terpene	30021-74-0	C15H24	1460	1477	93.0690	161.1310	105.0691
Valencen	Terpene	4630-07-3	C15H24	1485	1492	91.0520	133.0988	189.1622
Germacrene D	Terpene	23986-74-5	C15H24	1488	1481	161.1317	105.0694	119.0843
.alpha.-Cuprenene	Terpene	29621-78-1	C15H24	1507	1509	119.0844	105.0689	133.100
.beta.-Bisabolene	Terpene	495-61-4	C15H24	1512	1509	93.0687	161.1307	204.1867
Delta-cadinene	Terpene	483-76-1	C15H24	1529	1524	161.1308	119.0840	204.1867
E-Nerolidol	Terpene	40716-66-3	C15H26O	1566	1564	107.0842	121.0995	161.1300
Caryophyllene oxide	Terpene	1139-30-6	C15H24O	1591	1581	79.0539	91.0538	95.0852
Humulene epoxide I	Terpene	19888-33-6	C15H24O	1607	1604	93.0691	80.0607	121.0994
alpha-Cedrol	Terpene	77-53-2	C15H26O	1610	1631	150.1398	151.1466	95.0853
Humulene epoxide II	Terpene	19888-34-7	C15H26O	1618	1606	95.0850	135.1163	150.1398
11,11-Dimethyl-4,8-dimethylenebicyclo[7.2.0]undecan-3-ol	Terpene	79580-01-1	C15H24O	1644	1646	136.0866	91.0529	105.0688
Kusenol	Terpene	20489-45-6	C15H26O	1660	1661	161.1304	204.1856	135.1146
Zizanol	Terpene	28102-79-6	C15H24O	1665	1677	91.0528	105.0688	107.0841
.alpha.-Santalol	Terpene	115-71-9	C15H24O	1682	1681	94.0758	79.0526	107.0831
p-Camphorene	Terpene	20016-72-2	C20H32	1991	1995	93.0686	107.0839	229.1931

USC UNIVERSIDADE DE SANTIAGO DE COMPOSTELA

Table S4. Summary of compounds identified using the Carbowax column. Compounds in bold were confirmed with standards.

Compound	Chemical family	CAS number	Formula	LRI, exp.	LRI databases	Ion 1	Ion 2	Ion 3
3-Buten-2-ol, 2-methyl-	Alcohol	115-18-4	C5H10O	1069	1040	71.0495	59.0489	
4-Hexen-1-ol, (E)-	Alcohol	928-92-7	C6H12O	1398	1408	67.0540	82.0766	55.0537
3-Octanol	Alcohol	589-98-0	C8H18O	1403	1400	83.0802	59.0442	101.0902
Cyclopentanol, 2-methyl-	Alcohol	24070-77-7	C6H12O	1419	1430	57.0334	67.0543	82.0766
2-Furaldehyde	Aldehyde	98-01-1	C5H4O2	1488	1494	95.0123	96.0198	67.0173
Pyrazine, 2,3-dimethyl-	Alkaloid	5910-89-4	C6H8N2	1368	1357	108.0676	67.0410	93.0444
Toluene	Aromatic	108-88-3	C7H8	1079	1079	91.0554	92.0626	65.0394
Ethylbenzene	Aromatic	100-41-4	C8H10	1146	1147	91.0535	106.0763	77.0367
Benzene, chloro-	Aromatic	108-90-7	C6H5Cl	1237	1244	112.0067	77.0374	114.0035
Styrene	Aromatic	100-42-5	C8H8	1280	1282	104.0607	78.0451	103.0536
Benzoic acid, methyl ester	Aromatic	93-58-3	C8H8O2	1650	1650	105.0324	136.0518	92.0615
Estragole (p-allylanisole)	Aromatic	140-67-0	C10H12O	1782	1700	148.0866	147.0788	105.0680
Phenol, 3,5-bis(1,1-dimethylethyl)-	Aromatic	1138-52-9	C14H22O	2325	2310	191.1469	206.1656	163.1137
Propanoic acid	Carboxylic acid	79-09-4	C3H6O2	1554	1534	73.0272	74.0349	55.0177
Butanoic acid	Carboxylic acid	107-92-6	C4H8O2	1646	1647	60.0205	73.0273	55.0177
Hexanoic acid	Carboxylic acid	142-62-1	C6H12O2	1858	1858	60.0206	73.0278	87.0437
2-Hexenoic acid, (E)-	Carboxylic acid	13419-69-7	C6H10O2	1981	1961	73.0230	99.0379	81.0279
Butanoic acid, ethyl ester	Ester	105-54-4	C6H12O2	1072	1055	88.0496	73.0269	101.0571
Butanoic acid, 2-methyl-, ethyl ester	Ester	7452-79-1	C7H14O2	1081	1080	102.0673	74.0352	87.0431
Butanoic acid, 3-methyl-, ethyl ester (ethyl isovalerate)	Ester	108-64-5	C7H14O2	1089	1089	88.0510	70.0401	115.0735
1-Butanol, 3-methyl-, acetate (isoamyl acetate)	Ester	123-92-2	C7H14O2	1135	1137	55.0538	70.0766	87.0425
Heptanoic acid, ethyl ester	Ester	106-30-9	C9H18O2	1347	1351	88.0508	101.0589	113.0948
Propanoic acid, 2-hydroxy-, ethyl ester (ethyl lactate)	Ester	97-64-3	C5H10O3	1359	1369	45.0336	75.0069	
Allyl heptanoate	Ester	142-19-8	C10H18O2	1486	1468	85.1003	100.0515	113.0946
n-Valeric acid cis-3-hexenyl ester	Ester	35852-46-1	C11H20O2	1503	1518	67.0495	82.0723	85.0594
1,2-Ethanediol, monoacetate	Ester	542-59-6	C4H8O3	1659	1660.9	43.0144	74.0316	61.0241
Butanoic acid, 2-methyl-	Ester	116-53-0	C5H10O2	1685	1683	60.0202	87.0426	69.0322
Triethyl citrate	Ester	77-93-0	C12H20O7	2489	2496	157.0501	115.0390	129.0188

Compound	Chemical family	CAS number	Formula	LRI, exp.	LRI databases	Ion 1	Ion 2	Ion 3
2-Octanone	Ketone	111-13-7	C8H16O	1303	1297	58.0411	71.0478	85.0636
alpha Ionone	Ketone	6901-97-9	C13H20O	1876	1863	121.0641	93.0692	177.1271
2-Butanone, 4-(4-hydroxyphenyl)-	Ketone	5471-51-2	C10H12O2	3019	2982	107.0482	164.0830	94.0413
Dimethyl Sulfoxide	Sulfoxide	67-68-5	C2H6OS	1623	1596	62.9898	78.0130	44.9791
alpha-Thujene	Terpene	2867-05-2	C10H16	1067	1038	93.0689	91.0529	77.0371
Beta terpinene	Terpene	99-84-3	C10H16	1187	1206	93.0694	79.0531	107.0843
(E)-.beta.-Famesene	Terpene	18794-84-8	C15H24	1679	1673	133.0944	120.0863	161.1258
4-Hexen-1-ol, 5-methyl-2-(1-methylethenyl)-	Terpene	58461-27-1	C10H18O	1692	1687	69.0650	111.0748	13.1108
Beta-Terpineol	Terpene	138-87-4	C10H18O	1653	1603	93.0641	107.0796	121.0949
Verbenol	Terpene	473-67-6	C10H16O	1706	1672	109.0644	119.0850	81.0691

USC UNIVERSIDADE DE SANTIAGO DE COMPOSTELA

Fig. S1. Workflow of the data mining approach employed in the identification of e-liquid components from GC-TOF-MS data assisted by LC-MS experiments.

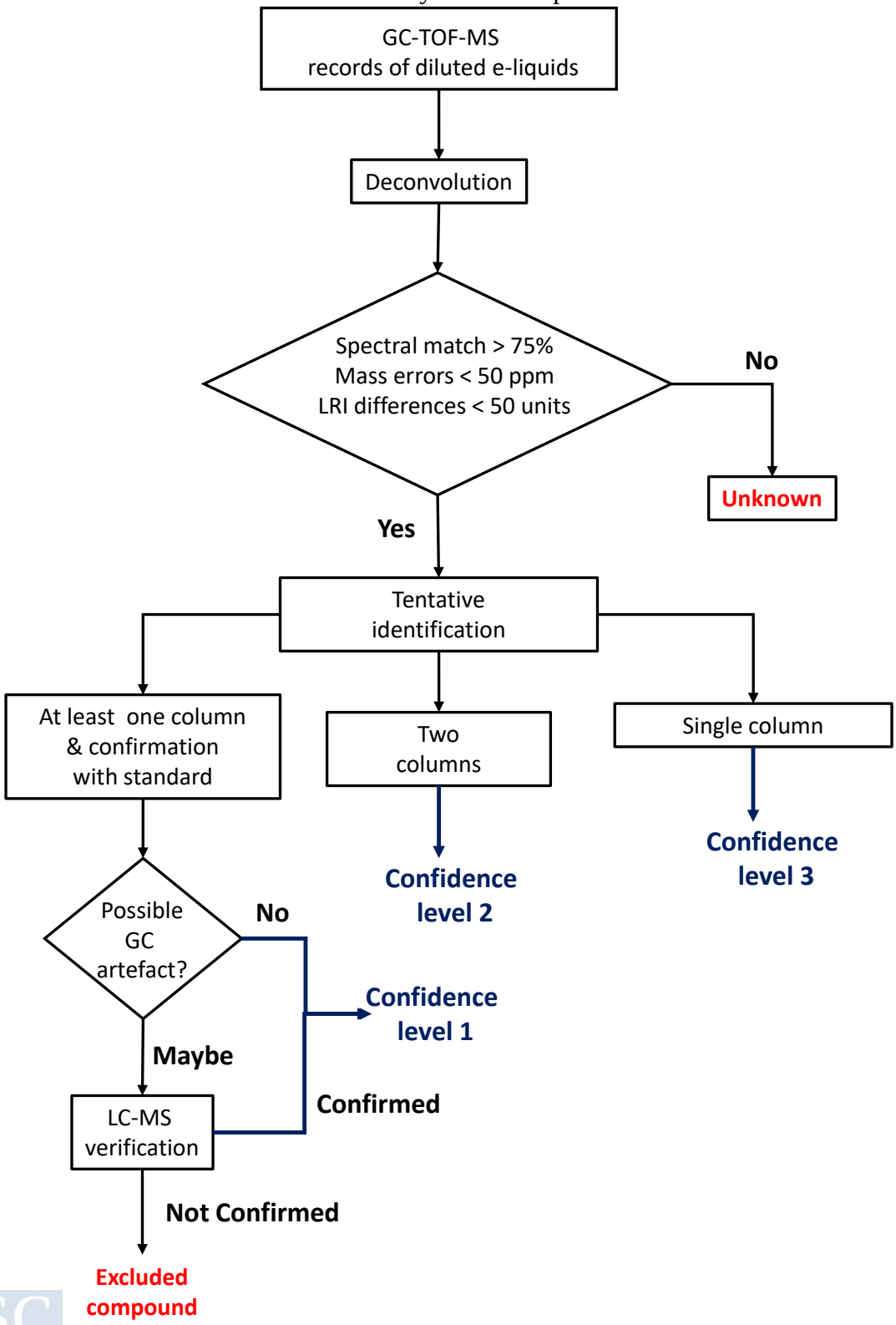
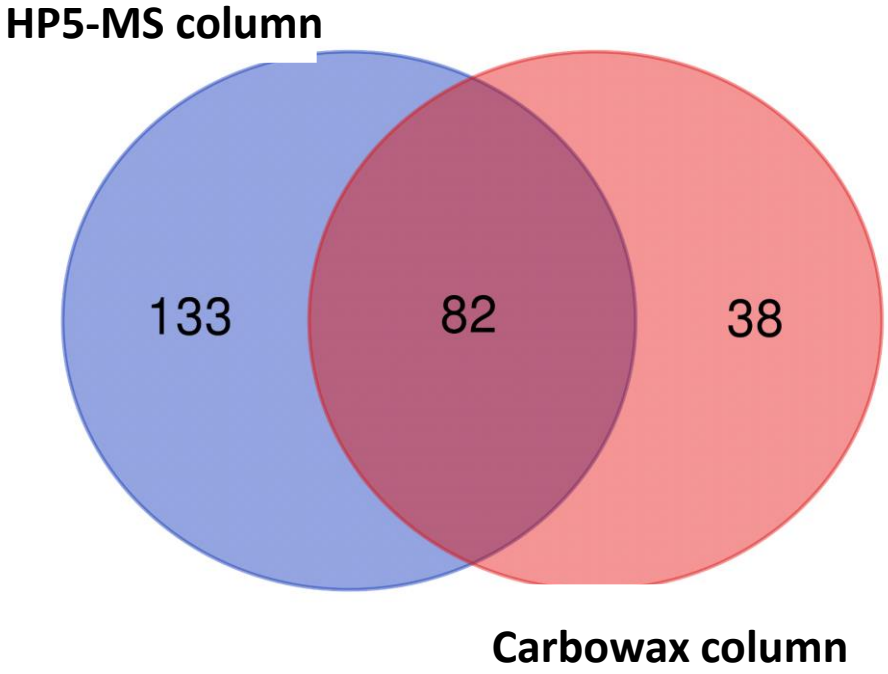


Fig. S2. Venn diagram with number of volatile and semi-volatile compounds identified with each of both columns.



USC
UNIVERSIDADE DE SANTIAGO DE COMPOSTELA

Fig. S3. Detail of GC-TOF-MS chromatograms obtained for e-liquid sample codes S28 (black trace) and S35 (red trace) using HP5-MS (A) and Carbowax (B) columns. Normalized responses for 1:100 diluted samples.

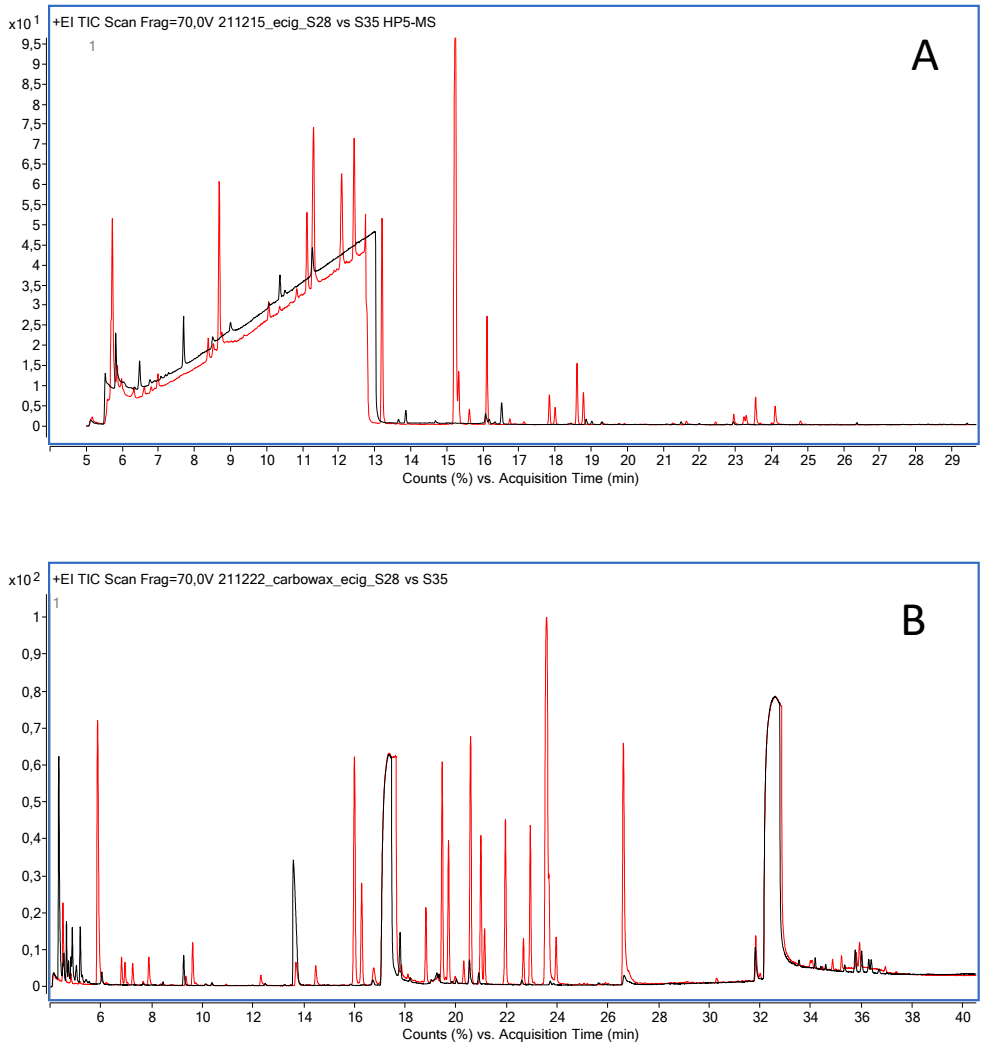
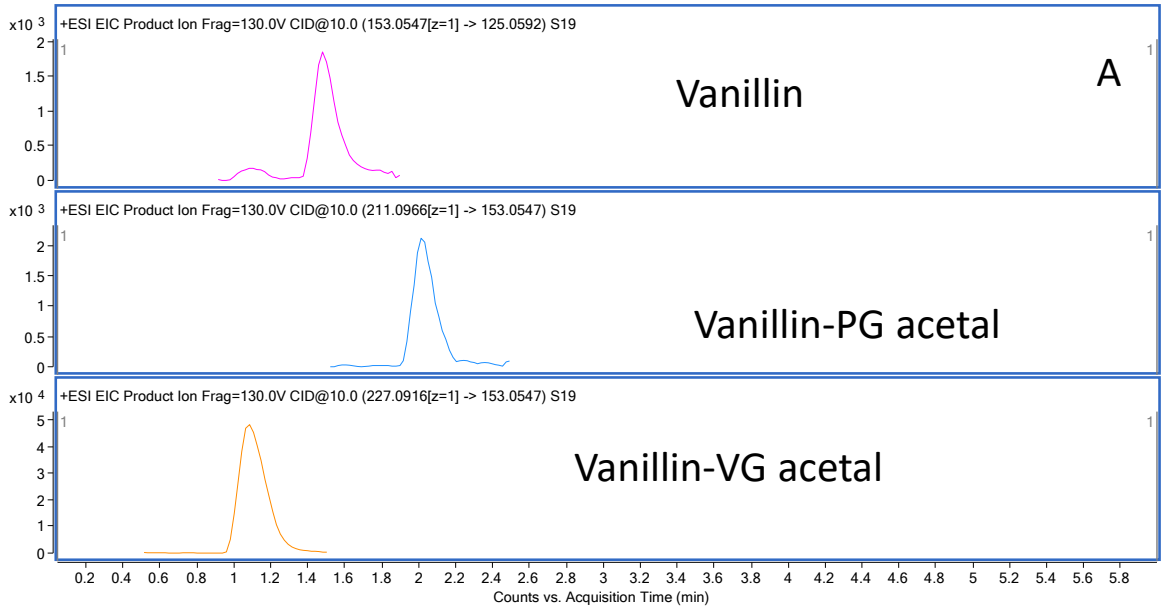
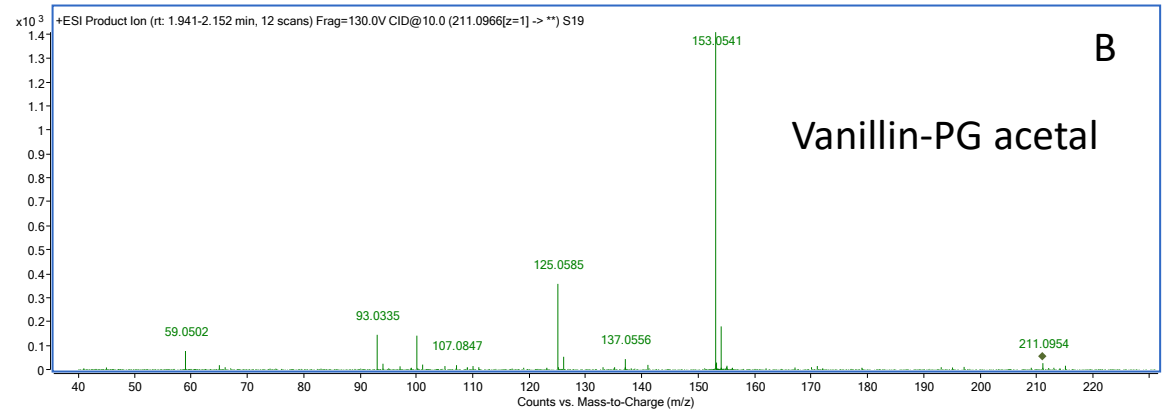
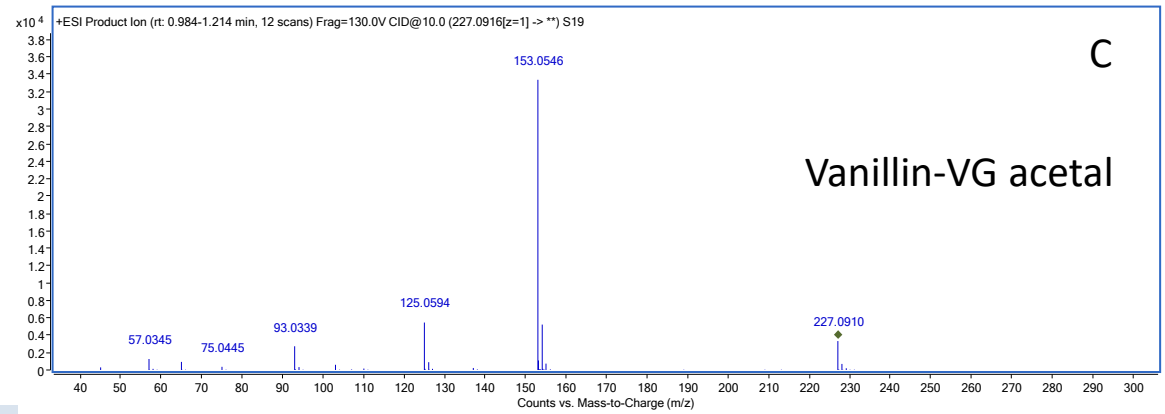


Fig. S4. A, LC-ESI-QTOF-MS chromatograms for the most intense product ions in the spectra of vanillin and its acetals with PG and VG, mass extraction window 20 ppm. B and C, accurate product ion spectra for both acetals. Data corresponding to a non-spiked e-liquid diluted 1:10 with methanol. See Text S1 for determination conditions.

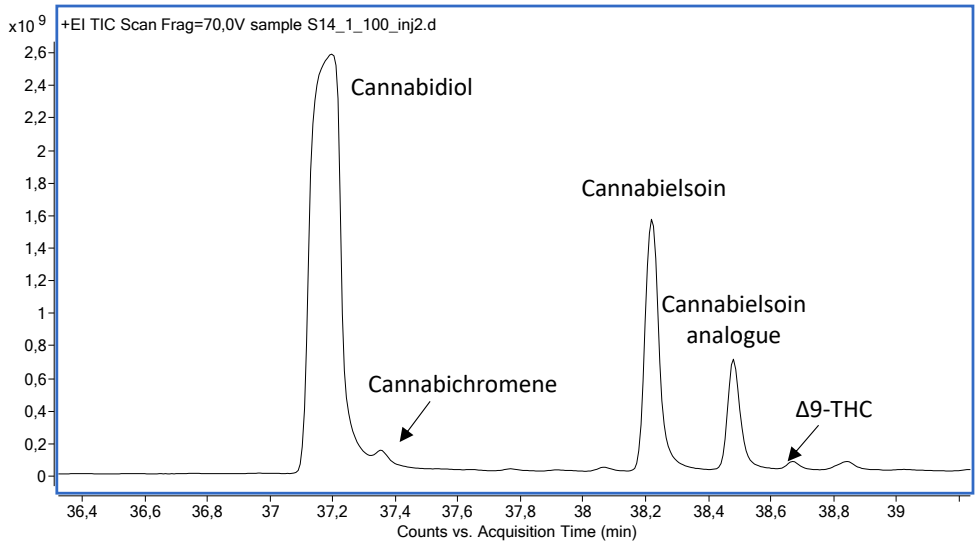






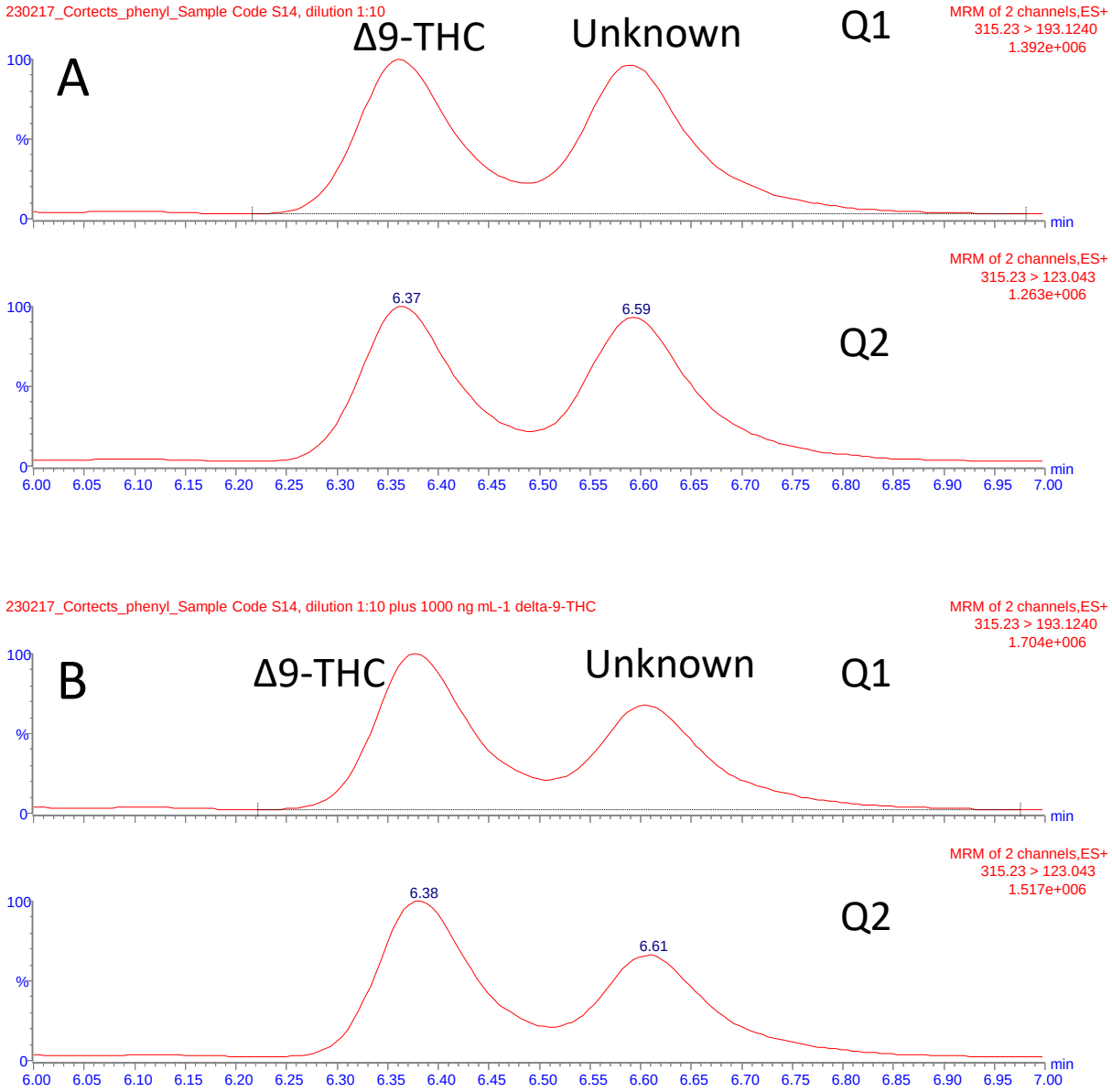
USC UNIVERSIDADE DE SANTIAGO DE COMPOSTELA

Fig. S5. Detail of TIC GC-TOF-MS chromatogram for major cannabinoids in e-liquid sample code S14.



USC UNIVERSIDADE DE SANTIAGO DE COMPOSTELA

Fig. S6. LC-MS-MS chromatograms, acquired in the multireaction monitoring mode (MRM) for a CBD containing e-liquid (sample code S14). A, injection of 1:10 diluted sample. B, injection of 1:10 diluted samples plus 1000 ng mL^{-1} of Δ9-THC. See text S2 for determination conditions.



Text S1. Conditions for LC-ESI-QTOF-MS identification of vanillin and its acetals.

Confirmation of the presence of acetals in e-liquids was obtained by LC-ESI-QTOF-MS. The employed system consisted of an Agilent 6520 QTOF MS instrument, combined with and Agilent 1290 LC instrument. Separations were performed in the isocratic mode (H_2O:ACN, 70:30,) at a flowrate of 0.3 mL min^{-1}, using a CORTECS Phenyl column (150 mm x 2.1 mm, 2.7 µm). The ESI source was operated in the positive ionization mode, with a needle voltage of 4000 V. The fragmentor was set at 120 V. Product ion scan spectra were recorded from the ([M+H]+) ion of each compound (vanillin, vanillin-PG and vanillin-VG acetals), using 10 V as collision energy.

USC UNIVERSIDADE DE SANTIAGO DE COMPOSTELA

Text S2. Conditions for LC-QqQ-MS determination of CBD and Δ9-THC in e-liquids.

The determination of CBD and Δ9-THC in e-liquids was carried out by LC-ESI-MS/MS, using a Xevo TQD instrument, acquired from Waters combined with a UPLC system from the same supplier. Compounds were separated using a CORTECS Phenyl column (150 mm x 2.1 mm, 2.7 µm) provided by Waters. The column was maintained at 40 ºC, using water (A) and acetonitrile (B), both 0.1% in formic acid, as mobile phases at a flowrate of 0.3 mL min^{-1}. The composition of phase B was programmed as follows 60% (0-10 min), 100% (11-13 min), 60% B (13.1-16 min). The ESI source was operated in the positive mode, considering a needle voltage of 1500 V. Two transitions 315.2>123.0 (35 eV) and 315.2>193.1 (25 eV) were used. The cone voltage was set at 40 eV. The retention order of cannabinoid standards was: CBD < Δ9-THC < CBC. Concentrations of CBD and Δ9-THC in e-liquids were determined using solvent-based calibration standards (20 – 1000 ng mL^{-1}), considering different dilution factors depending on the targeted compound, either CBD or Δ9-THC.

USC UNIVERSIDADE DE SANTIAGO DE COMPOSTELA

USC
UNIVERSIDADE
DE SANTIAGO
DE COMPOSTELA

PUBLICATION IV: COMPARISON OF UV, CHLORINATION, UV-HYDROGEN PEROXIDE AND UV-CHLORINE PROCESSES FOR TRAMADOL REMOVAL: KINETICS STUDY AND TRANSFORMATION PRODUCTS IDENTIFICATION

M. Cobo-Golpe, V. Fernández-Fernández, T. Arias, M. Ramil, R. Cela, I. Rodríguez
Journal of Environmental Chemical Engineering 10 (2022) 107854
DOI: 10.1016/j.jece.2022.107854

Impact factor: 7.7
Category: Engineering, chemical
Position: 16/142
Quartile: Q1

USC UNIVERSIDADE DE SANTIAGO DE COMPOSTELA

Journal of Environmental Chemical Engineering 10 (2022) 107854

Contents lists available at ScienceDirect

Journal of Environmental Chemical Engineering

journal homepage: www.elsevier.com/locate/jece

Comparison of UV, chlorination, UV-hydrogen peroxide and UV-chlorine processes for tramadol removal: Kinetics study and transformation products identification

M. Cobo-Golpe, V. Fernández-Fernández, T. Arias, M. Ramil, R. Cela, I. Rodríguez *

Department of Analytical Chemistry, Nutrition and Food Sciences, Research Institute on Chemical and Biological Analysis (IAQBUS), Universidade de Santiago de Compostela, 15782 Santiago de Compostela, Spain

ARTICLE INFO

Editor: Xin Yang

Keywords:
Tramadol
Oxidative processes
Liquid chromatography mass spectrometry
Removal efficiency
Transformation products

ABSTRACT

Tramadol (TRA) is a poorly biodegradable pharmaceutical, ubiquitously distributed in the aquatic environment. Herein, we present a thorough comparison of two conventional (UV and chlorination) and two advanced oxidative processes (UV-H_2O_2 and UV-chlorine), in terms of TRA removal efficiency and transformation products (TPs) formation. The performance of these processes was evaluated in different complexity water samples, previously adjusted at neutral pH. Using 1 mg L^{-1} as initial concentration of oxidant, UV-chlorine was the most effective process followed by UV-H_2O_2, direct photolysis and chlorination. The efficiency of the investigated treatments decreased for surface and wastewater samples compared to model solutions. Despite this limitation, the UV-chlorine treatment removed more than 70% of TRA measured in wastewater samples after 5 min of UV irradiation, in presence of 10 mg L^{-1} of chlorine. UV-chlorine involved additional degradation routes to those described for the rest of treatments, including the formation of tramadol-N-oxide, several chlorinated derivatives, and the volatile species chloroform, 1,1-dichloroacetone and anisole. Some of these specific TPs might pose a similar toxicity to that associated to the parent compound; however, their maximum formation yields remained below 2.5%, decreasing steady for reaction times longer than 5 min

1. Introduction

Tramadol (TRA) is a pharmaceutical prescribed for the treatment of pain. The parent drug and several human metabolites (i.e. N-desmethyl and O-desmethyl forms) are excreted through urine ending at urban sewage treatment plants (STPs) [1,2]. The low removal efficiency of TRA during biological treatments employed in these facilities (from activated sludge to bio-filtration) [3–5] leads to the discharge of this compound in the aquatic environment. Concentrations reported in this compartment range from the low ng mL^{-1} to dozens of ng L^{-1} in treated wastewater and surface water samples, respectively [5,6]. More specifically, Gurke and co-workers [3] reported a median level of 0.68 ng mL^{-1} for TRA during a 10-days sampling campaign of the effluent stream from the same STP. Average concentrations reported by other authors in the same matrix were in the range of 20 ng mL^{-1} [5,6]. TRA has been also noticed in soils, sediments and wetlands affected by sewage water discharges [7]; moreover, it shows limited attenuation during riverbank filtration of polluted waters [8]. To sum up, TRA is recognized as a persistent, relatively polar (log D −0.06 at pH 7) and mobile pollutant in the water phase.

In order to limit the discharges of TRA to the aquatic environment, several oxidative treatments are under evaluation. In spiked model solutions, TRA reacts with free chlorine with formation of N-desmethyl and carbonyl transformation products (TPs), a range of chlorinated derivatives with a close structure to that of the parent drug, and breakdown compounds generated through hydrolysis of the bond between cyclohexane and anisole rings [9]. Formation of hydroxylated and chlorinated derivatives has been also reported during UV irradiation of spiked water samples in presence of H_2O_2, using monochloramine as a source of chlorine [10]. As regards wastewater samples, the possibility to reduce the concentrations of TRA existing in this matrix has been proved using different sources of UV light, either employed alone [11] or combined with H_2O_2 in advanced oxidative processes (AOPs) [12,13]. Ozonization has been tested in pilot scale facilities [14]. In this study, authors highlighted the formation of N-oxide, as a concerning TP of TRA in wastewater. Same derivative was also noticed during photocatalytic

* Corresponding author.
E-mail address: isaac.rodriguez@usc.es (I. Rodríguez).

https://doi.org/10.1016/j.jece.2022.107854
Received 21 February 2022; Received in revised form 22 April 2022; Accepted 2 May 2022
Available online 5 May 2022
2213-3437/© 2022 The Author(s). Published by Elsevier Ltd. This is an open access article under the CC BY-NC-ND license (http://creativecommons.org/licenses/by-nc-nd/4.0/).

treatment of spiked water samples in presence of TiO_2 particles [15].

Despite these previous studies, a thorough comparison of the kinetics of TRA dissipation, its reaction routes and the generated TPs, when different oxidative treatments are applied to aliquots of the same water matrix, is missed. Moreover, to the best of our knowledge, the combination of UV irradiation and free chlorine ($HClO/ClO^-$) has not been evaluated for the removal of TRA, despite the fact that its efficiency has been demonstrated previously for other poorly biodegradable pharmaceuticals [16]. In addition to hydroxyl radicals ($HO^{\cdot}$), the photodecomposition of free chlorine generates a series of reactive chlorine species (RCS), with the chlorine radical ($Cl^{\cdot}$) being the most abundant one, and also that formed directly from free chlorine photodecomposition [17,18], Eq. (1). Both radicals ($HO^{\cdot}$ and $Cl^{\cdot}$) show high redox potentials and present complementary reactivity towards organic compounds; thus, the photochemical decomposition of free chlorine (Eqs. (1, 2)) might be more effective than the combined use of UV radiation and H_2O_2, which renders just $HO^{\cdot}$, Eq. (3). Moreover, at 254 nm, the molar extinction coefficient of free chlorine is about three times higher than that of H_2O_2 [18].

$$ClOH/ClO^- + UV\ (254\ nm) \rightarrow HO^{\cdot}/O^{\cdot-} + Cl \quad (1)$$

$$O^{\cdot-} + H_2O \rightarrow HO^{\cdot} + HO^- \quad (2)$$

$$H_2O_2 + UV\ (254\ nm) \rightarrow 2\ HO \quad (3)$$

Herein, we compare the efficiency of direct photolysis (using 254 nm light), chlorination ($HClO/ClO^-$), and the AOPs UV-H_2O_2, and UV-chlorine for the removal of TRA, reporting the suite of TPs generated during each treatment and their time-course stability. Procedures showing the best performance in model solutions were further evaluated with environmental samples of river and wastewater. The evolution of TRA during above treatments was followed by injection of water samples aliquots in a liquid chromatography (LC) quadrupole time-of-flight (QTOF) mass spectrometry (MS) system. Furthermore, gas chromatography (GC) TOF-MS was considered to assess the formation of volatile derivatives not amenable to electrospray (ESI) ionization.

2. Material and methods

2.1. Solvents, standards and samples

Methanol (MeOH), HPLC-grade purity, formic acid (FA, 98%) and pentane, trace analysis grade, were acquired from Merck (Darmstadt, Germany). Ultrapure deionized water (18.2 MΩ cm^{-1}) was obtained from a Geni U system (Rephile, Shanghai, China). Potassium phosphate salts (K_2HPO_4 and KH_2PO_4), ascorbic acid, potassium iodide, sodium sulfate, sodium bicarbonate, sodium chloride, sodium nitrate, H_2O_2, and sodium hypochlorite (6–14%) were provided by Sigma-Aldrich (Milwaukee, WI, USA). The exact concentration of the two later reagents were determined by titration, with standardized solutions of potassium permanganate and sodium thiosulfate (in presence of an excess of potassium iodide) for H_2O_2 and free chlorine analysis, respectively. Diluted solutions of sodium hypochlorite were prepared in ultrapure water and maintained at 4 °C for a maximum of 5 days. Before use, their concentrations were verified by reaction with N,N-diethyl-p-phenylenediamine with photometric detection [19].

TRA, its isotopically enriched analog (labeled in the methoxy moiety, TRA-^{13}C-d_3, 100 μg mL^{-1} in MeOH), tramadol-N-oxide and N-desmethyl tramadol, nitrobenzene (NB) and p-chlorobenzoic acid (CBA) were purchased from Sigma-Aldrich. Individual standards of these compounds were prepared in MeOH. Standards of anisole, 1,2-dibromopropane (1,2-DBP), a mixture of trihalomethanes and other volatile disinfection by-products (DBPs) were obtained from Sigma-Aldrich and Dr. Ehrenstorfer (Augsburg, Germany), Table S1. Diluted mixtures of volatile halogenated compounds (containing trihalomethanes and other DBPs) and anisole were prepared in MeOH and pentane.

Surface and treated wastewater samples were obtained from a local river, and two STPs equipped with primary and activated sludge treatments. Samples were filtered (using glass fiber and cellulose acetate 0.45 μm pore size filters) before being employed in degradation studies. Table S2 compiles some characteristics of these samples.

2.2. TRA oxidative treatments

Assays aiming for the removal of TRA were performed using different water samples. In a first series of experiments, TRA was added to model solutions of ultrapure water (previously buffered at pH 7) at concentrations of 0.005 and 0.5 mg L^{-1}, during investigation of its degradation rate and identification of potential TPs, respectively. The initial concentration of TRA employed during assessment of its degradation rate was within the range of values reported for this pollutant in treated wastewater samples [3,5,6]. Additional assays were carried out with spiked river water (0.005 mg L^{-1}) and non-spiked wastewater samples. The initial concentrations of oxidants varied between 1 and 10 mg L^{-1}, depending on the employed compound (H_2O_2 or free chlorine), the purpose of the assay (kinetics study or TPs identification), and the initial concentration of TRA.

Photodegradation experiments were carried out in a home-made UV reactor housing an 8 W low pressure mercury lamp (Philips reference G8T5), emitting at 254 nm and assembled orthogonally to a cylindrical quartz reaction vessel (200 mm length x 32 mm o.d., Afora, Barcelona, Spain), containing 25 mL of the considered water sample. The fluence of radiation on the water sample (1.04 $\times 10^{-6}$ Einstein L^{-1} s^{-1}) was experimentally determined using potassium iodide as chemical actinometer.

Spiked water samples were prepared directly in the photoreaction vessels. First, a small volume (10–100 μL) of a TRA standard in MeOH was disposed in the quartz tube. The organic solvent was evaporated at room temperature, using a gentle stream of nitrogen, and TRA was redissolved with the considered water matrix (25 mL), previously buffered at pH 7 by addition of 1 mL of a 0.3 M solution of K_2HPO_4/KH_2PO_4. Thereafter, vessels were either exposed to UV light (direct photolysis experiments), or spiked with the considered oxidant (free chlorine or H_2O_2). Zero time aliquots were taken before inserting the vessel in the photoreactor (case of AOPs), before addition of oxidant (chlorine or H_2O_2), or before UV irradiation (direct photolysis). Control experiments were prepared in absence of UV light and/or oxidant. Free chlorine oxidation experiments were carried out in same reaction vessels, not exposed to UV light.

Water aliquots (0.5 mL) were withdrawn at increasing reaction times and transferred to amber vessels containing 0.05 mL of a standard solution of TRA-^{13}C-d_3 in methanol, and 10 μL of ascorbic acid (60 mg L^{-1} in ultrapure water). Methanol served as quencher of radical species generated during AOPs [17], whilst ascorbic acid neutralized the excess of oxidant (H_2O_2 or chlorine) [20]. Concentrations of H_2O_2 and free chlorine during the time-course of AOPs experiments were controlled using colorimetric reactive strips (obtained from Sigma-Aldrich) and photometric detection, respectively [19], before quenching the oxidant with ascorbic acid. For the determination of the total organic carbon (TOC) content of treated samples following AOPs, the excess of oxidant was removed by addition of 0.25 mL of a 60 mg mL^{-1} solution of sodium thiosulphate and no methanol was added. TOC was determined using non-dispersive infrared spectroscopy, after acidification of treated water samples and CO_2 purge, followed by oxidation of organic matter.

Time-course of TRA, and formation of TPs closely related with the chemical structure of the parent compound, were measured by injection of different reaction times aliquots in a LC-QTOF-MS instrument. The ratio between peak areas for the $[M+H]^+$ ions of TRA (264.1963) and TRA-^{13}C-d_3 (268.2182, both extracted with a mass window of 10 ppm) were compared to those obtained for calibration standards of TRA in ultrapure water (0.05–100 μg L^{-1}). The $[M-H]^-$ ion used to follow the evolution of CBA in competitive kinetics was that at *m/z* 154.9900. The

USC UNIVERSIDADE DE SANTIAGO DE COMPOSTELA

Table 1
Observed reaction rate constants (k, min^{-1}), half-lives ($t_{1/2}$, min) and determination coefficients (R^2) for the natural logarithmic plots of TRA normalized concentrations versus reaction time in spiked (0.005 mg L^{-1}) ultrapure water solutions buffered at pH 7.

Treatment	Constant	Value (min^{-1})	$t_{½}$ (min^{-1})	R^2
Chlorine (1 mg L^{-1})	$k_{TRA\text{-}chlorine}$	0.0219	31.7	0.994
UV (254 nm)	$k_{TRA\text{-}UV}$	0.0475	14.4	0.990
UV-H_2O_2 (1 mg L^{-1})	$k_{obsTRA\text{-}UV\text{-}H2O2}$	0.2005	3.52	0.996
UV- chlorine (1 mg L^{-1})	$k_{obsTRA\text{-}UV\text{-}chlorine}$	0.3785	1.83	0.989

time-course of NB was followed by LC with UV detection, under conditions provided in the experimental section, Text S1.

In order to investigate the formation of volatile halogenated species, treated water samples were processed using a variation of EPA 551.1, LLE extraction method [21] (US-EPA 1995a). In brief, 5 mL aliquots were transferred to a 10 mL vessel and spiked with 1,2-DBP (as IS). After addition of 1 mL of n-pentane and 3.5 g of sodium sulfate, vessels were closed and shaken manually for 5 min. The organic layer was recovered and analyzed by GC-TOF-MS. Calibration standard solutions (5–500 μg L^{-1}) were prepared dissolving the commercial mixture of trihalomethanes, and other volatile DBPs in pentane. Detailed GC-TOF-MS determination conditions are given as supplementary information, Text S2, Table S1.

2.3. Equipment

The dissipation of TRA through the series of oxidative processes considered in this research, and the identification of most TPs were carried out using a UPLC-QTOF-MS instrument: Agilent 6550 model, furnished with an electrospray ionization source (ESI), and combined with a 1290 UPLC system from same supplier. Compounds were separated in a Zorbax Eclipse Plus C18 rapid resolution column (50 mm × 2.1 mm, 1.8 μm), acquired from Agilent Technologies. Column temperature was set at 40 °C and the injected volume was 5 μL (15 μL during investigation of TPs and kinetics experiments with unspiked wastewater samples). Ultrapure water (0.1% in FA, phase A) and MeOH (0.1% in FA, phase B) were employed as mobile phases, combined as follows: 2% B (0–2 min), 25% B (8 min), 100% B (15–16 min), 2% B (16.1–21 min). The LC-QTOF-MS instrument was operated in the 2 GHz, extended dynamic resolution mode, with continuous recalibration of the *m/z* axis using the following ions: 121.0508 and 922.0098 (ESI+); 112.9855 and 1033.9881 (ESI-). Typical mass resolution was 17,000 at *m/z* 322.

LC-ESI-TOF-MS records were processed with the MassHunter Qualitative and MassHunter Profinder software packages (Agilent) to identify those molecular features noticed in degradation experiments, which are absent in control assays. The chemical structures of identified TPs were proposed from their product ion spectra, recorded in further injections at different collision energies, considering also the existing background of TRA derivatives reported in previous degradation studies [9,10,15] and using in some photolysis experiments TRA-^{13}C-d_3 as parent compound to confirm the identities of certain TPs.

3. Results and discussion

3.1. Efficiency of oxidative treatments

The efficiency of different treatments for the removal of TRA in model solutions (ultrapure water adjusted at pH 7) was assessed with half-lives values ($t_{1/2}$, min) and observed reaction rate constants (k_{obs}, min^{-1}). In this study, the initial concentrations of oxidants (H_2O_2 or free chlorine) and TRA added to water solutions were 1 mg L^{-1} and 0.005 mg L^{-1}, respectively. TRA remained stable for more than 30 min when exposed to H_2O_2 under above conditions. As regards the rest of treatments, its stability decreased in the following order: free chlorine, UV irradiation, UV-H_2O_2 and UV-chlorine. In all cases, the time-course of TRA fitted a pseudo-first order kinetics model, with determination coefficients (R^2) above 0.98 for the natural logarithmic plots of normalized concentrations versus reaction time. Table 1 summarizes $t_{1/2}$, k_{obs} and R^2 values for each treatment.

During AOPs, k_{obs} values (k_{obsTRA}) reflect the sum of 1st order reaction rate constants of TRA with an excess of the considered oxidant

Table 2
Summary of transformation products generated from TRA noticed using UPLC-QTOF-MS.

Code	Tr (min)	Empirical formula [M+H]+	Experimental *m/z*	Calculated *m/z*	UV	Chlorine	UV-H_2O_2	UV-chlorine	Experimental *m/z* of product ions
TRA	6.25	$C_{16}H_{26}NO_2$	264.1967	264.1964					58.0655
TP142	1.15	$C_8H_{16}NO$	142.1225	142.1232		X	X	X	97.9687; 44.0497
TP156	1.26	$C_9H_{18}NO$	156.1377	156.1383	X		X	X	84.0658; 58.0652
TP170	4.75	$C_9H_{15}NO_2$	170.1173	170.1176				X	142.1226; 111.0802; 72.0448; 60.0444
TP172	1.40	$C_9H_{17}NO_2$	172.1329	172.1332				X	154.1226; 110.0964; 126.1277; 110.0964; 58.0651
TP206	2.08	$C_9H_{16}ClNO_2$	206.0943	206.0942				X	170.1174; 110.0960;92.0254; 84.0808; 58.0652
TP250a	3.93	$C_{15}H_{24}NO_2$	250.1783	250.1802	X		X		58.0652
TP250b	6.45	$C_{15}H_{24}NO_2$	250.1783	250.1802	X	X	X	X	232.1701; 201.1275; 189.1275; 159.0809; 147.0804; 121.0646; 81.0698
TP278	10.78	$C_{16}H_{24}NO_3$	278.1751	278.1756			X	X	201.1275; 159.0804; 121.0648; 72.0444
TP280a	6.63	$C_{16}H_{26}NO_3$	280.1907	280.1913				X	262.798; 201.1269; 135.0436; 121.0650; 58.0653
TP280b	3.50	$C_{16}H_{26}NO_3$	280.1904	280.1913	X		X		248.2447; 135.1161; 58.0652
TP280c	4.94	$C1_6H_{26}NO_3$	280.1546	280.1913	X		X		262.1432; 58.0653
TP280d	5.68	$C_{16}H_{26}NO_3$	280.1901	280.1913	X		X		262.1805; 217.1227; 58.0652
TP296a, d	3.03, 4.78	$C_{16}H_{26}NO_4$	296.1849	296.1862	X		X		58.0653
TP296b, c	4.02, 4.24	$C_{16}H_{26}NO_4$	296.1852	296.1862	X		X		114.0909; 58.0653
TP312a, b	2.12; 3.60	$C_{16}H_{26}NO_5$	312.1801	312.1811	X		X		58.0652
TP346a	2.53	$C_{16}H_{25}ClNO_5$	346.1410	346.1416				X	74.0600; 58.0652
TP346b	2.83	$C_{16}H_{25}ClNO_5$	346.1409	346.1416				X	310.1641; 58.0651
TP350a, b	1.80; 2.20	$C_{15}H_{22}Cl_2NO_4$	350.0921	350.092				X	314.1146; 296.1043; 270.1231; 252.1144; 216.1371; 173.0953; 92.0257; 74.0599; 58.0652; 44.0499
TP394a, b	2.65; 3.87	$C_{16}H_{22}Cl_2NO6$	394.0815	394.0819				X	344.0887; 314.1137; 299.092; 282.0895; 256.0734; 154.1224; 92.0257; 74.0598; 58.0653; 44.0499
TP396	3.33	$C_{16}H_{24}Cl_2NO_6$	396.0973	396.0975				X	378.0861; 58.0656

USC UNIVERSIDADE DE SANTIAGO DE COMPOSTELA

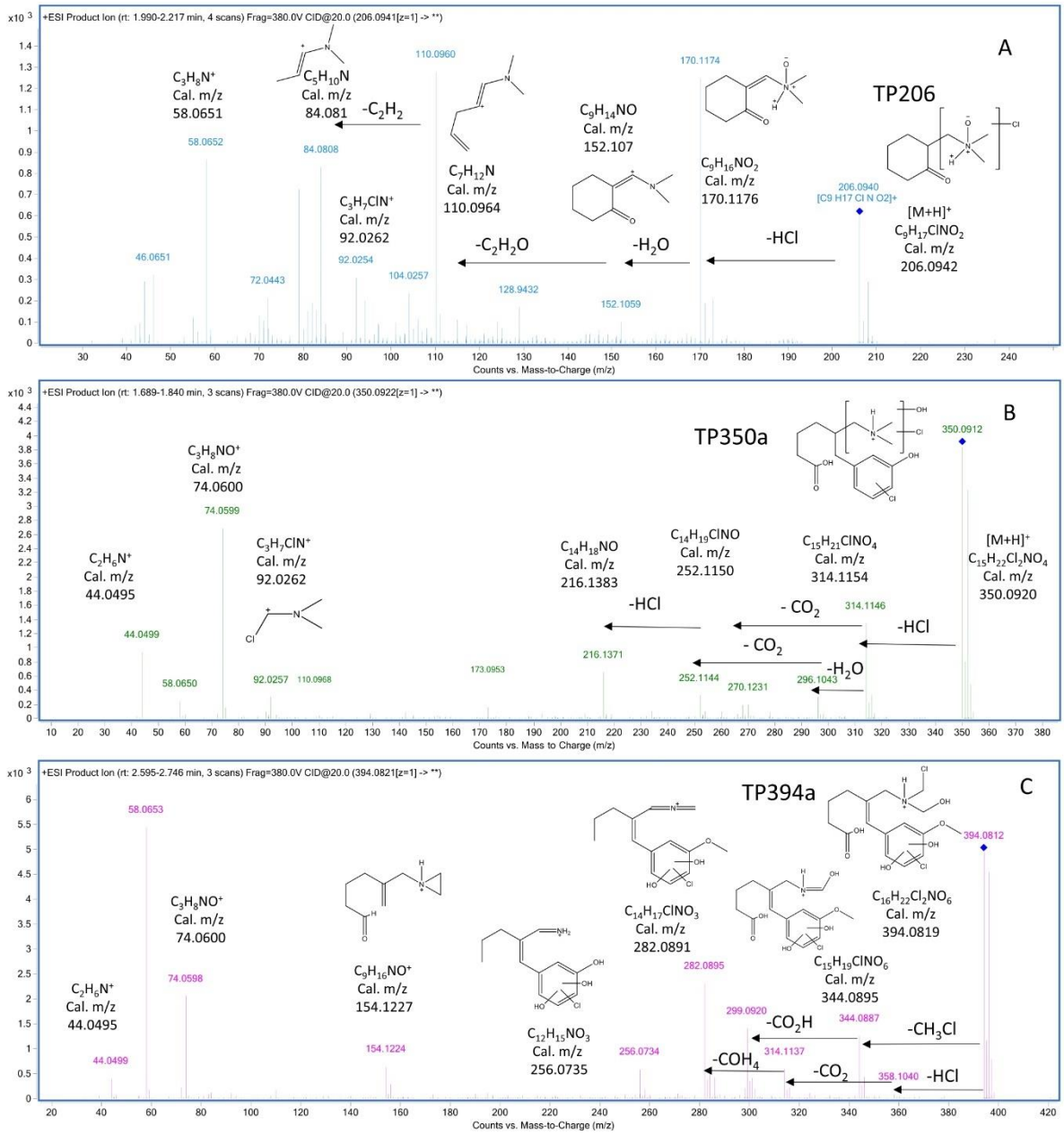


Fig. 1. Product ion spectra and chemical structures assigned to TRA transformation products TP206 (A), TP350a (B) and TP394a (C).

($k_{TRA\text{-}chlorine}$ or $k_{TRA\text{-}H2O2}$), UV light ($K_{TRA\text{-}UV}$) and 2nd order reaction rate with radical species generated during photodecomposition of the employed oxidant: $HO^{\cdot}$ in UV-H_2O_2, and $HO^{\cdot}$ and RCS in UV-chlorine processes. The reaction rate of TRA with $HO^{\cdot}$ ($k_{TRA\text{-}HO}$) was evaluated following a competitive kinetics experiment in presence of CBA. The assay was carried out as reported elsewhere [22], using 1 mM as the initial concentrations of H_2O_2, and 5 μM for TRA and CBA. Both compounds remained stable in contact with H_2O_2 (1 mM); thus, their observed reaction rate constants ($k_{obsCBA(TRA)\text{-}UV\text{-}H2O2}$ and $k_{obsTRA(CBA)\text{-}UV\text{-}H2O2}$) can be described using the following expressions (Eqs. (4 and 5)):

$$k_{obsCBA\ (TRA)\text{-}UV\text{-}H2O2} = k_{CBA\text{-}UV} + k'_{CBA\text{-}HO}\,[HO^{\cdot}] \quad (4)$$

$$k_{obsTRA(CBA)\text{-}UV\text{-}H2O2} = k_{TRA\text{-}UV} + k'_{TRA\text{-}HO}\,[HO^{\cdot}] \quad (5)$$

Table S3 summarized the experimental values of the observed reaction rate constants, and the direct photolysis rate constant of CBA ($k_{CBA\text{-}UV}$). Combining these data with the experimental $k_{TRA\text{-}UV}$ (Table 1), and the known value for the second order rate constant of CBA with $HO^{\cdot}$ ($k_{CBA\text{-}HO}$ 3.0 $\times 10^{11}$ M^{-1} min^{-1}) [22], the calculated value of $k_{TRA\text{-}HO}$ was 2.69 $\times$ 10^{11} M^{-1} min^{-1}.

Using a similar balance to those described by Eqs. (4 and 5), $k_{obsTRA\text{-}}$

USC UNIVERSIDADE DE SANTIAGO DE COMPOSTELA

$_{UV\text{-}chlorine}$ can be written as the sum of four contributions (Eq. (6)) [23]. The latter term in Eq. (6) represents the pseudo-first-order reaction rate constant of TRA with RCS species generated in the UV-chlorine treatment.

$$k_{obsTRA\text{-}UV\text{-}chlorine} = k_{TRA\text{-}chlorine} + k_{TRA\text{-}UV} + k'_{TRA\text{-}HO}\,[HO^{\cdot}] + k_{obs,\,RCS} \quad (6)$$

The concentration of $HO^{\cdot}$ radicals generated during the UV-chlorine treatment (using 1 mg L^{-1} of free chlorine, at pH 7) was calculated using NB as model compound. The 2nd order reaction rate of NB with $HO^{\cdot}$ ($K_{NB\text{-}HO^{\cdot}}$) has a value of 2.34×10^{11} $M^{-1}min^{-1}$. NB does not react with RCS [17,22]; moreover, it remained stable in presence of free chlorine levels up to 10 mg L^{-1} (Fig. S1). The experimental values of $k_{NB\text{-}UV}$ and $k_{obsNB\text{-}UV\text{-}chlorine}$ were 0.0016 and 0.041 min^{-1}, respectively, Fig. S1. Introducing these values in Eq. (7), we calculated that the concentration of $HO^{\cdot}$ radicals generated during UV decomposition of 1 mg L^{-1} of chlorine. The obtained value was 1.68×10^{-13} M. Combining this value with data compiled in Table 1, and applying Eq. (6), the $K_{obsTRA\text{-}RCS}$ has a value of 0.2639 min^{-1}. In summary, considering 1 mg L^{-1} as the initial concentration of free chlorine, at a UV light fluence reaching the sample of 1.04×10^{-6} Einstein $L^{-1}s^{-1}$, the relative contributions of chlorination, direct photolysis, $HO^{\cdot}$ radicals and RCS to the degradation of TRA were 5.8%, 12.5%, 12.0% and 69.7%, respectively. As discussed further, in Section 3.3, the importance of RCS during UV/free chlorine dissipation of TRA is in agreement with the identification of chlorinated transformation products, including the formation of chlorinated phenols and chlorination of alkyl chains bonded to the tertiary amine moiety in the molecule of tramadol.

$$k_{obsNB\text{-}UV\text{-}chlorine} = k_{NB\text{-}UV} + k'_{NB\text{-}HO}\,[HO^{\cdot}] \quad (7)$$

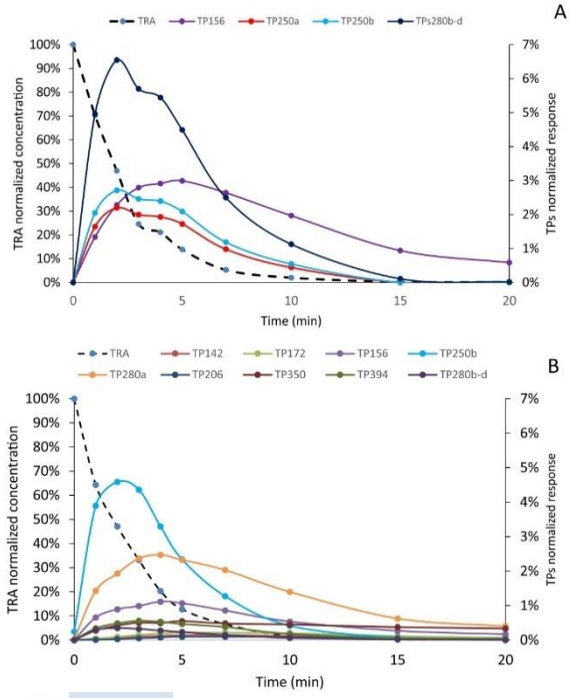


Fig. 2. Evolution of tramadol (left axis) and its main TPs (right axis) in model ultrapure water solutions. A, UV-H_2O_2. B, UV-chlorine.

3.2. Comparative study of transformation products

Table 2 summarizes the list of TPs identified by LC-QTOF-MS during different treatments (UV, chlorine, UV-H_2O_2 and UV-chlorine) applied to ultrapure water solutions, spiked with an initial concentration of TRA of 0.5 mg L^{-1}. Levels of oxidants were 10 mg L^{-1} (chlorine) and 5 mg L^{-1} (H_2O_2), equivalent to a molar concentration of 0.14 mM for both species.

TPs are labeled with a code corresponding to the nominal mass of their protonated molecules ($[M+H]^+$ ion). In addition to retention times and proposed formulae, the *m/z* values of most intense ions in their spectra (product ion) are also included in Table 2. All spectral data were recorded using ESI(+) ionization, since no TPs were noticed under ESI (-). The set of TPs was generated through different reaction routes involving N- and O-desmethylation, N-oxidation, hydroxylation, alkyl oxidation, chlorination, opening of the cyclohexane ring followed by oxidation, and cleavage of the bond between anisole and cyclohexane rings.

UV photolysis led to formation of both desmethylated TRA derivatives (TPs250a and 250b). TP250a was identified as the O-desmethyl species since same compound was formed from TRA and TRA-^{13}C-d_3, whilst TP250b was N-desmethyl TRA (confirmed with a commercial standard). TP156 was generated through hydrolysis of the bond connecting cyclohexane and anisole rings in the molecule of TRA. The three species have been previously reported as TPs of TRA. Their spectra are given in Fig. S2. Several hydroxylated derivatives containing one (TPs280b to 280d), two (TPs296a to 296d), or three hydroxyl moieties (TPs 312a and 312b) were also noticed during UV irradiation of TRA spiked water samples. The spectra of these hydroxylated TPs (Fig. S2) match those assigned to derivatives described during photocatalytic degradation of TRA in presence of TiO_2 [15]. However, the exact position of hydroxyl groups could not be identified since major MS/MS transitions reflected just the removal of H_2O from their $[M+H]^+$ ions, and a common fragment for the trimethyl amino ion ($[C_3H_8N]^+$, calculated *m/z* 58.0654).

Free chlorine led to formation of N-desmethyl TRA (TP250b) and its secondary hydrolysis derivative (TP142). Under employed conditions (samples buffered at pH 7, 10 mg L^{-1} of chlorine), we did not detect the formation of chlorinated species previously reported using higher chlorine doses, and samples buffered at pH values in the range from 4 to 9 units [9].

Combination of UV and H_2O_2 turned in similar TPs to those noticed under direct photolysis in addition to a carbonyl derivative of TRA (TP278) and TP142, Table 2. Regarding TP278, its product ion spectra (Fig. S2) did not permit to discriminate whether it corresponds to an aldehyde (resulting from oxidation of one of the primary carbons bonded to the atom of nitrogen) or to a ketone (oxidation in the secondary carbon). The aldehyde structure was described during free chlorine treatment of TRA spiked waters [9]; whilst formation of a ketone has been reported from the pharmaceutical venlafaxine, which shares the same tertiary amine group as TRA [24].

UV-chlorine treatment rendered the highest number of TPs. Among them, TPs 142, 156 and 170 are secondary hydrolysis derivatives of TP250b, TRA and TP278, respectively. TP280a was confirmed as the N-oxide of TRA, which has been previously reported during ozonization processes carried out at pilot scale [14]. TPs 172 and 206 are also specific for the UV-chlorine treatment. TP172 results from hydrolysis of TP280a, and TP206 is a chlorinated derivative of TP172. This assumption was confirmed with further UV-chlorine experiments using water samples spiked with a commercial standard of TRA N-oxide (TP280a). The spectra of TP206 contains a weak cluster of ions at *m/z* 92.0253, Fig. 1 A. The empirical formula assigned to this ion ($[C_3H_7ClN]^+$) suggests that TP206 is chlorinated in any of the carbons in alpha position to the atom of nitrogen. The O-desmethyl derivative of TRA (TP250a) was not observed during UV-chlorine treatment. We assume that this phenolic intermediate undergoes further, fast hydroxylation and/or chlorination reactions. This way, TPs350a and 350b might arise from

USC UNIVERSIDADE DE SANTIAGO DE COMPOSTELA

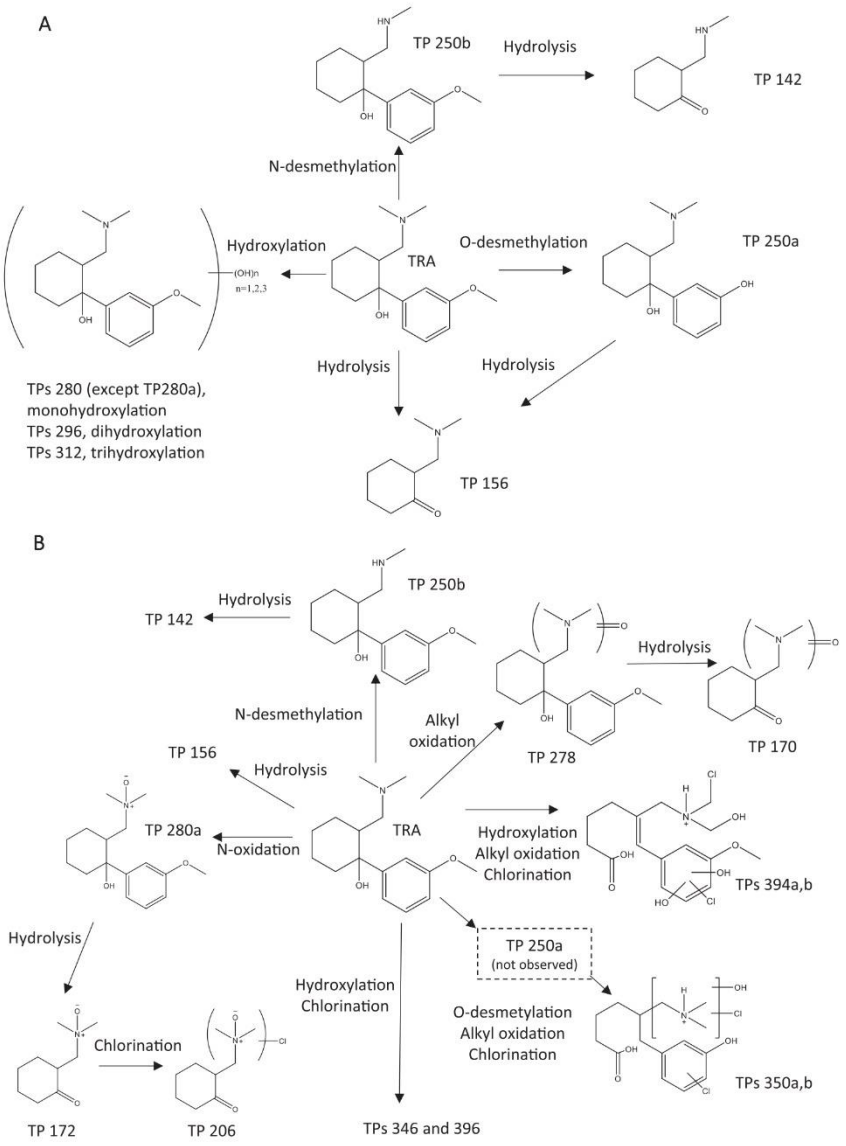


Fig. 3. Reaction routes of TRA in UV-H_2O_2 (A) and UV-chlorine (B) AOPs.

this intermediate. This assumption is made considering the electrophilic behavior of $HO^{\cdot}$ and $Cl^{\cdot}$ radicals, and the strong activation effect of the phenolic group to electrophilic substitution reactions [17,24]. Both, TPs350a and 350b presented the same spectra. Fig. 1B shows one of these spectra and a tentative structure of the TP. Again, the spectrum contains a weak product ion at *m/z* 92.0261, assigned to fragment ion $[C_3H_7ClN]^+$; moreover, some of the experimental transitions (314.1146 > 270.1231, 296.1043 > 252.1144) correspond to the removal of CO_2. Likely, formation of this compound involves hydroxylation of the aliphatic cycle followed by ring opening and further oxidation to a carboxylic acid. Likely, the second atom of chlorine is attached to the aromatic ring in ortho or para positions to the phenolic group, which explains the existence of two isomers.

TPs 394a and 394b are also dichloro derivatives of TRA, maintaining the same number of carbons as the parent compound and incorporating one additional unsaturation. The tentative structure assigned to these compounds and the spectrum of TP 394a are shown in Fig. 1 C. The observed transitions are compatible with chlorination in a terminal carbon (394.0812 > 344.0887) and CO_2 removal (358.1040 > 314.1137). TPs 394a and 394b are considered positional isomers, with two hydroxyls and one atom of chlorine attached to the anisole ring, whilst a third hydroxyl and another chlorine are in alpha to the tertiary amine group. The aliphatic part of the molecule includes a C-C double bond and a carboxylic group formed after opening of the cyclohexane ring.

Finally, spectra of TPs346a, 346b and 396 (mono and di-chlorinated species) do not contain useful information to identify positions of hydroxyl and chlorine substituents, Fig. S2. According to their empirical formulae, TPs346a and 346b are mono-chlorinated derivatives of a trihydroxylated form of TRA, and TP396 is a di-chlorinated and tetrahydroxylated derivative of TRA.

Fig. 2 shows the time-course of TRA and its TPs during UV-H_2O_2

USC UNIVERSIDADE DE SANTIAGO DE COMPOSTELA

(Fig. 2 A) and UV-chlorine (Fig. 2B) treatments, respectively. In the second case, data for TP346 and TP396 have not been included in the figure. Their maximum responses hardly represented 0.05% of that obtained for TRA at zero time. Whatever the water treatment, after 20 min, most of the TPs were either not detected, or their relative response represented less than 0.5% of that obtained for TRA at zero time. Therefore, TPs included in Fig. 2 are amenable to further degradation. In case of TPs 250b and 280a (N-desmethyl TRA and TRA-N-oxide, respectively), the responses provided by the LC-ESI-TOF-MS system for their $[M+H]^+$ ions were similar to that obtained for TRA; thus, normalized responses can be associated to normalized concentrations. Consequently, even though TP280a is known to have a higher toxicity than TRA, less than 0.5% of the initial TRA remains as TRA N-oxide after 20 min of treatment, Fig. 2B. The maximum yield of TPs 250b and 280a formation from TRA observed in this research was similar to that reported during photocatalytic treatment in presence of TiO_2 [15]; however, using UV-chlorine, the highest conversion rate was noticed at shorter irradiation times followed by steady decrease in the levels of both TPs.

During above AOPs, the concentration of H_2O_2 was checked to remain stable during 20 min (data not shown); whilst in case of UV-free chlorine, the level of oxidant decreased slowly, but steady with reaction time to 70% of its initial value after 20 min, see Fig. S3A. The TOC of reaction mixtures under UV/H_2O_2 and UV/free chlorine treatments are also provided as supplementary information, Fig. S3B. Data are shown as normalized values to the concentration measured at zero time. For the UV/H_2O_2 treatment, the content of organic carbon remained unchanged during the process; thus, mineralization is excluded. In case of UV/free chlorine, a reduction of TOC was appreciated after 10 min, despite the final value obtained after 20 min still represented 80% of that existing in the solution at the beginning of the experiment. Thus, additional compounds to those summarized in Table 2 (likely small molecules not amenable to LC-ESI-QTOF-MS determination) remain in the water solution.

The time-course profiles of TPs observed using direct photolysis and free chlorine alone are provided as supplementary information, Fig. S4. Major TPs noticed after 30 min were TP156 and TP250b for UV and free chlorine treatments, respectively. Their relative responses represented up to 20% of that of TRA in the zero time aliquot.

Regarding volatile species, after 20 min of UV-chlorine treatment of model solutions spiked with 0.5 mg L^{-1} and 10 mg L^{-1} of TRA and free chlorine, formation of chloroform, 1,1-dichloroacetone and anisole was noticed using LLE followed by GC-TOF-MS. Measured concentrations were in the range of 0.001–0.002 mg L^{-1} for the chlorinated compounds and 0.007 mg L^{-1} of anisole, respectively. These values represent between 0.2% and 1.4% of the concentration of TRA added to the aqueous solution.

Considering the spectral data of TPs, and the identities (confirmed or tentative) assigned to these compounds, the different routes observed during UV-H_2O_2 and UV-chlorine treatment of TRA spiked model aqueous solutions, buffered at pH 7, are shown in Fig. 3. Although UV-chlorine was the most effective treatment, it increased the potential reaction routes of TRA, leading to formation of several chlorinated species, some of them reported for the first time in this research.

3.3. Effect of inorganic species on UV-H_2O_2 and UV-chlorine kinetics

Anionic species, existing in environmental water samples, are scavengers of radicals generated in AOPs, reducing their efficiency. Particularly, bicarbonate (the major source of inorganic carbon in neutral pH waters) consumes $HO^{\cdot}$ and $Cl^{\cdot}$ species (Eqs. (8 and 9)) leading to formation of the carbonate radical, with a lower redox potential than precursor species [17,25].

$$HO^{\cdot} + HCO_3^- \rightarrow H_2O + CO_3^{\cdot-},\ k = 8{\cdot}5\times10^6\ M^{-1}s^{-1} \quad (8)$$

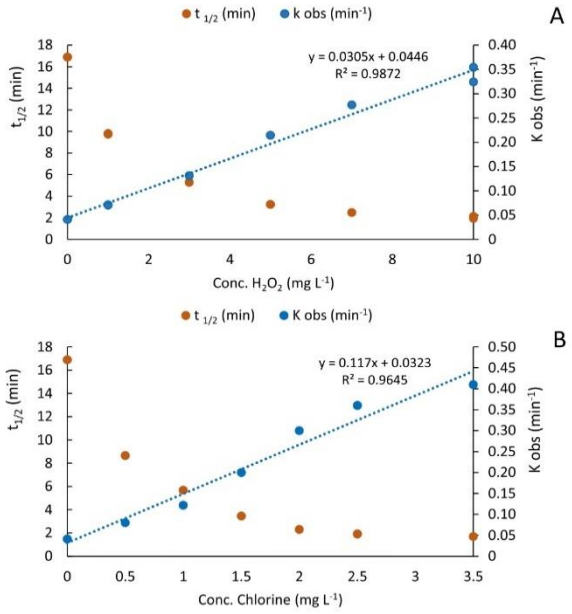


Fig. 4. Half-lives ($t_{1/2}$, min) and observed reaction rate constant (K_{obs}, min^{-1}) of TRA in spiked river water, pH 7, as function of the type and the concentration of oxidant. A, UV-H_2O_2. B, UV-chlorine.

$$Cl^{\cdot} + HCO_3^- \rightarrow HCl + CO_3^{\cdot-},\ k = 2{\cdot}2\times10^8\ M^{-1}s^{-1} \quad (9)$$

Chlorides and nitrates, participate in similar quenching reactions reducing the available amounts of $HO^{\cdot}$ and $Cl^{\cdot}$. On the other hand, ammonium combines with free chlorine producing chloramines; thus, it is expected to reduce the efficiency of UV-chlorine combined treatments [26]. The relative variations in the $t_{1/2}$ of TRA during UV-H_2O_2 and UV-chlorine processes (pH 7, using 1 mg L^{-1} as initial concentration of oxidant), in presence of the above species, versus values observed in model ultrapure water solutions are shown in Fig. S5. The added concentrations of ammonium, chloride or nitrate (1, 70 and 50 mg L^{-1}, respectively) were similar to their usual, or maximum values in treated wastewater and surface water (nitrates). The level of bicarbonate (200 mg L^{-1}) was twice higher than the equivalent inorganic carbon existing in further considered wastewater samples, Table S2. Bicarbonate showed a similar negative influence on the degradability of TRA under both AOPs. Efficiency of UV-H_2O_2 treatment was more sensitive to chlorides and nitrates than that of UV-chlorine. Finally, the negative impact of ammonium was significantly higher in case of UV-chlorine, Fig. S5.

3.4. Degradation efficiency in environmental water samples

The efficiencies of UV-chlorine and UV-H_2O_2 were re-evaluated with three environmental water matrices, corresponding to river water (spiked with TRA at 0.005 mg L^{-1}) and two samples of treated wastewater (TRA contents of 0.0019 mg L^{-1} and 0.0020 mg L^{-1}, samples code A and B, respectively) using different doses of the considered oxidant. The content in different anions in these samples, their total dissolved carbon, organic carbon and absorbance at 254 nm are given in Table S2. Fig. 4 shows the k_{obs} and $t_{1/2}$ of TRA in the river water matrix. The values of $k_{obsUV\text{-}H2O2}$ increased linearly with the concentration of oxidant in the range from 0 to 10 mg L^{-1}, Fig. 4 A. The $k_{obsUV\text{-}chlorine}$ increased also with the level of chlorine; however, no additional improvement was noticed for values above 3.5 mg L^{-1}, Fig. 4B. This finding suggests that the auto-quenching effects of radical species, by reaction with the excess of oxidant, were more relevant for the UV-

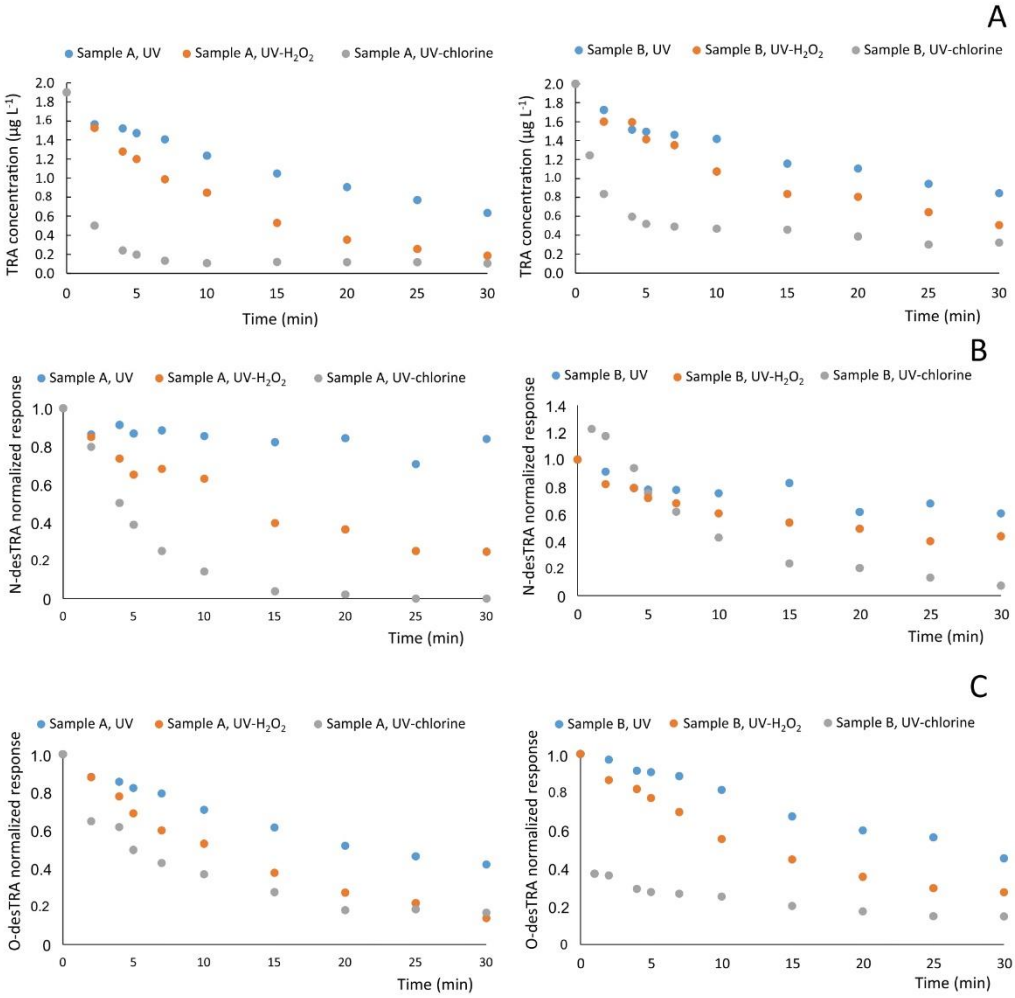


Fig. 5. Time-course plots of TRA concentrations (A), and N-desmethyl TRA (B) and O-desmethyl TRA (C) normalized responses in two non-spiked wastewater samples (left, sample code A; right, sample code B) under UV, UV-H_2O_2 and UV-chlorine treatments. Data for samples buffered at pH 7, using 10 mg L^{-1} as initial concentration of the selected oxidant.

chlorine system than for UV-H_2O_2 [16]. Under conditions considered in Fig. 4, the degradation of TRA fitted a first-order model; however, 3-times higher concentrations of oxidants were required to achieve similar $t_{1/2}$ values to those reported in Table 1 for model ultrapure water solutions.

Fig. 5 A shows the time-course of TRA concentrations in two unspiked wastewaters (left sample A, right sample B), buffered at pH 7, under direct photolysis, UV- H_2O_2, and UV-chlorine. Depicted data correspond to an initial concentration of oxidants of 10 mg L^{-1}. Using doses below 5 mg L^{-1}, no differences were noticed between the efficiency of UV irradiation and the two AOPs, data not shown. Whatever the tested treatment, for wastewater code A (showing the lower absorbance at 254 nm, Table S2), TRA was removed in a higher extent than in case of wastewater code B, Fig. 5 A. In both samples, the efficiency of the treatment increased following the same pattern as in ultrapure model solutions: UV < UV-H_2O_2 < UV-chlorine. The rate of TRA degradation using UV and UV-H_2O_2 fitted a first-order kinetics model; however, in the case of UV-chlorine, the degradation rate decreased significantly after 5 min. The photometric determination of available free chlorine showed levels of only 6 mg L^{-1}, at reaction times of 5 min, which further decreased to 1.3 mg L^{-1} at 15 min (data not shown); so, the reduction of tramadol dissipation rate observed in Fig. 5 (particularly for sample B) was in agreement with the fast consumption of free chlorine in wastewater samples. Despite this reduction, for irradiation times below 30 min, UV-chlorine demonstrated a higher efficiency than UV-H_2O_2. The difference in efficiencies is more evident at shorter reaction times (i.e. 5 min).

Regarding TPs compiled in Table 2, their formation was not observed during treatment of non-spiked wastewater samples. Assuming similar LOQs for these compounds to that obtained for TRA (0.04 μg L^{-1}), considering the initial concentration of TRA in the wastewater samples (ca. 2 μg L^{-1}) and transformation percentages shown in Fig. 2B, this was an expected result. For TP280a (TRA-N-oxide), the combination of a large volume injection method (0.1 mL) with a LC-QqQ-MS instrument, permitted to state that this TPs was not generated at concentrations above 0.002 μg L^{-1}. Formation of the desmethyl forms of TRA (TPs 250a and 250b) was most difficult to identify, since both compounds occurred in the wastewater samples. Their evolution during above treatments is shown in Fig. 5B (N-desmethyl TRA, TP250b) and Fig. 5 C (O-desmethyl TRA, TP250a). Their time-course profiles demonstrated again the higher

USC UNIVERSIDADE DE SANTIAGO DE COMPOSTELA

efficiency of UV-chlorine versus direct photolysis and UV-H_2O_2 to remove these active metabolites from wastewater samples. Again, faster dissipation was noticed in wastewater code A (left graphs) than in sample code B (right graphs). In case of N-desmethyl TRA (TP250b), an initial increase in the response of this compound was noticed during the first 2 min, in one of the wastewater samples (Fig. 5B, right), followed by a steady reduction. After 30 min of UV-chlorine treatment, the levels of N and O-desmethyl TRA existing in both wastewater samples were reduced in more than 80%.

4. Conclusions

At neutral pH values, the combination of UV with free chlorine was the most effective of the tested processes for the removal of TRA from spiked model solutions, surface and non-spiked wastewater samples previously submitted to a biological treatment. Shorter half-lives and higher observed reaction rate constants for UV-chlorine are coherent with the significant contribution of RCS to TRA degradation, the higher molar absorptivity of free chlorine compared to hydrogen peroxide, and the identification of specific reaction routes for UV-chlorine process not observed during UV-H_2O_2. Despite the fact that some of the TPs observed during UV-chlorine have been described as more concerning than the parent compound, i.e. TRA-N-oxide, maximum conversion rates found in this study remained below 3%. Regarding chlorinated derivatives (non-volatile and volatile ones) and other transformation products identified by GC-TOF-MS, their levels (concentrations in case of chloroform, 1,1-dichloroacetone and anisole) represented less than 2% of that measured for TRA in the non-treated samples. For the most complex of the water matrices considered in this research, a concentration of 10 mg L^{-1} of chlorine combined with UV irradiation, achieved a dramatic reduction in the levels of TRA, and its two human metabolites, found in wastewater samples, despite the rate of tramadol removal decreased significantly after 5 min. Further research is required to (1) correlate the composition of environmental water samples with the minimum concentration of oxidant required to enhance the efficiency of UV-chlorine versus direct photolysis, (2) scale-up and confirm the efficiency of UV-free chlorine at pilot plant level, and (3) using in-vitro studies to follow the time-course toxicity of complex reaction mixtures generated during UV/free chlorine treatment.

CRediT authorship contribution statement

M. Cobo: Investigation, Methodology, Writing – original draft. **V. Fernández**: Investigation, Methodology. **T. Arias**: Investigation. **M. Ramil**: Data curation, Formal analysis, Writing – review & editing. **R. Cela**: Project administration, Funding acquisition, Writing – review & editing. **I. Rodríguez**: Conceptualization, Supervision, Funding acquisition, Writing – original draft.

Declaration of Competing Interest

The authors declare that they have no known competing financial interests or personal relationships that could have appeared to influence the work reported in this paper.

Acknowledgements

This study was supported through grants PGC2018-094613-B-I00 and ED431C 2021/06, funded by Spanish Government (Ministry of Science, Innovation and Universities) and Xunta de Galicia, respectively. Both projects are co-funded by the EU FEDER program. M.C.G. thanks a FPI fellowship to the Ministry of Science and Education (Spain).

Appendix A. Supporting information

Supplementary data associated with this article can be found in the online version at doi:10.1016/j.jece.2022.107854.

References

[1] T. Boogaerts, M. Quireyns, A. Covaci, H. De Loof, A.L.N. van Nuijs, Analytical method for the simultaneous determination of a broad range of opioids in influent wastewater: optimization, validation and applicability to monitor consumption patterns, Talanta 232 (2021), 122443, https://doi.org/10.1016/j.talanta.2021.122443.
[2] K.S. Hakala, R. Kostiainen, R.A. Ketola, Feasibility of different mass spectrometric techniques and programs for automated metabolite profiling of tramadol in human urine, Rapid Commun. Mass Spectrom. 20 (2006) 2081–2090, https://doi.org/10.1002/rcm.2562.
[3] R. Gurke, M. Rößler, C. Marx, S. Diamond, S. Schubert, R. Oertel, J. Fauler, Occurrence and removal of frequently prescribed pharmaceuticals and corresponding metabolites in wastewater of a sewage treatment plant, Sci. Total Environ. 532 (2015) 762–770, https://doi.org/10.1016/j.scitotenv.2015.06.067.
[4] N. Hermes, K.S. Jewell, M. Schulz, J. Müller, U. Hübner, A. Wick, J.E. Drewes, T. A. Ternes, Elucidation of removal processes in sequential biofiltration (SBF) and soil aquifer treatment (SAT) by analysis of a broad range of trace organic chemicals (TOrCs) and their transformation products (TPs), Water Res. 163 (2019), 114857, https://doi.org/10.1016/j.watres.2019.114857.
[5] P. Verlicchi, M. Al Aukidy, E. Zambello, Occurrence of pharmaceutical compounds in urban wastewater: removal, mass load and environmental risk after a secondary treatment-a review, Sci. Total Environ. 429 (2012) 123–155, https://doi.org/10.1016/j.scitotenv.2012.04.028.
[6] B. Kasprzyk-Hordern, R.M. Dinsdale, A.J. Guwy, The removal of pharmaceuticals, personal care products, endocrine disruptors and illicit drugs during wastewater treatment and its impact on the quality of receiving waters, Water Res. 43 (2009) 363–380, https://doi.org/10.1016/j.watres.2008.10.047.
[7] D. Sadutto, V. Andreu, T. Ilo, J. Akkanen, Y. Picó, Pharmaceuticals and personal care products in a Mediterranean coastal wetland: impact of anthropogenic and spatial factors and environmental risk assessment, Environ. Pollut. 271 (2021), https://doi.org/10.1016/j.envpol.2020.116353.
[8] A.C. Kondor, G. Jakab, A. Vancsik, T. Filep, J. Szeberényi, L. Szabó, G. Maász, Á. Ferincz, P. Dobosy, Z. Szalai, Occurrence of pharmaceuticals in the danube and drinking water wells: efficiency of riverbank filtration, Environ. Pollut. 265 (2020), https://doi.org/10.1016/j.envpol.2020.114893.
[9] H. Cheng, D. Song, Y. Chang, H. Liu, J. Qu, Chlorination of tramadol: reaction kinetics, mechanism and genotoxicity evaluation, Chemosphere 141 (2015) 282–289, https://doi.org/10.1016/j.chemosphere.2015.06.034.
[10] J. Radjenovic, M.J. Farré, W. Gernjak, Effect of UV and UV/H2O2 in the presence of chloramines on NDMA formation potential of tramadol, Environ. Sci. Technol. 46 (2012) 8356–8364, https://doi.org/10.1021/es301625k.
[11] K.M. Blum, S.H. Norström, O. Golovko, R. Grabic, J.D. Järhult, O. Koba, H. Söderström Lindström, Removal of 30 active pharmaceutical ingredients in surface water under long-term artificial UV irradiation, Chemosphere 176 (2017) 175–182, https://doi.org/10.1016/j.chemosphere.2017.02.063.
[12] D.B. Miklos, R. Hartl, P. Michel, K.G. Linden, J.E. Drewes, U. Hübner, UV/H2O2 process stability and pilot-scale validation for trace organic chemical removal from wastewater treatment plant effluents, Water Res. 136 (2018) 169–179, https://doi.org/10.1016/j.watres.2018.02.044.
[13] B.A. Wols, C.H.M. Hofman-Caris, D.J.H. Harmsen, E.F. Beerendonk, Degradation of 40 selected pharmaceuticals by UV/H2O2, Water Res. 47 (2013) 5876–5888, https://doi.org/10.1016/j.watres.2013.07.008.
[14] S. Kharel, M. Stapf, U. Miehe, M. Ekblad, M. Cimbritz, P. Falås, J. Nilsson, R. Sehlén, K. Bester, Ozone dose dependent formation and removal of ozonation products of pharmaceuticals in pilot and full-scale municipal wastewater treatment plants, Sci. Total Environ. 731 (2020), https://doi.org/10.1016/j.scitotenv.2020.139064.
[15] M. Antonopoulou, I. Konstantinou, Photocatalytic degradation and mineralization of tramadol pharmaceutical in aqueous TiO2 suspensions: evaluation of kinetics, mechanisms and ecotoxicity, Appl. Catal. A Gen. 515 (2016) 136–143, https://doi.org/10.1016/j.apcata.2016.02.005.
[16] G. Castro, M. Ramil, R. Cela, I. Rodríguez, Assessment of UV combined with free chlorine for removal of valsartan acid from water samples, Sci. Total Environ. 762 (2021), 143173, https://doi.org/10.1016/j.scitotenv.2020.143173.
[17] N. Kishimoto, State of the art of UV/chlorine advanced oxidation processes: their mechanism, byproducts formation, process variation, and applications, J. Water Environ. Technol. 17 (2019) 302–335, https://doi.org/10.2965/jwet.19-021.
[18] X. Kong, J. Jiang, J. Ma, Y. Yang, W. Liu, Y. Liu, Degradation of atrazine by UV/chlorine: efficiency, influencing factors, and products, Water Res. 90 (2016) 15–23, https://doi.org/10.1016/j.watres.2015.11.068.
[19] M. Simmons George, Standard methods for the examination of water and waste water, J. N. Am. Benthol. Soc. 12 (1993) 308–309, https://doi.org/10.2307/1467470.
[20] I. Carpinteiro, G. Castro, I. Rodríguez, R. Cela, Free chlorine reactions of angiotensin II receptor antagonists: kinetics study, transformation products elucidation and in-silico ecotoxicity assessment, Sci. Total Environ. 647 (2019) 1000–1010, https://doi.org/10.1016/j.scitotenv.2018.08.082.
[21] D.P. Hautman, D.J. Munch, Development of U.S. EPA Method 551.1, J. Chromatogr. Sci. 35 (1997) 221–231, https://doi.org/10.1093/chromsci/35.5.221.
[22] Y. Yang, J. Jiang, X. Lu, J. Ma, Y. Liu, Production of sulfate radical and hydroxyl radical by reaction of ozone with peroxymonosulfate: a novel advanced oxidation

USC UNIVERSIDADE DE SANTIAGO DE COMPOSTELA

process, Environ. Sci. Technol. 49 (2015) 73307339, https://doi.org/10.1021/es506362e.
[23] Q. Li, C. Lai, J. Yu, J. Luo, J. Deng, G. Li, W. Chen, B. Li, G. Chen, Degradation of diclofenac sodium by the UV/chlorine process: reaction mechanism, influencing factors and toxicity evaluation, J. Photochem. Photobiol. A Chem. 425 (2022), 113667, https://doi.org/10.1016/j.jphotochem.2021.113667.
[24] T. Zhu, J. Deng, S. Zhu, A. Cai, C. Ye, X. Ling, H. Guo, Q. Wang, X. Li, Kinetic and mechanism insights into the degradation of venlafaxine by UV/chlorine process: a modelling study, Chem. Eng. J. 431 (2022), 133473, https://doi.org/10.1016/j.cej.2021.133473.
[25] B. Nikravesh, A. Shomalnasab, A. Nayyer, N. Aghababaei, R. Zarebi, F. Ghanbari, UV/Chlorine process for dye degradation in aqueous solution: mechanism, affecting factors and toxicity evaluation for textile wastewater, J. Environ. Chem. Eng. 8 (2020), https://doi.org/10.1016/j.jece.2020.104244.
[26] E. Rott, B. Kuch, C. Lange, P. Richter, R. Minke, Influence of ammonium ions, organic load and flow rate on the UV/chlorine AOP applied to effluent of a wastewater treatment plant at pilot scale, Int. J. Environ. Res. Public Health 15 (2018), https://doi.org/10.3390/ijerph15061276.

USC UNIVERSIDADE DE SANTIAGO DE COMPOSTELA

Supplementary information to manuscript:

Comparison of UV, chlorination, UV-hydrogen peroxide and UV-chlorine processes for tramadol removal: kinetics study and transformation products identification

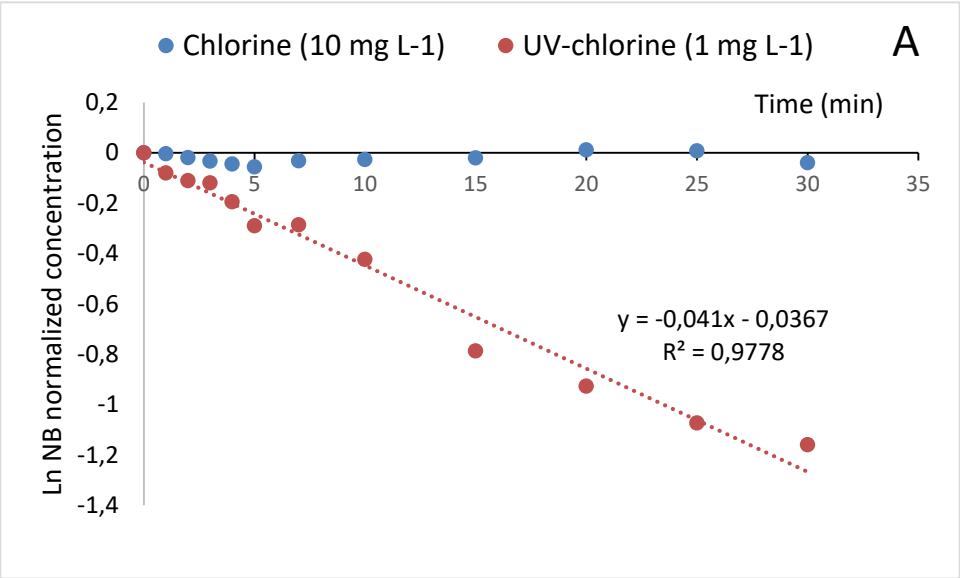
M. Cobo-Golpe, V. Fernández-Fernández, T. Arias, M. Ramil, R. Cela, I. Rodríguez*

Department of Analytical Chemistry, Nutrition and Food Sciences. Research Institute on Chemical and Biological Analysis (IAQBUS). Universidade de Santiago de Compostela, 15782-Santiago de Compostela, Spain.

*corresponding author
e-mail: isaac.rodriguez@usc.es

USC
UNIVERSIDADE DE SANTIAGO DE COMPOSTELA

Fig. S1. Natural logarithmic plots of nitrobenzene (NB) concentration versus time in model water solutions, at pH 7, in presence of free chlorine (10 mg L^{-1}) and UV-chlorine (1 mg L^{-1}) treatment (A), and UV photolysis (B).



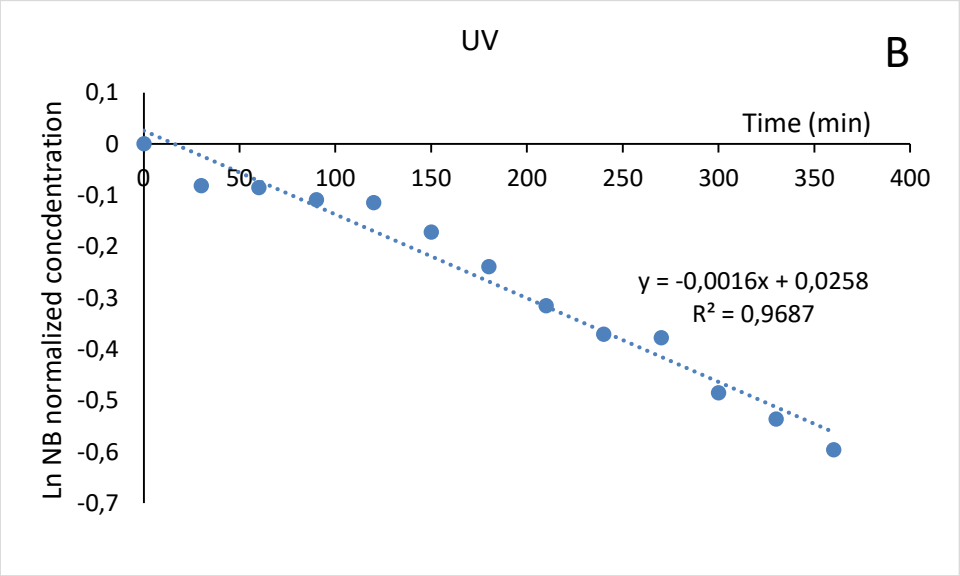


Fig. S2. Product ion spectra and possible structures of TRA transformation products amenable to LC-ESI-QTOF-MS detection.

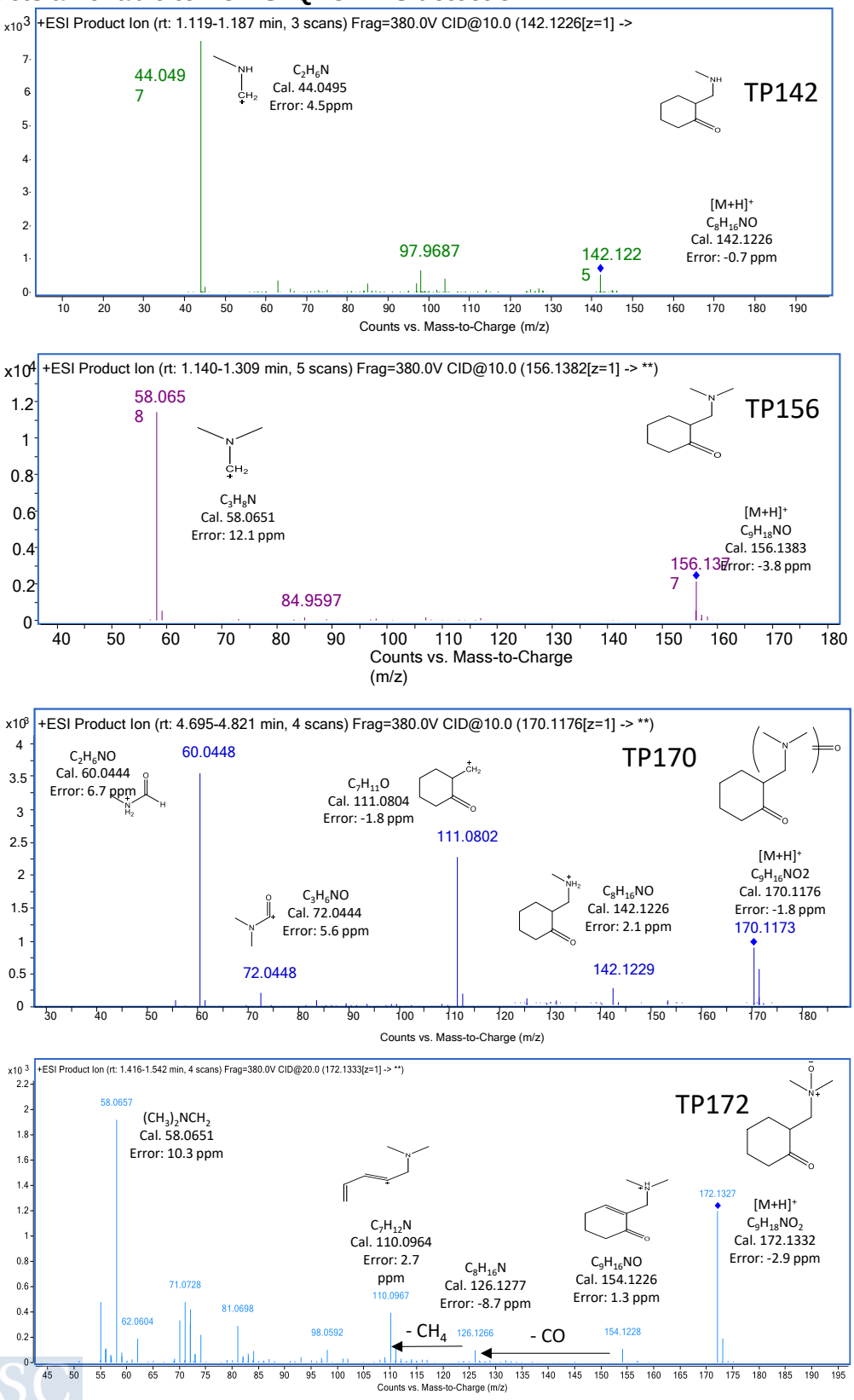
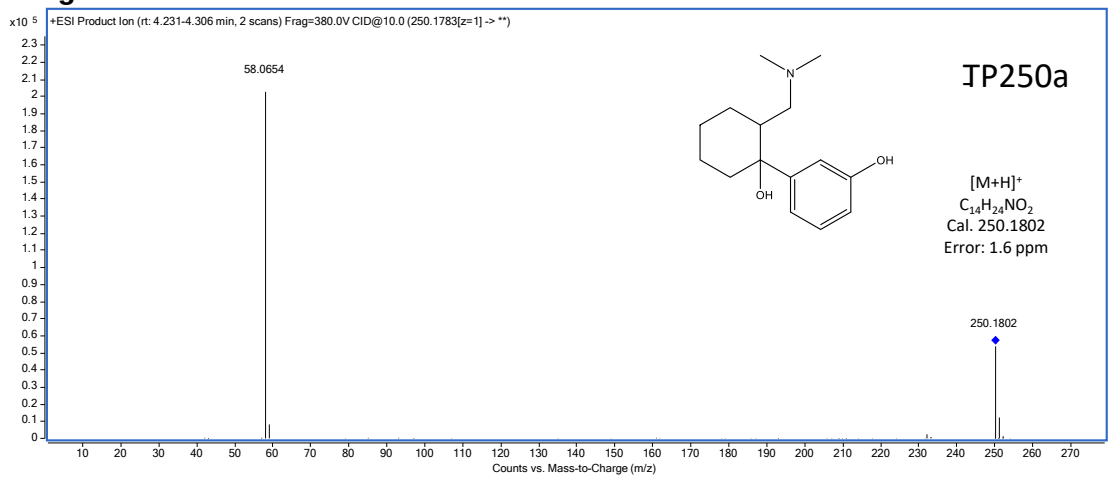
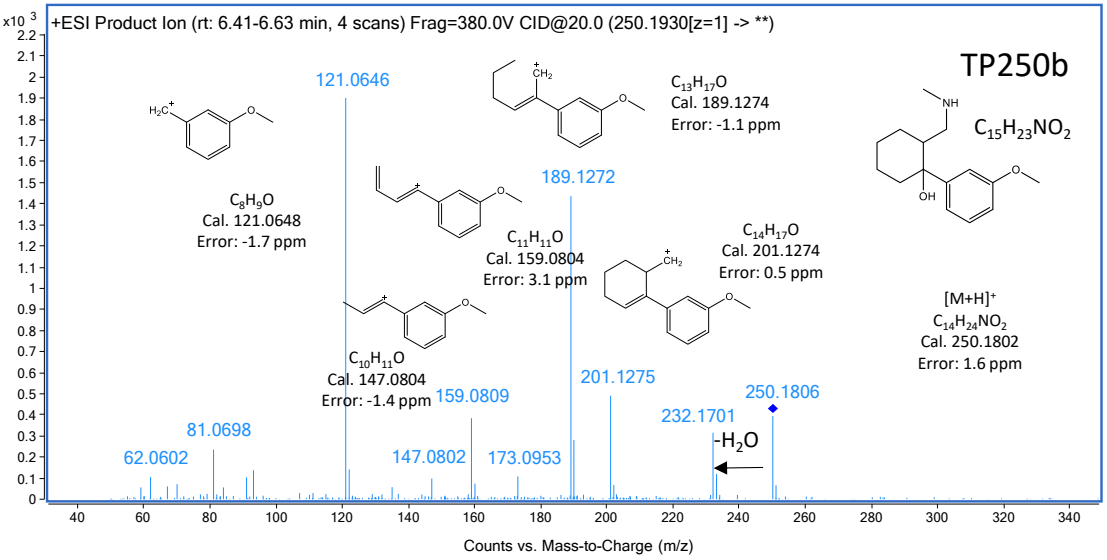


Fig. S2. Cont.


+ESI Product Ion (rt: 4.231-4.306 min, 2 scans) Frag=380.0V CID@10.0 (250.1783[z=1] -> **)
TP250a
58.0654
250.1802
[M+H]+
C14H24NO2
Cal. 250.1802
Error: 1.6 ppm
Counts vs. Mass-to-Charge (m/z)


+ESI Product Ion (rt: 6.41-6.63 min, 4 scans) Frag=380.0V CID@20.0 (250.1930[z=1] -> **)
TP250b
121.0646
189.1272
201.1275
250.1806
232.1701
159.0809
147.0802
173.0953
81.0698
62.0602
-H2O
C8H9O
Cal. 121.0648
Error: -1.7 ppm
C11H11O
Cal. 159.0804
Error: 3.1 ppm
C10H11O
Cal. 147.0804
Error: -1.4 ppm
C13H17O
Cal. 189.1274
Error: -1.1 ppm
C14H17O
Cal. 201.1274
Error: 0.5 ppm
C15H23NO2
[M+H]+
C14H24NO2
Cal. 250.1802
Error: 1.6 ppm
Counts vs. Mass-to-Charge (m/z)

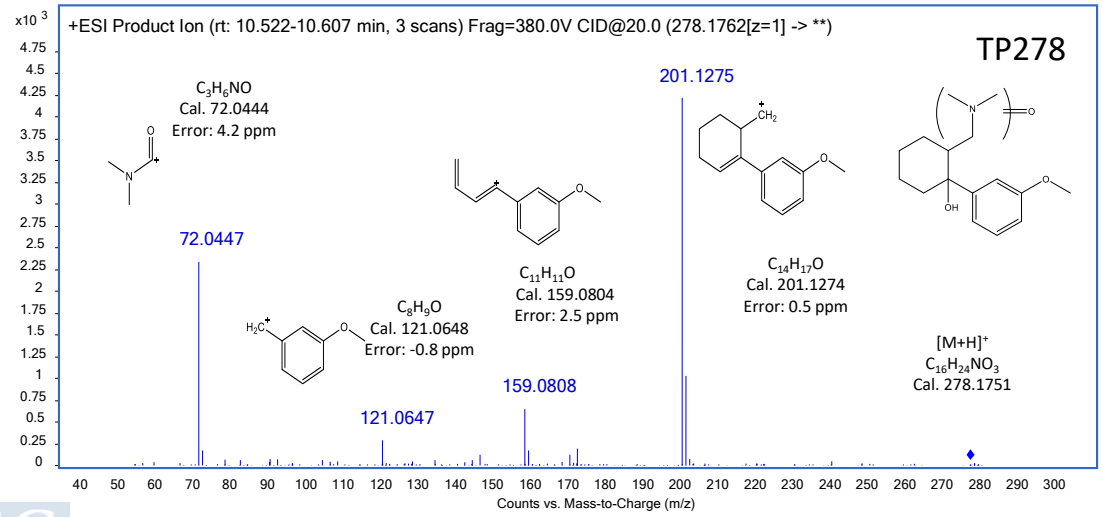
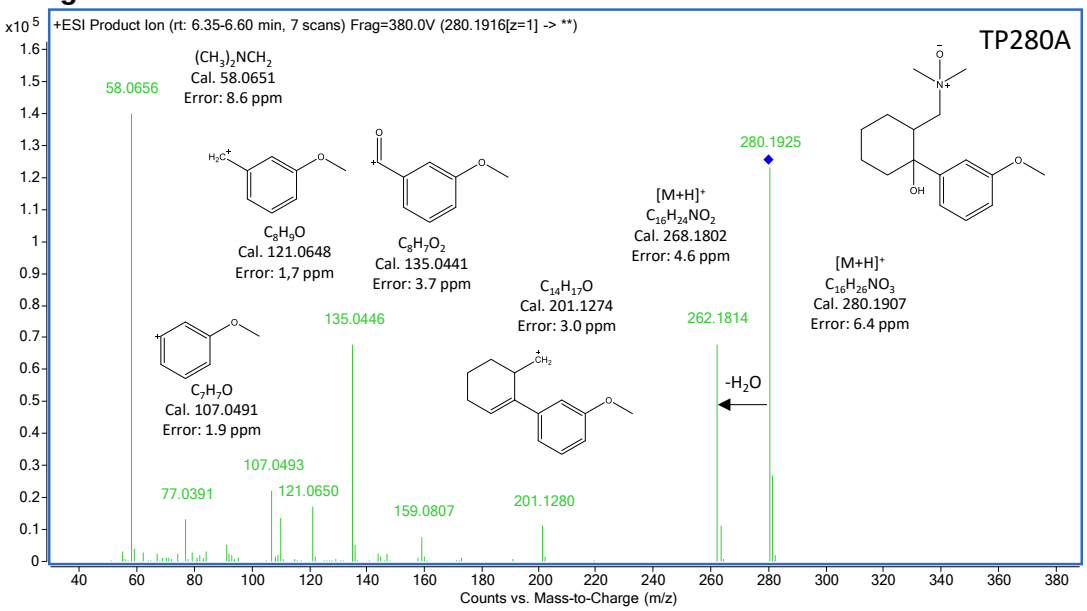
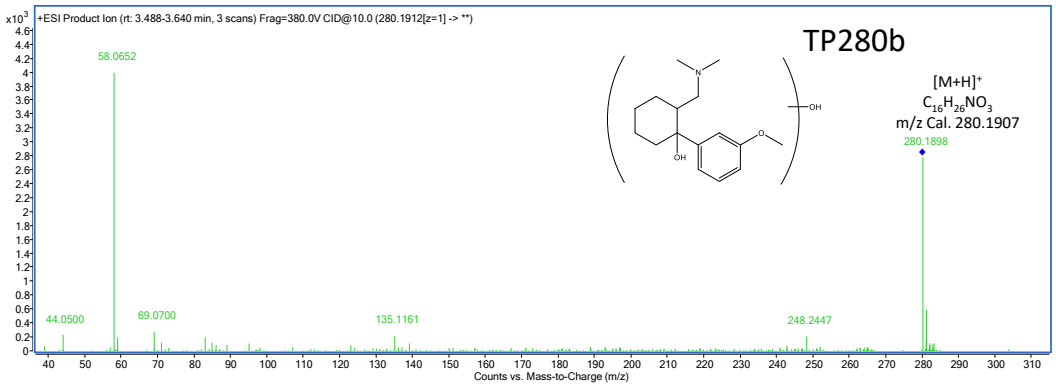

+ESI Product Ion (rt: 10.522-10.607 min, 3 scans) Frag=380.0V CID@20.0 (278.1762[z=1] -> **)
TP278
72.0447
121.0647
159.0808
201.1275
C3H6NO
Cal. 72.0444
Error: 4.2 ppm
C8H9O
Cal. 121.0648
Error: -0.8 ppm
C11H11O
Cal. 159.0804
Error: 2.5 ppm
C14H17O
Cal. 201.1274
Error: 0.5 ppm
[M+H]+
C16H24NO3
Cal. 278.1751
Counts vs. Mass-to-Charge (m/z)

Fig. S2. Cont.


+ESI Product Ion (rt: 6.35-6.60 min, 7 scans) Frag=380.0V (280.1916[z=1] -> **)
TP280A
58.0656
(CH3)2NCH2
Cal. 58.0651
Error: 8.6 ppm
C8H9O
Cal. 121.0648
Error: 1,7 ppm
C8H7O2
Cal. 135.0441
Error: 3.7 ppm
C14H17O
Cal. 201.1274
Error: 3.0 ppm
C7H7O
Cal. 107.0491
Error: 1.9 ppm
135.0446
107.0493
77.0391
121.0650
159.0807
201.1280
262.1814
-H2O
280.1925
[M+H]+
C16H24NO2
Cal. 268.1802
Error: 4.6 ppm
[M+H]+
C16H26NO3
Cal. 280.1907
Error: 6.4 ppm
Counts vs. Mass-to-Charge (m/z)


+ESI Product Ion (rt: 3.488-3.640 min, 3 scans) Frag=380.0V CID@10.0 (280.1912[z=1] -> **)
TP280b
58.0652
[M+H]+
C16H26NO3
m/z Cal. 280.1907
280.1898
44.0500
69.0700
135.1161
248.2447
Counts vs. Mass-to-Charge (m/z)

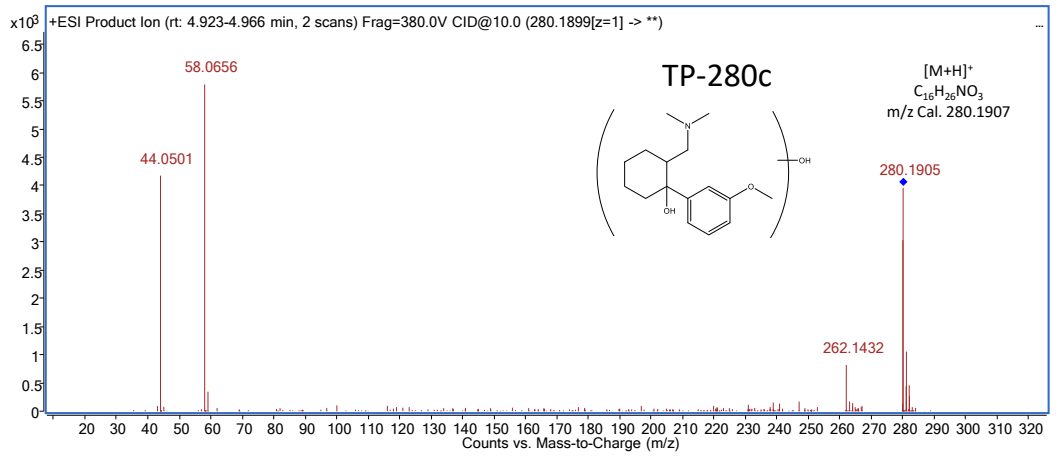
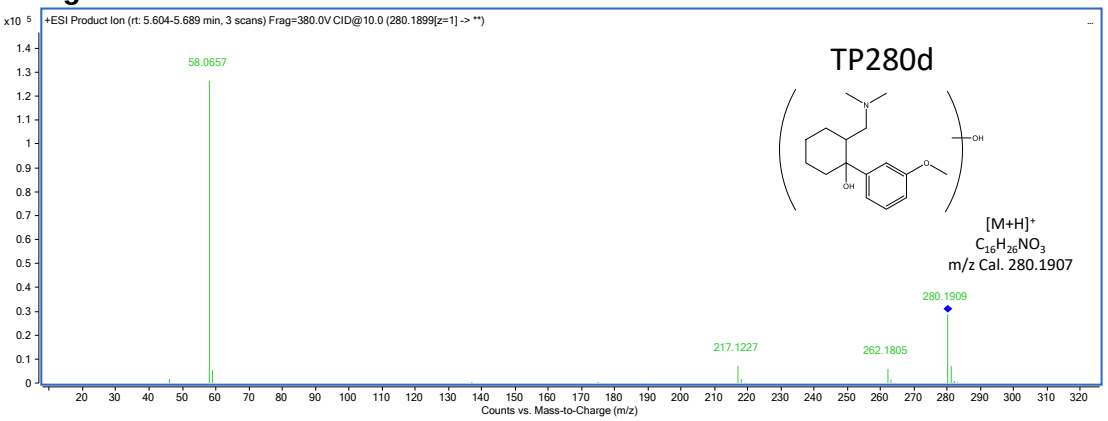
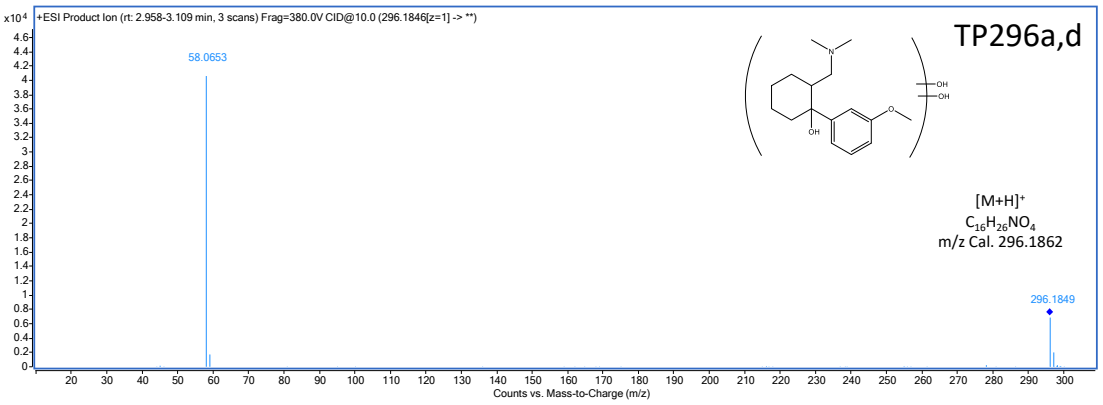

+ESI Product Ion (rt: 4.923-4.966 min, 2 scans) Frag=380.0V CID@10.0 (280.1899[z=1] -> **)
TP-280c
58.0656
44.0501
[M+H]+
C16H26NO3
m/z Cal. 280.1907
280.1905
262.1432
Counts vs. Mass-to-Charge (m/z)

Fig. S2. Cont.


+ESI Product Ion (rt: 5.604-5.689 min, 3 scans) Frag=380.0V CID@10.0 (280.1899[z=1] -> **)
TP280d
58.0657
217.1227
262.1805
280.1909
[M+H]+
C16H26NO3
m/z Cal. 280.1907
Counts vs. Mass-to-Charge (m/z)


+ESI Product Ion (rt: 2.958-3.109 min, 3 scans) Frag=380.0V CID@10.0 (296.1846[z=1] -> **)
TP296a,d
58.0653
296.1849
[M+H]+
C16H26NO4
m/z Cal. 296.1862
Counts vs. Mass-to-Charge (m/z)

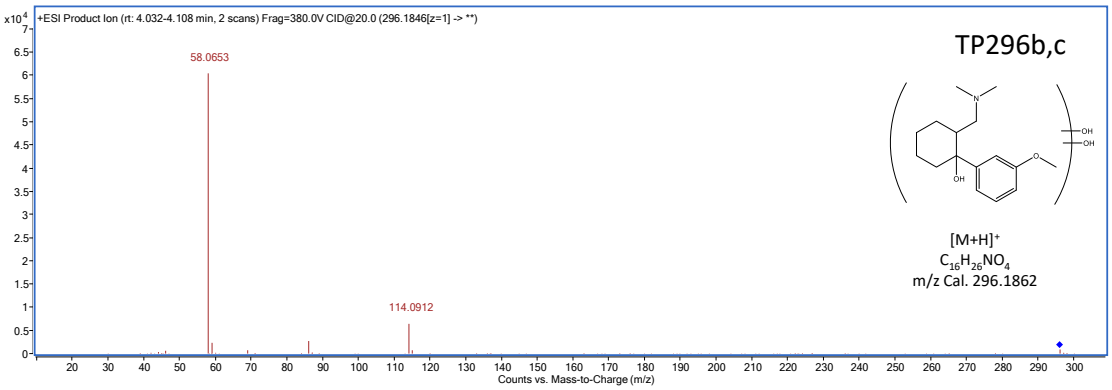
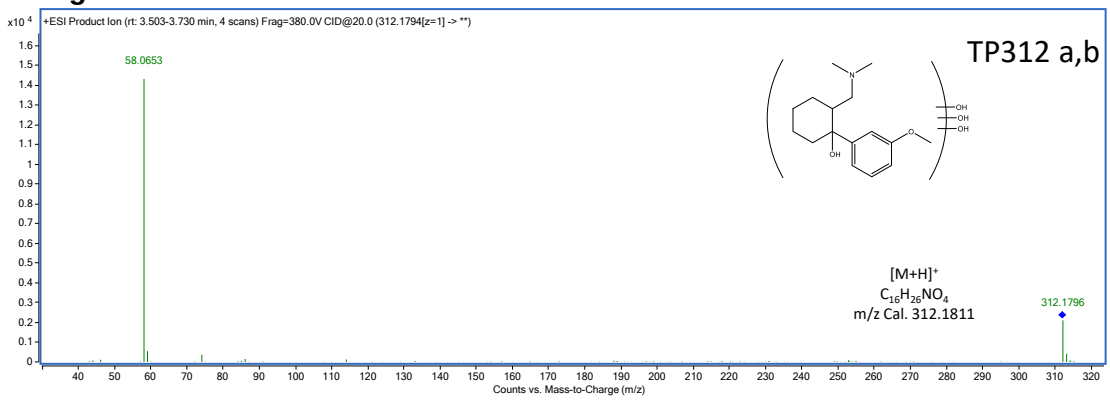
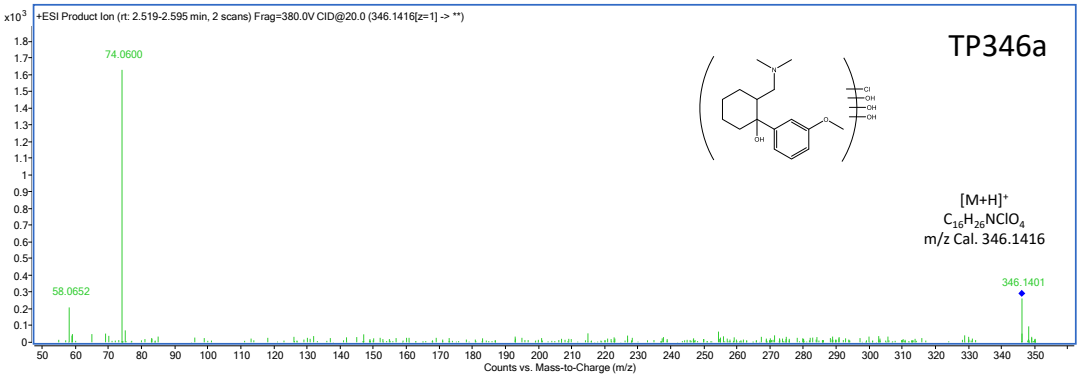
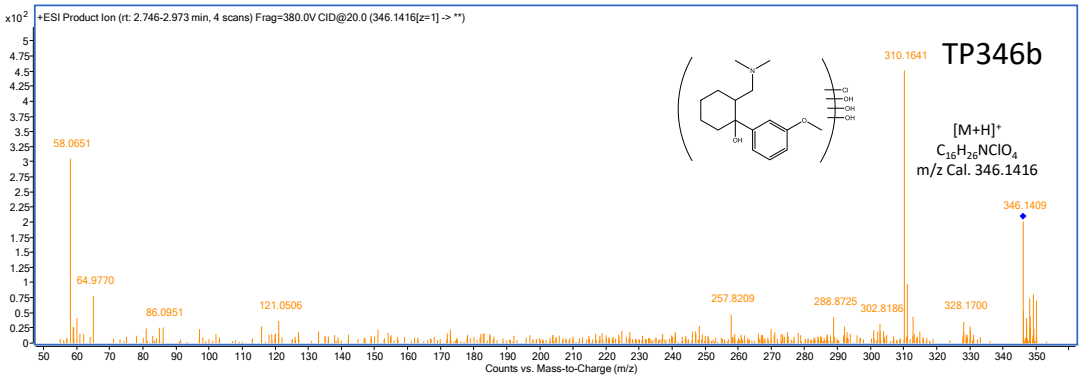

+ESI Product Ion (rt: 4.032-4.108 min, 2 scans) Frag=380.0V CID@20.0 (296.1846[z=1] -> **)
TP296b,c
58.0653
114.0912
[M+H]+
C16H26NO4
m/z Cal. 296.1862
Counts vs. Mass-to-Charge (m/z)

Fig. S2. Cont.


+ESI Product Ion (rt: 3.503-3.730 min, 4 scans) Frag=380.0V CID@20.0 (312.1794[z=1] -> **)
TP312 a,b
58.0653
[M+H]+
C16H26NO4
m/z Cal. 312.1811
312.1796
Counts vs. Mass-to-Charge (m/z)


+ESI Product Ion (rt: 2.519-2.595 min, 2 scans) Frag=380.0V CID@20.0 (346.1416[z=1] -> **)
TP346a
74.0600
58.0652
[M+H]+
C16H26NClO4
m/z Cal. 346.1416
346.1401
Counts vs. Mass-to-Charge (m/z)


+ESI Product Ion (rt: 2.746-2.973 min, 4 scans) Frag=380.0V CID@20.0 (346.1416[z=1] -> **)
TP346b
310.1641
58.0651
[M+H]+
C16H26NClO4
m/z Cal. 346.1416
346.1409
64.9770
86.0951
121.0506
257.8209
288.8725
302.8186
328.1700
Counts vs. Mass-to-Charge (m/z)

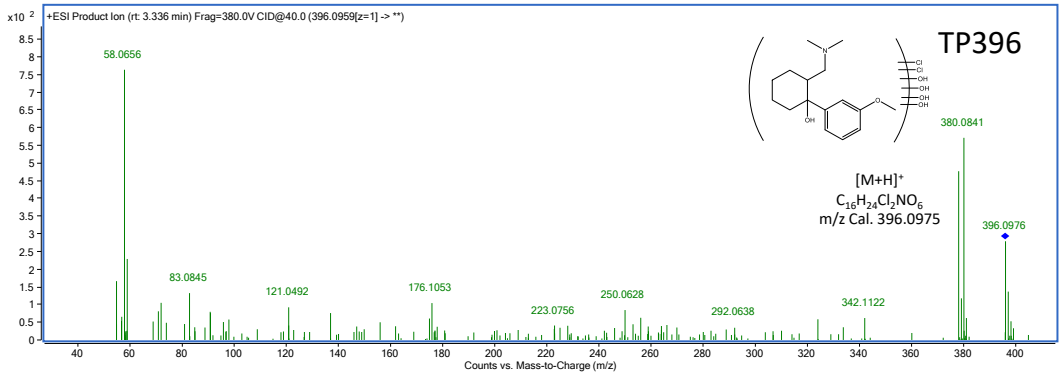
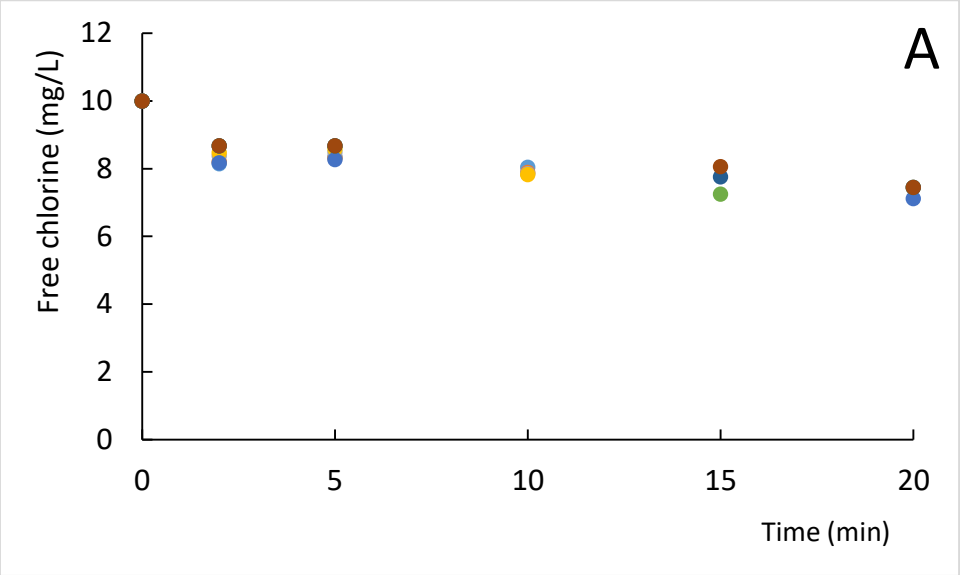
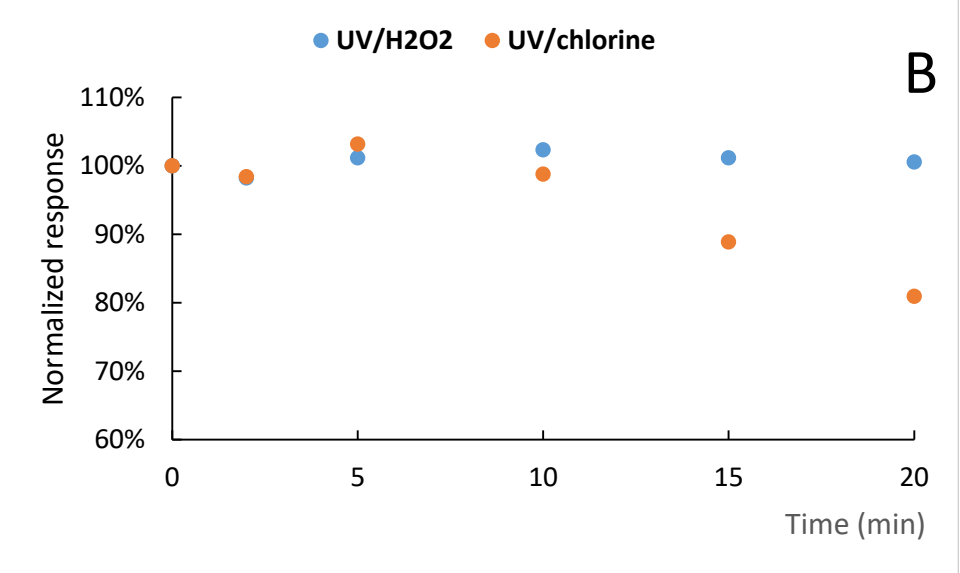

+ESI Product Ion (rt: 3.336 min) Frag=380.0V CID@40.0 (396.0959[z=1] -> **)
TP396
58.0656
380.0841
[M+H]+
C16H24Cl2NO6
m/z Cal. 396.0975
396.0976
83.0845
121.0492
176.1053
223.0756
250.0628
292.0638
342.1122
Counts vs. Mass-to-Charge (m/z)

Fig. S3. A, time-course of free chlorine during treatment of ultrapure water samples, spiked with 0.5 mg L^{-1} of tramadol. B, normalized values of total organic carbon (TOC) during UV/free chlorine and UV/H_2O_2 treatment of ultrapure water samples, at neutral pH, spiked with 0.5 mg L^{-1} of tramadol. Initial oxidant concentrations: 10 mg L^{-1} and 5 mg L^{-1} for free chlorine and H_2O_2, respectively.





USC
UNIVERSIDADE DE SANTIAGO DE COMPOSTELA

Fig. S4. Time-course of TRA and its TPs during chlorination (10 mg L^{-1}) (A), and direct photolysis (B) of spiked model solutions buffered at pH 7.

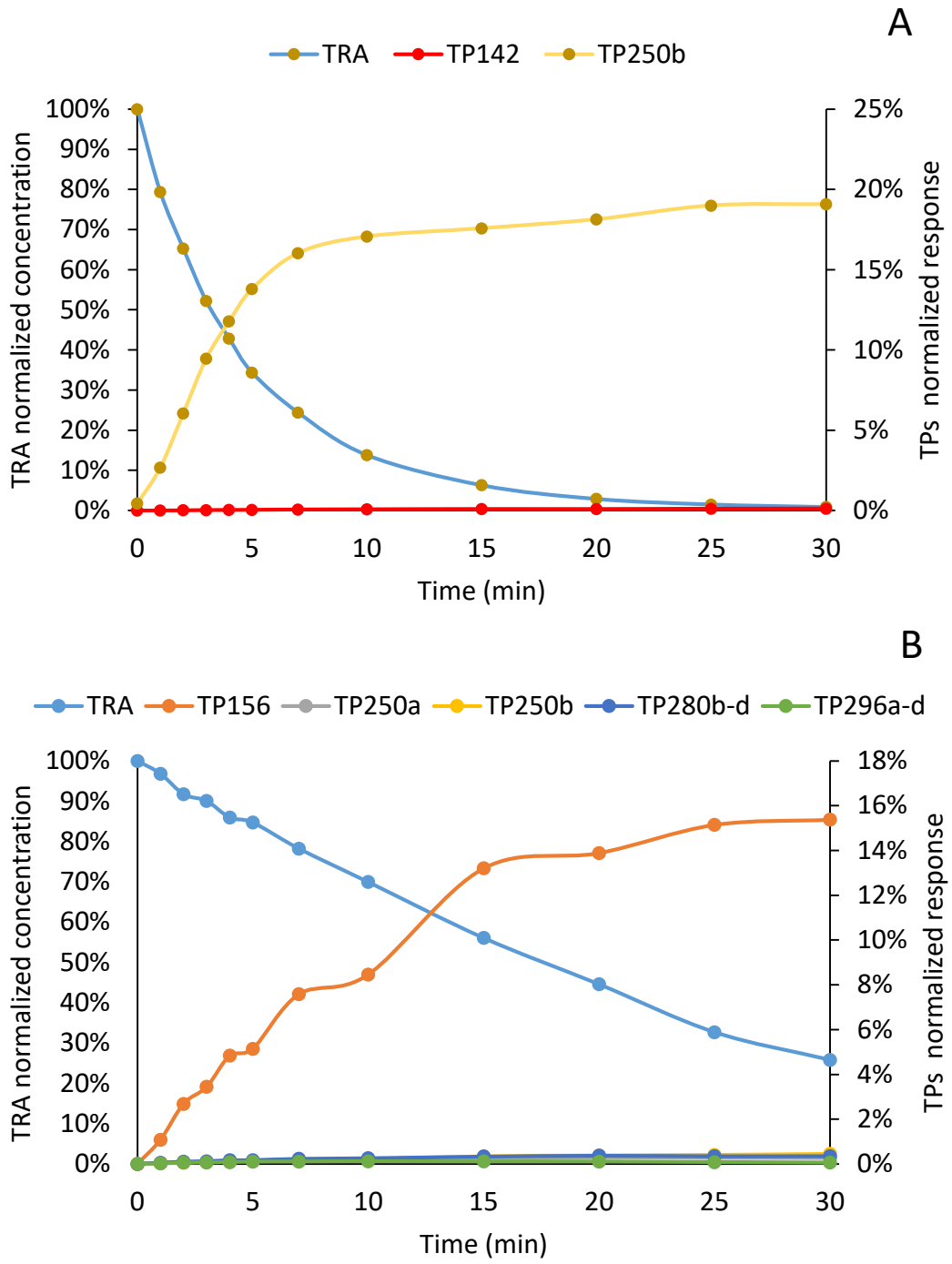
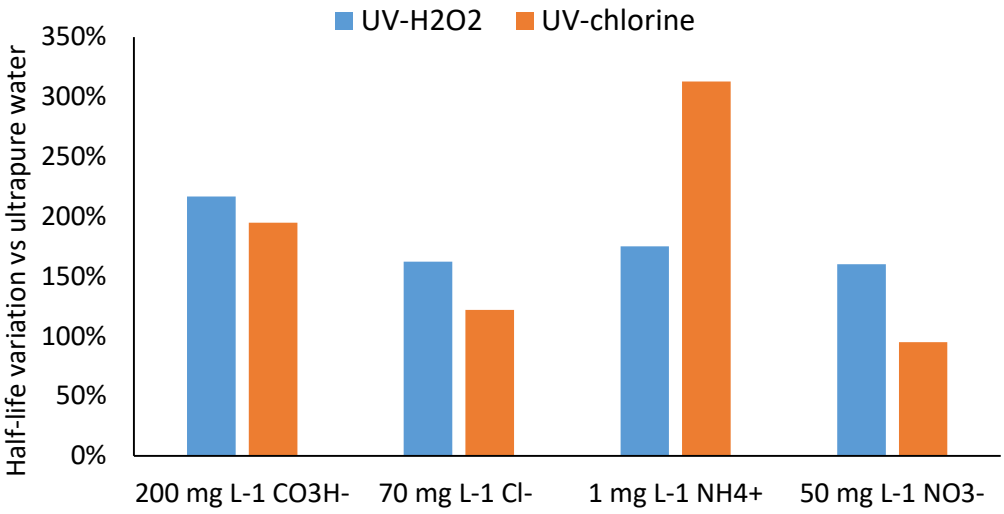


Fig. S5. Relative variations in the half-lives ($t_{1/2}$, min) of TRA, during UV-H_2O_2 and UV-chlorine processes, as function of species added to model water solutions buffered at pH 7.



USC UNIVERSIDADE DE SANTIAGO DE COMPOSTELA

Text S1. Determination of nitrobenzene by LC-UV.

The evolution of nitrobenzene (NB) in UV and UV-chlorine degradation studies was followed by LC-UV, using a XBridge C18 column (75 mm x 4.6 mm, 5 µm) acquired from Waters and operated in the isocratic mode, with ultrapure water: acetonitrile (50:50) as mobile phase. The column was maintained at 35 ºC, and the flowrate of mobile phase set at 1 mL min^{-1}. NB showed a retention time of 2.05 min. Absorbance was measured at 265 nm. The injected volume for different reaction time water aliquots was 50 µL.

Text S2. Determination of volatile by-products of tramadol by GC-MS.

The group of volatile disinfection by-products investigated during UV-chlorine processes includes the four legislated trihalomethanes (chloroform, dichlorobromethane, chlorodibromomethane and tribromomethane), 1,1-dichloroacetone, 1,1,1-trichloroacetone, and the following nitrogenated disinfection by-products: dichloro and trichloro acetonitrile, bromochloroacetonitrile and trichloronitromethane. Mixtures of these compounds, containing 1,2-dibromopropane (1,2-DBP) as surrogate standard, were prepared in pentane. Compounds were determined by gas chromatography-mass spectrometry (GC-MS), using a GC-TOF-MS instrument (Agilent 7200 model) with an electronic ionization source. Separations were carried out in a BP-1 type capillary column (30 m x 0.25 mm, 1 µm film thickness), purchased from Agilent. Injections (1 µL) were made in the splitless mode (purge time 0.6 min), with the injector maintained at 200 ºC. The flow of mobile phase (He) was 1.2 mL min^{-1}, and the temperature of the column was programmed as follows: 40 ºC (1 min), rated at 3 ºC min^{-1} until 60 ºC, second rate at 15 ºC min^{-1} to 240 ºC (5 min). Transfer line and EI source temperatures were 250 ºC and 230 ºC, respectively.

The retention times, quantification and qualification ions of each compound are compiled in the following table (Table S1). The limits of quantification of the procedure, considering LLE extraction of 10 mL water samples with pentane (1 mL), and further GC-MS analysis were 0.5 µg L^{-1}, and the linear response range extended up to 100 µg L^{-1} (both values are referred to the water sample). The *m/z* ratio of quantification and qualification ions were extracted using a mass window of 0.005 Da.

Conditions employed to determine the formation of anisole from hydrolysis of tramadol were the same as those described for volatile halogenated byproducts. The retention time and quantification- qualification ions of this compound are also given in Table S1.

USC UNIVERSIDADE DE SANTIAGO DE COMPOSTELA

Table S1. Retention times, quantification and qualification ions of volatile halogenated compounds, and anisole, using GC-EI-TOF-MS determination.

Compound	Retention time (min)	Quantification ion (m/z)	Qualification ion (m/z)
Chloroform	3.50	82.9443	84.9423
Bromodichloromethane	5.44	82.9443	128.8911
Dibromochloromethane	8.37	128.8911	126.8936
Tribromomethane	10.61	172.8419	174.8392
1,1-Dichloroacetone	6.19	82.9443	62.9993
1,1,1-Trichloroacetone	9.81	96.9599	124.9548
Trichloroacetonitrile	4.74	107.9401	109.9362
Dichloroacetonitrile	5.25	73.9791	81.9370
Bromochloroacetonitrile	8.34	73.9791	154.8945
Trichloronitromethane	8.16	116.9053	118.9023
Anisole	11.44	108.0577	78.0463
1,2-Dibromopropane	10.08	120.9649	122.9630

USC UNIVERSIDADE DE SANTIAGO DE COMPOSTELA

Table S2. Characteristics of environmental water samples employed in the study.

Parameter	River water	Wastewater A	Wastewater B
Chloride (mg L^{-1})	9.9	27.5	69.6
Nitrate (mg L^{-1})	7.8	< 0.1	12.4
Phosphate (mg L^{-1})	< 0.1	1.9	< 0.1
Sulfate (mg L^{-1})	7.4	29.6	32.7
Ammonium (mg L^{-1})	< 0.1	0.5	0.5
Total carbon (mg L^{-1})	7.5	39.2	34.1
Organic carbon (mg L^{-1})	4.8	23.9	26.6
UV absorbance (254 nm, cm^{-1})	0.023	0.165	0.32

USC UNIVERSIDADE DE SANTIAGO DE COMPOSTELA

Table S3. Direct photolysis rate constant and observed rate constants of CBA and TRA in competitive kinetics experiments using UV-H_2O_2 treatment. Data for ultrapure water solutions at pH 7. Initial concentrations 1 mM (H_2O_2) and 5 µM (CBA and TRA).

Constant	Value (min^{-1})	R^2
$k_{CBA\text{-}UV}$	0.0161	0.986
$k_{obsCBA(TRA)\text{-}UV\text{-}H2O2}$	0.3403	0.996
$k_{obsTRA(CBA)\text{-}UV\text{-}H2O2}$	0.3381	0.994

USC UNIVERSIDADE DE SANTIAGO DE COMPOSTELA

USC
UNIVERSIDADE
DE SANTIAGO
DE COMPOSTELA

CHAPTER 2. TARGET ANALYSIS OF SELECTED POLLUTANTS IN COMPLEX ENVIRONMENTAL MATRICES.

Emerging pollutants can be both natural and anthropogenic substances, that can cause damage to the environment and human health. Some emerging pollutants of special interest are pharmaceuticals and pesticides. As pharmaceuticals are designed to be highly stable for their intended effects on humans, their degradation in water treatment plants might be incomplete. Pesticides are also of great concern due to their possible non-target toxicity and persistence in the environment. Their presence in the environment can cause unexpected problems to many different non-target organisms.

In this chapter, different methodologies, based on target MS methods, for the determination of emerging pollutants, from different chemical families, were optimized and applied to evaluate their occurrence in several environmental compartments. First, a method for the selective and sensitive quantification of the bactericide chlorhexidine in sludge from WWTPs was developed. In the first part of the study, efforts were centred in improving the extraction efficiency, and the detectability of this high molecular weight, strong basic, compound by LC-MS/MS using a triple quadrupole instrument. The optimized procedure was applied to real samples, and the effects of chlorhexidine environmental levels in the development of plants, as well as its toxicity to model organisms, were assessed using in-vitro, standardized assays.

A direct analysis in real time methodology, using a DART ionization source, was explored for its capability of providing fast high resolution mass spectrometry data without the need of a chromatographic separation. In this study, several matrices with increasing complexity, from personal care products to sewage sludge, were considered for the fast quantitative determination of the antiseptic triclosan. Even if the main selling point of DART is the direct analysis on the own sample, when analysing very complex matrices, a pre-treatment of the sample is still necessary. The wastewater samples were extracted using a simple SPE protocol with HLB cartridges and ethyl acetate was used as the eluting solvent. Mouthwash samples were readily diluted with methanol and analysed thereafter and lastly, toothpaste and sludge samples were extracted using MSPD with C_{18} as the dispersant sorbent, followed by non-selective elution of triclosan using ethyl acetate. The study discusses those parameters affecting to capabilities of DART-QTOF-MS to discriminate the spectral signature of triclosan from those associated to organic species existing in these samples, or in their extracts, and effectively ionized in the DART source.

On the third publication compiled in this chapter, a determination methodology involving the enantiomeric separation of seven antimycotic drugs and three additional pharmaceuticals, from three different classes, was developed. The main objective was to evaluate potential changes in enantiomeric fraction that these chiral drugs can suffer during treatment of wastewater. To this end, influent and effluent wastewater samples collected on the same days were analysed, as well as sludge samples gathered in different regions of Galicia. The extraction of the liquid sample was done by SPE, with a mixed-mode cation exchanger, whereas the sludge samples were freeze-dried and extracted by MSPD, using a strong cation exchanger cartridge for clean-up purposes. In both cases, during extraction, compounds are isolated from other species without basic moieties in their structure. The article evaluates the performance of chiral

USC UNIVERSIDADE

SFC, combined with a QTOF-MS system, for the sensitive determination of the enantiomers of above compounds, assessing those parameters affecting the enantioselectivity of the separations, and the attained limits of quantification.

Lastly, a multianalyte target methodology, based on reversed-phase LC-MS/MS, was applied to assess the occurrence and the interaction between selected pesticides and plastic debris collected from agricultural fields. The selection of compounds was based on previous works made in the research group addressing the occurrence of pesticides in soils from vineyards. Moreover, a previous collaboration with researchers from CNRS (France) [98] focussed on the determination of organic compounds associated to marine microplastics suggested us the possibility that, end-of-life plastic for agricultural uses might contain relevant residues of the pesticides sprayed to crops and serve as carriers of these pollutants to other environmental compartments. After characterization of plastic litter collected from different places, conditions required to recover a pre-selection of pesticides from this matrix were investigated. Then, pesticide residues in plastics were compared to those existing in soils, and the effects of polymer aging and composition in the interaction with pesticides were assessed.

The published works regarding these studies can be found hereafter.

USC
UNIVERSIDADE DE SANTIAGO DE COMPOSTELA

PUBLICATION V: CHLORHEXIDINE RESIDUES IN SLUDGE FROM MUNICIPAL WASTEWATER TREATMENT PLANTS: ANALYTICAL DETERMINATION AND TOXICITY EVALUATION

Miguel Cobo Golpe, Gabriela Castro, Maria Ramil, Rafael Cela, Ysabel Santos, Isaac Rodríguez

Analytical and Bioanalytical Chemistry (2022) 414:6571–6580
DOI: 10.1007/s00216-022-04214-0



Impact factor: 4.3
Category: analytical chemistry
Position: 20/86
Quartile: Q1

USC UNIVERSIDADE DE SANTIAGO DE COMPOSTELA

Analytical and Bioanalytical Chemistry (2022) 414:6571–6580
https://doi.org/10.1007/s00216-022-04214-0

RESEARCH PAPER

Chlorhexidine residues in sludge from municipal wastewater treatment plants: analytical determination and toxicity evaluation

Miguel Cobo Golpe[1] · Gabriela Castro[1] · Maria Ramil[1] · Rafael Cela[1] · Ysabel Santos[1,2] · Isaac Rodríguez[1]

Received: 19 April 2022 / Revised: 22 June 2022 / Accepted: 4 July 2022 / Published online: 13 July 2022
© The Author(s) 2022

Abstract
In this work, a procedure for the sensitive and selective determination of chlorhexidine in sludge from municipal sewage treatment plants (STPs) based on matrix solid-phase dispersion (MSPD) and liquid chromatography coupled to tandem mass spectrometry (LC–MS/MS) was optimized and validated. Analysis of sewage sludge samples, obtained from different STPs in Northwest Spain from 2018 to 2021, showed that chlorhexidine was ubiquitous in this environmental compartment with concentrations between 0.3 and 16 μg g^{-1}. The toxicity of this pollutant was assessed in in vitro assays considering three different model organisms: *Candida albicans*, *Escherichia coli*, and *Staphylococcus aureus*. *C. albicans* was the most sensitive of the tested microorganisms to chlorhexidine with a lethal threshold concentration of 0.1 mg L^{-1}. Thus, the lowest observed sludge residue was 3 times higher than the acute toxicity threshold measured for *C. albicans*. Moreover, *E. coli* and *S. aureus* were also affected at chlorhexidine concentrations around 1.8 mg L^{-1} and 0.5 mg L^{-1}, respectively. So, chlorhexidine residues might affect the population of microorganisms existing in STPs. In addition, the potential phytotoxicity of the compound was evaluated with germination experiments using different model seeds. At the evaluated dose (10 μg g^{-1} dried soil), chlorhexidine did not affect the germination of *Sorghum saccharatum*, *Lepidium sativum*, or *Sinapis alba* seeds. Thus, amending agriculture soils with chlorhexidine containing sludge is unlikely to affect the germination of plants.

Keywords Chlorhexidine · Matrix solid-phase extraction · Liquid chromatography tandem mass spectrometry · Sludge · Ecotoxicity

Introduction

Emerging contaminants have been a concerning issue over the last two decades [1, 2]. These compounds comprise from pharmaceuticals to personal care products or high production volume chemicals. All of them are discharged in sewage and are only partially eliminated in sewage treatment plants (STPs) [3, 4]. Thus, they are introduced in the environment and in the water cycle causing different harmful effects to the wildlife [5–7].

✉ Maria Ramil
maria.ramil@usc.es

[1] Department of Analytical Chemistry, Nutrition and Food Sciences, IAQBUS - Institute of Research On Chemical and Biological Analysis, Universidade de Santiago de Compostela, R/Constantino Candeira SN, 15782 Santiago de Compostela, Spain

[2] Department of Microbiology and Parasitology, IAQBUS-Institute of Research On Chemical and Biological Analysis, Universidade de Santiago de Compostela, R/Constantino Candeira SN, 15782 Santiago de Compostela, Spain

Antiseptics and disinfectants present an increasing consumption in the last years and they have become target micropollutants in the aquatic environment [8]. Among them, chlorhexidine is employed as biocide and disinfectant in personal care, particularly mouth washes [9, 10], and household products [11]. It has been proven to be toxic to some animals such as rats by accidental ingestion [12], and it has been recently revealed to interfere with human sex hormone receptor pathways [13]. Moreover, chlorhexidine has already been reported as toxic for some aquatic organisms such as *P. subcapitata*, *D. magna*, *D. rerio*, and *V. fischeri* [14]. Effluent water from STPs contains just 1–2% of the total mass of chlorhexidine entering treatment plants [15–17]. However, owing to its large molecular weight, limited water solubility, and poor degradability [18, 19], this compound is expected to be accumulated in the sludge fraction of STPs.

As it has been already reported for antibiotics [20], biocides might also contribute to the development of resistant microorganisms [21]. In the environment of STPs, chlorhexidine has proved to be toxic for the microbiota involved in

USC UNIVERSIDADE DE SANTIAGO DE COMPOSTELA

the biodegradation of organic pollutants [21]. In this vein, Keerthisinghe et al. [21] have recently reported that chlorhexidine at environmentally relevant levels could lead to a significant reduction of *Comamonadaceae* and *Flavobacteriaceae*, core members of activated sludge and involved in major ecosystem functions (e.g., organic matter and nutrient removals and floc formation) of activated sludge processes. Further disposal of stabilized sludge in agriculture fields, as fertilizer, might also affect the microbiota of soil if relevant residues of this bactericide remain in the sludge matrix.

The above evidences justify the development of effective analytical methodologies allowing the fast and accurate determination of this biocide. Some specific features of chlorhexidine, such as its strong interaction with negatively charged compounds, large molecular size, and trend to ionize as a mixture of single and double charge species, merit to develop a tailored analytical approach. In general, typical multiresidue methods for water analysis including chlorhexidine are based simply on a SPE using a reversed-phase material such as OASIS HLB and the determination carried out by LC–MS [22, 23]. To the best of our knowledge, no optimized extraction conditions for chlorhexidine analysis in sludge have been reported to date.

The aim of this work was to evaluate for the first time the parameters affecting the yield of matrix solid-phase dispersion (MSPD), as sample preparation technique, for chlorhexidine extraction from freeze-dried sludge samples. Moreover, the effect of the LC column in the performance of the chlorhexidine chromatographic peak was also investigated. The optimized method was applied to determine the residues of this biocide in a selection of samples obtained from different urban STPs, in the Northwest of Spain in different years. The acute toxicity of the pollutant was assessed using in vitro assays considering three different model microorganisms: *Candida albicans*, *Escherichia coli*, and *Staphylococcus aureus*. Also, the potential phytotoxicity was investigated using a standardized germination test using *Sorghum saccharatum*, *Lepidium sativum*, and *Sinapis alba* seeds. Finally, environmental concentrations were compared to in vitro toxicity thresholds.

Material and methods

Material, solvents, and standards

Polypropylene syringes (12 mL volume) and polyethylene frits for MSPD extraction (20 µm, 15 mL) were supplied by International Sorbent Technology (Mid Glamorgan, UK). The dispersant sorbent (C18-bonded silica) was obtained from Agilent Technologies (Santa Clara, CA, USA). The co-sorbent, diatomaceous earth, was purchased from Sigma-Aldrich (Milwaukee, WI, USA). PTFE filters, 0.2 µm pore size, from Phenomenex (Cheshire, SK10 2BN, USA) were used.

Methanol (MeOH), HPLC-grade, ethanol, and formic acid (FA) were obtained from Merck (Darmstadt, Germany). Acetonitrile (ACN) was provided by VWR Chemicals (Radnor, PA). Ultrapure deionized water (18.2 MΩ cm^{-1}) was obtained from a Genie U system (Rephile, Shanghai, China).

The standard of chlorhexidine (98% purity) was purchased from Sigma-Aldrich and its deuterated analogue (chlorhexidine-d_8, employed as surrogate standard, SS) was obtained from Toronto Research Chemicals (North York, ON, Canada). Individual stock solutions of each compound were prepared in MeOH. Further dilutions were made in the same solvent.

The commercial Phytotoxkit, employed to investigate the potential phytotoxicity of chlorhexidine to three different model plants (*Sorghum saccharatum* (Sorgho), *Lepidium sativum* (garden cress) and *Sinapis alba* (mustard)), was purchased from Microbiotests (Gent, Belgium).

Samples and sample preparation

Grab sludge samples were obtained from 23 municipal STPs located in Galicia (Northwest of Spain) in the period 2018–2021. Figure S1 shows the geographic location of the STPs. After reception, samples were frozen, lyophilized, and then stored in glass vessels, at 4 °C, until analysis. MSPD sample preparation conditions were adapted from a previous protocol developed for the screening of emerging pollutants in sewage sludge [24]. In brief, a fraction of 0.5 g of lyophilized sludge, spiked with the SS, was dispersed using 2 g of C_{18} in a glass mortar, for 5 min. The mixture was loaded into a polypropylene syringe containing a polyethylene frit and 1 g of diatomaceous earth. The cartridge was compacted with a second frit on the top. Chlorhexidine was extracted passing MeOH-FA (99:1) (10 mL) through the MSPD cartridge. The obtained extract was passed through a PTFE filter, 0.2 µm pore size, and injected in the UPLC-MS/MS system without any additional treatment.

In order to evaluate the efficiency of the MSPD extraction, spiked samples were prepared by addition of the chlorhexidine standard to a pool of freeze-dried sludge samples (addition level 1 µg g^{-1}). Every 5 samples, procedural blanks (without any sludge in the MSPD packed syringe) were prepared in order to evaluate contamination problems during the extraction protocol.

Preliminary experiments were carried out using pressurized liquid extraction (PLE) with MeOH and MeOH-FA (1%) as extraction solvents. As in the case of MSPD, 0.5 g of sludge was dispersed with 2 g of C18 and 1 g of diatomaceous earth added in the bottom of the cell. Extraction was carried out at 90 °C and 1500 psi, during 2 cycles with 100%

USC UNIVERSIDADE DE SANTIAGO DE COMPOSTELA

MIGUEL COBO GOLPE

flush volume. A DIONEX (Sunnyvale, CA, USA) ASE 200 accelerated solvent extractor was used for PLE.

Toxicity tests

Microorganism and culture conditions

Quality control strains of *Escherichia coli* ATCC 25,922, *Staphylococcus aureus* ATCC25923, and *Candida albicans* ATCC 14,053 were used in the acute toxicity assay. The two bacterial strains were routinely cultured on Mueller–Hinton agar (MHA) and broth (MHB) media (Cultimed, Spain) at 37 °C, for 24 h. The fungal strain was cultured on yeast extract-peptone-dextrose agar (YPDA) and broth (YPDB) (Difco) media at 30 °C for 24 h.

The survival of *E. coli*, *S. aureus*, and *C. albicans* following chlorhexidine treatment was evaluated by a colorimetric assay based on the reduction of a tetrazolium salt (MTT method). Briefly, a stock solution of chlorhexidine of 578.5 mg L^{-1} in 96% ethanol was used to prepare a series of two fold solutions at concentrations ranging from 57.9 to 0.06 mg L^{-1} in yeast extract-peptone-dextrose (YPD) and Mueller–Hinton broth (MHC) media. Subsequently, the prepared solutions were dispensed in a volume of 90 µL into the appropriate wells of 96-well U-Bottom microplates. *E. coli*, *S. aureus*, and *C. albicans* suspensions, containing approximately 1 to 2×10^8 colony-forming units (CFU/mL) (OD_{620} of 0.08–0.13), were inoculated to each well in a 1:10 proportion. Colony counts on inoculum suspension were verified by the plate dilution method using MHA and YPDA plates and counting the bacterial/fungal colonies produced. Media with and without inoculum was used as positive and negative control of growth, respectively. MHB and YPDB with chlorhexidine were used as blank. The plates were incubated for 24 h at 37 °C (*E. coli* and *S. aureus* strains) and 30 °C (*C. albicans* strain). Viable bacteria or fungi present in the wells were quantified 30 min after addition of 10 µL of [3(4,5-dimethylthiazol-2-yl)-2,5-diphenyltetrazolium bromide] (MTT, 5 g L^{-1}), which is reduced in proportion to the number of viable cells present. Optical density was determined by eluting the dye with dimethyl sulfoxide and the spectrophotometric absorbance measured at 620 nm (Microplate Reader Model 680, BioRad). Experiments were carried out in triplicate. The results were expressed as percentage of mortality using the formula: Normalized mortality (%) = (1 − Absorbance treated samples/Absorbance control) × 100.

Phytotoxicity studies

The potential phytotoxicity of chlorhexidine was assessed using two types of dicotyl plants (garden cress (*Lepidium sativum*) and *mustard* (*Sinapis alba*)) and a monocotyl Sorgho (*Sorghum saccharatum*) as models, considering the effects of the biocide in seed germination and in the length of roots after a 3-day germination period. Assays were carried out using two different fractions of a model OECD soil. One of the fractions was used as control, whilst the other was spiked with a solution of chlorhexidine in MeOH at a concentration of 10 µg g^{-1}. Both fractions were stored at room temperature for 1 week to permit the evaporation of the organic solvent. Levels of chlorhexidine in the spiked soil were verified by MSPD extraction followed by LC–MS/MS determination. Thereafter, both soil fractions were saturated with water. Germination experiments were carried out in triplicate (three plates were prepared using unspiked and spiked soil samples), placing 10 seeds in each of the plates. Plates were placed vertically and maintained in the dark, at 25 °C, for 3 days before observing the germination of seeds.

Ecotoxicological risk assessment

Predicted environmental concentrations in amended soil (PEC_{soil}), estimated 1 year after one sludge-dose application, were calculated applying the following equation from the European Commission Technical Guidance Document on Risk Assessment EUR 20,418 EN/2 [25]:

$$PEC_{soil} = C_{sludge} \times APPL_{sludge} / (DEPTH_{soil} \times RHO_{soil})$$

where C_{sludge} is the concentration measured in digested sludge expressed as µg kg^{-1} dry mass; $APPL_{sludge}$ is the application rate of dry sludge onto soils (0.5 kg m^{-2} $year^{-1}$ for agricultural soils); $DEPTH_{soil}$ is the mixing depth (0.20 m for agricultural soils); and RHO_{soil} is the bulk density of wet soil (1700 kg m^{-3} for agricultural soils).

Instrumental analysis

In the current research, a UPLC-QqQ-MS instrument (Waters, Acquity UPLC Xevo TQD) furnished with a Z-ESI source was employed. The capillary voltage was set at 3.10 kV. The source temperature was maintained at 150 °C. Drying gas (N_2) flow and temperature were 650 L h^{-1} and 200 °C, respectively. Columns tested for chlorhexidine analysis were a Zorbax Eclipse Plus C_{18} rapid resolution (50 mm × 2.1 mm, 1.8 µm) column, acquired from Agilent Technologies (Wilmington, DE, USA), and a Kinetex PS C_{18} (50 mm × 2.1 mm, 2.6 µm) from Phenomenex (Torrance, CA, USA). The columns were protected with a C_{18} 2.1 mm i.d. Security Guard™ cartridge, supplied from Phenomenex. Column and precolumn were maintained at 40 °C. Ultrapure water (A) and MeOH (B), both containing 0.1% FA, were used as mobile phases at a flow of 0.4 mL min^{-1}. Under optimized conditions, the Kinetex PS column was used with the following gradient: 5% B (0 min), 20% B (3 min), 100%

USC UNIVERSIDADE DE SANTIAGO DE COMPOSTELA

B (6–7 min), 5% B (7.1–10 min). The injection volume for solvent-based standards and sludge extracts was 0.5 µL. The MS/MS transitions used to determine chlorhexidine and its deuterated analogue are given in Table 1.

A UPLC-QTOF-MS system (Agilent 6550 model, furnished with an electrospray ionization source (ESI), and combined with a 1290 UPLC system from the same supplier) was used to assess the molecular formula of chlorhexidine fragment ions. The instrument was operated in the 2 GHz, extended dynamic resolution mode, with continuous recalibration of the *m/z* axis using the following ions: 121.0508 and 922.0098 (ESI+). Typical mass resolution was 17,000 at *m/z* 322.

Results and discussion

Precursor ion and column selection

Ionization of chlorhexidine at ESI sources renders a mixture of $[M+H]^+$ and $[M+2H]^{2+}$ ions, which limits the sensitivity of its LC–MS determination. Furthermore, variations in the relative formation of mono- and di-protonated ions might affect method accuracy. Experiments were carried out using different ESI needle voltages (1.5–3.5 kV) and different compositions of the mobile phase in order to optimize the signal of the pseudomolecular ion. Figure S2 shows the MS spectra corresponding to a standard of chlorhexidine using two different capillary voltages. Whatever the considered ESI (+) conditions, the $[M+2H]^{2+}$ ion (*m/z* 253) showed a higher intensity than the $[M+H]^+$ one (*m/z* 505); therefore, it was selected as precursor to optimize MRM conditions. Several fragment ions were obtained from the *m/z* 253 precursor: one at *m/z* 170.0480 corresponding to the formula $[C_7H_9N_3Cl]^+$ was a monoprotonated ion derived from the break of the end part of the molecule including the chlorinated benzene ring and three amines, and it was used for quantitation. Another one, with *m/z* 125.1073 corresponding to the formula $[C_7H_{13}N_2]^+$, was common to the deuterated form, and therefore, it should correspond to the central-amine part of the molecule because the deuterium atoms were located at the benzene rings. It was used as qualifier. Other ions present in the MS/MS spectra corresponded to *m/z* 153.0214 with formula $[C_7H_6N_2Cl]^+$ obtained by NH_3^+ loss from the *m/z* 170.0480 and to *m/z* 142.1339 with formula $[C_7H_{16}N_3]^+$. All of them are monoprotonated ions.

Experimental findings showed that the shape of the chromatographic signal of chlorhexidine in the C_{18}-type column degraded very fast, leading to a tailing peak after a few injections. We assumed that the increasing peak tailing was the result of interaction between negatively charged silanol groups in silica particles, and the opposite sign charges in the molecule of chlorhexidine. As alternative, a column

Table 1 LC-ESI (+)-MS/MS conditions for chlorhexidine and chlorhexidine-d_8, linearity, and instrumental LOQ

Compound	Retention time (min)	Precursor ion $[M+2H]^{2+}$	Cone voltage (V)	Q1 (CE, eV)	Q2 (CE, eV)	Q2/Q1 ratio	Other ions	Calibration curve (5–250 µg L^{-1}; $n=7$ levels)	R^2	LOQ (µg L^{-1})
Chlorhexidine	4.9	253.1	40	170.0 (17)	125.1 (22)	0.45	153.0, 142.1	Slope: 0.0234 ± 0.0006 Intercept: − 0.0577 ± 0.0621	0.997	2
Chlorhexidine-d_8	4.9	257.1	40	174.1 (17)	125.1 (22)	0.45	157.0 142.1			

USC UNIVERSIDADE DE SANTIAGO DE COMPOSTELA

specifically designed to deal with strong basic compounds (Kinetex PS column) with a core–shell technology was evaluated to solve the above shortcoming. In this case, the positively charged groups introduced on the surface silica particles of this column avoid the above-described electrostatic interactions. Figure 1 shows the performance of the Kinetex column versus a conventional C_{18} reversed-phase one for a standard of chlorhexidine. Better peak shape and shorter retention were achieved using the Kinetex PS C18 column, which was selected for the rest of the study.

The LOQ and LOD of the QqQ instrument for chlorhexidine were established at 2 µg L^{-1} (Table 1) and 0.8 µg L^{-1} respectively. The LOQ corresponds to the lowest concentration standard providing a signal to noise (*S*/*N*) response of 10 for the less intense MRM transition (Q2), whilst the ratio between responses for qualification (Q2) and quantification (Q1) transitions remains within ± 30% of the average value showed in Table 1. Similarly, for LOD calculation, a signal to noise (*S*/*N*) response of 3 was taken into account. A lineal calibration range between 5 and 250 µg L^{-1} was attained with a determination coefficient of 0.997 using chlorhexidine-d8 at a constant concentration of 50 µg L^{-1} (see Table 1 and Supplementary information Figs. S3 and S4). The inter-day precision for $N = 10$ injections, in three different days, for standard containing100 µg L^{-1} of chlorhexidine was 5%.

The concentrations of chlorhexidine in the extracts from spiked and non-spiked sludge samples were determined

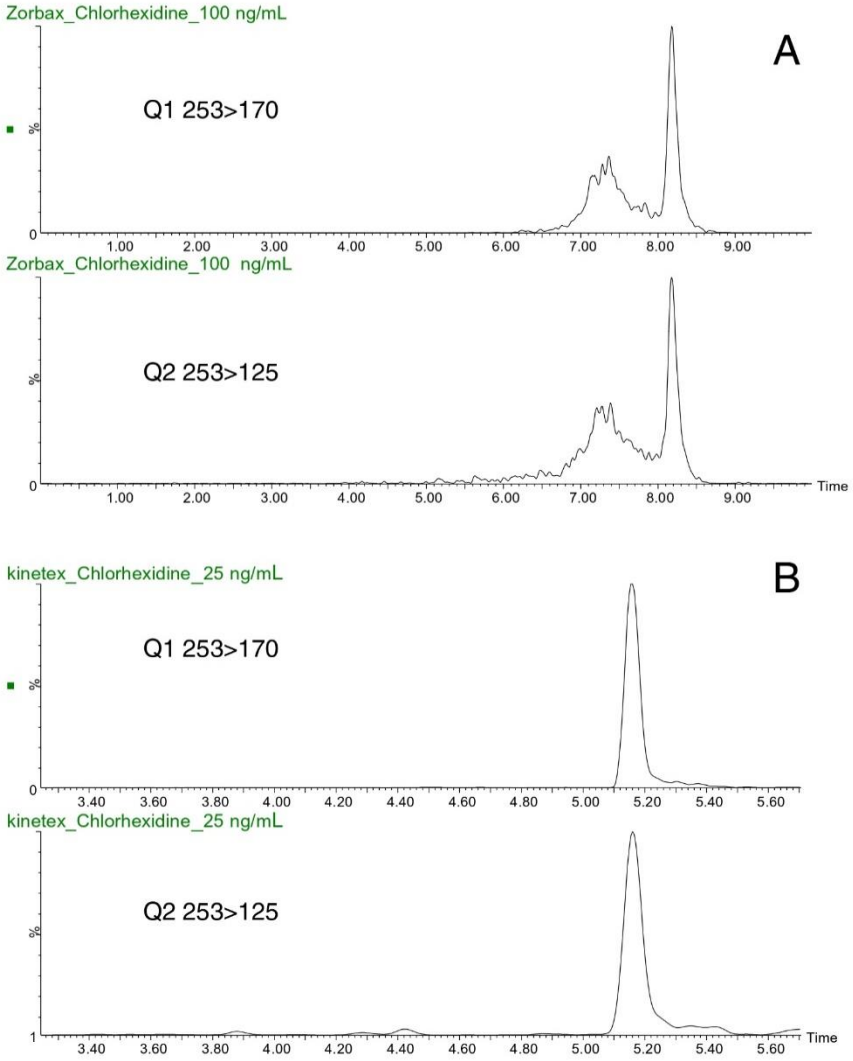


Fig. 1 Chromatograms of a standard solution of chlorhexidine in a conventional C18 column (100 µg L^{-1}) (A) versus a Kinetex PS one (25 µg L^{-1}) (B)

USC UNIVERSIDADE DE SANTIAGO DE COMPOSTELA

using solvent-based standards (5 to 250 µg L^{-1}), containing an equivalent concentration (50 µg L^{-1}) of deuterated chlorhexidine as SS.

MSPD extraction and performance of the method

Preliminary experiments with PLE of the sludge reported very low recoveries (25%) when using MeOH as extractant under standard extraction conditions (1500 psi and 90 °C) (Table 2). As a green and simpler alternative to PLE, a MSPD protocol was adapted from a previously reported work dealing with the determination of emerging contaminants in sludge [23]. Following this procedure, the freeze-dried sludge samples (0.5 g) were dispersed with 2 g of C18 over a layer of diatomaceous earth as clean-up sorbent. However, MeOH as eluting solvent failed again to recover quantitatively chlorhexidine from the sludge due to the strong lipophilic-ionic interaction between the compound and the matrix; ACN provided even lower recoveries (9%) (Table 2). Chlorhexidine values of pKa for the basic moieties range from 7.63 (pKa1) to 10.22 (pKa4), and the optimum pH for activated sludge is stated to remain between pH 6.5 and pH 8; therefore, chlorhexidine would be partially protonated in the sludge in the STP and an ionic interaction between the substance and the sludge matrix would take place. Thus, it was necessary to add 1% FA to MeOH to be able to release chlorhexidine from the matrix (Table 2). Probably, formic acid neutralizes some negatively charged sites at the sludge surface enabling the extraction of chlorhexidine. PLE with MeOH-FA provided recoveries of 73% versus 93% provided by MSPD using the same eluant; due to the simplicity of the latter approach, it was selected for the rest of the study.

The possible variation in the ionization efficiency of chlorhexidine in sludge extracts versus solvent-based standards was evaluated by comparing the slopes of calibration curves for spiked sludge extracts and solvent-based standards prepared in MeOH-FA (99.9:0.1). An average signal enhancement of 152% was obtained for two tested sludge samples (Table 2). In order to minimize this effect, the injection volume was reduced from 2 to 0.5 µL. As a result, just a slight increase in the response of the sludge matrix (115%) was observed (Fig. 2). The ratio of responses of chlorhexidine and an chlorhexidine-d8 was considered as response variable for the rest of the study.

The overall recoveries for the corrected responses were assessed for three different addition levels over pooled freeze-dried sludge samples: 2000 ng g^{-1}, 1000 ng g^{-1}, and 500 ng g^{-1}. For the lowest addition level, just sludge samples with relatively low levels of chlorhexidine were included in the pooled sludge. Results are compiled in Table 3. They were quantitative in all cases ranging from 94 ± 11% to 120 ± 6% and with a grand mean recovery of 105 ± 6%. The LOQ of the proposed methodology considering 0.5 g of freeze-dried sludge and 10 mL of eluting solvent were established in 40 ng g^{-1} (Fig. S5) and the LOD at 16 ng g^{-1}. As further shown, these values were

Table 2 Extraction efficiencies for chlorhexidine using PLE and MSPD with different eluents ($N = 3$) and matrix effects for two different injection volumes. Addition level: 2 µg g^{-1}

	PLE recovery		MSPD recovery			Matrix effects	
	MeOH	MeOH-FA (1%)	MeOH	ACN	MeOH-FA (1%)	Inj vol. 2 µL	Inj vol. 0.5 µL
Chlorhexidine	25 ± 5%	73 ± 9%	26 ± 4%	9 ± 2%	92.5 ± 7.5%	152 ± 4%	115 ± 3%

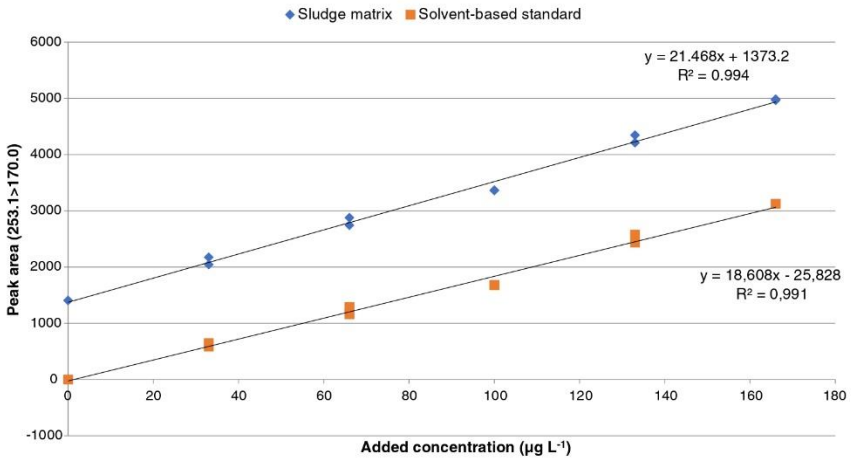


Fig. 2 Calibration curves obtained using matrix-matched (blue) and solvent-based (orange) standards. Peak areas for the Q1 transition, without surrogate standard correction, are plotted vs added concentration, duplicate injections

USC UNIVERSIDADE DE SANTIAGO DE COMPOSTELA

Table 3 Recoveries of chlorhexidine in three different pooled sludge samples ($N=3$) with different addition levels

Pooled sludge sample	Recoveries (%)		
	Addition level: 2000 ng g^{-1}	Addition level: 1000 ng g^{-1}	Addition level: 500 ng g^{-1}
1	109 ± 2%	94 ± 11%	101 ± 6%
2	120 ± 6%	101 ± 5%	115 ± 8%
3	97 ± 4%	96 ± 5%	112 ± 8%
Average	109 ± 4%	97 ± 7%	109 ± 7%
Grand mean	105 ± 6%		

lower than the residues of chlorhexidine found in the processed sludge samples, so verification of estimated procedural LOQ was carried out spiking the deuterated compound in sludge at a concentration of 50 ng g^{-1}. Fig. S5 shows the plots of Q1 and Q2 transitions for deuterated chlorhexidine spiked in sludge at 50 ng g^{-1}.

Analysis of real samples

Sludge samples were collected from 23 different STPs in Galicia (Northwest of Spain). Locations of each sampling site are plotted in Fig. S1. Samples were processed with the optimized MSPD protocol and found concentrations were in the range of 0.3–16 µg g^{-1} in the period 2018–2021 (Table S1). These concentrations are in agreement with those found by Östman et al. [16] in Swedish sludges (2.8–19 µg g^{-1}). Figure 3A compares the concentrations of chlorhexidine in sludge samples obtained from nine different STPs in, at least, two different years. Overall, concentrations found in the second sampling campaign were similar to, or higher than, those obtained in the sludge from the same STP in different years. Figure 3B shows the box-whisker plots with the distribution of chlorhexidine concentrations

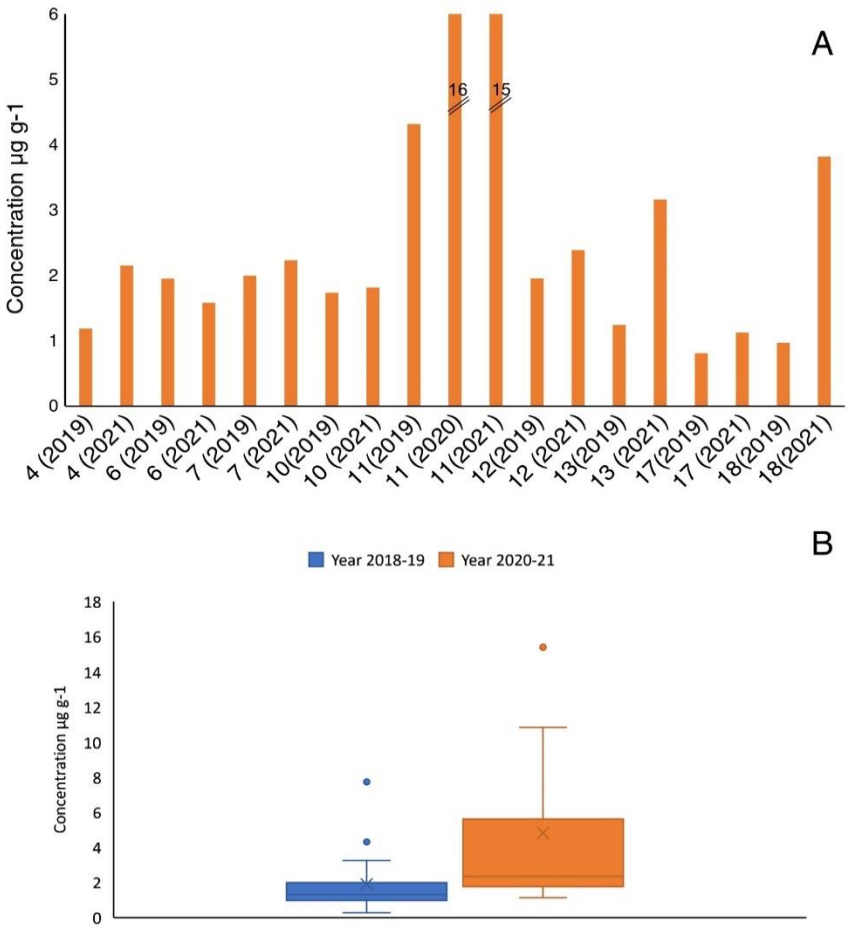


Fig. 3 Concentration of chlorhexidine in sludge samples from the same STPs in different years (2019–2021) (A). Box-whisker plots of chlorhexidine residues in sludge in the evaluated period, years 2018–2019 and 2020–2021 (B)

USC UNIVERSIDADE DE SANTIAGO DE COMPOSTELA

measured in sludge samples obtained before and after the outbreak of the COVID-19 disease. As appreciated, higher median and average concentrations were found in samples obtained during years 2020 and 2021, which point out to an increase in the consumption of the antiseptic.

Ecotoxicity

Three microorganisms were tested being exposed to decreasing concentrations of chlorhexidine: *Candida albicans*, *Escherichia coli*, and *Staphylococcus aureus*. The most sensitive of the tested microorganisms to chlorhexidine with lethal threshold concentrations lower than 0.1 mg L^{-1} was *C. albicans* (Fig. 4). *E. coli*, however, remained unaffected until concentrations around 1.8 mg L^{-1} and *Staphylococcus aureus* until 0.5 mg L^{-1} (Fig. 4). Considering a density of in vitro liquid toxicity assay solutions of 1 g mL^{-1}, above thresholds are equivalent to 0.1 µg g^{-1}, 1.8 µg g^{-1}, and 0.5 µg g^{-1} for *C. albicans*, *E. coli*, and *S. aureus*, respectively. Chlorhexidine was ubiquitous in the sludge samples analyzed and the lowest observed residue, referred to freeze-dried sludge and expressed in µg g^{-1} of dried sludge, was 3 times higher than the acute toxicity threshold measured for *C. albicans*. Furthermore, average concentrations referred to freeze-dried sludge stayed 5 times above the acute toxicity level observed for *S. aureus*, and they are two orders of magnitude higher than PNEC for freshwater sediment reported in the NORMAN data base (6.94 ng g^{-1} dw) [26]. Calculated PEC_{soil} (0.44–23.5 ng g^{-1}) are also at a similar level as the PNEC in freshwater sediment. In summary, chlorhexidine residues existing in STPs sludge might be high enough to modulate the microbiological communities existing either in STPs or in sludge amended soils.

Regarding plants toxicity, a test was carried out with *Sorghum saccharatum*, *Lepidium sativum*, and *Sinapis alba* in reference OECD soil spiked with chlorhexidine. In this case, chlorhexidine did not present toxicity towards these plant species even with a concentration as high as 10 µg g^{-1} (Fig. S6). Thus, considering PEC_{soil}, residues estimated from chlorhexidine measured in the processed sludge samples will not affect the germination of vegetables.

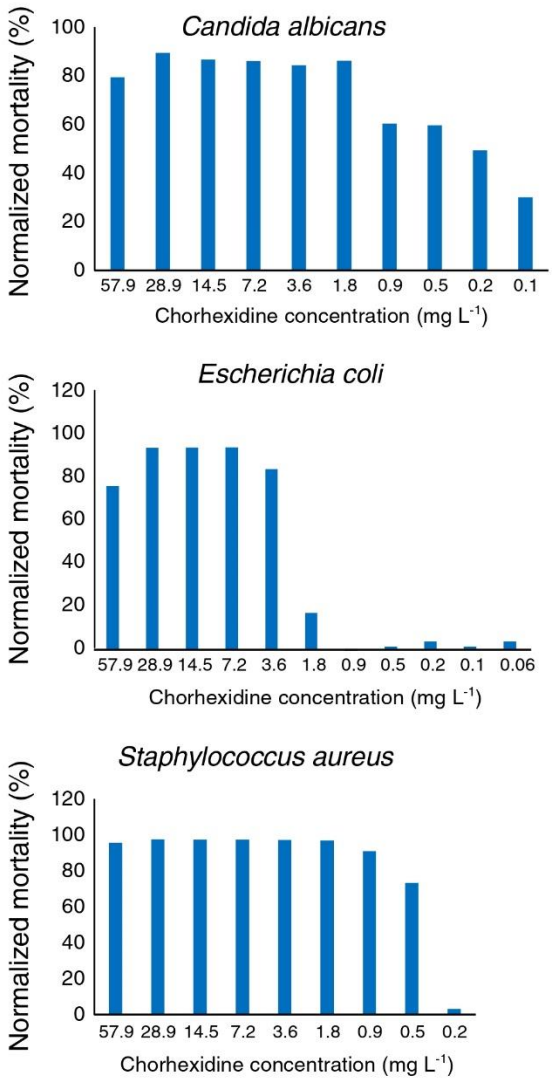


Fig. 4 Normalized mortalities for *Candida albicans*, *Escherichia coli*, and *Staphylococcus aureus* versus chlorhexidine concentration

Conclusions

Chlorhexidine has been confirmed to be ubiquitous in sludge samples. Sample preparation comprises MSPD extraction using methanol modified with formic acid in order to completely recover chlorhexidine from the matrix. Chromatographic performance is clearly improved by the use of columns specifically designed to cope with basic compounds. The chlorhexidine precursor duality, $[M+H]^+$ and $[M+2H]^{2+}$, favors the use of the latter ion in terms of intensity. Under optimized conditions, accurate concentration values can be obtained using solvent-based calibration standards. Concentrations up to 16 µg g^{-1} have been registered, and taken into account the experimental acute toxicity to some microorganism, as *C. albicans*, it can be concluded that chlorhexidine could alter the microbial population of the STP sludge and that existing in soil amended sludge. On the other hand, this pollutant would not affect seed germination.

Supplementary Information The online version contains supplementary material available at https://doi.org/10.1007/s00216-022-04214-0.

USC UNIVERSIDADE DE SANTIAGO DE COMPOSTELA

Funding Open Access funding provided thanks to the CRUE-CSIC agreement with Springer Nature. This study was supported by Spanish Government and Xunta de Galicia through grants PGC2018-094613-B-I00 and ED431C 2021/06, co-funded by the EU. M. Cobo Golpe received FPI fellowship from the Spanish Ministry of Science, Innovation and Universities.

Declarations

Conflict of interest The authors declare no competing interests.

Open Access This article is licensed under a Creative Commons Attribution 4.0 International License, which permits use, sharing, adaptation, distribution and reproduction in any medium or format, as long as you give appropriate credit to the original author(s) and the source, provide a link to the Creative Commons licence, and indicate if changes were made. The images or other third party material in this article are included in the article's Creative Commons licence, unless indicated otherwise in a credit line to the material. If material is not included in the article's Creative Commons licence and your intended use is not permitted by statutory regulation or exceeds the permitted use, you will need to obtain permission directly from the copyright holder. To view a copy of this licence, visit http://creativecommons.org/licenses/by/4.0/.

References

1. Ternes TA. Occurrence of drugs in German sewage treatment plants and rivers. Water Res. 1998;32:3245–60. https://doi.org/10.1016/S0043-1354(98)00099-2.
2. Hirsch R, Ternes TA, Haberer K, Mehlich A, Ballwanz F, Kratz KL. Determination of antibiotics in different water compartments via liquid chromatography-electrospray tandem mass spectrometry. J Chromatogr A. 1998;815:213–23. https://doi.org/10.1016/s0021-9673(98)00335-5.
3. Daughton CG, Ternes TA. Pharmaceuticals and personal care products in the environment: agents of subtle change? Environ Health Perspect. 1999;107:907–38. https://doi.org/10.1289/ehp.99107s6907.
4. Zwiener C, Frimmel FH. Oxidative treatment of pharmaceuticals in water. Water Res. 2000;34:1881–5. https://doi.org/10.1016/S0043-1354(99)00338-3.
5. Kidd KA, Blanchfield PJ, Mills KH, Palace VP, Evans RE, Lazorchak JM, Flick RW. Collapse of a fish population after exposure to a synthetic estrogen. 2007. Proc Matl Acad Sci USA. 2007; 104: 8897–8901. https://doi.org/10.1073/pnas.0609568104
6. Lange R, Hutchinson TH, Croudace CP, Siegmund F, Schweinfurth H, Hampe P, Panter GH, Sumpter JP. Effects of the synthetic estrogen 17 alphaethinylestradiol on the life-cycle of the fathead minnow (*Pimephales promelas*). Environ Toxicol Chem. 2001;20:1216–27. https://doi.org/10.1897/1551-5028(2001)020%3c1216:eotsee%3e2.0.co;2.
7. Oaks JL, Gilbert M, Virani MZ, Watson RT, Meteyer CU, Rideout BA, Shivaprasad HL, Ahmed S, Chaudhry MJ, Arshad M, Mahmood S, Ali A, Khan AA. Diclofenac residues as the cause of vulture population decline in Pakistan. Nature. 2004;427:630–3. https://doi.org/10.1038/nature02317.
8. Usage of mouthwash/dental rinse in the U.S. 2011–2024. Available online: https://www.statista.com/statistics/286902/usage-mouthwash-dental-rinse-us-trend (accessed on March 20th, 2022).
9. Manipal S, Hussain S, Wadgave U, Duraiswarny P, Ravi K. The mouthwash war-chlorhexidine vs. herbal mouth rinses: a meta-analysis. J Clin Diagn Res 2016; 10(5): ZC81-ZC83. https://doi.org/10.7860/jcdr/2016/16578.7815
10. Van Strydonck DAC, Slot DE, Van der Velden U, Van der Weijden F. Effect of a chlorhexidine mouthrinse on plaque, gingival inflammation and staining in gingivitis patients: a systematic review. J Clin Periodontol. 2012;39(11):1042–55. https://doi.org/10.1111/j.1600-051x.2012.01883.x.
11. Ram PK, Begum F, Crabtree-Ide C, Uddin MR, Weaver AM, Dostogir Harun MG, Allen JV, Kumar S, Nasreen S, Luby SP, El Arifeen S. Waterless hand cleansing with chlorhexidine during the neonatal period by mothers and other household members: findings from a randomized controlled trial. Am J Trop Med Hyg. 2020;103:2116–26. https://doi.org/10.4269/ajtmh.19-0773.
12. Xue Y, Zhang S, Tang M, Zhang T, Wang Y, Hieda Y, Takeshita H. Comparative study on toxic effects induced by oral or intravascular administration of commonly used disinfectants and surfactants in rats. J Appl Toxicol. 2012;32(7):480–7. https://doi.org/10.1002/jat.1662.
13. Michalíková K, Linhartová L, Ezechiáš M, Cajthaml T. Assessment of agonistic and antagonistic properties of widely used oral care antimicrobial substances toward steroid estrogenic and androgenic receptors. Chemosphere. 2019;217:534–41. https://doi.org/10.1016/j.chemosphere.2018.11.006.
14. Jesus FT, Oliveira R, Silva A, Catarino AL, Soares AMVM, Nogueira AJA, Domingues I. Lethal and sub lethal effects of the biocide chlorhexidine on aquatic organisms. Ecotoxicology. 2013;22:1348–58. https://doi.org/10.1007/s10646-013-1121-6.
15. Chakraborty T, Balusani D, Sabourin L, Renaud J, Sumarah M, Nakhla G, Ray MB. Fate of micropollutants in chemically enhanced primary treatment using recovered coagulants. J Environ Manage. 2020;269: 110815. https://doi.org/10.1016/j.jenvman.2020.110815.
16. Östman M, Lindberg RH, Fick J, Bjorn E, Tysklind M. Screening of biocides, metals and antibiotics in Swedish sewage sludge and wastewater. Water Res. 2017;115:318–28. https://doi.org/10.1016/j.watres.2017.03.011.
17. Östman M, Fick J, Tysklind M. Detailed mass flows and removal efficiencies for biocides and antibiotics in Swedish sewage treatment plants. Sci Total Environ. 2018;640–641:327–36. https://doi.org/10.1016/j.scitotenv.2018.05.304.
18. Linhartová L, Michalíková K, Šrédlová K, Cajthaml T. Biodegradability of dental care antimicrobial agents chlorhexidine and octenidine by ligninolytic fungi. Molecules. 2020;25:400. https://doi.org/10.3390/molecules25020400.
19. Sarkar S, Chakraborty S, Bhattacharjee C. Photocatalytic degradation of pharmaceutical wastes by alginate supported TiO_2 nanoparticles in packed bed photo reactor (PBPR). Ecotox Environ Safe. 2015;121:263–70. https://doi.org/10.1016/j.jecoenv.2015.02.035.
20. Bengtsson-Palme J, Hammarén R, Pal C, Östman M, Björlenius B, Flach CF, Fick J, Kristiansson E, Tysklind M, Larsson DGJ. Elucidating selection processes for antibiotic resistance in sewage treatment plants using metagenomics. Sci Total Environ. 2016;572:697–712. https://doi.org/10.1016/j.scitotenv.2016.06.228.
21. Keerthisinghe TP, Nguyen LN, Kwon EE, Oh S. Antiseptic chlorhexidine in activated sludge: biosorption, antimicrobial susceptibility, and alteration of community structure. J Environ Manage. 2019;237:629–35. https://doi.org/10.1016/j.jenvman.2019.02.043.
22. Boleda MR, Galcerán MT, Ventura F. Validation and uncertainty estimation of a multiresidue method for pharmaceuticals in surface and treated waters by liquid chromatography-tandem mass spectrometry. J Chromatogr A. 2013; 1286: 146–158. https://doi.org/10.1016/j.chroma.2013.02.077
23. Hernandez F, Ibanez M, Botero-Coy AM, Bade R, Bustos-Lopez MC, Rincon J, Moncayo A, Bijlsma L. LC-QTOF MS screening of more tan 1000 licit and illicit drugs and their metabolites in wastewater and surface waters from the area of Bogota, Colombia. Anal Bioanal Chem. 2015; 407 (21): 6405–6416. https://doi.org/10.1007/s00216-015-8796-x

USC UNIVERSIDADE DE SANTIAGO DE COMPOSTELA

24. Castro G, Ramil M, Cela R, Rodríguez I. Identification and determination of emerging pollutants in sewage sludge driven by UPLC-QTOF-MS data mining. Sci Total Environ. 2021;778: 146256. https://doi.org/10.1016/j.scitotenv.2021.146256.
25. Technical Guidance Document on Risk Assessment, Part II, EUR 20418 EN/2, European Commission, Joint Research Centre, 2003.
26. https://www.norman-network.com/nds/ecotox/lowestPnecsIndex.php (Accessed on March 30th, 2022)

Publisher's Note Springer Nature remains neutral with regard to jurisdictional claims in published maps and institutional affiliations.

USC UNIVERSIDADE DE SANTIAGO DE COMPOSTELA

Supplementary information to manuscript:

Chlorhexidine residues in sludge from municipal wastewater treatment plants: analytical determination and toxicity evaluation

M. Cobo Golpe[1]; G. Castro[1]; M. Ramil*[1]; R. Cela[1]; Y. Santos[2]; I. Rodríguez[1].

[1]Department of Analytical Chemistry, Nutrition and Food Sciences, IAQBUS - Institute of Research on Chemical and Biological Analysis, Universidade de Santiago de Compostela, R/Constantino Candeira SN, 15782 Santiago de Compostela, Spain

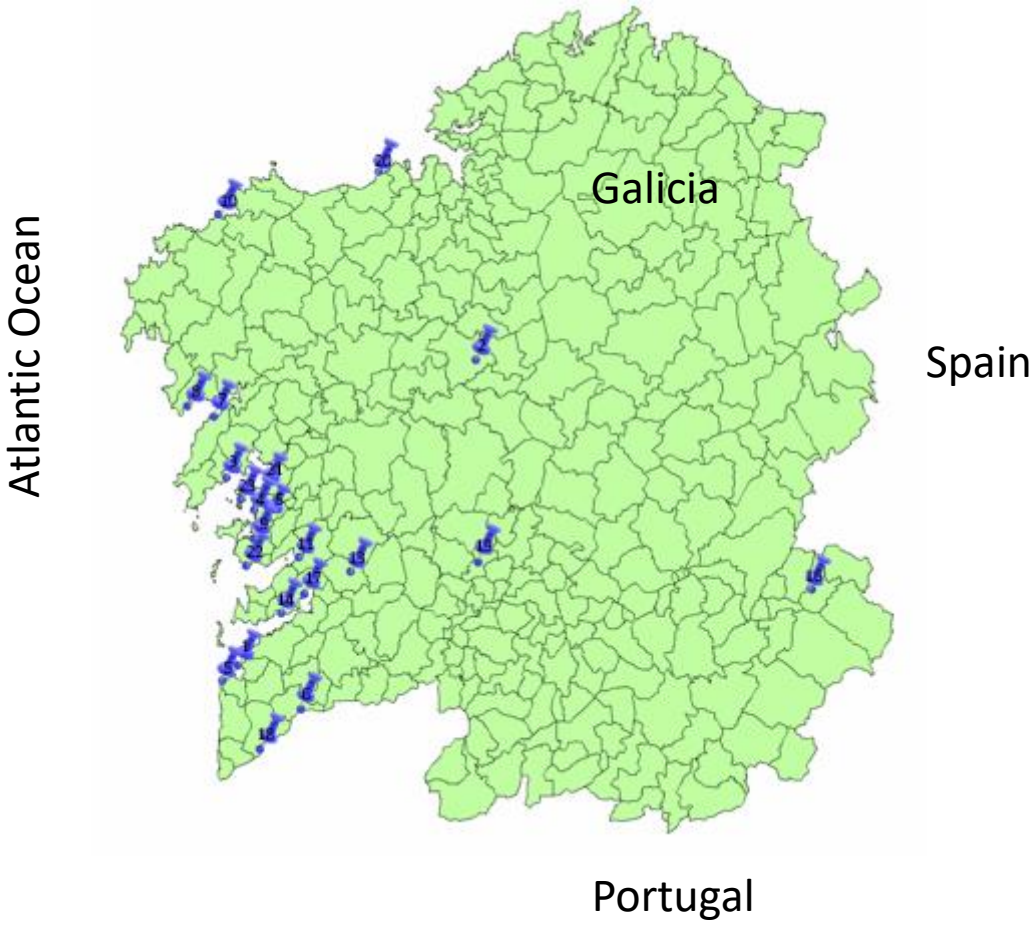
e-mail:maria.ramil@usc.es

[2]Department of Microbiology and Parasitology, IAQBUS - Institute of Research on Chemical and Biological Analysis, Universidade de Santiago de Compostela, R/Constantino Candeira SN, 15782 Santiago de Compostela, Spain

USC UNIVERSIDADE DE SANTIAGO DE COMPOSTELA

FIGURES:

Figure S1. Sampling locations in Galicia (Northwest of Spain).



USC
UNIVERSIDADE DE SANTIAGO DE COMPOSTELA

Figure S2: Mass spectra for a standard of chlorhexidine using two different voltages of the ESI needle.

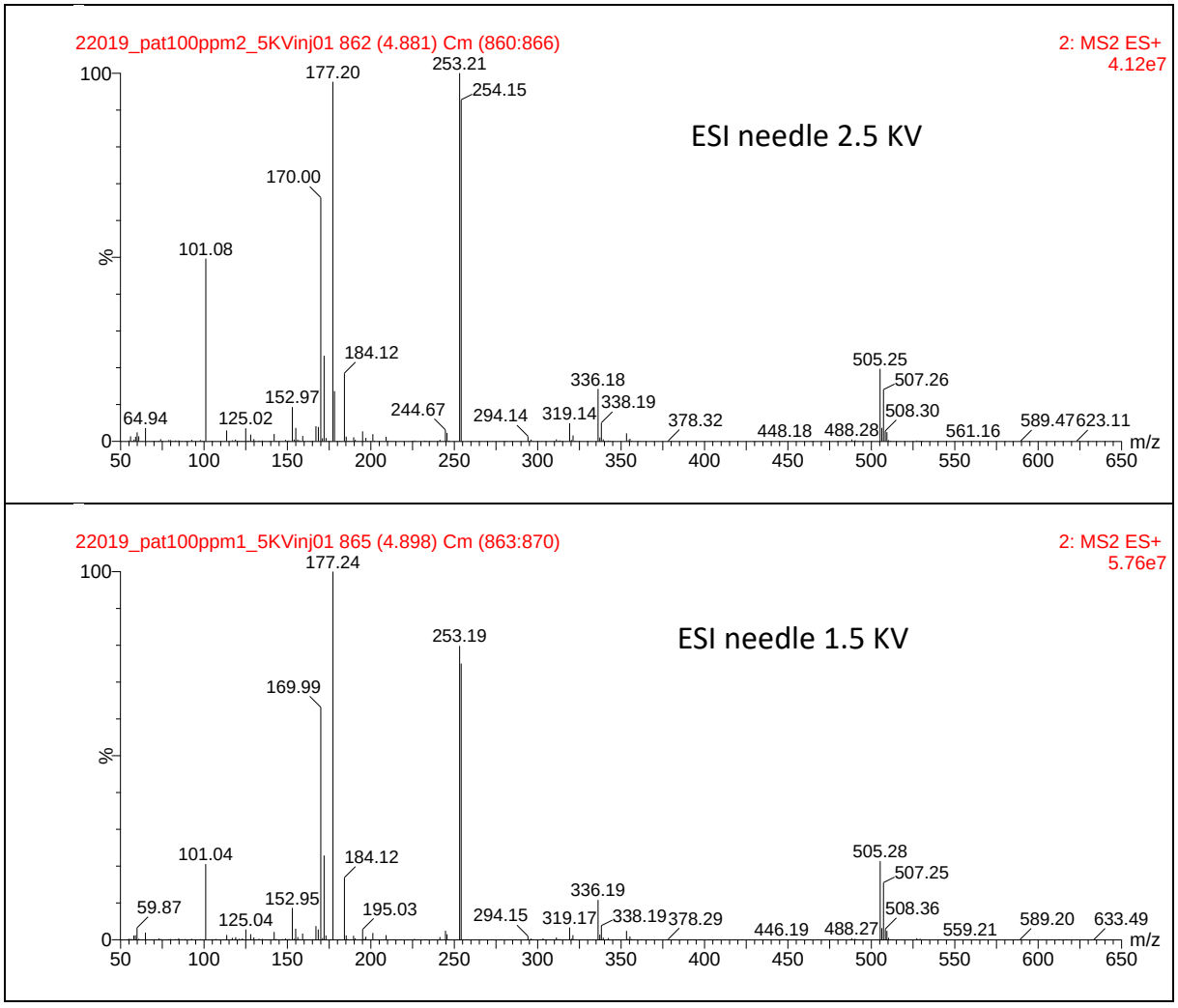


Figure S3: LC-MS/MS chromatogram of a standard solution of chlorhexidine close to the LOQ of the molecule (Concentration: 5 µg L^{-1})

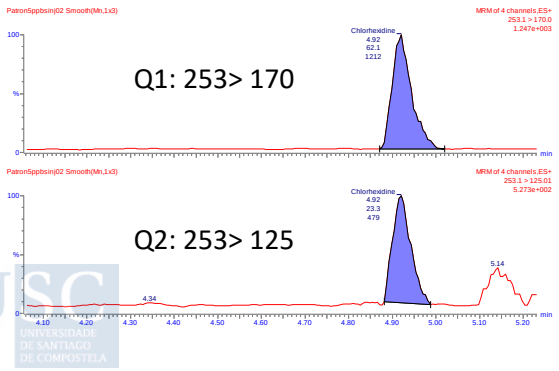


Figure S4: Calibration curve for standard solutions of chlorhexidine (Range: 5-250 µg L^{-1}).

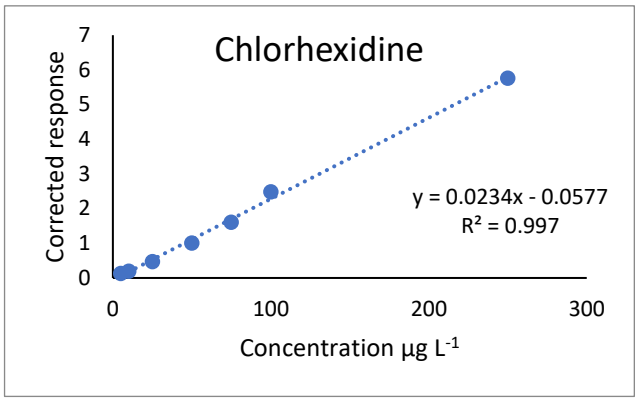


Figure S5: Chromatogram corresponding to the extract of a sludge spiked at 50 ng g^{-1} level with deuterated chlorhexidine (chlorhexidine-d_8).

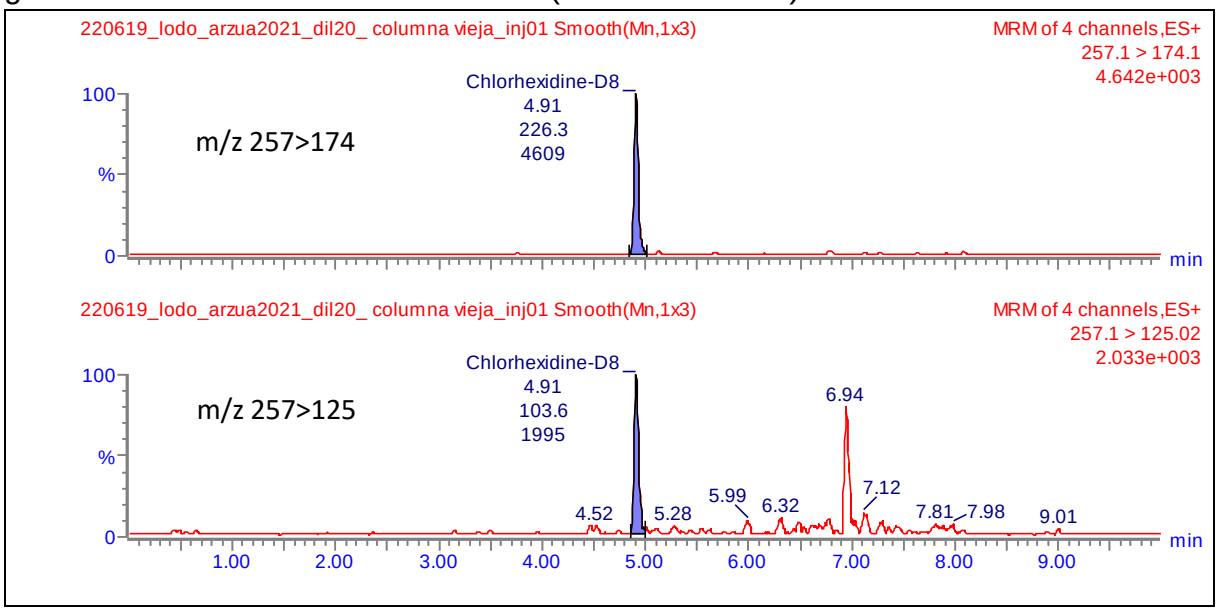
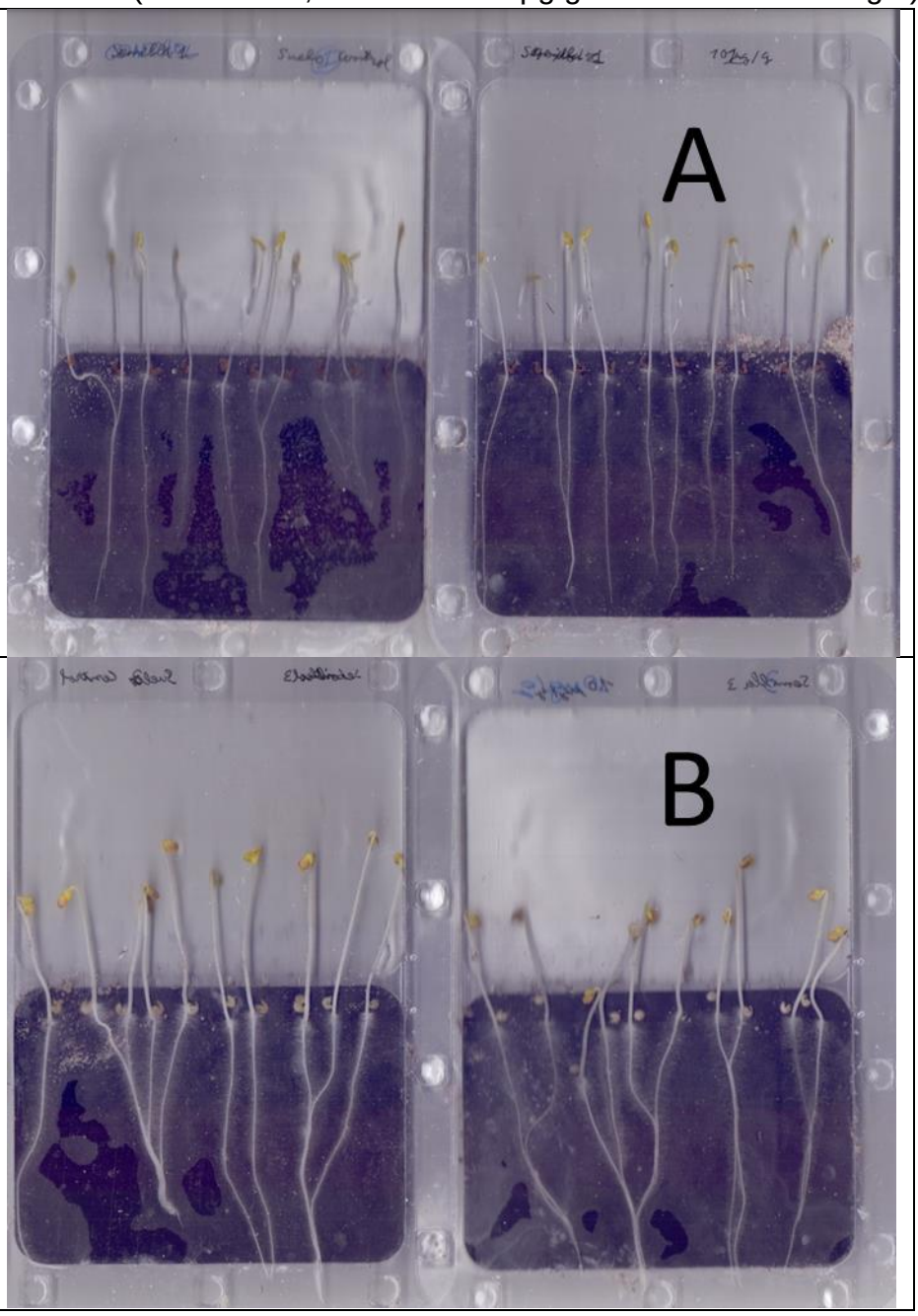


Figure S6. Lepidium sativum (A) and Sinapis alba (B) exposed to chlorhexidine amended soil (Control: left; addition of 10 µg g^{-1} of chlorhexidine: right).



TABLES:

Table S1: Concentrations of chlorhexidine in different STPs from Galicia (Spain) in the period 2018-2021.

	Concentration (µg g^{-1})			
STP Code	Year 2018	Year 2019	Year 2020	Year 2021
1	1.68			
2				1.17
3	1.05			
4		1.19		2.15
5	0.28			
6		1.95		1.58
7		2.00		2.23
8	1.30			
9	0.38			
10		1.73		1.81
11		4.32	15.51	15.40
12		1.96		2.39
13		1.24		3.16
14	0.79			
15	2.31			
16	7.74			
17		0.81		1.13
18		0.97		3.82
19	3.26			
20	10.86			
21	3.84			
22	2.31			
23	1.19			

USC UNIVERSIDADE DE SANTIAGO DE COMPOSTELA

USC
UNIVERSIDADE
DE SANTIAGO
DE COMPOSTELA

PUBLICATION VI: ASSESSMENT OF DIRECT ANALYSIS IN REAL TIME ACCURATE MASS SPECTROMETRY FOR THE DETERMINATION OF TRICLOSAN IN COMPLEX MATRICES

M. Cobo-Golpe, J. García-Martín, M. Ramil, R. Cela, I. Rodríguez1
Analytical and Bioanalytical Chemistry (2021) 413:6355–6364
DOI: 10.1007/s00216-021-03591-2

Impact factor: 4.478
Category: Analytical chemistry
Position: 22/87
Quartile: Q2

USC UNIVERSIDADE DE SANTIAGO DE COMPOSTELA

Analytical and Bioanalytical Chemistry (2021) 413:6355–6364
https://doi.org/10.1007/s00216-021-03591-2

RESEARCH PAPER

Assessment of direct analysis in real time accurate mass spectrometry for the determination of triclosan in complex matrices

M. Cobo-Golpe[1] · J. García-Martín[1] · M. Ramil[1] · R. Cela[1] · I. Rodríguez[1]

Received: 29 June 2021 / Revised: 27 July 2021 / Accepted: 29 July 2021 / Published online: 10 August 2021
© The Author(s) 2021

Abstract
In this work, the applicability of direct analysis in real time coupled to accurate mass spectrometry (DART-MS) to the quantitative determination of triclosan (TCS) in samples with increasing complexity, from personal care products to extracts from sewage, is investigated. In the first term, DART-MS spectra of TCS as free phenol and as derivatized species are characterized; thereafter, the effects of several instrumental variables in the detectability of TCS (i.e., temperature, solvent, and compound holder) are discussed. Under final selected conditions, TCS was determined from its $[M\text{-}H]^-$ ions, without need of derivatization, attaining an instrumental limit of quantification of 5 ng mL^{-1}, with a linear response range up to 1000 ng mL^{-1}. Complex matrices, such as solid-phase extracts obtained from environmental water samples, moderately inhibited the ionization efficiency of TCS, with signal attenuation percentages in the range of 6 to 57%, depending on the sample type and on the concentration factor provided by the SPE procedure. The accuracy of results obtained by DART-MS was evaluated using liquid chromatography (LC) with MS detection; in both cases, a time-of-flight (TOF) MS instrument was employed for the selective determination of the $[M{-}H]^-$ ions of TCS (*m/z* values 286.9439 and 288.9410) using a mass window of 20 ppm. DART-MS did not only provide enough sensitivity to detect the presence of TCS in environmental samples (raw and treated wastewater as well as freeze-dried sludge), but also measured concentrations matched those determined by LC-ESI-TOF-MS, with only slightly higher standard deviations. During analysis of personal care products, containing much higher concentrations of TCS in a less complex matrix, both techniques were equivalent in terms of accuracy and precision.

Keywords Ambient ionization · Triclosan · Direct analysis in real time (DART) · Accurate mass spectrometry · Environmental samples · Matrix effects

Introduction

Ambient ionization techniques, such as direct analysis in real time (DART) [1, 2], have been introduced recently coupled to mass spectrometry for rapid analysis of different kinds of samples. These techniques provide quantitative and qualitative information of different sample components, avoiding the chromatographic separation step and, sometimes, also sample preparation. Despite these inherent benefits, in the case of DART, the ionization process is rather complex, involving several competitive routes, which depend on the properties of each compound (energy of ionization, functional groups, and thermal stability), the matrix components, and the ambient atmospheric molecules. What is generally accepted is that compounds are first desorbed from the sample and then ionized in the gas phase. In practice, the possibility to determine a certain compound in a complex chemical matrix, such as an environmental sample, depends on several parameters: the efficiency of the ionization source to generate ions from the neutral molecules, the matrix effects in the yield of the ionization process, and the selectivity (resolution) provided by the mass spectrometer in order to discriminate the signal of the analyte from those of other simultaneously generated ions during ionization [1, 2]. These characteristics make DART suitable for qualitative/quantitative analysis of bulk material components, usually containing a reduced number of different species in a simple matrix [3, 4]. However, the number of applications reporting the determination of trace compounds

✉ M. Ramil
maria.ramil@usc.es

[1] Department of Analytical Chemistry, Nutrition and Food Sciences, IAQBUS - Institute of Research on Chemical and Biological Analysis, Universidade de Santiago de Compostela, R/Constantino Candeira SN, 15782 Santiago de Compostela, Spain

USC UNIVERSIDADE DE SANTIAGO DE COMPOSTELA

in complex matrices and/or in the concentrated extracts from environmental samples, i.e., wastewater, is still limited [5, 6].

Triclosan (TCS) is a synthetic antimicrobial agent which inhibits the activity of bacteria, viruses, and fungi [7]. It is widely used in various personal care products such as soaps, cosmetics, mouthwashes, and toothpaste [7, 8] and also in household items like toys, textiles, furniture, and kitchenware [9]. The above uses have led to the introduction of TCS in urban sewage and even in surface water due to its incomplete removal in wastewater treatment plants (STPs) [10–12]. The interaction of TCS with some water disinfectants has been correlated with the formation of halogenated disinfection by-products [13]. Moreover, its moderate lipophilic character, and chemical stability, have led to the distribution of this contaminant of concern in sewage sludge [14]. TCS has also been related to other environmental matrices, such as particulate matter or indoor dust [15]. Additionally to distribution studies, during the last years, the environmental risk assessment of triclosan has been widely investigated and harmful effects in aquatic plants [16] and fish [17] have been reported. More specifically, TCS has been found to be bioaccumulative in plants and earthworms [18–20], and correlated with the development of bacterial resistance [21, 22].

Thus, different analytical methodologies have been developed for the determination of triclosan in different products and environmental compartments. For aqueous samples, both solid-phase extraction [23, 24] and microextraction techniques [25–27] have been evaluated. Pressurized liquid extraction (PLE) [28] and matrix solid-phase dispersion (MSPD) [29] have been employed in the extraction of TCS from solid samples. In general, all these sample preparation techniques have been combined with an appropriate chromatographic technique, either gas chromatography or liquid chromatography, coupled to mass spectrometry. In some cases, the total protocol, sample preparation followed by chromatographic separation and detection, is rather time consuming. Furthermore, the use of a derivatization step in the case of GC-based techniques introduces an extra step in the analytical procedure.

To the best of our knowledge, to date, no thorough studies about triclosan determination by DART-MS have been carried out; therefore, the main objective of this work was to assess the possibilities of a DART source combined with a QTOF-MS instrument for the determination of this biocide in samples with different characteristics. These will include from personal care products, where the compound is added at concentrations of hundreds of milligrams per gram, to wastewater extracts and sewage sludge. In the case of environmental matrices, sample preparation protocols previously validated in combination with GC-MS/MS or LC-MS/MS have been used [30, 31]. Parameters affecting the detectability of TCS by DART-MS are optimized, and the accuracy of the results obtained during analysis of real samples is assessed using LC-ESI-QTOF-MS as reference technique.

Material and methods

Solvents, standards, and sorbents

Methanol (MeOH) (HPLC grade), acetonitrile, ethyl acetate, and formic acid were purchased from Merck (Darmstadt, Germany). Triclosan (TCS) and triclosan $^{13}C_6$ (TCS-$^{13}C_6$) were provided by Toronto Research Chemicals Inc. (North York, ON, Canada). Acetic anhydride and the silylation agent N-methyl-N-(tert-butyldimethylsilyl)-trifluoroacetamide (MTBSTFA) were provided by Sigma-Aldrich (Milwaukee, WI, USA). Individual stock standards of TCS and TCS-$^{13}C_6$ were prepared in MeOH. Further dilutions were made in the same solvent, and stored at − 20 °C. Calibration standards for DART were prepared in ethyl acetate from methanol stocks.

OASIS HLB cartridges (60 mg) were obtained from Waters (Milford, MA, USA), C_{18} was provided by Agilent (Wilmington, DE, USA), diatomaceous earth was provided by VWR Chemicals (Leicestershire, England), and 10-mL polypropylene syringes were purchased from Becton Dickinson (Franklin Lakes, NJ, USA).

Samples and sample preparation

Toothpaste and mouthwash samples were purchased in local supermarkets. Wastewater samples were collected in the effluent and influent of an urban sewage plant equipped with primary and secondary treatments. This plant receives the combined wastewater from a city of 125,000 inhabitants and also from a large hospital. Samples were passed through glass fiber filters and then stored at 4 °C until being analyzed. Sludge samples were collected from different STPs from Galicia (northwest of Spain) and freeze-dried after reception.

Mouthwash was simply diluted with methanol before analysis in order to bring TCS within the linear response range of DART-TOF-MS. Water samples were extracted by SPE using OASIS HLB cartridges (60 mg). Volumes of 200 and 400 mL were processed for influent and effluent samples, respectively. Samples were previously acidified at pH 3 and TCS-$^{13}C_6$ added before extraction. Elution of the cartridges was performed with 2 mL of ethyl acetate [30].

Sludge extraction was performed by MSPD. Briefly, approximately 500 mg of freeze-dried sludge, spiked with TCS-$^{13}C_6$, was dispersed over 2 g of C_{18} in a mortar and transferred to a polypropylene syringe containing 1 g of diatomaceous earth. The elution was carried out with 10 mL of ethyl acetate. This methodology was based on a generic MSPD extraction protocol developed in our group [31]. MSPD was also applied to the extraction of TCS from the toothpaste matrix. In this case, sample and dispersant (C18) masses were reduced to 0.2 and 1 g, respectively. The rest of the conditions were common to those employed for MSPD of freeze-dried sludge. Verification of the performance of both

USC UNIVERSIDADE DE SANTIAGO DE COMPOSTELA

MIGUEL COBO GOLPE

SPE and MSPD techniques rendered overall recoveries for wastewater and sludge higher than 88% (see Table S1).

Equipment and determination conditions

DART-QTOF-MS

A DART-SVP ion source (IonSense Inc. Saugus, MA, USA, model SVPS-200) equipped with a linear rail was used in this research. This module was employed to hold either *Quick Strip* transmission sample cards, with a 12-position frame of stainless steel, or a *Dip it* accessory with 12 positions for glass capillaries, both allowing the analysis of liquid samples. The DART source was coupled to a QTOF-MS, Agilent 6520 model acquired from Agilent Technologies (Wilmington, DE, USA), through the commercial Vapur chamber, which reduces the entrance of helium or nitrogen in the high-vacuum region of the MS instrument. Helium was used as volatilization and ionization gas, and N_2 was employed to refrigerate the source in the standby mode. In both cases, a flow rate of 2.5 mL min^{-1} was used. During method development, DART was operated in positive and negative ionization modes for native and derivatized TCS, applying a grid voltage of 350 V. The temperature of the source was set at 350 °C and the speed of the linear rail fixed at 0.3 mm s^{-1}. Standards and sample extracts (from 1 to 4 μL) were deposited in the stainless-steel mesh of cards, or at the capillary tip, using a 10-μL syringe. In both cases, the solvent was allowed to evaporate for about 5 min, before attaching the holding material (steel mesh or glass capillaries) to the linear rail module.

The QTOF instrument operated in the extended dynamic range (2 GHz) mode with a resolution of 7800 (FWHM) measured for the ion at *m/z* 301.9981. Under final working conditions, TCS was quantified in negative ionization mode, as underivatized compound, applying a capillary voltage of 1000 V. The fragmentor voltage was set at 130 V. Accurate mass data were recorded in the range of *m/z* values from 70 to 1700, at a rate of 2 spectra s^{-1} (6767 scans are accumulated in each spectrum). Continuous recalibration of the *m/z* axis in the QTOF system was carried out with signals obtained for ions at *m/z* values of 89.0234 and 255.2324. These ions were generated from species (polyethylene glycol derivatives) existing in the atmosphere of the laboratory [32]. In the experiments performed operating the DART source in the positive mode, the recalibration ions were 135.1016 and 391.2843 corresponding to diethylene glycol monoethyl ether and bis (ethylhexyl) phthalate ionization, respectively. Both species are recognized as ubiquitous in indoor environments and provided signals with enough intensity for continuous re-calibration of the TOF-MS analyzer.

LC-QTOF-MS

In this case, a UPLC chromatograph (Agilent Infinity 1290) coupled to a second QTOF-MS system (Agilent 6550) equipped with an ESI ionization source was used. The system was operated in the 2 GHz mode, with a typical resolution (FWHM) of 19,500, at *m/z* 301.9981, almost double than that obtained with the other QTOF instrument combined with the DART source. The separation of TCS was performed in a C18 type column, acquired from Agilent (Zorbax Eclipse Plus C18, 50 mm × 2.1 mm, 1.8 μm), employing water (A) and acetonitrile (B) (both 0.1% formic acid) as mobile phases with a flow of 0.4 mL min^{-1}. The gradient was as follows: 0–0.1 min (90% A), 6–7 min (0% A), and 7.1–10 min (90% A). The column temperature was fixed at 40 °C. The quantification ions were 286.9439 and 288.9410 for TCS and 292.9618 for TCS-$^{13}C_6$. The isolation window was 20 ppm and the injection volume, 2 μL.

Recovery assessment and sample quantification

The calibration range employed in the DART-QTOF-MS and UPLC-ESI-QTOF-MS systems was from 10 to 1000 ng mL^{-1}. The internal standard (IS, TCS-$^{13}C_6$) was kept at 100 ng mL^{-1}. Peak areas for the quantification ions were divided by the signal for the IS and plotted versus the concentration. The levels of TCS in the processed samples were calculated considering the concentrations measured in the calibration plots obtained for solvent-based standards, the mass (volume) of sample employed in the corresponding sample preparation approach, and the volume of extracts (2 and 10 mL in the case of SPE and MSPD extracts, respectively). TCS-$^{13}C_6$ was added to samples at the equivalent level to that used in calibration standards: 100 ng mL^{-1} referred to the final extract.

Matrix effects were evaluated by preparing standards in ethyl acetate and sample extracts (wastewater or sludge) in the same solvent. No IS correction was carried out. The slopes of the calibration curves for matrix-matched standards were normalized (divided) with those corresponding to solvent-based standards. Values lower than 100% indicate signal suppression and values higher than 100% correspond to an increase of the DART ionization efficiency for sample extracts versus solvent-based standards.

The accuracy of the results obtained by DART-QTOF-MS was evaluated using UPLC-ESI-QTOF-MS as reference technique, applied to the determination of the TCS concentration in the extracts obtained for non-spiked fractions of different samples. In the case of SPE and MSPD sample preparation, extracts were exchanged to MeOH before analysis. The aim of such comparison was to assess whether the measurements at the DART source are affected by isobaric interferences (ions with similar *m/z* ratios, not separated by the TOF mass

USC UNIVERSIDADE DE SANTIAGO DE COMPOSTELA

analyzer) proceeding from the ionization of other analytes present in the sample.

Results and discussion

DART-MS spectra of TCS

Previous studies [33] have demonstrated that certain phenols are fragmented in the DART source, likely during desorption, rendering ions with lower *m/z* ratios than the parent compound, leading to high limits of detection. In the case of bisphenols, this drawback was overcome considering compounds acetylation. Thus, the efficiency of TCS ionization was investigated as free compound and after acetylation and silylation (as dimethyl, tert-butyl silyl derivative), operating the TOF-MS instrument in positive and negative acquisition modes. TCS derivatives were prepared as described elsewhere [15, 34].

In Table 1, the identities and the *m/z* ratios of the main ions observed in the spectra of TCS without a derivatization step, or after derivatization, are shown. It is worth noticing that the completeness of derivatization reactions was assessed with the EI-MS spectra of TCS as silylated (dimethyl, tert-butyl silyl derivative) or acetylated species; see Supplementary information, Fig. S1 and S2. As regards the underivatized compound, no signal was noticed when operating the MS system in the positive mode, while the typical isotopic pattern of a trichlorinated phenolate $[M\text{-}H]^-$ was noticed in the negative mode. The silylated derivative was found to be unstable during the volatilization-ionization process; thus, the only cluster of ions observed was those associated to the deprotonated compound in the negative acquisition mode. Finally, the acetylated form led to an adduct with ammonium, observed when operating the MS spectrometer in the positive mode. Thus, conversely to the silylated forms, acetyl derivatives remain stable in the DART source leading to adducts with NH_4^+ ions, as it has been previously reported for bisphenol species [33].

The comparison of responses obtained for $[M-H]^-$ ions, observed for free TCS, and those for the adduct of the acetylated derivative with ammonium $[M+C_2OH_2+NH_4]^+$, reflected a significantly higher response for free TCS. So, derivatization was no longer considered.

Table 1 Identities of base ions in the DART spectra of TCS as a function of derivatization technique and polarity

Derivatization	Ionization	Ion	*m/z*
None	−	$[M-H]^-$	286.9439
Acetylation	+	$[M+C_2OH_2+NH_4]^+$	347.9956
Silylation	−	$[M-H]^-$	286.9439

Instrumental parameters of the DART source

One of the variables affecting the efficiency of the volatilization and ionization process at DART is the temperature of the excited helium atom current that incises over the sample holder. At the same time, the holder (Quick Strip or Dip It, Figs. S3–S6), where the species is deposited, might also affect the signal intensity. To assess the effect of the latter parameter, responses obtained for the $[M-H]^-$ ion of solvent-based standards with concentrations comprised between 50 and 400 ng mL^{-1} were evaluated. In both groups of experiments, the volume of standard deposited in the metal grid (Quick Strip Cards, Figs. S3–S4) or on the glass capillaries tip (Dip-It system, Figs. S5–S6) was 2 μL. Once the solvent was completely evaporated, the modules were incorporated to the mobile rail.

Figure 1 shows the obtained results (peak areas) for solvent-based standards with different concentrations from 50 to 400 ng mL^{-1}. The highest slopes were obtained with the Dip-It system. Likely, the metal mesh used in the transmission grids reduces the effective energy over the sample. For a desorption temperature of 350 °C, the obtained responses with the glass capillaries were three times higher than those obtained with the metal grid holder. Another drawback observed with the metal grid is that the holder interrupts the helium atom flow that reaches the inlet orifice of the vapor

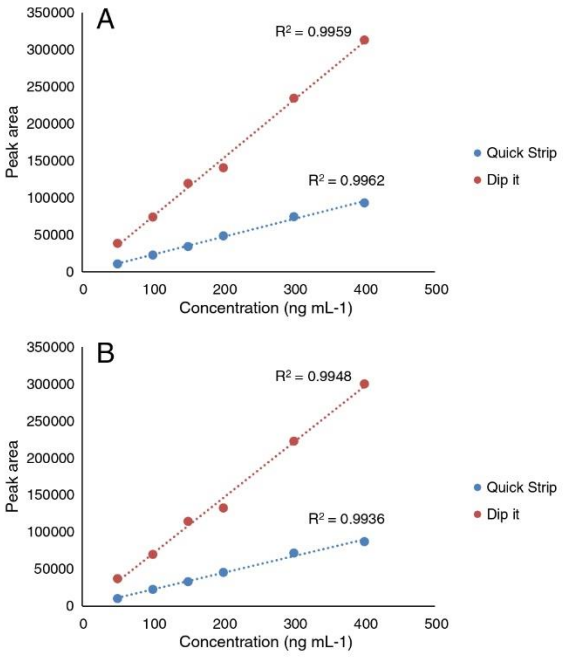


Fig. 1 Comparison of slopes obtained using different holders for standards ($n = 2$ replicates per calibration level) of TCS in ethyl acetate. Quantification ions *m/z* 286.9439 (**A**) and *m/z* 288.9410 (**B**). Mass extraction window 20 ppm

USC UNIVERSIDADE DE SANTIAGO DE COMPOSTELA

MIGUEL COBO GOLPE

chamber between sample spots; thus, there is not a continuous flow of background ions (some of them used to guarantee the stability of mass calibration) entering the MS spectrometer. Thus, the Dip-It system was selected for the study.

In order to choose the optimum working temperature, replicated samples were measured at different temperatures. In this case, a standard of 1 μg mL^{-1} of TCS was used and replicate determinations ($n = 3$), at temperatures between 150 and 400 °C, were performed. As it can be observed in Fig. 2, the response increases with the temperature till reaching a plateau at 300–350 °C. Thus, it was decided to operate at 350 °C for the rest of the study. Higher temperatures could lead to the thermal degradation of the compound.

Performance of DART-TOF-MS detection for TCS

The linearity of the system was investigated in the range of concentrations from 10 to 1000 ng mL^{-1}. Calibration curves were constructed for the ions with m/z 286.9439 and 288.9410, employing a mass extraction window of 20 ppm. As TCS is a trichlorinated species, the response ratio between both ions was close to the unit (experimental ratios were between 1.05 and 1.07, depending on the employed holder). This relationship must be constant during the real sample analysis. In both cases, the determination coefficients (R^2) were above 0.998 in the range of concentrations of two orders of magnitude. Figure 3 shows the plots of the DART-MS response vs time obtained for the quantification ions of TCS. The first observed signal (c.a. 1 min in the plot) corresponds to a calibration blank containing just the IS. The whole time required to obtain a calibration curve (9 calibration levels and 1 blank) was 6.6 min.

In Table 2, a comparison of slopes and R^2 values for calibrations in the same concentration range, and varying the solvent employed for the preparation of standards, is shown. As it can be noticed, the type of solvent affected the calibration curve slopes, ethyl acetate being the solvent which showed the highest sensitivity. Probably, changes in the obtained responses as a function of the solvent are related with TCS distribution on the surface of glass tips of the Dip-It module after solvent evaporation. Whatever the exact reason, ethyl acetate was maintained as calibration solvent, unless otherwise stated.

The instrumental limit of quantification (LOQ) of the DART-QTOF-MS was estimated from the signal to noise ratio obtained for the standard with the lowest concentration in the calibration. Thus, the minimum level of concentration that yields peaks with a signal to noise ratio of 10 was evaluated. The relationship between both quantification ions of TCS was kept at 1.0 ± 15%. In general, an instrumental LOQ of 5 ng mL^{-1} for a volume of 2 μL (Fig. S7) has been established.

The presence of organic and inorganic compounds in real samples (or in their extracts) can give rise to competence processes during TCS ionization. These processes could cause a significant attenuation of the TCS ionization in the DART source. Changes in the efficiency of TCS ionization could be expected to be more relevant than in LC-ESI-MS, since, in the absence of a chromatography separation step, all species present in the sample (in the case of environmental samples in the corresponding extract) are ionized simultaneously. This will produce a significant increase of the procedural LOQ, reducing the applicability of the methodology to real-sample analysis.

In this study, the comparison of slopes for SPE extracts of ultrapure water, river water, and treated and raw wastewater, after a 200-fold concentration factor by SPE (100-fold for raw wastewater), was carried out. Table 3 compiles the data corresponding to curve slopes, their determination coefficients (R^2), and the attenuation percentage in the signal for the real

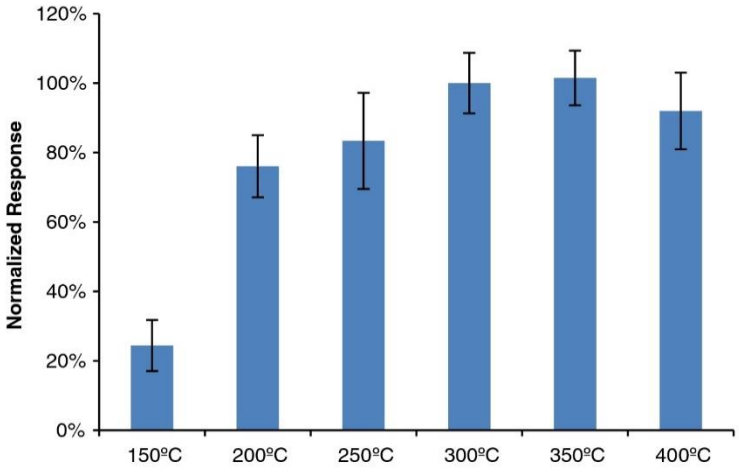


Fig. 2 Variations in the response of TCS as a function of DART temperature, $n = 3$ replicates

USC UNIVERSIDADE DE SANTIAGO DE COMPOSTELA

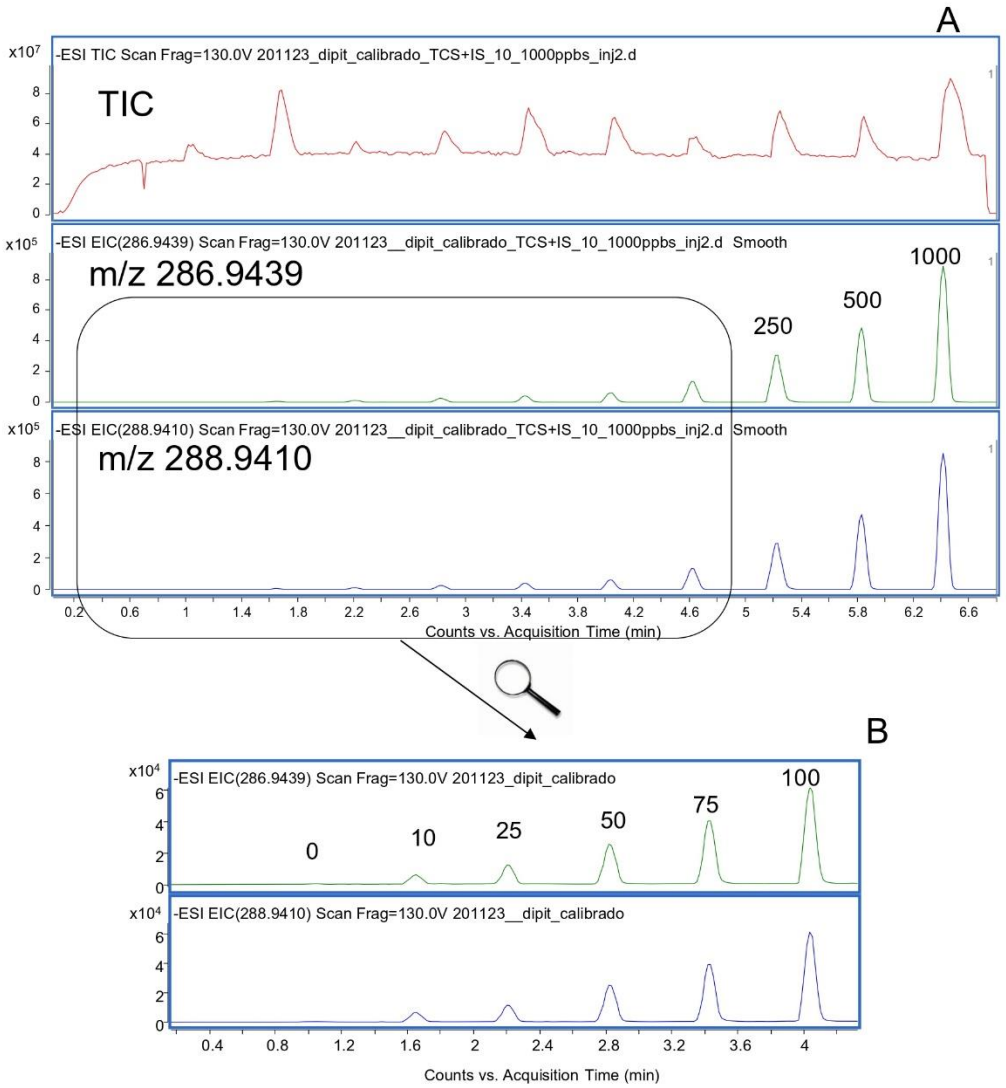


Fig. 3 **A** Plots of DART-QTOF-MS responses (negative mode) vs time obtained for a series of standards in ethyl acetate in the range of concentrations from 10 to 1000 ng mL^{-1}. Extraction ions, 286.9439 and 288.9410; mass window, 20 ppm. **B** Enlargement of the region 0.3–4.2 min

Table 2 Normalized slopes and determination coefficients (R^2) obtained with a calibration of TCS without internal standard and different solvents; quantification ion, 286.9439. (Range 10–1000 μg L^{-1}, 9 calibration levels)

Solvent	Normalized slopes	R^2
Ethyl acetate	1.000 ± 0.016	0.9983
MeOH	0.687 ± 0.015	0.9965
Chloroform	0.750 ± 0.027	0.9913
Ultrapure water	0.452 ± 0.010	0.9981

samples. The highest attenuation (around 56%) was observed for the influent sample. The plots of the DART-MS response vs time obtained for a spiked treated wastewater sample (50–400 ng mL^{-1} addition levels) are compiled in Fig. S8. Figure 4 shows a region of the spectra observed for the non-spiked and the spiked extracts (addition level 50 ng mL^{-1}) of a treated wastewater after 200-fold concentration by SPE. As observed, both spectra showed saturated bands with a baseline width of 0.2 Da at nominal m/z values of 287, 288, and 289 Da. Consequently, it becomes impossible to quantify any species rendering ions within those bands. The successful selective

USC UNIVERSIDADE DE SANTIAGO DE COMPOSTELA

Table 3 Slopes and determination coefficients (R^2) for matrix-matched calibration solutions prepared with SPE extracts from different water samples

Sample	Quantification ion	Slope	Intercept	R^2 (10–400 ng mL^{-1}, n=6 levels)	% Signal attenuation
Ultrapure water	286.9439	800.5	200	0.9869	–
	288.9399	761.9	190	0.9874	–
River water	286.9439	751.4	412	0.9974	6.1±0.2%
	288.9399	712.9	376	0.9927	6.4±0.3%
Raw wastewater	286.9439	354.4	2610	0.9789	56±3%
	288.9399	326.3	2273	0.9743	57±3%
Treated wastewater	286.9439	558.8	3110	0.9951	30±1%
	288.9399	533.4	2515	0.9961	30±1%

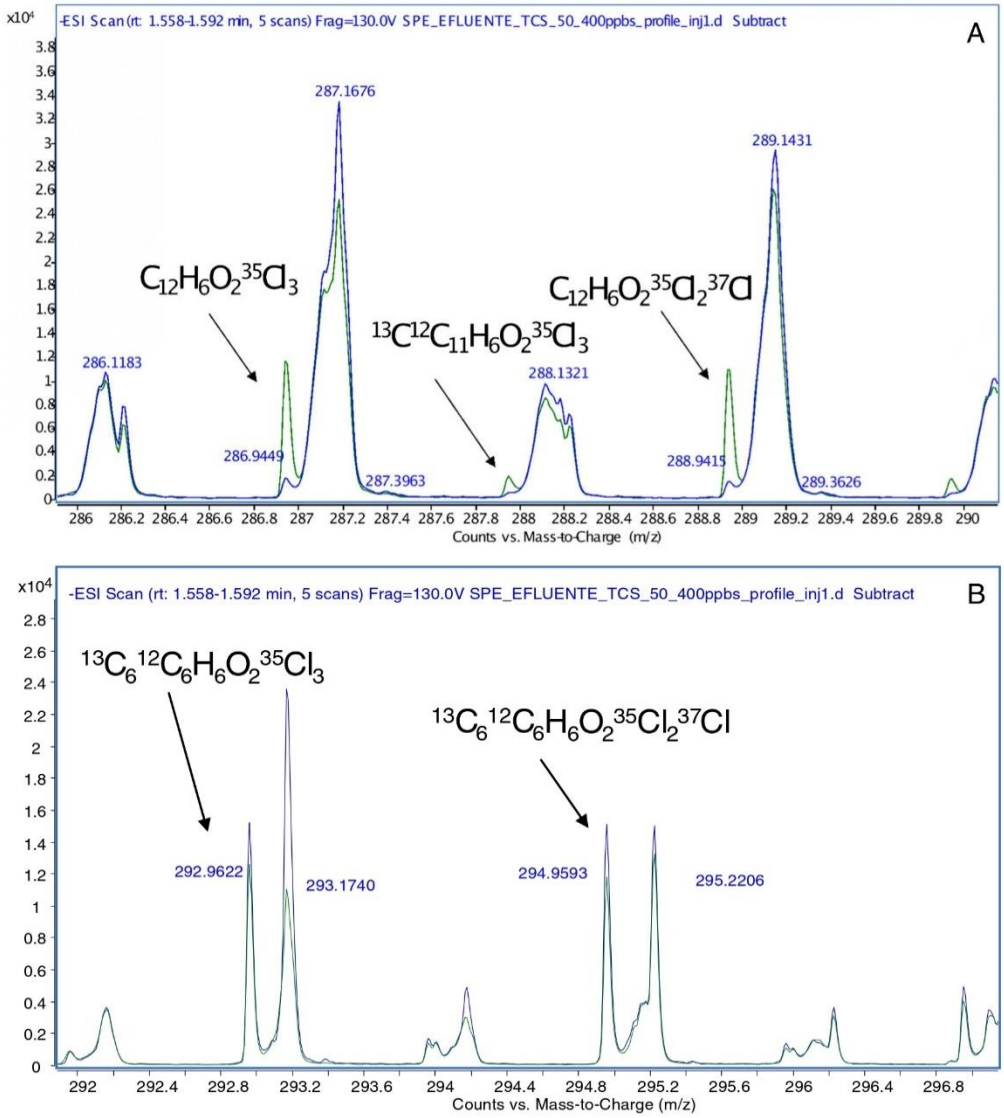


Fig. 4 Details of the mass spectra for TCS (**A**) and TCS-$^{13}C_6$ (**B**) in a spiked treated wastewater extract (50 ng mL^{-1}, green plot) versus a non-spiked extract from the same matrix (blue plot)

USC UNIVERSIDADE DE SANTIAGO DE COMPOSTELA

determination of TCS, and the isotopically labeled analogue TCS-$^{13}C_6$, is associated to the negative mass defect of this compound (ca. 56 and 59 mDa for $C_{12}H_6O_2{}^{35}Cl_3$ and $C_{12}H_6O_2{}^{35}Cl_2{}^{37}Cl$ ions, respectively); thus, the deprotonated molecular ions of this species show *m/z* ratios in a relatively clean spectral region. Thus, even the relatively poor resolution of masses provided by the first-generation TOF instrument combined with the DART source in this study permitted to discriminate TCS ions from co-extracted wastewater compounds.

In summary, considering the instrumental LOQs of DART-MS, the concentration factor provided by SPE (100- and 200-fold for raw and treated wastewater), and moderate attenuation in the efficiency of TCS ionization in the case of wastewater extracts, the estimated LOQs of the overall procedure are in the range of 100 to 35 ng L^{-1} for raw and treated wastewater, respectively. In the case of sludge, without considering signal attenuation effects, LOQ is estimated in the range of 100 ng g^{-1}. Such values might be low enough to permit the quantification of TCS in these environmental matrices.

Analysis of real samples

The accuracy of the DART-QTOF-MS system was investigated through the analysis of non-spiked samples, considering matrices with different complexity, and using UPLC-QTOF-MS as reference technique. In both cases, TCS-$^{13}C_6$ was used as surrogate standard added to samples before extraction (dilution in the case of mouthwashing formulations), and the concentration of TCS was estimated against solvent-based standards. In DART-MS, the only employed identification parameter was the ratio between responses for ions at *m/z* 286.9439 and 288.9410. When using UPLC-ESI-TOF-MS, retention time (window 0.1 min) was also considered for a positive identification. Pairs of wastewater samples (grab sampling) were obtained from the same STP at the end of 2020, while freeze-dried sludge samples correspond to four different STPs. Table 4 compiles the TCS concentration values and the standard deviation for the personal care product samples (mouthwash and toothpaste) and the environmental processed samples (raw and treated wastewater and sludge). In all the cases, data correspond to triplicate analysis of same extracts (samples). When required (personal care products) samples, or sample extracts, were diluted to accommodate the levels of TCS between 10 and 1000 ng mL^{-1}. In the case of personal care product samples, there is a good coincidence between the values (average concentrations with their standard deviations) obtained with both techniques. It is obvious that the complexity of DART-MS spectra for this kind of samples is significantly lower than that shown in Fig. 4 for SPE extracts of wastewater, which turns in a better precision (Fig. S9). On the other hand, for the wastewater and sludge samples, the concordance between average values is also acceptable.

Table 4 Concentration of TCS in personal care products and environmental samples obtained through analysis of obtained extracts by DART-TOF-MS and UPLC-ESI-TOF-MS, $n = 3$ replicates

Sample	TCS concentration (%, ng L^{-1} or ng g^{-1})	
	DART-QTOF-MS	UPLC-QTOF-MS
Mouthwash	0.20 ± 0.02%	0.21 ± 0.01%
Toothpaste	0.28 ± 0.07%	0.28 ± 0.01%
Effluent 1(26/11/20)	67 ± 13 ng/L	67 ± 3 ng/L
Effluent 2 (04/12/20)	75 ± 10 ng/L	66 ± 2 ng/L
Effluent 3 (09/12/20)	47 ± 10 ng/L	57 ± 1 ng/L
Influent 1 (26/11/20)	237 ± 20 ng/L	196 ± 19 ng/L
Influent 2 (04/12/20)	115 ± 10 ng/L	94 ± 2 ng/L
Influent 3 (09/12/20)	120 ± 10 ng/L	103 ± 5 ng/L
Sludge 1	136 ± 5 ng/g	162 ± 4 ng/g
Sludge 2	1004 ± 50 ng/g	981 ± 49 ng/g
Sludge 3	753 ± 98 ng/g	733 ± 44 ng/g
Sludge 4	324 ± 52 ng/g	426 ± 4 ng/g

Regarding repeatability, DART-TOF-MS renders worse results (higher dispersion). However, a suitable estimation of the TCS levels in those samples has been provided.

Data provided in Table 4 confirm that TCS is still present in the urban STPs despite the imposed restrictions to its use during the last years. On the other hand, the possibility of using a DART-QTOF-MS system to measure TCS at the concentration level existing in real samples without the spectral signals for TCS being affected is highlighted.

Conclusions

DART-MS allows the sensitive determination of TCS from its deprotonated ions, without the need of any derivatization reaction. The achieved instrumental LOQs are mainly affected by the temperature of the DART source and by the device employed to hold TCS solutions between the tip of the DART and the entrance of the Vapur interface connected to the MS spectrometer. For the particular application considered in the current research, the use of glass capillaries was advantageous to metallic frames. The level of spectral interferences observed when analyzing complex extracts from environmental samples was relatively low. The typical mass defect for chlorine isotopes is responsible for the selective determination of TCS. The signal suppression for complex environmental extracts was in the range of that obtained frequently by LC-ESI-MS. Therefore, in combination with the use of isotopically labeled analogue, DART-TOF-MS provides acceptable results in terms of precision and accuracy to determine TCS levels not only in personal care products but also in environmental samples.

USC UNIVERSIDADE DE SANTIAGO DE COMPOSTELA

Supplementary Information The online version contains supplementary material available at https://doi.org/10.1007/s00216-021-03591-2.

Acknowledgements This study was supported by the Spanish Government and Xunta de Galicia through grants PGC2018-094613-B-I00 and ED431C 2021/06, co-funded by the EU. M. Cobo-Golpe thanks the Spanish Ministry of Science, Innovation and Universities for a FPI fellowship.

Funding Open Access funding provided thanks to the CRUE-CSIC agreement with Springer Nature.

Declarations

Conflict of interest The authors declare no competing interests

Open Access This article is licensed under a Creative Commons Attribution 4.0 International License, which permits use, sharing, adaptation, distribution and reproduction in any medium or format, as long as you give appropriate credit to the original author(s) and the source, provide a link to the Creative Commons licence, and indicate if changes were made. The images or other third party material in this article are included in the article's Creative Commons licence, unless indicated otherwise in a credit line to the material. If material is not included in the article's Creative Commons licence and your intended use is not permitted by statutory regulation or exceeds the permitted use, you will need to obtain permission directly from the copyright holder. To view a copy of this licence, visit http://creativecommons.org/licenses/by/4.0/.

References

1. Gross JH. Direct analysis in real time- a critical review on DART-MS. Anal Bioanal Chem. 2014;406(1):63–80. https://doi.org/10.1007/s00216-013-7316-0.
2. Sisco E, Staymates ME, Forbes TP. Optimization of confined direct analysis in real time mass spectrometry (DART-MS). Analyst. 2020;145(7):2743–50. https://doi.org/10.1039/D0AN00031K.
3. Antal B, Kuki A, Nagy L, Nagy T, Zsuga M, Kéki S. Rapid detection of hazardous chemicals in textiles by direct analysis in real-time mass spectrometry (DART-MS). Anal Bioanal Chem. 2016;408:5189–98. https://doi.org/10.1007/s00216-016-9603-z.
4. Marić M, Marano J, Cody RB, Bridge C. DART-MS: a new analytical technique for forensic paint analysis. Anal Chem. 2018;90(11):6877–84. https://doi.org/10.1021/acs.analchem.8b01067.
5. Lei YT, Lu Y, Zhang TC, Qi Y, Lu YF. Rapid screening of testosterone in the aquatic environment using direct analysis in real-time (DART) mass spectrometry. Environ Earth Sci. 2016;75:1005. https://doi.org/10.1007/s12665-016-5830-z.
6. Wang X, Liu J, Liu CC, Zhang J, Shao B, Liu L. Rapid quantification of highly polar trimethyl phosphate in wastewater via direct analysis in real-time mass spectrometry. J Chromatogr A. 2014;1333:134–7. https://doi.org/10.1016/j.chroma.2014.01.076.
7. Dhillon GS, Kaur S, Pulicharla R, Brar SK, Cledón M, Verma M, Surampalli RY. Triclosan: current status, occurrence, environmental risks and bioaccumulation potential. Int J Environ Res Public Health. 2015;12(5):5657–84. https://doi.org/10.3390/ijerph120505657.
8. Jones RD, Jampani HB, Newman JL, Lee AS. Triclosan: a review of effectiveness and safety in health care settings. Am J Infect Control. 2000;28(2):184–96. https://doi.org/10.1067/mic.2000.102378.
9. Orhan M, Kut D, Gunesoglu C. Improving the antibacterial activity of cotton fabrics finished with triclosan by the use of 1,2,3,4-butanetetracarboxylic acid and citric acid. J Appl Polym Sci. 2009;111:1344–52. https://doi.org/10.1002/app.25083.
10. Bester K. Fate of triclosan and triclosan-methyl in sewage treatment plants and surface waters. Arch Environ Contam Toxicol. 2005;49(1):9–17. https://doi.org/10.1007/s00244-004-0155-4.
11. Coogan AM, Edziyie RE, La Point TW, Venables BJ. Algal bioaccumulation of triclocarban, triclosan, and methyl-triclosan in a North Texas wastewater treatment plant receiving stream. Chemosphere. 2007;67(10):1911–8. https://doi.org/10.1016/j.chemosphere.2006.12.027.
12. Buth MJ, Ross MR, McNeill K, Arnold WA. Removal and formation of chlorinated triclosan derivatives in wastewater treatment plants using chlorine and UV disinfection. Chemosphere. 2011;84(9):1238–43. https://doi.org/10.1016/j.chemosphere.2011.05.017.
13. Rule KL, Ebbett VR, Vikesland PJ. Formation of chloroform and chlorinated organics by free-chlorine-mediated oxidation of triclosan. Environ Sci Technol. 2005;39(9):3176–85. https://doi.org/10.1021/es048943+.
14. Langdon AK, Warne MSJ, Smernik RJ, Shareef A, Kookana RS. Selected personal care products and endocrine disruptors in biosolids: an Australia-wide survey. Sci Total Environ. 2011;409(6):1075–81. https://doi.org/10.1016/j.scitotenv.2010.12.013.
15. Canosa P, Rodríguez I, Rubí E, Cela R. Determination of parabens and triclosan in indoor dust using matrix solid-phase dispersion and gas chromatography with tandem mass spectrometry. Anal Chem. 2007;79(4):1675–81. https://doi.org/10.1021/ac061896e.
16. Reiss R, Mackay N, Habig C, Griffin J. An ecological risk assessment for triclosan in lotic systems following discharge from wastewater treatment plants in the United States. Environ Toxicol Chem. 2002;21(11):2483–92. https://doi.org/10.1002/etc.5620211130.
17. Schultz MM, Bartell SE, Schoenfuss HL. Effects of triclosan and triclocarban, two ubiquitous environmental contaminants, on anatomy, physiology, and behavior of the fathead minnow (Pimephales promelas). Arch Environ Contam Toxicol. 2012;63(1):114–24. https://doi.org/10.1007/s00244-011-9748-x.
18. Prosser RS, Lissemore L, Topp E, Sibley PK. Bioaccumulation of triclosan and triclocarban in plants grown in soils amended with municipal dewatered biosolids. Environ Toxicol Chem. 2014;33(5):975–84. https://doi.org/10.1002/etc.2505.
19. Higgins CP, Paesani ZJ, Chalew TE, Halden RU, Hundal LS. Persistence of triclocarban and triclosan in soils after land application of biosolids and bioaccumulation in Eisenia foetida. Environ Toxicol Chem. 2011;30(3):556–63. https://doi.org/10.1002/etc.416.
20. Coogan AM, La Point TW. Snail bioaccumulation of triclocarban, triclosan, and methyltriclosan in a North Texas, USA, stream affected by wastewater treatment plant runoff. Environ Toxicol Chem. 2008;27(8):1788–93. https://doi.org/10.1897/07-374.1.
21. Saleh S, Haddadin RNS, Baillie S, Collier PJ. Triclosan-an update. Lett Appl Microbiol. 2011;52(2):87–95. https://doi.org/10.1111/j.1472-765X.2010.02976.x.
22. Fraise AP. Susceptibility of antibiotic-resistant cocci to biocides. J Appl Microbiol. 2002;113(2):392–400. https://doi.org/10.1046/j.1365-2672.92.5s1.s.x.
23. Vanderford BJ, Snyder SA. Analysis of pharmaceuticals in water by isotope dilution liquid chromatography/tandem mass spectrometry. Environ Sci Technol. 2006;40(23):7312–20. https://doi.org/10.1021/es0613198.
24. Rodil R, Quintana JB, López-Mahía P, Muniategui-Lorenzo S, Prada-Rodríguez D. Multi-residue analytical method for the determination of emerging pollutants in water by solid-phase extraction

USC UNIVERSIDADE DE SANTIAGO DE COMPOSTELA

and liquid chromatography-tandem mass spectrometry. J Chromatogr A. 2009;1216(14):2958–69. https://doi.org/10.1016/j.chroma.2008.09.041.
25. Canosa P, Rodríguez I, Rubí E, Cela R. Optimization of solid-phase microextraction conditions for the determination of triclosan and posible related compounds in water samples. J Chromatogr A. 2005;1072(1):107–15. https://doi.org/10.1016/j.chroma.2004.11.032.
26. Guo JH, Li XH, Cao XL, Li Y, Wan XZ, Xu XB. Determination of triclosan, triclocarban and methyl-triclosan in aqueous samples by dispersive liquid-liquid microextraction combined with rapid liquid chromatography. J Chromatogr A. 2009;1216(15):3038–43. https://doi.org/10.1016/j.chroma.2009.02.021.
27. Zhao RS, Yuan JP, Li HF, Wang X, Jiang T, Lin JM. Nonequilibrium hollow-fiber liquid-phase microextraction with in situ derivatization for the measurement of triclosan in aqueous samples by gas chromatography-mass spectrometry. Anal Bioanal Chem. 2007;387(8):2911–5. https://doi.org/10.1007/s00216-007-1151-0.
28. Canosa P, Pérez-Palacios D, Garrido-López A, Tena MT, Rodríguez I, Rubí E, Cela R. Pressurized liquid extraction with in-cell clean-up followed by gas chromatography-tandem mass spectrometry for the selective determination of parabens and triclosan in indoor dust. J Chromatogr A. 2007;1161(1–2):105–12. https://doi.org/10.1016/j.chroma.2007.05.089.
29. Cerqueira MBR, Soares KL, Caldas SS, Primel EG. Sample as solid support in MSPD: a new possibility for determination of pharmaceuticals personal care and degradation products in sewage sludge. Chemosphere. 2018;211:875–83. https://doi.org/10.1016/j.chemosphere.2018.07.165.
30. Canosa P, Morales S, Rodríguez I, Rubí E, Cela R, Gómez M. Aquatic degradation of triclosan and formation of toxic chlorophenols in presence of low concentrations of free chlorine. Anal Bioanal Chem. 2005;383(7–8):1119–26. https://doi.org/10.1007/s00216-005-0116-4.
31. Celano R, Rodríguez I, Cela R, Rastrelli L, Piccinelli AL. Liquid chromatography quadrupole time-of-flight mass spectrometry quantification and screening of organophosphate compounds in sludge. Talanta. 2014;118:312–20. https://doi.org/10.1016/j.talanta.2013.10.024.
32. Cobo-Golpe M, Ramil M, Cela R, Rodríguez I. Portable dehumidifiers condensed water: a novel matrix for the screening of semi-volatile compounds in indoor air. Chemosphere. 2020;251:126346. https://doi.org/10.1016/j.chemosphere.2020.126346.
33. Castro G, Rodríguez I, Ramil M, Cela R. Direct analysis in real time accurate mass spectrometry determination of bisphenol A in thermal printing paper. Talanta. 2019;205:120086. https://doi.org/10.1016/j.talanta.2019.06.086.
34. Regueiro J, Llompart M, Psillakis E, García-Monteagudo JC, García-Jares C. Ultrasound-assisted emulsification-microextraction of phenolic preservatives in water. Talanta. 2009;79(5):1387–97. https://doi.org/10.1016/j.talanta.2009.06.015.

Publisher's note Springer Nature remains neutral with regard to jurisdictional claims in published maps and institutional affiliations.

USC UNIVERSIDADE DE SANTIAGO DE COMPOSTELA

Supplementary information to manuscript:

Assessment of Direct Analysis in Real Time accurate Mass Spectrometry for the Determination of Triclosan in Complex Matrices

Cobo Golpe, M.; García-Martín, J.; Ramil, M.*; Cela, R.; Rodríguez, I.
Department of Analytical Chemistry, Nutrition and Food Sciences, IAQBUS - Institute of Research on Chemical and Biological Analysis, Universidade de Santiago de Compostela, R/Constantino Candeira SN, 15782 Santiago de Compostela, Spain
e-mail:maria.ramil@usc.es

TABLES:

Table S1. Recoveries of SPE and MSPD for raw wastewater (addition level 500 ng/L) and freeze-dried sludge (addition level 500 ng/g), n=3 replicates.

Sample	Mean recovery (%)	SD
Raw wastewater	98	2
Freeze-dried sludge	88	13

USC UNIVERSIDADE DE SANTIAGO DE COMPOSTELA

FIGURES:

Figure S1. EI-MS spectrum of acetylated TCS, *m/z* range 40-380.

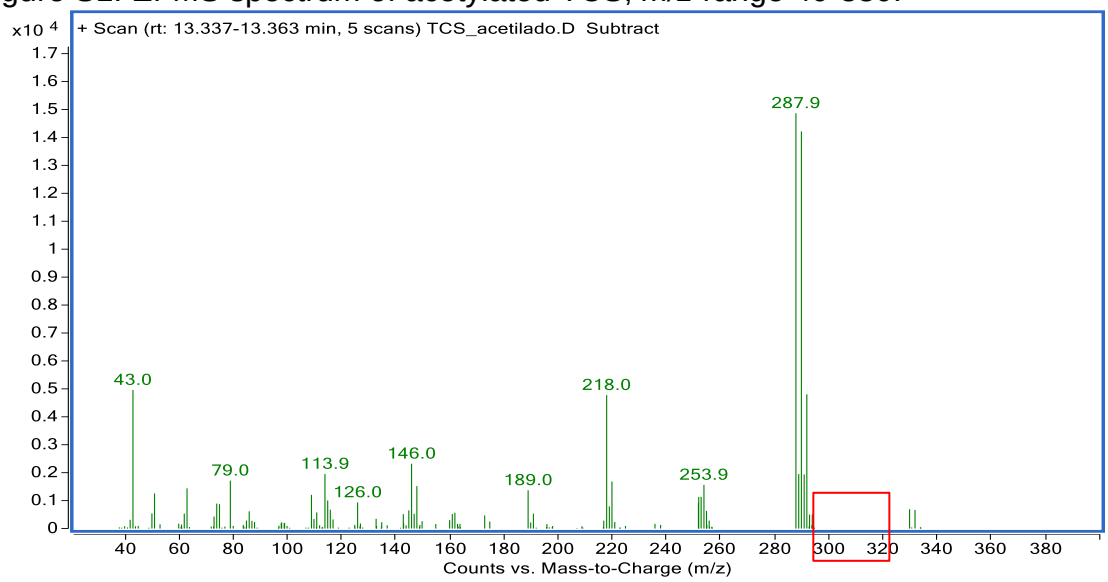


Figure S2. EI-MS spectrum of TCS as dimethyl tert.-butyl silyl derivative, *m/z* range 40- 440.

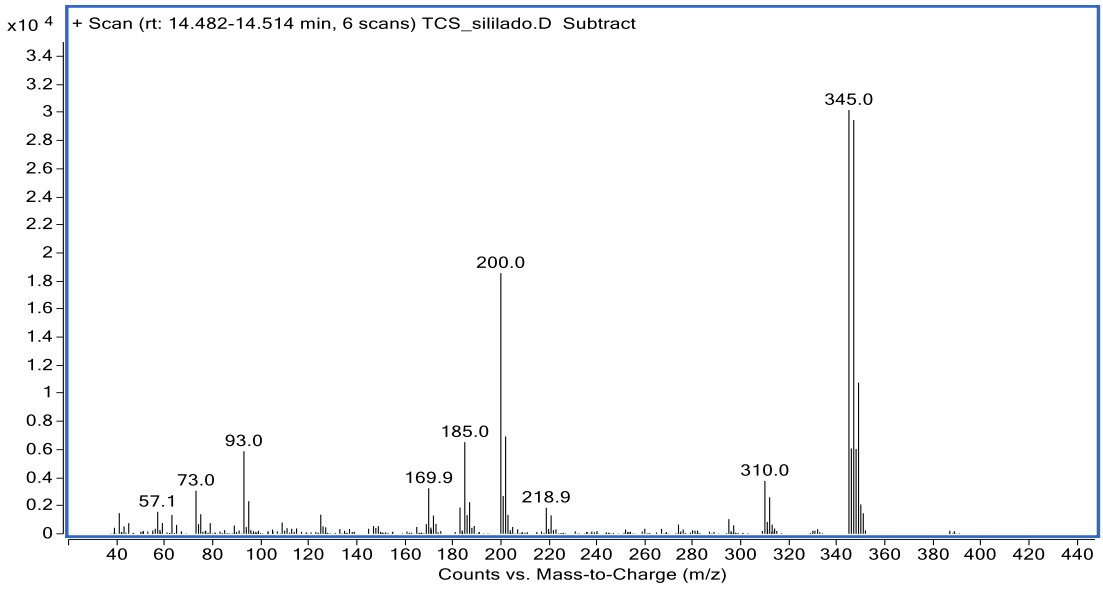


Figure S3. Metal grid (Quick Strip Card) picture



Figure S4.Quick Strip mobile rail and holder.

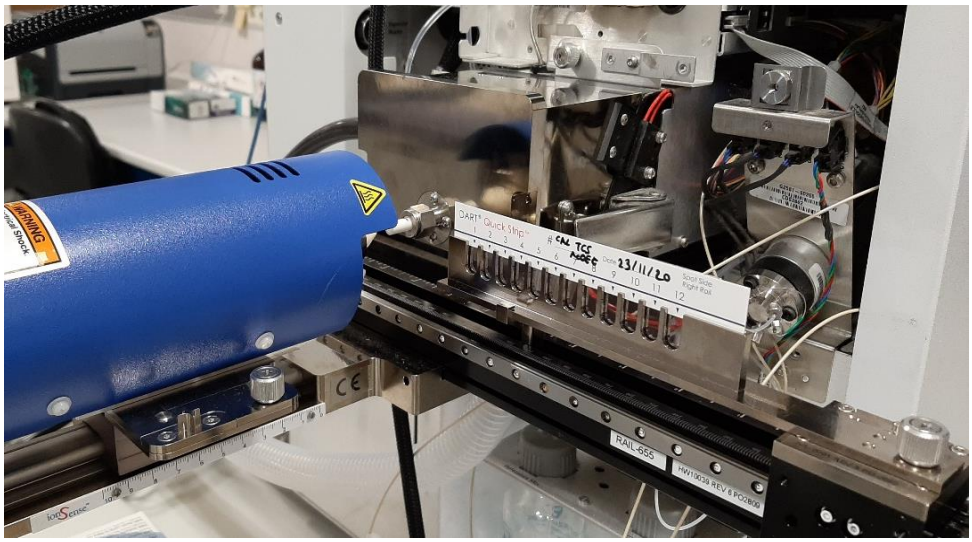


Figure S5: Glass capillaries configuration (Dip-It)

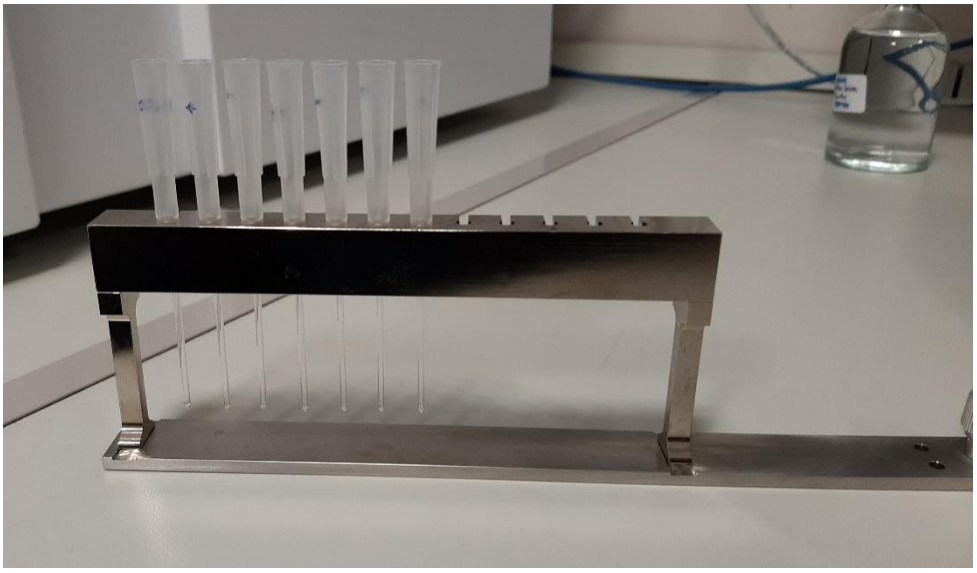
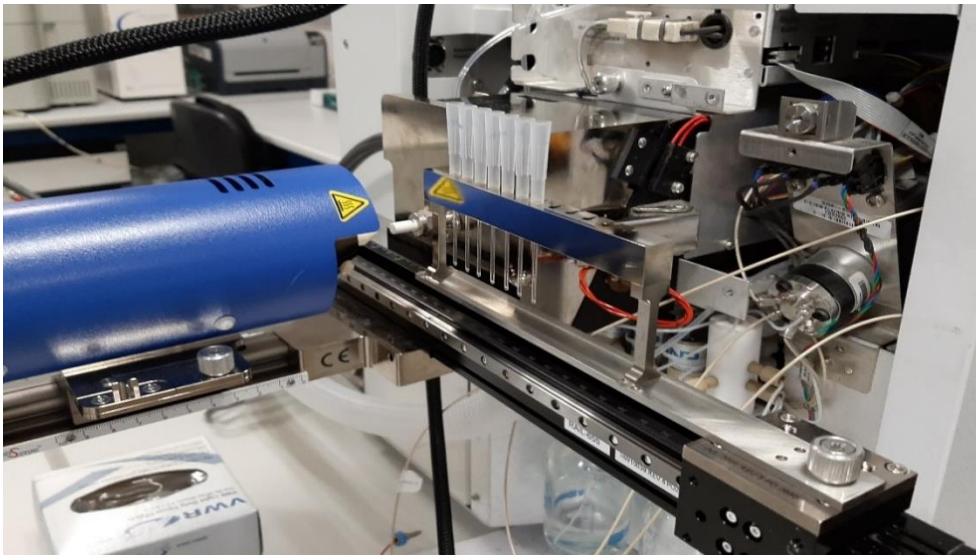


Figure S6: Dip-It mobile rail and holder.



USC UNIVERSIDADE DE SANTIAGO DE COMPOSTELA

Figure S7: Plot of DAR-TOF-MS responses versus time for TCS standards in ethyl acetate. Blank and 3 replicates of a 5 ng mL^{-1} standard. Quantification ions: m/z 286.9439 (A) and 288.9410 (B).

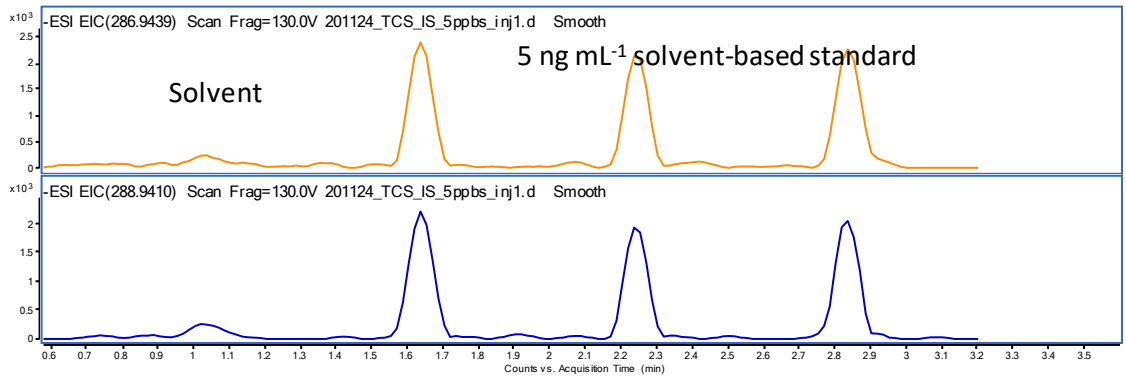


Figure S8: TIC and EIC (286.9439 and 288.9410) responses versus acquisition time forTCS in spiked extracts from treated wastewater (50-400 ng mL^{-1})

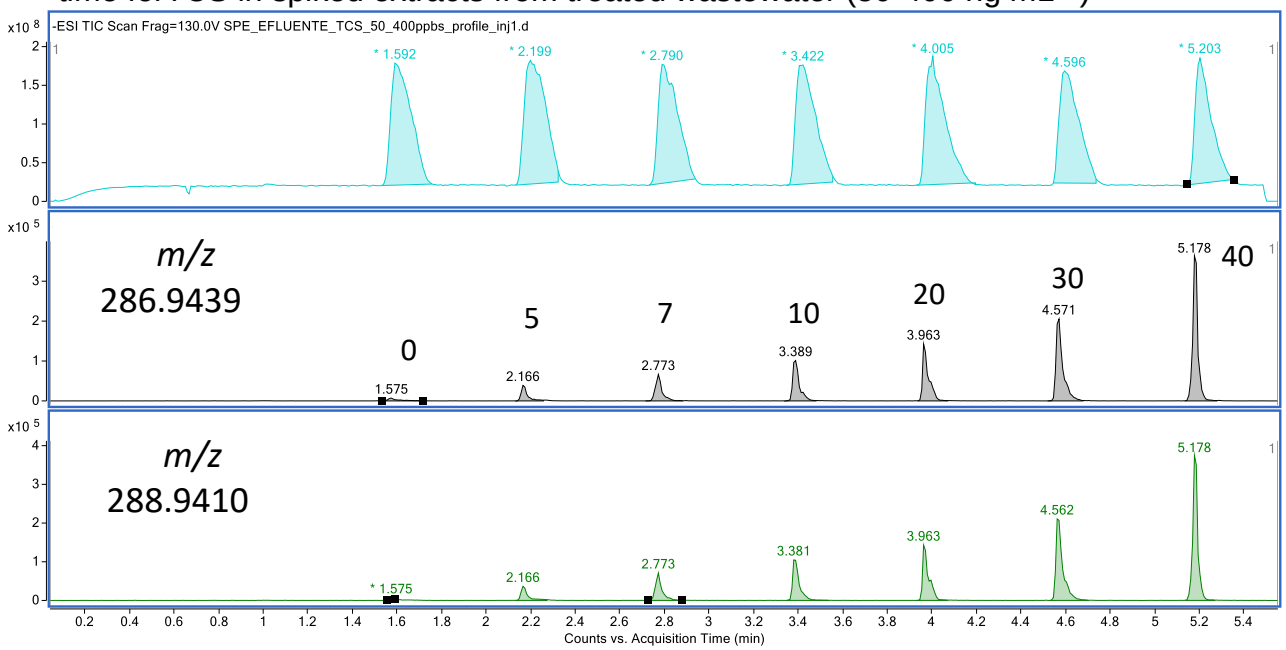
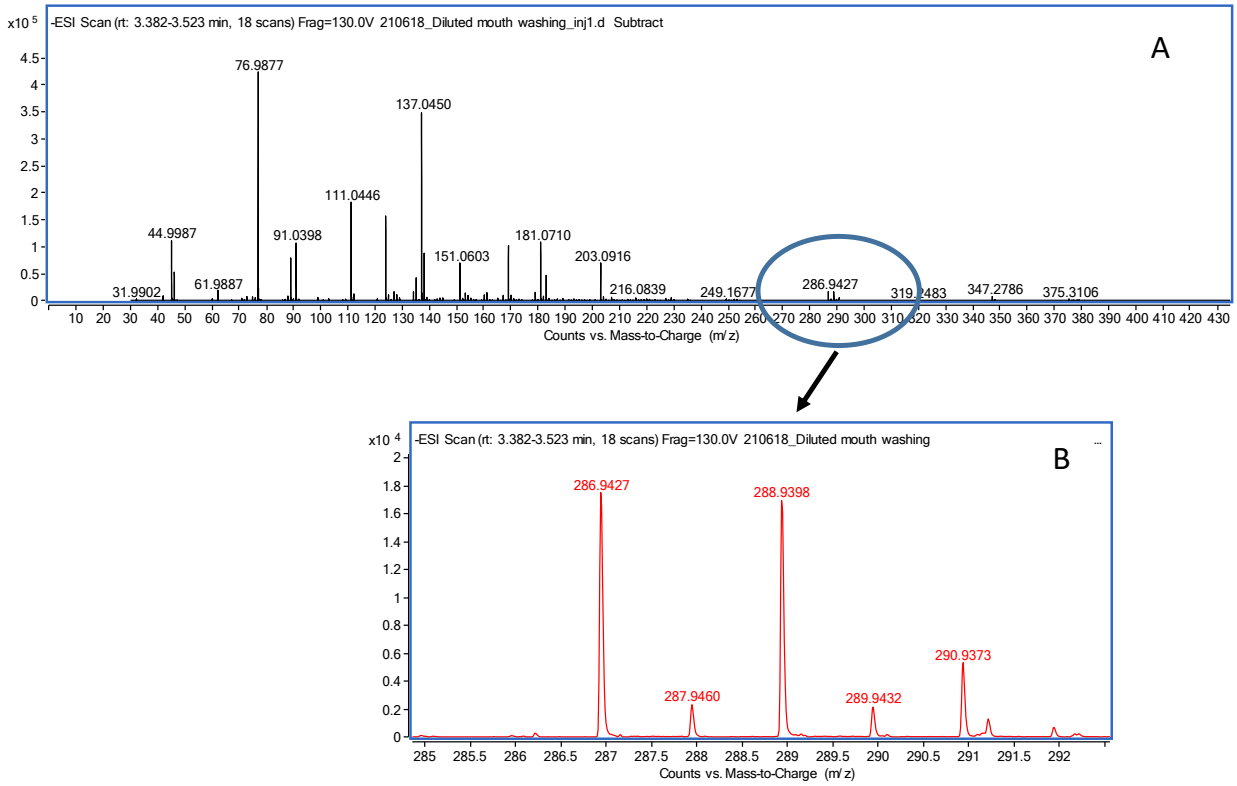


Fig. S9. A, profile spectrum obtained for a personal care sample (diluted mouth washing solution) by DART-TOF-MS. B, detail of the region corresponding to the $[M-H]^-$ ions of TCS.



PUBLICATION VII: SUPERCRITICAL FLUID CHROMATOGRAPHY TIME-OF-FLIGHT MASS SPECTROMETRY ENANTIOMERIC DETERMINATION OF BASIC DRUGS IN SEWAGE SAMPLES

M. Cobo-Golpe, M. Ramil, R. Cela, I. Rodríguez
Journal of Chromatography A 1673 (2022) 463088
DOI: 10.1016/j.chroma.2022.463088



Impact factor: 4.1
Category: Analytical chemistry
Position: 25/86
Quartile: Q2

USC UNIVERSIDADE DE SANTIAGO DE COMPOSTELA

Journal of Chromatography A 1673 (2022) 463088

Contents lists available at ScienceDirect

Journal of Chromatography A

journal homepage: www.elsevier.com/locate/chroma

Supercritical fluid chromatography time-of-flight mass spectrometry enantiomeric determination of basic drugs in sewage samples

M. Cobo-Golpe, M. Ramil, R. Cela, I. Rodríguez*

Department of Analytical Chemistry, Nutrition and Food Sciences, Research Institute on Chemical and Biological Analysis (IAQBUS), Universidade de Santiago de Compostela, Santiago de Compostela 15782, Spain

ARTICLE INFO

Article history:
Received 18 March 2022
Revised 21 April 2022
Accepted 23 April 2022
Available online 25 April 2022

Keywords:
Supercritical fluid chromatography
Chiral separations
Mass spectrometry
Basic pharmaceuticals
Wastewater
Sludge

ABSTRACT

Many pharmacologically active compounds are chiral species, and their therapeutic or toxicological effects might differ between isomers. Herein, we develop a fast and sensitive chiral analysis methodology for the determination of eight pharmaceuticals, considered as emerging environmental pollutants and belonging to two different chemical classes, in wastewater and sludge samples. Compounds were separated using supercritical fluid chromatography (SFC) combined with time-of-flight mass spectrometry (TOF-MS) detection. The stationary phase, the modifier and the additive combined with supercritical carbon dioxide (CO_2), in the SFC mobile phase, played a major effect in the enantiomeric resolution of selected compounds. Moreover, the composition of the mobile phase affected their ionization efficiency in the electrospray ionization source. Methanol (MeOH), containing a 0.1% of ammonia, was used as CO_2 modifier for the separation of compounds in a polysaccharide-type column. Total analysis time was 15.5 min, achieving resolution factors between 1.03 and 2.49 for the eight pairs of enantiomers. In combination with mixed-mode solid-phase extraction and matrix solid-phase dispersion protocols, compounds were determined in wastewater and sludge samples, with limits of quantification in the range of 0.010–0.020 μg L^{-1} and 3.7–11.1 ng g^{-1}, for aqueous and solid samples, respectively. The amine-type drugs (tramadol, propranolol and venlafaxine) were mostly found in wastewater samples, whilst azolic antimycotics were mainly quantified in sludge. The first group of compounds showed enantiomeric fractions significantly different to those existing in the commercial counterpart pharmaceuticals.

© 2022 The Author(s). Published by Elsevier B.V.
This is an open access article under the CC BY-NC-ND license
(http://creativecommons.org/licenses/by-nc-nd/4.0/)

1. Introduction

Many bioactive compounds designed by pharmaceutical and agrochemical industries are chiral molecules. Usually, the therapeutic and/or the toxicological effects of these species, on target and non-target organisms, differ significantly between isomers [1]. Even in case of compounds marketed as racemates, sometimes, their metabolization rates and their environmental biodegradability are enantioselective processes [2]. As a result, the enantiomeric fraction (EF) of these species in sewage samples might be different to that existing in the commercial formulations [3,4].

The development of chiral analysis methodologies is an emerging topic to characterize the enantiomeric purity of bioactive compounds, to understand the interaction of chiral compounds with biotic systems (vegetables, bacteria and animals) [2], and to discriminate the sources of some pollutants found in the aquatic media, as it has been reported for amphetamine-like drugs [5]. In the field of environmental analysis, chiral separations methods need to be combined with sensitive determination techniques allowing the quantification of these compounds in the ppb or sub-ppb range. Thus, the hyphenation of chiral separation techniques with mass spectrometry (MS) detection is the preferred approach to cope with complex extracts obtained from this kind of samples [1,2,6,7].

Chiral separations developed under supercritical fluid chromatography (SFC) conditions, are presented as a green alternative to liquid chromatographic (LC) methods [2], particularly to those using normal phase conditions. As separation technique, SFC employs higher flowrates than LC, it requires shorter column equilibration times, and the drop of pressure between both edges of the chromatographic column is lower than for the latter technique [8,9]. On the other hand, the yield of ionization processes, at the electrospray source, is less favorable for CO_2 rich mobile phases than for aqueous solutions of methanol (MeOH), or acetonitrile (ACN), employed in LC [6]. Consequently, hyphenation of SFC and MS requires the use of a make-up solution, whose composition

* Corresponding author.
E-mail address: isaac.rodriguez@usc.es (I. Rodríguez).

https://doi.org/10.1016/j.chroma.2022.463088
0021-9673/© 2022 The Author(s). Published by Elsevier B.V. This is an open access article under the CC BY-NC-ND license
(http://creativecommons.org/licenses/by-nc-nd/4.0/)

and flowrate affect the formation of ions in the ESI source and thus, the limits of quantification (LOQs) of SFC-ESI-MS methods. The make-up solution also prevents compound precipitation after CO_2 decompression [6,7]. In case of SFC-MS interfaces which divide the flow of mobile phase between the ESI source and a back-pressure regulator (BPR), i.e. the pre-BPR splitter design [6], sensitivity might be a challenge in environmental applications. Another challenge in chiral analysis is the development of multianalyte procedures, with separation times in the range of values employed when dealing with non-chiral separations. Despite the fact that the number of applications of chiral LC or SFC separations, combined with MS detection, is increasing steadily, only a reduced number of works consider more than one compound at a time, and just in a few cases, chiral separation methods involve the simultaneous determination of compounds from different families or chemical groups [9–12]. In most cases, a drawback of multianalyte chiral LC methods is the use of long isocratic separations, with run times in the range of 40–60 min [2,3,10,13].

In terms of occurrence, persistence and toxicity, azolic drugs are a relevant family of emerging environmental pollutants [14,15]. Many azolic drugs are chiral species, marketed as racemates and employed mainly as topic antimycotic prescription pharmaceuticals. Moreover, in some cases, they are included in the formulation of certain personal care products (i.e. climbazole, CBZ). In both uses, they are directly discharged into the network of urban sewers during showering. Upon arrival to sewage treatment plants (STPs), they distribute between wastewater and sludge depending on their polarities. The amino group is present in several groups of highly prescribed, chiral pharmaceuticals, such as beta-blockers, psychiatric drugs and pain relief medicaments, administrated as oral pills. Many drugs within the above prescription groups are recognized as ubiquitous in the aquatic environment, as it is the case of venlafaxine (VFX), tramadol (TRA) and some beta-blockers, i.e. propranolol (PRO). Although chiral separation methodologies have been proposed for some of the above compounds [13,16], either their performance was not investigated in combination with MS detection [17], or the chiral analysis of imidazolic and amine drugs, with very different water solubilities and pKa values, in the same chromatographic injection has not been reported, yet.

In this research, we assess the performance of SFC-ESI-MS for the chiral determination of five azolic antimycotics and three basic pharmaceuticals in wastewater and sludge samples obtained from urban STPs. The selection of compounds was made attending to their occurrence in water and sludge, combined with their reported environmental toxicity and risk assessment results [14,18–20]. Moreover, it was attempted to cover the analysis of chiral compounds with different polarities, water solubilities, and presence of basic functionalities with different strength (the weak basicity imidazole ring and the strongly basic amine moiety) in their structures. The aims of the study were to investigate the capability of the SFC-ESI-MS system to separate the enantiomers of selected compounds in the same chromatographic analysis, to achieve enough sensitivity to measure their enantiomeric fractions (EFs) in environmental matrices, and to identify possible variations in their EFs compared to those existing in commercial formulations.

2. Material and methods

2.1. Solvents, standards and sorbents

Methanol (MeOH), HPLC-grade purity, and formic acid (FA, 98%) were acquired from Merck (Darmstadt, Germany). Ammonia, 7 M solution in methanol, and diethyl amine (DEA) were purchased from Acros Organics (Geel, Belgium). Ultrapure deionized water (18.2 MΩ cm^{-1}) was obtained from a Geni U system (Rephile, Shanghai, China).

Racemic mixtures of miconazole (MCZ), CBZ, cis- TRA, their isotopically labeled analogues (miconazole-d_5, MCZ-d_5; climbazole-d_4, CBZ-d_4; and Tramadol-^{13}C-d_3, TRA-^{13}C-d_3), sertaconazole (STZ), tioconazole (TCZ), fenticonazole (FTZ), PRO, and VFX were acquired from Sigma-Aldrich (Milwaukee, WI, USA) and Toronto Research Chemicals (Ontario, Canada). The S-form of PRO (PRO-S) was purchased from Sigma-Aldrich. Chemical structures, log D values at neutral pH, and acidity constants of selected compounds are provided as supplementary information, Fig. S1. Individual standards of each compound were prepared in MeOH. Further mixtures were made in the same solvent. Enantiomers of target compounds were identified with codes 1 and 2, attending to their elution order under final working SFC conditions. Their identities were not confirmed, with the exception of those of PRO.

Polypropylene syringes (12 mL volume), and polyethylene frits (20 µm pore size, 15 mm diameter) for matrix solid-phase extraction (MSPD) were supplied by International Sorbent Technology (Mid Glamorgan, UK). The dispersant sorbent (C_{18}-bonded silica) was obtained from Agilent Technologies (Santa Clara, CA, USA). Primary and secondary amine (PSA), used as clean-up co-sorbent in the MSPD of sludge samples, was purchased from Sigma-Aldrich. Oasis mixed-mode (reversed-phase and cationic exchanger) cartridges (OASIS MCX-150 mg) were provided by Waters (Milford, MA, USA). This sorbent was employed for solid-phase extraction (SPE) of target compounds from water samples. Bond Elut Jr strong cation exchanger cartridges (SCX-150 mg) were acquired from Agilent Technologies.

2.2. Samples and sample preparation

Grab wastewater samples were obtained from several urban STPs located in Galicia (Northwest Spain) during year 2021. After reception, samples were spiked with the selection of labeled surrogate standards (SSs), adjusted at pH 3 using HCl (0.1 M solution), mixed with a 20% of MeOH, filtered and concentrated using MCX SPE cartridges, under conditions reported elsewhere for triazolic compounds [21]. In brief, water aliquots (200–400 mL) were passed through the cartridge, previously conditioned with MeOH and water at pH 3. Thereafter, the sorbent was rinsed with ultrapure water adjusted at pH 3 (5 mL), and dried using a stream of nitrogen. Neutral and acidic compounds were rinsed with 2 mL of MeOH containing a 0.1% of FA. Target compounds were recovered using 2 mL of MeOH: NH_3 (98:2). This extract was filtered (0.22 µm pore size) and stored at 4 °C until analysis.

Sludge samples (solid wastes after primary and secondary wastewater treatment) were obtained from six different STPs. After reception, they were frozen and lyophilized. Freeze-dried fractions (0.5 g) were spiked with SSs and allowed to stand overnight. Thereafter, they were thoroughly mixed with 2 g of C_{18} in a mortar, using a pestle, and packed in a polypropylene syringe containing 1 g of PSA as co-sorbent of acidic compounds [22]. The MSPD syringe was placed on top of a SCX cartridge. The modular combination of sorbents was first rinsed with MeOH (10 mL), which were discarded. Thereafter, the MSPD syringe, containing the packed samples, was de-attached from the SCX cartridge. Moderate and strong basic compounds were recovered from the latter sorbent using MeOH: NH_3 (98:2). This extract (5 mL) was evaporated to 2 mL, filtered, and maintained at 4 °C until analysis.

2.3. SFC-MS determination conditions

Compounds were determined using a QTOF-MS spectrometer (Agilent 6550 model), furnished with an electrospray ionization source (ESI), and coupled to 1260 infinity II SFC system from

USC UNIVERSIDADE DE SANTIAGO DE COMPOSTELA

Table 1
Retention times, quantification ions ($[M+H]^+$), determination coefficients (R^2), limits of quantification (LOQs), resolution factors (Rs) and peak widths for target compounds and their isotopically labeled analogues.

Compound	Retention time (min)	$[M+H]^+(m/z)$	R^2 (2–250 µg L^{-1})	LOQ (µg L-1)	Rs	Peak width (min)
PRO-R[a]	8.31	260.165	0.999	2	2.33	0.271
PRO-S[b]	8.86		0.999	2		0.203
TRA-1[a]	3.88	264.1963	0.999	1	1.37	0.44
TRA-2[b]	4.47		0.999	1		0.417
VFX-1[a]	4.36	278.212	0.999	1	1.09	0.417
VFX-2[b]	4.82		0.999	1		0.429
CBZ-1[c]	4.73	293.1057	0.999	1	1.25	0.406
CBZ-2[d]	5.23		0.998	1		0.395
TCZ-1[e]	7.68	386.9892	0.999	1	1.96	0.293
TCZ-2[f]	8.23		0.999	1		0.259
MCZ-1[e]	8.51	416.9905	0.999	1	2.17	0.327
MCZ-2[f]	9.24		0.999	1		0.35
STZ-1[e]	11.61	437.0049	0.999	1	1.03	0.372
STZ-2[f]	11.98		0.999	1		0.35
FTZ-1[e]	12.41	455.0752	0.999	1	2.49	0.485
FTZ-2[f]	13.45		0.999	1		0.35
TRA-^{13}C-d_3-1[a]	3.91	268.2182	-		1.36	0.417
TRA-^{13}C-d_3-2[b]	4.48		-			0.429
CBZ-d_4-1[c]	4.67	297.1302	-		1.34	0.383
CBZ-d_4-2[d]	5.23		-			0.44
MCZ-d_5-1[e]	8.45	422.0227	-		2.03	0.338
MCZ-d_5-2[f]	9.16					0.361

[a] to [f]Identify the surrogate standard associated to each compound.

the same supplier. The SFC was connected to the ESI source using a pre-BPR splitter interface, with an auxiliary sheath pump. Three different polysaccharide-based columns were tested for the separation of target compounds. They were the Lux Amylose-1 (3,5-dimethylphenyl carbamate), Lux i-Amylose-3 (3-chloro-5-methylphenyl carbamate) and Lux i-Cellulose-5 (3,5-dichlorophenyl carbamate) (150 mm x 3.0 mm, 3 µm) columns acquired from Phenomenex (Torrance, CA, USA). In the first case, the stationary phase was coated to the surface of silica particles, whilst the other two columns contained immobilized phases. Columns were used directly, without pre-column, connected to a metallic prefilter (0.2 µm). Under final working conditions, the Amylose-1 column was used. The mobile phase flowrate was adjusted at 1.5 mL min^{-1}, the column was maintained at 40 °C, and the injection volume was set at 2 µL. The mobile phase consisted of CO_2 (phase A) and MeOH with a 0.1% of NH_3 (phase B). Its composition was programmed as follows: 2% B (0–0.2 min), 8% B (0.3–6 min), 18% B (8–12 min), 25% B (12.1–13 min), 2% B (13.1–15.5 min). MeOH (0.5% in FA), at 0.1 mL min^{-1}, was employed as make-up solution, combined with the column flow before the splitter. The BPR pressure was set at 140 bar (60 °C), and the splitter was connected to the ESI source using a 0.5 m length, 0.050 mm i.d., silica capillary. The ESI source was operated in the positive mode (ESI+), using nitrogen as nebulizing and drying gas (35 psi and 15 L min^{-1}, 200 °C, respectively). The voltages of the ESI needle and the fragmentor were set at 3.5 KV and 380 V, respectively.

The QTOF-MS instrument was operated in the 2 GHz, extended Dynamic range resolution MS mode, with continuous recalibration of the *m/z* axis using the ions 121.0508 and 922.0098. The *m/z* ratio corresponding to the $[M+H]^+$ ion of each compound was extracted using a window of 10 ppm and employed for quantitative purposes, Table 1. Product ion scan spectra were used for confirmation purposes when required. Table S1 summarizes the most intense product ions of target compounds.

2.4. Characterization of SFC-ESI-MS methods

Performance of analytical procedures applied to wastewater and sludge analysis was characterized using chromatographic parameters, extraction efficiencies (EEs), matrix effects (MEs), accuracy and limits of quantification (LOQs). The efficiency of chiral separations was evaluated with resolution factors (Rs), calculated as defined in Eq. (1), being tr_2 and tr_1 the retention times of the later and earlier eluting enantiomer of each analyte. Baseline peak widths are represented by w_1 and w_2. Rs values above 1.0 indicate overlapping percentages below 2%, for equal intensity peaks. Values above 1.5 correspond to baseline separation.

$$Rs = 2(tr_2 - tr_1)/(w_1 + w_2), \quad (1)$$

The enantiomeric fractions (EFs) of chiral compounds are calculated as defined in Eq. (2) [4,5], with E_1 and E_2 corresponding to concentrations measured for the earlier and the later eluting enantiomer of each compound.

$$EF = E_1/(E_1 + E2), \quad (2)$$

The EEs of employed sample preparation procedures (SPE and MSPD for water and sludge samples, respectively) were defined as the ratio between the response (peak area without correction with responses obtained for SSs) of each compound in spiked samples and in extracts from same matrix, fortified at the end of the sample preparation process. MEs (%) represent the ratio between the slopes of calibration curves obtained for spiked extracts, from freeze-dried sludge and wastewater samples, and those corresponding to solvent-based standards. The closer the normalized ratio to 100%, the lower the variation between the efficiency of compound ionization in sample extracts versus solvent-based standards [23]. The accuracy of the overall method was evaluated dividing the difference of concentrations measured for spiked and non-spiked fractions of each sample by the added level. Concentrations were calculated against calibration curves obtained for solvent-based standards.

3. Results and discussion

3.1. Optimization of SFC-ESI-TOF-MS conditions

The success of environmental chiral SFC methods depends on two factors: the performance of the separation process itself, and the achieved LOQs, which are mainly controlled by the efficiency of compound ionization at the ESI source. In the earlier steps of

USC UNIVERSIDADE DE SANTIAGO DE COMPOSTELA

this study, chiral columns were operated using linear gradients between 2 and 30% of three different modifiers: MeOH, EtOH or ACN, either combined with ammonium acetate ($AcONH_4$, 5 mM) or DEA (0.1%), as neutral and basic additives, respectively. The total analysis time, including column re-equilibration, was limited to 10 min.

The retention and the enantiomeric resolution of antimycotic drugs were mainly affected by the modifier combined with CO_2. Their retention times varied in the following order: MeOH < EtOH < ACN, whilst enantiomeric resolution increased as follows: ACN < EtOH < MeOH. Fig. S2A illustrates this behavior using CBZ as model compound using the Amylose-1 column. Out of three tested columns, the Amylose-1 and the Cellulose-5 succeeded in separating (Rs > 1) the enantiomers of the five imidazole drugs, whilst the Amylose-3 failed to resolve those of STZ and TCZ. Retention and resolution between enantiomers of PRO, TRA and VFX were affected by the stationary phase of the chiral column, and the additive mixed with MeOH in the mobile phase. Better resolution and shorter retention times were observed using DEA instead of $AcONH_4$, as MeOH additive. Fig. S2B illustrated this behavior for the enantiomers of TRA using the Amylose-1 column. The effect of the additive was coherent with the strong basicity of amine-type compounds, and the acidic character of supercritical CO_2 [7]. Likely, DEA shields the non-stereospecific interactions of these strong bases with residual silanol groups in the stationary phase [8]. On the other hand, maintaining the same composition of the make-up solution (MeOH 0.5% in FA, 0.5 mL min^{-1}), DEA caused a significant attenuation in the ionization efficiency of all compounds (amine-type drugs and the imidazolic antimycotics) compared to that observed using $AcONH_4$ as additive in the mobile phase. Lower responses are linked to the high proton affinity of DEA [7], which limits the ionization of the compounds in the ESI (+) mode. This drawback was overcome replacing DEA by NH_3 (both 0.1%). The basicity of the latter additive was enough to improve the resolution between enantiomers of tertiary amine drugs in comparison to $AcONH_4$, without compromising their ionization efficiency as noticed for DEA, Fig. S2B. Moreover, the primary adduct between neutral molecules and the ammonium cation has been reported to evolve generating the $[M+H]^+$ species in the ESI source [24]. Whatever the exact mechanism enhancing compounds ionization, differences observed between the use of NH_3 and DEA in this study, are in agreement with previous results reported by Hamman et al. during determination of basic drugs by SFC-ESI-MS [24]. Using the same combination of modifier and additive (MeOH, 0.1% in NH_3), it was verified that the Cellulose-5 chiral column failed to resolve the isomers of PRO, TRA and VFX. The Amylose-3 separated the enantiomers of PRO and those of VFX; however, broad tailing peaks were observed for the latter species. On the other hand, it failed to resolve the stereoisomers of TRA. Thus, the Amylose-1 column was selected to continue with the study.

Once the SFC column, the mobile phase modifier and the additive were selected, different mobile phase gradients and temperatures (30–45 °C) were tested. Under final conditions described in Material and Methods section, compounds were separated in 15.5 min, with Rs values between 1.03 (STZ enantiomers) and 2.59 (FTZ enantiomers), Table 1. Total analysis time employed in this research was between twice [25] and four times [13] lower than those required in previous multianalyte methods using chiral LC as separation technique, under isocratic conditions; and in the range of values reported in other multianalyte SFC-MS applications [12]. Same SFC conditions were also tested to resolve the racemates of over the counter metabolites of TRA and VFX: N-desmethyl TRA and O-desmethyl VFX. Fully overlapped peaks were observed for N-desmethyl TRA enantiomers. The two isomers of O-desmethyl VFX were only partially resolved (Rs 0.7), but well separated from the stereoisomers of TRA (they appeared at longer retention times, c.a. 2 min). The latter is a relevant achievement since both compounds are ubiquitous in wastewater and they share identical MS and MS/MS spectra, with a single intense product ion ($[C_3H_8N]^+$) at *m/z* 58 [11].

As make-up solution, we considered the use of MeOH with a 0.5% of FA. The effect of its flowrate (from 0.1 to 0.75 mL min^{-1}) in the responses of target compounds was first investigated with solvent-based standards. Obtained data are provided as supplementary information, Fig. S3A. Increasing the make-up flowrate reduced the responses for all compounds without affecting other chromatography parameters, such as retention time repeatability, peak width or Rs factors. Depending on the compound, normalized responses were reduced between 20 and 50% when increasing the make-up flowrate from 0.1 to 0.75 mL min^{-1}, Fig. S3A. Thus, the dilution factor introduced by the increase in the make-up flowrate was partially compensated by a more effective ionization process. The trend observed for solvent-based standards, was similar to that noticed for a spiked sludge extract, Fig. S3B. Thus, the working value for this parameter was set at 0.1 mL min^{-1}. It is worth noting that, the make-up flowrate and the additive employed in the mobile phase are not independent parameters. As example, using MeOH (0.1% in DEA) in the mobile phase, higher responses were obtained for a make-up flow rate of 0.75 mL of MeOH:FA (99.5:0.5) than considering 0.1 mL min^{-1}, figure not shown. In this case, it is assumed that the increase in the amount of FA introduced in the ESI source, through the make-up solution, compensates in part the negative effect of DEA in the formation of $[M+H]^+$ ions.

Under optimized conditions, the repeatability of the injection, calculated as relative standard deviation of peak areas ($n = 5$, 10 µg L^{-1} standard), stayed between 1 and 4%. Relative standard deviations associated to the retention times of compounds varied between 0.1 and 1.02% for consecutive injection of calibration standards (2–250 µg L^{-1}), and between 0.2 and 1.3% for a quality control standard (100 µg L^{-1}) injected several times ($n = 16$ injections) during a 48 h sequence. Instrumental LOQs varied between 1 and 2 µg L^{-1}. The plots of normalized responses (compound peak area/SS peak area) versus concentration fitted a linear model, with determination coefficients above 0.998, within the range of concentrations from 2 to 250 µg L^{-1} per enantiomer, Table 1. Fig. 1 shows a chromatogram for a standard mixture of all compounds at a concentration level of 10 µg L^{-1} per isomer. Chromatograms obtained with the other two chiral columns tested in this research, under same SFC-MS conditions, are provided as supplementary information, Fig. S4.

3.2. Performance of analytical methodologies

The original mixed-mode SPE procedure, previously reported for extraction of antimycotic drugs from wastewater [21], was re-evaluated for the selection of compounds involved in this research. Polar, strong basic amine drugs were effectively retained by the mixed-mode sorbent during cartridge loading and clean-up steps; however, losses of moderately basic compounds (i.e. CBZ enantiomers) were noticed during the removal of neutrals with MeOH. This drawback was solved replacing MeOH by MeOH 0.1% in FA, as washing solvent, which reinforced the interaction between weak basic compounds and the negatively charged sites in the sorbent. The EEs of the SPE procedure for raw and treated wastewater were in the range from 82 to 113%, with standard deviations (SDs) below 11%, Table S2. The only exception was FTZ. The average EEs for the enantiomers of this compound in raw wastewater were 68%, Table S2. For this particular matrix, FTZ was partially lost due to breakthrough problems during concentration of 200 mL sample aliquots, Table S2. For freeze-dried sludge samples, the EEs of the modular MSPD procedure were between 83 and 117%, with standard deviations lower than 7%, Table S2.

USC UNIVERSIDADE DE SANTIAGO DE COMPOSTELA

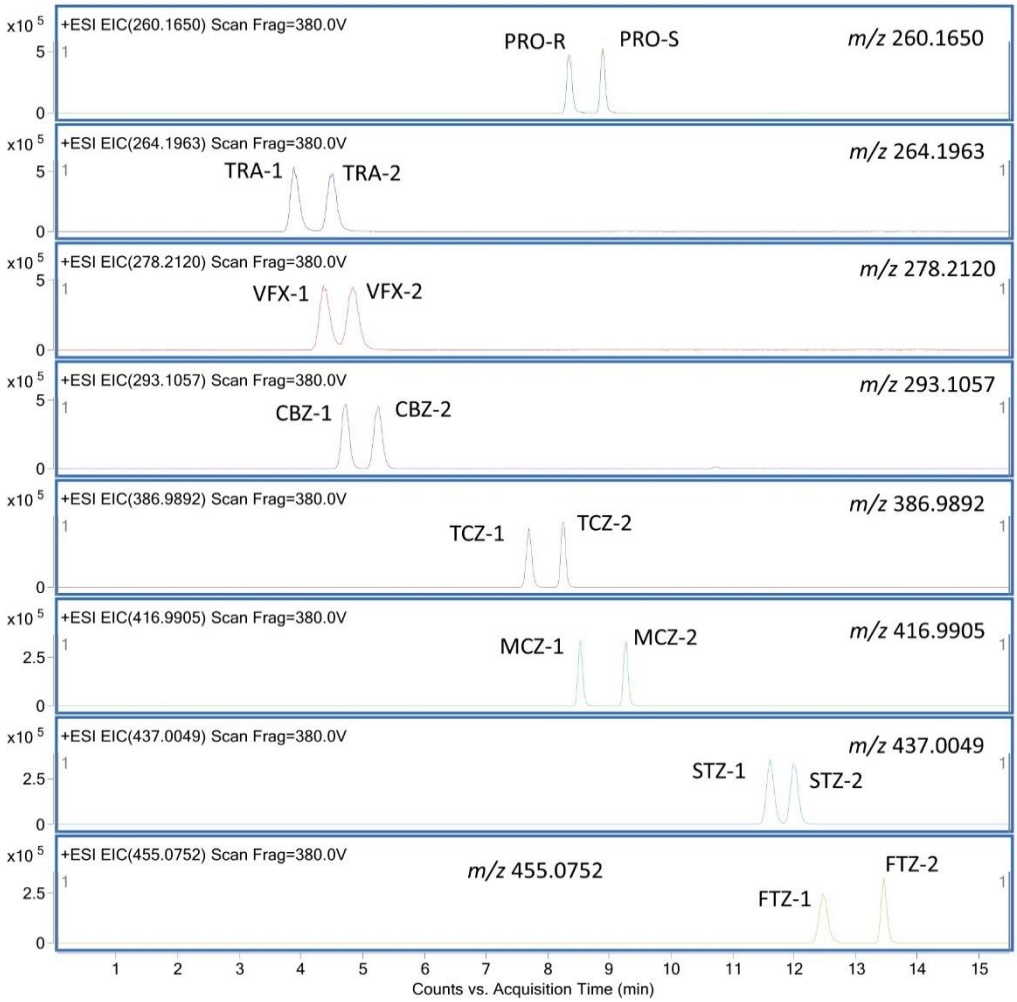


Fig. 1. Extracted ion chromatograms (mass window 10 ppm) for the $[M+H]^+$ ion of target compounds (10 μg L^{-1} per enantiomer) under optimized SFC-ESI-TOF-MS conditions using the Lux amylose-1 column with methanol (0.1% in NH_3) as modifier and additive of supercritical CO_2, respectively. Column temperature and mobile phase flow rate were 40 °C and 1.5 mL min^{-1}. The mobile phase gradient is given in Section 2.1.

The assessment of MEs became a major issue in this research. Changes in the efficiency of ionization between solvent-based standards and sample extracts affect the accuracy of the method; moreover, enantioselective MEs are a serious limitation when aiming to identify possible variations in the EFs of chiral compounds. Table 2 summarizes the MEs obtained for the most complex matrices involved in this research: raw wastewater and sludge. In the first case, MEs varied between 99 and 115%. Considering the definition of MEs reported in the Material and Methods section, these values point out to minor changes in the efficiency of compounds ionization between SPE extracts and solvent-based standards. For extracts obtained from sludge, moderate signal suppression (MEs in the range from 62 to 80%) was noticed for some species. The maximum differences between MEs for the enantiomers of a given pharmaceutical remained below 10%, Table 2.

Table 3 summarizes results obtained during evaluation of the accuracy of the SFC-ESI-TOF-MS method for water and sludge samples. For the first matrix, individual recoveries of each species, in the three considered water types, stayed between 80 and 115%, except in case of FTZ enantiomers with a value of 77% for the wastewater sample. It is worth noting that for the river water, the concentrated sample volume was increased to 400 mL, with satisfactory recoveries. The SD values associated to recoveries obtained for spiked water samples remained below 8%. In case of sludge, the enantiomers of VFX and MCZ showed overall recoveries between 120 and 133%, with associated SDs below 10%. For the rest of species, recoveries were in the range from 95 to 120%. The LOQs of the two analytical procedures are also shown in Table 3. Reported values were estimated from instrumental LOQs, considering the ratio between sample amount (200 mL and 0.5 g for wastewater and sludge, respectively) and the final volume (2 mL) of extracts obtained using SPE and MSPD extraction protocols. These ratios were corrected with EEs and MEs, when they stayed below 80%. The LOQs in raw wastewater were between 0.010 and 0.020 μg L^{-1}. Similar LOQs have been reported using chiral LC combined with a TOF-MS instrument [13], whilst lower values were achieved replacing the above system by a QqQ instrument [11]. Rice et al. [9] developed a SFC-QqQ-MS method for the determination of large se-

USC UNIVERSIDADE DE SANTIAGO DE COMPOSTELA

Table 2
Assessment of MEs (%) for raw wastewater and sludge samples. Normalized responses between slopes of calibration curves obtained for spiked extracts from raw wastewater, or sludge, and solvent-based standards (2–100 μg L^{-1}). Values within parenthesis are the standard deviations for slopes of calibration curves for matrix-matched standards.

Compound	Raw wastewater	Sludge
PRO-R	106% (1)	72% (4)
PRO-S	107% (1)	82% (5)
TRA-1	108% (2)	91% (7)
TRA-2	106% (1)	93% (6)
VFX-1	100% (3)	92% (6)
VFX-2	99% (3)	94% (6)
CBZ-1	115% (2)	107% (6)
CBZ-2	112% (2)	106% (5)
TCZ-1	104% (5)	70% (5)
TCZ-2	103% (2)	62% (5)
MCZ-1	104% (3)	81% (6)
MCZ-2	114% (2)	73% (4)
STZ-1	113% (3)	78% (6)
STZ-2	112% (1)	84% (6)
FTZ-1	108% (3)	80% (6)
FTZ-2	115% (3)	80% (5)

lection of non-chiral and nine chiral drugs in wastewater samples. The latter group included two compounds common to those considered in this study: PRO and TRA. For the 2nd species, authors failed to separate both enantiomers; moreover, their SPE method provided non-satisfactory recoveries for TRA in spiked wastewater samples [9]. In case of PRO, enantiomeric resolution was similar to that reported in this study, with equivalent LOQs (0.01-0-05 μg L^{-1}) despite using a more sensitive mass analyzer. LOQs compiled in Table 3 for sludge varied between 3.7 and 11.1 ng g^{-1}, referred to the dry sludge matrix. The linear response range of the method extended up to 2.5 μg L^{-1} and 1000 ng g^{-1} for wastewater and sludge, respectively.

3.3. Distribution in environmental samples

Chiral SFC-TOF-MS, combined with SPE and MSPD sample preparation methodologies, was applied to investigate the concentrations, and the EFs, of target compounds in sewage samples. Positive identifications were based on retention time and $[M+H]^+$ match (maximum differences 0.1 min and 10 ppm, respectively) with calibration standards. For compounds close to the LOQs of the method, their identities were confirmed in a second injection, using target MS/MS conditions reported in Table S1. Table 4 summarizes the concentrations measured for seven pairs of wastewater samples (raw and treated wastewater) obtained from four different STPs. Pharmaceuticals were ubiquitous in the environment of STPs. As a general observation, those showing high logD values (see Fig. S1) were mostly associated to sludge, whilst the amine-type pharmaceuticals were mainly found in water samples, Tables 4 and 5. Despite this global trend, one of the processed sludge samples contained a concentration of TRA enantiomers around 1000 ng g^{-1}, Table 5.

The concentrations of the enantiomers of TRA and VFX in wastewater ranged between 0.11 and 1.0 μg L^{-1}. Although data compiled in Table 4 correspond to grab samples, they confirm the poor biodegradability of both compounds at STPs. CBZ and PRO enantiomers were often above the LOQs of the method in wastewater; however, their concentrations remained one order of magnitude below those of TRA and VFX. Finally, MCZ enantiomers were just noticed in two raw wastewater samples, whilst TCZ, STZ and FTZ remained undetected.

As regards the sludge matrix, VFX and the imidazole antimycotic drugs were noticed in all samples above method LOQs. Given aside the high concentration of TRA found in sludge sample code S2, pollutants displaying the highest levels were MCZ and FTZ. The total concentration (sum of enantiomers) of the first compound varied between 0.44 and 1.57 μg g^{-1}. These concentrations are in the range of values found in sludge samples from other geographic areas, such as South America [26] and Asia [27]. In case of MCZ, they stay 3-order of magnitude above the lowest predicted non-effect concentration (PNEC) level compiled in the NORMAN ecotoxicity database for MCZ in freshwater sediments [28].

The EFs of above compounds in the set of processed samples are provided as supplementary information, Table S3. Fig. 2 shows the Box-Whisker plot for EFs measured in the set of processed sludge and wastewater samples. PRO, TRA and VFX showed EFs significantly different from 0.5. In the first case, environmental samples were enriched significantly in the latter eluting isomer (S-form), with average and median EF values of 0.40 and 0.41, respectively. This enantiomeric pattern agrees with that reported by Bagnall et al. [13] for environmental water samples. Rice et al. [9] have reported a value of 0.40 for the EF or PRO in raw and treated wastewater samples, but without identifying which enantiomeric form presented the higher concentration. The EFs of TRA showed a very narrow distribution of values, with an average of 0.53, which matched also the median value. In case of VFX, average and me-

Table 3
Accuracy of the analytical procedures for water and sludge samples. Recoveries obtained using solvent-based calibration standards, $n = 3$ replicates. Procedural LOQs estimated for raw wastewater and sludge.

	Water type (addition level)			Sludge (addition level)		LOQs	
Compound	Raw wastewater (0.5 μg L^{-1})	Treated wastewater (0.25 μg L^{-1})	River water (0.05 μg L^{-1})	(250 ng g^{-1})	(125 ng g^{-1})	Raw wastewater (μg L^{-1})	Sludge (ng g^{-1})
PRO-R	104% (2)	92% (5)	108% (4)	112% (6)	103% (7)	0.020	11.1
PRO-S	104% (2)	92% (5)	112% (5)	100% (4)	95% (8)	0.020	9.8
TRA-1	104% (2)	103% (4)	104% (2)	106% (1)	106% (4)	0.010	4.4
TRA-2	107% (2)	101% (3)	101% (4)	102% (2)	111% (5)	0.010	4.3
VFX-1	98% (5)	100% (5)	108% (2)	127% (8)	133% (7)	0.010	4.3
VFX-2	95% (3)	100% (5)	107% (3)	106% (3)	125% (4)	0.010	4.3
CBZ-1	115% (2)	95% (5)	100% (3)	105% (4)	112% (6)	0.010	3.7
CBZ-2	115% (2)	96% (4)	101% (3)	103% (1)	111% (7)	0.010	3.8
TCZ-1	110% (2)	89% (5)	98% (2)	98% (2)	117% (6)	0.010	5.7
TCZ-2	108% (2)	90% (7)	103% (2)	106% (4)	119% (6)	0.010	6.5
MCZ-1	108% (2)	88% (5)	102% (5)	125% (2)	128% (5)	0.010	4.9
MCZ-2	109% (1)	87% (6)	102% (3)	123% (5)	125% (4)	0.010	5.5
STZ-1	110% (2)	86% (8)	98% (2)	107% (4)	112% (7)	0.010	4.7
STZ-2	111% (1)	87% (8)	100% (2)	117% (7)	112% (5)	0.010	4.8
FTZ-1	98% (3)	77% (7)	88% (3)	102% (4)	108% (6)	0.015	5.0
FTZ-2	100% (2)	77% (8)	93% (4)	117% (4)	110% (6)	0.015	5.0

USC UNIVERSIDADE DE SANTIAGO DE COMPOSTELA

Table 4
Concentrations (μg L^{-1}) measured in wastewater samples. Average values for triplicate extractions, with standard deviations within parenthesis. Empty cells correspond to concentrations below procedural LOQs in wastewater.

Sample code	Compound									
	PRO-R	PRO-S	TRA-1	TRA-2	VFX-1	VFX-2	CBZ-1	CBZ-2	MCZ-1	MCZ-2
RW1	0.035 (0.005)	0.039 (0.003)	0.48 (0.03)	0.43 (0.02)	0.24 (0.01)	0.26 (0.01)	0.122 (0.009)	0.123 (0.008)		
TW1	0.051 (0.005)	0.086 (0.006)	0.48 (0.03)	0.42 (0.03)	0.24 (0.01)	0.29 (0.02)	0.035 (0.002)	0.036 (0.001)		
RW2	0.048 (0.003)	0.071 (0.004)	0.71 (0.05)	0.63 (0.05)	0.27 (0.02)	0.30 (0.01)	0.075 (0.004)	0.075 (0.003)		
TW2	0.048 (0.006)	0.068 (0.005)	0.40 (0.03)	0.35 (0.02)	0.18 (0.02)	0.20 (0.01)	0.029 (0.002)	0.030 (0.001)		
RW3	0.023 (0.002)	0.031 (0.002)	0.27 (0.03)	0.23 (0.01)	0.13 (0.01)	0.14 (0.01)	0.023 (0.001)	0.024 (0.002)	0.013 (0.001)	0.013 (0.002)
TW3			0.24 (0.01)	0.21 (0.01)	0.110 (0.008)	0.122 (0.004)	0.019 (0.001)	0.020 (0.002)		
RW4			0.50 (0.03)	0.41 (0.02)	0.21 (0.01)	0.23 (0.01)	0.068 (0.003)	0.070 (0.005)	0.032 (0.003)	0.026 (0.002)
TW4	0.021 (0.002)	0.031 (0.001)	0.34 (0.02)	0.30 (0.02)	0.15 (0.01)	0.17 (0.01)	0.022 (0.002)	0.022 (0.004)		
RW5	0.031 (0.001)	0.038 (0.003)	1.04 (0.02)	0.92 (0.03)	0.21 (0.01)	0.24 (0.01)	0.036 (0.002)	0.042 (0.002)		
TW5	0.029 (0.002)	0.029 (0.002)	0.75 (0.06)	0.63 (0.02)	0.25 (0.01)	0.26 (0.02)	0.025 (0.002)	0.031 (0.003)		
RW6			0.52 (0.06)	0.49 (0.02)	0.38 (0.02)	0.54 (0.03)	0.028 (0.001)	0.032 (0.002)		
TW6			0.56 (0.04)	0.48 (0.02)	0.41 (0.03)	0.52 (0.03)				
RW7	0.028 (0.002)	0.037 (0.002)	0.82 (0.09)	0.66 (0.03)	0.32 (0.01)	0.39 (0.02)	0.025 (0.001)	0.029 (0.002)		
TW7	0.021 (0.002)	0.027 (0.002)	0.75 (0.05)	0.66 (0.03)	0.25 (0.01)	0.31 (0.01)				

RW, raw wastewater.
TW, treated wastewater.

Table 5
Concentrations (ng g^{-1}, referred to dry weight) obtained in sludge samples. Average values for triplicate extractions, with standard deviation data. Empty cells correspond to concentrations below procedural LOQs in freeze-dried sludge.

Compound	Sample code					
	S1	S2	S3	S4	S5	S6
PRO-R	91.1 (0.9)				26.3 (2.1)	
PRO-S	113 (2)				37.5 (2.6)	
TRA-1	29.8 (1.7)	1067 (23)	136 (6)	92.2 (8.0)		
TRA-2	23.2 (1.9)	997 (30)	123 (4)	80.3 (8.2)		
VFX-1	20.4 (1.5)	133 (5)	112 (7)	43.8 (3.5)	11.8 (1.0)	8.7 (0.6)
VFX-2	23.0 (1.8)	133 (7)	119 (6)	50.6 (3.5)	12.8 (0.9)	9.2 (0.5)
CBZ-1	11.5 (0.9)	48.2 (2.4)	48.7 (3.5)	32.9 (2.7)	14.7 (1.0)	10.6 (0.9)
CBZ-2	12.8 (0.8)	48.8 (3.2)	47.7 (4.1)	35.1 (1.9)	15.1 (1.2)	11.1 (0.9)
TCZ-1	13.7 (0.9)	33.8 (2.7)	34.6 (2.7)	10.8 (0.9)	112 (7)	55.4 (4.8)
TCZ-2	13.8 (0.9)	41.1 (3.8)	45.0 (4.0)	10.5 (1.1)	110 (8)	68.8 (5.5)
MCZ-1	213 (11)	264 (15)	283 (19)	493 (20)	797 (35)	291 (16)
MCZ-2	229 (10)	303 (27)	310 (25)	418 (27)	782 (42)	305 (22)
STZ-1	20.2 (0.5)	34.5 (0.9)	39.6 (3.0)	4.8 (0.5)	74.7 (8.1)	10.9 (0.9)
STZ-2	25.4 (1.2)	48.5 (2.1)	56.6 (3.9)	5.0 (0.6)	73.6 (5.4)	11.0 (0.8)
FTZ-1	132 (7)	106 (6)	119 (9)	68.2 (5.4)	173 (12)	158 (9)
FTZ-2	153 (6)	137 (9)	154 (12)	72.9 (6.0)	165 (13)	150 (11)

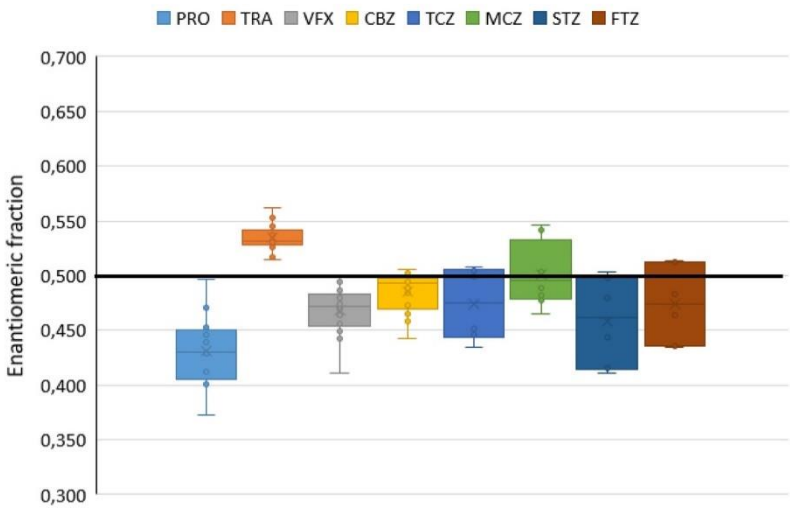


Fig. 2. Box-Whisker plot of enantiomeric fractions (EFs) for target compounds in samples (wastewater and sludge) above method LOQs.

USC UNIVERSIDADE DE SANTIAGO DE COMPOSTELA

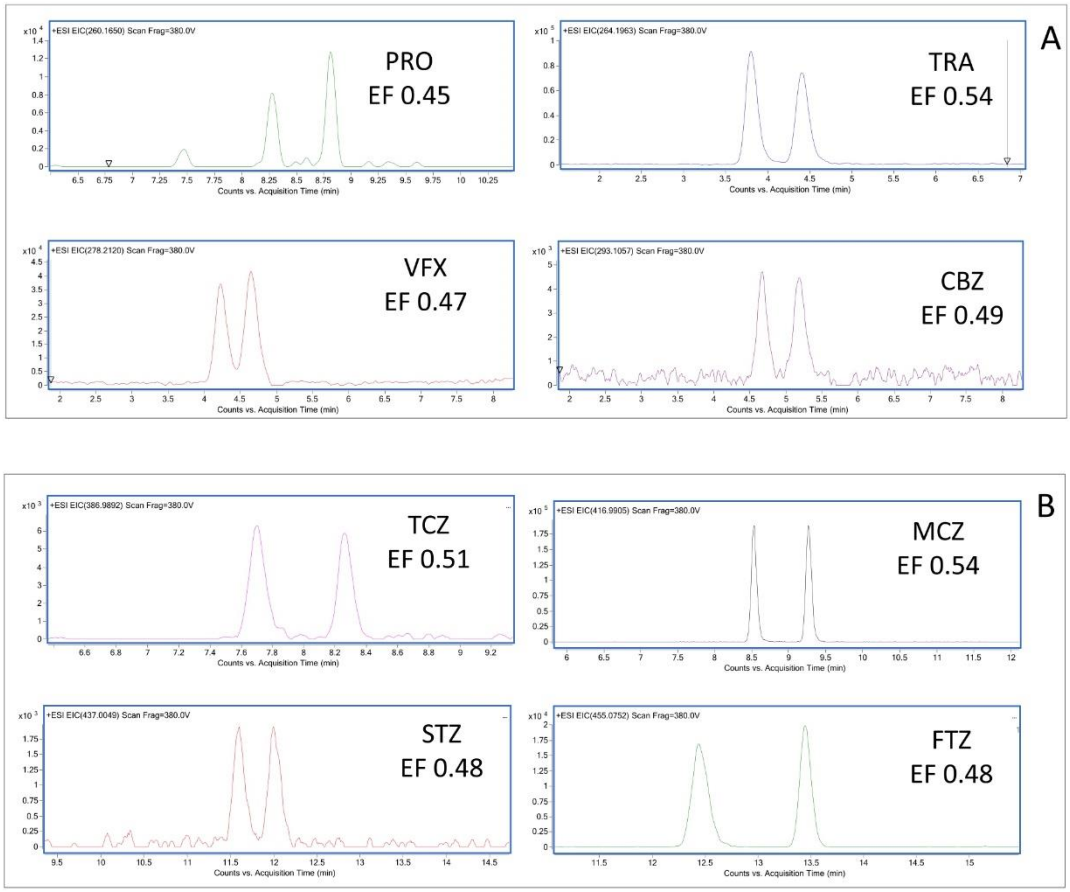


Fig. 3. Chromatograms for target compounds in non-spiked samples of wastewater (A, sample code TW2; PRO, TRA, VFX and CBZ) and sludge (B, sample code S4; TCZ, MCZ, STZ, FTZ), with EFs, calculated as ratio of concentration for the first eluting enantiomer and the sum of concentrations of both forms. Same SFC conditions as in Fig. 1.

dian EFs were below 0.5. In summary, the three pharmaceuticals showed a non-racemic distribution in the set of analyzed environmental samples. Their EFs were also calculated in three commercial medicaments, in this case, average values ranged from 0.501 to 0.507. We assume that changes in the EFs of these compounds did not occur at STPs, but they are the result of a differential metabolization between enantiomers. As regards the group of antimycotic pharmaceuticals (mainly found in sludge samples) their EFs showed a higher dispersion than those of amine-type pharmaceuticals. Considering the number of positive samples, no significant variations were noticed in their EFs compared to that expected for racemates (EF 0.5). As these compounds are mainly used in topic applications; thereafter, if they are partially biodegraded at STPs, EFs data obtained in this research suggest that the process was not enantioselective for investigated compounds. Fig. 3 shows the extracted ion chromatograms corresponding to the $[M+H]^+$ ion of each compound in two non-spiked samples of wastewater (Fig. 3A) and sludge (Fig. 3B), with the experimental EF values measured for each compound.

4. Conclusion

The SFC-QTOF-MS methodology optimized in this research permitted the rapid resolution of a selection of eight chiral compounds, with shorter analysis time and lower consumption of organic solvents than those employed in previous chiral applications using LC as separation technique. To the best of our knowledge, this research describes for the first time, the simultaneous enantiomeric resolution of azolic and amine-type drugs. Retention and enantiomeric resolution of the latter group of compounds were sensitive to the additive combined with MeOH in the mobile phase. Ammonia (0.1% in MeOH) provided the best balance between enantiomeric resolution and ionization efficiency of target compounds in the ESI source of the MS spectrometer. SFC-QTOF-MS combined with extraction-concentration methods isolating basic species from environmental samples, permitted to determine the concentrations and the EFs of target compounds in wastewater and sludge samples, with minor or moderate signal suppression effects. Residues of the three considered amine drugs (PRO, TRA and VFX) showed a non-racemic distribution in the investigated environmental samples, whilst EF values of azolic drugs remained around 0.5%. Very likely, enantioselective metabolization, rather than chiral selective biodegradation at STPs, is the responsible of the non-racemic distribution of PRO, TRA and VFX in the processed samples.

Declaration of Competing Interest

Authors declare no competing interest.

USC UNIVERSIDADE DE SANTIAGO DE COMPOSTELA

CRediT authorship contribution statement

M. Cobo-Golpe: Investigation, Methodology, Writing – original draft. **M. Ramil:** Supervision, Writing – review & editing. **R. Cela:** Project administration, Funding acquisition, Writing – review & editing. **I. Rodríguez:** Conceptualization, Supervision, Funding acquisition, Writing – original draft.

Acknowledgments

This study was supported through grants PGC2018-094613-B-I00 and ED431C 2021/06, funded by Spanish Government and Xunta de Galicia, respectively. Both projects are co-funded by the EU FEDER program. M.C.G. thanks a FPI fellowship to the Ministry of Science and Education (Spain).

Supplementary materials

Supplementary material associated with this article can be found, in the online version, at doi:10.1016/j.chroma.2022.463088.

References

[1] A. Dogan, D. Kempińska-Kupczyk, P. Kubica, A. Kot-Wasik, Analysis of chiral pharmaceutical residues in influent and effluent samples at racemic and enantiomeric level using liquid chromatography-tandem mass spectrometry, Microchem. J. 159 (2020), doi:10.1016/j.microc.2020.105517.
[2] Y. Fu, F. Borrull, R.M. Marcé, N. Fontanals, Enantiomeric fraction determination of chiral drugs in environmental samples using chiral liquid chromatography and mass spectrometry, Trends Environ. Anal. Chem. 29 (2021), doi:10.1016/j.teac.2021.e00115.
[3] M.M. Coelho, A.R. Lado Ribeiro, J.C.G. Sousa, C. Ribeiro, C. Fernandes, A.M.T. Silva, M.E. Tiritan, Dual enantioselective LC–MS/MS method to analyse chiral drugs in surface water: monitoring in Douro River estuary, J. Pharm. Biomed. Anal. 170 (2019) 89–101, doi:10.1016/j.jpba.2019.03.032.
[4] E. Sanganyado, Z. Lu, Q. Fu, D. Schlenk, J. Gan, Chiral pharmaceuticals: a review on their environmental occurrence and fate processes, Water Res. 124 (2017) 527–542, doi:10.1016/j.watres.2017.08.003.
[5] B. Kasprzyk-Hordern, D.R. Baker, Estimation of community-wide drugs use via stereoselective profiling of sewage, Sci. Total Environ. 423 (2012) 142–150, doi:10.1016/j.scitotenv.2012.02.019.
[6] G.L. Losacco, J.L. Veuthey, D. Guillarme, Supercritical fluid chromatography – mass spectrometry: recent evolution and current trends, TrAC Trends Anal. Chem. 118 (2019) 731–738, doi:10.1016/j.trac.2019.07.005.
[7] T. Gazárková, K. Plachká, F. Svec, L. Nováková, Current state of supercritical fluid chromatography-mass spectrometry, TrAC Trends Anal. Chem. 149 (2022), doi:10.1016/j.trac.2022.116544.
[8] K. De Klerck, D. Mangelings, Y.V. Heyden, Supercritical fluid chromatography for the enantioseparation of pharmaceuticals, J. Pharm. Biomed. Anal. 69 (2012) 77–92, doi:10.1016/j.jpba.2012.01.021.
[9] J. Rice, A. Lubben, B. Kasprzyk-Hordern, A multi-residue method by supercritical fluid chromatography coupled with tandem mass spectrometry method for the analysis of chiral and non-chiral chemicals of emerging concern in environmental samples, Anal. Bioanal. Chem. 412 (2020) 5563–5581, doi:10.1007/s00216-020-02780-9.
[10] S.L. MacLeod, P. Sudhir, C.S. Wong, Stereoisomer analysis of wastewater-derived β-blockers, selective serotonin re-uptake inhibitors, and salbutamol by high-performance liquid chromatography-tandem mass spectrometry, J. Chromatogr. A 1170 (2007) 23–33, doi:10.1016/j.chroma.2007.09.010.
[11] E. Castrignanò, A. Lubben, B. Kasprzyk-Hordern, Enantiomeric profiling of chiral drug biomarkers in wastewater with the usage of chiral liquid chromatography coupled with tandem mass spectrometry, J. Chromatogr. A 1438 (2016) 84–99, doi:10.1016/j.chroma.2016.02.015.
[12] V. Cutillas, M. García-Valverde, M.D.M. Gómez-Ramos, F.J. Díaz-Galiano, C. Ferrer, A.R. Fernández-Alba, Supercritical fluid chromatography separation of chiral pesticides: unique capabilities to study cyhalothrin and metalaxyl as examples, J. Chromatogr. A 1620 (2020), doi:10.1016/j.chroma.2020.461007.
[13] J.P. Bagnall, S.E. Evans, M.T. Wort, A.T. Lubben, B. Kasprzyk-Hordern, Using chiral liquid chromatography quadrupole time-of-flight mass spectrometry for the analysis of pharmaceuticals and illicit drugs in surface and wastewater at the enantiomeric level, J. Chromatogr. A 1249 (2012) 115–129, doi:10.1016/j.chroma.2012.06.012.
[14] Q. Huang, Z. Wang, C. Wang, X. Peng, Chiral profiling of azole antifungals in municipal wastewater and recipient rivers of the Pearl River Delta, China, Environ. Sci. Pollut. Res. 20 (2013) 8890–8899, doi:10.1007/s11356-013-1862-z.
[15] J. Bhagat, N. Singh, N. Nishimura, Y. Shimada, A comprehensive review on environmental toxicity of azole compounds to fish, Chemosphere 262 (2021) 128335, doi:10.1016/j.chemosphere.2020.128335.
[16] M. Brienza, S. Chiron, Enantioselective reductive transformation of climbazole: a concept towards quantitative biodegradation assessment in anaerobic biological treatment processes, Water Res. 116 (2017) 203–210, doi:10.1016/j.watres.2017.03.037.
[17] L. Toribio, J.L. Bernal, M.T. Martín, J. Bernal, M.J. del Nozal, Effects of organic modifier and temperature on the enantiomeric separation of several azole drugs using supercritical fluid chromatography and the Chiralpak AD column, Biomed. Chromatogr. 28 (2014) 152–158, doi:10.1002/bmc.3013.
[18] L.F. Angeles, R.R. Singh, P.J. Vikesland, D.S. Aga, Increased coverage and high confidence in suspect screening of emerging contaminants in global environmental samples, J. Hazard. Mater. 414 (2021) 125369, doi:10.1016/j.jhazmat.2021.125369.
[19] G. Castro, M. Roca, I. Rodríguez, M. Ramil, R. Cela, Identification and determination of chlorinated azoles in sludge using liquid chromatography quadrupole time-of-flight and triple quadrupole mass spectrometry platforms, J. Chromatogr. A 1476 (2016) 69–76, doi:10.1016/j.chroma.2016.11.020.
[20] F.J. Lopez, E. Pitarch, A.M. Botero-Coy, D. Fabregat-Safont, M. Ibáñez, J.M. Marin, A. Peruga, N. Ontañón, S. Martínez-Morcillo, A. Olalla, Y. Valcárcel, I. Varó, F. Hernández, Removal efficiency for emerging contaminants in a WWTP from Madrid (Spain) after secondary and tertiary treatment and environmental impact on the Manzanares River, Sci. Total Environ. 812 (2022), doi:10.1016/j.scitotenv.2021.152567.
[21] J. Casado, I. Rodríguez, M. Ramil, R. Cela, Selective determination of antimycotic drugs in environmental water samples by mixed-mode solid-phase extraction and liquid chromatography quadrupole time-of-flight mass spectrometry, J. Chromatogr. A 1339 (2014) 42–49, doi:10.1016/j.chroma.2014.02.087.
[22] J. Casado, G. Castro, I. Rodríguez, M. Ramil, R. Cela, Selective extraction of antimycotic drugs from sludge samples using matrix solid-phase dispersion followed by on-line clean-up, Anal. Bioanal. Chem. 407 (2015) 907–917, doi:10.1007/s00216-014-8167-z.
[23] B.K. Matuszewski, M.L. Constanzer, C.M. Chavez-Eng, Matrix effect in quantitative LC/MS/MS analyses of biological fluids: a method for determination of finasteride in human plasma at picogram per milliliter concentrations, Anal. Chem. 70 (1998) 882–889, doi:10.1021/ac971078+.
[24] C. Hamman, D.E. Schmidt, M. Wong, M. Hayes, The use of ammonium hydroxide as an additive in supercritical fluid chromatography for achiral and chiral separations and purifications of small, basic medicinal molecules, J. Chromatogr. A 1218 (2012) 7886–7894, doi:10.1016/j.chroma.2011.08.064.
[25] K. McKenzie, C.F. Moffat, C.F. Moffat, B. Petrie, Multi-residue enantioselective determination of emerging drug contaminants in seawater by solid phase extraction and liquid chromatography-tandem mass spectrometry, Anal. Methods 12 (2020) 2881–2892, doi:10.1039/d0ay00801j.
[26] M.B.R. Cerqueira, K.L. Soares, S.S. Caldas, E.G. Primel, Sample as solid support in MSPD: a new possibility for determination of pharmaceuticals, personal care and degradation products in sewage sludge, Chemosphere 211 (2018) 875–883, doi:10.1016/j.chemosphere.2018.07.165.
[27] X. Peng, Q. Huang, K. Zhang, Y. Yu, Z. Wang, C. Wang, Distribution, behavior and fate of azole antifungals during mechanical, biological, and chemical treatments in sewage treatment plants in China, Sci. Total Environ. 426 (2012) 311–317, doi:10.1016/j.scitotenv.2012.03.067.
[28] NORMAM Ecotoxicological Database. https://www.norman-network.com/nds/ecotox/lowestPnecsIndex.php (accessed 15 March 2022).

USC UNIVERSIDADE DE SANTIAGO DE COMPOSTELA

Supplementary information to manuscript:

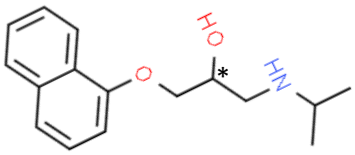
Supercritical fluid chromatography time-of-flight mass spectrometry enantiomeric determination of basic drugs in sewage samples

M. Cobo-Golpe, M. Ramil, R. Cela, I. Rodríguez*
Department of Analytical Chemistry, Nutrition and Food Sciences. Research Institute on Chemical and Biological Analysis (IAQBUS). Universidade de Santiago de Compostela, 15782-Santiago de Compostela, Spain.

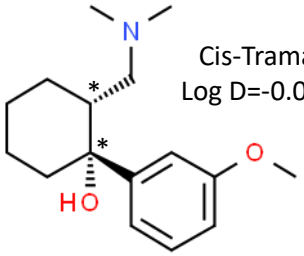
*Corresponding author: I. Rodríguez
e-mail: isaac.rodriguez@usc.es

USC UNIVERSIDADE DE SANTIAGO DE COMPOSTELA

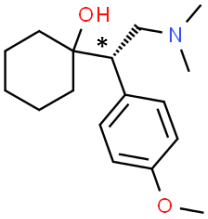
Fig. S1. Chemical structures, log D values at neutral pH, and pKa values of target compounds.



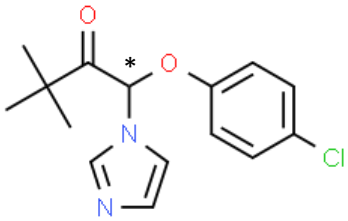
Propranolol (PRO)
Log D=0.45, pK_a= 9.67



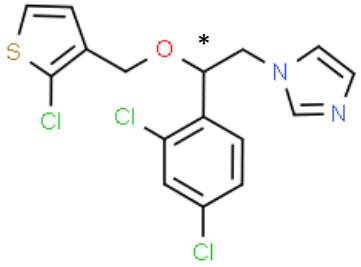
Cis-Tramadol (TRA)
Log D=-0.06, pK_a=9.41



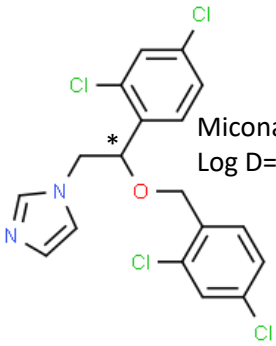
Venlafaxine (VFX)
Log D=0.39, pK_a=8.91



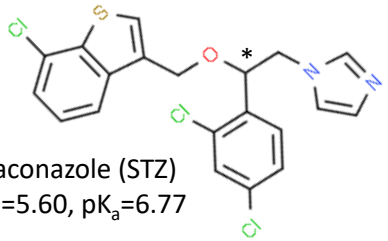
Climbazole (CBZ)
Log D =3.47, pK_a= 5.2



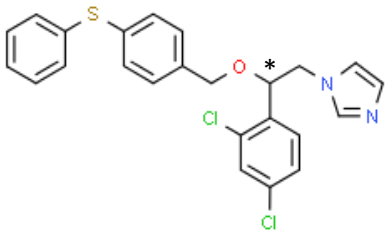
Tioconazole (TCZ)
Log D=4.11, pK_a=6.77



Miconazole (MCZ)
Log D=4.81, pK_a=6.77

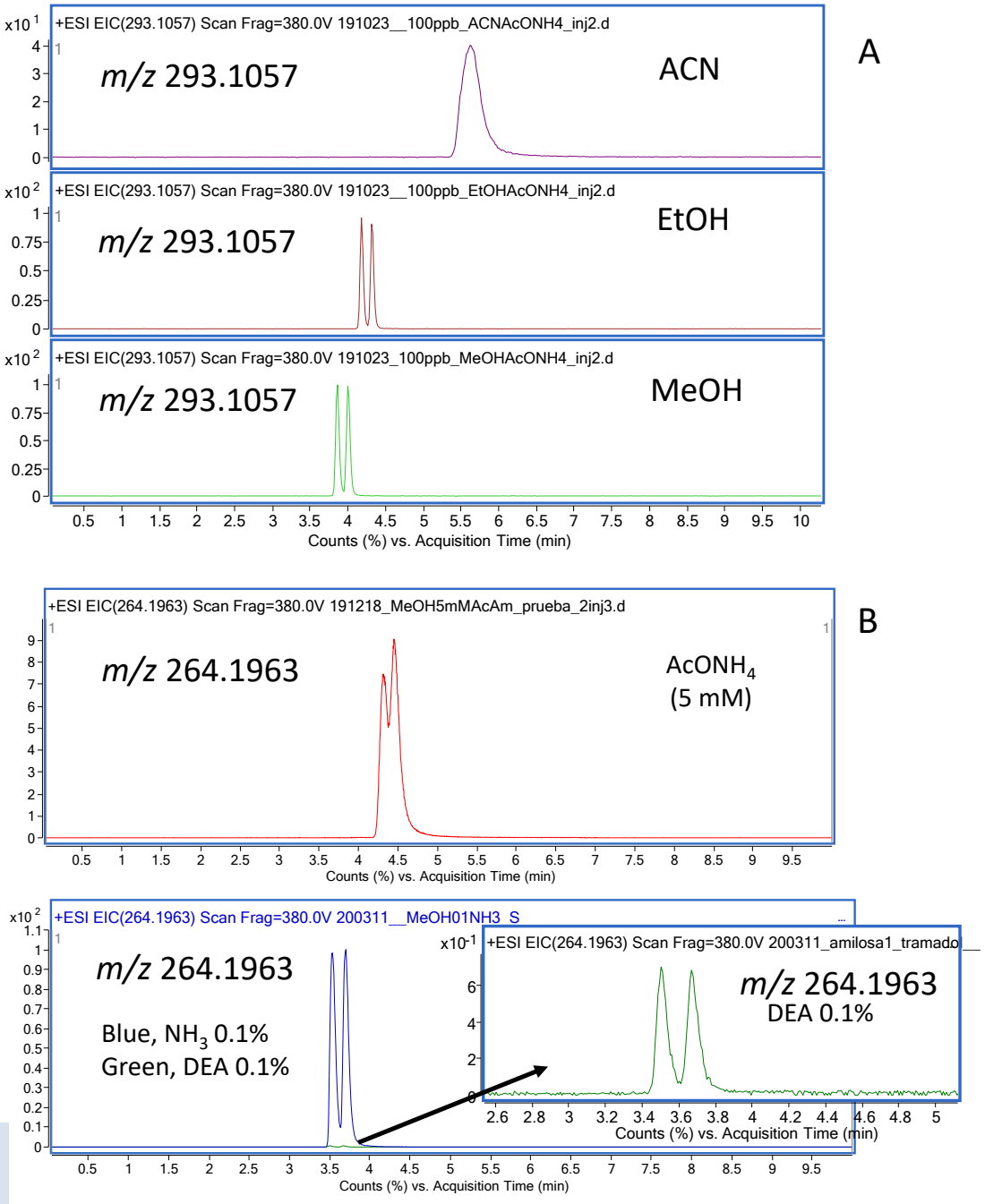


Sertaconazole (STZ)
Log D=5.60, pK_a=6.77



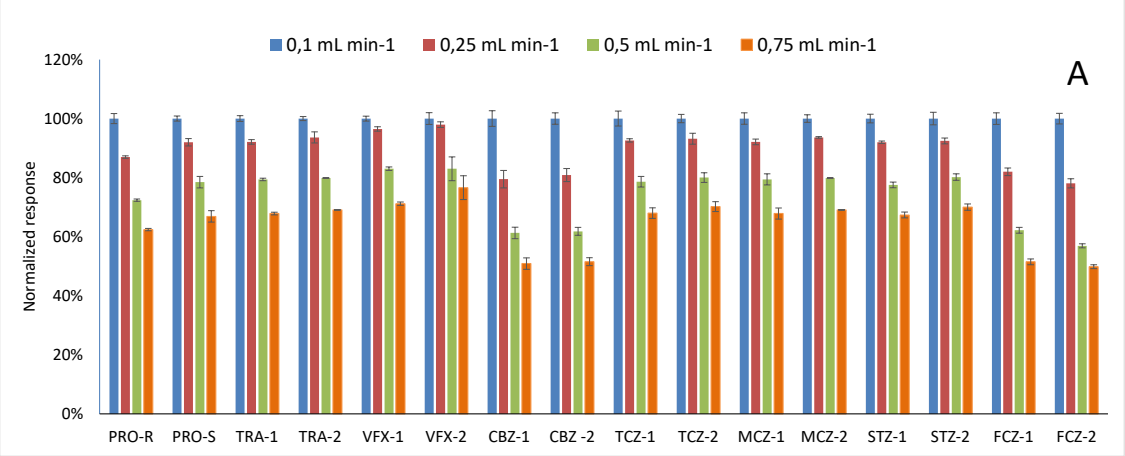
Fenticonazole (FTZ)
Log D= 4.56, pK_a=6.77

Fig. S2. SFC-ESI(+)-MS chromatograms for the $[M+H]^+$ ions of selected compounds using the amylose-1 column. A, Effect of the organic modifier in the retention and resolution of CBZ enantiomers. B, effect of the additive combined with MeOH (as mobile phase organic modifier) in the retention, resolution and ionization efficiency of TRA enantiomers. Mobile phase gradient (0-0.3 min, 2% of organic modifier; 0.2-7 min, 25% of modifier; 7.1-10 min, 2% modifier). Make-up solution MeOH: FA (99.5:0.5, 0.5 mL min^{-1}).



USC UNIVERSIDADE DE SANTIAGO DE COMPOSTELA

Fig. S3. Effect of the make-up solution (MeOH:FA, 99.5:0.5) flowrate in the response of compounds. A, data obtained for solvent-based standards. B, data obtained for a spiked sludge extract.



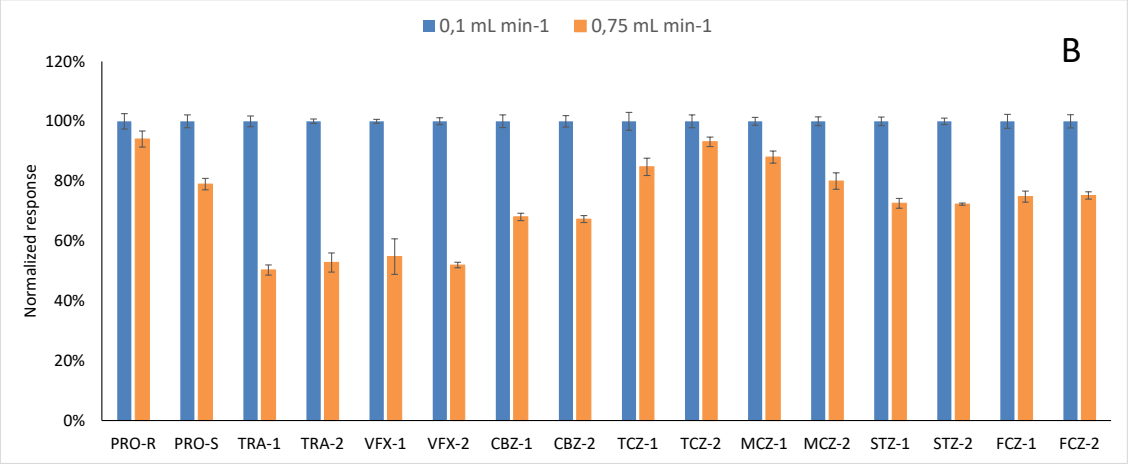


Fig. S4. Chromatographic separation obtained using Amylose-3 (A) and Cellulose-5 (B) columns under conditions reported in Fig. 1 as regards, mobile phase composition and gradient. Chromatograms for a 200 μg L^{-1} standard.

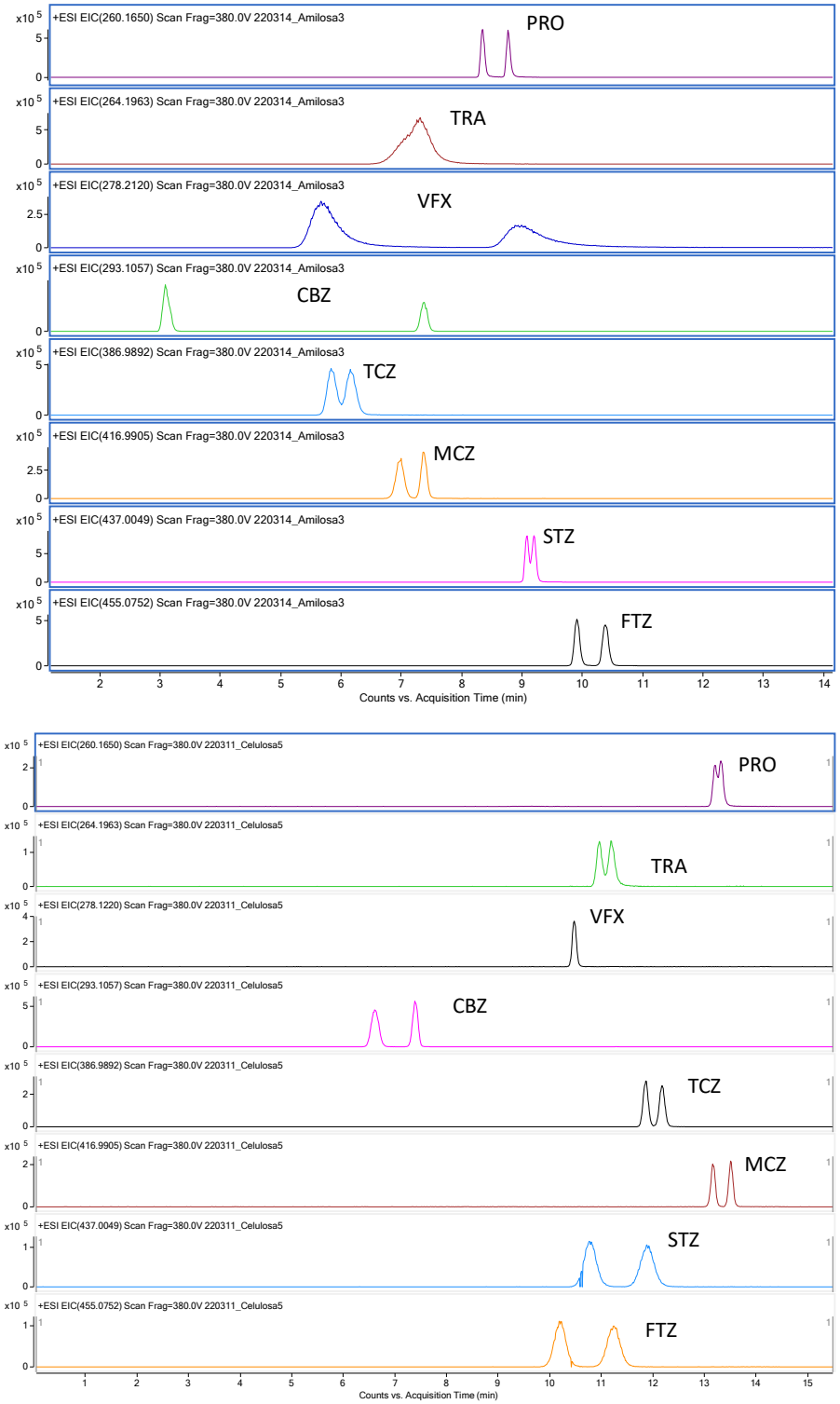


Table S1. Product ion scan parameters for target compounds

Compound	Precursor ion (m/z)	Collision Energy (eV)	Most intense product ion (m/z)	Other product ions (m/z)
PRO	260.1650	20	116.1068	183.0803; 72.0809; 56.0496
TRA	264.1963	10	58.0653	-
VFX	278.2120	20	58.0651	121.064
CBZ	293.1057	20	197.0725	69.0698
TCZ	386.9892	20	130.9715	69.0446; 199.0085
MCZ	416.9905	30	158.9759	69.0444
STZ	437.0049	30	180.9871	69.0446
FTZ	455.0752	30	199.0574	69.0446

USC UNIVERSIDADE DE SANTIAGO DE COMPOSTELA

Table S2. Extraction efficiencies (EEs, %), independent of matrix-effects, of mixed-mode SPE and MSPD procedures applied to wastewater and sludge samples, respectively, n= 3 replicates. Addition level 1 µg L^{-1} and 500 ng g^{-1} for water and sludge samples, respectively.

	Average recovery (%) with standard deviations		
Compound	Raw wastewater	Treated wastewater	Sludge
PRO-R	82% (6)	98% (8)	113% (5)
PRO-S	84% (7)	103% (8)	108% (4)
TRA-1	96% (3)	111% (10)	84% (2)
TRA-2	96% (3)	97% (5)	97% (4)
VFX-1	96%(2)	113% (5)	100% (7)
VFX-2	97% (2)	101% (6)	98% (4)
CBZ-1	98% (3)	103% (5)	84% (4)
CBZ-2	98% (2)	102% (4)	83% (4)
TCZ-1	92% (4)	104% (7)	105% (5)
TCZ-2	91% (4)	102% (5)	117% (3)
MCZ-1	87% (4)	100% (6)	116% (5)
MCZ-2	88% (4)	101% (5)	116% (5)
STZ-1	85% (4)	105% (9)	102% (6)
STZ-2	85% (5)	108% (9)	96% (7)
FTZ-1	68% (7)	94% (11)	95% (3)
FTZ-2	68% (8)	93% (10)	100% (5)

USC UNIVERSIDADE DE SANTIAGO DE COMPOSTELA

Table S3. Average EFs of compounds in samples above method LOQs.

	Compound							
Sample code	PRO	TRA	VFX	CBZ	TCZ	MCZ	STZ	FTZ
RW1	0.471	0.528	0.475	0.497				
TW1	0.372	0.531	0.453	0.497				
RW2	0.401	0.531	0.471	0.502				
TW2	0.415	0.538	0.473	0.489				
RW3	0.429	0.539	0.487	0.498		0.503		
TW3		0.526	0.475	0.494				
RW4		0.553	0.480	0.492		0.546		
TW4	0.402	0.532	0.471	0.495				
RW5	0.452	0.531	0.456	0.458				
TW5	0.497	0.545	0.494	0.443				
RW6		0.515	0.411	0.465				
TW6		0.541	0.443					
RW7	0.431	0.554	0.450	0.466				
TW7	0.439	0.532	0.445					
S1	0.446	0.562	0.470	0.473	0.499	0.482	0.443	0.464
S2		0.517	0.499	0.497	0.451	0.465	0.415	0.436
S3		0.526	0.484	0.505	0.435	0.477	0.411	0.435
S4		0.534	0.464	0.484	0.508	0.541		0.484
S5	0.412		0.480	0.494	0.504	0.505	0.504	0.513
S6			0.487	0.490	0.446	0.488	0.498	0.513
Average	0.431	0.535	0.468	0.485	0.474	0.501	0.454	0.474
Median	0.430	0.532	0.472	0.493	0.475	0.496	0.443	0.474
Min	0.372	0.515	0.411	0.443	0.435	0.465	0.411	0.435
Max	0.497	0.562	0.499	0.505	0.508	0.546	0.504	0.513

USC UNIVERSIDADE DE SANTIAGO DE COMPOSTELA

PUBLICATION VIII: ASSESSMENT OF THE OCCURRENCE AND INTERACTION BETWEEN PESTICIDES AND PLASTIC LITTER FROM VINEYARD PLOTS

M. Cobo-Golpe, P. Blanco, V. Fernández-Fernández, M. Ramil, I. Rodríguez
Science of the Total Environment 912 (2024) 169273
DOI: 10.1016/j.scitotenv.2023.169273



Impact factor: 8.2 (year 2023)
Category: Environmental sciences
Position: 28/359
Quartile: Q1

USC
UNIVERSIDADE DE SANTIAGO DE COMPOSTELA

Science of the Total Environment 912 (2024) 169273

Contents lists available at ScienceDirect

Science of the Total Environment

journal homepage: www.elsevier.com/locate/scitotenv

Assessment of the occurrence and interaction between pesticides and plastic litter from vineyard plots

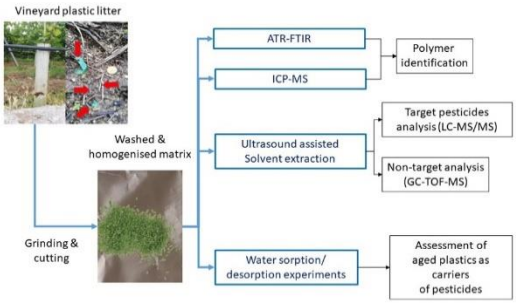
M. Cobo-Golpe [a], P. Blanco [b], V. Fernández-Fernández [a], M. Ramil [a], I. Rodríguez [a,*]

[a] Department of Analytical Chemistry, Nutrition and Food Sciences, IAQBUS - Institute of Research on Chemical and Biological Analysis, Universidade de Santiago de Compostela, R/Constantino Candeira SN, 15782 Santiago de Compostela, Spain
[b] Estación de Viticultura e Enoloxía de Galicia (EVEGA-AGACAL), Ponte San Clodio s/n, 32428 Leiro, Ourense, Spain

HIGHLIGHTS

- Aged plastics from vineyards were identified as polypropylene and polyethylene.
- Pesticides were absorbed inside aged debris of vineyard plastics.
- Different profiles of pesticides were noticed in plastic litter and vineyard soils.
- Aged plastics showed a higher interaction with pesticides than new counterparts.

GRAPHICAL ABSTRACT



ARTICLE INFO

Editor: Yolanda Picó

Keywords:
Agricultural plastics
Fungicides
Vineyard soil
Occurrence
Sorption

ABSTRACT

In this research, aged plastic fragments collected from vineyards were characterized in terms of composition, residues of pesticides, and their potential to exchange these compounds with the aquatic media. To this end, we employed the qualitative and quantitative information provided by complementary analytical techniques, including chromatography, organic and inorganic mass spectrometry, infrared spectroscopy and electronic microscopy. Debris of weathered plastics were identified as polypropylene and polyethylene, containing different types of additives, from organic UV stabilizers to inorganic fillers, such as calcium salts. Regardless of polymer type, plastic litter collected from vineyards contained residues of pesticides, and particularly of fungicides, with total concentrations in the range of values from 114 ng g^{-1} to 76.4 μg g^{-1}. Data obtained under different extraction conditions suggested that a fraction of these compounds was absorbed in aged polymers, penetrating inside the material. The parallel analysis of plastic litter and vineyard soils reflected higher pesticide residues in the former matrix. Furthermore, several fungicides, considered as labile in vineyard soils (i.e. zoxamide and folpet), were those showing the highest levels in plastic litter. Simulated sorption-desorption studies, with plastic debris in contact with surface water, demonstrated the higher affinity of aged materials by moderately polar pesticides than their new counterparts. For the first time, the manuscript highlights the presence of plastic litter in vineyards soils, reflecting the accumulation of several fungicides in this matrix, in some cases, with a different stability pattern to that observed in the soil from same vineyards.

* Corresponding author.
E-mail address: isaac.rodriguez@usc.es (I. Rodríguez).

https://doi.org/10.1016/j.scitotenv.2023.169273
Received 20 September 2023; Received in revised form 8 December 2023; Accepted 8 December 2023
Available online 10 December 2023
0048-9697/© 2023 The Authors. Published by Elsevier B.V. This is an open access article under the CC BY-NC-ND license (http://creativecommons.org/licenses/by-nc-nd/4.0/).

1. Introduction

Viticulture is a very important economic activity, with 80 % of worldwide wine production concentrated in well-defined areas, from just nine countries (Top wine-producing countries, 2022). The geographic concentration of vineyards makes this crop especially susceptible to pests, particularly to fungi and insect-transmitted infections. To treat and to prevent such diseases, under conventional agronomic managing, winegrowers make intensive use of pesticides, and particularly of fungicides and insecticides. The intensity of treatments applied to vineyards has been evaluated using different indicators, such as the so-called frequency treatment index (Fouillet et al., 2022), and it can be confirmed comparing the pesticide application rates to different crops, available in official websites (Statistics of pesticides consumption per crop in Spain, 2019). Moreover, regional (Pérez-Mayán et al., 2020) and supranational (Silva et al., 2019) survey campaigns, monitoring the presence of pesticides in different kinds of agriculture soils and the surrounding environment (Martin et al., 2022), confirmed the high intensity of treatments applied to vineyards.

The use of plastics in agriculture has become a common practice due to their positive effects in the productivity of crops and in the reduction of production costs (Gao et al., 2019). Degradation of these materials under environmental conditions contributes to the spread of smaller fragments in agriculture fields and, eventually, might lead to the production of micro and nanoplastics (Ramos et al., 2015; Steinmetz and Schröder, 2022). By themselves, plastic debris represent a hazard due to the risks of: (1) entering the terrestrial trophic chains through involuntary intake by soil invertebrates (Song et al., 2023), wild and livestock animals (Beriot et al., 2021; Thrift et al., 2022); and (2), migrating to surface and groundwater (Wanner, 2021). In addition, the fragments of plastics are recognized as a potential vector of concerning pollutants, either employed in the formulation of the original polymer (Hu et al., 2022; Li et al., 2021), or sorbed during their contact with crops (Fajardo et al., 2022), contributing to their spread in the environment.

Main types of plastics used in viticulture are guard tubes (Thomas et al., 2017), and tying items (mainly cord and tape). Plant protection tubes (PPT) are used just once when old vines are replaced by young plants. Usually, farmers do not care about these low cost items, which rest in vineyards for a long time, becoming fragile and leading to smaller size fragments, more difficult to collect and easily transported by run-off water and wind. Tying tape (TT) pieces represent a more concerning residue. These small size plastics (typically 1 cm width x 5–20 cm length) either reach the soil of vineyards at the end of winter, when vine canes are pruned; or they remain attached to wirelines existing in vineyards for years. Every new vegetative period of vines (spring and summer in the North hemisphere), new TT items are used. Due to this continuous use and their small size, they have become ubiquitous, difficult to recover and relatively mobile residues (due to wind and run-off water) on top soil of many vineyards. Obviously, both kinds of plastics are exposed to the range of pesticides applied to vineyards for years. Depending on the features of both, pesticides and plastic residues, certain compounds might present a higher stability in plastic debris than in soil and vine leaves. Moreover, the capability of aged plastic fragments to sorb pesticides sprayed on vineyards (mainly fungicides employed to treat mildium, oidium and botrytis infections) (Pérez-Mayán et al., 2020) might differ to that presented by the new polymers (Lan et al., 2021).

The aim of this research was contributing to understand the interactions between pesticides applied to vineyards and the two types of plastics systematically employed in this permanent crop: TT and PPT. This global aim includes evaluating the efficiency of different extraction conditions, the characterization of the residues of pesticides in plastic debris, and the assessment of the role of plastics as carriers of pesticides in the aquatic environment, identifying those parameters which control the distribution of these substances between vineyard plastics and surface water.

2. Materials and methods

2.1. Solvents and standards

Methanol (MeOH), HPLC grade purity was acquired from Merck (Darmstadt, Germany). Dichloromethane (DCM), hexane (Hex) and formic acid (FA) were purchased from VWR chemicals (Radnor, PA, USA). Acetonitrile (ACN) was provided by Thermo Fischer scientific (Waltham, MA, USA). Ultrapure deionized water (18.2 MΩ cm^{-1}) was obtained using a Geni-U system (Rephile, Shanghai, China). Hydrophilic and hydrophobic PTFE syringe filters (0.22 μm pore size, 13 mm diameter) were purchased from Phenomenex (Torrance, CA, USA). Glass fiber filters (0.7 μm cut-off limit, 47 mm diameter) were from Merck.

Standards for a group of 30 fungicides and insecticides were acquired from Sigma-Aldrich (Milwaukee, WI, USA) and Dr. Ehrenstorfer GmbH (Augsburg, Germany). Selection of target compounds was made considering information obtained from winegrowers, and data of occurrence in soil (Pérez-Mayán et al., 2020) and wine samples (Pérez-Mayán et al., 2021) obtained, or produced, from the same geographic area where plastic debris were taken. Labelled analogues (either deuterated or ^{13}C species) of some pesticides were provided by Sigma-Aldrich and Toronto Research Chemicals (North York, Canada). They were employed as surrogate standards (SSs) through the analytical procedures employed in this research. Table 1 summarizes the suite of pesticides considered for determination in plastic debris using a target, multiresidue liquid chromatography triple quadrupole mass spectrometry (LC-QqQ-MS) procedure. Data corresponding to retention times and transitions for each compound, including SSs, are also given in Table 1. Residues of the fungicide folpet in the extracts from plastic debris were investigated by gas chromatography mass spectrometry (GC–MS), using a time-of-flight (TOF) instrument, under conditions provided as Supplementary information, Text S1.

A series of calibration solutions, containing increasing concentrations of LC-MS/MS amenable pesticides (from 1 ng mL^{-1} to 200 ng mL^{-1}), and a constant level of isotopically labelled species (25 ng mL^{-1}) were made in MeOH:ACN (1:1). A second series of calibration standards was prepared in ultrapure water, from 50 ng L^{-1} to 5000 ng L^{-1}, with SSs maintained at 500 ng L^{-1}. In case of folpet, calibration standards were prepared in isooctane, within the range of concentrations from 10 ng mL^{-1} to 1000 ng mL^{-1}, with folpet-d_4 maintained at 500 ng mL^{-1}.

In addition to pesticides compiled in Table 1, standards of other organic compounds (either pesticides or plastic additives), tentatively identified in the extracts from aged plastics from their accurate EI-MS spectra, were used for confirmation purposes.

2.2. Sample collection

Plastic debris were collected from 22 different vineyard plots, within the Denomination of Origin Ribeiro, in Galicia (Northwest Spain). In some cultivars, plastics were collected at different dates and positions: from top soil or attached to vine canes. Overall, 34 samples of plastic litter were obtained in the period comprised between July 2022 to February 2023. All, but one, were obtained after grapes harvest. Attending to their uses, vineyard plastics were classified in two groups. The largest one, with 22 different specimens, corresponded to TT, with a width of 1 cm and different lengths from 1 cm to 20 cm. Most of them showed a green colour, although in one of the vineyards, debris of white TT were also noticed and sampled. Depending on their abundance, from 10 g to 50 g of fragments were collected per vineyard, considering a minimum of 10 square parcels (each 2 m × 2 m) distributed randomly in each cultivar The second group of samples corresponded to PPT. In this case fragments from weathered tubes, dispersed around the protected vines (10 plants per vineyard), were taken. Fig. S1 shows a picture of plastic litter residues commonly noticed at sampling places. Additional to aged materials, their new counterparts were acquired from local distributors. Composite samples of top soil (0–5 cm) were taken from

USC UNIVERSIDADE DE SANTIAGO DE COMPOSTELA

some of the vineyards, considering same sampling places, and dates, as those selected for collection of soil dispersed plastic debris. Each sample of soil corresponded to a minimum of 10 increments, with individual masses around 250 g.

2.3. Sample preparation

After reception, aged plastics were rinsed using ultrapure water and allowed to dry in a hood. PPT fragments were ground using a cutting mill (Retsch, model SM 100), furnished with a 2 mm mesh. After an additional sieving step, the fraction with particle sizes from 0.2 mm to 2 mm was selected for analysis and plastic-water sorption-desorption experiments. Debris of TT were classified attending to colour (green or white), and cut manually (it was not possible to grind this material following same approach used for PPT) in fragments with a size of 0.5 cm × 0.5 cm.

Sample preparation conditions used in the determination of pesticides associated to aged plastics involved extraction (0.5 g sample), with 10 mL of organic solvents, in an ultrasonic bath for 15 min (Elseblani et al., 2023; León et al., 2019). Under final working conditions, a mixture of Hex:DCM (1:1) was employed for extraction purposes. The primary extract was filtered (using lipophilic PTFE syringe filters), concentrated to a final volume of 2 mL, and divided in two fractions. One of them was exchanged to isooctane and used for the qualitative characterization of semi-volatile compounds (in most cases plastic additives), and quantitative determination of the fungicide folpet by GC-TOF-MS. The second fraction was evaporated to dryness, re-dissolved with 1 mL of MeOH:ACN (1:1) and analyzed by LC-MS/MS.

Soil samples were sieved immediately after sampling (in some cases a previous air-dry step was necessary). Thereafter, the fraction below 2 mm was freeze-dried, and stored at −20 °C until analysis. Soils showed a sandy-loam texture, with organic carbon contents in the range from 1.2 % to 2.8 %. Extraction of pesticides from the soil matrix was carried out by pressurized-liquid extraction (PLE), using a mixture of MeOH:ACN (70:30), under conditions reported elsewhere (Pérez-Mayán et al., 2020). The final extract was concentrated to 2 mL before LC-MS/MS analysis. Considering its limited thermal stability, extraction of folpet was carried out using the same protocol applied to aged plastics, in presence of folpet-d_4 as SS.

2.4. Sorption-desorption experiments

The potential of weathered plastic debris as carriers of pesticides in the aquatic environment was evaluated using surface water, obtained from a pristine stream, as model matrix. Accurately weighed samples of different types of plastics (0.40 g) were placed in contact with 200 mL of surface water (see Table S1 for physicochemical features of the water matrix) in closed glass vessels, under magnetic agitation. Vessels were maintained at room temperature (20 ± 2 °C) and protected from light with aluminum foil. Aliquots of water (5 mL) were taken at different times, from 0.5 to 56 h, spiked with SSs (500 ng L^{-1}), filtered and analyzed by LC-MS/MS under conditions reported in Section 2.5, but increasing the injected volume from 0.5 μL to 30 μL. After 56 h, the remaining solution was passed through a 47 mm glass fiber filter (cut-off

Table 1
Summary of retention times, LC-MS/MS determination conditions, and procedural LOQs of pesticides in vineyard soils and agriculture plastic litter.

Abbreviation	Compound	RT (min)	Precursor ion $[M+H]^+$ (*m/z*)	Cone (V)	Q1 (CE. eV)	Q2 (CE. eV)	Ratio (Q1/Q2)	SS	LOQ (ng g^{-1}, soil/plastic)
AME	Ametoctradin	3.18	276	60	70 (50)	176 (35)	0.16	MYC-d_4	0.1/1
AZO	Azoxystrobin	3.37	404	28	329 (30)	372 (15)	0.24	MYC-d_4	1/2
BEN	Benalaxyl	4.42	326.1	26	91 (34)	148 (20)	0.70	MET-$^{13}C_6$	0.5/1
CAR	Carbendazim	1.69	192	33	132 (28)	160 (18)	0.17	CAR-d_3	0.5/1
CHLOF	Clofentezine	4.84	303	28	102 (35)	138 (22)	0.8	MET-$^{13}C_6$	2/4
CHLOR	Chlorpyrifos	5.74	349.9	36	97 (32)	198 (20)	0.65	MYC-d_4	2/4
CHLORM	Chlorpyrifos Methyl	4.98	321.8	34	125 (20)	289.9 (16)	0.194	MYC-d_4	2/4
CYF	Cyflufenamid	5.23	413.2	36	203 (35)	295.1 (15)	0.55	MET-$^{13}C_6$	1/2
CYP	Cyprodinil	2.9	226	56	93 (33)	108 (25)	0.74	CYP-d_5	1/2
DIF	Difenoconazole	4.55	406	46	111.1 (60)	251.1 (25)	0.37	MYC-d_4	1/2
DIM	Dimethomorph	2.95/3.05	388.1	41	165 (30)	300.9 (20)	0.61/0.55	DIM-d_6	1/2
FLUO	Fluopicolide	3.62	383	40	172.9 (20)	365 (15)	0.076	MYC-d_4	1.5/3
IMI	Imidacloprid	2.10	256.1	34	175.1 (20)	209.1 (15)	1	IMI-d_4	5/10
IPROV	Iprovalicarb	3.30	321	28	119 (16)	203.1 (10)	0.32	MET-$^{13}C_6$	1/2
MAN	Mandipropamid	3.5	412	26	125 (35)	328 (16)	0.587	MET-$^{13}C_6$	1.5/3
MET	Metalaxyl	2.71	280.1	26	192.1 (17)	220.1 (13)	0.6	MET-$^{13}C_6$	0.5/1
METR	Metrafenone	5.15	409	28	209.1 (14)	226.9 (16)	0.45	MET-$^{13}C_6$	1/2
MYC	Myclobutanil	3.33	289.1	34	70.2 (18)	125.1 (32)	0.28	MYC-d_4	0.5/1
PEN	Penconazole	3.77	284	34	70.1 (16)	159 (34)	0.31	MYC-d_4	0.5/1
PROP	Propiconazole	4.05	342	46	69 (22)	159 (34)	0.53	MYC-d_4	1.5/3
PYRA	Pyraclostrobin	4.84	388.1	31	163 (25)	193.9 (12)	0.66	MYC-d_4	0.5/1
PYR	Pyrimethanil	2.53	200	51	82 (24)	107 (24)	1.3	PYR-d_5	0.5/1
QUIN	Quinoxyfen	5.07	308	61	161.9 (44)	197 (32)	0.70	MYC-d_4	0.5/1
TEBU	Tebuconazole	3.60	308	40	70.1 (22)	125 (40)	0.071	TEBU-d_9	1/2
TETRA	Tetraconazole	3.54	372	41	70.1 (20)	159 (30)	0.88	TEBU-d_9	1/2
TRIAF	Triadimefon	3.42	294.1	31	69.3 (20)	197.2 (15)	0.75	MYC-d_4	1/2
TRIAL	Triadimenol	3.00	296.1	21	70.2 (10)	99.1 (15)	0.11	MYC-d_4	1/2
TRIF	Trifloxystrobin	5.28	409	34	145 (40)	186 (16)	0.46	MYC-d_4	0.5/1
ZOX	Zoxamide	4.70	336	38	159 (38)	187 (16)	0.484	MYC-d_4	1/2
CAR-d_3	Carbendazim-d_3	1.69	195.1	33	132 (28)	160 (18)	0.201		
CYP-d_5	Cyprodinil-d_5	2.88	231	56	93 (33)	108 (25)	0.449		
DIM-d_6	Dimethomorph-d_6	2.94/3.03	394.2	40	171.1 (30)	307.1 (20)	0.5/0.5		
IMI-d_4	Imidacloprid-d_4	2.10	260.1	34	179.1 (20)	213.1 (15)	1.18		
MET-$^{13}C_6$	Metalaxyl-$^{13}C_6$	2.70	286.1	26	198.1 (17)	226.1 (13)	0.605		
MYC-d_4	Myclobutanil-d_4	3.31	293	34	70 (18)	129 (32)	0.15		
PYR-d_5	Pyrimethanil-d_5	2.52	205	51	82 (24)	107 (24)	0.82		
TEBU-d_9	Tebuconazole-d_9	3.56	317	40	70.1 (22)	125 (40)	0.076		

USC UNIVERSIDADE DE SANTIAGO DE COMPOSTELA

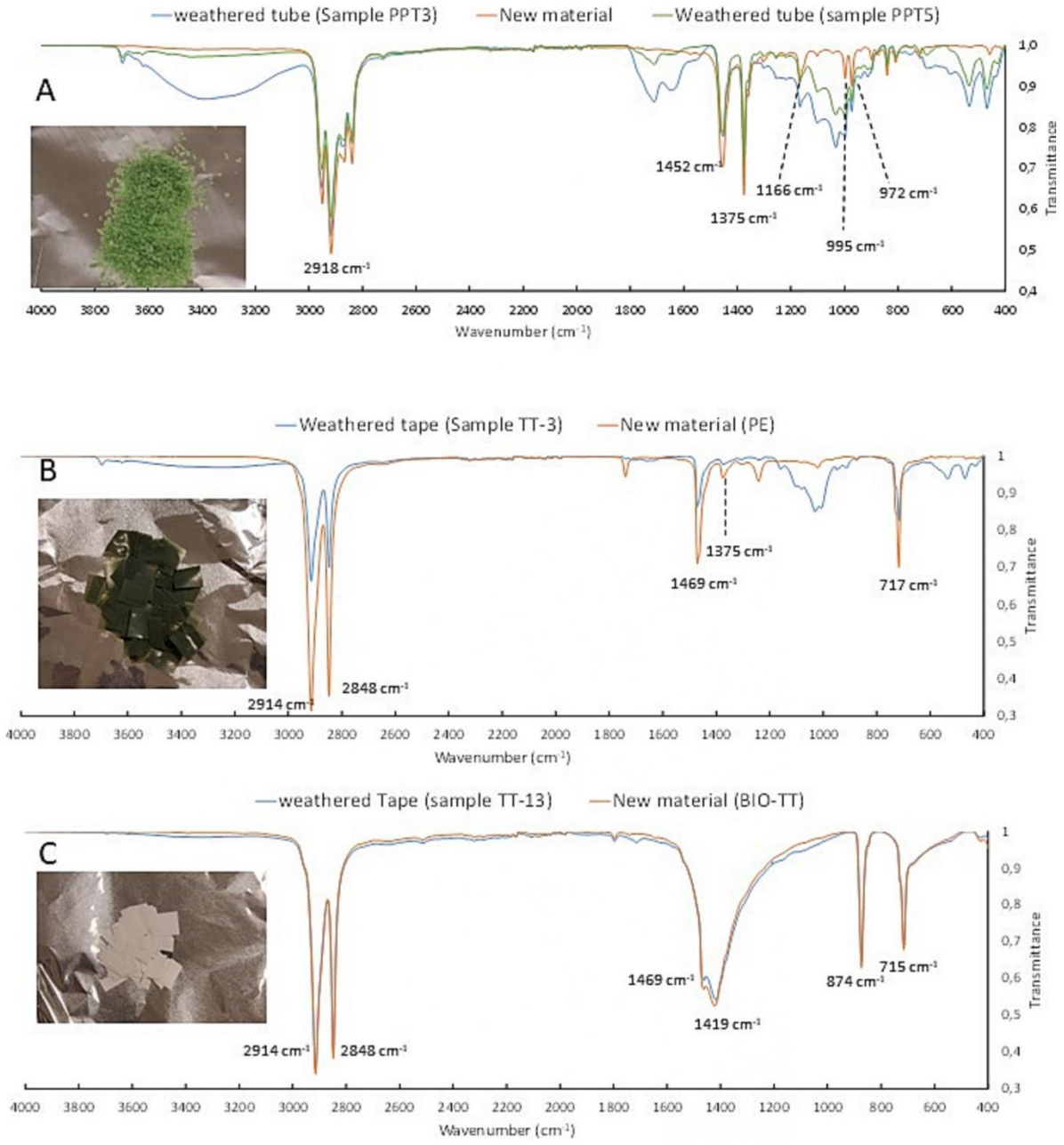


Fig. 1. Pictures of conditioned and ground (or cut) plastic debris collected from vineyards together with the FTIR-ATR spectra for aged materials and their new counterparts. A, Plant protection tube (PPT). B, Conventional tying tape (TT). C, Biodegradable-claimed TT.

threshold 0.7 μm) to recover plastic debris. The filter, with retained plastics, was rinsed with ultrapure water, spiked with SSs, and extracted with a mixture of Hex:DCM as reported in Section 2.3.

Sorption experiments were performed using new items, and previously cleaned (extracted) samples of aged PPT and TT, identified as polypropylene (PP) and polyethylene (PE), respectively. The volume of water and the mass of plastic were the same as in desorption assays. Surface water aliquots were spiked with target pesticides (2 ng mL^{-1}) and homogenized for 30 min before addition of plastic fragments. After 72 h of magnetic stirring, compounds remaining in the water phase and those sorbed on the plastic material were determined by LC-MS/MS as previously reported. Desorption and sorption experiments were carried out in triplicate. The Statgraphics 19 Centurion (The Plains, VA, USA) software package was used to assess the existence of significant differences among sorbed masses of each compound as function of the tested polymer and its degree of aging. To this end, analysis of variance and the least significant difference test were used.

USC UNIVERSIDADE DE SANTIAGO DE COMPOSTELA

2.5. Analytical techniques

LC-MS/MS was used as main technique to determine the residues of pesticides in aged plastic debris, soils, and to investigate the distribution of these compounds between the aqueous phase and plastic fragments in sorption and desorption experiments. The employed instrument consisted of an ultra-performance liquid chromatograph (UPLC) instrument combined with a triple quadrupole mass analyzer (Waters, Acquity UPLC Xevo TQD), equipped with an electrospray source (ESI). The LC column was a Zorbax Eclipse Plus C_{18} rapid resolution (50 mm × 2.1 mm, 1.8 μm) acquired from Agilent Technologies (Wilmington, DE, USA). The analytical column was protected with a C_{18} 2.1 mm i.d. Security Guard™ cartridge, supplied from Phenomenex (Torrance, CA, USA). Chromatographic separation conditions and ESI parameters are provided as Supplementary information, Text S2. Retention times and multiple reaction mode (MRM) detection conditions for native pesticides and isotopically labelled SSs are summarized in Table 1. LOQs achieved for soil and plastic samples are also given in Table 1. In case of water samples analyzed by LC-MS/MS, the concentration of the lowest level standard solution (50 ng L^{-1}) was adopted as the procedural LOQ for all compounds.

Quantification of folpet residues in plastic litter was performed by GC–MS, using an Agilent 7200, TOF instrument, equipped with an electronic ionization (EI) source. Chromatographic separations were carried out using a HP5-MS capillary column (30 m × 0.25 mm, 0.25 μm film thickness), with helium as carrier gas at a flow of 1.2 mL min^{-1}. Additional chromatographic conditions employed during determination of folpet and qualitative characterization of plastic extracts are given as Supplementary information, Text S1. Quantification (Q1) and qualification (Q2) ions for folpet and folpet-d_4 were 259.9334 and 261.9305; 265.9582 and 267.9534, respectively. The Q1 and Q2 ions were extracted using a window of 0.005 Da, and Q2 to Q1 ratios were 0.70 (folpet) and 0.15 (folpet-d_4). Whatever the determination technique (LC-MS/MS or GC–MS), compounds identification was based on retention times match with calibration standards (maximum deviation 0.1 min), and ratios between qualification and quantification product ions (fragments in case of EI-MS) within ±30 % of those obtained for calibration standards.

In addition to chromatography and mass spectrometry techniques, FTIR spectra, acquired in the total attenuated reflectance mode (ATR), were employed for identification of plastic debris collected from vineyards. This information was completed with images obtained using scanning electron microscopy (SEM), and elemental analysis by ICP-MS. In the latter case, samples (0.5 g) were digested with 25 mL of concentrated nitric acid, at atmospheric pressure, in a hot plate, for 4 h. Thereafter, the liquid phase was adjusted to 50 mL, further diluted with ultrapure water and analyzed by ICP-MS for identification and semi-quantitative determination of metallic elements (Elseblani et al., 2023).

2.6. Quality control procedures

Quality control experiments involved (1) the analysis of procedural blanks (either corresponding to river water employed in sorption, desorption experiments, or to the different solvents employed to recover pesticides from plastic litter and soil samples); (2) the assessment of the stability of pesticides in spiked surface water samples employed in sorption studies; (3) verification of the stability of the calibration curves by injection of a calibration standard every 10 injections; (4) comparison of responses for SSs in calibration standards versus extracts obtained from plastic litter; (5) assessing the repeatability of the extraction process for environmental polluted, aged plastics; and (6) testing the accuracy of the analytical procedure for spiked samples of agricultural soils.

3. Results and discussion

3.1. Characterization of plastic debris

The FTIR spectra for new and aged samples of PPT and two types of TT plastics collected from vineyards are shown in Fig. 1. Spectra of PPT items contain the characteristic bands of PP, with a group of four signals around 2918 cm^{-1}, corresponding to symmetric and asymmetric tension of the carbon hydrogen bond in methylene and methyl groups, and two additional intense absorption bands at 1452 cm^{-1} and 1375 cm^{-1}, respectively, Fig. 1A. Weathered samples of PPT, labelled as PPT-3 and PPT-5, presented extra bands in the regions above 3000 cm^{-1}, around 1700 cm^{-1}, and between 1200 cm^{-1} and 1000 cm^{-1}, which point out to oxidation of the hydrocarbon skeleton of PP, Fig. 1A. The experimental

Table 2
Concentrations of fungicides (ng g^{-1}), with standard deviations in parenthesis, measured in sub-samples of different aged plastic debris by LC-MS/MS as function of the extraction solvent, n = 3 replicates.

Sample code	Solvent	CYF	CYP	DIF	IPROV	MAN	MET	MYC	PEN	TEBU	TETRA	ZOX	SUM
PPT-08	MeOH: ACN		64.1 (19.4)		60.2 (11.4)	12.3 (4.0)	52.4 (14.0)	116.8 (22.1)	119.3 (35.1)	92.8 (11.1)	28.7 (3.4)	204.2 (26.4)	750.8
	Hex: DCM	17.1 (2.5)	106.3 (13.9)	22.4 (3.7)	186.9 (5.8)		150.0 (0.9)	191.7 (26.3)	179.2 (30.4)	142.1 (17.0)	50.4 (6.2)	208.9 (9.9)	1255.0
PPT-09	MeOH: ACN							191.6 (17.8)		92.2 (54.7)			283.8
	Hex: DCM							191.0 (11.5)		80.1 (4.9)			271.1
TT-18	MeOH: ACN		19.8 (2.3)					150.1 (11.5)					169.9
	Hex: DCM		106.4 (32.4)					194.0 (50.2)					300.4
TT-20	MeOH: ACN		138.4 (8.5)	12.7 (1.6)			737.5 (291.4)	100.0 (29.9)			20.3 (9.0)	1256.4 (472.7)	2265.3
	Hex: DCM		593.8 (110.4)	89.3 (22.5)			2089.8 (304.1)	590.7 (126.6)		62.8 (74.2)	87.0 (10.1)	2622.9 (500.7)	6136.3
TT-22	MeOH: ACN		43.1 (10.4)	13.5 (2.2)	10.4 (1.1)		5.7 (2.0)	65.9 (7.5)	61.2 (8.7)	89.2 (12.3)	28.9 (5.7)	222.8 (20.0)	540.7
	Hex: DCM	51.5 (10.6)	305.0 (40.3)	65.5 (8.0)	201.3 (20.4)		12.8 (1.3)	334.9 (45.0)	283.5 (7.0)	376.3 (35.2)	193.7 (6.0)	1987.0 (197.5)	3811.5
TT-23	MeOH: ACN		4.6 (1.3)					17.5 (3.7)		17.1 (4.9)			39.2
	Hex: DCM		96.9 (18.7)					50.7 (3.4)		74.2 (13.2)			221.8

USC UNIVERSIDADE DE SANTIAGO DE COMPOSTELA

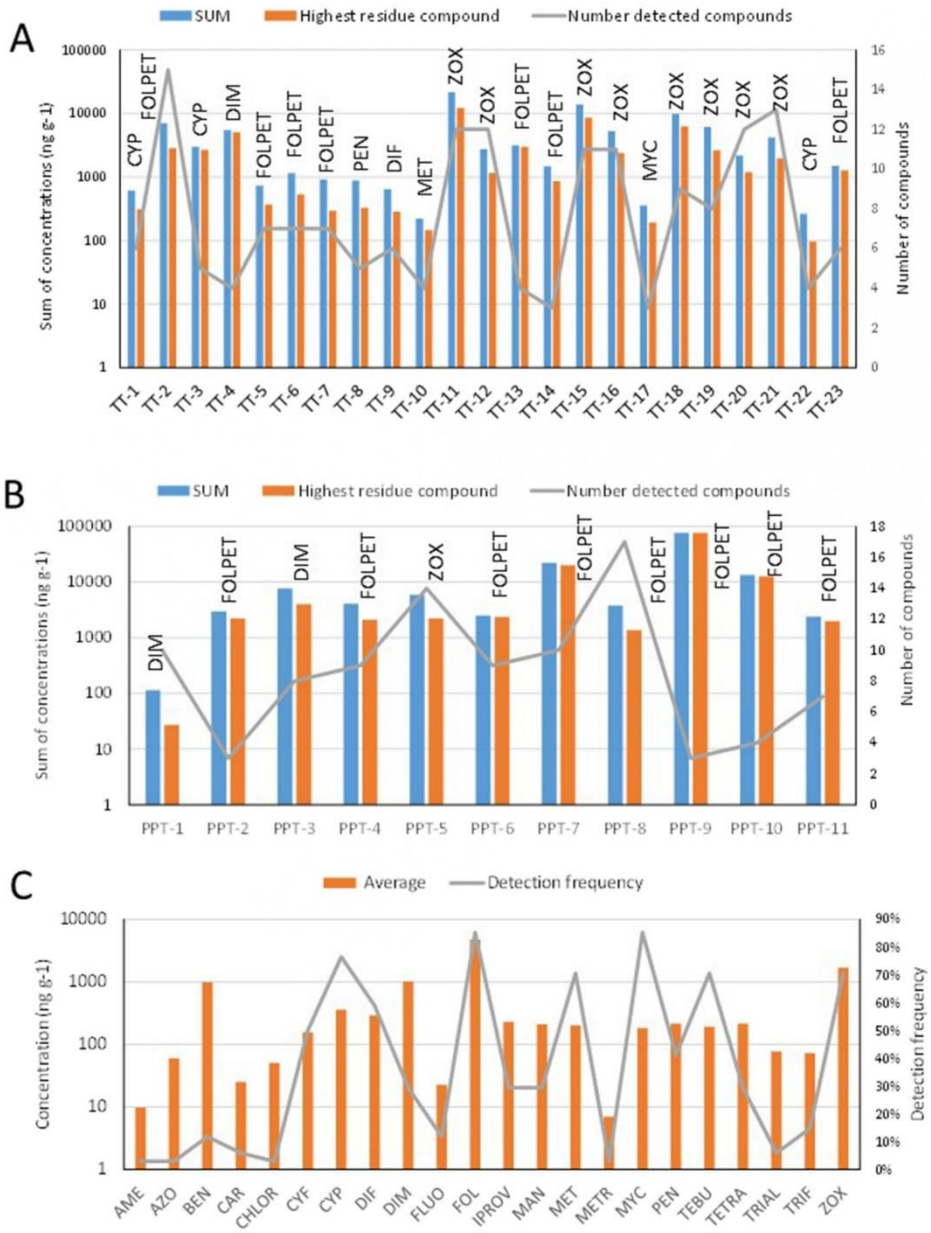


Fig. 2. Summary of total pesticide residues (data in ng g^{-1}) in debris of plastics collected from vineyards. A, Tying tape samples. B, Plant protection tubes. C, Average concentrations of individual pesticides and detection frequencies in all samples.

spectra of a new green-colour TT fitted that of PE, likely low-density PE, considering the low intensity band at 1375 cm^{-1}, Fig. 1B. The record for the aged material keeps most of these bands, showing a moderate degree of oxidation, Fig. 1B. Spectra of TT debris collected from most vineyards matched those shown in Fig. 1B; confirming the prevalent use of PE as material to tie the canes of vines. Fig. 1C presents the spectra for a second type of TT, of white colour, identified just in one of the sampled vineyards. According to the feedback provided by the winegrower, and the available commercial information for new items of the same material, it was sold as biodegradable tying tape. The IR spectra for new and aged pieces of this material retained the four most intense bands noticed in the spectra of conventional PE, Fig. 1B. Moreover, two extra signals at 1419 cm^{-1} and 874 cm^{-1} were present, Fig. 1C.

GC-TOF-MS, ICP-MS and SEM analysis showed also some relevant differences among the three types of plastics. The GC-TOF-MS records for new, green colour, PE tape reflected the presence of TINUVIN-326 as UV absorber. Analysis of weathered samples of TT, with the same colour, confirmed the residues of the UV filter in most samples. In some cases, other UV absorbers belonging to the benzotriazole chemical family (i.e. TINUVIN-328 and TINUVIN-327) were also identified. In the extracts from PPT, a steric hindered amine, termed as TINUVIN-770, was often detected. This compound is also employed as UV filter. The chemical

USC UNIVERSIDADE DE SANTIAGO DE COMPOSTELA

structures, accurate EI-MS spectra, and linear retention index of these compounds are provided as Supplementary information, Fig. S2. None of these UV absorbers were noticed in samples of the biodegradable-claimed tape.

Images obtained by SEM reflected that this later material showed a rough, irregular surface compared to the smooth one of the conventional PE TT, Fig. S3. ICP-MS analysis of both types of TT reflected higher concentrations of Na, Zn, Mg, and particularly Ca, in the tape commercialized with the biodegradable stamp than in the conventional one, Table S2. Calcium content accounted for 4.3 % of the mass of the former polymer. Calcium carbonate is often used as white dye, and filler in polymeric materials. The database IR spectra of this salt contains a broad, intense absorption band at 1425 cm^{-1} and narrow, medium and low intensity ones at 875 cm^{-1} and 712 cm^{-1} (On-line database of infrared and Raman spectra, 2023), which matched extra bands shown in Fig. 1C versus those existing in the spectrum of conventional PE. Some previous studies suggested that the biotic degradation of PE containing calcium carbonate as filler is advantageous compared to that of conventional PE (Croitoru et al., 2017; Husarova et al., 2010). This fact, combined with the absence of UV absorbers in this kind of TT and its rough surface, which might favour microbiological colonization of the material, contributing to its degradation. However, from an academic perspective, PE is not within the list of biodegradable polymers designed for agriculture uses (Serrano-Ruiz et al., 2021).

3.2. Extraction of pesticides from plastic debris

The extraction of pesticides from weathered agricultural plastics (PPT and TT) was assessed using two different mixtures of solvents: MeOH:ACN (1:1) and Hex:DCM (1:1). The first combination of polar solvents has been employed to recover pesticides from vineyard soils (Pérez-Mayán et al., 2020). Moreover, MeOH has been previously applied to the extraction of organic compounds from marine-origin microplastics (León et al., 2019). Combinations of alkanes and DCM are also proposed to recover organic compounds from plastic debris and microplastics collected from different environmental compartments (Elseblani et al., 2023). Extractions were performed in triplicate, with aged plastics (0.5 g) soaked with 10 mL of solvent for 15 min. Regardless of the employed mixture of solvents, responses obtained in consecutive extractions of the same sample remained below 10 % of those obtained in the 1st cycle. Thus, the volume of solvent and the number of extraction cycles were limited to 10 mL and 1 cycle, respectively.

Table 2 summarizes average concentrations, with their standard deviations, for a group of 11 fungicides noticed in six different samples, extracted in triplicate using two different mixtures of solvents. Considering 0.5 g of sample and adjusting the obtained extract to a final volume of 2 mL, the limits of quantification of the LC-MS/MS procedure ranged from 1 ng g^{-1} to 10 ng g^{-1}, depending on the compound (Table 1), with a linear response range up to 800 ng g^{-1}. Samples above this value required a further dilution of the primary extract before quantification. The combination of Hex and DCM led to higher concentrations than the mixture of polar solvents, Table 2. The exception was noticed for sample code PPT-9. In this case, both solutions led to similar residues of the fungicides myclobutanil (MYC) and tebuconazole (TEB).

GC–MS chromatograms corresponding to extracts obtained from the same sample in both mixtures of solvents are provided as Supplementary information, Fig. S4. Whatever the type of polymer (PE or PP), the total ion current (TIC) chromatograms corresponding to the Hex:DCM solution were more complex than those recorded for extracts in MeOH:ACN. The extracted chromatograms (EICs) for characteristic ions of alkanes (m/z values of 57.0698, 71.0855 and 85.1012) in Hex:DCM extracts showed peaks at increasing retention times. Thus, both polyolefins not only swell, but they are partially solubilized in contact with the mixture of Hex:DCM.

Considering data summarized in Table 2, and GC–MS profiles in Fig. S4, it seems feasible that pesticides sprayed in vineyards are not only retained on the surface of plastic debris, but they penetrate inside the polymer. That is, at least one fraction of fungicides identified in the aged debris of PPT and TT is absorbed by the polymeric materials. This assumption agrees also with data reported for non-polar insecticides in laboratory experiments carried out with films of undisturbed PE (Ramos et al., 2015).

If we assume that the interaction between pesticides and aged plastics is different to that observed for new materials, and that the strength of the interaction increases with contact time, assessing the accuracy of data obtained for polluted plastic debris becomes a very difficult task. Considering responses obtained for isotopically labelled compounds, added to samples before extraction, absolute recoveries measured for TT and PPT ranged from 79 % to 114 %, Table S3. The average relative standard deviations of the sample preparation procedure (n = 6 replicates of 0.5 g fractions from two different aged plastics) for compounds noticed above their LOQs were 17 % and 20 %, Table S4.

Table 3
Comparison of average concentrations (ng g^{-1}) measured for pesticides in top-soil samples and soil-dispersed plastic fragments obtained from different vineyards by LC-MS/MS. Average values for duplicate extractions.

Sampling site	1		2		3		4		5			6		7	
Sample type	TT	Soil	TT	Soil	TT	Soil	TT	Soil	TT	PPT	Soil	PPT	Soil	TT	Soil
AZO		6.5		3.8		2.5		92.9			17.0				
BEN										858.0					
CAR						30.0		95.5	41.3	8.6	37.0				
CYF	95.0	15.9	63.0				115.0		51.5	17.1					
CYP	150.8		134.7		593.8	30.3	62.0	6.0	305.0	106.3	11.8			106.4	90.5
DIF	201.6	42.8	222.5	21.3	89.3		1407.8		65.5	22.4	2.8				
DIM		16.7		14.0		32.8		115.0		100.2	36.7		10.0		
FLUO									44.1	16.9	46.3				
IPROV	22.6		14.3				42.6		201.3	186.9					
MAN	32.2	45.3	29.6	21.0			34.4				49.5	563.1	6.9		
MET	13.2	64.5	8.7		2089.8	34.8	56.2	20.6	12.8	150.0	8.8	130.9	6.5		
MYC	36.6	54.5	4.6	30.8	590.7	79.8	48.6	105.3	334.9	191.7	57.0		92.8	194.0	205.8
PEN	75.8	8.4	85.9	4.23					283.5	179.2	21.8				
TEBU	157.0	146.6	189.2	88.5	62.8	14.3	313.4	166.0	376.3	142.1	59.0				
TETRA	26.6		19.9		87.0	2.5	663.2		193.7	50.4	3.8				
TRIAL										151.8					
TRIF					10.6					35.5					
ZOX	1157.4	51.6	1190.7		2622.9		2370.0		1987.0	208.9	5.2	112.2	2.5		
SUM	1968.8	452.8	1963.1	183.5	6146.9	226.8	5113.2	610.4	3896.9	2426	415.5	806.2	128.7	300.4	296.3

USC UNIVERSIDADE DE SANTIAGO DE COMPOSTELA

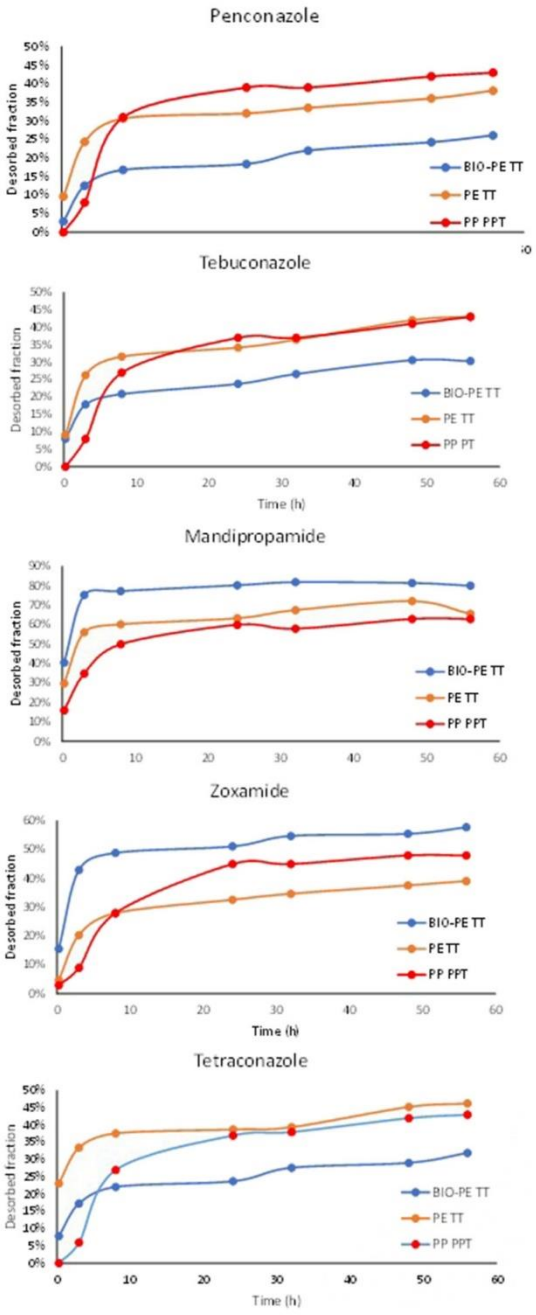


Fig. 3. Time-course of desorbed pesticides fractions from weathered agriculture plastics (0.4000 g) in contact with river water (200 mL). Average values (fraction desorbed to the water phase) for triplicate experiments with each material.

3.3. Occurrence of pesticides in agriculture plastics

Fig. 2 summarizes data of pesticides found in the set of 34 samples of aged plastic debris obtained from different vineyards, processed in duplicate. Values corresponding to TT fragments are shown in Fig. 2A and those measured in PPT in Fig. 2B. The set of compounds investigated in the processed samples were those included in the multiresidue LC-MS/MS procedure (Table 1) plus folpet, determined by GC-TOF-MS. LOQs of the LC-MS/MS method for plastic debris varied between 1 ng g^{-1} and 10 ng g^{-1}. Regarding folpet, a LOQ of 40 ng g^{-1} and a linear range up to 4000 ng g^{-1} was obtained using GC-TOF-MS detection. Every sample of plastic debris contained residues of at least one of the considered pesticides, with a maximum of 17 compounds above their LOQs in sample code PPT-8. Total pesticide residues ranged from 114 ng g^{-1} to above 76,000 ng g^{-1}, case of samples PPT-1 and PPT-9, respectively. Concentrations measured for each individual compound are given as Supplementary information, Table S5. All residues found in aged plastics, except chlorpyrifos, corresponded to fungicides. Species showing detection frequencies equal or above 50 % were cyflufenamid (CYF), cyprodinil (CYP), difenoconazole (DIF), folpet, metalaxyl (MET), myclobutanil (MYC), tebuconazole (TEB) and zoxamide (ZOX), Fig. 2C. Among them, the highest average concentrations corresponded to ZOX and folpet. Folpet is a non-systemic fungicide, included in the formulation of commercial mixtures applied to vineyards at concentrations up to 40 %. It is hardly transferred to wine (Cabras et al., 1997), and shows a limited stability in soil (Bermudez-Couso et al., 2007). On the other hand, folpet has been pinpointed as one of the most often detected compounds in air samples obtained close to arable fields (Zaller et al., 2022), and particularly in the vicinity of vineyards (Martin et al., 2022). ZOX is also regarded as non-persistent in soil (Liu et al., 2023). To the best of our knowledge, none of both fungicides were previously reported in samples of aged agriculture plastics.

In addition to pesticide residues quantified in aged plastics, traces of two fungicides (propiconazole, PROP; and MET) were noticed in new samples of TT and PPT at concentrations between the LOQs of the method and 10 ng g^{-1}. The origin of these compounds remains unclear, and it is not straightforward to determine if agriculture plastics were contaminated with these compounds during production or later, in the distribution process. Both possibilities seem feasible due to recycling of end-of-life agriculture plastics (Martínez Urreaga et al., 2020) and commercialization of new materials in locals which stock and sell commercial fungicide formulations. Conversely to the low residue levels of both fungicides, metrafenone (METR) was quantified in different items of new TT, at levels in the range of 3700 ng g^{-1} to 4000 ng g^{-1}. Such values were considered too high to be regarded as an accidental contamination. Thus, we assume that the fungicide was intentionally included in the formulation of this material. Levels of METR in new items decreased in more than 90 %, when the PE material was exposed to outdoors conditions for 48 h. This behavior agrees with the fast dissipation of the pesticide under simulated solar light (López-Fernández et al., 2018); moreover, it explains why METR was hardly identified in aged samples of agriculture plastics, Table S5.

Deconvolution of GC-TOF-MS records for extracts of aged plastics reflected the existence of some additional pesticides. In brief, 50 % of the analyzed PPT contained residues of the fungicide dichlofluanid; moreover, the herbicide oxyfluorfen was often noticed in this type of plastics and the insecticide deltramethrin in fragments of TT. Although their concentrations were not determined, the identity of these species was confirmed using authentic standards. Dichlofluanid lost the authorization of use by 2009; thus, its presence in weathered debris of PP confirms the stability of both, the fungicide and the debris of PP in the environment of vineyards. Another example of a non-currently authorized fungicide, quantified in aged fragments of PPT was triadimenol, Table S5. Regarding oxyfluorfen, according to the Spanish Ministry of Agriculture (Statistics of pesticides consumption per crop in Spain, 2019), this is one of the most often used herbicides to control vegetation in vineyards. Considering that PPT are in direct contact with soil, it is not strange that this material retains residues of herbicides sprayed on vineyards.

USC UNIVERSIDADE DE SANTIAGO DE COMPOSTELA

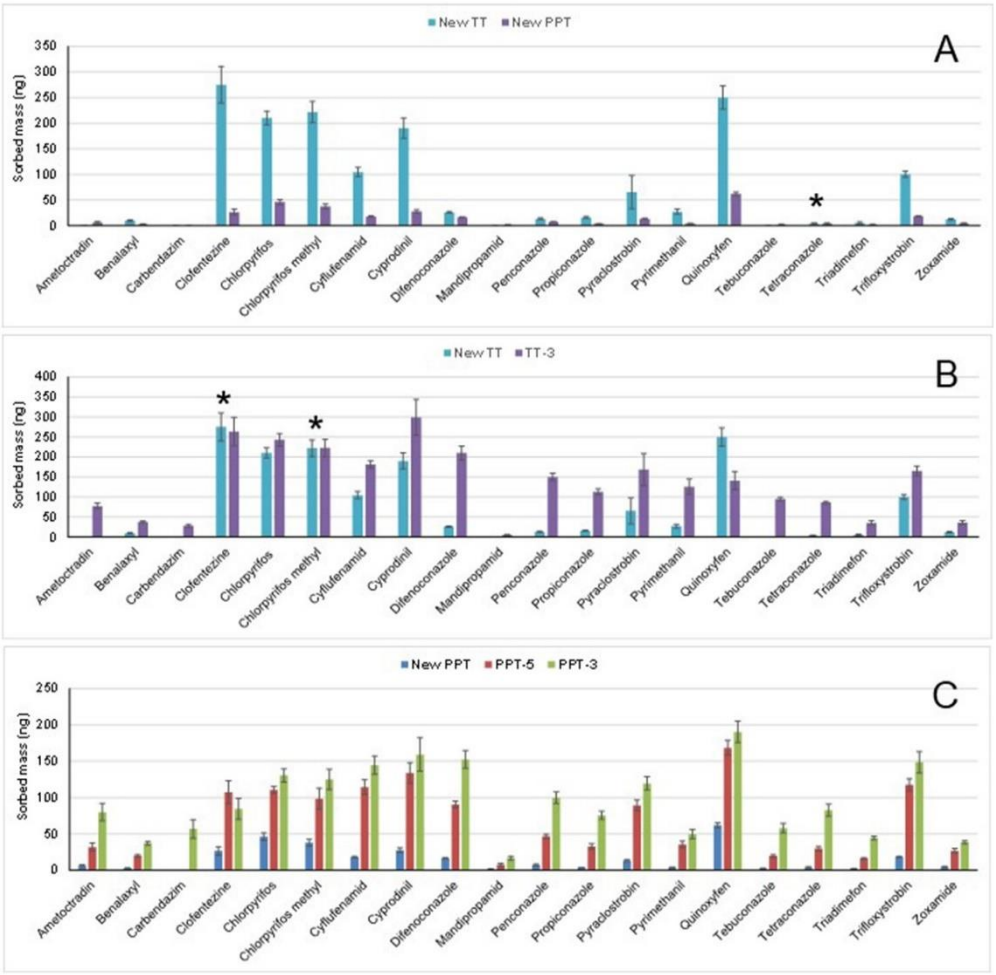


Fig. 4. Comparison of sorbed amounts (mass in ng) of pesticides in PE-made tying tape (TT) and PP plants protection tubes (PPT) in contact with pesticide spiked river water (200 mL, addition level 2 ng mL^{-1}). Average data with standard deviations ($n = 3$ replicates). A, Comparison of new polymers. B, Effect of aging in the masses sorbed by TT made of low-density PE. C, Effect of aging in masses sorbed by PPT made of PP. Asterisk marked bars correspond to non-significative differences (95 % confidence level) of sorbed masses between investigated conditions.

3.4. Pesticide residues in plastics versus soil

To confirm the different levels of pesticides in aged plastics, in direct contact with the soil of vineyards, and soils, samples of both matrices were simultaneously taken in seven cultivars and analyzed using LC-MS/MS as determination technique. Accuracy of results obtained from soil samples were evaluated with samples spiked at two different concentration levels (10 ng g^{-1} and 100 ng g^{-1}), processed in triplicate. Recoveries varied between 75 % and 111 %, with average standard deviation values of 16 % and 7 % for low and high addition levels, respectively, Table S6. In case of folpet, using GC–MS analysis, the recovery for soil spiked at 800 ng g^{-1} was 118 %, with a standard deviation of 6 %. Table 3 summarizes the concentrations of LC-MS/MS amenable pesticides in these pairs of samples. Folpet was not included in this Table 3, since this compound was found only in aged plastic debris but not in soil samples at concentrations above its LOQ (25 ng g^{-1}). Even without considering the contribution of this compound, the sum of concentrations for the rest of pesticides found in plastic were higher than those existing in soils, except for samples obtained at site number 7. As expected, concentrations of ZOX were significantly higher in plastic debris than in soil. Apart from the parent compound, potential degradation products of ZOX (sharing the most intense fragment ion in the spectra of the parent fungicide for the methyl-dichloro-benzamide moiety) were tentatively identified in GC-TOF-MS chromatograms corresponding to aged plastics. Their experimental accurate EI-MS spectra are given as Supplementary information, Fig. S5. On the other hand, azoxystrobin and carbendazim were quantified in soil from several fields; however, they remained undetected in plastics collected from same sites, Table 3. It is worth to note that, the range of values for total pesticide residues in vineyard soils (from 129 ng g^{-1} to 610 ng g^{-1}) was similar to that reported in our former study from year 2020, for top soil samples collected between 2017 and 2019 (Pérez-Mayán et al., 2020). On the other hand, literature references to compare residues measured in plastic debris could not be found. Overall, data in Table 3 suggest that the relative stabilities, and the degradation routes of fungicides in vineyard soil and plastic debris show significant differences.

USC UNIVERSIDADE DE SANTIAGO DE COMPOSTELA

3.5. Desorption and sorption experiments

Fragmented plastics noticed in the soil of vineyards are susceptible of migration to surface water due to run-off; thus, we investigated the potential transference of pesticides from weathered, partially oxidized, plastics to the water phase. The study was limited to LC-MS/MS amenable compounds, so migration of folpet was not assessed. Fig. 3 shows the average water migration fraction ($n = 3$ replicates) for a selection of fungicides noticed in the three different types of weathered plastics identified in this research. Time-course fractions for compounds whose desorption could be followed in one of the investigated materials are provided as Supplementary information, Fig. S6. As a general statement, the equilibrium between desorbed concentrations and pesticide residues associated to plastic litter was achieved after 24 h, with little (case of penconazole and TEB), or null increase in dissolved concentrations (mandipropamide, ZOX and tetraconazole) at longer times. In some cases, significant desorbed percentages were noticed just after 0.5 h. This behavior points out to a readily available adsorbed fraction of pesticides in some plastics, whilst further desorption processes require the migration of the compounds from inside the materials to the bond with the water sample. For pesticides in Fig. 3, equilibrium desorbed fractions ranged from 20 % to 80 %, depending on the considered compound and the type of plastic. Likely, the lower the polarity and the water solubility of a pesticide, the smaller the fraction released to the water phase. On the other hand, the type of polymer, and its oxidation degree might also affect the desorption equilibria. In this vein, polar compounds might be more strongly retained by highly oxidized polymers than by their new, lipophilic polyolefin (PE or PP) counterparts.

To verify the latter hypothesis a 2nd series of experiments was carried out. In this case, the sorption capabilities of new and aged materials were compared. The employed samples corresponded to PP PPT and conventional PE TT, whose IR spectra are shown in Fig. 1A and B, respectively. Fig. 4 summarizes the masses of 20 compounds found in the plastic residue above their LOQs after 72 h. Eight pesticides (azoxystrobin, dimethomorph, fluopicolide, imidacloprid, iprovalicarb, MET, MYC and triadimenol) remained under their LOQs in plastic material. Thus, taking into account their initial amount in the water solution (400 ng) and their LOQs for plastics (Table 1), it can be concluded that the sorption efficiencies of these eight compounds remained below 2.5 %. METR was also excluded from Fig. 4 since it could not be completely removed from the new TT material. The influence of the type of polymer on pesticides sorption capabilities is shown in Fig. 4A. In general, pieces (0.5 cm × 0.5 cm) of new PE tape showed a higher sorption capability (95 % confidence level) than ground new PP guard tubes. The only exception corresponded to tetraconazole. In this case, no significant differences were noticed between amounts sorbed by the two polymers. The effect of environmental oxidation in the sorption capability of each material are shown in Fig. 4B and C. For PE-made TT, the sorbed amounts of less polar compounds (clofentezine, and methyl chlorpyrifos; log D values from 3.8 to 5.0, at pH 7) were equivalent (95 % confidence level) for new and aged PE, for quinoxyfen (log D 5.2 at pH 7) the sorbed amount decreased for the aged polymer, and the rest of compounds showed a higher, statistically significant affinity to pieces of aged PE tape than to the new items, Fig. 4B. In case of PP, the sorbed masses of every compound (except clofentezine) increased significantly with the oxidation degree of the polymer, Fig. 4C. That is, in general, changes in the composition of both kinds of agricultural plastics (PE and PP) under environmental conditions increase significantly (95 % confidence level) their capability to sorb medium polarity fungicides used to protect vines against mildium, oidium and botrytis infections.

4. Conclusions

Most of the residues of tying tape and plant protection tubes collected from vineyards corresponded to low-density PE and PP polymers. The analysis of these materials reflected the presence of significant levels of several pesticides, particularly fungicides, including compounds considered as non-persistent in soils, as it is the case of folpet and ZOX. Assessment of extraction conditions applied to aged plastics reflected that fungicides are not only adsorbed on the surface, but also absorbed inside the polymeric materials. The strength of the interaction plastic-pesticide is function of the type of plastic and the features of the pesticides. Moreover, aging of tying tape and plant protection tubes polymers significantly increased their capability to sorb medium polarity compounds from model surface water solutions. On the opposite direction, migration of same compounds from aged, polluted plastic litter to surface water is expected to be also affected by the previous weathering of the host materials. Despite sorption studies reflecting a low affinity of new and aged plastic residues by medium polarity fungicides (i.e. MET, MYC, ZOX), most of these compounds were found in aged plastic debris collected from vineyards, suggesting a good environmental stability when sprayed directly on these materials.

Findings obtained in this manuscript reveal the need to adopt an unambiguous definition of biodegradable plastics developed for agricultural uses, including information of the employed polymer. It is also advised to be aware of the existence of pesticide residues in vineyard plastics before considering the possibility of being recycled to produce new goods. Further research on other kinds of agricultural plastics, employed in higher amounts (i.e. greenhouse and mulching films), must be performed to assess the extent of pesticide residues in these materials.

CRediT authorship contribution statement

M. Cobo-Golpe: Investigation, Methodology, Writing – review & editing. **P. Blanco:** Investigation, Methodology, Writing – review & editing. **V. Fernández-Fernández:** Investigation, Methodology, Writing – review & editing. **M. Ramil:** Funding acquisition, Investigation, Supervision, Writing – review & editing. **I. Rodríguez:** Conceptualization, Funding acquisition, Project administration, Supervision, Writing – original draft.

Declaration of competing interest

The authors declare that they have no known competing financial interests or personal relationships that could have appeared to influence the work reported in this paper.

Data availability

Data will be made available on request.

Acknowledgements

Economic support from projects TED2021-129962B-C42, funded by the Spanish Ministry of Science and Innovation, through the UE Next Generation program; and ED431C2021/06, from Xunta de Galicia, co-financed the EU FEDER program, is acknowledged. M.C. thanks a FPI contract to the Spanish Ministry of Science and Innovation. We thank Prof. A. Moreda for ICP-MS analysis of digested polyethylene tying tape.

Appendix A. Supplementary data

Supplementary data to this article can be found online at https://doi.org/10.1016/j.scitotenv.2023.169273.

References

Beriot, N., Peek, J., Zornoza, R., Geissen, V., Huerta Lwanga, E., 2021. Low density-microplastics detected in sheep faeces and soil: a case study from the intensive vegetable farming in Southeast Spain. Sci. Total Environ. 755, 142653 https://doi.org/10.1016/j.scitotenv.2020.142653.

UNIVERSIDADE DE SANTIAGO DE COMPOSTELA

Bermudez-Couso, A., Arias-Estévez, M., Nóvoa-Muñoz, J.C., López-Periago, E., Soto-González, B., J.S.-G., 2007. Seasonal distributions of fungicides in soils and sediments of a small river basin partially devoted to vineyards. Water Res. 41, 4515–4525. https://doi.org/10.1016/j.watres.2007.06.029.

Cabras, P., Angioni, A., Garau, V.L., Melis, M., Pirisi, F.M., Farris, G.A., Sotgiu, C., Minelli, E.V., 1997. Persistence and metabolism of folpet in grapes and wine. J. Agric. Food Chem. 45, 476–479. https://doi.org/10.1021/jf960353a.

Croitoru, C., Pascu, A., Roata, I.C., Stanciu, E.M., 2017. Obtaining and characterization of polyolefin-filled calcium carbonate composites modified with stearic acid. IOP Conf. Ser. Mater. Sci. Eng. 209, 012041 https://doi.org/10.1088/1757-899X/209/1/012041.

Elseblani, R., Cobo-Golpe, M., Godin, S., Jimenez-lamana, J., Fakhri, M., Rodríguez, I., Szpunar, J., 2023. Study of metal and organic contaminants transported by microplastics in the Lebanese coastal environment using ICP-MS, GC-MS, and LC-MS. Sci. Total Environ. 887, 164111 https://doi.org/10.1016/j.scitotenv.2023.164111.

Fajardo, C., Martín, C., Costa, G., Sánchez-Fortún, S., Rodríguez, C., de Lucas Burneo, J. J., Nande, M., Mengs, G., Martín, M., 2022. Assessing the role of polyethylene microplastics as a vector for organic pollutants in soil: ecotoxicological and molecular approaches. Chemosphere 288, 132460. https://doi.org/10.1016/j.chemosphere.2021.132460.

Fouillet, E., Deliere, L., Chartier, N., Munier-Jolain, N., Cortel, S., Rapidel, B., Merot, A., 2022. Reducing pesticide use in vineyards. Evidence from the analysis of the French DEPHY network. European. J. Agron. 136, 126503 https://doi.org/10.1016/j.eja.2022.126503.

Gao, H., Yan, C., Liu, Q., Ding, W., Chen, B., Li, Z., 2019. Effects of plastic mulching and plastic residue on agricultural production: a meta-analysis. Sci. Total Environ. 651, 484–492. https://doi.org/10.1016/j.scitotenv.2018.09.105.

On-line database of infrared and Raman spectra [WWW Document]. URL. http://www.irug.org (accessed 9.13.23).

Top wine-producing countries [WWW Document]. URL. https://italianwinecentral.com/top-fifteen-wine-producing-countries/ (accessed 9.13.23).

Statistics of pesticides consumption per crop in Spain [WWW Document]. URL. https://www.mapa.gob.es/es/estadistica/temas/estadisticas-agrarias/agricultura/estadisticas-medios-produccion/fitosanitarios.aspx (accessed 9.13.23).

Hu, X., Yu, Q., Gatheru Waigi, M., Ling, W., Qin, C., Wang, J., Gao, Y., 2022. Microplastics-sorbed phenanthrene and its derivatives are highly bioaccessible and may induce human cancer risks. Environ. Int. 168, 107459 https://doi.org/10.1016/j.envint.2022.107459.

Husarova, L., Machovsky, M., Gerych, P., Houser, J., Koutny, M., 2010. Aerobic biodegradation of calcium carbonate filled polyethylene film containing pro-oxidant additives. Polym. Degrad. Stab. 95, 1794–1799. https://doi.org/10.1016/j.polymdegradstab.2010.05.009.

Lan, T., Wang, T., Cao, F., Yu, C., Chu, Q., Wang, F., 2021. A comparative study on the adsorption behavior of pesticides by pristine and aged microplastics from agricultural polyethylene soil films. Ecotoxicol. Environ. Saf. 209, 111781 https://doi.org/10.1016/j.ecoenv.2020.111781.

León, V.M., García-Agüera, I., Moltó, V., Fernández-González, V., Llorca-Pérez, L., Andrade, J.M., Muniategui-Lorenzo, S., Campillo, J.A., 2019. PAHs, pesticides, personal care products and plastic additives in plastic debris from Spanish Mediterranean beaches. Sci. Total Environ. 670, 672–684. https://doi.org/10.1016/j.scitotenv.2019.03.216.

Li, Q., Zeng, A., Jiang, X., Gu, X., 2021. Are microplastics correlated to phthalates in facility agriculture soil? J. Hazard. Mater. 412, 125164 https://doi.org/10.1016/j.jhazmat.2021.125164.

Liu, H., Wang, Y., Shi, X., 2023. Co-existing antibiotics alter the enantioselective dissipation characteristics of zoxamide and drive combined impact on soil microenvironment. J. Environ. Manag. 344, 118340 https://doi.org/10.1016/j.jenvman.2023.118340.

López-Fernández, O., Pose-Juan, E., Yáñez, R., Rial-Otero, R., Simal-Gándara, J., 2018. Modelling the isothermal degradation kinetics of metrafenone and mepanipyrim in a grape juice analog. Food Res. Int. 108, 339–346. https://doi.org/10.1016/j.foodres.2018.03.058.

Martin, S., Dévier, M.H., Cruz, J., Duporté, G., Barron, E., Gaillard, J., Le Menach, K., Pardon, P., Augagneur, S., Flaud, P.M., Villenave, É., Budzinski, H., 2022. Passive sampling as a tool to assess atmospheric pesticide contamination related to vineyard land use. Atmosphere (Basel) 13, 504. https://doi.org/10.3390/atmos13040504.

Martínez Urreaga, J., Beltrán, F.R., Acosta, J., Aguinaco, T., Fonseca, C., Ochoa, A., Oliet Palá, J.A., González-Sánchez, C., de la Orden, M.U., 2020. Tube shelters from agricultural plastic waste: an example of circular economy. J. Clean. Prod. 268, 122401 https://doi.org/10.1016/j.jclepro.2020.122401.

Pérez-Mayán, L., Ramil, M., Cela, R., Rodríguez, I., 2020. Multiresidue procedure to assess the occurrence and dissipation of fungicides and insecticides in vineyard soils from Northwest Spain. Chemosphere 261, 127696. https://doi.org/10.1016/j.chemosphere.2020.127696.

Pérez-Mayán, L., Ramil, M., Cela, R., Rodríguez, I., 2021. Determination of pesticide residues in wine by solid-phase extraction on-line combined with liquid chromatography tandem mass spectrometry. J. Food Compos. Anal. 104, 104184 https://doi.org/10.1016/j.jfca.2021.104184.

Ramos, L., Berenstein, G., Hughes, E.A., Zalts, A., Montserrat, J.M., 2015. Polyethylene film incorporation into the horticultural soil of small periurban production units in Argentina. Sci. Total Environ. 523, 74–81. https://doi.org/10.1016/j.scitotenv.2015.03.142.

Serrano-Ruiz, H., Martin-Closas, L., Pelacho, A.M., 2021. Biodegradable plastic mulches: impact on the agricultural biotic environment. Sci. Total Environ. 750, 141228 https://doi.org/10.1016/j.scitotenv.2020.141228.

Silva, V., Mol, H.G.J., Zomer, P., Tienstra, M., Ritsema, C.J., Geissen, V., 2019. Pesticide residues in European agricultural soils – a hidden reality unfolded. Sci. Total Environ. 653, 1532–1545. https://doi.org/10.1016/j.scitotenv.2018.10.441.

Song, W., Du, Y., Li, D., Xiao, Z., Li, B., Wei, J., Huang, X., Zheng, C., Wang, Jinhua, Wang, Jun, Zhu, L., 2023. Polyethylene mulch film-derived microplastics enhance the bioaccumulation of atrazine in two earthworm species (Eisenia fetida and Metaphire guillelmi) via carrier effects. J. Hazard. Mater. 455, 131603 https://doi.org/10.1016/j.jhazmat.2023.131603.

Steinmetz, Z., Schröder, H., 2022. Plastic debris in plastic-mulched soil-a screening study from western Germany. PeerJ 10, 13781. https://doi.org/10.7717/peerj.13781.

Thomas, A.L., Harris, J.L., Bergmeier, E.A., Striegler, R.K., 2017. Establishment technique and rootstock impact 'chambourcin' grapevine morphology and production in Missouri. Horttechnology 27, 248–256. https://doi.org/10.21273/HORTTECH03610-16.

Thrift, E., Porter, A., Galloway, T.S., Coomber, F.G., Mathews, F., 2022. Ingestion of plastics by terrestrial small mammals. Sci. Total Environ. 842, 156679 https://doi.org/10.1016/j.scitotenv.2022.156679.

Wanner, P., 2021. Plastic in agricultural soils – a global risk for groundwater systems and drinking water supplies? – a review. Chemosphere 264, 128453. https://doi.org/10.1016/j.chemosphere.2020.128453.

Zaller, J.G., Kruse-Plaß, M., Schlechtriemen, U., Gruber, E., Peer, M., Nadeem, I., Formayer, H., Hutter, H.P., Landler, L., 2022. Pesticides in ambient air, influenced by surrounding land use and weather, pose a potential threat to biodiversity and humans. Sci. Total Environ. 838, 156012 https://doi.org/10.1016/j.scitotenv.2022.156012.

USC UNIVERSIDADE DE SANTIAGO DE COMPOSTELA

Supplementary information to manuscript:

Assessment of the occurrence and interaction between pesticides and plastic litter from vineyard plots

M. Cobo-Golpe[a], P. Blanco[b], V. Fernández-Fernández[a], M. Ramil[a], I. Rodríguez[a]*

[a] *Department of Analytical Chemistry, Nutrition and Food Sciences, IAQBUS - Institute of Research on Chemical and Biological Analysis, Universidade de Santiago de Compostela, R/Constantino Candeira SN, 15782 Santiago de Compostela, Spain.*

[b] *Estación de Viticultura e Enoloxía de Galicia (EVEGA-AGACAL), Ponte San Clodio s/n, 32428, Leiro-Ourense.*

*Corresponding author
e-mail: isaac.rodriguez@usc.es

USC UNIVERSIDADE DE SANTIAGO DE COMPOSTELA

Text S1. GC-TOF-MS determination conditions

Quantitative determination of folpet residues and identification of semi-volatile additives and pesticides in extracts from plastic debris was carried-out by GC-MS, using a quadrupole, time-of-flight mass instrument (Agilent GC-TOF-MS model 7200), operated in the single MS mode. Spectra were recorded in the profile mode, within the range from 60 to 700 Da, at a rate of 5 spectra s^{-1}. The injection volume was 1 μL, with the injector operated in the splitless mode (purge time 60 mL min^{-1} after 1 min). Injector and transfer line temperatures were set at 280 ºC. The temperatures of the electron ionization (EI) source and the quadrupole were 230 ºC and 150 ºC, respectively. Two different oven temperature programs were employed. During screening of additives and pesticides sorbed on aged plastic debris the temperature of the column was varied as follows: 65 ºC (1 min), 5 ºC min^{-1} to 290 ºC (8 min). For the quantitative determination of folpet, same initial and final oven temperature were employed, with a gradient of 12 ºC min^{-1}.

Instrumental limits of quantification for folpet and linear response range were 10 ng mL^{-1} and 1000 ng mL^{-1}, with a determination coefficient of 0.995 considering six-level calibration standards prepared in isooctane. The procedural LOQs for Folpet analysis in soil and plastic debris were 25 ng g^{-1} and 40 ng g^{-1}, respectively. Corrected recoveries for extraction of Folpet from spiked soils (addition level 250 ng g^{-1}) were 108 %, with a standard deviation of 5%.

Identification of polymer additives (UV stabilizers) and additional pesticides in extracts from plastic litter was carried out as described elsewhere [101]. In brief, raw chromatograms were deconvoluted using the *Unknowns Analysis* software (part of MassHunter Quantitative package); then, accurate spectra were compared to those compiled in the low resolution NIST17 EI-MS database, and accurate EI-MS libraries provided by Agilent. When commercially available, identities of tentatively identified pesticides were confirmed with authentic standards.

References:

Cobo-Golpe, M., Ramil, M., Cela, R., Rodríguez, I., 2020. Portable dehumidifiers condensed water: A novel matrix for the screening of semi-volatile compounds in indoor air. Chemosphere 251, 126346. https://doi.org/10.1016/j.chemosphere.2020.126346

USC UNIVERSIDADE DE SANTIAGO DE COMPOSTELA

Test S2. Multiresidue determination of pesticides by LC-ESI-MS/MS

During LC-MS/MS determination of pesticides, the temperatures of the pre-column and the analytical column were maintained at 40 ºC. Ultrapure water (A) and ACN (B), both containing 0.1% FA, were employed as mobile phases. The optimized conditions for the successful separation of the studied pesticides were as follows: 2% B (0 min) 50% B (1.3 – 2.8 min), 100% B (6.4 – 7.5 min), 2% B (7.6 – 10 min). The injection volume of plastic and soil extracts was 0.5 µL. For water samples, corresponding to sorption-desorption experiments, the injection volume of filtered samples was 30 µL.

The voltage of the ESI needle was set at 1.5 KV and the temperature of the source maintained at 150 ºC. Drying gas (N_2) flow and temperature were 1000 L h^{-1} and 450 ºC, respectively.

USC UNIVERSIDADE DE SANTIAGO DE COMPOSTELA

Table S1**.** Physical-chemical properties of river water matrix employed in pesticide sorption-desorption experiments.

Parameter	Value
pH	6.9
Chloride (mg L^{-1})	9.9
Nitrate (mg L^{-1})	7.8
Phosphate (mg L^{-1})	< 0.1
Sulphate (mg L^{-1})	7.4
Ammonium (mg L^{-1})	< 0.1
Total carbon (mg L^{-1})	7.5
Organic carbon (mg L^{-1})	4.8
UV absorbance (254 nm, cm^{-1})	0.023

USC UNIVERSIDADE DE SANTIAGO DE COMPOSTELA

Table S2. Concentrations of selected elements in new items of conventional and biodegradable-labelled tying tape. Data in μg g^{-1}.

Analyte	Conventional	Biodegradable-labelled
	μg/g	μg/g
Ni	0.8	0.8
Mn	0.2	0.8
Cr	1.4	3.4
Ti	0.2	6.0
Sr	0.2	9.2
B	0.8	9.8
S	---	12.6
Fe	11.0	24.8
K	31.8	34.0
Al	13.2	49.8
Na	93.2	154.8
Zn	3.0	166.8
Mg	5.2	338.4
Ca	224.6	42814.4

USC UNIVERSIDADE DE SANTIAGO DE COMPOSTELA

Table S3. Absolute recoveries, with standard deviations (SD), for isotopically labelled compounds added to aged plastics before extraction. Addition level (100 ng g^{-1}), n= 6 replicates.

Compound	Tying tape		Vine protection tube	
	Average recovery (%)	SD (%)	Average recovery (%)	SD (%)
CAR-d3	79	13	106	8
IMI-d4	86	17	93	20
MET-13C6	90	9	108	10
CYP-d5	89	13	106	10
PYR-d5	95	14	114	11
DIM-d6	93	10	98	16
TEBU-d9	90	7	97	9
MYC-d4	99	5	103	11

USC UNIVERSIDADE DE SANTIAGO DE COMPOSTELA

Table S4. Repeatability of the sample preparation procedure for pesticides quantified in two different samples of aged plastics obtained from vineyards. Mean concentrations (ng g^{-1}) and relative standard deviation values (RSDs, %) corresponding to n=6 replicate extractions.

Concentration (ng g^{-1})	Sample type			
	PPT (PP)		Tying tape (PE)	
	Average (ng g^{-1})	RSD (%)	Average (ng g^{-1})	RSD(%)
CYF			95.0	17
CYP	21.0	19	150.8	9
DIF			201.6	27
Folpet	2370.5	12	778.0	17
IPROV			22.6	22
MAN	8.7	32	32.2	17
MET	26.1	16	13.2	9
MYC	25.9	20	36.6	9
PEN	16.7	13	75.8	19
TEBU	20.0	20	157.0	20
TETRA	4.0	26	26.6	23
ZOX	15.9	24	1157.4	15

USC UNIVERSIDADE DE SANTIAGO DE COMPOSTELA

Table S5. Summary of pesticide concentrations (ng g-1) determined in plastic litter by LC-MS/MS (except Folpet determined by GC-TOF-MS). Average values for duplicate extractions.

Sample Code	Sampling date	Polymer	AME	AZO	BEN	CAR	CHLOR	CYF	CYP	DIF	DIM	FLUO	Folpet	IPROV	MAN	MET	METR	MYC	PEN	TEBU	TETRA	TRIAL	TRIF	ZOX
TT-1	17/07/2022	PE						6.8	310.2							8.6		249.7		9.2				32.1
TT-2	11/09/2022	PE	9.8				50.6		632.5	4.1	601.5	16.1	2839.6	1609.2		11.1	7.0	177.9	7.9	494.7			230.9	308.2
TT-3	11/09/2022	PE						60.8	2664.9	116.7			103.8					44.3						
TT-4	11/09/2022	PE							28.0		5093.6		289.9			45.8								
TT-5	25/09/2022	PE						48.9	247.9	46.8	5.0		370.0			8.9		4.6						
TT-6	25/09/2022	PE						50.4	147.4	88.9			535.5		8.8					49.6				269.6
TT-7	01/10/2022	PE			29.3			285.1		258.9	26.3		296.0					10.7						6.1
TT-8	15/10/2022	PE							203.0	162.4								184.4	327.0					
TT-9	16/10/2022	PE							93.0	286.6			40.7					96.6		55.8				74.8
TT-10	29/01/2023	PE							50.7							146.8		14.0						8.7
TT-11	26/10/2022	PE						1138.2	1682.8	623.0			3754.8	37.8	349.8	49.0		97.4	542.0	638.6	229.0			12374.6
TT-12	26/10/2022	PE						95.0	150.8	201.6			778.0	22.6	32.2	13.2		36.6	75.8	157.0	26.6			1157.4
TT-13	26/10/2022	aPE							32.8				3020.6							24.4				63.0
TT-14	26/10/2022	aPE											857.1					552.2		76.2				
TT-15	26/10/2022	PE						104.8	186.0	1259.2			1704.7	22.8	555.2	20.4		52.8		710.6	658.2			8620.2
TT-16	26/10/2022	PE						115.0	62.0	1407.8			151.2	42.6	34.4	56.2		48.6		313.4	663.2			2370.0
TT-17	15/02/2023	PE							106.4				56.5					194.0						
TT-18	15/02/2023	PE						441.4	491.4	505.8			949.3			95.1		53.1	442.1	693.5				6278.5
TT-19	15/02/2023	PE							593.8	89.3						2089.8		590.7		62.8	87.0		10.6	2622.9
TT-20	15/02/2023	PE						63.0	134.7	222.5			207.4	14.3	29.6	8.7		4.6	85.9	189.2	19.9			1190.7
TT-21	03/02/2023	PE				41.3		51.5	305.0	65.5		44.1	304.2	201.3		12.8		334.9	283.5	376.3	193.7			1987.0
TT-22	03/02/2023	PE							96.9				42.0					50.7		74.2				
TT-23	03/02/2023	PE							10.0		62.9		1267.8			22.6		93.3		50.8				

UDC UNIVERSIDADE DE SANTIAGO DE COMPOSTELA

Sample Code	Sampling date	Polymer	AME	AZO	BEN	CAR	CHLOR	CYF	CYP	DIF	DIM	FLUO	Folpet	IPROV	MAN	MET	METR	MYC	PEN	TEBU	TETRA	TRIAL	TRIF	ZOX
PPT-1	**17/07/2022**	PP									27.1	13.0		11.3		8.5		6.2	24.4	7.4		3.7	7.1	4.9
PPT-2	**25/09/2022**	PP											2221.0			356.6		394.0						
PPT-3	**01/10/2022**	PP			2402.1			33.2		79.6	4022.4				43.5	1039.0			8.3					14.5
PPT-4	**15/10/2022**	PP							325.2	224.8	119.2		2097.6			317.0		309.2	458.6	25.0				215.0
PPT-5	**26/10/2022**	PP		59.4				44.8	614.6	141.4			844.1	148.4	478.2	154.2		422.6	237.4	283.8	221.2		79.4	2229.4
PPT-6	**27/11/2022**	PP							21.0				2370.5		8.7	26.1		25.9	16.7	20.0	4.0			15.9
PPT-7	**04/12/2022**	PP			636.3			77.3	25.0		35.3		20271.3			56.9		776.1	319.1	4.5				9.9
PPT-8	**03/02/2023**	PP			858.0	8.6		17.1	106.3	22.4	100.2	16.9	1365.0	186.9		150.0		191.7	179.2	142.1	50.4	151.8	35.5	208.9
PPT-9	**03/02/2023**	PP											76079.6					191.6		92.2				
PPT-10	**03/02/2023**	PP											12653.0		563.1	130.9								112.2
PPT-11	**03/02/2023**	PP						15.7		43.5			1992.9			38.3		38.1		48.9				223.6

[a]PE with calcium salt filler

Empty cells correspond to compounds below LOQs given in Table 1.

Table S6. Assessment of the accuracy of the analytical procedure for spiked soil samples. N=3 replicates at each addition level.

Compound	Addition level			
	10 ng g-1		100 ng g-1	
	Recovery (%)	SD(%)	Recovery (%)	SD(%)
AME	83	17	97	5
AZO	90	10	105	8
BEN	87	22	98	6
CAR	96	21	95	5
CHLOF	105	14	105	6
CHLOR	79	22	97	5
CHLORM	97	22	101	10
CYF	93	8	103	3
CYP	111	21	109	6
DIF	91	11	100	7
DIM	105	19	99	6
FLUO	95	17	101	9
IMI	80	24	104	12
IPROV	102	6	96	8
MAN	96	28	98	9
MET	105	7	100	6
METR	101	19	97	6
MYC	86	15	98	7
PEN	91	18	99	6
PROP	99	15	103	4
PYRA	108	9	103	8
PYR	99	12	98	3
QUIN	110	13	98	8
TEBU	75	8	105	5
TETRA	81	16	104	10
TRIAF	102	23	97	3
TRIAL	103	17	102	10
TRIF	90	8	109	8
ZOX	93	19	104	9

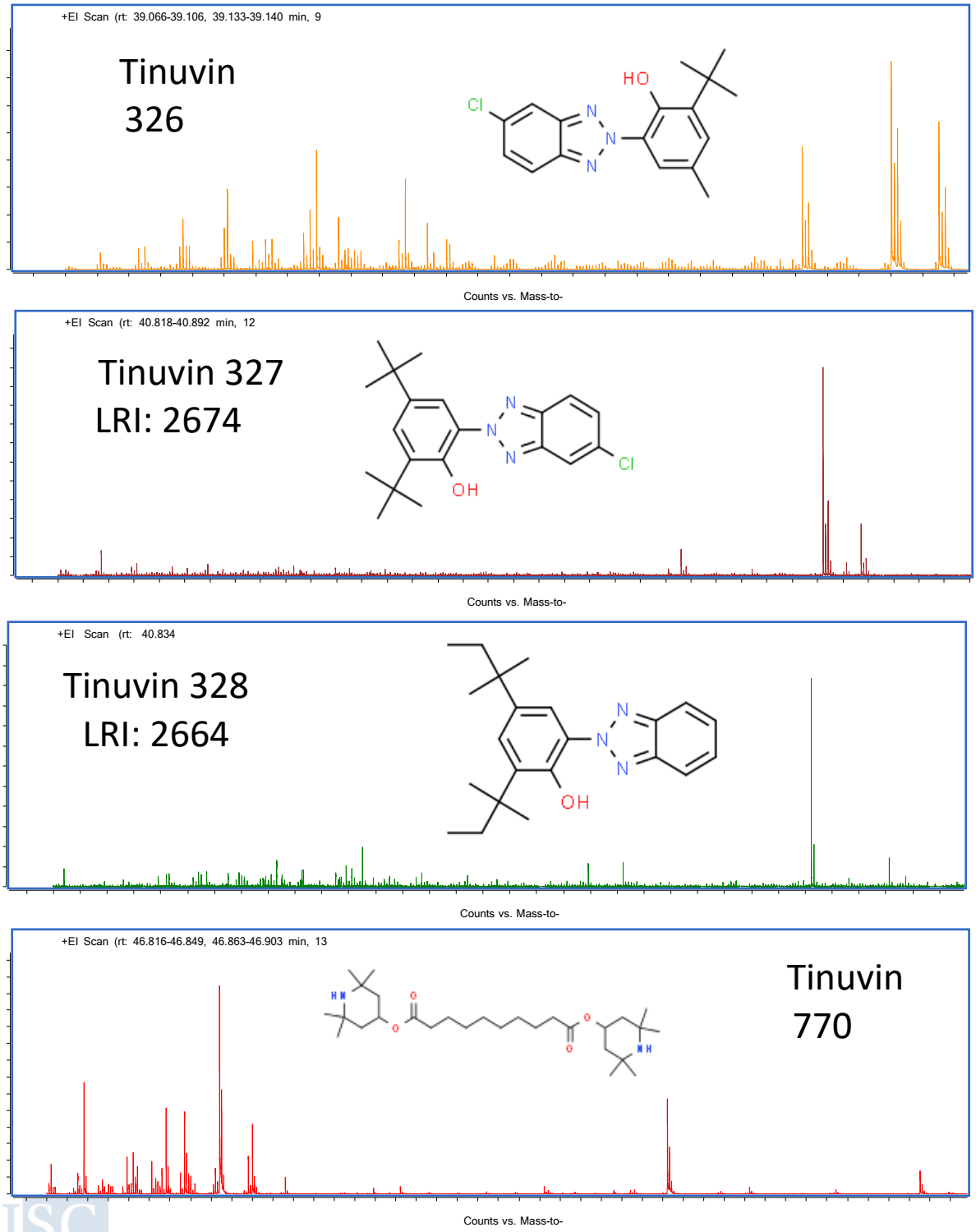
USC UNIVERSIDADE DE SANTIAGO DE COMPOSTELA

Fig. S1. Pictures of tying tape litter holding vineyard canes in autumn 2022 (A); residues of same material on a vineyard soil (B); new and weathered fragments of vine protection tubes.



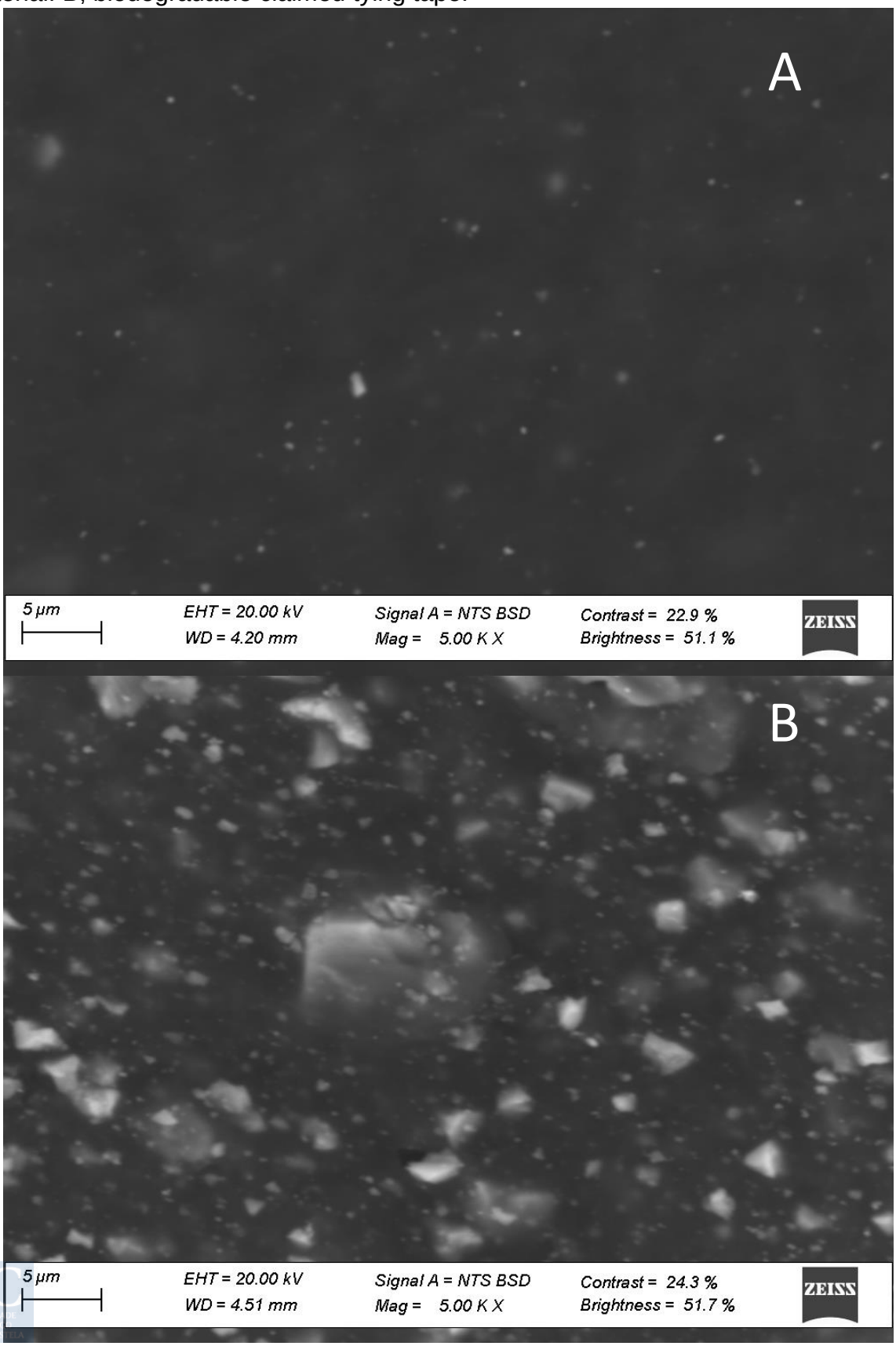
USC
UNIVERSIDADE DE SANTIAGO DE COMPOSTELA

Fig. S2. Chemical structures, experimental linear retention index (LRI) and EI-TOF-MS spectra for polymer additives identified in weathered plastics from vineyards.



USC
UNIVERSIDADE
DE SANTIAGO
DE COMPOSTELA

Fig. S3. SEM images of two types of new tying tape polymers. A, conventional material. B, biodegradable claimed tying tape.



USC UNIVERSIDADE DE SANTIAGO DE COMPOSTELA

Fig. S4. A and B, TIC chromatograms for extracts of TT (polyethylene) and PPT (polypropylene). Red, extract in Hex:DCM. Black, extract in MeOH: ACN. C, EIC chromatograms for ions at m/z 57.0698, 71.0855 and 85.1012 for the extract of PPT in Hex: DCM, mass extraction window 0.005 Da.

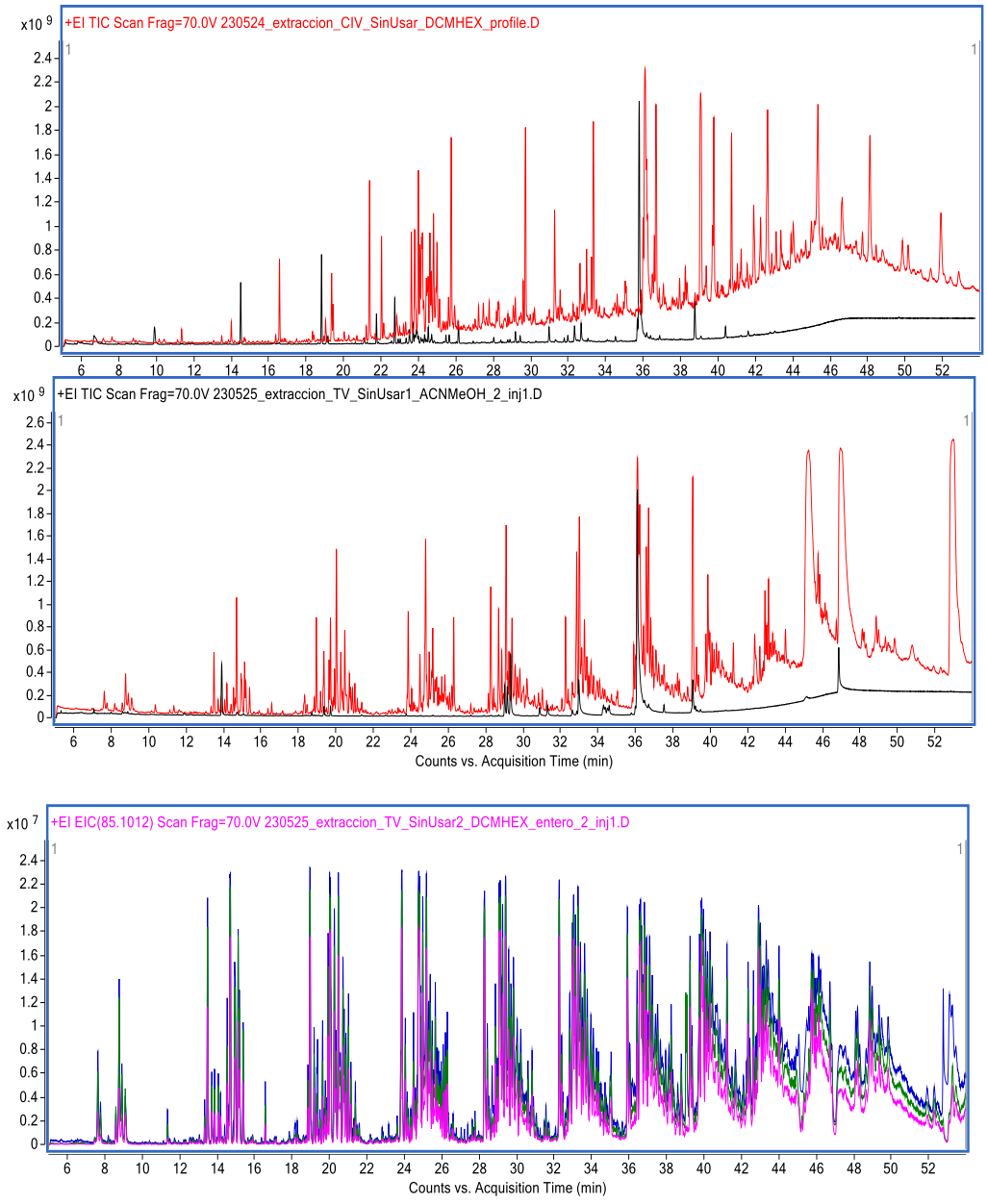


Fig. S5. A, extracted ion chromatogram for the base peak in the EI-MS spectrum of zoxamide (ZOX), mass extraction window 0.005 Da. B to E, deconvoluted spectra for ZOX and potentially related transformation products identified in agriculture plastic litter from vineyards.

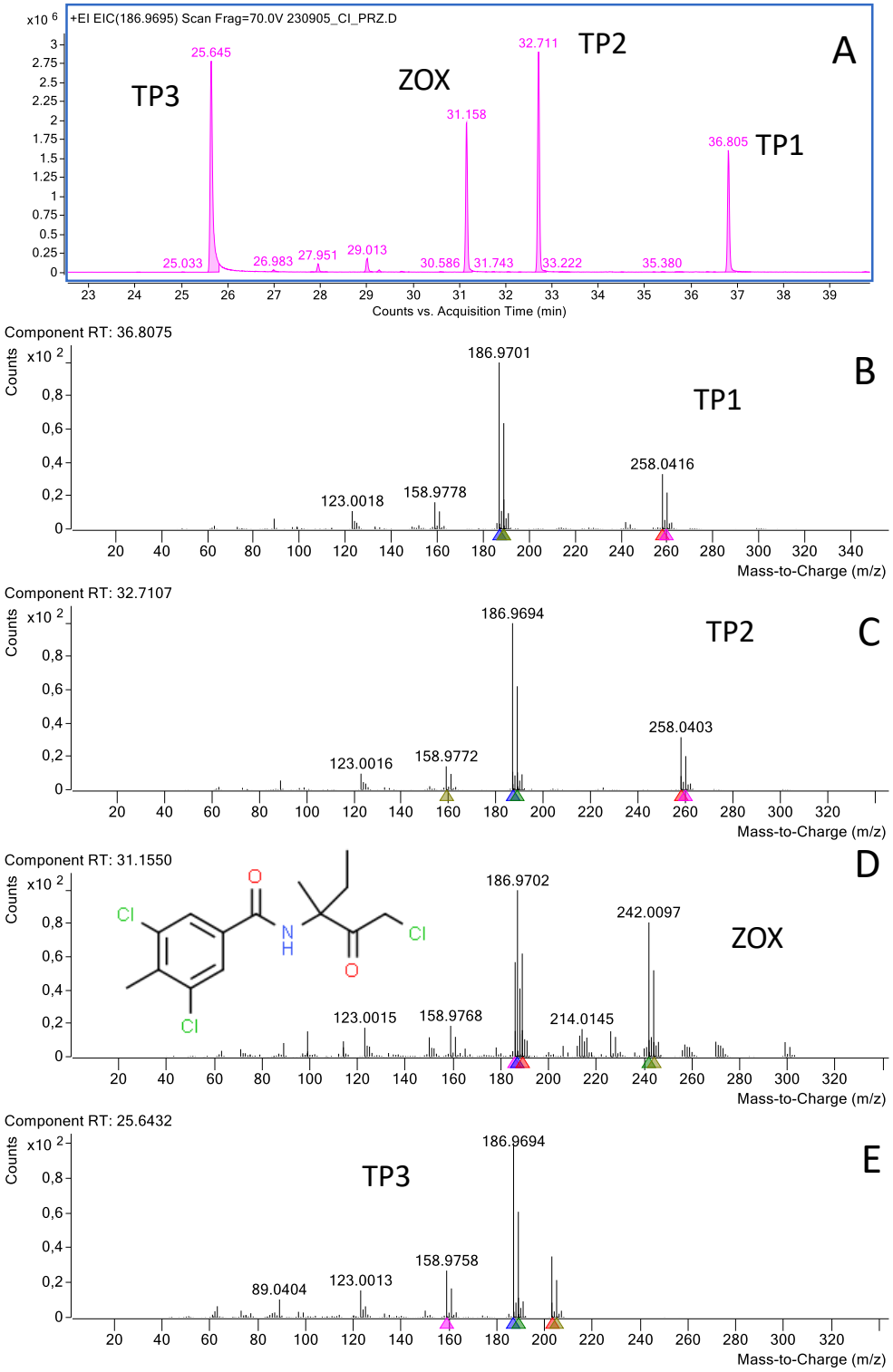
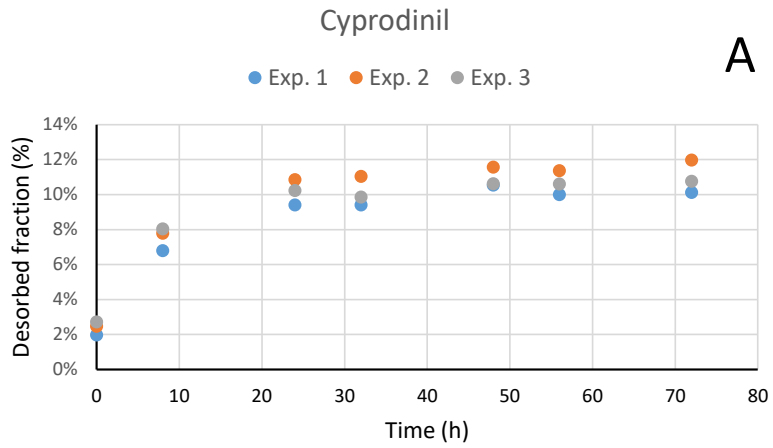
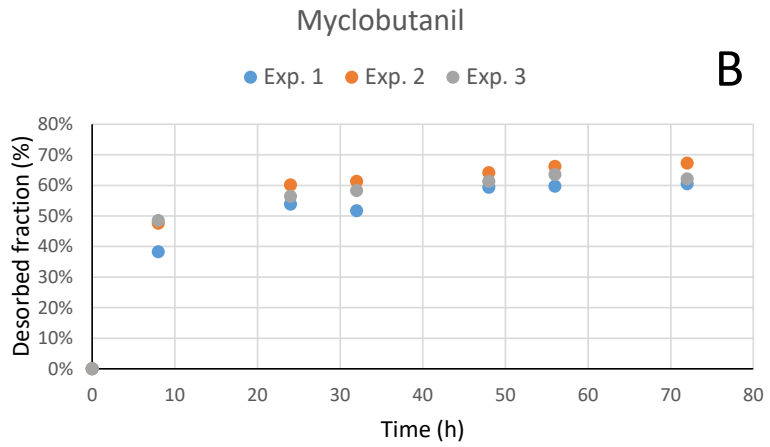
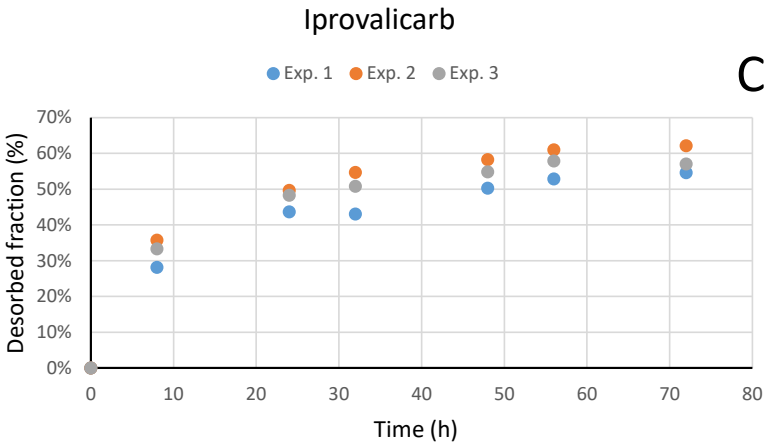


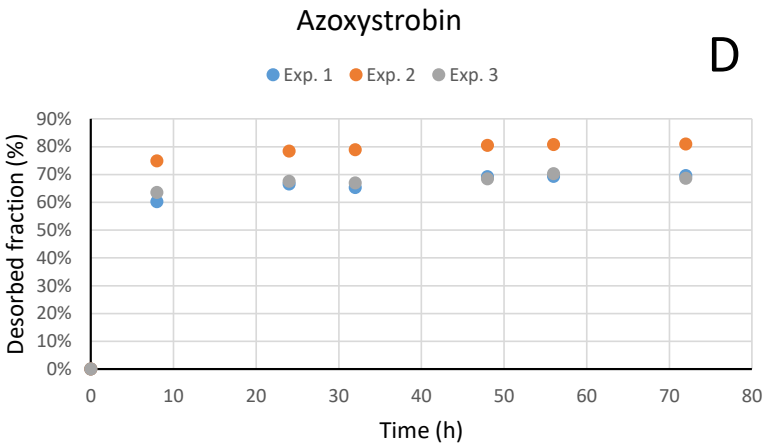
Fig. S6. Desorption kinetics of selected pesticides from aged plastics in contact with river water. Data for experiments in triplicate. A to F, desorption from PE tying tape. G to H, desorption kinetics from the so-called biodegradable tying tape material.

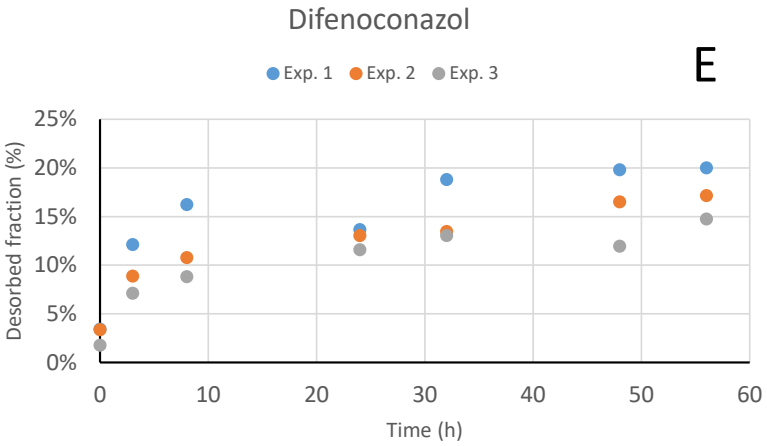


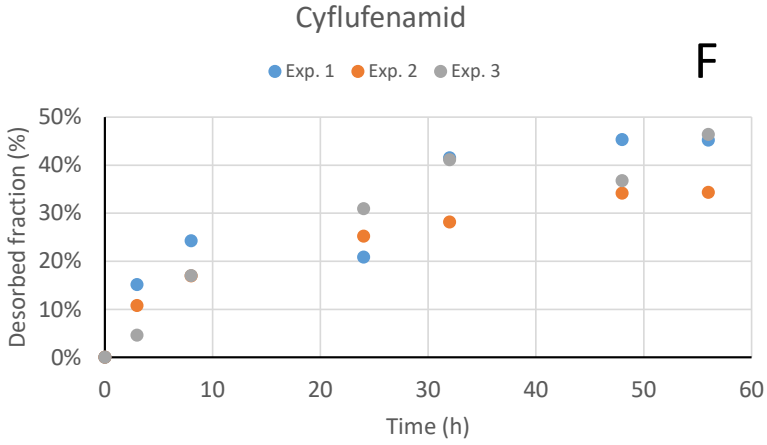




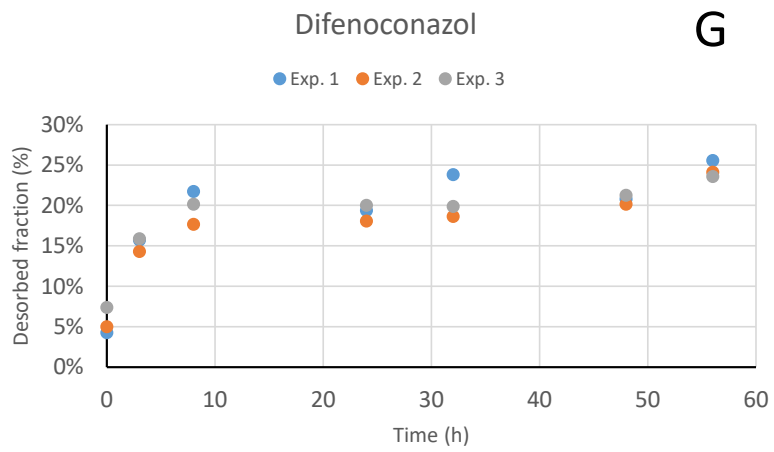
USC
UNIVERSIDADE DE SANTIAGO DE COMPOSTELA

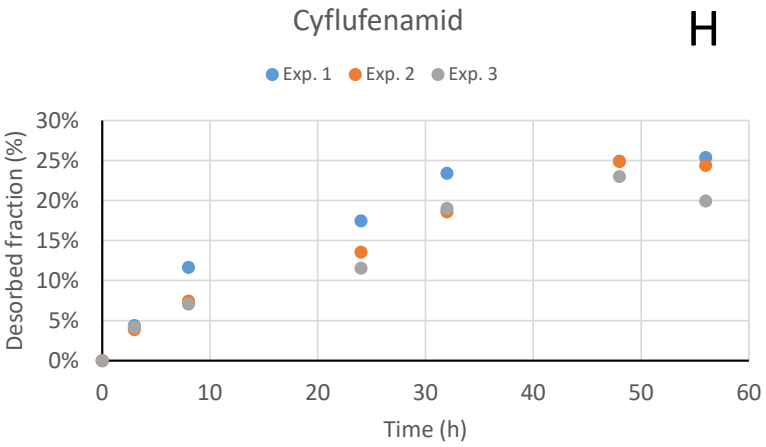






USC
UNIVERSIDADE DE SANTIAGO DE COMPOSTELA


Difenoconazol
G
Exp. 1
Exp. 2
Exp. 3
Desorbed fraction (%)
30%
25%
20%
15%
10%
5%
0%
0
10
20
30
40
50
60
Time (h)


Cyflufenamid
H
Exp. 1
Exp. 2
Exp. 3
Desorbed fraction (%)
30%
25%
20%
15%
10%
5%
0%
0
10
20
30
40
50
60
Time (h)

5 INTEGRATIVE DISCUSSION

The studies carried out during this Thesis are separated into two chapters regarding the main purpose of the mass spectrometry application. Many different environmental and consumer-ready products were employed as samples to evaluate the accuracy, and selectivity of different sampling and extraction techniques hyphenated to MS applied to many different molecules of environmental and health concern.

The first chapter was focused on the non-targeted analysis of various different environmental samples and commercial products to which humans are regularly exposed to. The aim was to have a better understanding of their composition, which can provide invaluable information of the possible adverse effects that a prolonged exposure can have on human health and/or to the environment, as it is the case of incomplete degradation of pharmaceuticals in wastewater treatment plants, which can cause environmental problems or even leading to pollution of drinking water, either with parent pollutants and/or with their transformation products.

The second chapter of this Thesis was focused on showcasing the quantitative capabilities of MS when applied to several different matrices and combined with different ionization and separation techniques. Analyte selection was based on their environmental concern and occurrence data available from previous studies. The matrices selected for this chapter are all of environmental importance, including sludge, wastewater and end of life agricultural plastics, which were judged to contain relevant amounts of pesticides and might serve as carriers of these pollutants through different environmental compartments.

The analysis of complex matrices normally requires some kind of sample treatment to eliminate unwanted components, concentrate the analytes and make the solvent compatible with the selected chromatographic technique. During this Thesis, sample preparation techniques were selected according to the complexity and state of the samples, in brief, the selected treatments were SPE for wastewater samples, MSPD for freeze-dried sludge, PLE for vineyard soils and UAE for samples of plastic litter. A dilute and shoot approach was employed to avoid the loss of information during e-liquid characterization, as LLE resulted in a cleaner GC-MS record at the cost of losing most polar components present in them.

The compounds determined in this Thesis are mostly of organic nature, from many different families, with different physico-chemical properties. The most volatile ones, not amenable to LC, were determined by GC. To ensure the most comprehensive sample characterization, two different columns were employed: a semi-polar siloxane-type HP-5MS column (30 m x 0.25 mm, 0.25 µm), and a polar Carbowax, polyethylene glycol-type (DB-WAXetr), with the same dimensions as the HP-5MS column, but with a film thickness of 0.50 µm.

For the determination of the rest of the analytes, the column selection was dependent on their characteristics; for most pesticides, the employed column was a Zorbax Eclipse Plus C18 rapid resolution (50 mm × 2.1 mm, 1.8 µm), protected with a C18 2.1 mm i.d. Security Guard™ cartridge. In the case of Chlorhexidine, a Kinetex PS C_{18} (50 mm × 2.1 mm, 2.6 µm) column

USC
DE SANTIAGO
DE COMPOSTELA

was needed to obtain a suitable peak shape. For the chiral separation of antimycotics and basic drugs, a Lux Amylose 1 (3,5-dimethylphenyl carbamate) was employed for the successful enantiomeric separation. Lastly, for the analysis of triclosan, a DART system with a Dip-it sample carrier was used to achieve great selectivity.

Following these procedures, through the non-target analysis of indoor air, a total of 141 compounds were identified, out of which 98 were confirmed against standards; including fragrances (some of which are known allergens), solvents, plasticizers, flame retardants and intermediates in the production of polymeric materials. Their LRI was calculated as well, for two different columns. Afterwards, air water distribution constants were obtained for 14 of the previously confirmed compounds, and a proof of concept for their estimation in air using water condensates was proposed successfully. Thus, an easy to obtain matrix was proposed to determine trace levels of semi-volatile compounds in air from indoor atmospheres.

During e-liquid characterization, a total of 250 compounds were identified with different levels of confidence, using two columns with different polarities for a more exhaustive characterization. This study was performed with 39 different e-liquid samples of different flavours.

A more effective, degradation methodology for the pharmaceutical tramadol, recognized as an ubiquitous pharmaceutical in the aquatic environment, was proposed and new transformation products were discovered, with possible structures being proposed for them.

During the quantitative approaches in chapter two, limits of quantification of 40 ng/g of chlorhexidine in sludge were achieved, while concentration in samples ranged from 300 to 16000 ng/g. During triclosan analysis through DART, LOQs were on the range of 100 ng/L to 35 ng/L depending on the wastewater matrix, and 100 ng/g in sludge samples. Concentrations in samples varied in the range from 47 to 237 ng/L for water samples, and between 136 and 1004 ng/g in sludge samples.

An effective and fast enantiomeric separation was achieved for a group of eight chiral pharmaceuticals, with resolution factors ranging from 1.03 to 2.49 and LOQs in the range of 10–20 ng/L and 3.7–11.1 ng/g, for water and solid samples, respectively. Concentration ranges in samples were in the range of 0.013-1.04 µg/L and 8.7-1067 ng/g in water and sludge, respectively (concentrations referring to individual enantiomers).

Lastly, a total of 29 pesticides were quantified in aged plastics collected from vineyards and related soils, with LOQs in the range of 0.1-5 ng/g and 1-10 ng/g in soil and plastic samples, respectively; concentrations in plastics remained in the range between 114 ng/g to 74.6 µg/g.

The development and application of these methodologies, together with main findings obtained in these studies, will be explained in detail in the following sections. Fig. 25 shows the connections among each particular study, with the corresponding chapter of the memory, and with mass spectrometry as the central topic in my Thesis.

USC
UNIVERSIDADE DE SANTIAGO DE COMPOSTELA

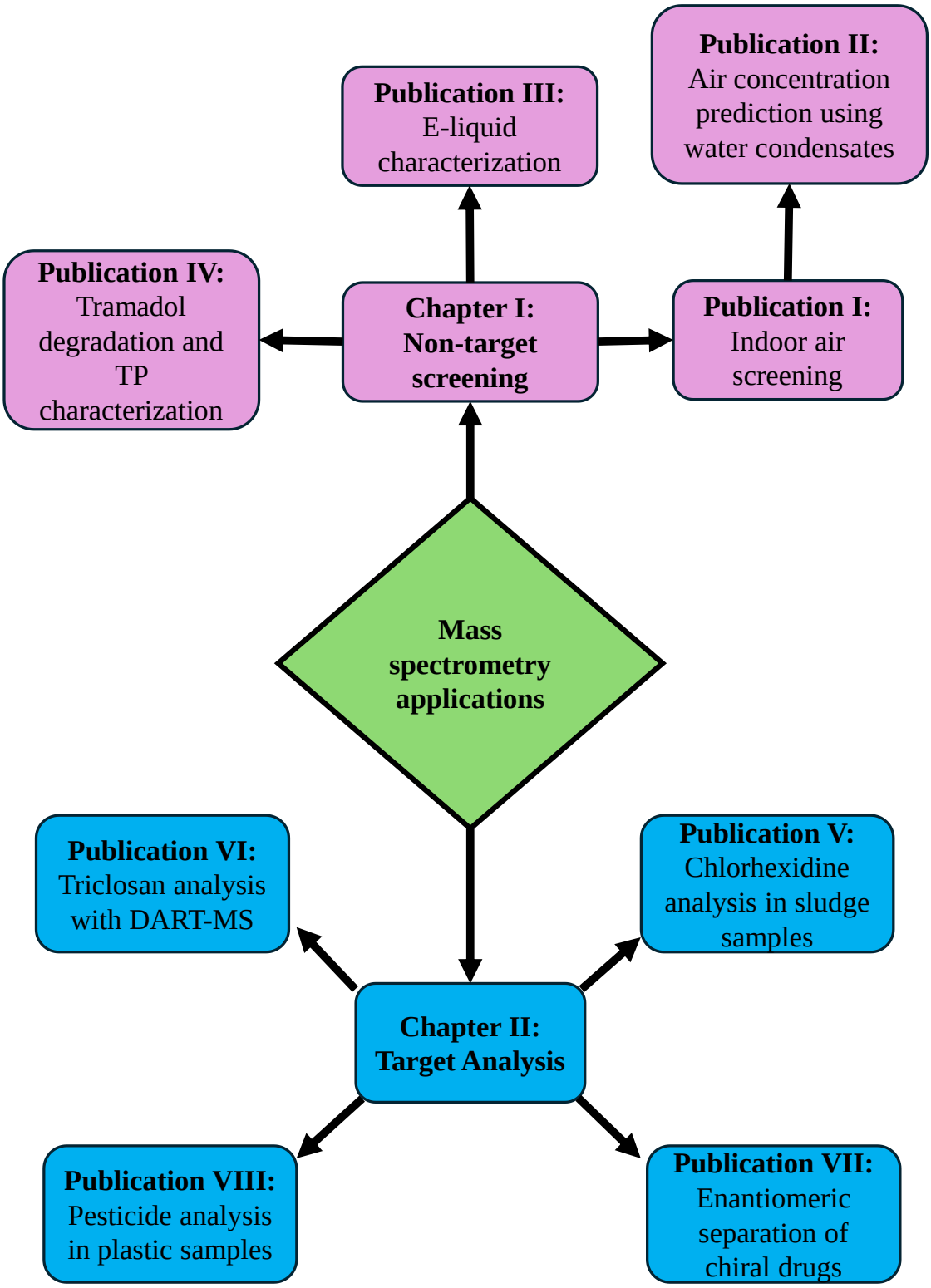


Figure 25: Scheme of the studies carried out during the current Thesis.

USC UNIVERSIDADE DE SANTIAGO DE COMPOSTELA

CHAPTER 1: DEVELOPMENT OF NON-TARGET SCREENING METHODOLOGIES USING HIGH RESOLUTION MASS SPECTROMETRY FOR A COMPREHENSIVE CHARACTERIZATION OF ENVIRONMENTAL AND COMMERCIALLY AVAILABLE SAMPLES.

Methodologies optimized in this chapter were focused on extracting the most amount of information from samples with mostly unknown compositions, following non-target screening approaches.

Despite its importance in human health and everyday life, few publications exist regarding an extensive characterization of indoor air, as most studies are focused on the identification and determination of compounds sorbed to dust and particulate matter; moreover, direct sampling of air requires the use of a vacuum pump, which is a noisy device and can disturb people present during the sampling; to help mitigate these problems, the first research **(Publication I)** was focused on assessing the capabilities of water condensates, obtained from a dehumidifier system, for the screening of semi-volatile compounds present in air. To this end, the sampling steps, sample treatment and chromatographic separation needed to be optimized. For the sampling step, sampling time and air flow (in the case of direct sampling) where optimized. Since the combination of both parameters influences the amount of air that goes through the sorbent, a flow of 1 m^3/h was selected. That way, the exact amount of air volume that goes through the cartridge can be easily controlled by increasing or decreasing sampling time. An air volume of 5 m^3 was used as a compromise between sampling time and concentration factor. The dehumidifier was operated at the same time as the direct sampling took place. For the extraction of water condensates, the chosen methodology was SPE, using an Oasis HLB cartridge for concentration. In this research, the HLB cartridges were conditioned using ethyl acetate, followed by methanol and water (2 mL each); the final volume of water to concentrate was 300 mL; the loaded cartridge was later dried using a gentle stream of nitrogen and eluted using 2 mL of AcOEt. In order to have comparable results, the cartridge used as sorbent for direct sampling was also an OASIS HLB cartridge, conditioned with AcOEt and eluted also using 2 mL AcOEt.

The resulting extracts were analysed using gas chromatography coupled to a quadrupole time-of-flight mass spectrometry, equipped with an electronic ionization source (GC-EI-QTOF-MS). The data-mining workflow was based on the use of the *unknowns analysis* algorithm for spectral deconvolution of the GC-MS spectra. This algorithm was employed in **publications I** and **III,** with small modifications, according to the objective of each publication. In first place, deconvoluted accurate EI-MS spectra were compared to the nominal resolution NIST database to have a possible identification of compounds present in the different indoor atmospheres. Thereafter, tentative identifications were confirmed by injection of standards using the same chromatographic conditions, or by comparing to available libraries with exact mass spectra and LRIs.

Publication II was intended as a continuation to **publication I**, showing a proof of concept using water condensates as an indirect way of predicting compounds found in air, not disturbed with the fraction of same species associated to particulate matter. To this end, the air water partition constants (K_{aw}) were estimated for 14 different compounds previously determined in **Publication I**. Taking into account that different environmental parameters may affect K_{aw}, these values were estimated based on the results of 20 pairs of samples taken from different rooms, and with two different sampled air volumes: 1.5 and 3 m^3. Different experiments were carried out to assess the importance of the room temperature in analyte solubility in water.

USC DE COMPOSTELA

Afterwards, thirteen new pairs of samples were obtained from seven different rooms and the air and water extracts were analysed separately. Then, using the calculated K_{aw} constants, the concentration in air was estimated using the concentrations found in water condensates, obtaining a good correlation between measured and predicted concentrations for all 14 analytes. The main conclusion from both publications is that the composition of water condensates was correlated to the composition of indoor atmospheres, being feasible to calculate the corresponding air-water partition coefficients. As a general statement, analysis of condensed water might be favourable in terms of sensitivity for semi-volatile species and/or highly polar species. Examples of compounds for which analysis of water condensates was most favourable than active air sampling are the most volatile phthalates (diethyl, dibutyl and diisobutyl phthalate, benzothiazole and the halogenated flame retardant TCPP). An accurate control of the temperature in the condenser of the dehumidifier emerged as the most relevant issue to obtain repeatable results among different sampling units (dehumidifiers). The replacement of polymer surfaces by metallic ones could be necessary to bring down procedural LOQs of polymer additive compounds existing in the vapor phase of indoor areas.

E-liquids for electronic cigarettes have gained popularity in recent years, in principle, as a mean to stop smoking, however, little is known about their composition except the few declared ingredients; for that reason, **Publication III** was focused on obtaining an in-depth characterization of a relevant number of e-liquids (39 samples) with different flavours and from different brands. The e-liquid base solutions generally consists of a mixture of vegetal glycerine and propylene glycol (the percentage of each component can vary depending on the manufacturer), making them extremely thermostable and viscous, which makes them unsuitable for direct injection on CG-MS systems; for this reason, we opted for a dilute-and-shoot approach, with a factor of 1:100 (1:1000 when quantification of major components was addressed) when working with them. This approach was the best to ensure that all the components in the e-liquid are correctly introduced into the GC-MS system; however, due to the high concentration of glycerine and propylene glycol, very broad bands corresponding to these two substances were present in the chromatograms. Such broad signals mask the peaks of minor components present in the e-liquids; to avoid that, a liquid-liquid extraction diluting the e-liquids in water and using AcOEt as extractant was proposed. This methodology allowed for the elimination of both glycerine and propylene glycol, resulting in cleaner chromatograms; however, most polar components were also lost during this procedure. In the end, we opted with following the dilute-and-shoot approach and applied the above-mentioned deconvolution algorithm for a preliminary identification.

During this publication, identifications were made with three different confidence levels: level 1 was the highest level, compounds fulfilling both LRI, spectral and accurate mass match with library data, and were also confirmed with a standard in any of the two columns that were assigned to this level; Level 2 corresponded to compounds not verified against standards, but matching spectral and retention time requirements in both columns. And level 3 was assigned to compounds tentatively identified using just one of the columns. This level mostly corresponds to highly volatile species, poorly retained by the HP5-MS column, noticed just in the chromatograms from the Carbowax-type column; as well as to compounds detected in both columns, but without an available reference LRI in one of them. The compounds that were identified with confidence levels 1 and 2 were compiled into two libraries, one for each of the columns used and they are available online in the Zenodo repository (https://zenodo.org ; doi: 10.5281/zenodo. 7738079).

For some compounds that were identified with confidence level 1 in GC analysis, it was considered necessary to perform confirmation experiments via UHPLC-MS to verify if they

USC DE COMPOSTELA

were present on the e-liquid, or if they were formed in the hot injector of the GC by re-arrangement of the molecular structures of the precursors. These separations were carried out using a CORTECS Phenyl column (150 mm x 2.1 mm, 2.7 μm) using ultrapure water and ACN, both with 0.1 % FA and with a constant flow of 0.3 mL min^{-1} with different gradients according to the analysed substance. These experiments resulted in the confirmation of the presence (and quantification) of different acetals of aldehydes and non-declared cannabinoids, including Δ^9-THC, in e-liquids. Thus, our study highlighted the complementary features of both techniques for a more comprehensive characterization of complex matrices, and to avoid possible false positives associated to the features of each one of them. Relevant findings of the study requiring further research are the assessment of the e-liquid storage conditions on the formation of irritant acetals, and the estimation between acetals/precursor aldehydes ratios in e-liquid and aerosols formed during the e-smoking process.

The last application of MS for non-target screening carried out in this Thesis was the evaluation, at laboratory scale, of a degradation methodology for the pharmaceutical tramadol (TRA) (**Publication IV**). The main aims of this study were achieving the complete elimination of tramadol, as well as identifying the different transformation products formed during the different degradation experiments carried out, and their fate during said experiments. Degradation experiments done during this study included photolysis, UV/free chlorine and UV/peroxide.

All photodegradation experiments were carried out in a home-made UV reactor housing an 8 W low pressure mercury lamp (the lamp was partially covered to allow for a more controlled irradiation of the sample), emitting at 254 nm and assembled orthogonally to a cylindrical quartz reaction vessel, containing 25 mL of the considered water sample. The fluence of radiation on the water sample was experimentally determined using potassium iodide as chemical actinometer, the obtained value was 1.04×10^{-6} Einstein L^{-1} s^{-1}.

Spiked model water solutions were prepared directly in the photoreactor vessel adding a small amount of a standard solution of tramadol in methanol and letting it dry before adding the water sample. The different aliquots of 0.5 mL were taken at increasing reaction times and were poured into vials containing 0.05 mL of a standard solution of TRA^{13}C-d_3 in MeOH, which was used as a quencher of radical species produced during the degradation reactions regardless of the experiment (excess free chlorine was eliminated using ascorbic acid). The different aliquots were then injected into a liquid chromatograph coupled to a quadrupole time-of-flight mass spectrometer using electrospray as the ionization source (LC-ESI-QTOF-MS) in the all-ions mode. All degradation experiments were performed in spiked samples of ultrapure water, river water, and filtered wastewater to assess their efficiency in different matrices with increasing complexity.

The efficiency of different treatments for the removal of TRA was assessed with half-lives values ($t_{1/2}$, min) and observed reaction rate constants (k_{obs}, min^{-1}). TRA stability decreased in the following order: free chlorine, UV irradiation, UV-H_2O_2 and UV-chlorine.

The identification of transformation products was done performing the different degradation experiments in ultrapure water, using a pure tramadol standard, as such, after injecting the standard before degradation, we were able to locate the peaks corresponding to the possible transformation products easily and perform a target MS/MS analysis on them. Depending on the advanced oxidative treatment applied, different transformation products were formed, for example, many chlorinated TPs were formed during the UV/free chlorine experiments that were absent from the UV/peroxide experiments, however, some TPs remained constant in all degradations, as is the case with N-demethyl tramadol and O-demethyl tramadol. Some of the more well-known and major TPs identities were confirmed using standards, for the

other ones, possible structures were proposed according to their accurate product ion spectra. Although for some of the TPs, the exact structure could not be defined, as the molecular formula fit many possible isomeric structures. Some volatile chlorinated by-products were also found during UV/chlorine degradation by analysis using GC-QTOF, they included four legislated trihalomethanes (chloroform, dichlorobromethane, chlorodibromomethane and tribromomethane), 1,1-dichloroacetone, 1,1,1-trichloroacetone, and the nitrogenated disinfection by-products: dichloro and trichloro acetonitrile, bromochloroacetonitrile and trichloronitromethane and, lastly, anisole. Despite the inherent toxicity of these species, the conversion rate remained between 0.2% and 1.4% of the initial concentration of tramadol. Again, the complementary use of LC-QTOF-MS and GC-QTOF-MS was necessary for the exhaustive characterization of by-products generated by tramadol. Thus, the systematic use of these screening tools is recommended if AOPs, such as UV-free chlorine, are transferred to pilot plant scale, using real water samples where a range of low concentration, poorly biodegradable emerging pollutants, is expected.

Finally, different degradation routes were proposed for the UV/free chlorine and UV/H_2O_2 degradations according to the different transformation products detected in each of the processes.

USC
UNIVERSIDADE DE SANTIAGO DE COMPOSTELA

CHAPTER 2: TARGET ANALYSIS OF SELECTED POLLUTANTS IN COMPLEX ENVIRONMENTAL MATRICES.

The methodologies developed during this chapter are focused on the separation and sensitive determination of a number of preselected compounds in samples of environmental concern. The quantitative capabilities of mass spectrometry were tested with complex matrices, using different sample introduction techniques, including LC, SFC and DART, identifying the possibilities, but also their limitations, for each of the considered scenarios.

The first study in this chapter was focused on the quantitative extraction of the bactericide chlorhexidine from sludge samples, and the assessment of its toxicity towards model plants and microorganisms. For the extraction of chlorhexidine from the sludge samples, the selected methodology was MSPD. MSPD extraction conditions were adapted from a previous protocol developed in our research group for the screening of emerging pollutants in sludge. Freeze dried sludge samples (0.5 g) were dispersed in 2 g of C_{18} in a mortar for 5 minutes, afterwards, this mixture was poured into a polypropylene syringe containing a polyethylene frit and 1 g of diatomaceous earth. After compacting the cartridge with another frit, chlorhexidine was eluted using a mixture of MeOH-FA (99:1), the extract was then filtered through a PTFE filter, 0.2 μm pore size, and injected in the LC-MS/MS system.

Toxicity assessment for chlorhexidine was performed on three model microorganisms: *Escherichia coli, Staphylococcus aureus* and *Candida albicans*; and on three model plants: *Lepidium sativum, Sinapis alba,* and *Sorghum saccharatum*. For the microorganisms acute toxicity was measured using a colorimetric standardized test. In the case of plants phytotoxicity assays, we considered chlorhexidine effects in seed germination and root length after a three-day germination period. These experiments were carried out using two different fractions of a model OECD soil, one of the fractions was used as control, and the other one was spiked with chlorhexidine in the range of concentrations expected in sludge amended soils, taking into account the levels of the bactericide reported in the first part of the study. The most sensitive of the tested microorganisms to chlorhexidine with lethal threshold concentrations lower than 0.1 mg/L was the fungi *C. albicans*. On the other hand, *E. coli*, remained unaffected until concentrations around 1.8 mg/L and *Staphylococcus aureus* until 0.5 mg/L. From an analytical perspective, our results highlighted the difficulties to determine, strongly basic, relatively large and symmetric molecules, due to (1) their strong interaction with silanol groups in conventional reversed-phase columns, and (2) potential changes in the ratios between single and multiple charge ions observed during ESI ionization. Polar modified reversed-phase columns improved peak shape and detectability of chlorhexidine. Although the performance of the column was lost after several dozens of injections of sludge extracts, the column was recovered by pumping a solution of ammonium bicarbonate (50 mM) in water: acetonitrile (1:1) for 40 min. Likely, this treatment elutes compounds blocking the positively charged sites in the stationary phase, eluting species with anionic groups. Moreover, the use of isotopically labelled analogues was mandatory to minimize the contribution of non-repeatable ionization in the accuracy of quantitative data. From an environmental point of view, levels of chlorhexidine measured in sludge support the controversy about the safety of urban sewage sludge as a source of nutrients in agriculture. Despite found concentrations of the bactericide being unlikely to affect the germination of plants, in-vitro toxicity results suggest the possibility to modify the microbiome

of soils, due to a negative impact in the survival of most sensitive bacteria and/or fungi, as found in the assays with *C. albicans*.

The second study performed in this chapter was the evaluation of Direct Analysis in Real Time coupled to time-of-flight mass spectrometry (DART-MS) for the selective quantification of triclosan in very complex environmental samples such as wastewater and sludge. Same samples were also analysed using a UHPLC-QTOF instrument as a means to verify the accuracy of concentrations obtained using the DART-TOF-MS system, another method of verifying DART-MS accuracy was analysing personal care products with a declared concentration of the biocide triclosan.

Some conclusions derived from this research are related to the difficulty to predict ionization mechanisms of DART sources, depending on the features of the considered analyte. Thus, the ionization behaviour of triclosan was different to that observed in previous works of the group for bisphenol-like structure compounds. A difficulty related to the configuration of the source employed in this research is that related to stability of mass calibration in the TOF-MS instrument during its combination with the DART source. At difference with the normal operational mode, the reference calibration solution cannot be directly introduced in the spray chamber through a second ESI probe. Obviously, during combination of DART-MS for analysis of trace compounds in a complex chemical environment, the MS system is the only responsible of the selectivity of the method. Even when DART-MS was able to detect concentrations in the low ng per mL in solvent-based solutions, LOQs are expected to be much higher during application to complex samples, or sample extracts, where a high number of isobaric interferences are observed. On the other hand, the effect of the sample matrix is expected to show a much lower impact for detection of compounds with a negative mass defect, as in the case of triclosan and other polyhalogenated compounds, rendering ions in relative clean spectral regions as reflected in our study. Finally, despite triclosan having been regarded as a controversial bactericide from the beginning of the current century, and its uses in personal care products having been restricted, environmental samples, such as sewage water and sludge, still contained relevant concentrations of the biocide

The objective of the third study carried out during this chapter was to develop a multiresidue method for the chiral analysis of a group of selected drugs at levels presented in wastewater and sludge (**Publication VII**). On one hand, the study pursuits to assess the performance of the combination between SFC and QTOF-MS for the effective, rapid separation of selected compounds. Furthermore, the effect on the pre-backpressure split interface on the sensitivity and the matrix effects of the method was investigated.

Matrices contemplated for this study were raw and treated wastewater, as well as sludge. Wastewater samples were extracted using SPE, as it is the most commonly used methodology for these kinds of samples. For the extraction, the sorbent used was a mixed-mode OASIS MCX, conditioned with methanol and water at pH 3. Before the extraction, the samples were spiked with a mixture of SSs, acidified to pH 3 to ensure all the analytes were protonated, and 20% of volume in MeOH was added before filtration to avoid the loss of the most lipophilic species. Once the cartridges were dried under a light stream of nitrogen, the neutral and acidic compounds were first eluted using 3 mL of a mixture MeOH containing 0,1% FA and afterwards the analytes were eluted using a mixture of MeOH:NH_3 (98:2). Recoveries for these matrices remained between 80 and 115% except in the case of fenticonazole (FTZ) enantiomers, which showed only a 77%.

USC DE COMPOSTELA

Sludge samples were extracted using MSPD; freeze-dried sludge samples were dispersed in C_{18} and poured into a polypropylene syringe with diatomaceous earth and a polyethylene frit, the mixture was then compacted using another frit. For the elution, OASIS SCX cartridges were connected in-line to the above-mentioned MSPD cartridge; both cartridges were then eluted with 10 mL of MeOH, which was discarded, and then the SCX cartridge was eluted using a mixture of MeOH:NH_3 (98:2), this extract was then filtered with a PTFE filter, 0.2 μm pore size and injected into the UHPLC system. Recoveries in sludge samples remained between 95 to 120%, except in the case of venlafaxine (VFX) and miconazole (MCZ) with recoveries between 120 and 133%.

The study identified a number of critical parameters during development of chiral separations by SFC-MS, using polysaccharide columns. As happens in chiral LC methods, chiral stationary phase and selector were the most important parameters controlling the success of chiral separation. Among the tested columns, the Amylose-1 was the best performing one. Moreover, CO_2 modifiers played a relevant predictable role in the elution strength of the mobile phase, and a non-predictable one in the enantioselectivity of the column. Depending on compounds basicity, the additive also played a relevant role in the efficiency of the separation process. The moderately basic azolic compounds were non sensitive to changes in the pH of the mobile phase; however, the more basic drugs, with an amino group in their structure, showed non-reversible interactions with the stationary phase under acidic conditions, which has been described during SFC separations using combinations of supercritical CO_2 with methanol. Basic additives overcome the aforementioned chromatographic problems. However, the choice of the additive needs to be carefully balanced since it might impair the ionization of compounds when the ESI source is operated in the positive mode. The findings of this study pointed out to the use of ammonia as the most suitable additive to enhance the enantiomeric separation and ESI(+) ionization of the amino-type drugs: venlafaxine, tramadol and propranolol. Out of all the analytes, only tramadol, venlafaxine and propranolol showed significant differences in their enantiomeric fractions in wastewater samples when compared to the commercial standards, and also to those determined in pharmaceuticals containing these active molecules. Likely, variations in their EF values are related to different metabolization and excretion of both enantiomers.

The last study in this chapter and Thesis is summarized in **publication VIII**. The aim of this study was to evaluate the potential of plastic debris, found in vineyards from the Northwest of Spain, to accumulate pesticides and to act as carriers for them. Infrared spectroscopy, in the attenuated total reflection mode (ATR-IR), permitted to classify most of the plastic litter by comparison with database spectra and those obtained from new counterparts. In addition, aged materials showed extra bands, suggesting oxidation of the hydrocarbon skeleton of polypropylene and polyethylene materials. On the other hand, characterization of the composition of some of the debris required to combine information obtained from multiple techniques, leading to conclusions different to those stated in advertising labels. In particular, a modified polyethylene agriculture use tape film was labelled as a biodegradable polymer, which turned out to be untrue, or at least, inaccurate information.

Since most plastics were in contact with soil at the time of sampling, they were cleaned using ultrapure water when they were received and left to dry protected from dust in a vacuum chamber at ambient temperature; afterwards, samples of polyethylene tape were cut to fragments of size 0.5 cm x 0.5 cm; pieces of plant protection tubes, made in polypropylene,

were instead shredded and sieved to a size between 0.2 mm and 2 mm to ensure a better homogeneity. A problem related to sample preparation (homogenization) of polyethylene film was the difficulty to reduce the size of this material. Pieces of tape film collected from vineyards showed small dimensions, with widths around 0.9-1cm and lengths from 0.5 cm to 15 cm. Cutting mills failed to crush this material without melting. So, debris was manually cut and combined in an attempt to obtain homogeneous subsamples from the same plot. On the other hand, polypropylene debris turned to be relatively fragile, being easily homogenized without risk of melting.

The pesticides selected for study were chosen based on knowledge of their application to vineyards thanks to previous studies performed in the research group and based on literature; as such, LC separation and MS determination steps were already optimized in previous studies. In brief, a UPLC reversed-phase column was combined with a QqQ instrument for the analysis of 30 pre-selected pesticides, including a suite of labelled surrogate standards, in 10 min. Analysis of pesticide residues in plastic litter reported several interesting findings. In first term, pesticides showed a strong interaction with the matrix of the polymer, particularly in case of polyethylene litter. This observation was supported by the fact that polar solvents (methanol, acetonitrile and their combinations), previously employed for pesticides extraction from agricultural soils, do not perform well with aged plastics. Thus, they led to lower concentrated extracts than those achieved by the combination of hexane and dichloromethane. Using a GC-MS as complementary technique, it was found that these latter solvents lead to polymer swelling, releasing more pesticides than non-polar ones.

Another relevant findings of the study were the high levels and stability of pesticides in plastic litter. On one hand, qualitative data, again derived from GC-TOF-MS analysis, permitted identifying some fungicides phased out more than 10 years ago in aged materials, such is the case of the fungicide dichlofluanid. Quantitative analysis by LC-QqQ-MS determined much higher residues of pesticides in plastic litter from vineyard soils than in the soil matrix from the same plots. Even more, some fungicides known to be extremely labile in soil, as it is the case of Folpet with half-lives of few days, was identified at concentrations of dozens of mg per Kg in plastic litter collected several months after application of fungicides to vineyards.

Sorption and desorption studies of selected pesticides in agricultural plastics revealed that the affinity of given compound by the plastic material was function of its original composition and its degradation state. As a rule, polyethylene was more retentive than polypropylene. Moreover, the affinity of moderately polar fungicides to both polymers was higher in case of aged materials (likely due to interaction with polar groups, identified from extra bands, assigned of carbonyl and hydroxyl groups in their IR spectra) than for new counterparts. Thus, aged, polluted plastic debris are expected to be excellent carriers of pesticides once they reach a size small enough to be transported by run-off water and/or wind.

A final finding of this publication was the identification of pesticides in new items of agricultural plastics purchased from different suppliers. In a few cases, relevant concentrations were identified as for the fungicide metrafenone in polyethylene tying tape. The source of these residues are currently under study in the research group. Although the first hypothesis was that the fungicide was intentionally added to the polymer, at the moment of preparing this memory, the most probable source is the use of recycled PE for the elaboration of the tape material.

USC
UNIVERSIDADE DE SANTIAGO DE COMPOSTELA

USC
UNIVERSIDADE
DE SANTIAGO
DE COMPOSTELA

6 CONCLUSIONS

The capabilities of mass spectrometry as a determination technique have been thoroughly assessed during this Thesis. Several applications for non-target screening analysis of substances of interest, which could cause serious issues to human health and to the environment, were developed. In addition, a degradation methodology for the elimination, and discovery of transformation products, of the pharmaceutical tramadol, selected attending to its poor biodegradability and ubiquity in the aquatic media, was also proposed. Target applications to pesticides and drugs present in complex environmental samples, such as sludge or wastewater, as well as the assessment of plastic debris as carriers of pesticides were also developed.

The most critical issues in the combination of different sample introduction, and chromatographic techniques, with mass spectrometry were also identified during the development of above cited applications.

The general conclusions extracted from each chapter are found hereafter.

Chapter 1: Development of non-target screening methodologies using high resolution mass spectrometry for the characterization of environmental and commercially available samples.

- A total of 141 semi-volatile compounds were identified in indoor air by GC-EI-QTOF-MS with the help of water condensate samples obtained from a dehumidifier system. The existence of correlations between compounds existing in indoor air and those accumulated in condensed water samples was confirmed with: (1) repeatable GC-TOF-MS records obtained during consecutive sampling experiments, carried out in the same room; and (2) by the different GC-MS profiles of water condensates from different indoor areas, as well as the differences in composition observed in samples from different indoor spaces.
- The usefulness of portable dehumidifiers for the characterization of indoor air were further evaluated for the possibility of obtaining semi-quantitative analysis for a suite of 14 volatile and semi-volatile compounds, generally present in indoor air from offices and homes. Their air-water distribution constants were calculated by extensive sampling, using different air volumes and environmental temperatures to ensure more reliable values. The calculated constants were then employed for the estimation of concentrations in air for said compounds present in a total of 13 pairs of samples collected from seven different sites. All compounds showed a high correlation, which proves the potential of portable dehumidifiers for the semi-quantitative analysis of air samples.
- More than 250 compounds were identified in the formulation of e-liquid samples by GC-EI-QTOF-MS using two different columns. Among them, respiratory pro-

USC UNIVERSIDADE DE SANTIAGO DE COMPOSTELA

inflammatory compounds, such as the acetals of propylene glycol and glycerine with aldehydes; nicotine-related and non-related alkaloids, and psychoactive cannabinoids were confirmed as concerning compounds present in e-liquid samples.

- Two different databases (one for each column) which contain compound names, retention indexes, structures and accurate EI mass spectra were created. They are expected to be of usefulness for further characterization of substances present in e-liquid studies.
- Several oxidative treatments were assessed at laboratory scale, for the removal of tramadol from water samples. The most effective one was the combination of UV light and chlorination, yielding removal rates near 100% in 30 minutes.
- The formation of transformation products considered more concerning than tramadol (i.e. tramadol-N-oxide) remained below 3% of the initial concentration of tramadol. Other volatile chlorinated TPs also remained below 2% of tramadol concentration.
- Transformation routes were proposed for two of the oxidative treatments carried out, one for UV/peroxide and another one for UV/chlorine, according to the TPs reported during this study.

The non-target screening applications performed in this Thesis permitted to identify many different substances present in complex samples. The data mining procedure for non-target screening from GC-EI-MS accurate m/z records is well-established and robust, as demonstrated with applications focussed on air from indoor atmospheres and e-liquids. Nevertheless, there are some limitations to fully exploit the information derived from de-convoluted EI-accurate MS data. The most important ones are (1) the lack of high resolution/accurate EI-MS databases, and (2) the need to combine accurate EI-MS spectral information with chromatographic retention indexes, preferably for different stationary phases, to achieve the discrimination of compounds with common fragment ions (a relatively often situation in case of natural origin, volatile compounds).

Chapter 2: Target analysis of selected emerging pollutants in complex environmental matrices using different sample introduction/chromatographic techniques.

- Chlorhexidine was found to be ubiquitous in sludge samples from the Northwest of Spain, with concentrations up to 16 μg g^{-1} being registered. Despite the relatively high levels existing in this matrix, the strong basicity and lipophilic characteristics of this bactericide are the most challenging issues for its determination.
- After several toxicological tests, it was found that chlorhexidine concentrations existing in sludge did not cause any harm to any of the three model plants, as higher concentrations were tested with no effect on their germination; however, chlorhexidine proved to be very toxic to the three model microorganisms it was tested on, at concentrations lower than those found in sludge samples. So, it can be assumed that chlorhexidine can have an important impact on the microbial population present in WWTP sludge.
- The use of DART-MS allowed the selective and sensitive determination of triclosan in complex environmental samples, partly due to the chloride mass defect of the compound.

USC UNIVERSIDADE DE SANTIAGO DE COMPOSTELA

- The optimized conditions allowed for the quantification of triclosan in samples using solvent calibration thanks to the use of an isotopically labelled analogue of triclosan.
- Enantiomeric separation of eight different pharmaceuticals was achieved by SFC-ESI-QTOF-MS, and their quantification was done in wastewater and sludge samples. The chromatography separation procedure operated under "green chemistry" conditions given that the major component of the mobile phase was CO_2. However, as mobile phase flowrates are higher than in reversed-phase chiral LC analysis, and an additional make-up solution was required to enhance their ionization, both approaches (chiral SFC-MS and chiral LC-MS, operated under reversed-phase conditions) consume similar volumes of organic solvents. As a whole, the developed SFC-ESI-QTOF-MS was very effective in terms of total analysis time, enantiomeric resolution and limits of quantification.
- Differences in the enantiomeric fractions between the commercial pharmaceuticals and the ones present in raw and treated wastewater of three out of the eight pharmaceuticals were reported.
- High concentrations of pesticides were reported in plastic debris collected from vineyards. Residues in aged plastics were much higher than those found on the soil from same plots, showcasing the role of plastics as collectors and carriers of pesticides.
- The capabilities of plastics to accumulate and release pesticides from, and to, the water phase were assessed via sorption and desorption experiments. The obtained results showed that, the more weathered the plastic, the higher its absorption capabilities; it was also observed that the different polymers showed different affinity for pesticides. As a rule, polyethylene debris turned to be more retentive towards pesticides than polypropylene. Thus, the combination of thermal and mechanical processes, involved in the recycling of previously washed agricultural polyethylene films, might be of limited usefulness to remove pesticide residues associated to end of life agricultural plastics. So, a further issue is to determine if pesticides associated to microplastics collected from aquatic environments were concentrated by these solid wastes from the water phase; or, if their correspond to the non-desorbed fraction of residues existing in microplastics, which migrated from the terrestrial environment to the aquatic one.

USC
UNIVERSIDADE DE SANTIAGO DE COMPOSTELA

USC
UNIVERSIDADE
DE SANTIAGO
DE COMPOSTELA

ANNEX 1: LIST OF PUBLICATIONS AND CONTRIBUTION STATEMENTS

Data collected from the journal of citation reports on July 8th 2024

1. Miguel Cobo Golpe, María Ramil Criado, Rafael Cela Torrijos, Isaac Rodríguez Pereiro. Portable dehumidifiers condensed water: A novel matrix for the screening of semi-volatile compounds in indoor air. Chemosphere 251 (2020) 126346. DOI: https://doi.org/10.1016/j.chemosphere.2020.126346
   Impact factor (2020): 7.086
   Journal ranking (2020): environmental sciences, 30/274, Q1
   Contribution statement: I carried out all laboratory experiments, including the optimization, validation, and application of the developed analytical methodology with chromatographic analysis, processed experimental data, data treatment and drafted the manuscript. All authors provided critical feedback and helped shape to the final version of the manuscript.
2. Miguel Cobo Golpe, María Ramil Criado, Leticia Perez Mayán, Isaac Rodríguez Pereiro. Predicting concentrations of volatile and semi-volatile compounds in indoor areas through analysis of condensed water samples. A proof of concept. Chemsphere 360 (2024) 142403. DOI: https://doi.org/10.1016/j.chemosphere.2024.142403
   Impact factor (2023): 8.1
   Journal ranking (2023): environmental sciences, 32/358, Q1
   Contribution statement: I carried out all laboratory experiments, including the optimization, validation, and application of the developed analytical methodology with chromatographic analysis, processed experimental data, data treatment and drafted the manuscript. All authors provided critical feedback and helped shape to the final version of the manuscript.
3. Miguel Cobo Golpe, María Ramil Criado, Isaac Rodríguez Pereiro. Comprehensive characterization of volatile and semi-volatile compounds in e-liquids for electronic cigarette using gas chromatography accurate mass spectrometry. Journal of chromatography A 1703 (2023) 464114 DOI: https://doi.org/10.1016/j.chroma.2023.464114
   Impact factor (2023): 3.8
   Journal ranking (2023): Analytical chemistry, 26/106, Q1
   Contribution statement: I carried out all laboratory experiments, including the optimization, validation, and application of the developed analytical methodology with chromatographic analysis, processed experimental data, data treatment and drafted the manuscript. All authors provided critical feedback and helped shape to the final version of the manuscript.
4. Miguel Cobo Golpe, Victoria Fernández Fernández, Tania Arias Cailleau María Ramil Criado, Isaac Rodríguez Pereiro. Comparison of UV, chlorination, UV-hydrogen peroxide and UV-chlorine processes for tramadol removal: Kinetics study and transformation products identification. Journal of Environmental

USC UNIVERSIDADE DE SANTIAGO DE COMPOSTELA

Chemical Engineering Volume 10 Issue 3 (2022) 107854. DOI: https://doi.org/10.1016/j.jece.2022.107854
Impact factor (2022): 7.7
Journal ranking (2022): Engineering, chemical, 16/142, Q1
Contribution statement: I carried most of the laboratory experiments, including the optimization, validation, and application of the developed analytical methodology with chromatographic analysis, processed experimental data, data treatment and drafted the manuscript. All authors provided critical feedback and helped shape to the final version of the manuscript.

5. Miguel Cobo Golpe, Gabriela Castro Varela, María Ramil Criado, Ysabel Santos, Isaac Rodríguez Pereiro. Chlorhexidine residues in sludge from municipal wastewater treatment plants: analytical determination and toxicity evaluation. Analytical and Bioanalytical Chemistry. 414 (2022) 6571-6580. DOI: 10.1007/s00216-022-04214-0
Impact factor: (2022): 4.3
Journal ranking (2022): Analytical chemistry, 20/86, Q1
Contribution statement: I carried most of the laboratory experiments, including the optimization, validation, and application of the developed analytical methodology with chromatographic analysis, processed experimental data, data treatment and drafted the manuscript. Phytotoxicity assays were carried out by me while microbiological tests were carried out by an associated laboratory. All authors provided critical feedback and helped shape to the final version of the manuscript.
6. Miguel Cobo Golpe, Jennifer García Martín María Ramil Criado, Rafael Cela Torrijos, Isaac Rodríguez Pereiro. Assessment of direct analysis in real time accurate mass spectrometry for the determination of triclosan in complex matrices. Analytical and Bioanalytical Chemistry 413 (2021) 6355–6364 DOI: 10.1007/s00216-021-03591-2
Impact factor (2021): 4.478
Journal ranking (2021): Analytical chemistry, 22/87, Q2
Contribution statement: I carried most of the laboratory experiments, including the optimization, validation, and application of the developed analytical methodology with chromatographic analysis, processed experimental data, data treatment and drafted the manuscript. All authors provided critical feedback and helped shape to the final version of the manuscript.
7. Miguel Cobo Golpe, María Ramil Criado, Rafael Cela Torrijos, Isaac Rodríguez Pereiro. Supercritical fluid chromatography time-of-flight mass spectrometry enantiomeric determination of basic drugs in sewage samples. Journal of Chromatography A 1673 (2022). 463880. DOI: https://doi.org/10.1016/j.chroma.2022.463088.
Impact factor (2022): 4.1
Journal ranking (2022): Analytical chemistry, 25/86, Q2
Contribution statement: I carried out all laboratory experiments, including the optimization, validation, and application of the developed analytical methodology with chromatographic analysis, processed experimental data, data treatment and

USC UNIVERSIDADE DE SANTIAGO DE COMPOSTELA

drafted the manuscript. All authors provided critical feedback and helped shape to the final version of the manuscript.

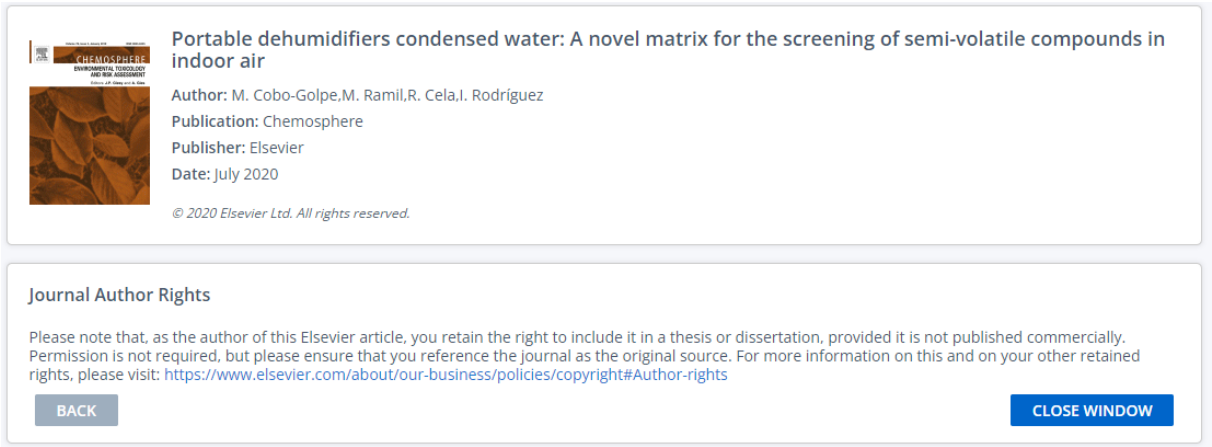
8. Miguel Cobo Golpe, Pilar Blanco, Victoria Fernández Fernández, María Ramil Criado, Isaac Rodríguez Pereiro. Assessment of the occurrence and interaction between pesticides and plastic litter from vineyard plots. Science of The Total Environment 912 (2024) 169273 DOI: https://doi.org/10.1016/j.scitotenv.2023.169273
   Impact factor (2023): 8.2
   Journal ranking (2023): Environmental sciences, 28/359, Q1
   Contribution statement: I carried most of the laboratory experiments, including the optimization, validation, and application of the developed analytical methodology with chromatographic analysis, processed experimental data, data treatment and drafted the manuscript. All authors provided critical feedback and helped shape to the final version of the manuscript.

USC UNIVERSIDADE DE SANTIAGO DE COMPOSTELA

USC
UNIVERSIDADE
DE SANTIAGO
DE COMPOSTELA

ANNEX 2: REPRODUCTION PERMISSIONS

Miguel Cobo Golpe, María Ramil Criado, Rafael Cela Torrijos, Isaac Rodríguez Pereiro. Portable dehumidifiers condensed water: A novel matrix for the screening of semi-volatile compounds in indoor air. Chemosphere 251 (2020) 126346. DOI: https://doi.org/10.1016/j.chemosphere.2020.126346 (refers to Chapter1, publication I)



Portable dehumidifiers condensed water: A novel matrix for the screening of semi-volatile compounds in indoor air

Author: M. Cobo-Golpe,M. Ramil,R. Cela,I. Rodríguez
Publication: Chemosphere
Publisher: Elsevier
Date: July 2020

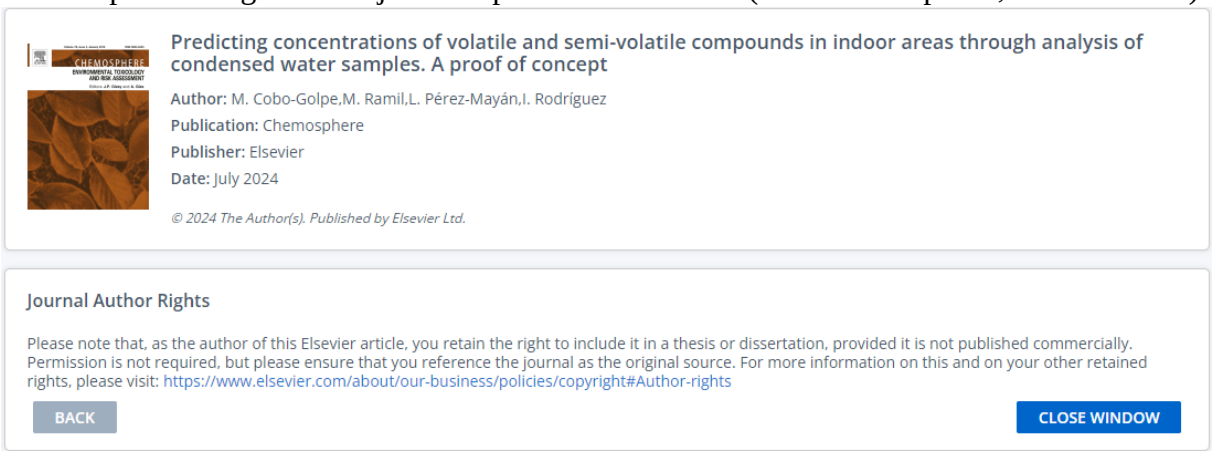
© 2020 Elsevier Ltd. All rights reserved.

Journal Author Rights

Please note that, as the author of this Elsevier article, you retain the right to include it in a thesis or dissertation, provided it is not published commercially. Permission is not required, but please ensure that you reference the journal as the original source. For more information on this and on your other retained rights, please visit: https://www.elsevier.com/about/our-business/policies/copyright#Author-rights

BACK CLOSE WINDOW

Miguel Cobo Golpe, María Ramil Criado, Leticia Perez Mayán, Isaac Rodríguez Pereiro. Predicting concentrations of volatile and semi-volatile compounds in indoor areas through analysis of condensed water samples. A proof of concept. Chemsphere 360 (2024) 142403. DOI: https://doi.org/10.1016/j.chemosphere.2024.142403 (refers to Chapter 1, Publication II)



Predicting concentrations of volatile and semi-volatile compounds in indoor areas through analysis of condensed water samples. A proof of concept

Author: M. Cobo-Golpe,M. Ramil,L. Pérez-Mayán,I. Rodríguez
Publication: Chemosphere
Publisher: Elsevier
Date: July 2024

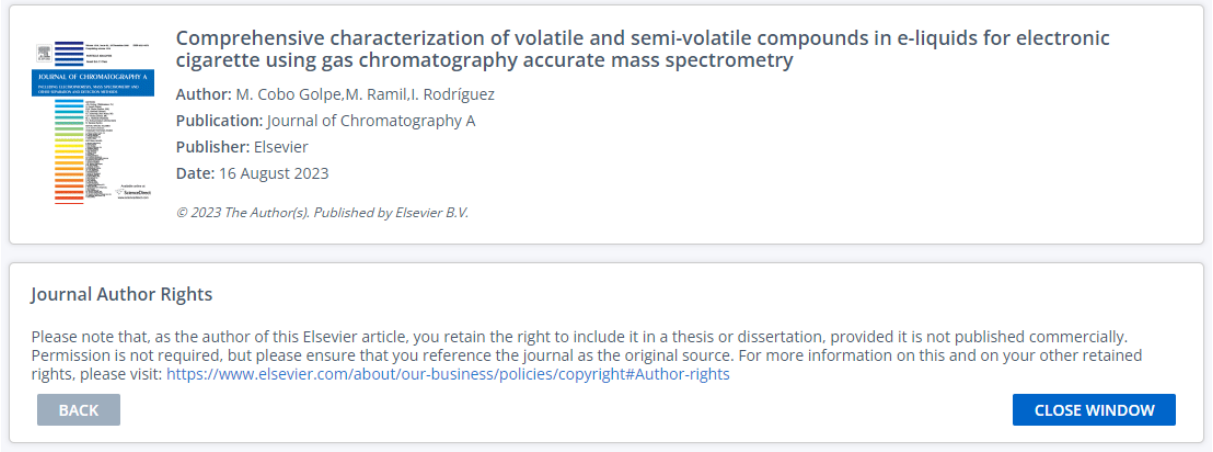
© 2024 The Author(s). Published by Elsevier Ltd.

Journal Author Rights

Please note that, as the author of this Elsevier article, you retain the right to include it in a thesis or dissertation, provided it is not published commercially. Permission is not required, but please ensure that you reference the journal as the original source. For more information on this and on your other retained rights, please visit: https://www.elsevier.com/about/our-business/policies/copyright#Author-rights

BACK CLOSE WINDOW

Miguel Cobo Golpe, María Ramil Criado, Isaac Rodríguez Pereiro. Comprehensive characterization of volatile and semi-volatile compounds in e-liquids for electronic cigarette using gas chromatography accurate mass spectrometry. Journal of chromatography A 1703 (2023) 464114 DOI: https://doi.org/10.1016/j.chroma.2023.464114 (refers to chapter 1, publication III)



Comprehensive characterization of volatile and semi-volatile compounds in e-liquids for electronic cigarette using gas chromatography accurate mass spectrometry

Author: M. Cobo Golpe,M. Ramil,I. Rodríguez
Publication: Journal of Chromatography A
Publisher: Elsevier
Date: 16 August 2023

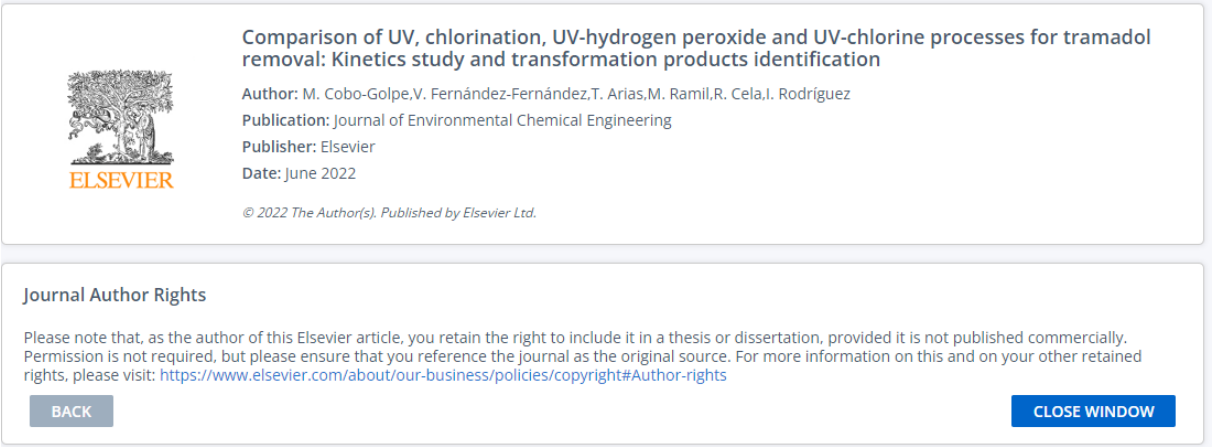
© 2023 The Author(s). Published by Elsevier B.V.

Journal Author Rights

Please note that, as the author of this Elsevier article, you retain the right to include it in a thesis or dissertation, provided it is not published commercially. Permission is not required, but please ensure that you reference the journal as the original source. For more information on this and on your other retained rights, please visit: https://www.elsevier.com/about/our-business/policies/copyright#Author-rights

BACK CLOSE WINDOW

Miguel Cobo Golpe, Victoria Fernández Fernández, Tania Arias Cailleau María Ramil Criado, Isaac Rodríguez Pereiro. Comparison of UV, chlorination, UV-hydrogen peroxide and UV-chlorine processes for tramadol removal: Kinetics study and transformation products identification. Journal of Environmental Chemical Engineering Volume 10 Issue 3 (2022) 107854. DOI: https://doi.org/10.1016/j.jece.2022.107854 (refers to Chapter 1, Publication IV)



Comparison of UV, chlorination, UV-hydrogen peroxide and UV-chlorine processes for tramadol removal: Kinetics study and transformation products identification

Author: M. Cobo-Golpe,V. Fernández-Fernández,T. Arias,M. Ramil,R. Cela,I. Rodríguez
Publication: Journal of Environmental Chemical Engineering
Publisher: Elsevier
Date: June 2022

© 2022 The Author(s). Published by Elsevier Ltd.

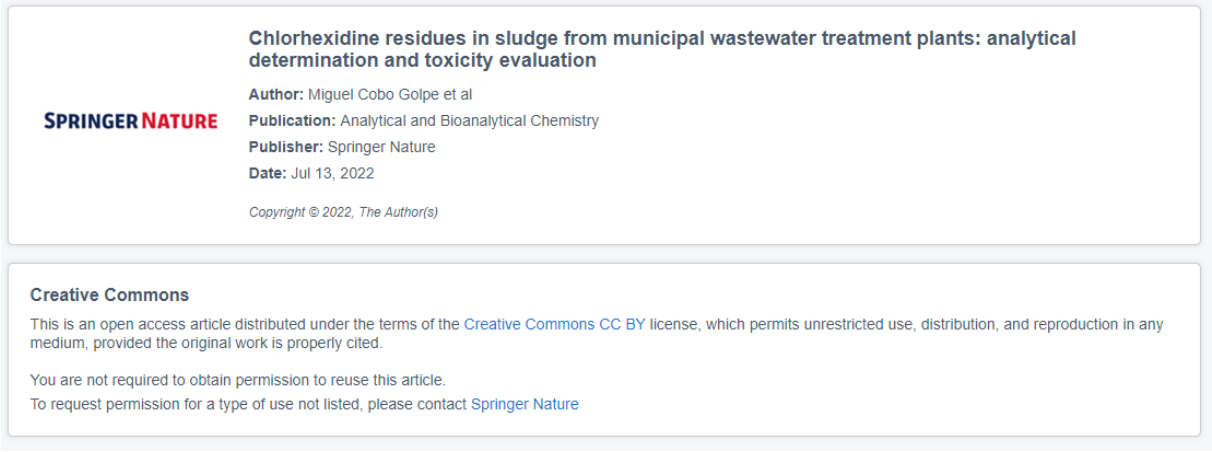
Journal Author Rights

Please note that, as the author of this Elsevier article, you retain the right to include it in a thesis or dissertation, provided it is not published commercially. Permission is not required, but please ensure that you reference the journal as the original source. For more information on this and on your other retained rights, please visit: https://www.elsevier.com/about/our-business/policies/copyright#Author-rights

BACK CLOSE WINDOW

Miguel Cobo Golpe, Gabriela Castro Varela, María Ramil Criado, Ysabel Santos, Isaac Rodríguez Pereiro. Chlorhexidine residues in sludge from municipal wastewater treatment plants: analytical determination and toxicity evaluation. Analytical and Bioanalytical Chemistry. 414 (2022) 6571-6580. DOI: 10.1007/s00216-022-04214-0 (refers to Chapter 2, Publication V)

USC UNIVERSIDADE DE SANTIAGO DE COMPOSTELA



Chlorhexidine residues in sludge from municipal wastewater treatment plants: analytical determination and toxicity evaluation

Author: Miguel Cobo Golpe et al
Publication: Analytical and Bioanalytical Chemistry
Publisher: Springer Nature
Date: Jul 13, 2022

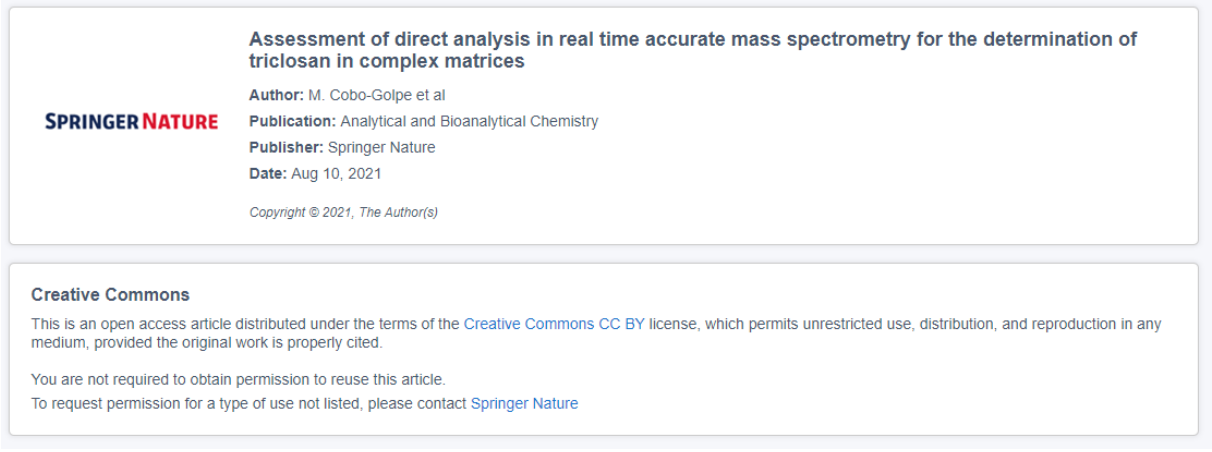
Copyright © 2022, The Author(s)

Creative Commons

This is an open access article distributed under the terms of the Creative Commons CC BY license, which permits unrestricted use, distribution, and reproduction in any medium, provided the original work is properly cited.

You are not required to obtain permission to reuse this article.
To request permission for a type of use not listed, please contact Springer Nature

Miguel Cobo Golpe, Jennifer García Martín María Ramil Criado, Rafael Cela Torrijos, Isaac Rodríguez Pereiro. Assessment of direct analysis in real time accurate mass spectrometry for the determination of triclosan in complex matrices. Analytical and Bioanalytical Chemistry 413 (2021) 6355–6364 DOI: 10.1007/s00216-021-03591-2 (refers to Chapter 2, Publication VI)



Assessment of direct analysis in real time accurate mass spectrometry for the determination of triclosan in complex matrices

Author: M. Cobo-Golpe et al
Publication: Analytical and Bioanalytical Chemistry
Publisher: Springer Nature
Date: Aug 10, 2021

Copyright © 2021, The Author(s)

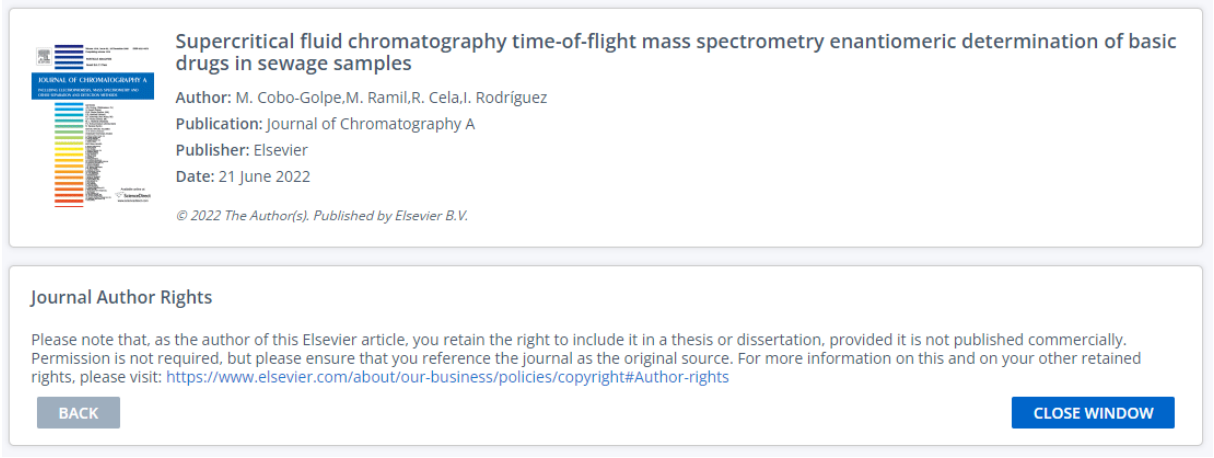
Creative Commons

This is an open access article distributed under the terms of the Creative Commons CC BY license, which permits unrestricted use, distribution, and reproduction in any medium, provided the original work is properly cited.

You are not required to obtain permission to reuse this article.
To request permission for a type of use not listed, please contact Springer Nature

Miguel Cobo Golpe, María Ramil Criado, Rafael Cela Torrijos, Isaac Rodríguez Pereiro. Supercritical fluid chromatography time-of-flight mass spectrometry enantiomeric determination of basic drugs in sewage samples. Journal of Chromatography A 1673 (2022). 463880. DOI: https://doi.org/10.1016/j.chroma.2022.463088. (refers to Chapter 2, Publication VII)

USC UNIVERSIDADE DE SANTIAGO DE COMPOSTELA



Supercritical fluid chromatography time-of-flight mass spectrometry enantiomeric determination of basic drugs in sewage samples

Author: M. Cobo-Golpe,M. Ramil,R. Cela,I. Rodríguez
Publication: Journal of Chromatography A
Publisher: Elsevier
Date: 21 June 2022

© 2022 The Author(s). Published by Elsevier B.V.

Journal Author Rights

Please note that, as the author of this Elsevier article, you retain the right to include it in a thesis or dissertation, provided it is not published commercially. Permission is not required, but please ensure that you reference the journal as the original source. For more information on this and on your other retained rights, please visit: https://www.elsevier.com/about/our-business/policies/copyright#Author-rights

BACK CLOSE WINDOW

Miguel Cobo Golpe, Pilar Blanco, Victoria Fernández Fernández, María Ramil Criado, Isaac Rodríguez Pereiro. Assessment of the occurrence and interaction between pesticides and plastic litter from vineyard plots. Science of The Total Environment 912 (2024) 169273 DOI: https://doi.org/10.1016/j.scitotenv.2023.169273. (refers to Chapter 2, Publication VIII)



Assessment of the occurrence and interaction between pesticides and plastic litter from vineyard plots

Author: M. Cobo-Golpe,P. Blanco,V. Fernández-Fernández,M. Ramil,I. Rodríguez
Publication: Science of The Total Environment
Publisher: Elsevier
Date: 20 February 2024

© 2023 The Authors. Published by Elsevier B.V.

Journal Author Rights

Please note that, as the author of this Elsevier article, you retain the right to include it in a thesis or dissertation, provided it is not published commercially. Permission is not required, but please ensure that you reference the journal as the original source. For more information on this and on your other retained rights, please visit: https://www.elsevier.com/about/our-business/policies/copyright#Author-rights

BACK CLOSE WINDOW

USC
UNIVERSIDADE
DE SANTIAGO
DE COMPOSTELA





The use of chemical substances has become a necessity to maintain our current lifestyle. However, they can cause undesired effects in the environment and human beings. This Thesis addresses the development of mass spectrometry applications, using complementary analytical platforms, for target and non-target analysis of different kinds of compounds. Application of the developed methods has contributed to the comprehensive characterization of volatile compounds in complex samples, such as indoor air and e-liquids; the identification of the degradation routes of tramadol, under oxidative treatments; and the quantification of several groups of concerning chemicals in sludge, wastewater and end-of-life plastic wastes. Results were reflected in eight publications in international scientific journals.